Measurement of Venous Blood Flow Using Photoplethysmography

Gareth W John

PRIFYSGOL CYMRU
UNIVERSITY OF WALES

PhD Thesis

2005

CARDIFF UNIVERSITY
PRIFYSGOL CAERDYDD

coleg meddygaeth cymru
wales college of medicine

PRIFYSGOL CYMRU
UNIVERSITY OF WALES

UMI Number: U200853

All rights reserved

INFORMATION TO ALL USERS
The quality of this reproduction is dependent upon the quality of the copy submitted.

In the unlikely event that the author did not send a complete manuscript
and there are missing pages, these will be noted. Also, if material had to be removed,
a note will indicate the deletion.

UMI U200853
Published by ProQuest LLC 2013. Copyright in the Dissertation held by the Author.
Microform Edition © ProQuest LLC.
All rights reserved. This work is protected against
unauthorized copying under Title 17, United States Code.

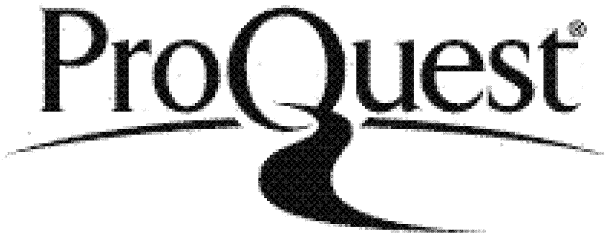

ProQuest LLC
789 East Eisenhower Parkway
P.O. Box 1346
Ann Arbor, MI 48106-1346

Acknowledgements

There are numerous people who I would like to thank for their help during my work on this study. Firstly, my supervisor, Professor JP Woodcock for giving me the opportunity to undertake the research, for his continuing encouragement and trust, and for always making time to listen. Thanks also to Dr Nigel Gough whose ideas and suggestions helped a great deal and to Huntleigh Technology PLC for financing the project. I would also like to thank the all the staff at the Department of Medical Physics and Bioengineering at the University Hospital of Wales for their help during my time there and for providing me with the patients required for the study.

My special thanks extend to all my family whose encouragement, support, understanding and patience are abundant and never faltering.

Gareth.

List of Abbreviations

ADC	Analogue-to-digital converter
AK	Above knee
AV	Arteriovenous
AVP	Ambulatory venous pressure
BK	Below knee
CDM	Complex demodulation
COM	Communications
cpm	Cycles per minute
DFT	Discrete Fourier transform
dp	Decimal places
DPPG	Digital photoplethysmography
DUS	Doppler ultrasound
DVT	Deep vein thrombosis
ECG	Electrocardiogram
FFT	Fast Fourier transform
IIR	Infinite impulse response
IR	Infrared
LED	Light emitting diode
LPF	Low pass filter
LRR	Light reflection rheography
MAAD	Mean absolute amplitude difference
MAPD	Mean absolute phase difference
MPD	Mean phase difference
MRI	Magnetic resonance imaging
NPV	Negative predicting value
PC	Personal computer
PE	Pulmonary embolism
PI	Preliminary investigation
PPG	Photoplethysmography
PPV	Positive predicting value
RT	Refill time
sf	Significant figures
UHW	University Hospital of Wales
UV	Ultraviolet
VP	Venous pump

Abstract

In this study, a new test for lower limb deep vein thrombosis (DVT) is developed using digital photoplethysmography (DPPG). Signal processing techniques are used to analyse DPPG signals collected from the feet of 142 patients (65 with DVT and 77 without DVT) while they rested in a supine position for 10 minutes.
Fourier analysis is used to investigate the frequency content of the signals and, by reference to the literature, the frequencies are associated with corresponding physiological processes. It is established that the signals contain three important frequency bands representing neurogenic and local controls of microcirculation blood flow, the influence of breathing and cardiac pulsations.
Following this, complex demodulation is used to analyse the amplitude and phase of selected frequencies within the signals. For the breathing frequencies, a greater phase difference is identified statistically between the signals taken from the feet of the patients with DVT, compared to those without the condition. Consequently, it is shown that the phase difference can be used as an indicator of lower limb DVT by empirically setting a threshold value to distinguish between the two patient groups. Using the data from the 142 patients, the new test is shown to have sensitivity 100%, positive predicting value 49.5%, specificity 27.5%, negative predicting value 100% and accuracy 57.6%.

This simple, non-invasive test will reduce the patient numbers requiring the more time-consuming ultrasound examination, by screening out a high proportion of individuals who definitely do not have lower limb DVT. However, further signal processing methods should be investigated to improve the specificity of the test.

Contents

Chapter 1

Anatomy and Physiology of the Circulatory System

The role of the circulatory system is to service the body's tissues and to maintain a suitable environment for them to be able to function. The circulatory system is essentially a network of tubes throughout the body. These conduits transport blood around the body, driven by a central pump, the heart. The blood consists of red blood cells, white blood cells, and platelets, suspended in plasma. Oxygen and nutrients are transported around the body to the tissues while carbon dioxide and other waste products are removed.

The circulatory system is divided into two sections – pulmonary and systemic. The pulmonary circulation provides a blood supply to the lungs whereas the systemic circulation supplies all other parts of the body (the systemic circulation is sometimes called the greater or peripheral circulation).

Since this project is concerned with blood flow in the lower limbs, it is the systemic circulation that this chapter will be primarily concerned with.

1.1 Components of the systemic circulation

The blood vessels vary in diameter in different parts of the circulation (table 1.1) and are categorised depending on whether they carry blood to or away from the heart. Generally, the arteries carry blood away from the heart towards the other tissues/organs of the body, whereas the veins transport blood from the tissues/organs back towards the heart.

Table 1.1: Generalisation of the physical dimensions of the blood vessels.

Vessel	Approximate internal diameter (cm) *(Berne and Levy, 1998)*	Approximate vessel wall thickness (cm) *(Berne and Levy, 1998)*	Approximate total cross sectional area (cm^2) *(Guyton, 2000)*
Aorta	2.5	0.2	4.5
Arteries	0.4	0.1	20
Arterioles	30×10^{-4}	6×10^{-4}	40
Capillaries	8×10^{-4}	0.5×10^{-4}	2500
Venules	20×10^{-4}	1×10^{-4}	250
Veins	0.5	0.05	80
Venae cavae	3	0.15	8

The largest artery in the systemic circulation is the aorta, which leaves the heart and travels though the thorax and abdomen. Numerous smaller arteries branch off from the aorta, which in turn split into smaller branches carrying blood to all parts of the body. As the blood travels further from the heart and more and more branches develop, the arteries gradually decrease in diameter, eventually becoming arterioles. These very small diameter vessels have a strong muscular wall, enabling them to constrict or dilate to control the volume of blood flowing through their lumen. Such control is essential for moderating blood pressure and controlling flow through to the capillaries. The capillaries have the smallest diameter of all the vessels in the circulatory system. It is here that the essential exchange takes place between the blood and interstitial fluid. The capillaries have very thin walls (one cell layer thick) containing many pores, through which the exchange of nutrients, waste products and other substances takes place. Subsequent to the capillaries, vessel diameter begins to increase again as the blood enters the venous side of the circulation. The blood from the capillaries flows into the venules. These are essentially small collection conduits, the diameter of which increases steadily as they combine to become larger veins. The function of the veins is twofold. Firstly they act as conduits for returning blood back to the heart. Secondly, they act as reservoirs of blood and may hold more than 60% of the total blood volume in the circulation at any one time (table 1.2). The amount of blood stored in these pools has an appreciable effect on cardiac output since the heart can only pump out what is delivered to it from the venous system.

Table 1.2: Distribution of blood throughout the body.

Section of the circulatory system	Percentage of total blood volume *(Guyton, 2000)*	Percentage of total blood volume when supine *(Bray et al., 1999)*
Pulmonary Circulation	9	16
Heart	7	8
Arteries	13	12
Arterioles and capillaries	7	9
Veins, venules and venous sinuses	64	55

The veins have highly elastic walls, which gives them the ability to expand like balloons. Systemic veins are about 8 times as distensible and have a compliance of approximately 24 times greater than the corresponding systemic arteries (Guyton, 2000). In addition, the total cross sectional area of the veins is approximately four times that of the arteries (table 1.1). The most distensible veins of the lower extremities are those of the superficial system, which can dilate to accommodate large volumes of blood with little increase in back pressure. The volume of blood within such veins at any moment can vary by a factor of two or more without interfering with the normal function of the vein. Deep veins below the deep fascia tend to be thicker walled and surrounded by muscle. This reduces their extensibility somewhat.

1.2 Pressure and flow through the circulatory system

The approximate pressures and velocities of blood in the circulatory system of a supine person are shown in figure 1.1.

Fig 1.1: Pressure and velocity variations as blood flows through the systemic circulation of a supine person. *Adapted from Ganong (1999).*

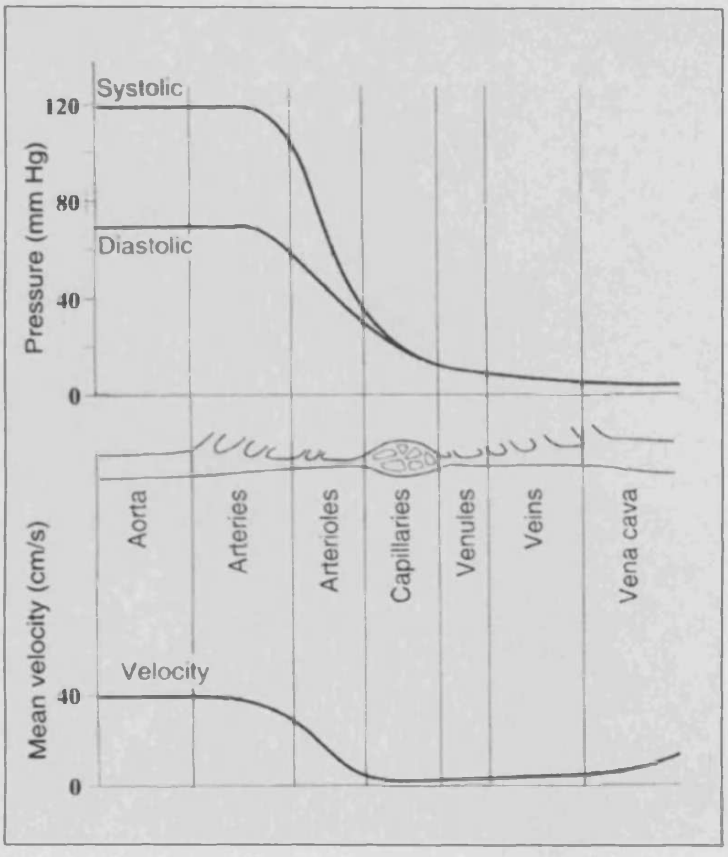

Moving from the aorta, through the arterial system to the venous system and eventually the vena cava, there is an overall decrease in blood pressure (because of the resistance of the vessels to blood flow). The mean pressure in the aorta is approximately 100mmHg, falling to around 30mmHg at the arterioles*. On the venous side of the circulation the pressure continues to fall from around 10mmHg in the venules to almost 0mmHg at the right atrium. However, there is still a sufficient pressure gradient to drive blood back to the heart through the low resistance venous vessels, when supine. Pressure variations are greatest in the aorta where the pumping action of the heart forces blood into the artery at approximately 120mmHg at systole and approximately 80mmHg at diastole, in a typical person. The pressure variations, caused by the pumping action of the heart, become damped as blood flows through the arteries, eventually disappearing at the capillaries.

* 1mmHg=133.32Pa (2dp)

Vessel diameter also decreases from the aorta to the capillaries with a consequent increase in the resistance to blood flow and a decrease in blood velocity. The diameter of the arteries, which may be more than a centimetre, decreases to micrometres at the arterioles. The arterioles offer major resistance to blood flow in the normal circulation. Through sympathetic nervous control of their strong muscular walls they have the ability to constrict and direct flow to regions where blood is required the most. For example, during periods of heavy exercise, constriction of the arterioles supplying the skin allows extra blood to be directed to the skeletal muscles. Control of blood flow by the arterioles is discussed further in section 1.5.2, where the microcirculation is described in greater detail.

The capillaries have the smallest diameter of all the blood vessels. Therefore, blood velocity is slower here than in any other part of the body (about 1000 times slower than the blood velocity in the aorta (Guyton, 2000)). Slow flow is necessary to allow the exchange of nutrients and waste products to take place in the tissues. In addition, the total surface area of the capillaries is greater than any other vessel (table 1.1), which is essential in order to supply the body's vast nutritional requirements.

On the venous side of the capillary network, vessel diameter begins to increase again as the venules coalesce to form veins, which may have diameters of the order of centimetres. Resistance decreases and blood velocity increases, even though venous pressure continues to fall when the body is relaxed and the veins are undisturbed.

An important point to note here is that the above description applies to a supine person. The situation changes when a person stands up. In this case, venous blood pressure in the lower limbs increases due to the weight of the column of blood in the veins. The hydrostatic pressure causes venous blood pressure in the feet to rise to approximately 90mmHg (Guyton, 2000). Consequently, the human body has to employ additional methods to increase the return of venous blood to the heart and to prevent swelling of the limbs. These are described below.

1.3 Return of venous blood to the heart

The walls of the deep veins contain valves whose function is to keep the blood flowing in one direction only (fig 1.2). The valves are oriented in the direction of the blood flow. When open, the valves allow venous blood flow towards the heart with only little

reduction of the vessel lumen. However, if the blood attempts retrograde flow, the valves are pushed back, completely blocking the lumen and preventing reflux. In this way, venous blood is kept flowing in one direction only.

Fig 1.2: The action of a venous valve.
Arrows indicate the direction of blood flow.

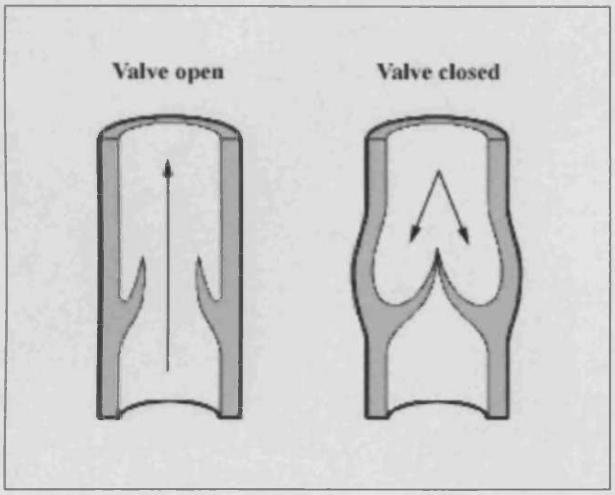

The blood is helped through the veins by the "muscle pump" mechanism. Contraction of the muscles compresses the veins and, since the blood has to go somewhere, it is moved in a direction towards the heart. The venous valves prevent any flow in the opposite direction. Subsequent relaxation of the muscles results in a decreased venous pressure in the section of the vein that was compressed (due to the expulsion of blood). The blood then flows from distal regions of higher pressure, through the one-way valves towards the heart.
In a person with fully functioning venous valves, blood pressure in the veins of the legs is maintained at less than 25mmHg during walking as a result of the muscle pump mechanism (Guyton, 2000).

Another mechanism that aids venous return to the heart is breathing (e.g., Berne and Levy, 1998). During inspiration, intrathoracic pressure decreases and less pressure acts on the walls of the veins within the thoracic cavity. Central venous pressure decreases and the pressure gradient between the intrathoracic and extrathoracic veins increases. As a consequence, there is a net movement of blood from the abdominal to the thoracic

veins. During expiration, blood flow into the thoracic veins decreases. However, reverse flow does not occur because of the presence of venous valves. The net effect is a phasic flow of blood towards the heart, synchronous with breathing. This phasic flow is communicated to the deep veins of the lower limbs and can be detected by, e.g., Doppler examination of the deep veins of the thigh.

However, the relative amount of blood flow during inspiration and expiration depends on the extent to which the abdominal muscles are used during breathing. In normal, spontaneous breathing, movement of the diaphragm up and down shortens and lengthens the chest cavity (Guyton, 2000). On the other hand, during heavy breathing, contraction of the abdominal muscles can help raise the diaphragm by pushing the contents of the abdomen against it. Murray et al. (1996) state that, during "abdominal breathing", there is reduced blood flow back to the heart during inspiration.

1.4 Anatomy of the circulatory system in the lower limbs

This section describes the anatomy of the blood vessels in the lower limbs. Since this study is concerned with venous thrombosis, the emphasis will be on venous anatomy. However, in general, for every deep vein (or pair of veins in the calf) there is usually a corresponding artery. Therefore, the arterial anatomy will not be significantly different from that of the deep veins.

The venous system in the leg can be thought of as comprised of two parts; the deep and the superficial system. The deep system is so called because the vessels exist deep inside the muscles of the body, whereas the superficial system exists just below the skin. There are also perforating veins that connect the deep and the superficial systems. A schematic diagram of the anatomy of the venous system of the lower limbs is shown in figure 1.3. The diagram represents the venous anatomy that will be found in the majority of individuals. However, this is not universal. There are many forms that the anatomy could take, e.g. veins may be duplicated, non-existent or link together in different ways.

Fig 1.3: Diagram of the main veins of the lower limbs and the tissues drained by the veins.
Superficial veins are marked "(sv)".

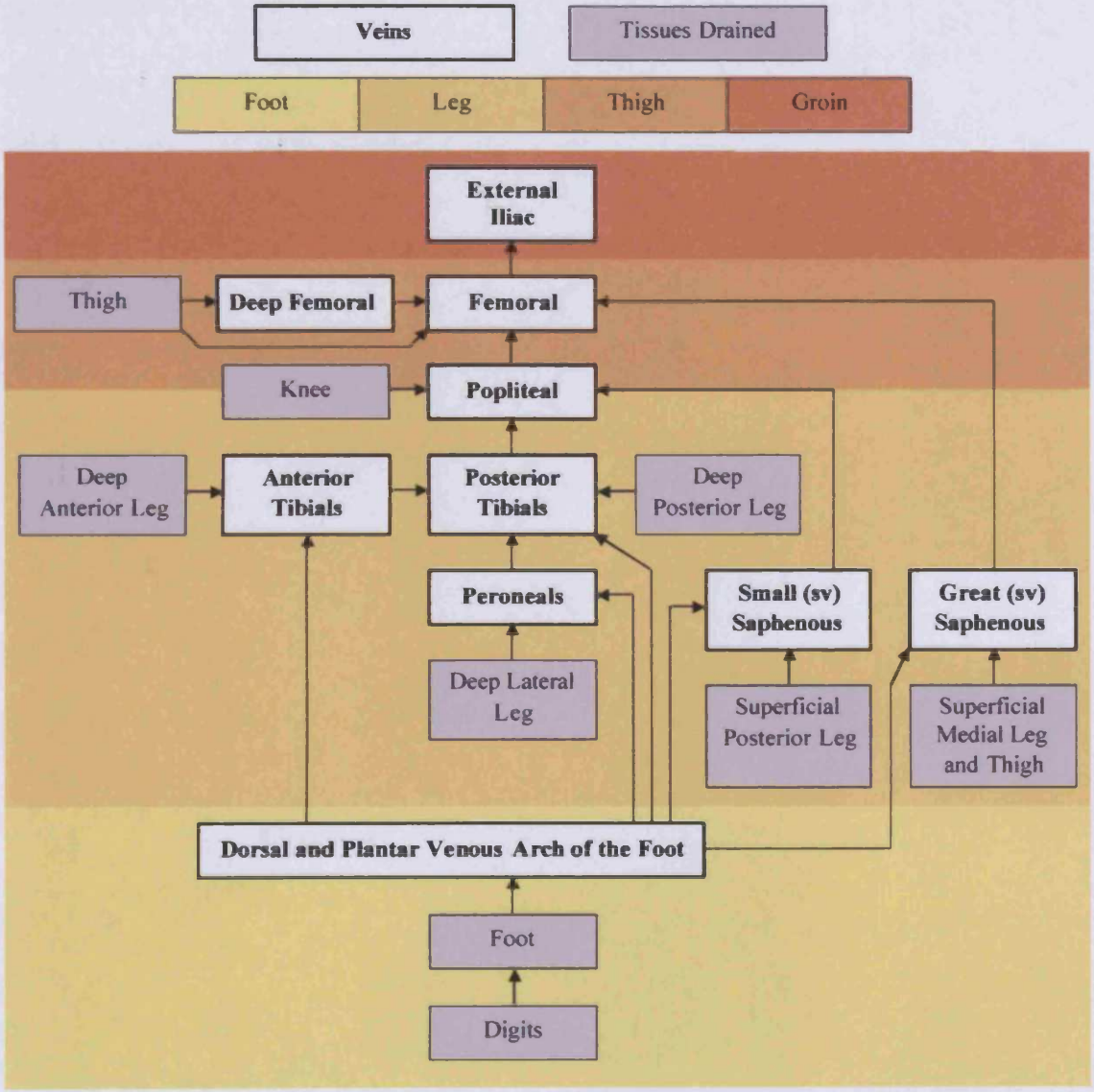

1.4.1 The superficial venous system of the lower limbs

The superficial venous system of the lower limbs contains many veins. These act as conduits, moving blood to the deep venous system ready for return to the heart. The number and location of the various superficial veins varies from person to person. In fact, the variability is so great that many are not even named. There are, however, two long veins that are typically found; the small saphenous vein and the great saphenous vein. The small saphenous vein originates in the foot and runs laterally along the leg

before, in most cases, draining into the popliteal vein at the level of the knee. However, in some cases, the small saphenous vein may drain into the deep venous system of the thigh or even into the great saphenous vein. The great saphenous vein also originates in the foot but runs along the medial line of the leg and thigh before eventually draining into the femoral vein just before it enters into the pelvic region. The great saphenous vein is the longest vein in the human body

The confluence of the small saphenous vein with the popliteal vein and the great saphenous vein with the femoral vein are called the spahenopopliteal and the saphenofemoral junctions respectively.

There are also perforating veins that take blood directly from the superficial to the deep venous system, through the deep fascia. Valves in the walls of the perforating veins maintain one way flow from the superficial to the deep system. Again, only a few of the perforating veins are ever consistent in location, with the majority being variable and therefore not named.

1.4.2 The deep venous system of the lower limbs

The deep veins of the lower limbs are the main conduits for storing blood before being returned to the heart. Below the knee, three main groups of deep veins exist; the anterior tibial veins, the posterior tibial veins and the peroneal veins. In most cases, these are actually pairs of veins running parallel to the correspondingly named artery. Venous sinusoids within the gastrocnemius and soleus muscles also merge to form part of the deep venous system and drain into the peroneal vein at the mid-calf level. Just below the knee, the anterior and posterior tibial veins join with the peroneal veins and become the single popliteal vein. This large vein forms the main outflow channel of blood from the leg. Although it is one long vessel, its name changes as it continues through to the thigh. Passing through the adductor canal at the level of the knee, the popliteal vein becomes the femoral vein with the accolade of being the longest deep vein in the lower extremity. The *deep* femoral vein supplies a tributary to the femoral vein, connecting with it at the proximal thigh level. This short vein usually has its origin in the terminal deep muscle tributaries in the lateral thigh. In some cases, the deep femoral vein may instead join with the popliteal vein. The merging of the femoral

and deep femoral veins forms the common femoral vein, which travels, towards the pelvis, eventually becoming the external iliac vein at the groin.

1.5 The microcirculation

Presented below is a more detailed description of the components of the microcirculation together with the processes that control blood flow through the vessels. The general microcirculation is described. However, since this study is primarily concerned with blood flow through the microcirculation of the skin, any differences are specifically highlighted.

1.5.1 The structure of the microcirculation

The microcirculation is a multifunctional network of vessels playing a crucial role in the regulation of metabolic, haemodynamic and thermal processes in the body. In the case of the skin, the most important of these is thermoregulatory control.

The microcirculation consists of three main types of blood vessels; arterioles, capillaries and venules. The vessel diameters are of the order of 1-100μm and are some of the smallest in the body. Also on this scale, and working closely with the microcirculation, is the lymphatic system. This is a network of lymph vessels that carry, amongst other things, proteins, water and electrolytes from the tissues and returns them to the blood stream via the thoracic duct and the innominate veins of the neck. The lymph vessels do not contain blood.

Blood flows from the arteries, into the arterioles. These are small vessels with an internal diameter between 5-100μm and similar vessel wall thickness (Berne and Levy, 1998). The arterioles arise from the continual branching of the larger arteries. They have highly muscular walls and the ability to significantly alter their diameter to control flow. The arterioles are important resistance vessels and are directly associated with the maintenance of arterial blood pressure. They directly control the rate of blood flow from the arteries through to the capillaries and the venous system. As they pass further into the microcirculation, the arterioles become smaller in diameter, eventually becoming capillaries.

After passing through the arterioles, the blood enters the capillaries via metarterioles or terminal arterioles. Metarterioles are vessels that have a structure somewhere between that of an arteriole and a capillary. Their walls are not as muscular as the arterioles and only have intermittent smooth muscle fibres surrounding the vessel. Flow into the capillaries is also controlled by pre-capillary sphincters. Here, a smooth muscle fibre around the capillary wall controls the blood flow from the metarterioles.

The capillaries have an internal diameter of around 4-9μm and are the smallest blood vessels in the body (e.g., Guyton, 2000). The diameter of some of the smallest capillaries is such that erythrocytes have to deform their shape in order to pass through. The capillary wall consists only of a single layer of endothelial cells, which acts as a semi-permeable membrane. Their main function is to allow the diffusion of substances including oxygen, carbon dioxide and nutrients etc. between the blood and the tissues. The capillaries pervade a huge area within the body and are so essential to the tissues that every single functioning cell is typically no more than 20-30μm away (Guyton, 2000).

Following the passage through the capillaries, the blood drains into a series of venules. These vessels are generally larger than the arterioles but have a weaker muscular wall. (However, because of the small blood pressure here, the venules still have the ability to constrict.) Many venules merge to form the larger veins. Therefore, the venules are fundamentally conducting vessels that channel blood from the microcirculation into the main veins of the body.

In some areas of the body, another type of vessel, called arteriovenous (AV) anastomoses, can be found in the microcirculation. These vessels have thick muscular walls and shunt blood directly from the arterioles to the venules, bypassing the capillary network. They are commonly found in the skin of the ears, the hands and the feet. Such a system is important in the skin for temperature regulation. Here, large amounts of blood need to be moved through the microcirculation, bypassing the capillaries, since not all the blood is needed for metabolism.

The microcirculation supplies many different body tissues, each requiring different quantities of blood flow at different times. For example, the skeletal muscle may require increased blood flow during exercise. The microcirculation adjusts the blood flow through its vessels to provide each particular tissue with just the right amount to

match its requirements. This is achieved primarily by constriction of the arterioles. In this way, blood is diverted to the tissues that require it the most. Such subtle regulation allows the heart to do only a minimum amount of work to adequately supply blood to all the tissues of the body. If a large microcirculation blood flow existed at all times through all tissues, the amount of blood required to supply the flow would be more than the heart could cope with (Guyton 2000).

A summary of the factors that influence blood flow in the microcirculation and the way in which it is controlled is outlined below.

1.5.2 Control of microcirculation blood flow

There are several mechanisms that control blood flow through the microcirculation. These can be broadly split into two categories, i.e., local and central control.
Local control depends on factors in the neighbourhood of the vessels concerned. Here, the tissue itself can influence blood flow to meet its own specific requirements.
Central control is mainly directed by the nervous system and responds to the global requirements of the body, e.g., control of blood pressure and body temperature.

1.5.2.1 Local controls of microcirculation blood flow

Local controls include intrinsic mechanisms, related to the vascular smooth muscle itself. These perform auto regulatory controls where the vessels maintain steady blood flow by adjusting their resistance. These are,

1. Myogenic regulation of the diameter of arterioles. Stretching the vessel's wall induces a constrictive response in the vascular smooth muscle and vice versa. It is currently unclear why this response occurs (Berne and Levy, 1998).
2. Regulation via the endothelium lining the arterioles and larger upstream arteries. As flow increases through the vessels, the increased drag puts the walls under stress. This triggers the release of factors that induce dilatation of the vessel. The chemical thought to be primarily responsible for this effect is nitric oxide (Berne and Levy, 1998).

3. Metabolic regulation governs blood flow by monitoring the local oxygen content in the tissues.

   The vasodilator theory suggests that any oxygen deficiency will trigger the release of chemicals from the tissue that cause dilatation of the vessels and therefore increased blood flow and oxygen supply to the affected area. Again, it is uncertain which chemicals cause this effect.

   Alternatively, the oxygen lack theory postulates that when there is a lack of oxygen and other nutrients, the muscles of the vessels themselves do not have the required energy to maintain their constricted state and instead naturally dilate. This, in turn, results in more oxygenated blood reaching the vessels, enabling constriction once again.

   These mechanisms lead to cyclic opening and closing of the arterioles, metarterioles and the precapillary sphincters, called vasomotion.

All of the above processes are acute controls of blood flow and are able to react within a few seconds or minutes to changing local conditions. They are temporary solutions. There are also long-term controls of the microcirculation's blood supply that act over days, weeks or months and give a more complete regulation of blood flow. These involve the growth of new blood vessels to supply the tissues.

1.5.2.2 Central controls of microcirculation blood flow

1.5.2.2.1 Arterial blood pressure control

Central control of microcirculation blood flow is mainly via the autonomic nervous system. Of the two main components of this system, the most important is sympathetic control. Parasympathetic regulation of the circulation plays an important role in the control of heart functions, but its role in the microcirculation is non-existent in some areas, including the skin or muscle.

The sympathetic nervous system provides an important, rapid control over arterial blood pressure. Sympathetic innervation extends to both arteries and veins. In the microcirculation, the arterioles, venules, AV anastomoses and some metarterioles are sympathetically innervated but not the capillaries. It is believed that the pre-capillary sphincters are not innervated but opening and closing is caused by local conditions in the tissues, such as oxygen concentration (Guyton 2000). The vasomotor centre,

located in the medulla oblongata controls the firing of sympathetic nerves throughout the body. The vasomotor centre is responsible for maintaining vasomotor tone in the vessels by continuous, slow firing of the sympathetic nerve fibres at a rate of 1.5-2Hz (Guyton, 2000). In the skin, the basal tone of the vessels is lower than in muscle and they have a greater sensitivity to sympathetic nervous stimulation than the large veins (Berne and Levy, 1998).

When the arterial blood pressure falls too low, very nearly all the arterioles together with the other large vessels, especially the veins, are almost immediately constricted. In addition, the heart rate and contractile force of the heart is increased. This effect is also important during heavy exercise where arterial pressure rises about 30-40%, increasing blood flow to the working muscles (Guyton, 2000).

1.5.2.2.1.1 Baroreceptor reflex

One of the most important nervous system controls affecting the microcirculation is the baroreceptor reflex. The baroreceptors are nerve endings found in several large systemic arteries, but are most prevalent in the carotid sinuses and the aortic arch. When arterial blood pressure rises, the baroreceptors are stretched and the vasomotor center is inhibited. Within seconds, the arterioles and veins become dilated and the heart rate and contractile strength is reduced. Conversely, when arterial pressure falls, the inhibitory effect of the baroreceptors is lost and blood pressure rises. The baroreceptors monitor short term changes in arterial pressure, responding more strongly when pressure changes are more rapid. This maintains arterial pressure around a constant value. However, the baroreceptors are "reset" every few days and essentially forget what value the arterial pressure was previously maintained at. Any gradual drift in arterial pressure, upwards or downwards, over time results in the baroreceptors endeavoring to maintain arterial pressure at its new value. Therefore, baroreceptor control of arterial blood pressure is only effective in the short term.

1.5.2.2.1.2 Chemoreceptor reflex and other controls

There is another arterial pressure control system that works in the same way as the baroreceptor control but, instead of using stretch receptors, uses chemoreceptors to detect lack of oxygen, increase of carbon dioxide or excess hydrogen ions. (However,

the chemoreceptors are much less important in arterial pressure control than they are in respiratory control.) The chemoreceptors, located in the carotid bodies and aortic bodies, are always in close contact with the arterial blood. A fall in arterial pressure, and subsequent reduced blood flow, is accompanied by a lack of oxygen and build up of carbon dioxide and hydrogen ions. Responding to these changes, signals are sent from the chemoreceptors to the vasomotor centre which correspondingly alters the constriction of the arterioles via the sympathetic nervous system. However, over normal pressures, the chemoreceptor reflex is not as important as the baroreceptor control since the response only figures prominently once the pressure falls to below ~80mmHg.

Other arterial pressure control systems include the atrial and pulmonary artery reflexes that, via stretch receptors in their walls, are able to react to pressure changes caused by changes in blood volume. However, the receptors are unable to monitor systemic arterial pressure.

Arterial blood pressure is controlled primarily by the above mechanisms. Even though the vasomotor center in the brain coordinates the response to the signals sent to it by the baroreceptors, chemoreceptors and low pressure receptors, all of these receptors are found outside the brain, in the peripheral circulation. However, when blood flow to the vasomotor centre itself is reduced, such that there becomes a nutritional deficiency, the neurons in the vasomotor center itself become excited and respond by greatly raising the arterial blood pressure. This is known as the central nervous system ischemic response. However, the response only acts in emergency situations whenever blood flow to the brain falls to dangerously low levels.

1.5.2.2.2 Hypothalamus and temperature control

Temperature control in the body can be thought of in terms of two components – core temperature and skin temperature. In the absence of fever, the core temperature deep within the body is kept remarkably constant, within $\pm 0.6^{\circ}C$ over a range of external temperatures (Guyton 2000). This is not the case for the skin, the temperature of which depends on its surroundings. This situation is vital as it enables a temperature gradient to be set up between the body and the surroundings, which enables the body to loose

heat when it becomes too hot. The skin therefore plays an important role in temperature regulation of the body because the rate of heat loss from the body depends on how quickly heat can be lost from the skin to the surroundings (and also the rate at which heat can be conducted from deep within the body to the skin). Heat loss from the skin occurs via radiation, at wavelengths between approximately 5-20μm (Guyton 2000), evaporation, and conduction to solid objects and to the air which is subsequently carried away by convection.

Blood flow in the microcirculation of the skin plays a vital role in maintaining a stable core body temperature. The rate of blood flow into the venous plexus determines the rate at which heat can be conducted from deep within the body to the skin. The higher the flow, the greater is the conduction. In some of the more exposed areas of the body, e.g. the ears, hands and feet, the direct connection between the arterioles and venules made by the AV anastomoses facilitates this flow by bypassing the capillaries and therefore enabling greater heat conduction. The rate of blood flow into the skin's venous plexus can vary from almost zero to around 30% of total cardiac output (Guyton 2000).

The temperature control mechanisms are directed mainly by the hypothalamus via nervous system feedback. Depending on the temperature of the blood perfusing through itself, the hypothalamus controls the core body temperature. However, temperature receptors that monitor the core body temperature are also found within the body, e.g., in the spinal chord and around the great veins in the upper abdomen and thorax. There are also temperature receptors in the skin, which monitor the body's surface temperature. However, there are many more cold receptors than warmth receptors (Guyton, 2000). Both skin and deep body temperature sensors provide information to the hypothalamus which then reacts accordingly. The hypothalamus responds to any increase in temperature by causing vasodilatation in nearly all the skin blood vessels, stimulating sweating and inhibiting heat generating mechanisms, such as shivering. When the body is too cold, the skin blood vessels become constricted, piloerection is induced and heat production mechanisms, such as shivering, become active.

However, the skin is also capable of providing temperature control in very local areas of the body. Local decreases in temperature, e.g. by placing the foot in an ice bucket will cause local vasoconstriction. Conversely, subjecting only a small part of the body to

heat will result in local vasodilatation and mild sweating. These effects are caused by the reaction of the local blood vessels to the changing temperature and also by nervous impulses sent from temperature receptors in the skin to the spinal cord and back to the same area. These local controls work in conjunction with the hypothalamus, to maintain a constant body temperature.

Chapter 2

Deep Vein Thrombosis

Deep vein thrombosis (DVT) is a coagulation of blood in the deep veins, forming a clot (thrombus). The thrombus forms a solid mass in the affected vein segment, which may partially or completely occlude the vessel lumen.

However, thrombus in the venous system is not limited to the deep veins. In the superficial system the condition is known as thrombophlebitis and follows inflammation of the wall of the vein. Historically, superficial thrombophlebitis has been considered to pose little threat. However propagation of the thrombus into the deep veins can occur (Chengelis et al., 1996). Thrombosis in the deep veins is a serious condition with the potential to cause life-threatening complications.

DVT most commonly occurs in the deep veins of the lower limbs, however, thrombus can potentially form anywhere in the deep venous system. In the upper limbs, the axillary or subclavian veins are usually affected, often resulting from unusual strenuous use of the arm and shoulder, genetic disposition or the use of venous catheters. Nevertheless, DVT in the lower limbs is much more common and is the focus of this chapter.

2.1 Incidence of DVT

Historically, DVT is an elusive disease. According to Mannucci (2002), there are no clearly reported cases of DVT in antiquity or representations of the disease in any pieces of art from ancient Egypt, Greece, Rome, Persia or South America. There are, however, descriptions and representations of varicose veins, ulcers and leg oedema. According to Dexter and Folch-Pi (1974), the first well documented case of venous thrombosis is believed to be found in a 13th century manuscript currently residing at the Bibliothèque Nationale in Paris. The manuscript depicts a young, 20 year old man who seemingly had a DVT extending from the ankle to the thigh. After consultation with his surgeon, the man was advised to "wait and see". Later, a visit the tomb of Saint Louis was recommended where he was to confess his sins and pray. While there, he chose to collect dust from the tomb and apply some to his open wounds, which subsequently

began to heal. Eleven years later, although still experiencing some pain, the man was able to walk again without the aid of a cane.

In the present day, DVT is a widespread condition. However, because of the sometimes silent nature of the disease it is still difficult to establish its true incidence in the general population. All figures are likely to underestimate the actual incidence since many cases of DVT are never diagnosed. Most studies find an incidence averaging around 1 in every 1000 people[+], although this figure tends to increase with age (e.g., Hansson et al. 1997). Fowkes et al. (2003) conducted a systematic review to look at the incidence of DVT in the general population. They concluded that, on average, the condition affects 1 in 2000 of the general population and that the incidence increases dramatically with age, from around 1 in 4000 for those aged 30-49 years to around 1 in 500 for those aged between 70 and 79 years.

The condition is also estimated to affect around 1%-2% of all hospitalised patients (e.g., Anderson and Wheeler, 1992) and may be responsible for around 5% of deaths in such patients (e.g., Harris et al., 1997). Surgery is one of the biggest risk factors for acquiring DVT. Clagett et al. (1995) find that patients undergoing general surgery have a 16%-30% risk of developing DVT when they do not receive prophylactic treatment. However, for those who undergo elective hip or knee replacement or hip fracture surgery, the risk of postoperative DVT is at least 40%.

2.2 Causes of DVT

DVT can form anywhere in the deep venous system of the lower limbs, from the small veins of the calf (distal DVT) to the level of the popliteal vein at the knee and up to the femoral vein or extending up into the iliac veins of the groin (proximal DVT). However, many studies suggest that DVT commonly originates below the level of the knee (except possibly after surgery where the DVT may be confined to the sites of high trauma (e.g., Jackson, 1998)). For example, Kearon (2001) states that two thirds of asymptomatic DVTs are confined to the calf veins. Most seem to originate either at the location of venous valves or in the small soleal sinusoids (Jackson, 1998).

[+] For example, see The House of Lords Select Committee on Science and Technology, Fifth Report, Air Travel and Health, November 2000.
(http://www.publications.parliament.uk/pa/ld199900/ldselect/ldsctech/121/12101.htm)

The process of DVT formation is still quite uncertain. It is believed that many thrombi begin life behind the valve cusps in the veins. As the blood passes the valves, the flow becomes disrupted and slows down behind the cusps. It is possible that a stagnant pool of blood may form behind the valve cusp encouraging deposition of platelets, red blood cells and fibrin over time. This small deposition may then act as a nucleus, encouraging thrombus growth. Coagulation factors in the blood enable the accumulation of these deposits and thrombus formation results.

This may be one of the reasons why leg mobilisation or compression, either intermittent pneumatic compression or compression stockings, are often effective in DVT prophylaxis (e.g. Vanek, 1998). An increased volume or speed of blood flow may "wash out" any stagnant deposits of blood before any significant accumulation of thrombus takes place. There is also evidence that intermittent pneumatic compression increases systemic fibrinolysis (e.g., Tarnay et al., 1980).

At first, the thrombus is small and may go unnoticed. However, once the thrombus begins to form, there are two courses that it could take. The thrombus may adhere to the wall of the vessel, growing ever larger along the vein in the direction of the blood flow, eventually completely occluding the vessel lumen. Without treatment, the thrombus may grow to a considerable length, sometimes extending from the calf, past the knee and into the thigh. In this case, treatment is necessary to remove or dissolve the DVT and to avoid dangerous complications. On the other hand, if the thrombus does not take hold of the vessel endothelium in the early stages, natural anticoagulants in the blood may dissolve it so that it retracts in size and eventually disappears altogether. This process usually begins 5 to 10 days after the thrombus begins to form (Line, 2001).

2.3 Risk factors for DVT

There are a myriad of risk factors that are thought to predispose certain groups of people to DVT. Virchow, in 1856, listed a triad of causes.

i. Blood vessel wall damage.
ii. Alteration in the hypercoagulability of the blood.
iii. Slow blood flow or stasis.

These are still considered to be the causes of DVT and any person having one or more of these conditions will be vulnerable. Damage to the blood vessel wall releases clotting factors into the blood that promote coagulation. Various genetic disorders, such as Factor V Leiden, increase the susceptibility of the blood to coagulate and encourage DVT formation (table 2.1). At least one of these inherited disorders can be found in 40%-60% of patients with a first episode of DVT (Lensing et al., 1999). Combined with low blood flow, allowing coagulation factors to accumulate, these conditions are ideal for thrombus formation.

There are a numerous situations in which any of the three components of Virchow's triad may exist. Examples of these are listed in table 2.2, which shows a selection of the large number of risk factors for DVT.

Table 2.1: Examples of inherited thrombophilic defects and estimates of their prevalence in patients with confirmed DVT and in the general population. *Taken from Lensing et al. (1999).*

	Patients with venous thrombosis (%)	General population (%)
Antithrombin deficiency	1–2	0·1–0·3
Protein C deficiency	2–3	0·2–0·5
Protein S deficiency	2–3	0·2–0·5
Factor V Leiden	10–20	3–7
Hyperhomocysteinaemia	10–20	2–6
Prothrombin 20210A	5–6	1–3
High factor VIII concentrations	10–15	6–8

Table 2.2: Major risk factors for DVT formation.

Virchow's triad i. Damage to blood vessel wall ii. Hypercoagulability of blood iii. Slow blood flow or stasis	
Muscular inactivity: Immobilisation (e.g., paralysed by a stroke) Prolonged bedrest (e.g post operation) Prolonged sitting Age: Risk increases risk with age, especially over 40 years old Recent surgery: Especially those involving major trauma and immobility, such as orthopaedic surgery Recent trauma to the blood vessels: For example, sporting injuries or surgery Hereditary genetic disorders: For example, Factor V Leiden	Oral conraceptive pills or hormone replacement therapy Pregnancy and the following few months Cancer and its therapy Infections and inflammatory diseases that stimulate the clotting process: For example, rheumatoid arthritis or Crohn's disease Heart failure Smoking Dehydration Previous DVT

Recent surgery probably poses the greatest risk of DVT (especially orthopaedic surgery involving the hips or lower limbs) because of the major trauma involved combined with prolonged periods of immobilisation (e.g., Claggett et al. (1995) or Kearon (2001)). Assuming everything else to be equal, the risk of developing DVT does not seem to differ greatly between men and women (White, 2003) but does increase with age in both genders; being greatest in those over 40 years old. Anderson et al. (1991) find that the risk of DVT increases exponentially with age in the general population. However, even young, otherwise healthy individuals can be at risk and there is not always a clear reason for why the condition develops. Hereditary genetic disorders that increase the

tendency of the blood to clot may play a part, combined with conditions experienced in everyday life. For example, many people experience long periods of inactivity, whether sitting at their desk in the office or travelling long distances while seated with limited room to move. Such conditions may promote to low blood flow and increase the risk of DVT, especially when hereditary coagulation disorders are present. Beasley et al. (2003) reported one of the first cases of "eThrombosis". Here, DVT (and pulmonary embolism) was believed to be the result of regularly working at a computer terminal for 12-18 hrs per day and, on occasions, for up to 6 hours without standing.

Recent media interest in DVT, especially airline DVT, has highlighted these problems and resulted in a much improved awareness of the condition. The colloquially dubbed "economy class syndrome" has highlighted to many people the dangers of this sly, often silent and potentially fatal disease.

2.4 Complications associated with DVT

As mentioned above, most DVTs begin life in the calf veins. Initially the thrombus is very small. However, without treatment, it may grow in size, propagating proximally along the vein, forming a partial or complete occlusion of the vessel lumen. At this stage, the leg may become red and swollen, causing the patient some discomfort. However, apart from the aches and pains and the possible displeasing appearance of the leg, the DVT itself is not a serious problem. If the vein is not totally occluded, blood will still be able to flow back to the heart. Even in the case of a complete occlusion of the vessel lumen, collateral channels often develop allowing an alternative route for the blood to flow. It is the complications that arise from DVT that one has to be aware of and which necessitate early diagnosis and treatment.

The major complication following DVT, and the reason why the condition has to be taken extremely seriously, is pulmonary embolism (PE). Here, bits of the thrombus in the deep veins break off, travel with the blood though the venous system and eventually become lodged in the pulmonary artery of the lungs, causing an embolism[♦]. Large pulmonary emboli are potentially fatal and can lead to sudden death. Smaller emboli may only result in the death of a section of lung tissue or cause pleurisy or coughing up

[♦] Less common, the embolus may settle in organs other than the lungs, such as the brain, causing a stroke, or in the heart, causing a myocardial infarction. However, these complications are extremely rare, existing only in patients with a septal defect (hole in the heart). Otherwise the thrombus fragment never makes it past the lungs.

of blood (in some cases, very small emboli may go unnoticed). In both cases however, quick treatment is essential. It may be possible to dissolve the smaller emboli with drugs but larger obstructions may require surgery.

It is difficult to find reliable figures for the incidence of PE subsequent to DVT because many DVTs go undetected. Sandler and Martin (1989) showed that on post mortem of 2388 patients dying in hospitals, 10% of deaths were due to PE. Of those, 83% were found to have DVT in the legs but only 19% of these had symptoms of DVT before death and even fewer, only 3%, underwent investigation for DVT.
Clagett et al. (1995) find that patients undergoing general surgery have a 1.6% incidence of PE when they do not receive prophylactic treatment. For those undergoing elective hip or knee replacement or hip fracture surgery, the risk of postoperative PE ranges from 1.8% to 30%.

There has always been some disagreement over the relationship between DVT location in the lower limbs and its potential to cause to PE. It has always been accepted that a DVT in the popliteal vein and more proximal regions poses a threat of PE. For example, Moser et al. (1994) suggest that the risk of PE after proximal DVT is as high as 50%. However, there is less of a consensus as to whether a DVT distal to the level of the knee poses such an immediate threat. Although there is no doubt that pulmonary emboli do arise from below knee DVTs (e.g. Passman et al., 1997), these tend to be smaller than those arising from proximal DVTs, and are usually not fatal (e.g., Philbrick et al. (1988), Moser and LeMoine (1981)). However, if small, below knee DVTs do not dissolve spontaneously, there is always the possibility of the thrombus growing in size and propagating to more proximal veins. For example, Philbrick et al. (1988) find that up to 20% of isolated calf vein DVTs continue to extend into the proximal veins and Line (2001) states that 20%-30% of untreated, symptomatic, calf vein DVTs may extend into the popliteal vein. Therefore, it seems that there is always a risk of developing PE subsequent to a DVT. This is not only true for large proximal thrombi, but also for smaller, below knee thrombi because they have the potential to grow and propagate into more proximal regions.

There are other unwelcome but less serious complications that arise from DVT, after the thrombus has been dissolved. The post-thrombotic syndrome may affect up to three

quarters of those who have had DVT*. The condition arises as a result of damage to the venous valves caused by the thrombus. The valves become unable to maintain a one-way flow of blood through the veins. Instead, reflux of blood away from the heart leads to venous hypertension and ultimately results in the veins becoming incompetent. This may cause pain, discolouration and swelling of the leg together with varicose veins.

Kahn and Ginsberg (2004) state that 20%-50% of patients with symptomatic DVT develop the post-thrombotic syndrome within 2 years and Brandjes et al. (1997) find this figure to be 60% for symptomatic, proximal DVT. The development of the post-thrombotic syndrome does not seem to depend on the location of the thrombus (Bank et al., 2003), however Prandoni et al. (1996) find that repeated ipsilateral DVT increases the risk of occurrence by 6-fold.

Ankle ulcerations may develop in 5%-10% of those patients who develop chronic venous insufficiency (Jackson, 1998). However, such an outcome may be avoided by using appropriate prophylaxis, e.g. elastic compression stockings. Brandjes et al. (1997) find that continued application of graded compression stockings within 2-3 weeks after the initial diagnosis of proximal DVT reduces the likelihood of developing the post-thrombotic syndrome by 50%.

2.5 Diagnosis of DVT

Clinical diagnosis of DVT is subjective and unreliable (e.g., Anand et al., 1998). In addition to pain when moving, indications of DVT may include swelling of the leg combined with reddening and warmth. However, the signs and symptoms often associated with a DVT do not necessarily indicate its presence because they are common to many other conditions (e.g. cellulitis or venous insufficiency). Conversely, a DVT may be present even in the absence of any signs and symptoms. Clinical diagnosis can be improved by consideration of the individual's risk factors for DVT. However, when a DVT is clinically suspected, the patient is always sent for follow-up objective diagnostic tests.

* http://www.medinfo.co.uk/conditions/dvt.html

Venography is commonly considered the gold standard for DVT diagnosis but is no longer routinely used because of its invasive nature. Recently, Doppler ultrasound* has become more popular. The test is non-invasive and technological advances have resulted in its accuracy rivalling venography for the diagnosis of DVT. However, the significant disadvantages of both tests are that they require highly trained operators and can only be performed in a hospital setting.

The difficulty in diagnosing DVT clinically leads to a large number of referrals for objective testing, many of which turn out to be negative. For example, it has been reported that as many as 70%-90% of patients tested for DVT using Doppler ultrasound do not have the condition (e.g., Markel et al. (1992), Messina et al. (1993), Rubin et al. (1994), Fowl et al. (1996)). This places a considerable strain on resources in test centres, not only financially, but also in terms of the time taken to perform all the scans.

A simple, quick, reliable screening test for DVT that can be performed anywhere and at any time is extremely desirable. Such a test could be performed, e.g., in the doctor's surgery, or in the emergency department of a hospital to rule out DVT and reduce the number of unnecessary Doppler ultrasound or venography scans. There has been considerable interest in the use of D-dimer testing to perform such a task. Photoplethysmography techniques have also aroused interest. The sensitivities of these tests for diagnosing DVT do not match the more established tests of venography or Doppler ultrasound. However they may prove useful as a screening test to rule out DVT, possibly combined with a clinical scoring system.

The above-mentioned tests for DVT are described in greater detail below (together with magnetic resonance imaging, plethysmographic techniques, radioactive-labelled fibrinogen scans and thermography).

2.5.1 Contrast venography

Venography allows direct imaging of the venous system. The procedure involves taking an x-ray image of the body part under investigation following injection of a

* The term "Doppler ultrasound" refers to ultrasound imaging with the use of Doppler techniques to assess blood flow.

contrast medium to delineate the veins. There are two types of venography; ascending and descending. The ascending type is the most popular and involves injection of the contrast medium into a superficial vein of the foot. Application of a tourniquet around the leg occludes the superficial veins and directs the contrast medium to the deep venous system. DVT is identified from the resulting image by observing the parts of the venous system not containing contrast medium, indicating an obstruction.
Descending venography is often used to evaluate venous reflux. In this test, the contrast medium is injected directly into a deep vein (usually the common femoral vein when investigating the lower limbs). The competence of the venous valves is determined by observing the extent of distal reflux of the contrast medium.

Venography has always been considered the gold standard for DVT diagnosis. Provided the deep veins are completely visualised, the technique is almost 100% sensitive and specific (Tapson et al., 1999) and is effective in diagnosing both proximal and calf vein DVT (e.g., Jackson 1998).
However, there are many disadvantages associated with venography. The test requires specially trained operators. It is invasive, uncomfortable, time-consuming, carries a significant risk of an allergic reaction to the contrast agent and also morbidity, especially phlebitis. There is also a risk of developing DVT as a result of the procedure, although this is uncommon. It is therefore undesirable to refer all suspected DVT patients for a scan of this type if clinical diagnosis is so unreliable that the majority of the referrals turn out to be negative. For this reason, non-invasive tests, e.g., Doppler ultrasound, are generally attempted first. However, venography might still be utilised if non-invasive testing is inconclusive or if a negative result contradicts high clinical suspicion.

2.5.2 Doppler ultrasound

Doppler ultrasound is currently the favoured diagnostic test for DVT. The technique allows non-invasive, direct imaging of the veins and other structures in the body via ultrasound reflections from the various tissue surfaces. A handheld probe is used to direct the ultrasound waves into the body and also acts as a receiver. The amplitude of the ultrasound signal returning to the probe enables an image of the internal body

structures to be formed on an observation screen. The Doppler shift of the returning signals may also be used to investigate blood flow within the blood vessels.

Therefore, a DVT can either be directly visualised or inferred from its effect on the blood flow in the vessel. Such effects may include lack of venous flow, continuous flow instead of phasic flow with breathing or diminished flow following distal compression of the limb. The presence of thrombus may also be deduced from lack of vessel compressibility when pressure is applied to the vein by the examiner pressing on the leg with the probe.

The large, deep veins of the leg, i.e., the popliteal, femoral or iliac veins are easily located with the technique, although the smaller calf veins may be more difficult to find. According to Zierler (2004), ultrasonography has a sensitivity and specificity of 97% and 94% respectively, compared to venography, when detecting symptomatic thrombus in the proximal veins. However, it has been reported that the technique is less well suited to detect thrombus in the calf veins. For example, Rose et al. (1990) reported a sensitivity of 80% and specificity of 100% in diagnosing DVT limited to the calf veins but also reported that the calf veins were adequately visualised in only 60% of the total number (75) of patients investigated. Nevertheless, ultrasound equipment is constantly improving, resulting in clearer images and more accurate blood flow measurements so that calf vein visualisation is becoming less problematic. Obtaining satisfactory results also depends heavily on the experience of the operator and some studies have reported sensitivities and specificities for detecting calf vein DVT that are comparable to those for proximal DVT (e.g., Bradley et al., 1993).

2.5.3 D-dimer

D-dimer is a specific degradation product of cross linked fibrin, produced when the body attempts naturally to dissolve blood clots. The level of D-dimer in the blood can be measured following a simple blood test and elevated levels indicate a possible thrombus. Several types of assay are available to do this. Some require the blood to be tested in a laboratory. Others can be performed at the patient's side and are reasonably quick. The latest assays produce results within a few minutes of taking the blood sample.

The sensitivity and specificity of D-dimer tests vary depending on the type of assay used (e.g. Kelly et al. (2002) and Bounameaux et al. (1994)). The tests are usually quite

sensitive to venous thrombosis with sensitivities greater than 90% often reported. However, the tests tend to produce many false positive results, indicating an inability to differentiate DVT from other conditions that may produce high levels of D-dimer in the blood (e.g. malignancy, pregnancy or post operation). Specificity is often quoted to be quite low; between 30% and 50% (e.g., Brotman et al. (2003), Diamond et al. (2005)). Nevertheless, reasonably high negative predictive values, approaching 100%, indicates that a negative test result does seem to be good at ruling out the presence of DVT. As such, the principle use of D-dimer seems to be as a screening tool for DVT.

It has been suggested that the usefulness of D-dimer in DVT screening may be improved by combining it with a clinical scoring system (described in greater detail in section 2.5.5).

The major disadvantage of the D-dimer test is its invasive nature due to the requirement of a blood sample. The test also tends to perform less well when detecting below knee DVTs and may only be suitable for use within a couple of weeks after initial thrombus formation, before D-dimer levels begin to normalise (Kelly et al., 2002). In addition, Brotman et al. (2003) have shown that the tests perform less well in elderly patients (>60 years of age) or those hospitalised for more than 3 days.

2.5.4 Photoplethysmography

A non invasive alternative to D-dimer for DVT diagnosis/screening is photoplethysmography. The device uses an optical system to measure blood volume changes in the skin (described in greater detail in Chapter 3). The technique has the potential to provide a simple, portable, non-invasive test for DVT that is not associated with significant pain or side effects.

Photoplethysmography has been available for many years and has found application in numerous areas including lower limb venous investigations, where it has been used to monitor venous insufficiency in the legs (see section 3.6). The technique has also been considered as a possible test for DVT. In the most common test, a single probe is placed on the skin, 10cm above the level of the medial malleolus, and the patient performs numerous dorsiflexions of the foot. This exercise reduces the volume of blood in the lower limbs as a result of the muscle pump. Infrared light is used to measure the time taken for the microcirculation plexus under the probe to refill with blood following the exercise. The refill time is reduced in the presence of a DVT since the obstruction

reduces the volume of blood that is expelled from the leg during the exercise. (The volume of blood expelled during the exercise is itself sometimes used as an indicator for DVT.)

Tan and da Silva (1999) investigated the use of digital photoplethysmography, combined with the standard dorsiflexion test, to diagnose DVT. Using Doppler ultrasound as their gold standard, they performed the photoplethysmography test on 100 hospital inpatients. A venous refilling time of less than 21 seconds was found to best identify DVT. This gave the photoplethysmography test a sensitivity of 100%, specificity of 47%, positive predictive value (PPV) of 51% and a negative predictive value (NPV) of 100%. These results suggest that digital photoplethysmography may be well suited as a screening test for DVT, since all those patients that tested negative were correctly diagnosed (NPV 100%). However, although the sensitivity of the test was 100% (all DVTs were detected), only 51% of those that tested positive with digital photoplethysmography were also positive with respect to the gold standard. Therefore, on the basis of these results, digital photoplethysmography alone could not be used to diagnose DVT since 49% of the patients who tested positive would have been unnecessarily treated for the condition.

One of the main problems with the photoplethysmography test is patient compliance. It is often painful to move the foot when there is a DVT present in the calf and it is impossible to perform the test on immobile patients (who are at high risk of developing DVT). Also, elderly patients in particular have difficulty executing the dorsiflexions in time with the metronome signal. The test is very sensitive to patient movement during the post exercise phase where muscle contractions may cause extra blood to be expelled from the leg, increasing the refill time. In addition, other conditions, such as venous insufficiency, may produce false positive results because they affect venous outflow from the limb.

Nevertheless, when the test is able to be performed, and when it is performed well, the system does seem capable of definitively ruling out DVT (or venous insufficiency). However, it is clear is that photoplethysmography, like D-dimer, is currently unable to replace venography or Doppler ultrasound as the gold standard for DVT diagnosis. Rather, its function seems to be suited to a relatively quick and inexpensive screening

test to reduce the number of patients that are referred for venography or Doppler ultrasound scans.

Even though the sensitivities of photoplethysmography and D-dimer are high (which is necessary to minimise the possibility of missing any cases of DVT), the tests tend to give many false positive results. The reason for this may be that both D-dimer and photoplethysmography look at the secondary effects of the DVT rather than looking for the thrombus itself. D-dimer looks for the degradation products of blood clots and plethysmography looks at venous blood volume changes. Both these factors can be influenced by conditions other than DVT. This situation is similar to that in the clinical diagnosis of DVT where the signs and symptoms are similar to those of many other diseases and consequently makes the diagnosis unreliable.

2.5.5 Clinical scores

In an attempt to improve the efficiency of DVT testing, especially when detecting small DVTs confined to the calf veins, it has been suggested that a clinical scoring system could by used. Prior to objective testing, the physician considers a checklist of relevant questions, the answers to which are assigned a numerical value and the final score is deemed to give an indication of the risk of that patient for developing DVT. This risk assessment is then taken into consideration when performing the Doppler ultrasound, D-dimer or plethysmography test (or any other diagnostic test for DVT).

The most well known clinical scoring system is probably the Wells test, which was first described in 1995 (Wells et al., 1995). The original model consisted of a checklist of signs and symptoms and risk factors for DVT, constructed by consultation of the literature up to that time and utilising the experience of the investigators in the study. These included active cancer, paralysis, thigh and calf swelling, recent trauma, erythema and so on. This list was split into major and minor features and, depending on how many of each type were found on examination, the patient was classified as low, medium or high risk of developing DVT. Later, Wells et al. (1997) simplified the clinical model and the refined form is shown in table 2.3. This model forms the basis of most clinical scoring models used today. As before, the Wells score is evaluated and the patient is categorised accordingly as having a low, medium or high risk of developing DVT. A score of three or more is considered a high risk for DVT, while a

score of zero or less is categorised as low risk. Patients with a score of one or two are considered at moderate risk of developing DVT.

Table 2.3: Clinical model used in the Wells test for determining the risk of a patient developing DVT (taken from Wells et al., 1997).

Clinical feature*	Score
Active cancer (treatment ongoing or within previous 6 months or palliative)	1
Paralysis, paresis, or recent plaster immobilisation of the lower extremities	1
Recently bedridden for more than 3 days or major surgery within 4 weeks	1
Localised tenderness along the distribution of the deep venous system	1
Entire leg swollen	1
Calf swelling by more than 3 cm when compared with the asymptomatic leg (measured 10 cm below tibial tuberosity)	1
Pitting oedema (greater in the symptomatic leg)	1
Collateral superficial veins (non-varicose)	1
Alternative diagnosis as likely or greater than that of deep-vein thrombosis	-2

*In patients with symptoms in both legs, the more symptomatic leg is used.

Wells et al. (1997) used their clinical scoring system in conjunction with Doppler ultrasound and venography to investigate its effectiveness in predicting the probability of DVT. They found that out of 329 patients classified as having low risk of DVT only 3% actually developed venous thromboembolism. For 193 patients classified as moderate risk and 71 patients classified as high risk, 17% and 75% developed venous thromboembolism respectively. These results suggest that the Wells score is a reasonable indication of the likelihood of a person developing DVT.

However, since the original Wells test, there have been numerous modifications of the clinical scoring system. Wells et al. (2003) have also recently simplified the original to remove the moderate risk category. In the new model, a score of 1 or less is classified as low risk and 2 or more is high risk. The new score also takes into account whether the patient has had a previous incidence of DVT and assigns a score of 1 in such a case.

Since no standard scoring system exists at present and there is no standard way in which clinical scoring systems are implemented in diagnostic strategies for DVT, caution must be utilised when applying the clinical scores in practice. In addition, for the Wells test to provide consistent results, there requires a good interobserver agreement when scoring each patient. However, some categories in the test are less than objective, e.g.,

the last category in table 2.3, states that a mark of -2 should be awarded when "alternative diagnosis is as likely or greater than that of deep-vein thrombosis".

Nevertheless, there have been a number of studies that suggest that a clinical scoring system, in combination with a non-invasive test, may improve the efficiency of DVT screening. For example, Wells et al. (2003) find that it is safe to exclude DVT based on a low clinical probability score when combined with a negative D-dimer result. Using this criterion, they concluded that further diagnostic tests were unnecessary in 39% of 562 outpatients who were suspected of having DVT. On follow up, DVT developed in only two of these patients.

Using a similar clinical test, Janes and Ashford (2001) found that it was safe to withhold treatment in 23% of 431 outpatients with suspected DVT (based on a low clinical probability score combined with a negative D-dimer result). Of these, only one patient was subsequently admitted to hospital, 5 months later, with PE.

2.5.6 Magnetic resonance imaging

Magnetic resonance imaging (MRI) produces a 3-dimensional image of the limbs with excellent discrimination of the tissues and blood vessels within. The technique is non-invasive and does not require the use of contrast agents. In its simplest terms, application of a magnetic field and radio frequencies to the body cause specific atoms to resonate. This process changes the magnetic properties of the atoms and induces an electric current in a receiving coil, which is used to build up a picture of the internal body structures.

In the most common imaging sequence, moving blood appears as a bright area on a darker background and thrombus is detected via filling defects in the veins. However, recent studies have shown that it is also possible to image the thrombus directly. Using the direct imaging technique, Fraser et al. (2002) have reported sensitivities and specificities greater than 90% for detecting isolated calf DVT, femoropopliteal DVT and ileofemoral DVT.

The main disadvantages of MRI are availability of the large machines, the requirement of trained personnel to operate them and the cost of the scan.

2.5.7 Plethysmographic techniques

The plethysmographic techniques are all non-invasive. Their initial role in DVT testing was to replace, or work alongside, invasive venography. However, the tests are no longer used to a great extent. Various types of plethysmography are possible including strain gauge, electrical impedance, air and water plethysmography. Each method measures volume changes in whole limbs. Photoelectric plethysmography (photoplethysmography), described in section 2.5.4, is a special kind of plethysmography since the technique measures skin blood volume variations only.
Although non-invasive, a major disadvantage with all the plethysmographic techniques is that they require considerable operator involvement to set up the tests. They are also unreliable for detecting small non-occluding thrombi, especially in the calf veins where multiple channels exist for the blood to flow.

2.5.7.1 Strain gauge plethysmography

In strain gauge plethysmography, the circumference of the calf is monitored by a strip of electric conducting material wrapped around the limb, e.g., rubber filled with mercury. As the strain gauge is stretched, its electrical resistance alters. Therefore, any change in calf circumference can be detected and measured. The changes in calf circumference can attributed to blood volume variations in the limb (assuming the time taken to perform the investigation is small).
In a DVT test using this system, the patient is examined in a supine position. The leg under examination is raised slightly to empty the veins and a strain gauge is placed around the calf. Venous blood flow is then occluded by inflating a thigh cuff, causing a distal increase in blood volume (the compression pressure applied is not large enough to prevent arterial inflow). Venous blood volume continues to increase until the venous blood pressure reaches the thigh compression pressure. At this point, there is sufficient pressure to allow venous blood to flow past the cuff. An equilibrium is established between arterial inflow and venous outflow such that the distal blood volume does not change.
The pressure in the thigh cuff is then released and the rate of outflow of blood is measured indirectly by monitoring the rate of change of calf circumference, measured by the strain gauge (fig 2.1). Any obstruction to the venous outflow, e.g. a DVT in the

leg, reduces the rate at which the calf circumference decreases when the thigh pressure is released. The test may be computer controlled and performed in a few minutes.

Sensitivities greater than 90% have been reported for detecting proximal DVTs. However the figure is much lower for distal DVTs. For example, Maskell et al. (2002) report a sensitivity of 66% (specificity was 73% for proximal DVTs and 80% for distal DVTs).

Fig 2.1: Illustration of a typical curve recorded during strain gauge plethysmography showing the change in calf circumference when venous blood flow is occluded by an inflatable cuff at the thigh.

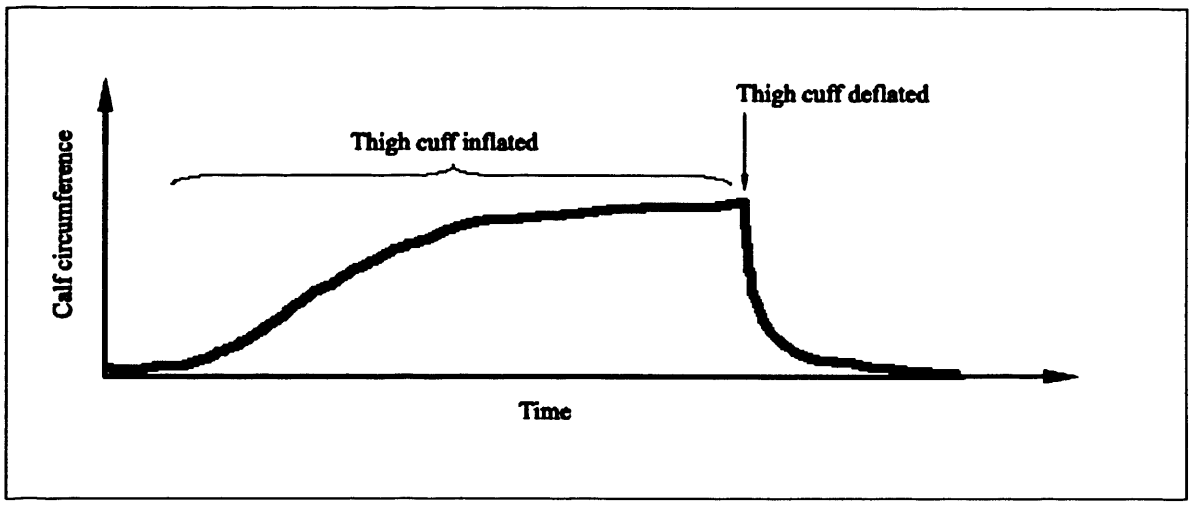

2.5.7.2 Impedance plethysmography

Impedance plethysmography makes use of the electrical conducting properties of the circulation. Pairs of electrodes are attached to the leg, which apply a low amplitude (~0.1mA), high frequency (~22kHz) alternating current to the body (e.g., Browse et al., 1999). The amplitude of the current is too low to be sensed by the patient. The blood is the preferred path of any electrical current in the body and over the short time of the investigation (~minutes) it is the blood volume that mostly affects the impedance between the electrodes. As the volume of blood in the limb increases, the impedance between the electrodes falls. Therefore, voltage changes between the electrodes can be used to monitor blood volume variations.

As in strain gauge plethysmography, investigations of the leg often involve the use of a tourniquet to impede venous blood flow, causing a distal increase in blood volume. On release of the cuff pressure, the rate of increase of impedance gives an indirect measure

of the rate of venous outflow from the limb. Again, this is slower when a DVT is present in the leg.

The sensitivity of impedance plethysmography has been reported to be around 83% - 93%, with specificity in a similar range (White et al., 1989). However, more recent studies have found the sensitivity for detecting proximal DVT to be around 65% (e.g, Anderson et al., 1993 and Ginsberg et al., 1994). Results seem to vary between centres as the technique is highly operator dependent.

2.5.7.3 Air and water plethysmography

Air and water plethysmography use air and water filled chambers to measure volume changes in whole limbs. Both techniques work in a similar way. The whole limb is placed in a long air/water filled, non-distensible chamber (fig 2.2). As the volume of the limb increases or decreases, the air or water is forced out of the chamber. The quantity of fluid displaced is measured and used to infer the limb volume change.

Fig 2.2: An example of a typical experimental set-up for air plethysmography.
A similar set-up is used for water plethysmography, with the air filled cuff replaced by a water filled chamber.
(Picture from Belcaro et al., 1995)

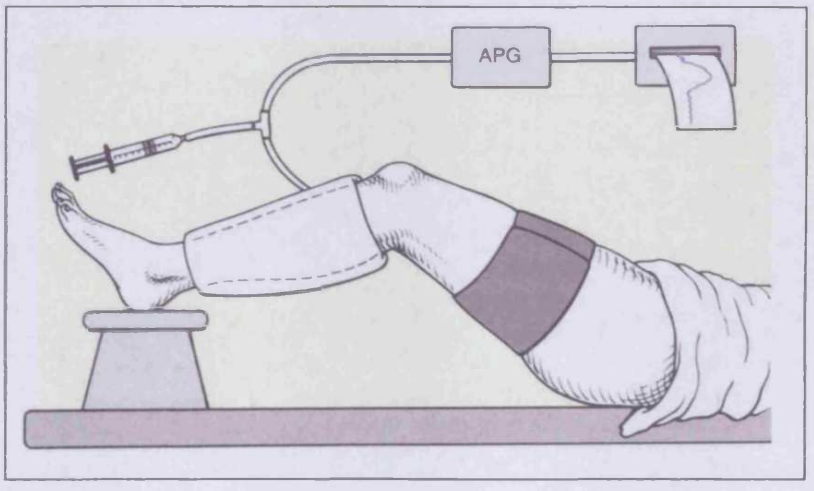

2.5.8 Radioactive-labelled fibrinogen scan

In this test, radioactive fibrinogen is used as a tracer of DVT. It is injected into the bloodstream and its progress through the body is monitored by a scintillation counter. If

a DVT is present in the leg, uptake of the radioactive fibrinogen by the developing thrombus results in a large signal at that location.

However, the technique is invasive and the presence of other conditions such as superficial thrombophlebitis, ulceration, wounds or arthritis will increase radioactivity and may produce false positive results. In addition, the technique is not useful for scanning the pelvic regions because of background radioactivity from the bladder (Nicolaides and Sumner, 1991).

2.5.9 Thermography

DVT can cause an increase in the temperature of the affected limb and this effect has been utilised in thermography. A picture of the limbs is taken that displays the skin's surface temperature. A temperature difference of around 0.7°C between the limbs is taken as positive for venous disease (Nicolaides and Sumner, 1991).

The procedure is non-invasive and quick to perform and, over the years, bulky, expensive infrared cameras have been replaced by colour liquid crystal devices. However, like the plethysmographic techniques, small DVTs are difficult to detect. This is also true for chronic thrombi. False positive results may be caused by other conditions that cause a build up of fluid in the limbs, such as superficial thrombophlebitis, varicose veins, ruptured Baker's cysts and cellulites.

2.6 Treatment of DVT

The initial aim of any treatment for DVT is to prevent the thrombus from propagating and causing a PE. The ultimate goal is to reduce the size of the thrombus, eventually dissolving it completely and returning the venous system to its pre diseased state.

It is accepted that large DVTs in the proximal regions of the leg require immediate treatment because of their potential to fragment and cause a fatal PE (see section 2.4). However, there is some ambiguity about whether small, below knee DVTs should be treated immediately or whether to wait and see if they dissolve spontaneously, favouring repeat scans to check the progress. This "wait and see" approach may prevent costly rescans and administration of unnecessary drugs but it can be risky. As described above (section 2.4), there is always the possibility of a DVT in the calf

growing in size and propagating to more proximal regions, increasing the risk of developing a fatal PE. Therefore, there now seems to be an inclination towards the need to treat all DVTs regardless of the location in the lower limb. For example, recommendations for treatment of venous thromboembolism at the Sixth American College of Chest Physicians' Consensus Conference on Antithrombotic Therapy stated that both proximal and symptomatic calf vein DVT should be treated (Hyers et al. 2001).

Treatment is usually via the anticoagulant drugs heparin or warfarin. These inhibit clotting factors in the blood and prevent further thrombus formation, aiding the body to naturally dissolve the DVT. Direct injection of heparin is initially used together with oral warfarin. Then, after a week or two, the warfarin is continued alone. Usually, the treatment continues for several months. Ideally the treatment would continue as long as necessary to dissolve the DVT, but prolonged use of anticoagulant drugs runs the risk of bleeding complications. Therefore, the treatment is only administered for as long as the benefits outweigh the risks. This is true for anyone treated with anticoagulant drugs but is particularly important in the case of post operative patients. Large continued doses of anticoagulant drugs run the risk of bleeding at the site of the surgery. This risk has to be balanced against the chance of developing PE or recurrent thrombus.

When treatment is eventually stopped, there is always the threat of DVT reoccurring. The probability of recurrence depends on the risk factors for DVT in each individual patient but decreases with time after the initial episode of DVT (Baglin et al., 2003). If the treatment is inadequate, i.e. stopped prematurely, the probability of recurrence is higher. In such cases, Line (2001) states that, within 3 months, the frequency of recurrence of proximal thrombi is 47% and greater than 20% for symptomatic calf vein thrombi. With adequate treatment, proximal DVT recurrence rate is around 2%. Lensing et al. (1999) reports that several studies indicate that patients with idiopathic DVT, genetic susceptibility or cancer have the highest rate of reoccurrence after an initial episode.

However, even following complete removal of the DVT, the post-thrombotic syndrome is always a threat because of the damage to the venous valves.

Other treatment options for DVT include fibrinolytic/thrombolytic therapy (which chemically breaks down the thrombus) or surgical thrombectomy in the case of particularly large thrombi, although these treatments are less often used.

Chapter 3

Photoplethysmography

Photoplethysmography (PPG) is an optical-electronic system for investigating tissue blood perfusion. Its origins can be traced back to the 1930s when analogue PPG systems were first developed. The technique is based on the absorption of light by biological tissue. During initial tests, using rabbit skin, the light absorption was found to correlate with blood volume variations in the tissue. Consequently, the technique was developed and used to investigate skin blood perfusion in humans.

Current PPG apparatus consist of a small probe, a few cm in diameter, which houses a light source (usually an infrared light emitting diode, LED) and a photodetector. Light is shone onto the tissue under investigation and any light that is not absorbed by the tissue is detected by the photodetector. The photodetector signal is relayed back to the main unit (which may be computer controlled) and the intensity variations are displayed on a screen or recorded in the device for further analysis.

The history of the development of PPG is outlined below, together with a detailed description of how the system works and its current uses.

3.1 A brief history of PPG

The origins of PPG can be traced back to the 1930s. Prior to this, there was no really good method to investigate the microcirculation non-invasively and in real time. Two available methods were indirect observation using plethysmography and direct observation of the microcirculation vessels using microscopy.

Plethysmography measures changes in the volume of whole limbs. The volume changes are then used to infer information about blood flowing into and out of the limb. There are many forms of plethysmography, each of which are discussed in more detail in section 2.5.7. However, in the 1930s, only air or water plethysmography was available. The shortcoming of all plethysmography techniques is that the investigations record net changes in limb volume, which could be affected by several different factors including blood flow in all types of vessels, lymph flow, intercellular exchange etc. The

technique cannot differentiate between specific vessels or processes that cause the changes in limb volume. The method is also very sensitive to muscle contractions, producing artefacts that mask the changes due to natural volume variations.

Microscopy, however, allowed direct visualisation of the vessels in the microcirculation, i.e. arterioles, venules and capillaries. Its disadvantages were primarily related to the extremely small size of the vessels being imaged. Any small but significant changes in vessel diameter were likely to be missed and a summation of these could lead to appreciable blood volume changes within the limb. In the 1930s it was possible to produce a permanent and continuous record of the vessels by micro-cinematography, however this required costly equipment. Also, photographic records have the disadvantage of not being able to be visualised while the experiment is taking place.

The development of PPG helped to overcome some of the difficulties in the study of the microcirculation (table 3.1). It provided a means to investigate the small microcirculation vessels only (arteries, venules and capillaries) and to continually record changes in blood volume. The readings could be viewed as the experiment was taking place using a pen and chart recorder.

Some of the earliest pioneers were Molitor and Kniajuk (1936) who measured microcirculation circulatory changes in a rabbit's ear. The device they constructed was based on the principle that any variation of blood volume within the microcirculation of the skin would result in a change to its colour and transparency (as a consequence of a change in light absorption) or its temperature (since thermoregulatory processes take place mainly in the microcirculation of the skin). Consequently, they constructed a device that allowed measurements of light intensity following it's interaction with tissue (and also included a facility to take temperature measurements). The apparatus consisted of a photocell, a 2½ V flashlight bulb as a light source, an amplifier and a mechanical recorder. The tissue to be investigated was usually placed between the light source and the photocell, although it was also possible to use the system in reflection mode with the light source and detector on the same side. The tissue was illuminated and any light that was able to pass completely through the sample was detected at the photocell. The change in light intensity, measured by the photocell, was converted to a change in voltage and used to drive a pen chart recorder. Additional use of a thermocouple incorporated into the apparatus enabled Molitor and Kniajuk to make simultaneous measurements of temperature. Using the combined light intensity and

temperature measurements, they were able to distinguish between active hyperaemia and congestion. In active hyperaemia, they observed that light transmission through the rabbit's ear decreased due to increased light absorption from an increased blood volume. This was accompanied by a temperature increase. Congestion was also observed to be associated with a decrease in light transmission. However, this was not accompanied by a temperature increase. Such a distinction between active hyperaemia and congestion was not possible with conventional plethysmography and was one of the first described uses of the new technique.

Another application envisaged for the new technique (because of its ability to detect very small volume changes) was investigations of the effects of new drugs, including vasoconstricting and vasodilating drugs. Light transmission through rabbit's ears was again used to demonstrate this. Also reported was the visualisation of Traube-Hering waves in the signal, resulting from nervous system control of the microcirculation.

Table 3.1: Summary of the main advantages and disadvantages of the available techniques for observing microcirculation blood volume changes in the mid-1930s.

	Advantages	Disadvantages
Plethysmography	• *Non-invasive.* • *Recordings can be taken while the experiment is in progress via a pen chart recorder.*	• *Records net volume changes in the limb. Therefore cannot differentiate between deep, superficial or microcirculation blood flow or, e.g., between blood and lymph flow.* • *Very sensitive to muscle contractions. Therefore, live animals need to be sedated.*
Microscopy	• *Non-invasive.* • *Visualises the vessels of the microcirculation directly.*	• *Photographic records are expensive and cannot be analysed while the experiment is being performed.* • *Difficult to observe very small changes in vessel diameter.*
PPG	• *Non-invasive.* • *Sensitive to blood volume changes in the vessels of the microcirculation only.* • *Recordings can be taken while the experiment is in progress via a pen chart recorder.* • *Easy to use.* • *Cheap to build - the original device costing less than $250 (Molitor & Kniajuk, 1936).*	• *Sensitive to movement.*

The new system was cheap to manufacture (less than $250 for all the parts) and easy to use. Encouraged by the early tests, others began investigating the potential of the new technology. Hertzman (1938) attempted to find a quantitative relationship between blood volume and the intensity of the light reflected from the skin. A diagram of the apparatus used is shown in figure 3.1. The technique was named photoelectric plethysmography (which has subsequently been shortened to photoplethysmography, PPG). Hertzman concluded that there exists a complex relationship between the PPG signal and the blood volume that is difficult to quantify because of numerous sources of

error including movement of the skin with respect to the photocell, contact pressure of the photocell on the skin, variation of intensity and the spectrum of the light source. Nevertheless, the study demonstrated that it was possible to use the reflection of light from the surface of the skin, rather than transmission, to investigate its blood content. Molitor and Kniajuk (1936) also report obtaining satisfactory reflection results using their apparatus but they specify a preference for placing the skin between the light source and photodetector. However, this is only possible for tissue that is thin enough to allow transmission of light through its volume and is restricted to parts of the body such as the fingers and ears. Measurement of backscattered light allows PPG to be performed anywhere on the human body.

Fig 3.1: Diagram of early photoelectric plethysmography apparatus used by Hertzman (1938).
The apparatus are carried by rack and pinion on a heavy stand, then brought into light contact with the skin.

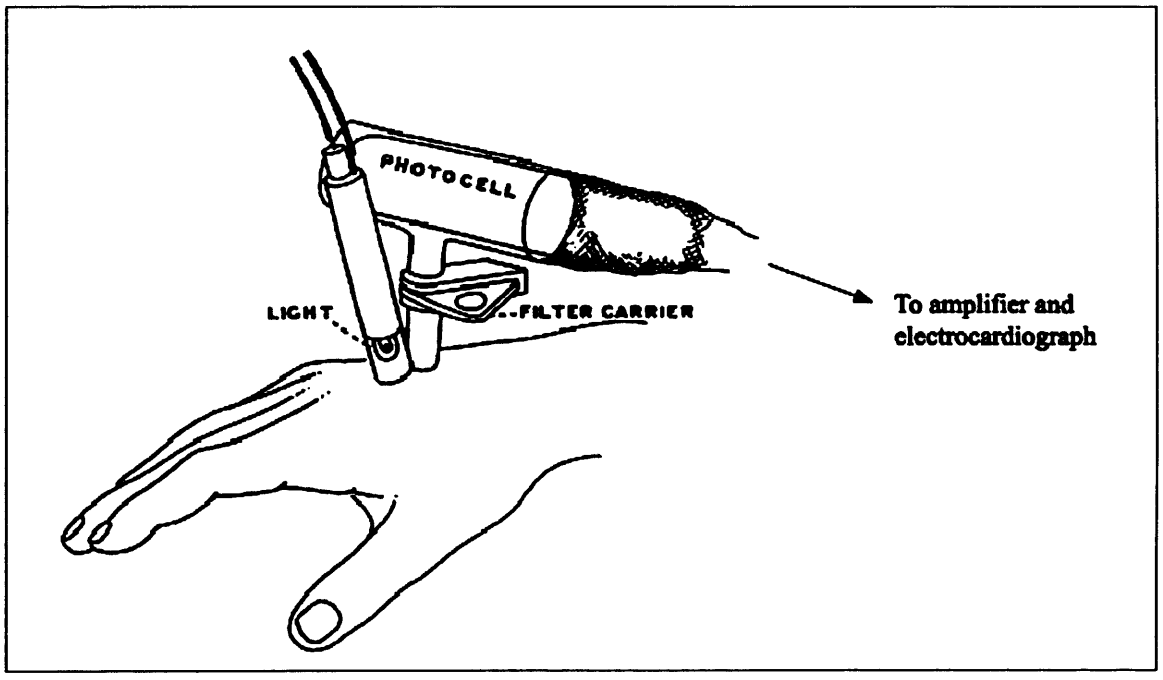

Hertzman and Dillon (1940a) used the system to investigate peripheral arterial disease by monitoring blood volume changes in the skin during exercise and when exposed to different temperatures. They also illustrated (Hertzman and Dillon, 1940b) two very different components of the photoplethysmograph signal; a rapidly changing "a.c." component corresponding to pulsations of blood as it is driven through the

microcirculation by the heart and a "d.c." component consisting of larger amplitude, longer period undulations. The "d.c." component was postulated to be the result of bulk changes in the total volume of blood in the microcirculation, caused by varying arterial tone or venous volume changes (caused by venous congestion or venous tone).

From the 1970s onwards, the system was used increasingly for non-invasive venous investigations, especially of the calf muscle pump. The investigations usually required the patient to undertake a small exercise. For example Abramowitz et al. (1979) describe patients sitting on the side of a bed with legs dangling over the edge while performing dorsiflexions and plantarflexions of the foot. Nicolaides and Miles (1987) describe patients standing up and performing tip-toe exercises. Whichever exercise was chosen, the result was to reduce the volume of blood in the leg by activation of the muscle pump. At the same time, PPG was used to measure microcirculation blood volume changes in the skin. Common measurement sites were at the dorsum of the foot or on the leg, just above the medial malleolus. During the exercise, a reduction in microcirculation blood volume was observed. At the end of the exercise, the time taken for the microcirculation to recoup the loss was measured and used as an indicator for the condition of the veins. A rapid refill time was taken as indicative of venous insufficiency where incompetent venous valves allow retrograde flow through the veins, filling them quicker than would be expected from arterial inflow alone.

Such measurements of microcirculation refill time after standardised exercise were shown to correlate well with invasive venous pressure recovery measurements. Abramowitz et al. (1979) were one of the first to conduct such an experiment. They compared PPG refill times taken from near the medial malleolus with venous pressure recovery times taken from a cannulated vein at the dorsum of the foot. A high correlation was found between the two measurements when 338 refill times were compared from 24 normal, 25 post-thrombotic, and 14 varicose vein limbs. Invasive vein pressure measurements have long been a trusted assessment of venous insufficiency in the leg (e.g., Belcaro et al., 1995). A normal recovery time is usually considered to be greater than 20s (although this depends on the characteristics of the method used to empty the veins or the vigour at which the chosen exercise test is performed). However, the method is invasive and requires trained personnel to perform the test. Therefore, Abramowitz et al. suggested that PPG could provide an alternative, non-invasive, simple assessment of venous insufficiency. They also suggested that,

through the use of a tourniquet to occlude superficial venous flow, it was not only possible to diagnose venous insufficiency but also to distinguish between superficial and deep venous insufficiency.

However, others have suggested that although PPG can give an indication of venous insufficiency, it cannot be used to grade its severity. Nicolaides and Miles (1987) found a non-linear relationship between PPG refill time and ambulatory venous pressure (AVP), which was defined as the lowest mean pressure, measured in a cannulated vein at the dorsum of the foot, during a 30 second tiptoe exercise. They found that, although there was an excellent relationship between PPG refill time and venous pressure recovery time, the PPG refill time did not correlate with absolute values of AVP. Therefore, they concluded that PPG could only be used to detect venous insufficiency, not grade its severity. They suggested that PPG should be primarily used as a screening device to rule out venous disease.

Despite this, it is probably fair to say that the correlation between the recovery times measured with non-invasive PPG and those obtained by invasive vein pressure measurements was a key driving factor behind the development of PPG. The system provided a non-invasive, simple, low risk and painless technique to study venous haemodynamics, which was extremely desirable. In addition, the introduction of the LED meant that both the light source and detector could be incorporated into a single measurement probe, which could be made smaller and more manageable. (The LEDs also lasted longer than the early tungsten bulbs and produced less heat, reducing any changes to the microcirculation blood flow caused by local vasodilatations.)

In the early 1980s, light reflection rheography (LRR) was developed. According to Veraart et al. (1994), the main protagonists were Wienert and Blazek. The system is almost identical to reflection PPG and is based on the same principle, measuring the intensity of light returning to a detector following illumination of the skin's surface. However, instead of a single light source and detector, the measurement probe incorporates three infrared LEDs, a photodetector and a thermocouple (fig 3.2).

Fig 3.2: Diagram of the measurement probe used in LRR.
The probe, which is only a few centimetres in diameter, is attached to the skin using sticky tape.

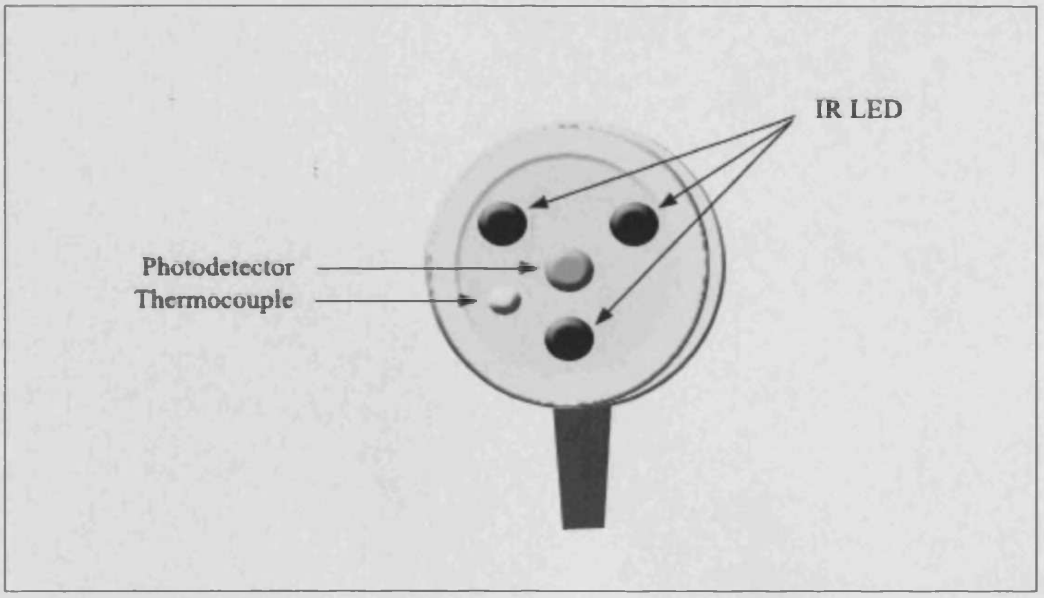

The introduction of the thermocouple into the probe is the only major difference between LRR and PPG. The reason for its inclusion was an attempt to take into account that blood flow through the vessels of the skin is highly dependent on its temperature, since the skin forms an integral part of the body's thermoregulatory control system. In fact, Mukherjee et al. (1991) suggest that LRR investigations are only meaningful if the temperature of the skin is between 25°C and 33°C. Sproule et al. (1997) also advise against investigations being conducted when the ambient skin temperature of the leg falls below 25°C. They suggest that constriction of the microcirculation vessels, associated with such low temperatures, may produce erroneously normal refill times following dorsiflexion exercises to empty the blood from the venous plexus of the calf. Like PPG, microcirculation refill times following exercise or occlusion of the large veins showed good correlation with venous pressure recovery measurements and the system seemed well suited for investigations of venous insufficiency.

The next stage in the development of PPG came in the late 1980s. Until then, PPG and devices based on the principles of PPG, were analogue systems and had significant problems with calibration. This restricted their usefulness to measuring time related

parameters. It was not possible to make inter-person comparisons of the amplitude of the PPG signal. This was because the absorption of infrared light depends on, amongst other things, skin pigmentation, thickness and also on the amount of blood initially in the measurement volume. These problems were overcome by the development of digital photoplethysmography (DPPG) by Blažek and Schultz-Ehrenburg. The new DPPG system used a probe similar to LRR, but slightly smaller, incorporating only a single infrared LED and a photodetector, with no thermocouple (fig 3.3).

Fig 3.3: Diagram of the measurement probe used in DPPG. *The probe, which is only a few centimetres in diameter, is attached to the skin using sticky tape.*

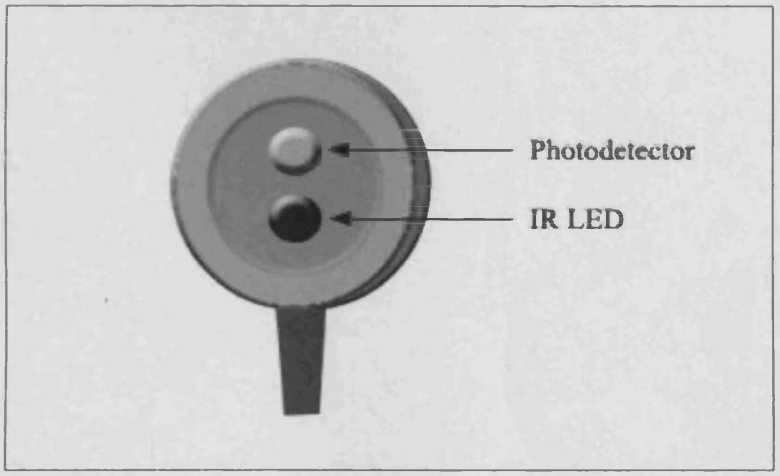

However, the major improvement over previous systems was that DPPG is computer controlled. A microprocessor adjusts the incident infrared light intensity so that the intensity received at the photodetector at the start of the measurements is exactly the same for each person. The intensity at the photodetector is then converted to a digital signal and the data can be analysed automatically by a central processing unit and the results stored in an inbuilt memory, recorded via an external printer or visualised on a display screen. Therefore, results are instantaneously available to the investigator.

3.2 Transmission and reflection PPG

There are two types of PPG; transmission and reflection. The two techniques do not greatly differ, except for the position of the light source and photodetector (fig 3.4).

In transmission PPG, the light source and photodetector are placed on opposite sides of the tissue under investigation. Therefore, the technique can only be used to investigate samples that allow light transmission all the way through the tissue. This technique is often used for monitoring blood volume variations in the digits or the ear lobes, e.g., Nakajima et al. (1996), Nitzan et al. (1999).

In reflection PPG, the light source and photodetector are on the same side of the tissue and so there is less restriction on which parts of the body can be investigated. The technique can be used on the skin's surface in most areas of the body.

From this point onwards, only reflection PPG as applied to the skin's surface will be described as this technique is employed in this study. However, the basic principles apply to both types.

Fig 3.4: Transmission and reflection PPG.
The blue line illustrates the path of a photon that is successful in finding its way from the light source to the photodetector.

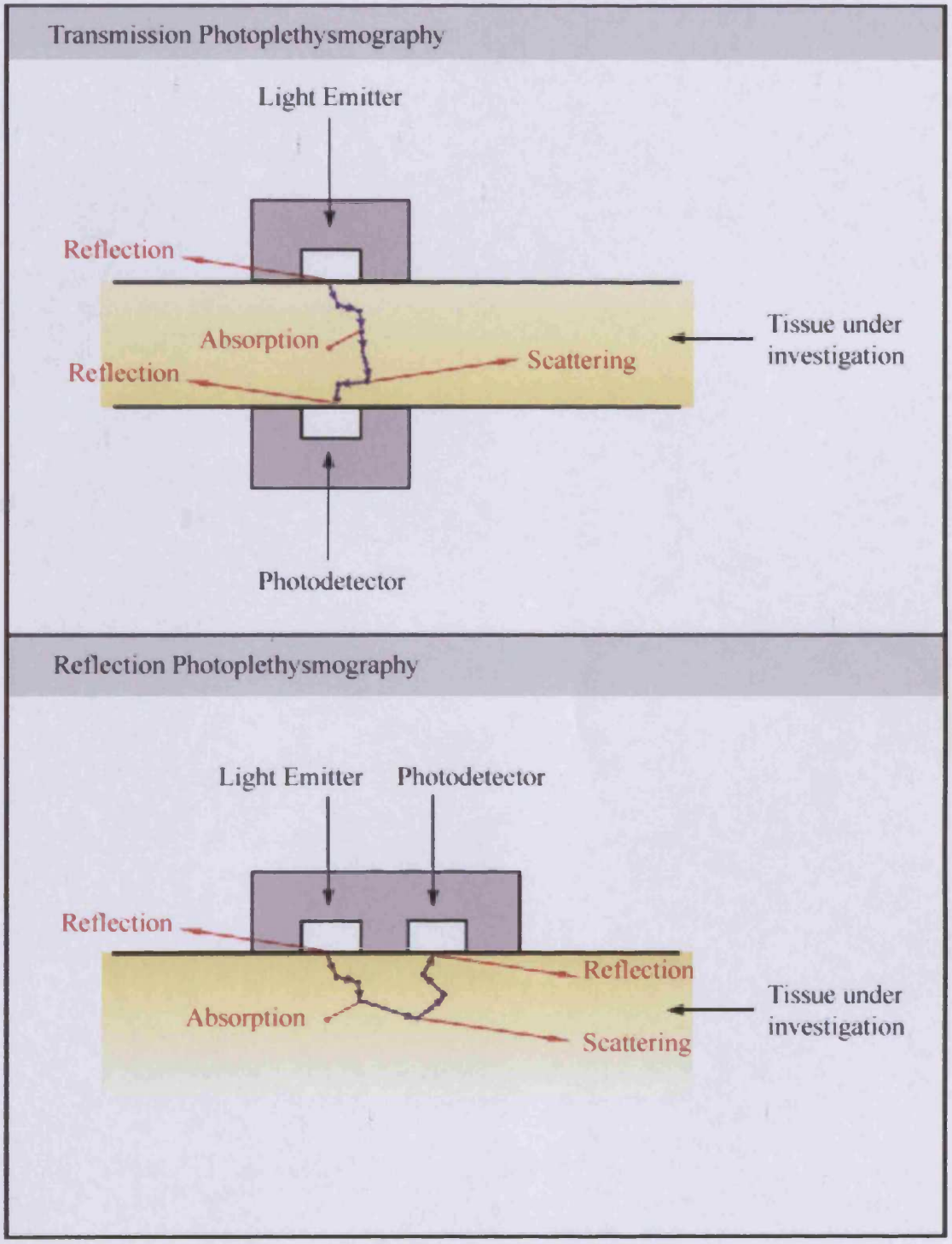

3.3 The origin of the PPG signal

The fundamental principle that PPG is based upon is the absorption of light by biological tissue. Infrared (IR) light is commonly used (the reason for this is described in greater detail below) and is directed onto the skin by a LED incorporated into a small probe (fig 3.5).

Fig 3.5: Diagram illustrating a PPG probe placed on the surface of the skin.

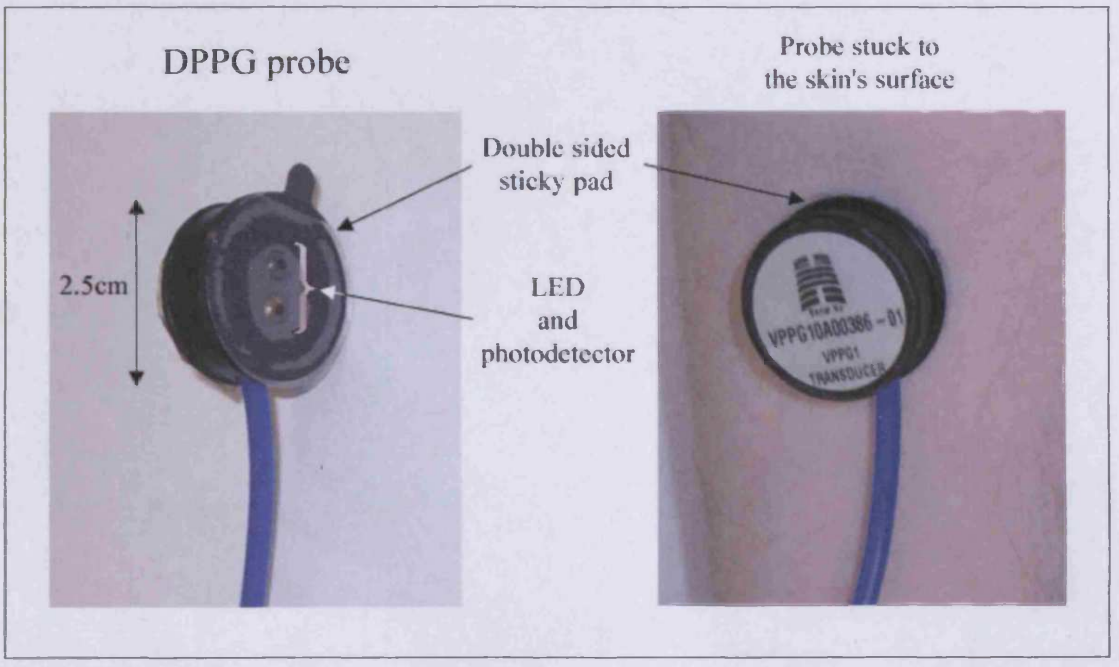

Any IR light that is not reflected by the skin's surface penetrates into the body where it is scattered and absorbed by the biological material through which it traverses, including tissue, blood vessels, blood etc. (There may also be photons that pass straight through without interaction, called ballistic photons). Eventually, some IR light finds its way out of the skin and is received at the photodetector (fig 3.4).

The IR light penetrates to a depth of approximately 2mm below the skin's surface, depending on the wavelength of light used (see section 3.4.2). This allows investigation of the skin's dermal vessel plexus, including the arterioles, capillaries and venules. Over the time taken to conduct the investigation, usually on the scale of minutes, the only component likely to undergo any significant change is the blood volume. Therefore, the variation of IR intensity at the photodetector is believed to correspond to the varying blood volume in the path of the IR light as it advances from emitter to

detector. Blažek and Schultz-Ehrenburg (1996) estimate that, at the lower extremities, 10% of the incident IR light (at 940nm) is absorbed by the tissue and around 90% is absorbed by the arterial and venous blood volumes. However, PPG makes no distinction between arterial and venous blood, i.e., both arterial and venous blood contributes to the PPG signal via absorption of IR light. Nevertheless, there is a difference between the absorption properties of oxygenated and deoxygenated blood depending on the wavelength of the light used (fig 3.6). This property is utilised in pulse oximetry.

Fig 3.6: Absorption coefficient of oxygenated and deoxygenated haemoglobin. *Adapted from Moyle (2002).*

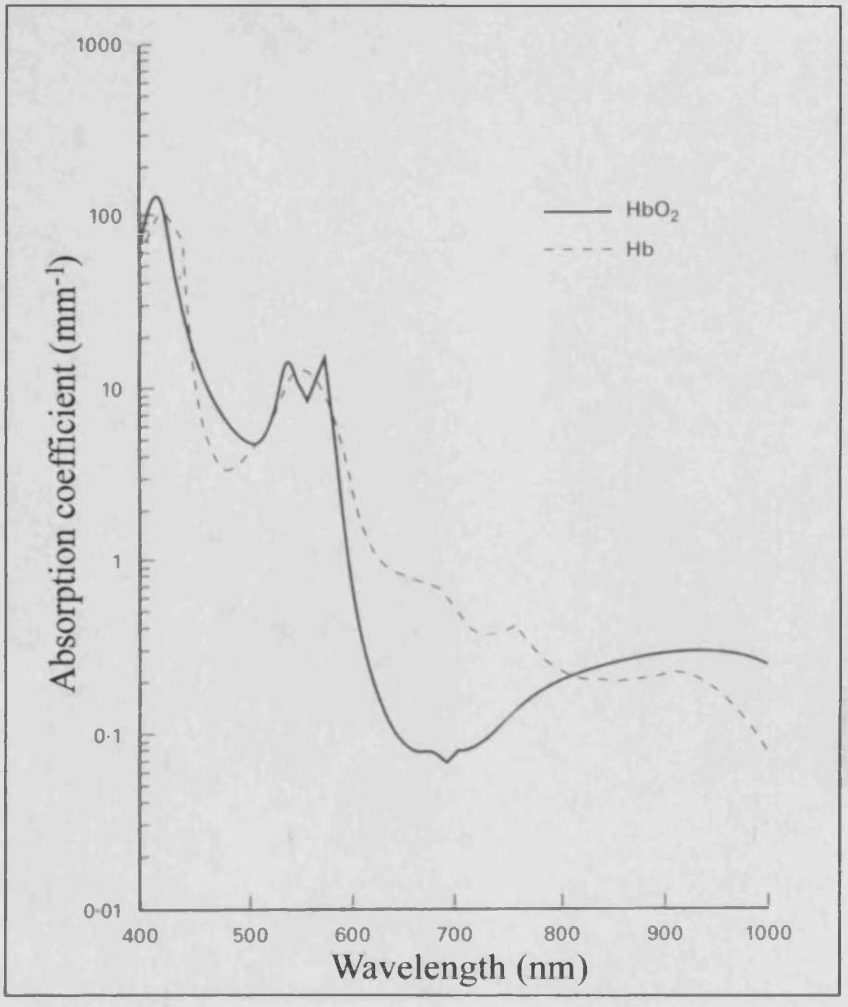

According to Lindberg and Öberg (1991), the effect of blood oxygenation on the PPG signal is uncertain. However, they refer to a study by Challoner in 1979, who compared

PPG signals obtained using light at wavelengths of 650nm and 805nm (the latter being one of the isobestic wavelengths, i.e., independent of the degree of oxygenation). Challoner found that the amplitude of intensity fluctuations within the PPG signal (caused by changing blood volume under the probe) remained the same when oxygen concentration was altered but the baseline amplitude (representing total absorption from all tissues and blood) varied substantially.

It has also been suggested that the absorption of IR light in PPG may depend on the orientation of the erythrocytes within the vessel (Moyle, 2002). During diastole, the erythrocytes tend to align parallel to the direction of blood flow but perpendicular during systole, increasing the absorption path length.

3.4 A closer look at the interaction between light and the skin

The first barrier to light, incident on the surface of the skin, is the air-skin interface. When optical radiation reaches this interface, reflection occurs due to change of refractive index between the air and the outer layer of the skin, the stratum corneum (1 and ~1.55 respectively). At near-normal incidence, approximately 4%-7% of the light may be reflected (Anderson and Parrish, 1981). This reflectance occurs over the entire spectrum from 250nm-3000nm for all skin colours. Variation in water content on the skin during, e.g., sweat gland secretion, will alter the refractive index and therefore the percentage of reflected light. The angle at which the light strikes the skin's surface will also affect the amount of reflection. By the same token, reflection at the skin-air interface will cause reflection, preventing light escaping from the skin. Structures on the surface of the skin may also impede the progress of the incident light, e.g., hairs or calluses.

The light that succeeds in passing though the skin's surface is absorbed and scattered by the underlying layers. This is described in greater detail below.

3.4.1 Absorption and scattering in the epidermis and dermis

The skin consists of an outer layer, the epidermis, and an inner layer, the dermis. Beneath the dermis is a subcutaneous layer of fatty tissue containing, sweat glands and blood vessels (fig 3.7). Any radiation that is successful in penetrating through the

skin's surface is scattered and absorbed by various structures and chromophores within these layers.

Fig 3.7: Diagram of the structure of the skin.

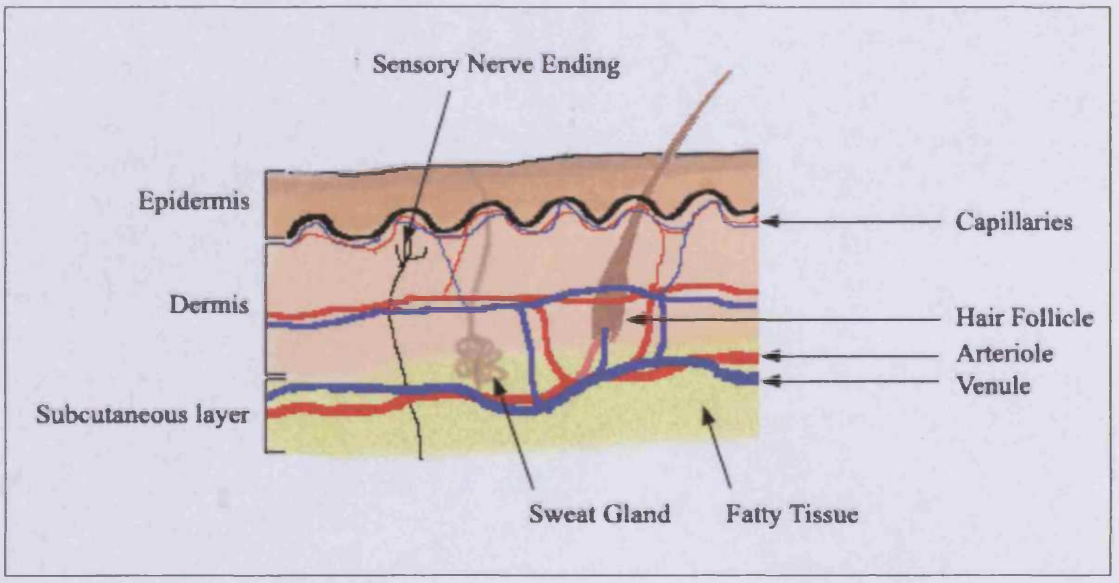

Epidermis: The thickness of the epidermis varies between approximately 50μm and 150 μm (Giltvedt et al., 1984). It is thickest on the palms of the hands and the soles of the feet. The epidermis has no blood vessels and is divided into four layers. The innermost layer, stratum germinativum, consists of continuously dividing cells. These cells are used to renew those in the upper three layers of the stratum granulosum, stratum lucidum and the outermost stratum corneum. The stratum corneum consists of dead cells.

In the epidermis, melanin is a strong absorber of short wavelength visible and ultraviolet (UV) light but has decreasing influence at longer wavelengths, becoming almost negligible at wavelengths greater than 1100nm (Anderson and Parrish, 1981). Scattering is not considered important in this layer.

Dermis: The thickness of the dermis varies between approximately 1mm and 4mm (Giltvedt et al., 1984). Like the epidermis, it is thickest at the palms of the hands and the soles of the feet. The dermis consists mainly of loose connective tissue. Within

the dermal layer are blood and lymph vessels, sensory nerve endings, sweat and sebaceous glands, hail follicles and smooth muscle fibres.

Scattering of optical radiation is of major importance in the dermal layer. The process is inversely proportional to wavelength and dictates the depth to which electromagnetic radiation can penetrate the dermis. Chromophores in the blood, including haemoglobin, oxy-haemoglobin, beta-carotene and bilirubin are the major absorbers of visible radiation in the dermis (Anderson and Parrish, 1981).

3.4.2 Penetration depth of optical radiation

The depth to which optical radiation can penetrate into biological tissue depends on its wavelength (in addition, penetration depth may also depend on the angle of incidence). The penetration depth through the dermis for various wavelengths was calculated by Anderson and Parrish (1981). Their results for fair Caucasian skin are shown in table 3.2 (these are theoretical values calculated from a simplistic model of radiation transfer in biological tissue). The figures would be different for different skin colours because a highly pigmented epidermis increases absorption, especially at shorter wavelengths. However, the results show a clear trend. Longer wavelengths have a greater penetrating power in the dermis and may be used to probe the capillary network, the superficial and deep plexuses and the communicating vessels between them whereas shorter wavelengths may only probe the superficial vessel plexus and capillary network.

Table 3.2: Approximate penetration depth of optical radiation in fair Caucasian skin to a value of 1/e (37%) of the incident energy density. *(Anderson and Parrish, 1981).*

Wavelength (nm)	Depth (μm)	Wavelength (nm)	Depth (μm)
250	2	500	230
280	1.5	600	550
300	6	700	750
350	60	800	1200
400	90	1000	1600
450	150	1200	2200

Giltvedt et al. (1984) investigated the different penetration depths of green (560nm) and IR (950nm) light. They used PPG on the lower arm to investigate the arterial pulsations

in the skin's microcirculation. A blood pressure cuff was wrapped around the arm (and over the PPG probe) to occlude arterial inflow. Then, by gradually releasing the pressure, they noted when arterial pulsations began to reappear in the PPG signals. They found that, because of the difference in penetration depth, the pulsations began to reappear in the PPG signals obtained with IR light before those obtained with the green light. They suggested that this was evidence of decreasing systolic pressure as one moves outwards from the deep plexus of the skin to the more superficial plexus and the capillaries. Such a decrease in systolic pressure from the large arteries, to the arterioles and capillaries is well known (e.g. Guyton, 2000).

The relatively large penetration depth of IR light is one of the reasons for its use in PPG. This allows a greater volume of the microcirculation to be investigated. In addition, wavelengths of this order provide maximum contrast between absorption due to blood and bloodless skin. In fact, full blood vessels reflect around 10 times less IR light than bloodless tissue (Blažek and Schultz-Ehrenburg, 1996). The absorption at the epidermis is also minimal at IR wavelengths and therefore a large percentage of incident photons are able to penetrate the skin's surface (fig 3.8).

Fig 3.8: Diagram illustrating the absorption and reflection of light incident on the skin, as function of wavelength.
The shaded region indicates the wavelengths often used in PPG.
(Adapted from Blažek and Schultz-Ehrenburg, 1996.)

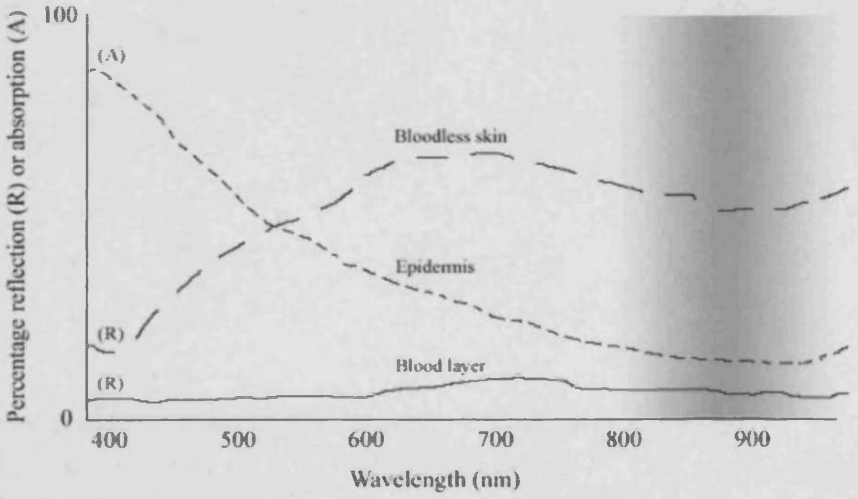

3.5 Calibration in digital photoplethysmography

As alluded to at the end of section 3.1, modern PPG systems are computer controlled. In order to indicate this, the prefix "digital" is added to the name. Digital photoplethysmography (DPPG) systems allow automatic collection and analysis of data. The data can be analysed by a central processing unit, saved in an inbuilt memory, recorded via an external printer or visualised on a screen.

DPPG can also perform automatic self-calibration. This procedure ensures that the DPPG reflection signal, measured at the start of each investigation, is within the instrument's measurement range. (The measurement range of the instrument is limited by its electronics, explained further in section 4.3.1.1, where the DPPG device used in this study is described in detail.)

Such a procedure is necessary because, as described above, the absorption of IR light by the skin depends on its pigmentation and thickness (and also on the initial quantity blood in the measurement volume). For example, Nitzan et al. (1998), using transmission PPG without calibration, found that the PPG baseline signal was higher in females when compared to males. This was assumed to be due to lower tissue volume (and therefore lower blood content) in the fingers of females and therefore less IR absorption. These problems are overcome by DPPG self-calibration through adjustment of the IR intensity incident on the skin's surface so that the intensity received at the photodetector, at the start of the investigation, is exactly the same for each person regardless of skin type, colour and thickness.

However, calibration does not make it possible to obtain a quantitative measure of the absolute volume of blood within the illuminated tissue. This is because the IR light is reflected, scattered and absorbed by various other structures and chemical compounds in the tissue (section 3.4). Therefore, the intensity of IR light returning to the probe depends on multiple interactions, not just with the blood. In addition, factors such as the haematocrit (the percentage of total blood volume that exists as erythrocytes) will affect the light absorption (e.g., Nijboer et al., 1981).

3.6 Current uses of PPG

PPG has the advantages of being, non-invasive, painless, low risk, without side effects, inexpensive, simple and easy to operate (not requiring highly skilled operators). In

addition, PPG is portable and can be performed anywhere. These properties make PPG an attractive technique for investigating the human body. The following are examples of current uses of PPG and technologies that are based on the principles of PPG.

- Investigating venous function including:
  - *The calf muscle pump*
  - *Venous insufficiency*
  - *Deep vein thrombosis*

PPG is commonly used to investigate venous insufficiency and the efficiency of the calf muscle pump (e.g., Fronek and Vanderweijer, 2003). The most common test involves a reflection PPG probe placed on the skin, 10cm above the medial malleolus. The patient, who remains seated, is instructed to perform a simple exercise routine (usually multiple dorsiflexions of the foot) during which a reduction in microcirculation blood volume is shown by the PPG signal. Following the exercise, the time taken for the microcirculation to recoup the loss is measured and used as an indicator for the condition of the veins. Very short refill times indicate venous reflux due to incompetent venous valves.

The technique has also been considered as a test for DVT where the amount of blood expelled from the limb (indicated by the change in PPG signal during the dorsiflexion exercise) is used as an indicator of the condition. A low venous output indicates obstruction in the veins. It has also been suggested that the refill time after exercise can be used as an indicator for DVT.

(Venous examinations using DPPG are described in greater detail in section 4.1.1, where the specific DPPG device used in this study is considered. For a more detailed consideration of the role of DPPG in DVT diagnosis, see section 2.5.4)

However, the results for diseased limbs are sometimes ambiguous and a positive test result may not be able to differentiate between diseases. For example, a reduced venous refilling time may indicate venous insufficiency or DVT. In addition, some investigators believe that PPG is not useful in assessing the severity of venous insufficiency (e.g., Nicolaides and Miles, 1987) and others have questioned the reproducibility of the test (e.g., Rutgers et al., 1993). In DVT diagnosis, even if the

technique could detect its presence, it would be difficult to assess the location of the thrombus.

Therefore, the technique has not gained widespread acceptance as a diagnostic tool but is often used as a screening device to reduce the burden on more conventional techniques such as Doppler ultrasound imaging.

- Monitoring heart and breathing rates

There has been interest in using PPG to monitor heart and breathing rates, replacing more conventional techniques such as ECG and transthoracic impedance. PPG may provide a simple monitoring system using a single probe placed on the most convenient site of the patient. For example, Olsson et al. (2000) suggest that a single PPG probe may be used to monitor both the heart and breathing rates of newborn infants with the same degree of accuracy as conventional ECG and transthoracic impedance. As the apparatus are easily portable, this simple technique means that monitoring of long-term conditions could take place away from the hospital setting.

Lindberg et al. (1992) lists other circumstances where breathing and heart rate monitoring by PPG may be important. These include the postoperative period (see also Nilsson et al., 2000), in the intensive care unit, during MRI investigations where optical devices are unaffected by the strong radio frequencies and magnetic fields or in noisy electromagnetic environments away from the hospital setting (e.g., cars and electric trains). PPG has also been considered for use in monitoring anaesthetised patients during operations, e.g., Dorlas and Nijboer, 1985.

- Measuring blood pressure

PPG systems can be used to measure systolic blood pressure (e.g., Chawla et al., 1992). Transmission PPG probes are usually used and are clamped over the digits (however, there is no reason why reflection PPG probes could not be used). A compression cuff is wrapped around the arm or the leg. When the cuff is inflated with air to above systolic pressure, the arterial pulsations in the PPG signal disappear. The cuff pressure is deflated slowly and systolic blood pressure is taken to be the pressure in the cuff when the arterial pulsations begin to reappear in the PPG signal.

It has been suggested that the ankle/brachial index can be calculated using a simple, automated PPG test, rather than Doppler ultrasound, as a means of investigating peripheral arterial occlusive disease (Sadiq and Chithriki, 2001).

- Pulse oximetry

The principles behind PPG have been used for many years in pulse oximetry. The absorption of light at two different wavelengths is used to measure the proportion of oxygenated haemoglobin in the blood (e.g., Moyle, 2002).

- Investigating the sympathetic nervous system

Since all blood vessels are innervated, including the small microcirculation vessels, there is growing evidence to suggest that PPG signals from the skin may be used to provide an insight into the functioning of the sympathetic nervous system. Possible uses include the investigation of autonomic neuropathy in diabetes; a condition in which the nervous system becomes dysfunctional (e.g. Nitzan et al., 1998 and Bernardi et al., 1996).

3.7 Artefacts in the PPG signal

There are many factors that influence the PPG signal during an investigation. Firstly, there are those intrinsic to the tissue under investigation and these have been described above. In addition, physiological factors influence blood flow and hence the volume of blood in the microcirculation. However, there are other factors, external to the body, which could produce artefacts in the PPG signal and some of these are described below.

- The ambient light intensity in the room where the test is conducted

This effect was important during early investigations with PPG but only arises when the light emitter and detector are not placed in direct contact with the tissue under investigation. In this case, the ambient light may contribute to the intensity measured at the photodetector. In fact, Rutgers et al. (1993) stated that a lighted lamp within 1m from the PPG apparatus could disturb the signal by a magnitude comparable to the original, unaffected signal. However, in most modern PPG techniques, the measurement probes are placed in direct contact with the skin. This arrangement

prevents any ambient light from reaching the photodetector. In addition, the use of IR light in modern PPG alleviates the problem.

- Skin and environmental temperature

The skin performs a major role in the body's thermoregulatory control (see section 1.5.2.2.2). Changes in body temperature may significantly alter blood flow through the skin. Cold temperatures result in constriction of skin blood vessels, reduced blood flow and reduced heat loss from the body. Conversely, warmer temperatures result in dilatation of the skin blood vessels, increased blood flow and increased heat loss through the skin's surface. However, the skin has more cold than warmth receptors, so protection from falling temperatures is more important.
Therefore, in experiments with PPG, the temperature of exposed skin surfaces should be prevented from falling too low. This maintains adequate skin blood flow and a good PPG signal. For example, Tan and da Silva (1999) attempt to "maintain a stable temperature" of the foot by simply insulating with a towel.

- Pressure at which the PPG probe is attached to the skin

If the PPG probe is attached too firmly to the skin, compression of the small microcirculation vessels will affect the blood flow. Rutgers et al. (1993) point to studies which show that different attachment pressures can give substantially different recordings. However, in some reflection PPG apparatus, the measurement probe is attached to the skin using double sided sticky tape. This keeps the probe in position without any unnecessary pressure on the skin's surface.

- Movement artefacts

Patient movement will cause large changes in the PPG signal because of blood volume shifts in the circulation (for example, when dorsiflexing the foot). This can cause significant artefacts in the signal, especially when the movement concerns the part of the body under investigation.

Chapter 4

Description of the Equipment Used in This Study

This chapter describes the equipment used in this study. The basic commercial DPPG device is described, together with the way in which the instrument was modified to meet the requirements of the study. Also described is the method used to transfer the DPPG data to a personal computer and the corrections required before the data could be analysed further.

4.1 The DPPG device

The DPPG device used in this study was the Huntleigh PPG Assist• (Huntleigh Technology PLC, Luton, UK). The main unit (fig 4.1) has dimensions approximately 25cm x 15cm x 5cm and is powered by a rechargeable battery with a lifetime of approximately 4hrs. Alternatively, the unit can be powered by the mains electricity supply. The unit weighs 1.6kg and is therefore easily portable. However, for convenience, the unit can be connected to a docking station (fig 4.2). Although the docking station is not required, it is useful for holding the unit firmly in place during an investigation and also has a compartment to store small items, such as the measurement probes or the sticky pads required to attach the probes to the skin. The docking station also provides recharging, printing and sound capabilities.

• For further technical specifications, see http://www.huntleigh-healthcare.co.uk

Fig 4.1: Huntleigh PPG Assist.

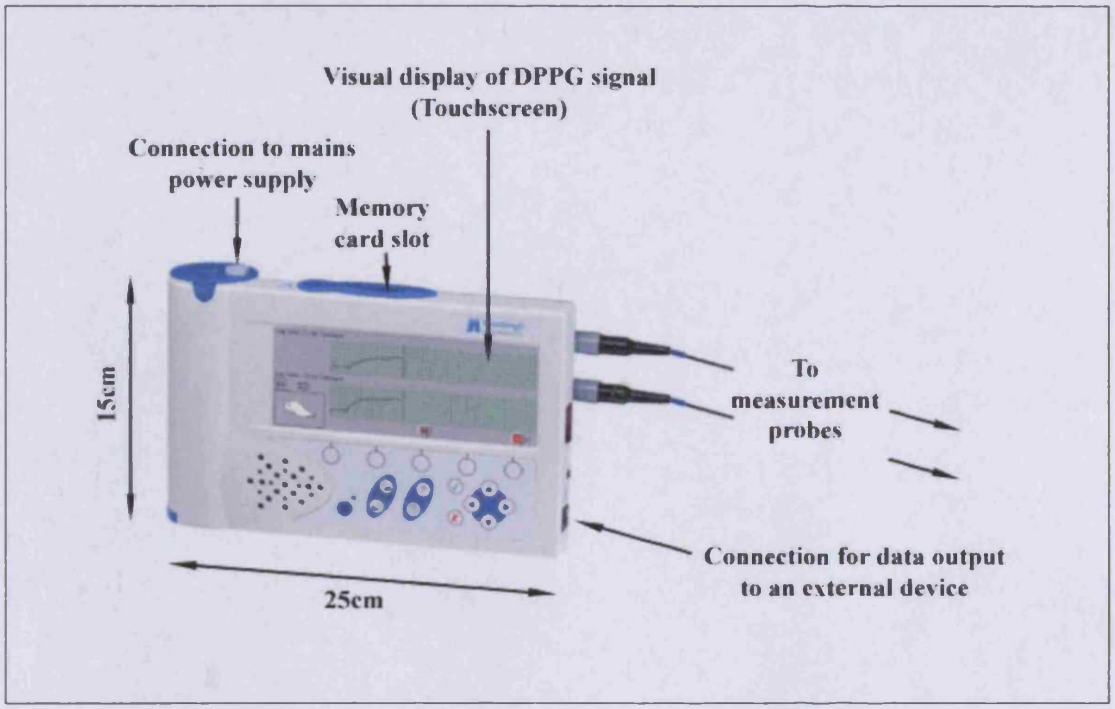

Fig 4.2: Optional docking station.

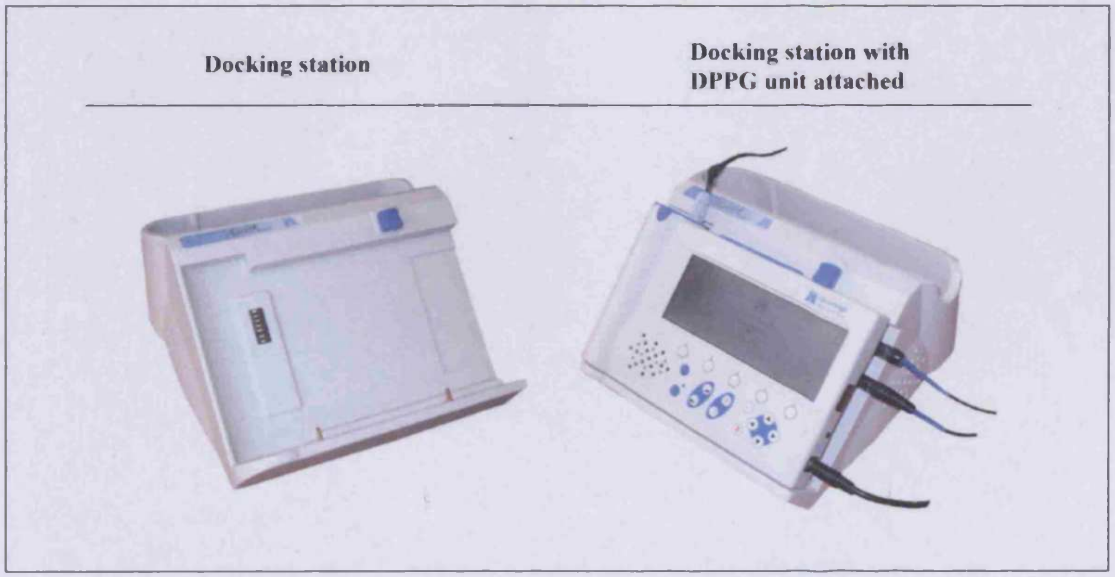

The unit has connectors for two measurement probes and can be used in a single or dual probe configuration, allowing investigation of up to two body regions simultaneously. Each probe has a cylindrical head measuring approximately 2.5cm in diameter with a

depth of 1cm (fig 4.3). Built into each probe is an IR emitter (LED) and photodetector. The probes are attached to the region of investigation on the skin via a thin, transparent sticky pad (fig 4.3) and connected to the main DPPG unit via electrical wires.

Fig 4.3: The measurement probe used with the Huntleigh PPG Assist.

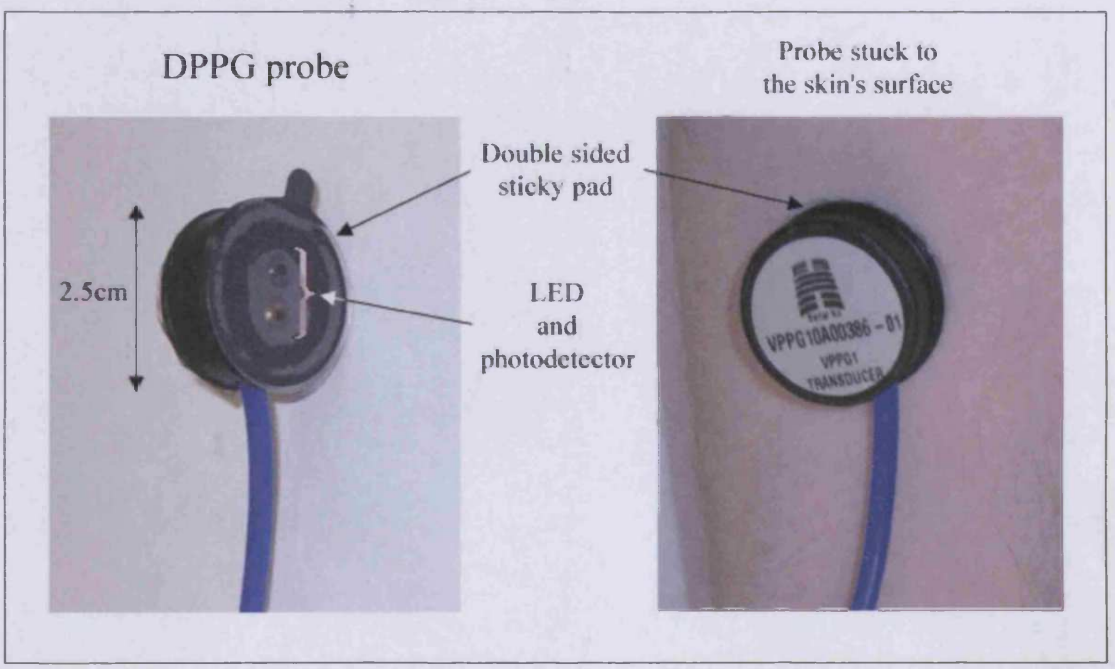

IR light of wavelength 940nm is emitted from the LED and this interacts with the skin directly below the probe. Here, it is absorbed, scattered and reflected in the manner described in sections 3.3 and 3.4. Any IR light that returns to the probe is detected by the photodetector where the IR intensity is converted into an electrical signal. The signal is passed to the main unit where it can be viewed on the display screen as the data is acquired or output directly to an external device for storage and further analysis (e.g., see section 4.3).

4.1.1 Standard DPPG test

The Huntleigh PPG Assist was designed and manufactured to be used in lower limb venous investigations. It can be used as an indicator of venous insufficiency and also DVT. The standard test for lower limb venous disease using the device is described below.

Ideally, the patient sits on a chair with their upper body tilted slightly back. The feet should be placed flat on the floor such that the angle at the knee joint is approximately 120° (fig 4.4). This body position helps to minimise any crimping of the blood vessels, especially the veins, at the level of the groin and the knee. This, in turn, prevents any unwanted disturbances to the blood flow that may influence the results.

Fig 4.4: Set-up for the standard lower limb venous investigation using the PPG Assist.

One measurement probe is attached to the leg under investigation. The probe is positioned 10cm above the level of the medial malleolus, measured by a strip of blue plastic fixed onto the wire of the measurement probe (fig 4.4). The probe is attached to the leg using double sided sticky pads, which are provided with the DPPG device.
The patient is asked to relax, while maintaining the same body position, until instructed to dorsiflex the foot. When the patient is comfortable and relaxed, the test is started.

This begins with the DPPG device performing self-calibration, which can take between a few seconds up to a maximum of 90 seconds to complete, depending on the stability of the microcirculation blood volume. Calibration requires that the DPPG signal does not show any net increase or decrease with time. If a stable signal is not observed during the 90s, the device displays a warning indicating that readings may be misleading. Calibration adjusts the intensity of the incident IR light so that the intensity received at the photodetector is within the possible measurement range of the DPPG device (which is limited by its electronics, see section 4.3.1.1). Calibration also ensures that the amplitude of the DPPG signal at the start of the investigation is the same for all skin types (colour and thickness) and towards the lower level of the possible measurement range so that any large amplitude changes during dorsiflexion of the foot (described below) can be accommodated.

Following calibration, the device emits an audible sound and the patient is instructed to begin dorsiflexion exercises. This involves raising and lowering the front part of the foot while the heel maintains contact with the ground (fig 4.5). Ten dorsiflexions are performed in 15 seconds. To maintain the correct rate, the patient is instructed to dorsiflex in time with a small moving image of a foot on the display screen of the DPPG device. There is also an audible metronome signal indicating the correct dorsiflexion rate.

Fig 4.5: Illustrating the dorsiflexion exercises performed during the standard lower limb venous investigation using the PPG Assist.

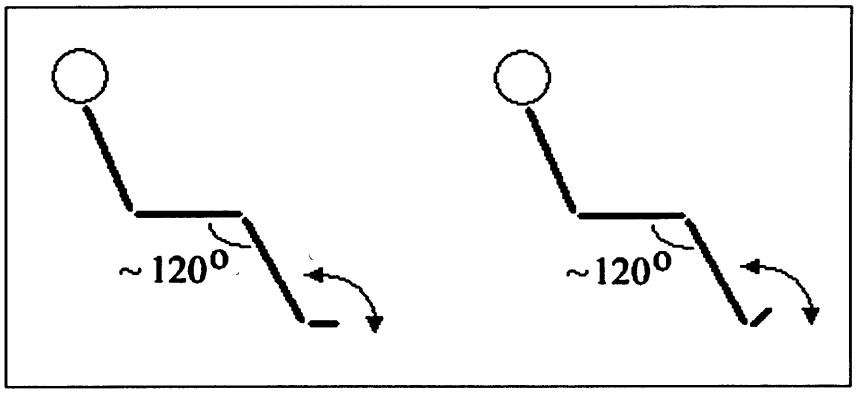

The dorsiflexion exercises utilise the calf muscle pump to expel blood from the veins of the lower limb. As a result, the microcirculation blood volume is reduced and an increase in the DPPG signal amplitude is observed on the display screen.

Following the dorsiflexion exercises, the patient is again instructed to remain still for the remainder of the investigation, with the foot placed flat on the floor. During this time, the microcirculation blood volume returns to its pre-dorsiflexion level and the DPPG device continues to record data while this takes place. Total test time (following calibration) is 65seconds. At the end of the test, an emptying-refilling curve is displayed on the display screen (fig 4.6).

Fig 4.6: Typical DPPG emptying-refilling curve recorded during a dorsiflexion test with the probe placed 10cm above the medial malleolus.

- **Tdorsiflexion** *is the time during which the patient performs the dorsiflexion exercises.*
- **A_0** *is the DPPG amplitude before the dorsiflexions begin.*
- **A_1** *Is the DPPG amplitude following 10 dorsiflexions of the foot.*
- **δAd** *is the DPPG amplitude change corresponding to a single dorsiflexion.*
- **VP** *gives a value proportional to the volume of blood expelled from the microcirculation as a result of the dorsiflexion exercises.*
- **T_{RT}** *is the time taken from the microcirculation blood volume to return to its initial level following the dorsiflexion exercises.*
- **$T_{1/2RT}$** *is the time taken for the DPPG signal to return from A_1 to 50% of VP.*

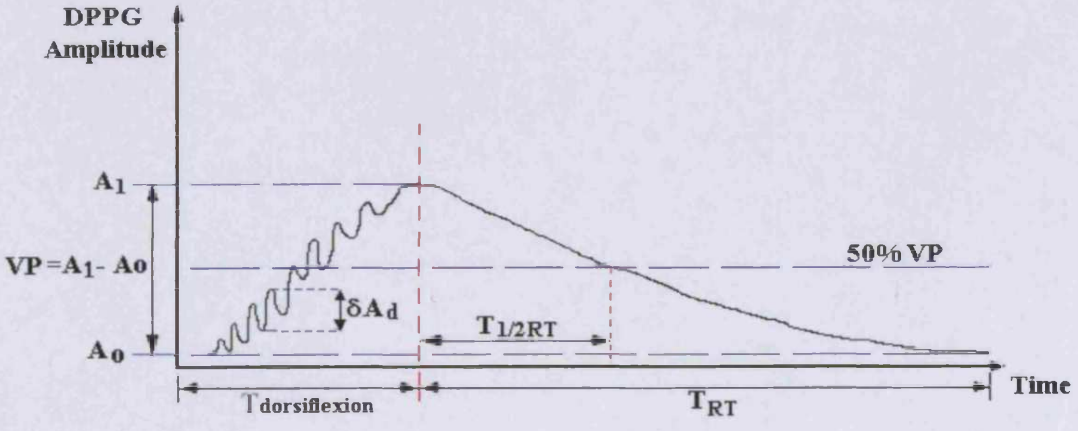

The maximum amplitude change of the DPPG signal, called the venous pump (VP), is proportional to the volume of blood expelled from the microcirculation as a result of the

dorsiflexion exercises. The time taken for the microcirculation plexus to refill following the dorsiflexions is called the refill time (RT). These two parameters are used as an indicator for venous disease in the leg.

Both venous insufficiency and DVT cause a reduction in RT and VP, compared to normal values (fig 4.7). Venous refill is normally caused by arterial inflow since venous valves prevent reverse flow of blood. However, when the venous valves are incompetent, as with venous insufficiency, reverse flow is allowed through the veins. This reduces RT. Since the efficiency with which the muscle pump expels blood from the veins is also reduced when venous insufficiency is present, VP may also decrease.

A DVT in the leg obstructs venous outflow, reducing VP. As a consequence, RT will also decrease since less blood is required to refill the veins.

Using a similar DPPG device[♦], Tan and da Silva (1999) found that a refill time less than 21s was optimal for use in DVT diagnosis. They also found the optimum value for VP to be less than 36 (in arbitrary units, specific to the DPPG device used in their investigation). Nevertheless, the cut-off values of RT ad VP are by no means fixed and should be determined by each centre that performs the test. A combination of the two values may provide a more accurate diagnosis.

♦ Rheo Dopplex II (Huntleigh Technology PLC, Luton, UK).

Fig 4.7: Illustration of emptying-refilling curves for different lower limb venous diseases.

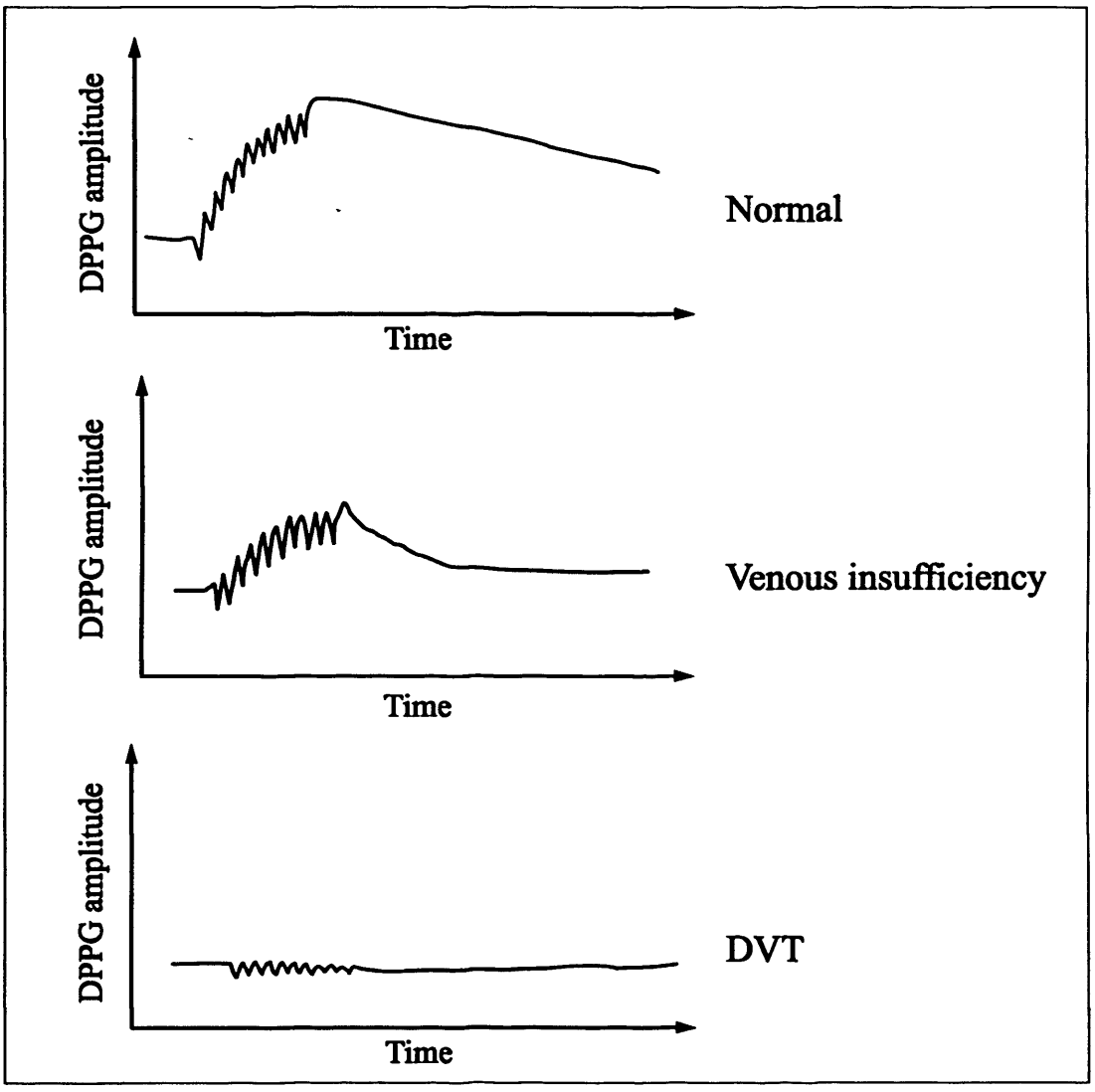

4.1.1.1 Limitations of the standard test

Despite the obvious advantages of the DPPG test (low cost, non-invasive, portable, quick and simple to perform with minimal training) there are limitations. For example, there is no way of quantifying the vigour at which the dorsiflexions are performed. Particularity less dynamic dorsiflexions may not eject as much blood from the leg, compared to more vigorous dorsiflexions, affecting the VP and RT values.

In addition, the test is only suitable for those patients who are able to comply with the dorsiflexion exercises. Patients with poor ankle mobility or confused, elderly patients may have difficulty dorsiflexing the foot at the required rate. Similarly, the test cannot

be performed on immobile patients. This is a clear disadvantage since these patients are at a high risk of developing DVT (see section 2.3).

As described in section 4.1.1, a reduced RT and VP may be caused by DVT or venous insufficiency. Therefore, it is sometimes difficult to differentiate between the diseases. Other conditions may also affect the DPPG emptying-refilling curve. For example, a Baker's cyst at the knee may compress the popliteal vein and impede the displacement of blood during the dorsiflexion exercise. The latter stages of pregnancy may also disrupt venous flow due to compression of the pelvic veins.

Even for those without venous disease, the measured RT tends to decrease with age (Stacey et al., 1996). This may be caused by a deterioration of the effectiveness of the calf muscle pump, possibly due to a reduction in muscle mass available to compress the veins or restricted movement at the ankle joint.

Arterial disease may also affect the emptying-refilling curve by reducing arterial inflow, although Tan and da Silva (1999) and Stacey (1996) find this to be unlikely.

4.2 Modification of the DPPG device

Since the Huntleigh PPG Assist was designed to investigate venous function by generating an emptying-refilling curve like that shown in figure 4.6, the device only acquires data for 65s (following calibration). After this period, data collection automatically stops. However, for this study, it was necessary to record microcirculation changes over a longer period of time. This was not possible using the commercial device, which had to be continually restarted, resulting in significant gaps in the recorded data.

To overcome this problem, the manufacturers were asked to modify the operating software so that longer recording times were allowed. The modified device is fundamentally the same as the original except that it allows continuous real-time collection of DPPG data for an indefinite period.

4.3 Connecting the DPPG device to a personal computer

As well as recording DPPG data for long periods of time, it was also necessary to transfer the data to a personal computer (PC) for analysis. Since the (modified) DPPG device could not store data in its internal memory, the data had to be streamed to the PC

in real time. This was achieved via the data output connection on the side of the DPPG device (fig 4.8). The data was streamed straight to the serial communications (COM) port on the PC and data capture was controlled by a "SerialSampler" program*.

* Custom program supplied by Huntleigh (Huntleigh Technology PLC, Luton, UK).

Fig 4.8: The DPPG-PC set-up.

(The screenshot shows the serial sampler program while capturing a DPPG signal.)

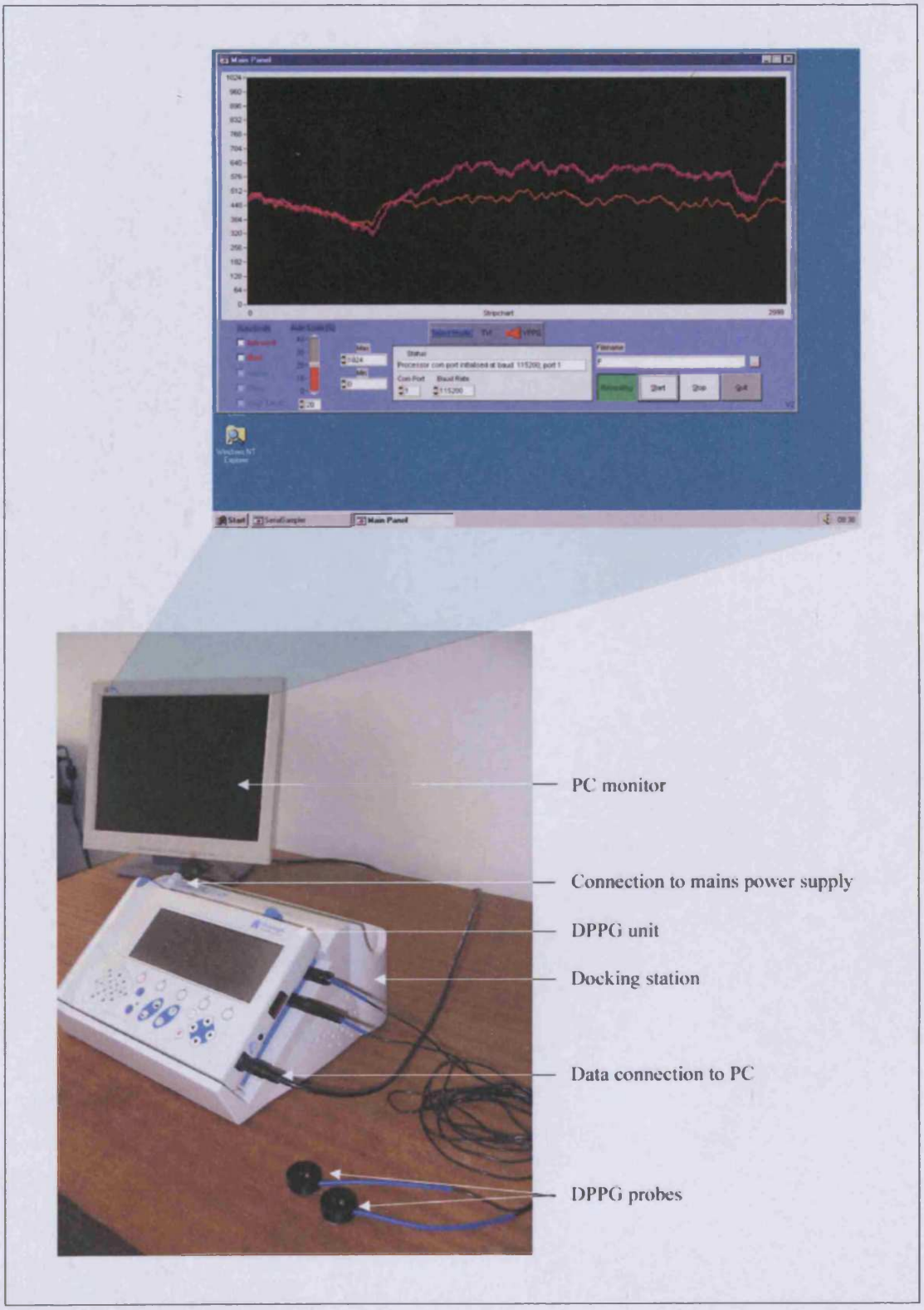

4.3.1 Data transfer from the DPPG device to the PC

4.3.1.1 Conversion from an analogue to a digital signal

Before the DPPG data can be passed to the PC, the signal received from the photodetector, representing the intensity of the IR light, must be digitised. This process converts a continuous, analogue signal to a digital signal consisting of a series of discrete values. To do this, the analogue intensity signal is sampled by the DPPG device at a frequency of 6.25Hz and then converted to a series of representative numbers by an analogue-to-digital converter (ADC). The ADC used in the DPPG device has a 10-bit precision, able to produce 2^{10} integer numbers from 0 to 1023. This means the continuous intensity signal can be quantised into a possible 1024 levels, where each level is labelled by an integer number representing a small intensity range. It is these numbers that form the DPPG signal. However, conversion from analogue to digital data is associated with two well known effects:

i) As a result of quantisation, errors are introduced that appear to be like random noise superimposed on the data. After the intensity signal is sampled, the ADC assigns an integer number to any intensity value that falls between a particular range. Therefore, each digitised number is associated with a maximum error of ±½.

ii) The ADC imposes a limitation on the measurement range of the DPPG device since it can only generate 1024 different digital numbers to represent the sampled intensity values. If the intensity continues to rise so that the ADC must produce higher numbers to represent it, there comes a point where no more numbers are available and the recording saturates (fig 4.9). The same is true for prolonged decreases in intensity.

Fig 4.9: An example of DPPG signal saturation.

(Each point represents digitised output from the ADC. Sampling frequency is 6.25Hz.)

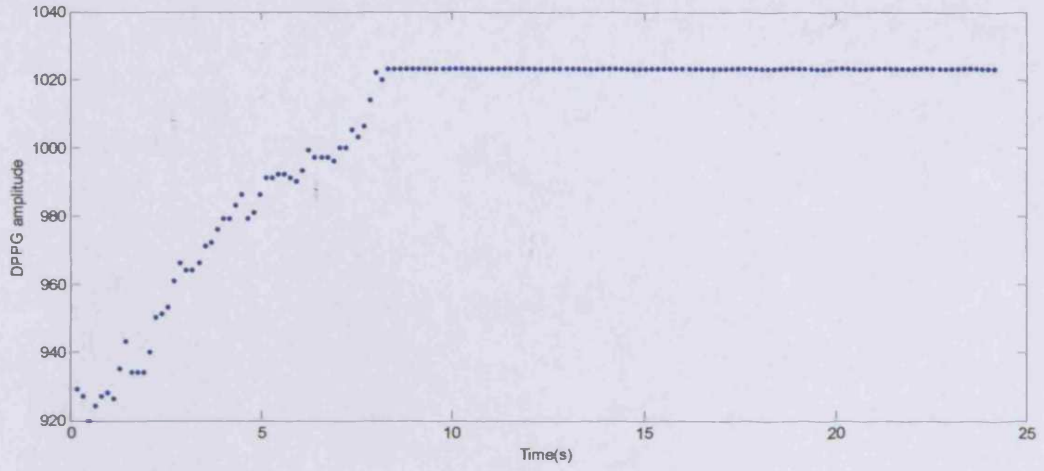

The discrete set of integer numbers between 0 and 1023 form the DPPG signal. It is these numbers that are passed to the PC for further analysis. The transfer of these data from the DPPG unit to the PC is described below.

4.3.1.2 Data collection using two DPPG probes (the "dual sampling" artefact)

When two measurement probes are attached to the DPPG unit, the photodetector signals from both channels are sampled simultaneously (sampling frequency, 6.25Hz). Following digitisation by the ADC, the data from both channels are ready to be sent to the PC. However, the data cannot be sent simultaneously because the DPPG unit is connected to the serial port. Data from each channel must be sent separately and this leads to an artefact in the data stored on the PC, appearing that each point has been sampled twice.

Each time the photodetector signal is sampled and digitised by the ADC, the data are tagged to indicate which channel they come from before being sent to the PC. The PC allocates two different memory locations for data storage and places the data from each DPPG channel in the corresponding memory location.

However, because the data from each channel are sent to the PC separately, only one channel in the PC memory is updated each time. The other channel does not get

updated but retains the value of the previous datum sent by the DPPG device. The process is illustrated in figure 4.10.

Consequently, a "dual sampling" artefact appears in the data stored on the PC. An example of DPPG data captured by the PC while the DPPG device was used in the dual channel mode is shown in figure 4.11. The "dual sampling" artefact is clearly seen. This artefact must be corrected before the DPPG data is analysed further and the way in which this was achieved is described in section 4.3.1.4.

Fig 4.10: Diagram illustrating the transfer of data to the PC from the DPPG unit, when used in dual channel mode.

- *The letters indicate the sampling order. For example, an A-A' pair indicates that data from channels 1 and 2 were sampled at the same time (sampling frequency, 6.25Hz).*
- *The vertical arrows indicate data transfer from the DPPG unit to the PC, following digitisation by the ADC.*
- *The shaded circles represent data that are copied from the previous values in the PC's memory location.*

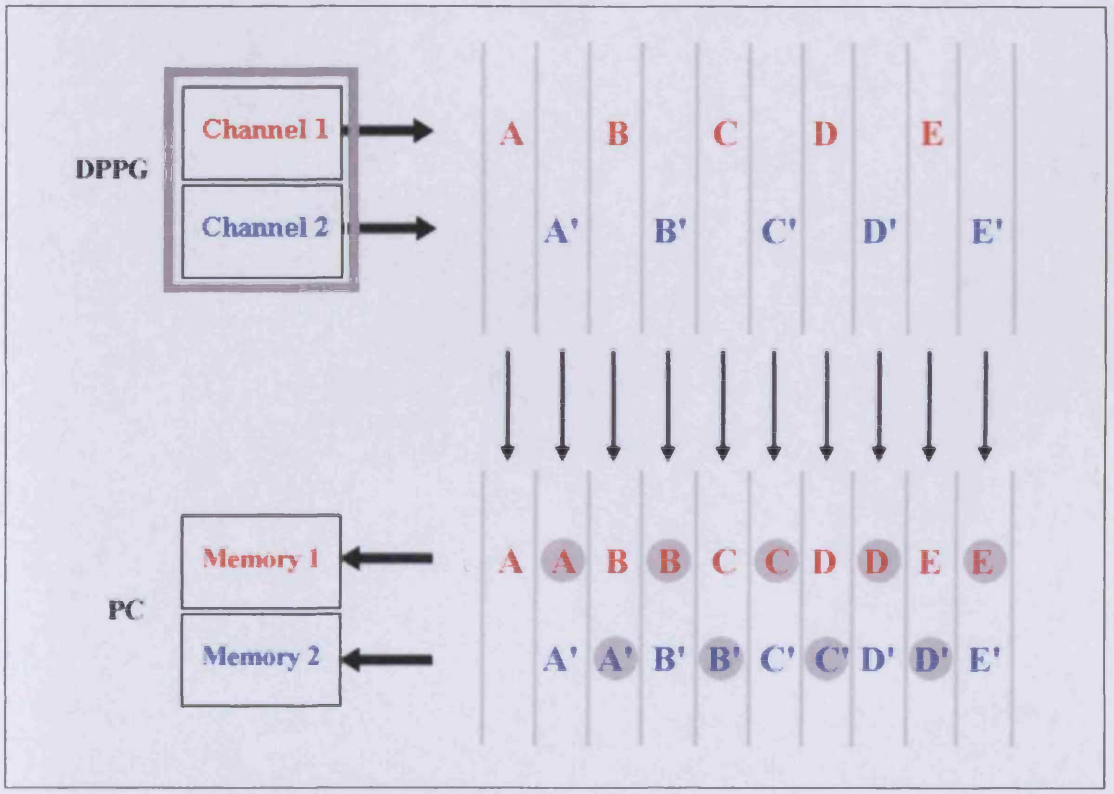

Fig 4.11: An example of data sent to the PC by the DPPG device when used in dual channel mode.

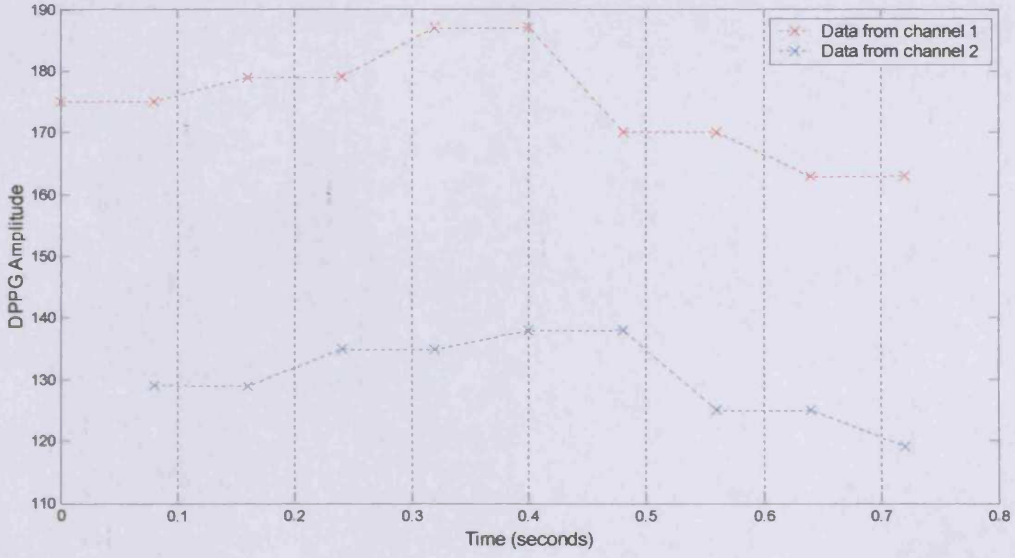

4.3.1.3 Data collection using a single DPPG probe

When only one measurement probe is attached to the DPPG unit, the photodetector signal from the single channel is sampled, digitised and sent to the PC once every 0.16s (sampling frequency, 6.25Hz). The PC receives the data, which it stores in a single memory location. Therefore, no duplication of data takes place and the "dual sampling" artefact observed when two DPPG probes are used does not occur. The process is illustrated in figure 4.12.

Fig 4.12: Diagram illustrating the transfer of data to the PC from the DPPG unit, when used in single channel mode.

- *The letters indicate the sampling order (sampling frequency, 6.25Hz).*
- *The vertical arrows indicate data transfer from the DPPG unit to the PC, following digitisation by the ADC.*

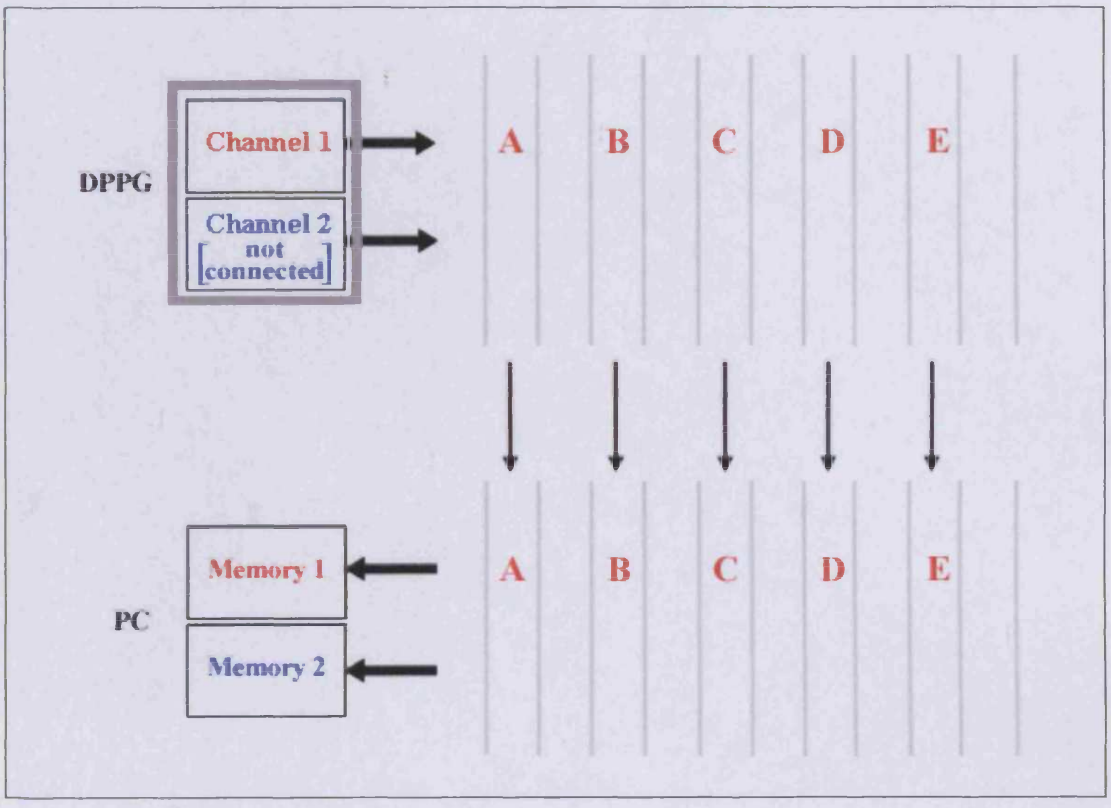

4.3.1.4 Correcting the captured data

When the DPPG device is used in single channel mode, no corrections to the captured data on the PC are necessary because the data exactly match those output from the ADC.

However, when the DPPG device is used in the dual channel configuration, some data manipulation is required to remove the "dual sampling" artefact described in section 4.3.1.2.

This was achieved by simply deleting alternate values from the data stored on the PC (fig 4.13). This process does not remove any information content from the data since the deleted values are only copies created by the PC (cf. fig 4.10).

Subsequent to this, the remaining data were aligned (fig 4.14). The resulting data exactly matches those output from the ADC of the DPPG device.

Fig 4.13: Illustrating the values to be removed from the DPPG data stored on the PC.

The plot is the same as that shown in figure 4.11, except that the circles illustrate the data that will be deleted.

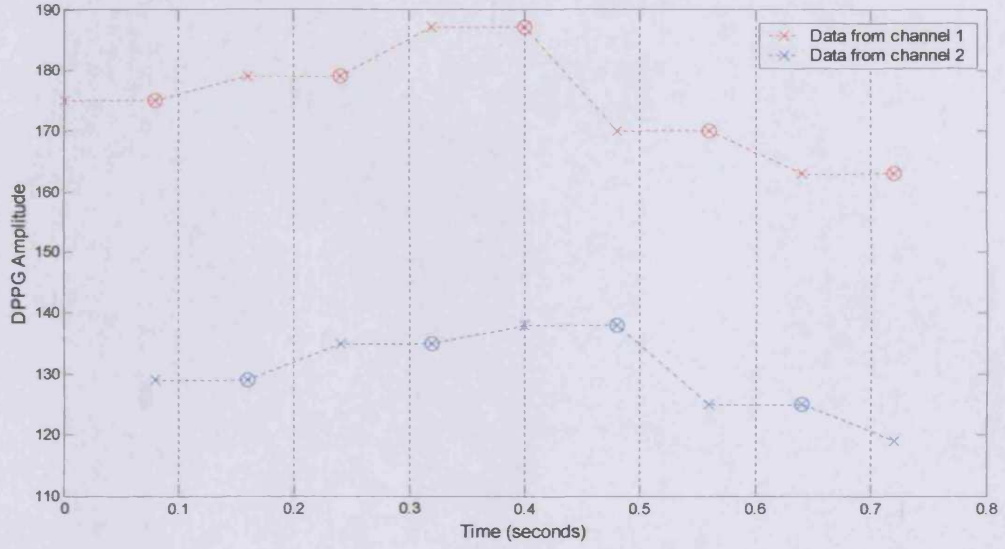

Fig 4.14: The DPPG data following the modification described in figure 4.13.

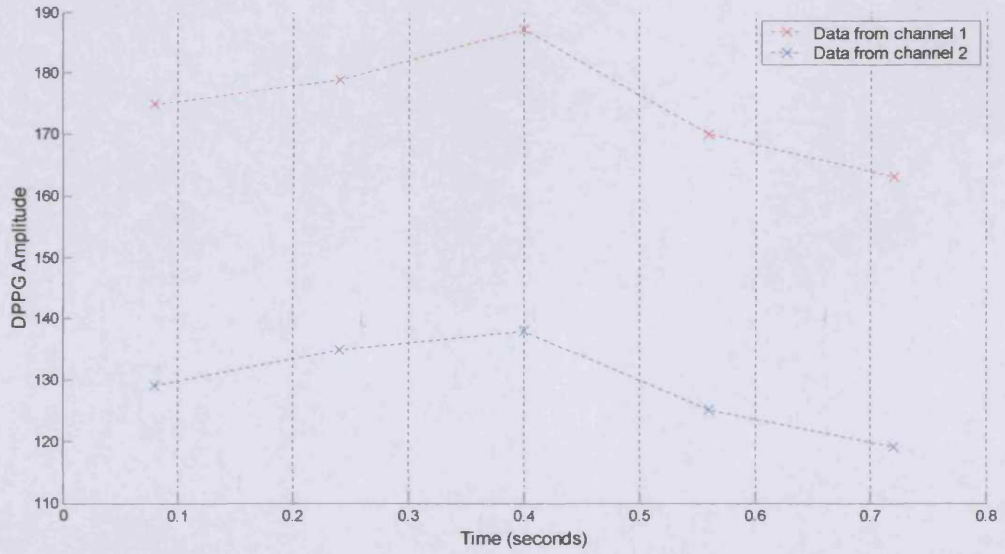

Chapter 5

Analysis Methods Used in This Study

This chapter describes the methods used in this study to analyse the DPPG signals. Firstly, Fourier analysis is considered together with its limitations. This technique can be used to obtain a general idea about the frequency content of the DPPG signal but is not appropriate to assess how the frequency components vary over time.

To achieve this, the technique of complex demodulation was introduced. Using this method, it is possible to calculate the temporal variation in amplitude and phase of a single, selected frequency in the DPPG signal. The theory and limitations of this technique are also discussed below together with the use of digital filters.

Finally, the implementation of these analysis techniques, using MATLAB software, is described.

5.1 Fourier analysis

Fourier analysis is named after the French mathematician and physicist Jean Baptiste Joseph Fourier (1768-1830) for his mathematical contribution and realisation of practical uses for the technique (Lynn, 1993). The technique is based on the principle that any continuous, periodic signal can be represented by the sum of sinusoidal waves of different frequencies, called a Fourier series. The original signal, in the time domain, is completely represented by the amplitude of its constituent frequency components. It is also possible to reconstruct the original time domain signal from the frequency information and the process of converting between time and frequency domains is called transformation.

A similar method also exists for analysing continuous signals that are aperiodic (e.g. decaying exponentials), called the Fourier Transform.

5.1.1 Digital signal processing – The discrete Fourier transform

Fourier analysis assumes that the signals are infinite in length (since it is impossible to construct a finite length signal from the sum of sinusoidal waves, which are, by definition, infinite in length). However, infinite signals do not occur in real life

situations. Furthermore, in digital signal processing, the signals are not continuous. The signals are sampled and stored on a computer for future analysis.

In order to apply Fourier analysis to real life, finite length, discrete signals an approximation has to be used. In digital signal processing, this is provided by the Discrete Fourier Transform (DFT). Here, the original, discrete signal is imagined as repeating itself an infinite number of times. This creates an illusion of an infinitely long, periodic signal with a wavelength equal to that of the original, finite length signal. The DFT is usually calculated using a complicated but extremely fast algorithm called the Fast Fourier Transform (FFT). Calculating the DFT in this way is typically hundreds of times faster than other methods. Lynn (1993) states that the time taken to calculate the DFT of a signal with N values is proportional to N^2. This reduces to $N\log_2(N)$ when the FFT is used. However, the actual time depends on the computer hardware, software and the efficiency of the computer code. In general, the FFT of a sequence of real numbers is a sequence of complex numbers. A suitably scaled plot of the magnitude of the complex numbers, commonly known as a power spectrum, gives information about the frequency components in the signal (fig 5.1).

Fig 5.1: Performing a FFT on a time domain signal.
The signal on the left is a superposition of random noise with two sine waves (frequency 0.5Hz and 1.5Hz with amplitude 1 and 2 respectively). The signal was sampled at 6.25Hz.
The plot on the right is the power spectrum of the signal after performing a FFT using MATLAB (discussed in section 5.4.1).

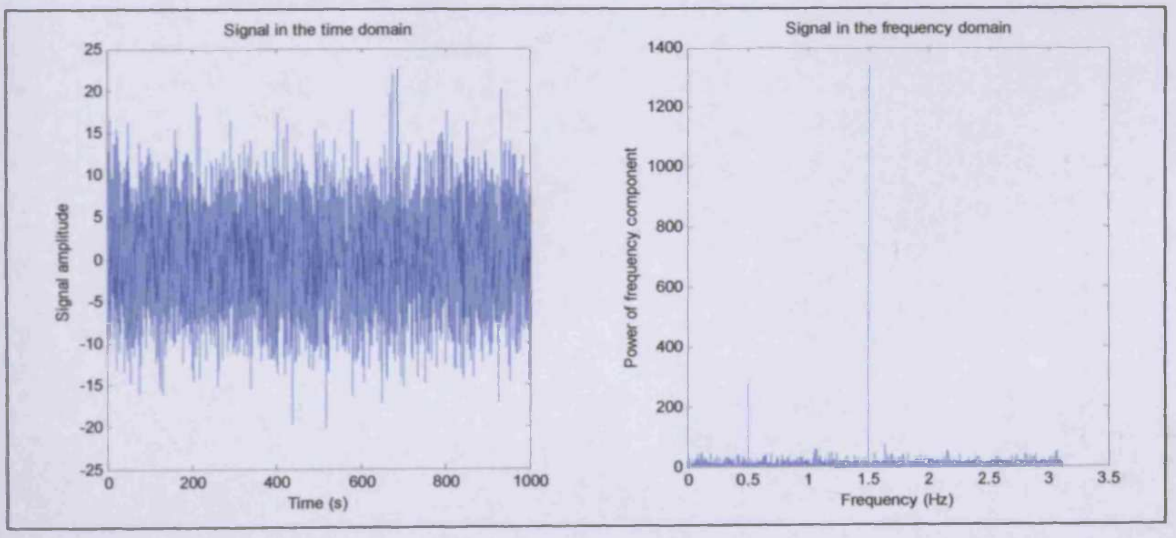

5.1.2 Limitations of Fourier analysis

Fourier analysis of a time domain signal gives information about the signal's frequency content. However, it does not say anything about the time when the frequency components exist in the signal. For this reason, the technique is only really suitable for analysis of stationary signals, i.e., where the frequency content does not change over time. For these signals, it is not necessary to know when frequencies appear and disappear in the time domain because they are always present. However, this situation is unlikely to exist when, e.g., biological signals are considered. Here, various frequency components may appear/disappear with time or the frequency of an individual process may change over the duration of the signal. For example, the frequency of cardiac pulsations may vary about some mean value. In such cases, Fourier analysis may only be suitable to identify the frequency content of the signal, giving limited information about what time in the signal the frequency components exist. However, some insight may be gained from the power spectrum of the signal. The power will depend on the "amount" of the frequency in the time domain. When a FFT is taken of the whole signal, any frequency that exists for only a short time will have a smaller power in the frequency domain compared to frequencies that last for a longer time, even if the amplitudes in the time domain are equal (fig 5.2). The power in the frequency domain may also depend on the whether the short-lived frequency exists at the central portions of the time domain data or at the extremes.

Fig 5.2: Non-stationary signals and the FFT.
The top plot is a superposition of three equal amplitude sine waves. Wave 1 exists between 0-20s. Wave 2 exists between 0-40s. Wave 3 exists throughout the entire signal (0-60s). The signal was sampled at 6.25Hz.
Wave 1: Amplitude=1, frequency=0.5Hz
Wave 2: Amplitude=1, frequency=1.5Hz
Wave 3: Amplitude=1, frequency=2.0Hz
The bottom plot is the power spectrum of the signal after performing a FFT using MATLAB (discussed in section 5.4.1).

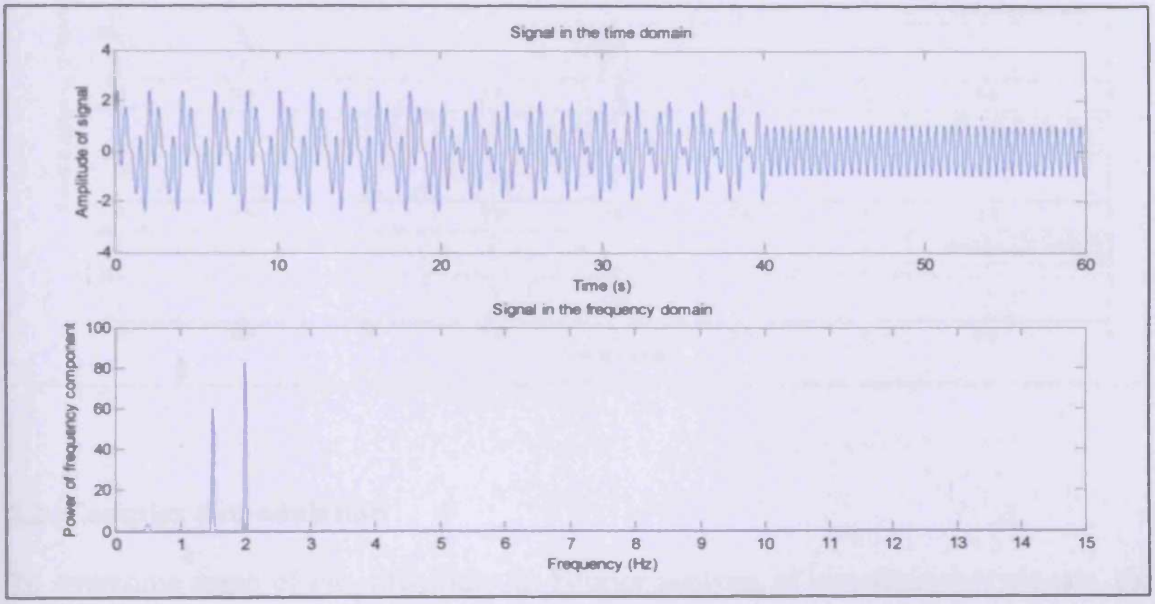

The problem of varying frequencies within a signal can be overcome to a certain extent by "windowing". The original time domain signal may be split into smaller segments (windows) and the FFT calculated for each segment. By observing how the FFT changes from one window to the next, it is possible to gain some information about the variation in frequency content over time. However, greater time resolution is at the expense of frequency resolution (fig 5.3). To obtain good frequency resolution, the FFT must be calculated over many wavelengths.

Fig 5.3: The change in the power spectrum of the signal in figure 5.2 when the FFT is calculated over consecutive 20s intervals.
(For clarity, the range of the vertical axis has been reduced in the bottom 3 plots.)

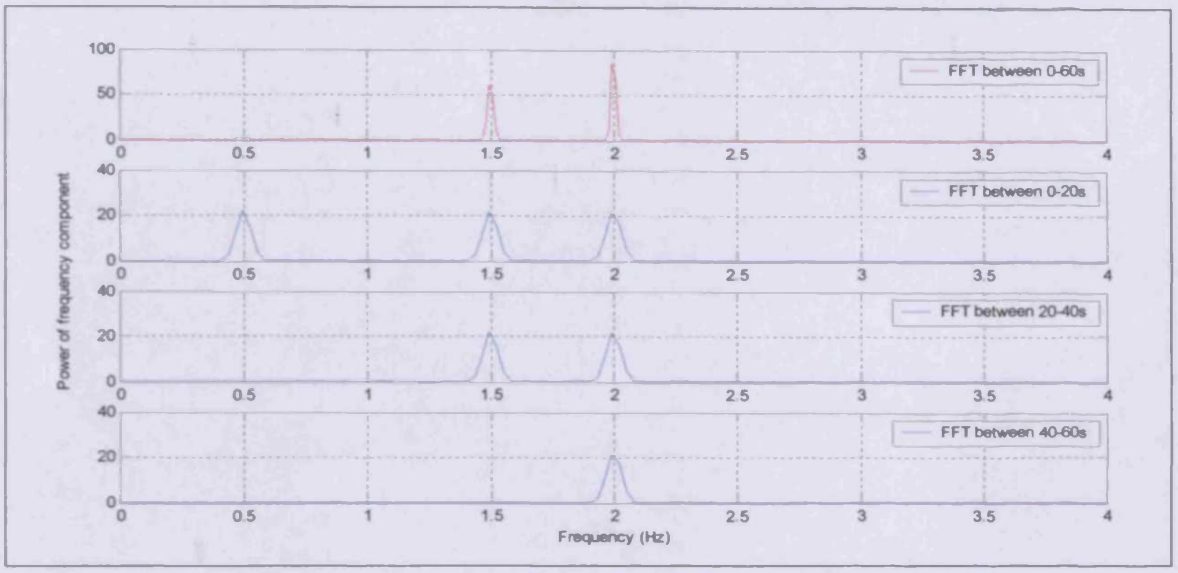

5.2 Complex demodulation

To overcome some of the difficulties in Fourier analysis of non-stationary signals, the technique of complex demodulation (CDM) was introduced. The method is similar to Fourier analysis but instead of analysing the whole spectra of frequencies, the technique focuses on a "single" frequency, which is chosen beforehand. The output from CDM is the amplitude and phase variation of the selected frequency as function of time.

However, as in Fourier analysis, there is always a trade-off between resolution in the time and frequency domain. Obtaining detailed information about amplitude and phase variations over time means that frequency resolution is compromised. One of the limitations of CDM is that it is not strictly possible to look at one specific frequency. Even though a single frequency is selected for analysis, the chosen frequency is isolated from the signal using an appropriate filter. As no filter can be made infinitely narrow, a band of frequencies is actually analysed in practice. The width of the filter dictates how close the results will be to describing the behaviour of the selected frequency.

5.2.1 The mathematics of CDM

Consider a real signal, X(t). (This may be the variation of light intensity over time as measured by DPPG.) The signal is likely to be composed of an amalgam of individual components oscillating at different frequencies, which may fluctuate in amplitude and phase. The purpose of CDM is to describe the temporal amplitude and phase variation of a selected frequency component of X(t).

The original signal, X(t), can be written as a superposition of its individual frequency components (cf. Fourier analysis above.). If x_t is the component of interest, with frequency f_s, and z_t represents all other frequency components of X(t), then the original signal may be written as:

$$X(t) = x_t+z_t = A_t\cos(\omega t+\phi_t) + z_t \qquad \text{Equation 5.1}$$

where: x_t ≡ component of X(t) with frequency f_s

z_t ≡ contribution to X(t) from all other frequency components other than x_t (may also contain a noise component)

A_t ≡ time varying amplitude of x_t

ϕ_t ≡ time varying phase of x_t

ω ≡ $2\pi f_s$

(Subscript t denotes a time varying component.)

Using the following trigonometric identities, the real signal can be written in terms of complex exponentials,

$$\exp(i\theta)=\cos(\theta)+i\sin(\theta) \qquad \text{and} \qquad \exp(-i\theta)=\cos(\theta)-i\sin(\theta)$$

gives,

$$\cos(\theta)=[\exp(i\theta)+\exp(-i\theta)]/2$$

Substituting for cos(θ) in equation 5.1 gives the complex form,

$$X(t)=A_t\{\exp[i(\omega t+\phi_t)]+\exp(-i[\omega t+\phi_t)]\}/2 + z_t \qquad \text{Equation 5.2}$$

The goal of CDM is to extract A_t and ϕ_t as these give the temporal amplitude and phase variations of x_t (the component of X(t) with frequency f_s).

In order to achieve this, equation 5.2 is firstly multiplied by $2\exp(-i\omega t)$,

$$Y(t)=2X(t).\exp(-i\omega t)$$

$$Y(t)=A_t\{\exp[i(\omega t+\phi_t)]+\exp(-i[\omega t+\phi_t)]\}\exp(-i\omega t) + 2z_t\exp(-i\omega t)$$

$$Y(t)=A_t[\exp(i\omega t+i\phi_t-i\omega t)+\exp(-i\omega t-i\phi_t-i\omega t)] + 2z_t\exp(-i\omega t)$$

$$Y(t)=A_t\exp(i\phi_t)+A_t\exp[-i(2\omega t+\phi_t)] + 2z_t\exp(-i\omega t) \qquad \text{Equation 5.3}$$

The multiplication converts the real signal, X(t), into a complex signal, Y(t), and has the effect of shifting the entire power spectrum of the signal by a magnitude of f_s in the negative direction.

This is illustrated in figure 5.4. In the power spectrum of the original, real signal (fig 5.4[a]) the component x_t is represented by the peaks R2 and R3*. An additional, higher frequency component is represented by R1 and R4. This component, together with the noise in the signal, is the term z_t in equation 5.1.

Figure 5.4[b] is the power spectrum of the complex signal formed by the multiplication of the real signal by $2\exp(-i\omega t)$. The frequency component at 0Hz (C3) is caused by the first term in equation 5.3. The frequency component, C2, is caused by the second term in equation 5.3. Together, these two components represent the shift of x_t, within the power spectrum, by $-f_s$ (from R2 and R3 in figure 5.4[a]). The third term in equation 5.3, if expanded, would show that the same effect happens for all other frequencies in the original signal, i.e., the corresponding frequency in the power spectrum is shifted by $-f_s$ (e.g., the frequency component represented by R1 and R4 in figure 5.4[a] appears to shift to the positions indicated by C1 and C4 in figure 5.4[b]).

* For a real signal, the frequency components in the negative region of its power spectrum are always a "mirror image" of those in the positive region. This is not the case for complex signals, for which the positive and negative frequencies are independent.

Fig 5.4: An example of the power spectrum of a real signal and the corresponding complex signal following multiplication by $2\exp(-i\omega t)$.
The complex signal looks like the original, real signal but shifted in the frequency domain.
(For clarity, the range of the vertical axis is different in the two plots.)

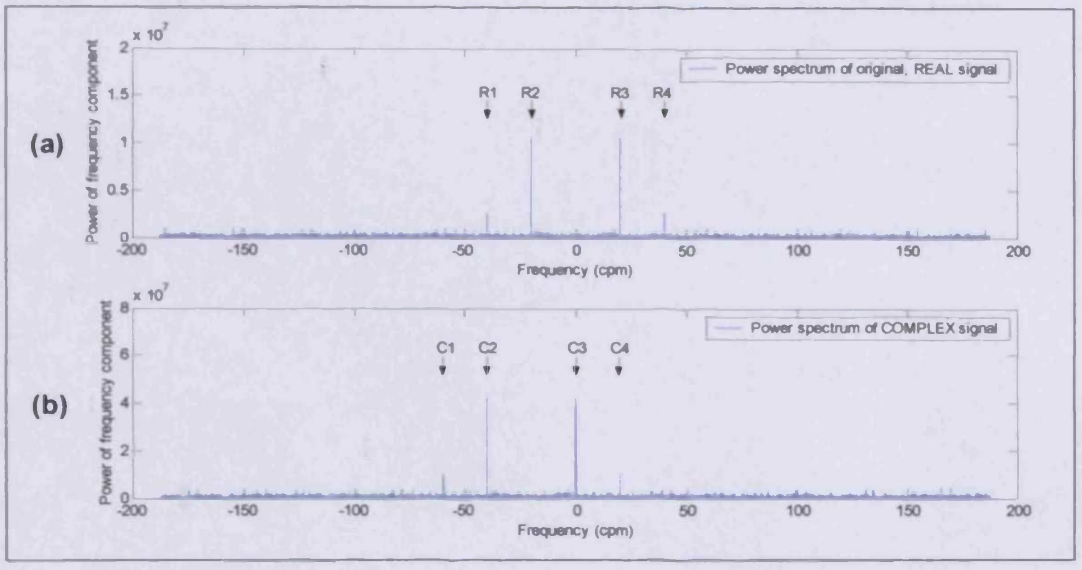

The aim of CDM is to extract A_t and ϕ_t. This can now be easily achieved via the complex signal (equation 5.3), where the first term contains all the required information. However, the contributions from all the other terms must first be removed.

This is achieved using a low pass filter and the knowledge that the whole power spectrum of X(t) is shifted such that the frequency of interest is now centred at 0Hz. A suitable low pass filter will remove all but a narrow band of frequencies centred on 0Hz. Provided the filter width is narrower than $2f_s$, the second term of equation 5.3 will be removed. If the filter is made even narrower, the majority of the components that make up z_t in equation 5.3 are also likely to be filtered out. Equation 5.3 then becomes,

$$Y(t) \approx A_t \exp(i\phi_t) \qquad \text{Equation 5.4}$$

The temporal amplitude and phase variations (A_t and ϕ_t) of the component of X(t) with frequency f_s can then be easily obtained in the usual way for complex numbers (e.g., see Appendix A).

The narrower the low pass filter is made, the closer A_t and ϕ_t will be to representing the temporal amplitude and phase variations of the selected frequency, f_s. However, the low pass filter cannot be made infinitely narrow and always has a finite width. Therefore, the filter width imposes a limitation on the effectiveness of CDM to analyse a single frequency when there are other "significant" frequencies nearby. Components of X(t) that have frequencies close to f_s may still remain in the narrow band of frequencies after filtering. Therefore, in practice, CDM can only provide an estimate of the amplitude and phase variation of x_t. The filtering process and the consequence of residual frequencies remaining after filtering is considered further in Appendix B.

5.3 Digital filters

A filter is a frequency selective device or process. On input of a signal, the filter transmits a defined range of frequencies and blocks others. Analogue filters act on continuous signals and are constructed from electrical components. Digital filters act on sampled signals and can be implemented using a PC and appropriate software. The performance of digital filters tends to be vastly superior to their analogue counterparts (Smith, 1999). Digital filters are used in this study to analyse the DPPG signals and, from this point onwards, the term filter will refer to digital filter.

Generally, filters may be classified as low pass, high pass, band pass or band stop depending on the range of frequencies passed and blocked (fig 5.5).

Fig 5.5: The idealised frequency responses of four different filter types.
The shaded areas indicate the frequencies passed by the filter.

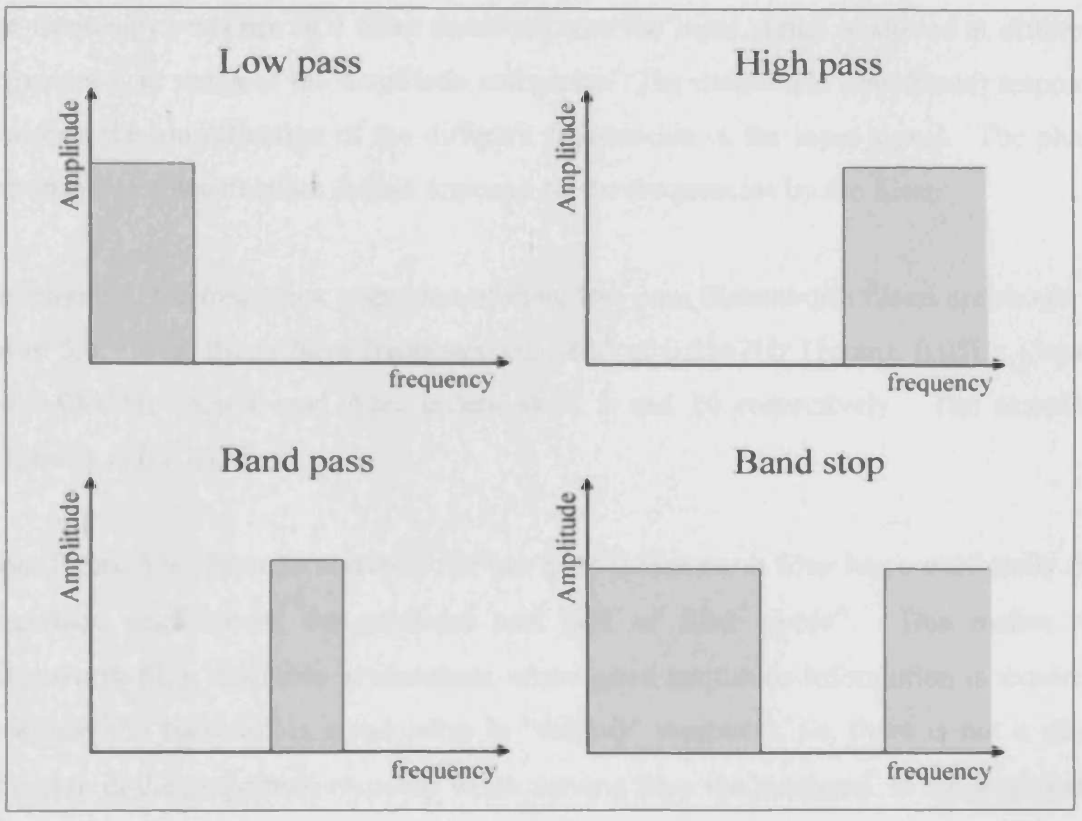

The ability of the filter to pass or block frequencies depends on its design. There are many different filter designs that can be used to implement the above processes, e.g., Butterworth, Chebyshev type I, Chebyshev type II, elliptic, Bessel etc. Each of these has advantages and disadvantages depending on their effectiveness to pass or block appropriate frequency bands and the disruptive influence the filter has on the input signal. These properties are described below, with particular reference to the low pass Butterworth filter since this type was chosen for the CDM analyses in this study.

5.3.1 Filters characteristics

The characteristics of a filter can be described in the frequency domain or the time domain. Each is considered below. There is always a trade-off in filter performance between both domains. Good performance in one results in poorer performance in the other.

5.3.1.1 The frequency domain (The frequency response)

The frequency response of a filter describes how the input signal is altered at different frequencies, in terms of the amplitude and phase. The magnitude (amplitude) response describes the amplification of the different frequencies in the input signal. The phase response describes the time delays imposed on the frequencies by the filter.

For example, the frequency responses of three low pass Butterworth filters are shown in figure 5.6. (The filters have frequency cut offs[§] of 0.0167Hz (1cpm), 0.05Hz (3cpm) and 0.0833Hz (5cpm) and filter orders of 3, 5 and 10 respectively. The sampling frequency is 6.25Hz.)

From figure 5.6, it can be seen that the low pass Butterworth filter has a maximally flat magnitude response in the passband and lack of filter ripple[♠]. This makes the Butterworth filter desirable in situations where good amplitude information is required. However, the trade off is a reduction in "roll-off" steepness, i.e. there is not a sharp reduction in the magnitude response when moving from the passband[•] to the stopband[♦]. (A negative magnitude response indicates a reduction in the amplitude of the filtered signal compared to the input signal.)

The phase response of a Butterworth filter is not constant. A time lag is introduced between the filter output and the original input signal (an example of this effect can be seen in figure 5.9). The phase delay between the input and output signal increases with increasing frequency, as shown in figure 5.6 (negative values indicate that the filtered signal lags behind the original input signal).

---

§ Cut off: The frequency at which the magnitude response is -3dB. (In a low pass filter, all frequencies below the cut off are said to be "passed by the filter".)

♠ Ripple: Undulations in the magnitude response of a filter.

• Passband: The range of frequencies passed by the filter.

♦ Stopband: The range of frequencies blocked by the filter.

Fig 5.6: The magnitude and phase response of three, low pass, Butterworth digital filters.
The bottom two plots show an enlarged view of the top two plots, corresponding to the green shaded area.

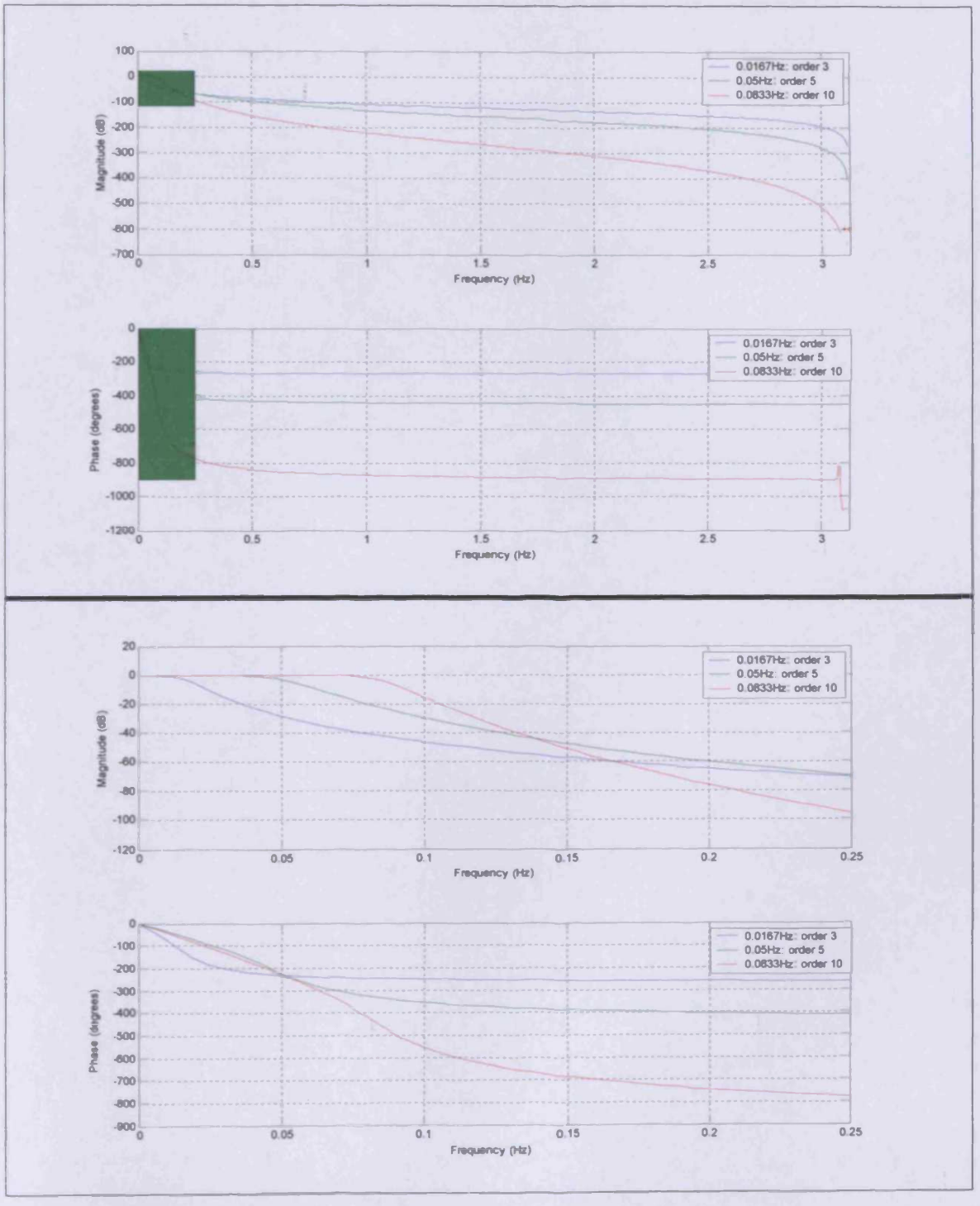

5.3.1.2 The time domain (The impulse response)

Application of a filter to a signal is accompanied by transient effects. It takes some time for the filtered signal to "settle" before a steady state is reached. This effect is sometimes called "ringing". The impulse response of the filter illustrates these transient effects. The impulse response is the output waveform when an unit impulse is applied to the filter (fig 5.7). For discrete signals, the unit impulse is defined as,

$$\delta[t] = \begin{cases} 1 & t = m \\ 0 & t \neq m \end{cases}$$

Fig 5.7: An example of an impulse response from a 5th order low pass Butterworth filter with cut off frequency 0.05Hz (sampling frequency = 6.25Hz).

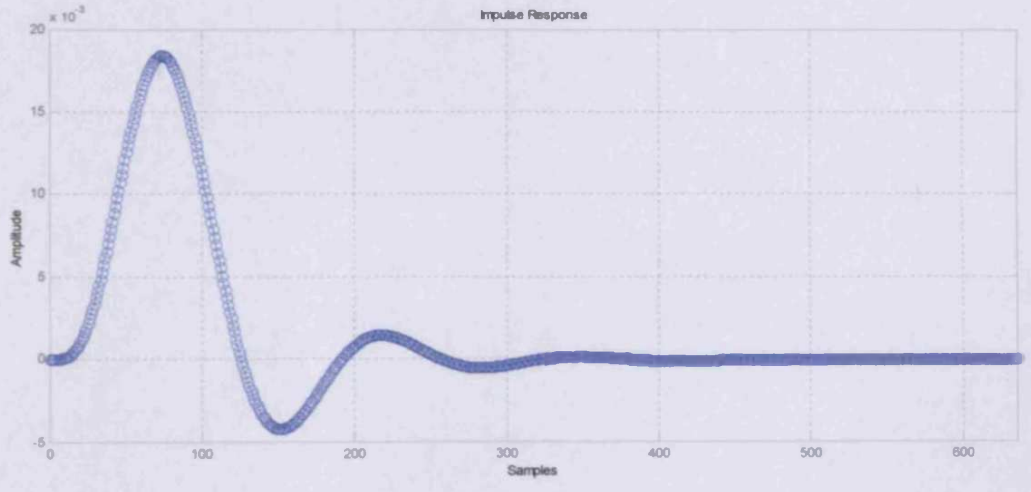

In the case of the Butterworth filter, the "ringing" continues indefinitely and for this reason the filter is called an infinite impulse response (IIR) filter. However, the impulse response amplitude decays exponentially so that, after a while, the effect becomes negligible. The period of significant transient ringing increases with decreasing filter passband and increasing filter order.

Another quantity used to define the performance of the filter is the overshoot. This is amount by which the filtered signal exceeds its steady-state output on its initial rise. Overshoot increases with increasing passband and the impulse response tends to the unit impulse as the filter width approaches the Nyquist frequency.

5.3.2 Summary of the characteristics of the low pass Butterworth filter

i. The filter's magnitude response is maximally flat and gives an ideal response of unity in the passband and zero in the stopband. There is no ripple in the passband.
ii. The magnitude response is smooth and decreases monotonically with frequency outside the passband.
iii. Around the cut-off frequency, the roll-off in the magnitude response just outside the passband is not as steep as other filters (e.g., Chebyshev). Steepness increases with filter order, but there is a trade-off with the length of filter "ringing".
iv. There are moderate amounts of phase distortion.
v. The impulse response shows a large overshoot and fairly long settling times.

The Butterworth filter was chosen for use in the CDM analyses because it was felt that the filter's smooth frequency response and lack of ripple in the passband justified having a more gradual "roll-off" than might have been provided by other filter types.

5.4 Use of MATLAB software

5.4.1 Implementation of Fourier analysis in MATLAB

MATLAB 6.1 (The MathWorks Inc, Natick, Massachusetts, USA) was used to implement Fourier analysis of the DPPG signals. The DFT is calculated using a FFT algorithm[§§]. Table 5.1 lists the lines of code that were written to implement the process. There then follows an explanation of each line of the code.

[§§] A detailed description of the FFT algorithm employed by MATLAB is beyond the scope of this discussion. For further information, the reader is referred to the documentation supplied with the software.

Table 5.1: Fourier analysis in MATLAB.

	MATLAB code
1	FFTdata=FFTdata-mean(FFTdata);
2	FFTdata = FFTdata .* hanning(N);
3	ft=fft(FFTdata,N);
4	P=ft.*conj(ft)/N;
5	f=samplefreq/N*(0:N/2);

Explanation of variables:

FFTdata:	The DPPG data do be analysed
N:	Number of samples in "FFTdata"
Samplefreq:	Frequency at which "FFTdata" is sampled (Hz)

Explanation of the lines of code in table 5.1:

(The line numbers below correspond to those in the table.)

1. The mean value of "FFTdata" is calculated. This mean value is then subtracted from each value in FFTdata. This process removes any large "d.c. offset" in the signal, preventing a large peak at the 0Hz frequency in the power spectrum.
2. "FFTdata" is multiplied by a N-point Hanning window. In the time domain, this procedure reduces the amplitude of "FFTdata" from the centre of the signal to zero at the start and the end. The result is an improved frequency resolution in the power spectrum of the DPPG data[**](fig 5.8).
3. Calculates the N-point DFT using a FFT algorithm. The result is placed in "ft".
4. Calculates the power spectrum of the signal by multiplying "ft" with its complex conjugate.
5. Calculates frequency values for plotting the power spectrum.

** A finite time sample of a signal may not include an integral number of oscillations of its frequency components. Performing a FFT on such data results in smearing (or leakage) in the frequency domain. Multiplication of the data by an appropriate window can reduce such effects (the effects may also be reduced by increasing the time that the data is sampled for). The window, in effect, forces the sampled data to look periodic and this provides better resolution in the frequency domain.

Fig 5.8: The effect of multiplying a time domain signal by a Hanning window.
The top three plots illustrate the process in the time domain.
The bottom two plots illustrate the process the frequency domain.
(Note: The range of the vertical axis in the power spectrum of the "Original signal x Hanning window" is reduced for clarity.)

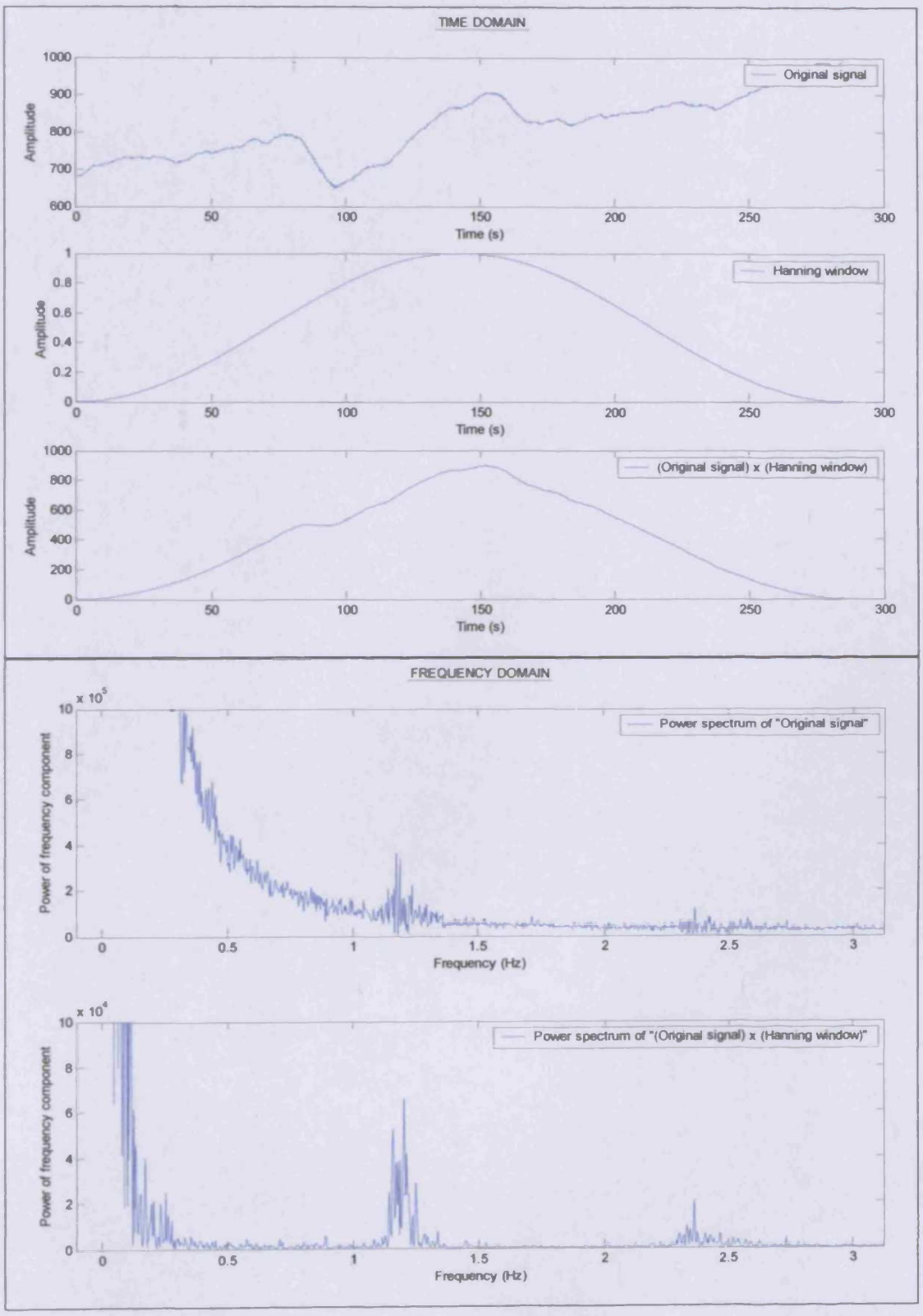

5.4.2 Implementation of CDM in MATLAB

MATLAB 6.1 was used to write the computer code for CDM. Table 5.2 lists the lines of code that were written to implement the process. The complete computer code used to analyse the DPPG data collected in the main study of this project (Chapter 9) is given in Appendix C.

Table 5.2: Implementation of CDM in MATLAB.

MATLAB code	**Explanation of the line of code**
cdm=2*data.*exp(-i*w*t);	Multiplication of the original data by 2exp(-iωt)
cdm_filt = filtfilt(B, A, cdm);	Application of the low pass filter
amplitude = abs(cdm_filt);	Calculation of temporal amplitude variation
phase = angle(cdm_filt);	Calculation of temporal phase variation
Explanation of variables: data: The real signal, X(t), to be analysed by CDM w: $2\pi f_s$, where f_s is the frequency chosen to be analysed by CDM i: Imaginary number where $i^2 = -1$ t: A list of the times when "data" was sampled A, B: Low pass filter coefficients	

Explanation of the MATLAB code:

A Butterworth filter was chosen for the CDM analysis. The low pass filter coefficients, "A" and "B", were calculated using the MATLAB function "butter",

[B,A] = butter(n,f_c,'low')

Where:

n: Filter order

f_c: Cut off frequency (i.e., the frequency at which the magnitude response is -3dB) as a fraction of the Nyquist frequency.

'low': Defines the filter as "low pass"

The MATLAB function "filtfilt" performs the low pass filtering. The function produces a zero phase shifted output, with double the filter order. Start-up and end transients are also minimised (fig 5.9).

The function works by filtering the input signal twice. The signal is filtered in the forward direction, the output from which is reversed and sent through the filter again. Finally, the output from the second filtering process is reversed and this gives the required filtered signal. Such "dual filtering" prevents phase differences that would otherwise be introduced in the filtering process (one pass filtering induces a time lag between the filter output and the original signal, as defined by the frequency response of the filter, e.g., figure 5.6).

Fig 5.9: Low pass filtering using the MATLAB "filtfilt" function.
The blue line represents a signal with frequency 2cpm.
The green line represents the output from the application of a low pass Butterworth filter with a 3cpm cut off.
The red line represents the output using a 3cpm low pass Butterworth filter, implemented using "filtfilt".

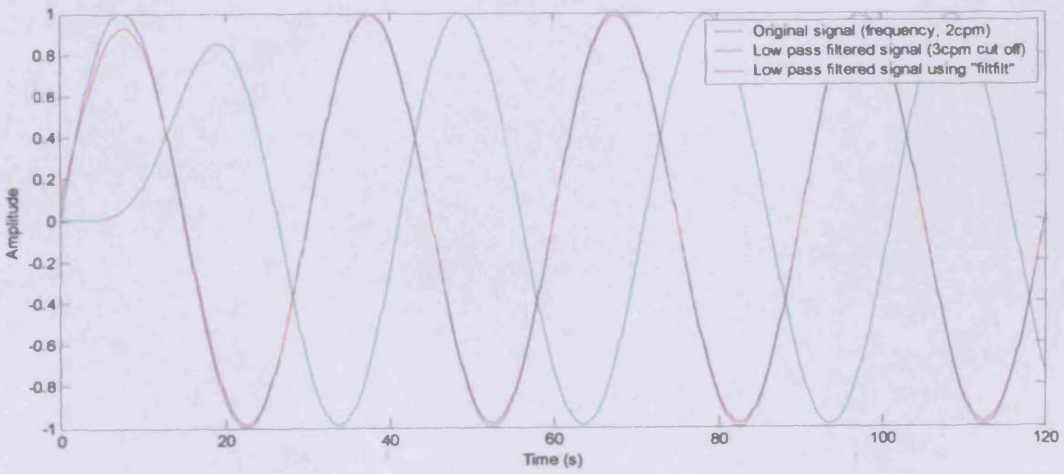

The "abs" function calculates the magnitude of a complex number (Appendix A). When applied to the filtered signal, the result is the temporal amplitude variation, A_t, of the chosen CDM frequency.

The "angle" function calculates the argument of a complex number (Appendix A), in radians, between the range $-\pi < \arg ument \leq \pi$. When applied to the filtered signal, the result is the temporal phase variation, ϕ_t, of the chosen CDM frequency.

In addition to the lines of code in table 5.2, the following lines were used to remove sections of the CDM outputs significantly affected by filter ringing:

```
amplitude( L-R+1 : L ) = [ ];
amplitude(1:R) = [ ];

phase( L-R+1 : L ) = [ ];
phase(1:R) = [ ];
```

"L" is the number of data in the "amplitude" or "phase" array. The first and last "R" values are removed from both the amplitude and phase results. "R" was defined by the length of data during which the absolute amplitude of the filter's impulse response was greater than 0.5% of the initial overshoot (this is described in greater detail in Appendix D). Since the signal is passed through the "filtfilt" function in the forward and reverse directions, a large transient effect occurs at the beginning and at the end of the filtered signal.

Chapter 6

Introduction to the Experimental Procedures

The initial objectives of this study were to investigate the current use of PPG in lower limb DVT diagnosis, to determine its value and improve the test. Current PPG tests for lower limb DVT require active patient participation involving a small exercise (see, e.g., section 4.1.1). This is usually dorsiflexions of the foot, which activates the muscle pump mechanism and reduces the volume of blood in the leg. PPG probes are usually placed on the leg, approximately 10cm above the medial malleolus, and monitor the amount of blood expelled from the microcirculation during the exercise (venous pump, VP) and the time taken for the microcirculation to recoup the loss when the exercise is stopped (refill time, RT).

However, there are problems with the use of an exercise test. Firstly, it is difficult to standardise. Although the patient is instructed to perform a fixed number of dorsiflexions within a certain time, the VP and RT may depend on the vigour at which the exercise is performed or the muscle mass in the leg, leading to inconsistent results. Also, the dorsiflexion test is unsuitable for those who find it difficult to move their foot at the required rate (e.g., confused, elderly patients) or those who cannot move their ankle (e.g., amputees or immobile patients). In addition, other conditions, such as venous insufficiency, may cause changes to VP and RT, masquerading as DVT (see section 4.1.1).

Initially, this study intended to concentrate on improving the existing method of the PPG test. Intermittent pneumatic compression of the calf was considered as a substitute for the dorsiflexion exercise to eliminate active patient participation. Standardising the magnitude of each compression, as well as the total number and duration, may have improved the reproducibility of the test and increased its scope to include the categories of patients excluded in the old system. However, the added complexity of setting up compression cuffs and a pneumatic pump would probably reduce the appeal of the test in a busy clinical setting and the portability of the apparatus would be compromised by the additional components.

The current, most useful role PPG has in the diagnosis of lower limb DVT is to provide a simple, quick screening test that can be used alongside more established tests such as venography or Doppler ultrasound. It was noted in section 2.5 that clinical diagnosis is unreliable and as many as 70%-90% of patients sent for objective testing are negative. A test that can be performed quickly and easily, with minimal training, could help to reduce the burden on relatively time consuming and expensive tests such as venography and Doppler ultrasound. Therefore, the PPG test not only needs to be reliable but also simple and quick to use, otherwise there will be little point in incorporating it into DVT diagnosis procedures.

Ultimately, it was decided to take a fresh approach to DVT diagnosis using PPG, looking in more detail at the PPG signal itself. The idea was to develop a test for DVT that not only eliminates patient movement but is also easy to set up, quick and straightforward to perform. The ideal test envisaged was one where a single PPG probe, placed on the surface of the skin, is able to detect a DVT while the patient remains relaxed and motionless in any position, supine or sitting. The test, as well as being non-invasive and non-intrusive, would be suitable for all categories of patients including the elderly or immobile patients or those on the operating table.
Therefore, the challenge was to look for a signature of DVT within the PPG signal itself. For example, this could be the result of any effect a DVT has on blood flow in the deep veins. If these disturbances are transmitted to the microcirculation, they may be detectable with PPG. On the other hand, the presence of DVT may be inferred by observing microcirculation changes that occur if any physiological processes within the body are affected by its presence in the lower limb (e.g., blood pressure regulation, cardiac rate due to changes in venous return etc.).

To look for possible indicators of DVT, the signal processing techniques described in Chapter 5 were used to analyse DPPG signals taken from resting patients, with and without DVT. The experimental protocol and data analyses used in the patient study are described in Chapter 9.
However, before any patients were recruited to take part in the study, preliminary investigations were conducted to investigate the feasibility of using DPPG in such a way. These investigations are outlined in Chapters 7 and 8. The goals were:

1. To analyse, in detail, the DPPG signal from the microcirculation of the skin and to understand what physiological processes contribute to its appearance.
DPPG data were taken from the legs of 5 normal volunteers while sitting still and relaxed. The power spectra of the DPPG data were analysed to look for characteristic frequency components. By reference to the literature, the frequency components were associated with physiological processes.

2. To determine whether there is a relationship between deep venous blood flow and microcirculation blood volume changes measured by DPPG.
Ultrasound imaging with colour Doppler analysis was used to look at the deep veins of the thigh directly beneath a custom-made compression cuff. Concurrently, DPPG was used on the leg and the foot to monitor the skin's microcirculation for any changes when the thigh was compressed.

Chapter 7

Preliminary Investigation 1

(Investigating the DPPG signal)

The DPPG device used in this study was originally intended to investigate venous function by generating emptying-refilling curves of the kind described in section 4.1.1. These are very low frequency, large amplitude changes in the DPPG signal corresponding to bulk movement of blood into and out of the limb during dorsiflexion exercises. However, by transferring the DPPG signals to a PC, it is possible to examine them in greater detail.

The investigation described in this chapter was carried out to obtain a general idea about the kind of information that can be extracted from the DPPG signal taken from the surface of the skin. There are many processes that directly influence blood flow through the microcirculation, including local vessel controls, leading to vasomotion, and central controls of blood pressure and temperature via the autonomic nervous system (described in section 1.5.2). There are also factors that indirectly affect microcirculation blood flow, e.g. cardiac pulsations and breathing.
The aim of this investigation was to determine whether the influence of these processes can be detected in DPPG signals taken from normal, resting volunteers. If so, it may then be possible to observe whether their effect on the DPPG signal is altered by the presence of a DVT in the leg. This may form the basis of a test for DVT. Even if this is not the case, there may still be other features, intrinsic to the DVT itself, which show up in the DPPG signal and act as a marker of the condition. Knowing the characteristics of the DPPG signal should help to identify such markers.

7.1 Experimental protocol

Ten minutes of DPPG data were taken from the legs of five normal (non-patient) volunteers while sitting still and relaxed on a chair (fig 7.1). The volunteers were selected from those in the Department of Medical Physics and Bioengineering at the University Hospital of Wales (UHW). None of the volunteers had any known vascular

disease in the lower limbs (although no tests were carried out to confirm this). The age range was 25 to 60 years old.

Fig 7.1: Diagram of experiment set-up.

The DPPG data were streamed straight to the PC in real-time by the method described in section 4.3.

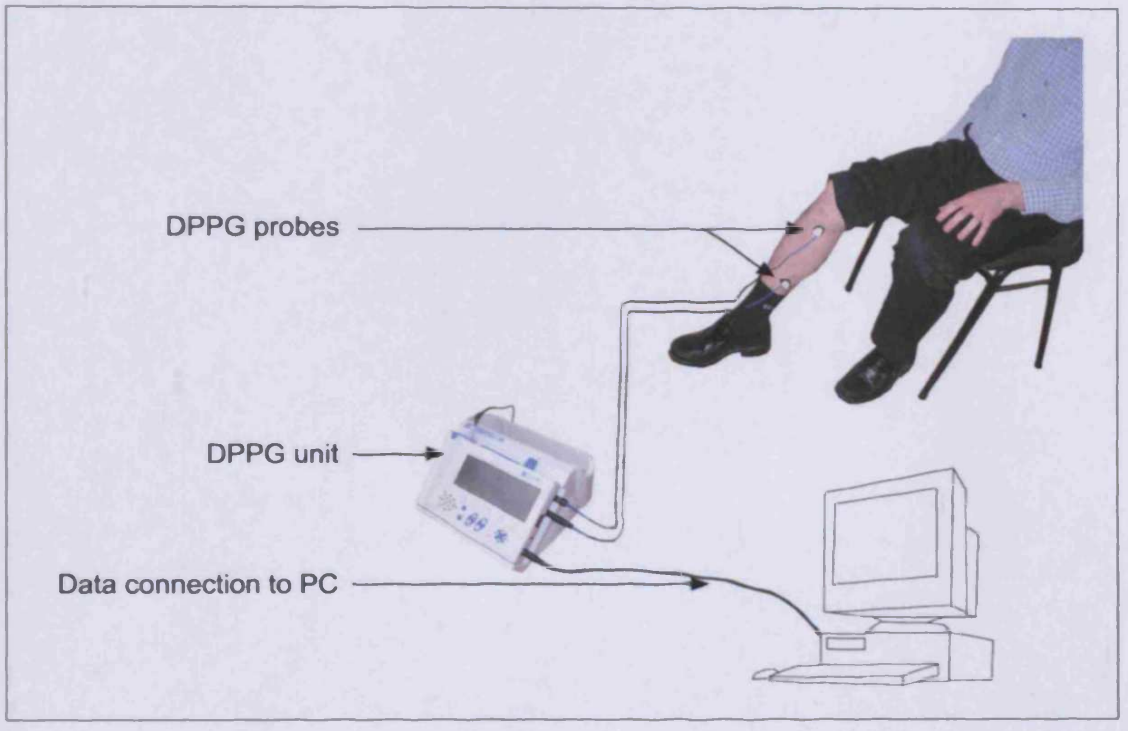

Two DPPG probes were attached to the right leg of each volunteer. (The right leg was arbitrarily chosen since there is no obvious reason why the haemodynamics should be any different to those in the left leg.) One DPPG probe was placed 10cm above the medial malleolus because this is the standard probe position for lower limb investigations using the DPPG device (see section 4.1.1). The other DPPG probe was placed on the medial aspect of the same leg, just below the level of the knee. This position was chosen to determine whether there is any difference in the DPPG signal taken from a different part of the leg. The probes were stuck to the leg using the standard double-sided sticky pads supplied by the manufacturer of the DPPG device.

Each volunteer was asked to assume the position they would adopt in a standard DPPG test, but not to perform any dorsiflexions of the foot. Ideally, this would involve sitting

on the chair with their upper body tilted back slightly and their feet placed flat on the floor such that the angle at the knee joint is approximately 120°. This position minimises disturbances in the blood flow by preventing crimping of the blood vessels, especially the veins, at the ankle, knee and hip level. However, the body position of the volunteers was not measured accurately. They were only asked to tilt their back slightly and increase the angle at the knee joint to slightly greater than 90°. Greater emphasis was placed on comfort and the ability to maintain a relaxed posture for 10 minutes, while the DPPG device was recording. This was considered more important than standardising body positions, since the discomfort that can be caused by trying to maintain an unnatural posture for 10 minutes may have induced unwelcome physiological effects (e.g., increased blood pressure, tensing of muscles etc.). These would have been undesirable complications to a test that sets out to investigate the physiological information contained in the DPPG signal from relaxed subjects.

7.2 Analysis of the DPPG data

The DPPG data collected from each volunteer are presented in Appendix E. In all cases the signals seem to be less than simple. Just by looking at the signals they seem to be composed of several superimposed frequencies (e.g., figure 7.2). There are very low frequency components with only a few oscillations per minute and also higher frequency components with periods ranging from a few seconds down to fractions of a second.

These overlying frequencies suggest that the DPPG signal may indeed be influenced by the physiological processes that control blood flow in the microcirculation. To investigate the frequency components in more detail, and attempt to associate them with a corresponding physiological process, Fourier analysis was used. For each subject, the whole of the collected data were used to calculate the power spectrum (excluding parts of the signal affected by calibration of the DPPG device). The reason for doing this was to obtain a general ideal about what frequencies are contained in the signal and whether there are any frequencies that dominate the power spectrum. Since the signals are likely to be non-stationary, Fourier analysis, in effect, gives an "average" result over the period that the data were collected and favours detection of frequencies that are predominant, i.e., last longest or have the largest amplitude (section 5.1). Analysing

numerous smaller sections of the data may have provided information about how the frequencies change with time but this has limitations with respect to frequency resolution. For the purpose of obtaining a general knowledge about the frequency content of the signal, it was considered to be more appropriate, in the first instance, to analyse the DPPG signal as a whole.

The power spectra obtained by doing this are shown in Appendix F. The results show predominant frequencies lying within specific bands. The origins of these oscillations are probably related to the processes controlling blood flow in the microcirculation. An attempt to associate the frequency components to their causes is presented below.

7.2.1 The frequency content of the DPPG signals

Just by looking at the power spectra of the DPPG signals (Appendix F) it seems that the predominant frequencies can be broadly split into 3 bands (see also fig 7.3).

High frequencies (>~40cpm): These frequencies, which are always clearly visible, are believed to be associated with cardiac pulsations within the arterioles of the microcirculation.

Low frequencies (<~10cpm): These frequencies tend to have the largest amplitude in the power spectra and are thought to be primarily associated with nervous system or local control of the microcirculation.

Mid range frequencies: Between the high and low frequency bands is a region where frequencies seem to appear at the breathing rate of the subject.

Each frequency band is discussed in greater detail below.

Fig 7.2: A DPPG signal taken from the surface of the skin.
(The signal is taken from volunteer 4.)

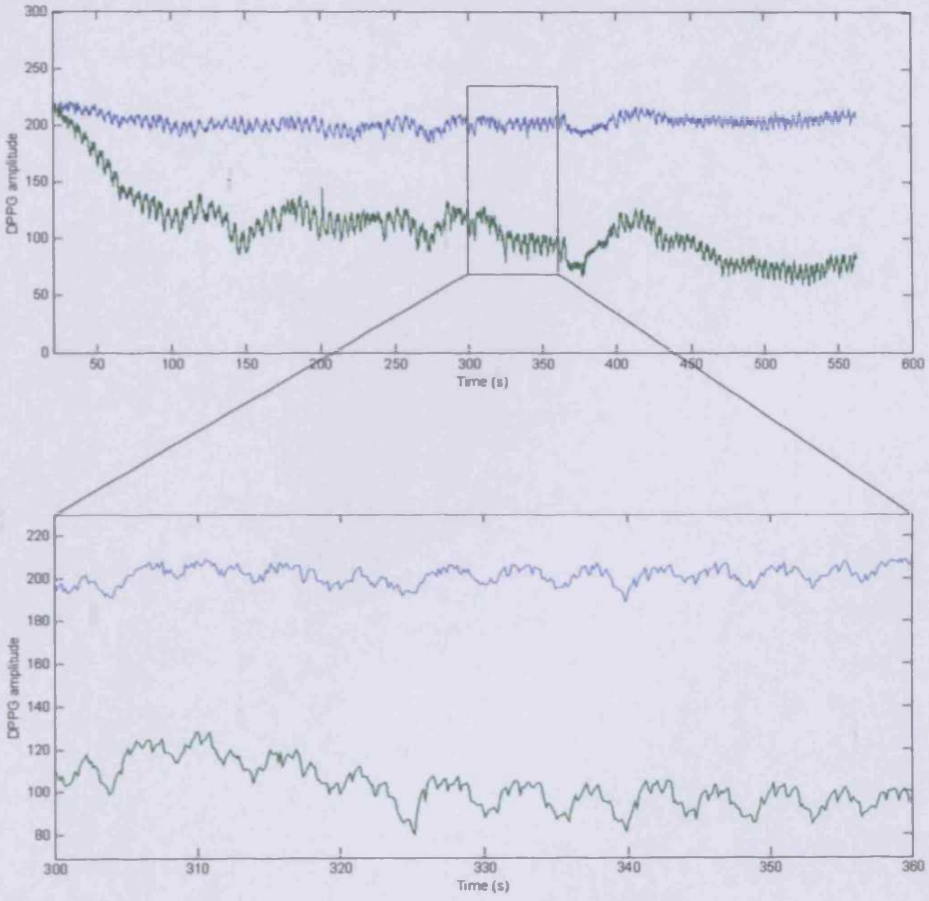

Fig 7.3: Power spectrum of the DPPG signal in figure 7.2.

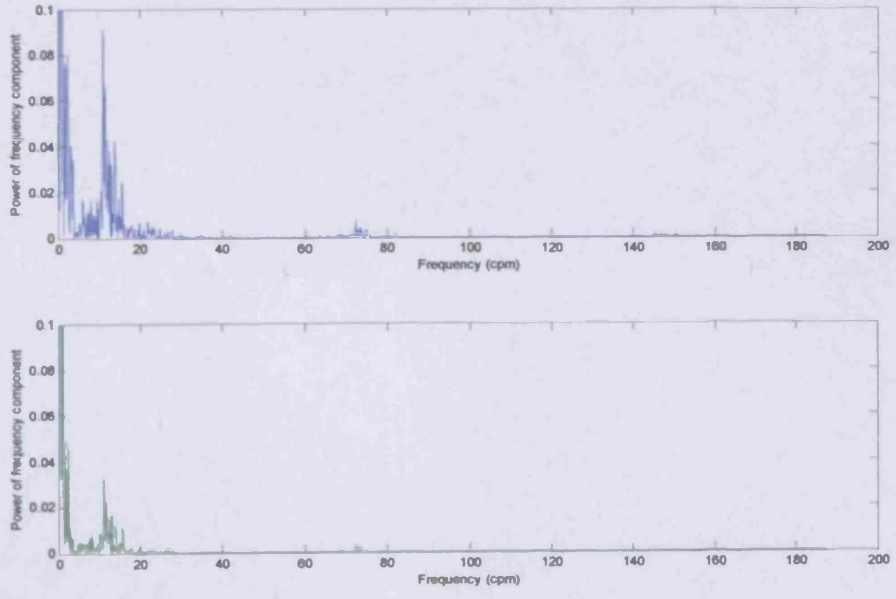

7.2.1.1 The high frequency band (>~40cpm)

Frequencies above 40cpm correspond to the rate of cardiac pulsations, with the fundamental cardiac frequency accompanied by higher harmonics. These microcirculation oscillations are believed to be the result of pressure variations in the arterioles, before significant damping occurs in the capillaries.

Studies have shown a high correlation between heart beats measured by PPG and ECG. For example, Olsson et al. (2000) found a high correlation coefficient (~0.993) between PPG and ECG cardiac pulses when investigating newborn infants. Also, Nitzan et al. (1999) state evidence for a high correlation (>0.98) between the fluctuations observed in cardiac signal periods measured with PPG and ECG.

7.2.1.2 The low frequency band (<~10cpm)

The low frequency band is defined here as the part of the power spectrum with frequencies less than approximately 10cpm. These oscillations are believed to be derived from both local and global controls of microcirculation blood flow.

Comparing the power spectra of the DPPG signals taken from the two different parts of the leg, it can be seen that peaks often occur in both spectra at the same frequency (albeit with different power) and these may be the result of global processes. However, there are also some low frequency peaks in the power spectra of the data taken from one part of the leg that do not appear in the other (e.g., around 4cpm in volunteer 1), which may be the result of some local influence on the microcirculation.

It is believed that the origin of the low frequencies can be attributed to sympathetic nervous system control and/or local vasomotion.

The sympathetic nervous system has a global effect on the body and is postulated to be the cause of the identical frequency components in the DPPG signals taken from different sites on the body, e.g., Bernardi et al. (1996), Nitzan et al. (1998), Nitzan et al. (1999). The oscillations may be attributed to Traube-Hering-Mayer waves, which are the result of oscillations in nervous activity. Here, high arterial pressure stimulates the baroreceptors, which inhibit the sympathetic nervous system and lowers the pressure. This, in turn, reduces the baroreceptor excitement causing arterial pressure to rise once

again and the cycle continues. The control mechanism oscillates due to a strong "feedback" and a delay in the response to the pressure variations. The period of these oscillations is typically 7-10s (Guyton, 2000).

The non-identical low frequency components in the DPPG signals from different locations may be explained by vasomotion, e.g., Nitzan et al. (1998). This cyclic opening and closing of the arterioles, metarterioles and the precapillary sphincters usually occurs at a rate of a few cycles per minute (Guyton, 2000). Vasomotion is caused by conditions local to the vessels and neurogenic control is not involved (see section 1.5.2.1).

Low frequency oscillations may also be caused by thermoregulatory controls (either local or global).

7.2.1.3 The "breathing frequency" band

Between the two abovementioned frequency bands is another region where frequencies stand out in the power spectra of the DPPG signals. These frequencies are clearly visible in 3 of the 5 power spectra in Appendix F (volunteer 1, 3 and 4) but not in the other two. Where they are visible, the peaks occur at the same frequency in the data from both positions on the leg, suggesting a single origin.

The frequencies are believed to correspond to the breathing frequency of the subject from which the signal was obtained. However, this could not be verified in this investigation because no independent measurement of the breathing frequency was made. Nevertheless, the link between breathing and the corresponding frequency in the DPPG signal can be demonstrated by having the subject hold their breath for a short time. During this period, the DPPG frequency is observed to disappear, only to reappear when breathing is resumed. Therefore, there is no doubt that this frequency component is caused by breathing. However, the route to its manifestation in the microcirculation still somewhat uncertain. There are two main thoughts regarding this.

The first is related to the phasic flow observed in the large veins during breathing. Variations in thoracic and abdominal pressure during inspiration and expiration cause phasic blood flow, which can be observed in the large veins of the lower limbs by, e.g., ultrasound examination with colour Doppler analysis (see section 1.3).

It is often postulated that the phasic blood flow in the large veins is somehow conveyed to the microcirculation through the small veins and venules (e.g., Dorlas and Nijboer, 1985). The blood volume changes then appear as the undulations in the PPG signal at the breathing frequency (Murray and Foster, 1996).

The second theory to explain blood volume changes in the microcirculation at the breathing frequency relates to the arterial side of the circulation. However, the effect is also related to the changes in venous return during breathing. Arterial blood pressure, heart rate and stroke volume have all been shown to vary with respiration (e.g., see Nilsson et al. (2003) or Guyton (2000)). Bernardi et al. (1996) find that the breathing fluctuations observed in PPG signals taken from the ear and the finger lag behind those in arterial blood pressure. Therefore, they suggest that the breathing component in PPG is, to a large extent, caused by passive transmission from the large arteries to the microcirculation.

Therefore, while it is agreed that frequencies around approximately 10-30cpm are related to breathing, the process (or processes) that causes their appearance in the microcirculation is still a matter for debate.

7.3 Comparison with a similar investigation of the microcirculation

Although it is appreciated that five subjects is not a large enough number for rigorous scientific analysis, the idea in this investigation was to develop a feel for what the DPPG signal looks like and to develop a basic understanding of what physiological information is contained in the signal. Similar investigations of microcirculation characteristics have been described by others throughout the literature and a comparison with the results of one of these studies is presented below.

Stefanovska et al. (1999) applied a wavelet analysis technique to laser Doppler signals taken from the skin to analyse the range of frequencies associated with microcirculation

blood flow*. Using this technique, they identified five characteristic oscillations that occur within specific frequency bands in the microcirculation. In addition, they attempted to associate the oscillations with appropriate physiological processes by reference to various sources in the literature. Their results, which are summarised in table 7.1, are similar to those found in this study using DPPG data. The cardiac and breathing frequency bands have been identified together with the very low frequency oscillations.

Table 7.1: Characteristic microcirculation frequencies and suggested origin. *(From Stefanovska et al., 1999.)*

Frequency band		**Suggested cause**
0.0095 - 0.02Hz	(0.57 - 1.2cpm)	Origin unclear.
0.02 - 0.06Hz	(1.2 - 3.6cpm)	Blood pressure regulation by neurogenic control of vessel diameter.
0.06 - 0.15Hz	(3.6 - 9.0cpm)	Blood pressure regulation by myogenic regulation of vessel diameter.
0.15 - 0.4Hz	(9.0 - 24cpm)	Breathing. Frequency correlates with measurements of lung movements during breathing.
0.4 - 1.6Hz	(24 - 96cpm)	Heart pump. Frequency correlates with ECG measurements.

7.4 Conclusions

Microcirculation blood volume changes, measured with DPPG, contain oscillations that occur within common frequency bands. The frequencies of the oscillations seem to be characteristic of the various physiological processes that control microcirculation blood flow. It is therefore conceivable that that the microcirculation may provide a window for non-invasive study of these physiological processes. For example, observing the low frequency band with DPPG may provide an insight into the functioning of the

* It must be remembered here that blood perfusion, measured by laser Doppler, is not the same as blood volume changes measured by PPG. Laser Doppler output is due to the Doppler shift of laser light as it interacts with moving structures within its path (mainly erythrocytes in the case of skin blood flow measurements). The output measure is proportional to the product of the local speed and concentration of the moving cells. However, PPG measures the absorption of infrared light by biological tissue. It is assumed that the variation of light intensity returning to the PPG detector is a result of changing blood volume in the region under investigation. Therefore, the PPG signal is proportional to the blood volume (see sections 3.3 and 3.4 for a more detailed discussion of the PPG signal).

sympathetic nervous system. The DPPG device may also be used to monitor breathing or cardiac function (section 3.6).

As a test for DVT, DPPG may be able to provide much more information than a simple refill time following a dorsiflexion exercise. The results of this investigation show that the DPPG signal is influenced by many different physiological processes, which can be investigated by simply placing a single probe on the surface of the skin. If any disease, such as DVT, influences these processes, it may be possible to detect its presence by observing a change in the DPPG signal.

Chapter 8

Preliminary Investigation 2

(Investigating the relationship between deep venous blood flow and microcirculation blood volume changes)

The purpose of this investigation was to explore whether disruption of the blood flow in the deep veins of the lower limbs causes microcirculation blood volume changes in the skin that can be detected with DPPG.

The femoral vein was compressed using a pneumatic compression cuff around the thigh. Changes in vessel diameter and blood flow were observed using ultrasound imaging with colour Doppler analysis. At the same time, microcirculation blood volume changes were monitored by DPPG probes placed on the skin of the leg and the foot.

To establish what happens to the deep veins directly beneath the applied pressure, it was necessary to scan through the compression cuff. This was not possible with conventional pneumatic cuffs because the layer of air between the cuff walls prevents ultrasound transmission. Therefore, before the investigation could be performed, a special compression cuff had to be designed and constructed. This is described below.

8.1 Design of the compression cuff

The most important requirement of the compression cuff was to have no air between the ultrasound probe and the leg. Several different designs were considered including one where the bladder of the cuff was expanded by filling it with water rather than air. However, this was found to be less than manageable, so it was decided to revert back to using air to inflate the cuff.

Two air filled cuff designs were considered. The first was constructed from a thin sheet of PVC material that was wrapped around the thigh. An inflatable bladder, attached across the width of one of the ends, provided asymmetric compression. The cuff was designed for the bladder to be positioned between the leg and the non-inflatable layer (fig 8.1). Inflation of the bladder caused compression by pulling the non-inflated

section taut. Velcro strips along the cuff prevented unravelling when the bladder was inflated.

Fig 8.1: Asymmetric compression cuff design.

The cuff wraps around the thigh and over the inflatable bladder. The bladder is inflated using a mechanical air pump, which is connected with a plastic tube. A standard ultrasound scan can be performed through the thin, non-inflated region.

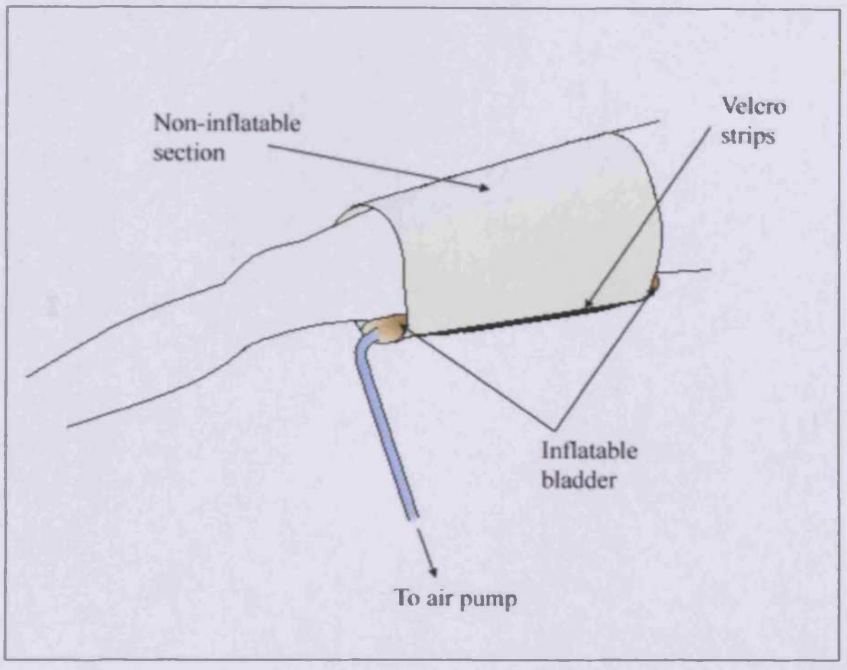

Initial tests using the asymmetric compression design found that the cuff was ineffective at compressing the deep veins of the thigh. Ultrasound investigations with Doppler analysis showed substantial blood flow through the femoral vein directly below the cuff even when the gauge on the air pump indicated that more than 100mmHg pressure was applied. Since venous pressure in the lower limbs is normally much less than this when a person rests supine (e.g., Guyton, 2000) there was uncertainty about the ability of this cuff design to provide effective compression of the deep veins in the thigh.

Therefore, an alternative cuff was constructed that was designed to apply circumferentially symmetric compression to the thigh. The cuff, taking the form of a tube, slips up the leg and over the thigh in one piece (fig 8.2). The cuff was constructed to the correct size and shape to fit one person so that it would form a well fitting cover

around the thigh, when not inflated, without exerting any compression. The cuff is comprised of two connected layers. The inner layer is an inflatable bladder. The outer layer is made from a non-stretching synthetic material that prevents outward expansion of the cuff when the bladder is inflated. Therefore, all the air pressure in the bladder is used to compress the leg. The only part of the cuff that does not inflate is a small window of thin PVC material, approximately 5cm in diameter, on the side of the cuff. When the cuff is inflated, this window lies flat against the thigh and allows an ultrasound investigation of the veins directly below.

Fig 8.2: Symmetric compression cuff design.

A standard ultrasound scan can be performed through the plastic window.

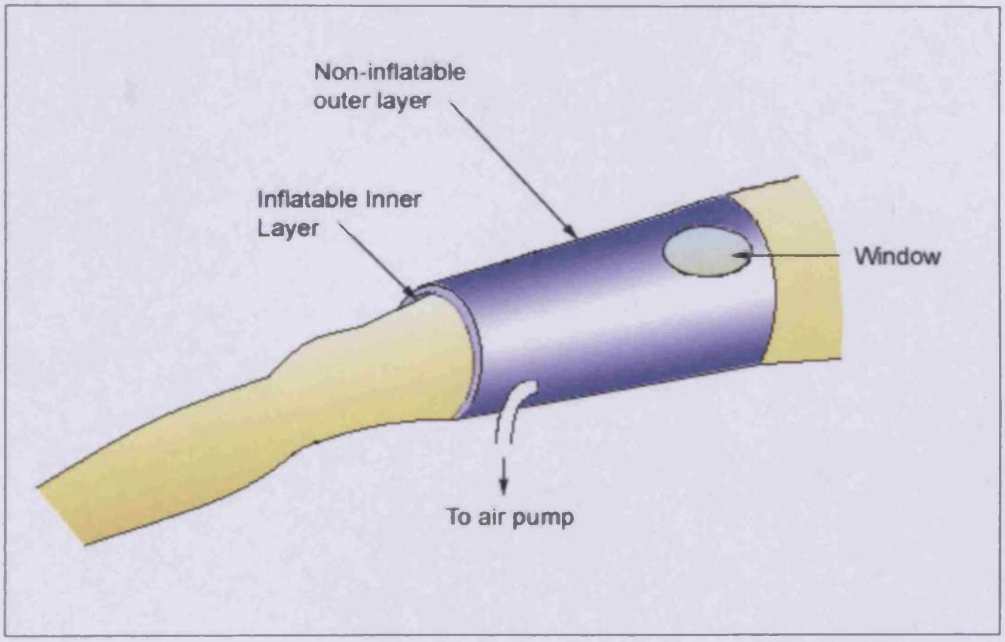

Initial tests using this cuff design found it to be much more effective at compressing the thigh than the asymmetric compression design. Ultrasound imaging through the window of the cuff showed collapse of the femoral vein when the cuff was inflated to only 30mmHg (the effect of the compression on deep venous blood flow in the thigh is described in greater detail below). Therefore, it was decided that the symmetric compression cuff design was the most appropriate to use in this investigation.

8.2 Experimental protocol for the thigh compression investigation

The investigation was carried out according to the protocol described below. The subject was a 24 year old male from the Department of Medical Physics and Bioengineering at the UHW with no known vascular disease in the lower limbs. Ethical approval for the investigation was provided by permission already granted to the department for a previous study by Morris (2000).

Fig 8.3: Diagram of experiment set-up.

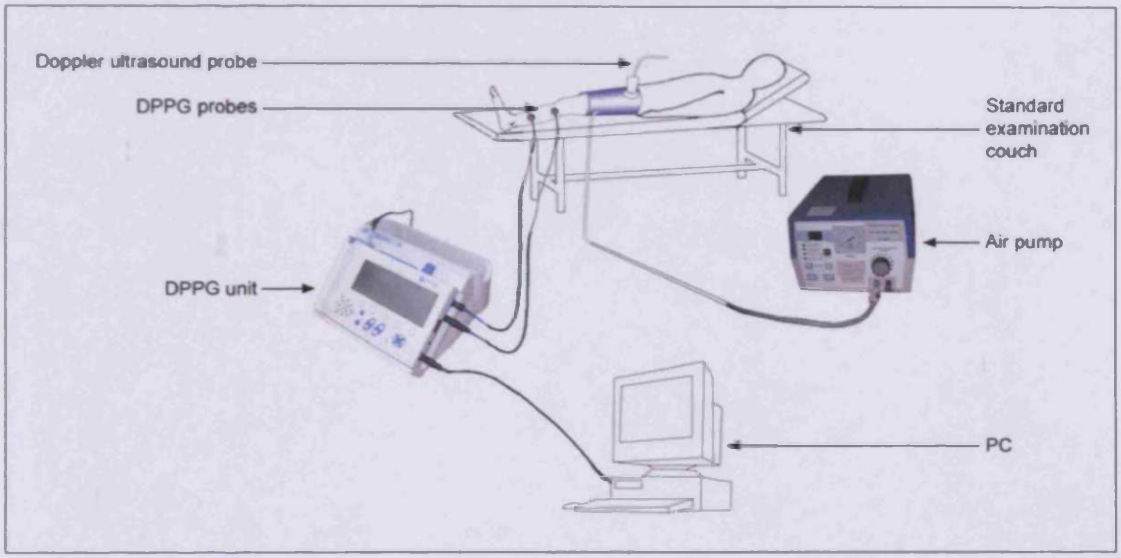

- The subject was asked to remove their shoes and trousers and to lay relaxed and motionless in a supine position on a standard examination couch (fig 8.3).
- The cuff was positioned over the right thigh and attached to an air pump*, but not inflated. (There was no particular reason why the right limb was chosen in preference to the left limb, other than consistency with preliminary investigation 1 (PI-1) and ease of performing the ultrasound investigation because the right limb was nearer to the operator when the subject was lying on the examination couch.)
- Two DPPG probes were attached to the medial aspect of the ipsilateral leg using the standard double-sided sticky pads provided with the DPPG equipment. One was

* The air pump used was the Huntleigh Flowpac (Huntleigh Technology PLC, Luton, UK), which had been modified to allow sustained inflation for up to 9½ minutes. For further information about this pump, see Morris (2000).

positioned 10cm above the medial malleolus (the standard DPPG test position) and the other was positioned just below the knee joint.

The exact location of the DPPG probes was not considered critical because the aim of the investigation was only to determine if compression of the deep veins affects the DPPG signal in some way. However, one probe was intentionally placed closer to the compression cuff than the other in order to gain some idea about whether the distance between the probe and the compression cuff has any influence on the DPPG signal.

- Before any measurements were taken, the subject relaxed for five minutes. This was necessary to allow the circulation to stabilise, which not only permits collection of data in the resting state but also expedites the DPPG calibration procedure.
- The DPPG device was then set running. After a period of self-calibration, which usually takes less than 30s, the DPPG device automatically starts recording.
- Following DPPG calibration, the data logger on the PC was started and the DPPG data were streamed straight to the PC in real time via a serial connection (described in section 4.3).
- The ultrasound probe was placed against the window of the cuff and its orientation adjusted until a good image of the femoral vein was observed on the viewing screen. Since the author had no previous experience in conducting ultrasound investigations, this procedure was performed by an experienced operator within the department of Medical Physics and Bioengineering.

Ultrasound imaging (with colour Doppler analysis) and DPPG recordings were made continuously throughout the procedure described below. All ultrasound images and blood flow measurements were recorded on video tape and the DPPG data were saved on the PC.

- After a period of initial recording, without cuff inflation, pressure in the cuff was increased to 30mmHg[♦] and maintained for 9½ minutes (which was the maximum

[♦] The cuff inflation pressure is set on the air pump by rotating a dial (possible error, ±2mmHg). It takes the air pump approximately 1.5s to reach 30mmHg pressure, 2s to reach 45mmHg pressure and similar times to deflate to 0mmHg (Morris, 2000).

inflation time provided by the pump) or until a steady blood flow and DPPG signal was observed.

- The cuff was then deflated and transition back to the normal, resting state was observed by ultrasound and DPPG.
- The same procedure was repeated using 45mmHg compression pressure.

8.3 Results of the thigh compression investigation

The DPPG data recorded on the PC was compared with the video taped ultrasound examination to look for a connection between microcirculation blood volume and deep venous blood flow changes during the thigh compression. (Since blood pressure in the arteries is normally greater than 60mmHg (section 1.2), it was assumed that thigh compression at 30mmHg or 45mmHg would not have a great effect on arterial inflow.)

The DPPG data acquired during the 30mmHg compression and 45mmHg compression are displayed in figure 8.4.

Fig 8.4: DPPG amplitude versus time during application of 30mmHg (top plot) and 45mmHg (bottom plot) compression pressure to the thigh.
The red line represents data from the DPPG probe placed just below the knee.
The blue line represents data from the DPPG probe placed 10cm above the medial malleolus.

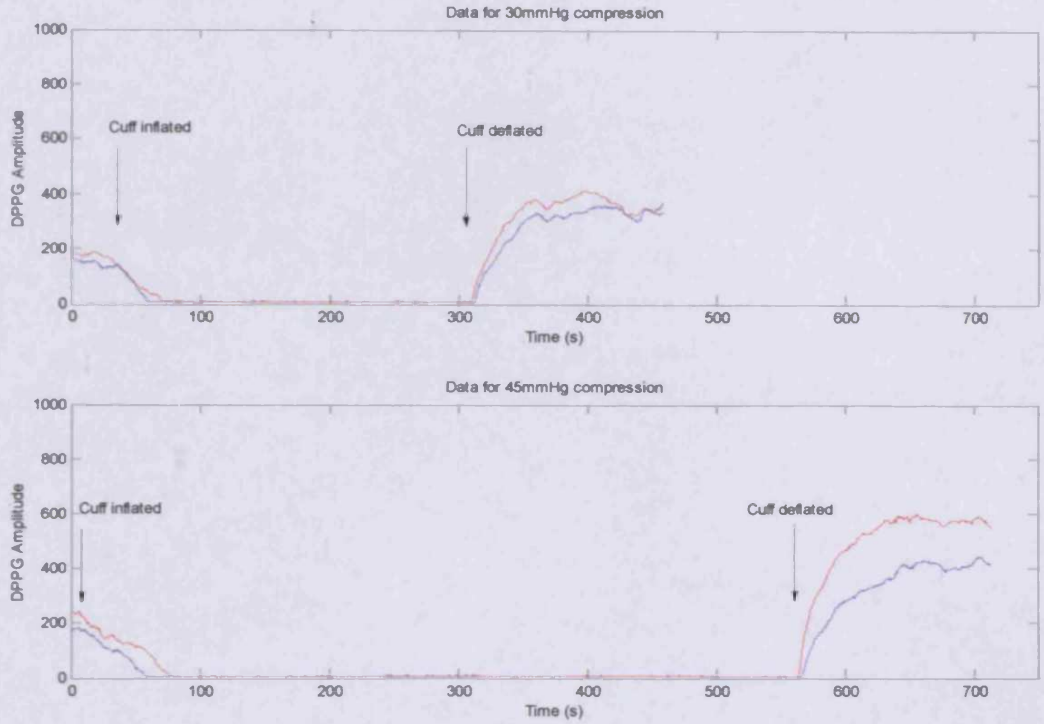

Before compression:

Ultrasound with colour Doppler analysis showed blood flow through the deep femoral vein to be in phase with breathing. A peak velocity of approximately 20cm s^{-1} was observed. The DPPG signals from the microcirculation were similar to those recorded in PI-1 and similar to what would be expected in the normal resting state, i.e. a superposition of components at different frequencies with no abrupt changes in DPPG amplitude.

During compression:

30mmHg:

When the cuff was inflated to 30mmHg, ultrasound imaging showed that the femoral vein initially collapsed. The vessel became totally occluded and blood flow through the

vein ceased. This was expected since physiology theory predicts that venous blood pressure in the lower limbs of a supine person is normally less than 30mmHg (section 1.2).

Thigh compression was followed by a decrease in the DPPG signal, indicating an increasing blood volume in the microcirculation of skin. This was assumed to be caused by damming of venous blood distal to the compression of the femoral vein (and all other veins under the cuff) since the occlusion prevents the blood from flowing past the cuff. The decrease in DPPG amplitude occurred almost immediately after thigh compression was applied and appeared to happen first in the data taken from the probe placed just below the knee, although it was difficult to tell.

A short while after the cuff was inflated (approximately 30 seconds) Doppler measurements showed blood flow beginning to reappear through the compressed vein. However, instead of the phasic flow observed before compression, the flow was continuous with a velocity of approximately 20cm s^{-1}. Around 2min later, the blood velocity began to increase again until a steady 50cm s^{-1} was reached. The re-emergence of flow was assumed to be a result of pressure building up in the dam of blood distal to the compressed vein segment. As the pressure rises, it becomes sufficient to counteract the external pressure acting on the vein and squeezes blood through the lumen. At this point, equilibrium is established between arterial inflow and venous outflow, which prevents the continual accumulation of blood in the limb.

Ultrasound imaging during the time when the flow was continuous seemed to show the diameter of the femoral vein to be smaller than its pre-compression size. However, it was not always easy to see the outline of the vein, even though Doppler analysis could still measure the blood flow. Throughout this period, it was impossible to determine what was happening to the DPPG signal because the amplitude had fallen below the lowest value that could be recorded with the instrument. However, the fact that the DPPG signal did not reappear suggests that there was still a greater microcirculation blood volume compared to before compression.

45mmHg:

Results for 45mmHg compression were similar to those for 30mmHg. Following inflation of the compression cuff, there was an almost immediate decrease in the DPPG signal, indicating an increased microcirculation blood volume. Ultrasound and Doppler

analysis showed initial collapse of the femoral vein and cessation of venous blood flow. Approximately 2 minutes after thigh compression was applied, blood flow was again observed in the vein. The flow was continuous with a velocity of approximately 30cm s^{-1}. As with the 30mmHg compression, the flow remained continuous but the velocity varied a little throughout the duration of the recording. The vein diameter seemed to be reduced compared to before compression. The amplitude of the DPPG signal was outside the instrument's measurement range for most part of the compression period.

After compression:

When the cuff was deflated and the compression pressure removed from the thigh, Doppler measurements showed an initial, large gush of blood through the femoral vein. Within one minute, the venous blood flow returned to its pre-compression state, i.e., phasic with breathing and a peak velocity of approximately 20cm s^{-1}. The initial gush of blood was assumed to be due to the sudden release of the pool of blood accumulated behind the vein during the compression.

There was an increase in the DPPG signal from both probes as the cuff pressure was removed, indicating decreasing microcirculation blood volume. Eventually the DPPG amplitude stopped increasing but the resting level following compression was greater than that before compression. This may have been the consequence of an overly large venous flow when the compression was removed as the body tries to establish a new resting level for blood flow out of the limb.

8.4 Further compression investigations following a modification to the DPPG device

The initial investigations, described above, showed clear changes in the DPPG signal as the thigh was compressed and when the compression pressure was removed. However, a major problem was that the DPPG signals always went off the bottom of the display screen and out of the measurement range not long after the compression was applied. Therefore, changes in the signals could not be observed throughout the entire duration of compression. This was a consequence of the DPPG self-calibration procedure and the finite measurement range of the instrument, due to limitations of the ADC (described in section 4.3.1.1). Self-calibration adjusted the IR intensity emitted onto the

skin's surface so that the recorded DPPG signal was close to the lower end of the possible measurement range at the start of each investigation. This was necessary for what the instrument was initially designed to do, i.e., to generate an emptying-refilling curve during dorsiflexions of the foot (section 4.1.1). Since the dorsiflexions cause an increase in the DPPG signal, due to a decrease in microcirculation blood volume, the starting DPPG amplitude must be quite low to accommodate a large increase without going out of the measurement range.

To correct this problem, the manufacturers were asked to make a modification to the software running the device so that the recorded DPPG signal was set to the centre of the measurement range during self-calibration. As a result of this, it was hoped that any large changes in the DPPG signal could be followed.

Therefore, the compression experiment described above was repeated using the modified DPPG device. However, this time, the DPPG probes were placed on the sole of each foot, rather than on the leg. This reason for doing this was to investigate whether microcirculation changes during thigh compression could be detected at probe locations as far away as the foot. Also, it was interesting to investigate whether signals taken from the non-compressed limb showed any changes during compression of the contralateral limb. The DPPG signals recorded during the investigation are shown in figure 8.5.

Fig 8.5: DPPG amplitude versus time during application of 30mmHg and 45mmHg compression pressure to the thigh.

The green line represents data from the DPPG probe placed on the sole of the foot of the limb ***with*** *the compression cuff.*
The blue line represents data from the DPPG probe placed on the sole of the foot of the limb ***without*** *the compression cuff.*

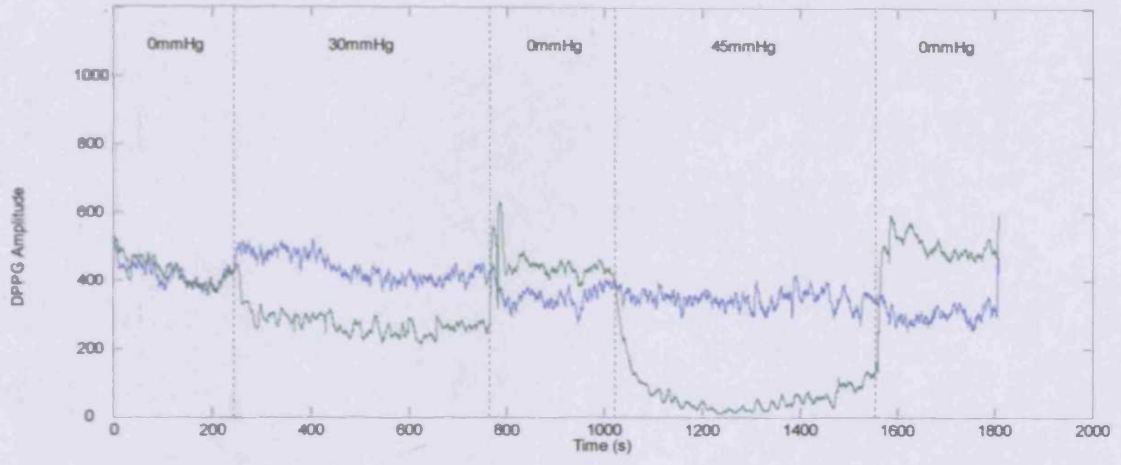

Before considering what happens to the DPPG signals during compression, it is interesting to note that, overall, the DPPG amplitude fluctuations seem to be much more pronounced in these results (fig 8.5) than in the previous set (fig 8.4). The reason for this may be a greater number of microcirculation vessels in the feet compared to the leg. For example, it is known that the feet, hands and ears have more AV anastomoses than other parts of the body (section 1.5.1). More blood vessels in the measurement volume leads to larger blood volume variations and greater IR absorption.

From figure 8.5 it can be seen that the modified DPPG device provides additional information about what happens to the DPPG signal during compression. The DPPG signal does not move out of the measurement range at any time during which the compression pressure is applied. Therefore, DPPG changes can be followed throughout 30mmHg and 45mmHg compression periods.

During thigh compression, large changes in the DPPG amplitude do not occur in the signal taken from the non-compressed limb. The signal remains at a relatively constant level even when compression is applied to the contralateral limb.

However, when considering the DPPG data taken from the limb with the compression cuff attached, significant changes can be seen when the thigh is compressed. In agreement with the observations made before the DPPG device was modified, there is an immediate reduction in DPPG amplitude when compression begins and the signal remains at a lower amplitude throughout the compression period. When the compression is stopped, the signal rises rapidly and overshoots the initial resting level. The resting level following the 45mmHg compression is slightly larger than the resting level following the 30mmHg compression (when considering both the mean and median DPPG amplitude over each of the three non-compressed periods. Mean values are 425.5, 436.2 and 501.2. Median values are 425, 435 and 491 for the consecutive non-compressed periods).

The appearance of the DPPG data taken from the limb with the cuff attached seems to change when the cuff is inflated. During the periods when compression is applied, the data appears to be 'smoother' than during the periods of no compression. It was thought that this could be due to a change in the frequency content of the signal. Therefore, to investigate this further, the power spectra of the data were considered. The power spectra of the signals, during the various stages of compression, are shown in figure 8.6 and figure 8.7.

Fig 8.6: Power spectra of sections of the DPPG data taken from the limb ***with*** the cuff, during the various stages of compression.

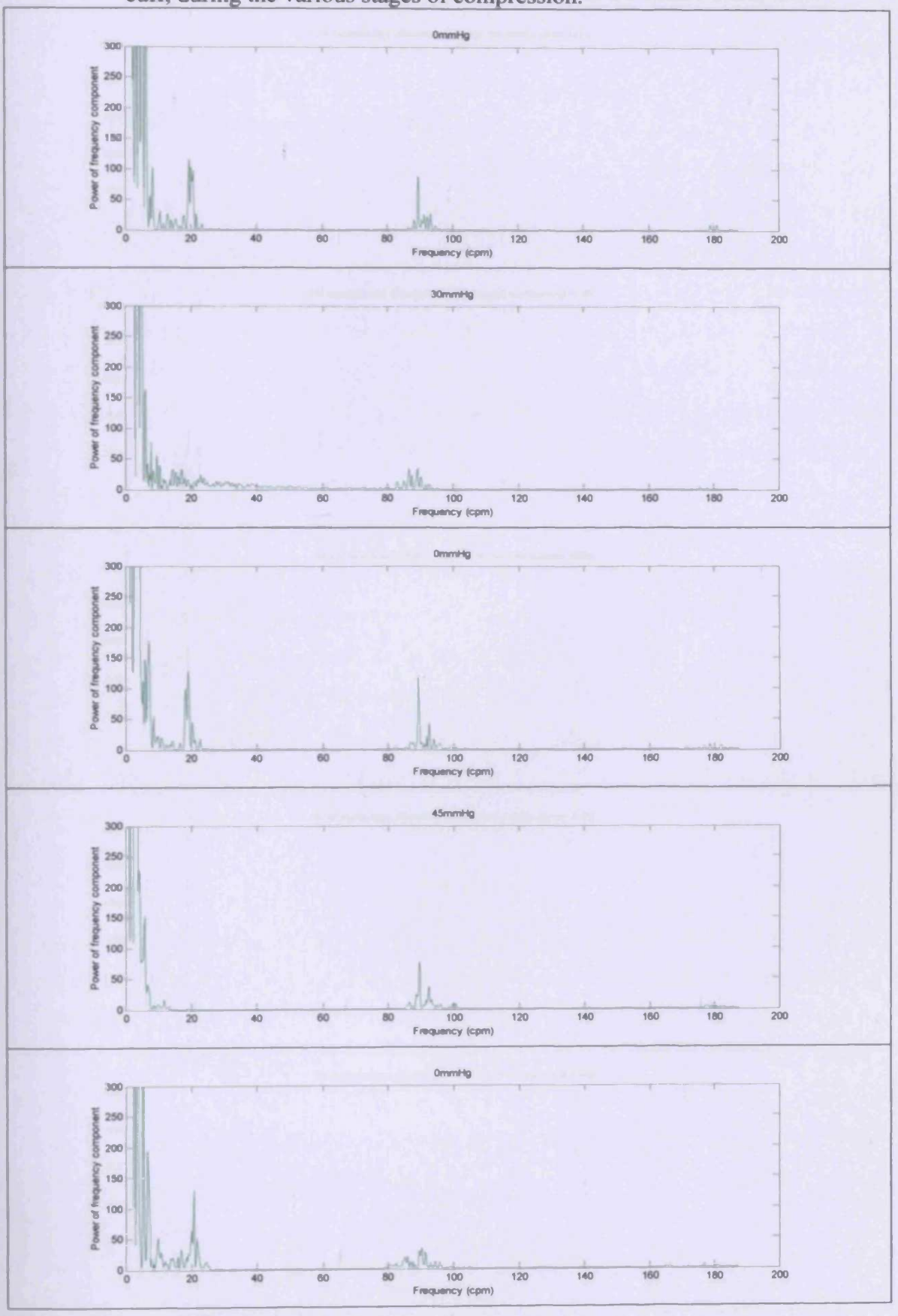

Fig 8.7: Power spectra of sections of the DPPG data taken from the limb ***without*** the cuff, during the various stages of compression of the contralateral limb.

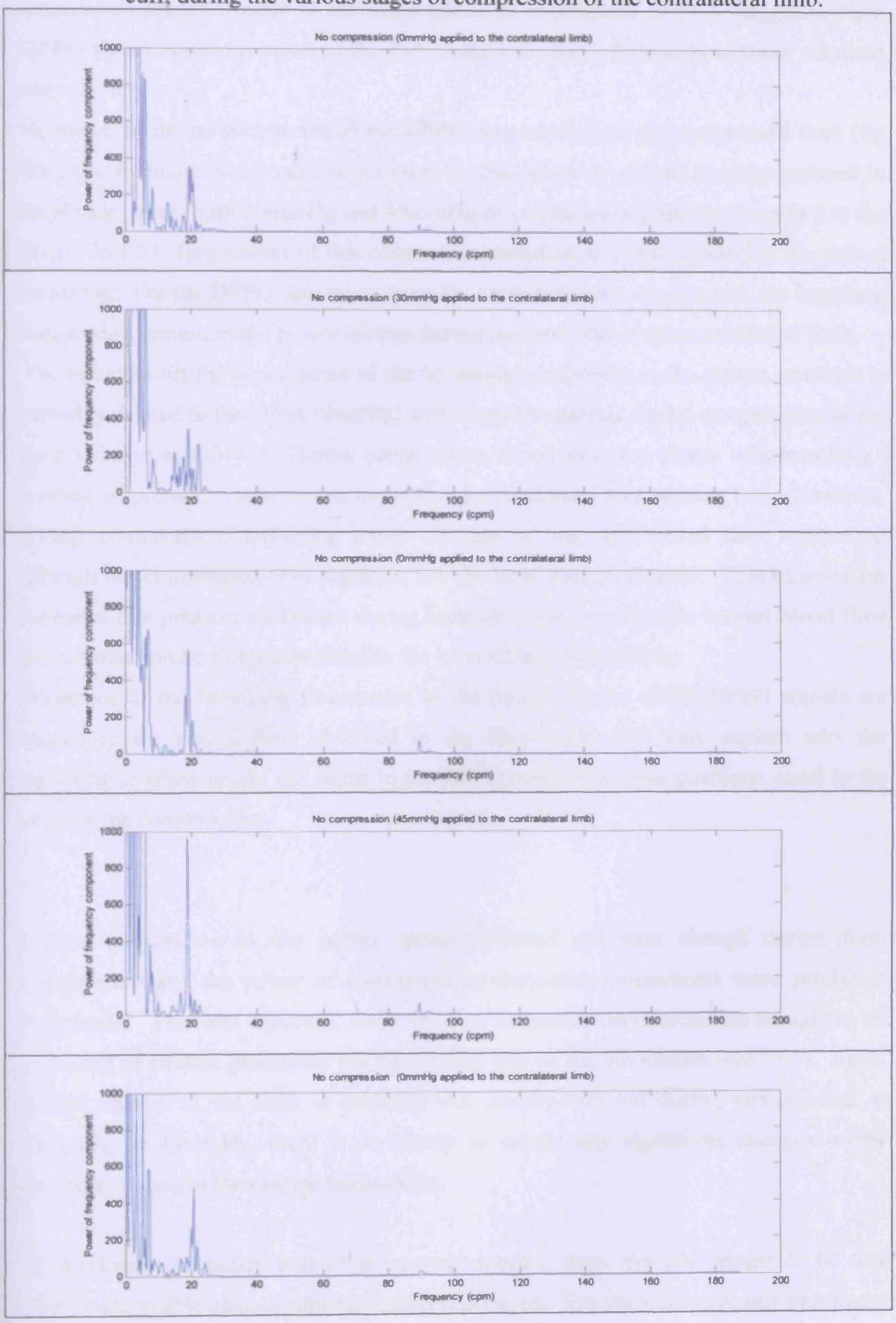

The first thing to notice from the power spectra (fig 8.6 and fig 8.7) is that dominant frequencies seem to occur in the same bands as highlighted in PI-1, suggesting that DPPG signals from the soles of the feet contain similar information to those acquired from the leg.

However, in the power spectra of the DPPG data taken from the compressed limb (fig 8.6), the frequencies around 20cpm seem to disappear, or at least become reduced in amplitude, when both 30mmHg and 45mmHg of compression pressure is applied to the thigh. In PI-1, frequencies of this order were identified as corresponding to the rate of breathing. For the DPPG data taken from the limb that is not compressed, the breathing frequencies remain in the power spectra during compression of the contralateral limb.

The reduction in the prominence of the breathing component in the power spectrum is probably related to the effect observed with Doppler analysis during compression of the deep veins in section 8.3. Before compression, blood flow was phasic with breathing - a result of pressure variations in the thorax and abdomen (see section 1.3). However, during compression, following initial collapse of the vein, blood flow reappeared through the compressed vein segment, but the flow was continuous. This observation indicates that pressure variations during breathing that cause phasic venous blood flow are not transmitted to regions distal to the level of the compression.

Therefore, if the breathing frequencies in the power spectra of the DPPG signals are related to the phasic flow observed in the deep veins, this may explain why the breathing frequencies do not occur in the DPPG data taken from positions distal to the level of the compression.

Higher frequencies in the power spectra showed no great change during limb compression and the power of corresponding frequency components were similar in both limbs. This was expected, since the high frequency oscillations are thought to be the result of cardiac pulsations via the arterial side of the circulation (see PI-1). Since arterial inflow to the limb is probably not greatly affected during compression at 30mmHg or 45mmHg, there is no reason to expect any significant changes in the microcirculation at the cardiac frequencies.

At the lower frequency end of the power spectra, there did not appear to be any significant, visible changes during limb compression. For the most part, any prominent

frequency components seemed to match up between the data from the both limbs during the periods when the cuff was inflated and deflated. However, the frequencies of the prominent components were not constant but varied slightly over the different compression periods. Nonetheless, the fact that the frequencies change in the same way in the data taken from both the limbs suggests that they are caused by global physiological processes within the body (e.g., it was suggested in PI-1 that the sympathetic nervous system has a major influence in the lower frequency band of the DPPG power spectrum). In addition, taking multiple FFTs for each period when the limb was compressed and not compressed also showed low frequency changes occurring in the same way in both legs, suggesting that the changes are related to some global physiological processes in the body and not to the thigh compression.

8.5 Conclusions

While it is realised that all the experiments in this section were only conducted on one individual (albeit multiple times) and therefore the results may not have considerable scientific weight, the experiments at least indicate that disruptions to the deep venous blood flow in the femoral vein cause changes in the microcirculation that can be detected by a DPPG probe placed on the leg or on the foot.

Application of compression pressure to the thigh was accompanied by collapse of the femoral vein and a decrease in DPPG amplitude. On closer inspection of the power spectra of the DPPG data taken from the compressed limb, significant changes seemed to occur at the band of frequencies associated with breathing, where application of the thigh compression reduced the power in the band. However, this did not occur in the contralateral limb, where the breathing frequency band seemingly remained unaffected.

It was felt that these results could contribute in a positive way to the development of a DVT test using DPPG. Even though thigh compression may not be a very accurate model for DVT*, the results suggest that it may be possible to use DPPG on the skin's surface to detect a disruption to the deep venous blood flow caused by DVT. This may

* Thigh compression affects all body structures under the cuff, including the deep *and* superficial veins. However, DVT affects the deep veins only and partial occlusion of the vessel lumen or the development of collateral channels (possibly via the superficial veins) enables blood to return to the heart. If this did not occur, continuing arterial inflow would increase the net volume of blood in the leg, leading to extreme swelling.

lead to a DPPG test for DVT that requires no active patient participation. In particular, it was felt that the effect the compression had on the breathing frequencies in the power spectra deserved further consideration.

Chapter 9

Patient Investigation

(To investigate DPPG signals taken from the soles of the feet of patients with and without lower limb DVT)

It was established in preliminary investigation 1 (PI-1) that the power spectra of DPPG signals, taken from various points on the leg, contain information about the physiological processes that control microcirculation blood flow.
Preliminary investigation 2 (PI-2) showed a clear change in the DPPG signal when the thigh was compressed using a pneumatic compression cuff. Although mechanical compression may not be an accurate model for DVT, the investigation at least demonstrated that disruption to deep venous blood flow in the lower limbs can be detected by a DPPG probe placed on the surface of the skin, as distal as the sole of the foot.

From the conclusions of these investigations, it seemed feasible that a DVT causing disruption to the deep venous blood flow may influence the DPPG signal obtained by a probe placed on the surface of the skin. This could be a change in the frequency bands of the power spectra highlighted in PI-1 (low frequency, breathing or cardiac), or some other feature, intrinsic to the DVT itself, that acts as a marker of the condition.

To develop these ideas further, it was necessary to collect DPPG signals from patients with confirmed lower limb DVT. DPPG signals were also collected from patients who were diagnosed as not having the condition but who were sent for objective testing on the basis of a clinical suspicion of DVT. The idea was to look for any difference in the DPPG signals acquired from the two groups of patients which, if associated with the presence of a DVT in the limb, could be used as an indicator of the condition in a diagnostic test.

9.1 Description of the patient investigation

Approval for the investigation was granted by the Bro Taf Local Research Ethics Committee and took place in the Doppler Ultrasound Unit of the Department of Medical Physics and Bioengineering at the University Hospital of Wales (UHW). Patients were

selected from those visiting the department for a scan to investigate suspected lower limb DVT. Doppler ultrasound* was chosen as the gold standard for DVT diagnosis because it is the primary test for DVT in the UHW and would therefore produce a high yield of patients for the study. Contrast venography is less frequently used. Also, as described in section 2.5.2, the sensitivity and specificity of Doppler ultrasound has been reported to be greater than 90% and some have suggested that it could be used in addition to venography as a gold standard in DVT diagnosis, e.g., Tan and da Silva (1999), Phillips (2000).

As many patients as possible were recruited to take part in the study between 5 June 2003 and 3 September 2004. These were mainly outpatient GP referrals. However, on occasion, inpatients were also asked to take part in the study, provided they were physically and mentally able to do so. No payment was made to any participant and all freely agreed to take part. Both males and females over 18 years of age were recruited with only a few exclusion criteria. All patients attending for a scan were asked to take part except for those unable to understand what was being asked (because of deafness, confusion, etc), unable to read or sign a consent form or those who were unable to transfer onto a standard examination couch, e.g., immobile patients. It was thought unnecessary to exclude any patient because of evidence of vascular disease other than DVT. For patients who are clinically suspected of having DVT but are diagnosed as free from the condition, the discomfort may be ascribed to other causes such as venous insufficiency, phlebitis, Baker's cysts etc. For those who are diagnosed as having DVT, associated conditions such as varicose veins or the post-thrombotic syndrome arising from previous DVTs etc. are common. Therefore, it was thought likely that excluding patients with any vascular disease other than DVT would significantly reduce the number of patients eligible to take part, increasing the time needed to recruit a reasonable number (time which was not available). Instead, each patient was asked about any present or past vascular disease or any other condition, recent operations, medications etc. that may have influenced blood flow in the lower limbs. In addition, in response to a question on a consent form, the patients gave permission for their medical history to be accessed. Consequently, a search was made through the hospital's computer records for any previous ultrasound scans of the lower limbs. These were

* The term "Doppler ultrasound" refers to ultrasound imaging with the use of Doppler techniques to assess blood flow.

noted together with the results of their present scan and any relevant details on the request form filled in by the referring physician.

On arrival at the UHW, the Clinical Scientists gave the patients the requested Doppler Ultrasound scan before referring them to myself to discuss their possible inclusion in the study. (Patients were invited to take part whether they tested positive or negative for DVT.) The Doppler ultrasound scan was carried out according to the standard protocols adopted in the department. This involved an investigation of the whole lower limb, including the calf veins (except the anterior tibial veins, which are difficult to visualise with the technique). All scans started at the iliac vein in the groin, working distally along the limb to the calf veins. However, if a proximal DVT was detected, the scan was stopped since additional investigation of more distal regions was considered unnecessary. DVT visualisation, vein compression and blood flow were assessed. However, bilateral scanning was not undertaken unless requested by the referring physician or if PE was suspected.

Following the referral of each patient to myself, the investigation was carried out according to the following protocol (time to complete: approximately 20-25 minutes).

9.2 Experimental protocol

Fig 9.1: Diagram of experiment set-up.

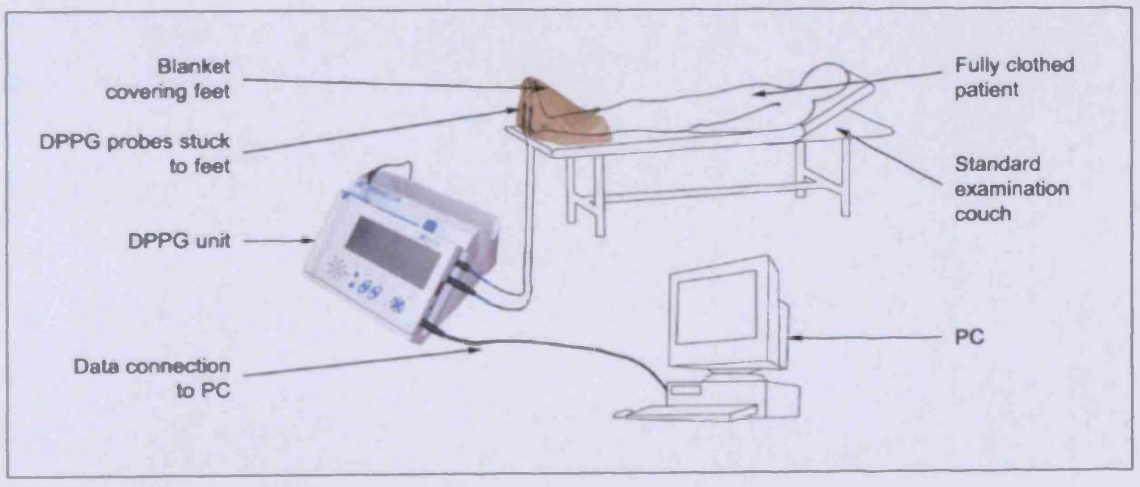

- The patient was asked to sit down and given an oral explanation of why the study was being conducted and what was expected of them during the investigation. The patient was then given an information sheet to read and a few minutes to decide whether or not they would like to take part. If they agreed, they were asked to complete and sign a consent form (copies of the information sheet and consent form are given in Appendix G).
- The patient was asked to remove their shoes, and anything else covering the feet, and to lie on a standard examination couch in a supine position with both feet on the couch. Following this, the patient was instructed to relax, not to talk and try to minimise movement, especially of the lower extremities.
- One DPPG probe was attached to the plantar surface of each foot. The probes were attached using the double-sided sticky pads supplied with the DPPG device and positioned as close as possible to the centre of the sole of each foot (fig 9.2). The DPPG probes were labelled so that the same probe was always attached to the same foot; left or right. (This made it easier to keep track of which foot the DPPG signals came from when analysed on the PC.)

Fig 9.2: Positioning the DPPG probe on the sole of the foot.

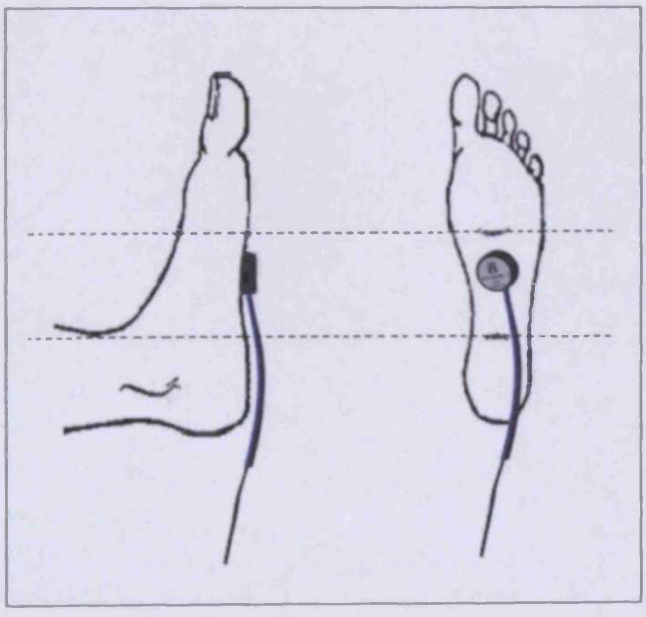

- The feet were covered with a blanket to prevent excessive cooling and constriction of the blood vessels in the microcirculation. It was hoped that this would also

minimise temperature variations in the foot, which could influence microcirculation blood flow.

- The patient was allowed five minutes to relax before any DPPG readings were taken. This allowed the microcirculation blood flow to stabilise following exertion of the patient and also helped expedite the DPPG calibration procedure.
- The DPPG device was then started. At first, the device performs self-calibration, which sets the initial IR intensity recorded by the probes to the same starting value for each foot (see section 3.5). Calibration completes when a stable IR intensity is detected at the probes. Following this procedure, which usually takes less than 30s, the DPPG device automatically starts recording data. (Successful calibration was taken to indicate that, at that time, the patient was sufficiently relaxed and microcirculation blood flow was stable enough for data collection to begin.)
- Once the DPPG calibration procedure had completed, the data logger on the PC was set running. Data were streamed from the DPPG device directly to the PC in real-time via a serial connection (described in section 4.3).
- DPPG data were collected for 10min following the start of the data logger on the PC. This was timed by observing a clock on the PC screen.

The investigations were performed in a room which was not temperature controlled. The reason for this was lack of convenient access to such a facility. Some control of room temperature would have been desirable because it is known that blood flow in the skin plays an important role in temperature regulation of the body (section 1.5.2.2.2). Nevertheless, an attempt was made to minimise extreme temperature fluctuations during the investigations by closing windows and doors where possible. It was thought that preventing excessive cooling of the body was most important, avoiding considerable vasoconstriction of the blood vessels in the skin and any consequent change to the DPPG signal intensity (as well as preventing physiological effects such as shivering). Therefore, the patients remained fully clothed and a blanket was placed over the exposed feet for the duration of the investigation.

Placement of a blanket on the feet should not have affected the DPPG signal. Due to the position of the feet on the examination couch (pointing perpendicular to the surface

of the couch) and the location of the DPPG probes on the soles of the feet, the blanket did not place any direct pressure on the DPPG probes (see figures 9.1 and 9.2).

The soles of the feet were chosen as the measurement site because it is known that the skin in this area (as well as the hands and the ears) is very vascular, i.e., has a high density of microcirculation vessels (see section 1.5.1). Therefore, it was thought that this location would provide the best quality DPPG signals (e.g., PI-2 showed more pronounced amplitude fluctuations in the DPPG signals taken from the soles of the feet compared to those taken from the leg). Another reason for choosing the soles of the feet as the measurement site involved a little foresight. The purpose of collecting DPPG data in this investigation was to determine if a DVT in the lower limb has any effect on the frequency bands in the power spectra of the DPPG signals, described in PI-1. One of these bands is thought to be related to the influence of breathing on venous blood flow. In PI-2, compression of the thigh was shown to diminish the breathing component of the DPPG signal when the probe was placed distal to the level of the compression. Simultaneous Doppler ultrasound examinations demonstrated that blood flow in the deep veins, initially phasic with breathing, became continuous when the compression was applied. A similar effect is exploited in the diagnosis of lower limb DVT using Doppler ultrasound. Phasic flow in the deep veins is often disrupted when a DVT is present. A reduction in the phasic nature of the flow is often observed around, and distal to, the level of the thrombus (section 2.5.2). Therefore, if similar changes also occur in the microcirculation, it was thought that the best location for the DPPG probe would be distal to the level of any DVT in the limb. Since DVT can potentially occur anywhere in the lower limb, the probe was positioned at the most distal site, i.e., the sole of the foot. The proximity of the DPPG probe to any DVT in the limb was not thought to be critical since PI-2 showed clear changes in the DPPG signal during thigh compression with the probe placed at various points along the leg and at the foot. Also, PI-1 and PI-2 showed that the power spectra of DPPG signals taken from positions along the leg are similar to those taken from the soles of the feet when no disease is present. Both contain cardiac, breathing and low frequency terms.

The DPPG probes were placed on the central part of the arch of the foot (fig 9.2). The reason for choosing this area, rather than the heal or the ball of the foot, was that this area is relatively protected from pressures and abrasions when walking etc. The heal

and the ball of the foot are most likely to develop callosity and the thick layer of dead skin associated with the condition may reduce the quality of the DPPG signal.

Placing the probes on the toes was also thought to be unwise because the DPPG device is very sensitive to movement artefacts and the toes are likely to move much more than the sole of the foot during the data collection. Also, it was likely that the blanket, when draped over the feet, would have rubbed against probes on the toes causing artefacts in the signal or the probes to become detached (since they were only attached to the skin using a double sided sticky pad).

Slight variation in the position of the probes on the soles of the feet was not thought likely to cause significant variations in the DPPG signal. For example, Kamal et al. (1989) refers to a previous study which demonstrated that reflection PPG probes of a reasonable size (not fibre optics or miniature transducers) using two uncollimated light sources with a photodetector in between are relatively insensitive to changes in probe position when placed over a diffuse vascular bed.

9.3 Analysis of the DPPG data

The following sections describe the analysis of the DPPG data collected in the patient investigation. The aim was to determine whether DPPG signals, taken from the soles of the feet, can give an indication of the presence of DVT in the lower limbs.
Firstly, a description of the patient group is presented. The DPPG data acquired from this group is then analysed to look for any differences between the patients with DVT (confirmed with Doppler ultrasound) and those without the condition.
Fourier analysis is used to give an indication of any effect DVT has on the components of the power spectra of the DPPG signals. Complex demodulation is then used to examine specific frequency components in greater detail and the results are used to develop a new DPPG test for DVT.
Finally, the statistics of the test are discussed, together with its possible role in DVT diagnosis and/or screening.

9.3.1 Description of the patient group used in the study

A table summarising the Doppler ultrasound (DUS) scan results and relevant medical history of all those patients who took part in the study is given in Appendix H. Each patient is labelled with a number and, from this point onwards, when a patient is referred to in the text, the patient will be described by their DUS scan result, i.e., positive or negative for DVT and the corresponding patient number.

A total of 142 patients agreed to take part in the investigation, of whom 55 were male and 87 were female. Of these patients, the DUS examination was positive for DVT in 65 cases and negative for DVT in 77 cases. The male to female ratio for the positive cases was 36:29, while the ratio for the negative cases was 19:58. Basic statistics describing the ages within the group of 142 patients are summarised in table 9.1. A histogram illustrating the age distribution is given in figure 9.3.
Seven patients declined to take part in the investigation after being asked. Three did not have a DVT (one giving a reason of time pressure and two others indicating nervousness about medical tests). Four did have a DVT (of which, two were eager to receive treatment after being diagnosed with DVT, one was unable to read and sign the consent form due to poor eyesight, and the other gave no reason for declining to take part).

Table 9.1: Basic statistics describing the patient group used in the investigation. (There was one patient, negative for DVT, whose date of birth could not be obtained.)

	Negative DUS	Positive DUS
Number of patients	76	65
Minimum age (years)	18	26
Maximum age (years)	83	88
Mean age (years, 2sf)	54	59
Standard deviation of ages (years, 2sf)	17	17

Fig 9.3: Histogram illustrating the age distribution of the patient group used in the investigation. (There was one patient, negative for DVT, whose date of birth could not be obtained.)

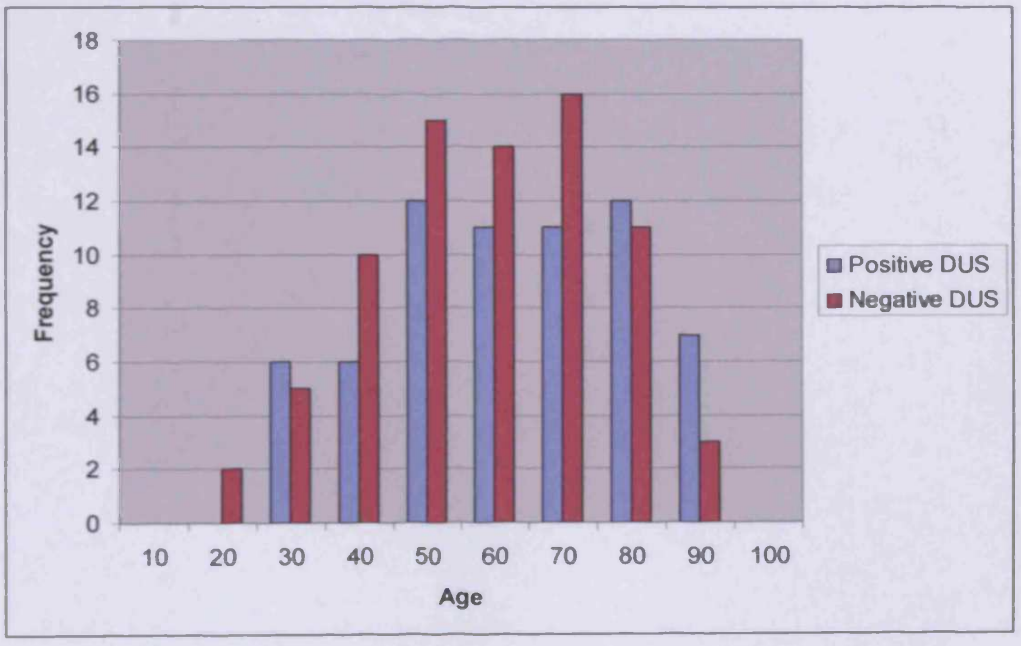

Of the patients with DVT, 41/65 had the thrombus at the level of the popliteal vein or above (proximal or "above knee" DVT) and 23/65 had a DVT below the level of the popliteal vein (distal or "below knee" DVT). Thirty patients had DVT in the left limb and 34 patients had a DVT in the right limb. In addition, there was one case of bilateral DVT (femoral DVT in the left limb and posterior tibial vein DVT in the right limb; both partially recanalised.) A more detailed description of the DVT locations is given in figure 9.4.

Fig 9.4: The location of DVT in patients diagnosed as positive with DUS (excluding a case of bilateral DVT where there the thrombus was in the femoral vein in the left limb and in the posterior tibial vein in the right limb).
BK=Below Knee; AK=Above Knee.

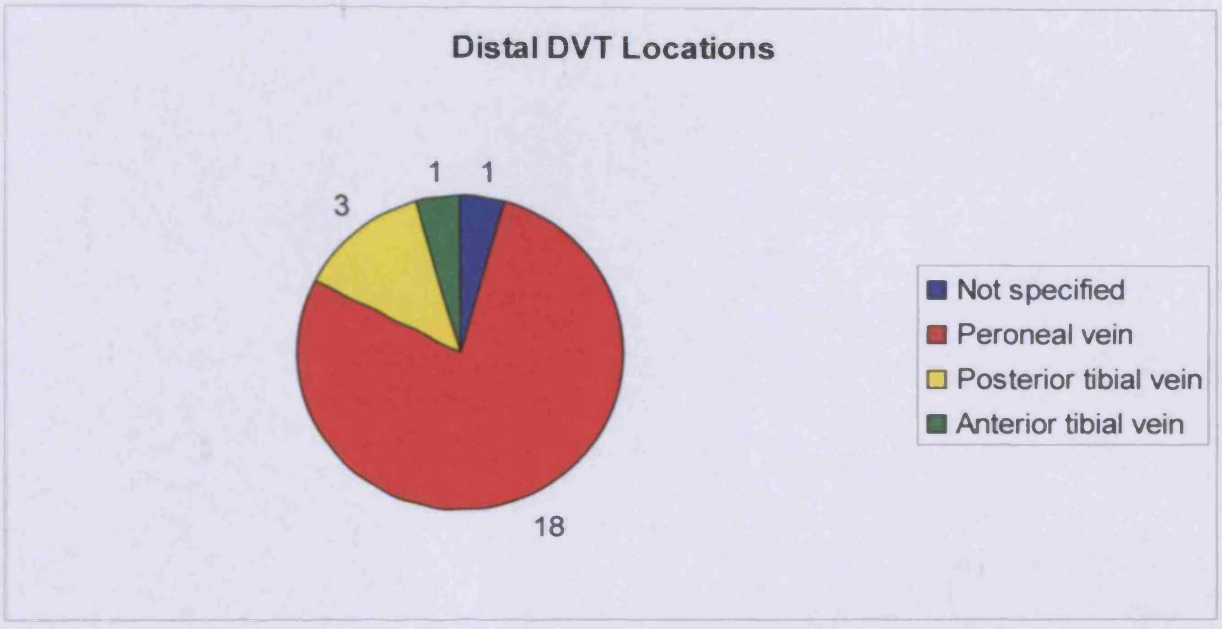

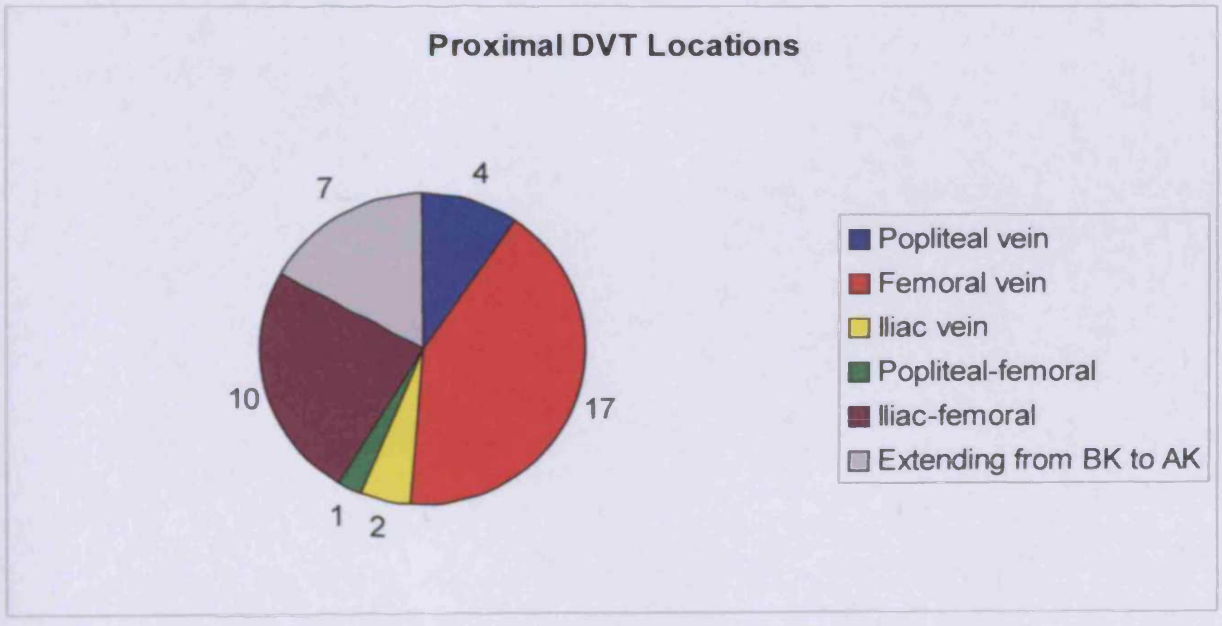

Each patient who agreed to take part in the study underwent the DPPG investigation described in section 9.2. During the investigation, as much information as possible was recorded about factors that may have influenced the DPPG signal. Examples include

patient movement, talking, recalibration of the DPPG device, callosity on the feet, limbs in plaster or bandaged etc.

In addition, conditions such as pregnancy, phlebitis, varicose veins, Baker's cyst and medications such as anticoagulants could alter the haemodynamics in the leg and therefore influence the DPPG signal. For each patient, as much information as possible was recorded about such conditions by examining the DUS scan result and any previous scan results, the details on the doctor's request form and by speaking to the patient directly (however, there was no list of pre-prepared questions). Table 9.2 lists a summary of the findings.

Table 9.2: Summary of the factors that may have affected the DPPG signals collected in the patient investigation.

Possible influencing factor	**Number of patients affected**
Previous DVT (possibility of long term damage to veins disrupting venous flow)	23
Post-thrombotic changes	12
Superficial thrombophlebitis	8
(Ruptured) Baker's cyst	5
Deep venous reflux	3
Cellulites	2
Pregnancy	2
Resolving chronic thrombus	1
Gross oedema below knee	1
Fluid effusion behind knee and proximal calf	1
Enlarged lymph nodes and lymph obstruction in the groin	1
Polycythaemia	1
Abdominal aortic aneurysm	1
Gout in foot	1
Factors noted during the test	
Feet shaking	3
Foot callosity	3
Patient restless	3
Patient not refraining from talking	8
DPPG recalibration	22

9.3.2 Looking at the DPPG signals by eye

The DPPG signals collected from the feet of each patient are displayed in Appendix I. By looking at the signals from all the patients (both positive and negative for DVT), the overall pattern seems to be much the same as that described in PI-1, i.e., a superposition of low (<~10cpm), medium (~10<cpm<~40) and high frequency (>~40cpm) components.

However, for the patients with confirmed DVT (by DUS), large amplitude, low frequency changes are sometimes more prominent in the DPPG data taken from the limb with the DVT. For an example, see figure 9.5 and also positive patient numbers 14, 16, 19, 25 and 42 in Appendix I. All these patients had a DVT at, or proximal to, the level of the popliteal vein. The oscillations occur at a frequency of a few cycles per minute and were postulated to be the result of blood accumulating distal to the obstruction in the veins, which causes venous blood pressure to increase. When the pressure becomes large enough to force the blood past the obstruction, the volume of blood in the distal reservoir decreases, until the blood is again no longer able to flow and the cycle starts once more.

However, similar low frequency oscillations can also be seen in the DPPG signals taken from the non-thrombosed leg of some DVT patients (e.g., positive patient number 7, 10, 38, 46 and 49), although the absence of bilateral DVT can only be assumed since it was not standard protocol to routinely scan both legs in the DUS examination (unless requested by the referring clinician). Only patient number 49 was noted to have had previous, extensive, below knee, bilateral post-thrombotic changes in both legs.

Additionally, similar low frequency oscillations can sometimes be observed in the DPPG data taken from those patients who were diagnosed as not having DVT (e.g., negative patient numbers 11, 15, 33, 34, 38, 39 and 58). For these patients, only number 15 had a noted previous history of DVT. Therefore the source of the oscillations may not necessarily be related to the presence of a DVT but possibly linked to some other local condition or physiological process. For example, negative patient number 11 was noted to have superficial thrombophlebitis in the long saphenous vein and a history of varicose veins. Number 34 had a history of thrombophlebitis in the short saphenous vein, number 38 had a history of varicose veins and number 58 had a Baker's cyst in the medial aspect of the knee.

Fig 9.5: An example of DPPG data taken from a patient with an acute femoral DVT. *(Positive patient number 14)*

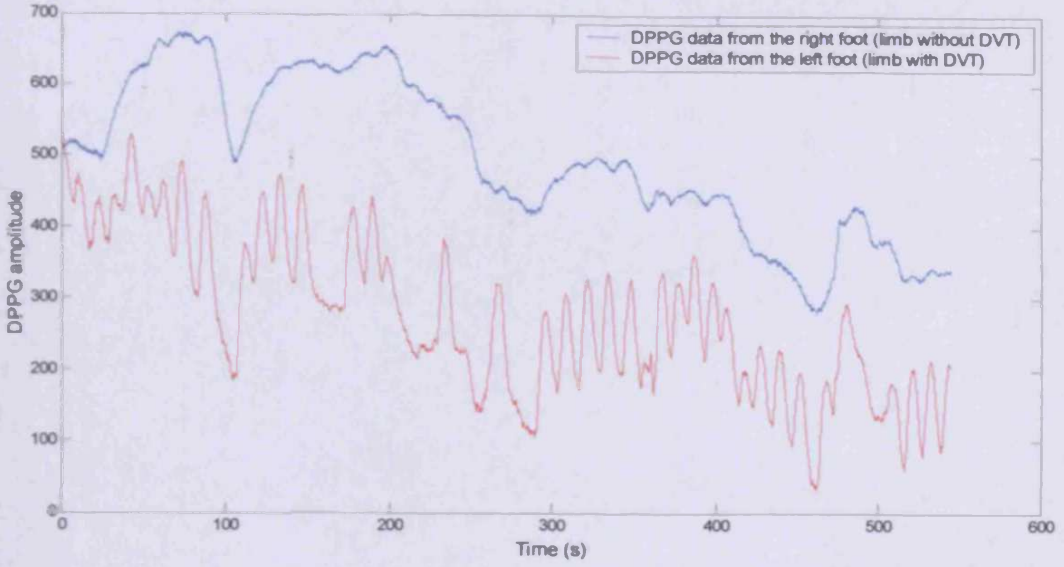

In addition to the low frequency oscillations, the baseline amplitude of the DPPG signals did not always remain constant throughout the period that the data were collected but sometimes tended to drift. Occasionally, this resulted in a gradual, continual increase or decrease of the DPPG signal. However, in some cases, the drift was such that that the signal went out of the measurement range of the DPPG device (positive patient numbers 5, 7, 11, 19, 37, 39, 46, 48, 57, 58, 61, 62, 63 and 65; negative patient numbers 7, 32, 64, 70, 71, 72, 73 and 77). Recalibration of the DPPG device was then necessary before the test could continue.

It is unlikely that the drift was caused by the DPPG equipment itself. The device was tested by the manufacturer (Huntleigh Technology PLC, Luton, UK) and shown to produce a constant output in the absence of any external influence.

Therefore the source of the drift was probably physiological, but not occurring rapidly enough to prevent calibration at the start of the data collection. The DPPG device will not complete its self-calibration procedure unless a reasonably stable baseline amplitude is detected. However, calibration usually completes within one minute and, in most cases, within 10 seconds. Therefore, a drift in baseline amplitude occurring over 10 minutes may not be sufficient to prevent the calibration from completing.

9.3.3 The power spectra of the DPPG signals

In PI-1, it was established that the effects of cardiac pulsations, breathing, neurogenic and local blood flow controls can all be seen in the power spectra of DPPG signals taken from the surface of the skin. Therefore, as an initial step in developing a DVT test, it seemed sensible to look for any changes in the power spectra of the DPPG signals when there is a DVT present in the limb. As a simple first attempt to investigate this, the power spectra of the DPPG signals, taken from the feet of the patients, were compared by eye to look for any obvious differences.

The power spectra were calculated as described in PI-1 and section 5.4.1. The whole DPPG signal from each patient was used to produce the spectra (excluding parts of the signal affected by recalibration). The reason for this was to obtain, in effect, an "average" spectrum, giving a general idea about what frequencies make up the DPPG signal and whether any specific frequency component dominates over its length. The results are described below.

9.3.3.1 Low frequencies (<~10cpm)

The low frequency region of the power spectra commonly show components that appear at the same (symmetrical) frequency in the DPPG data taken from the both feet. This observation holds true for all patients, i.e., for those with and without lower limb DVT. Such symmetrical frequencies were also observed in the power spectra of DPPG data taken from volunteers without venous disease in PI-1 and were suggested to be the result of neurogenic control of the microcirculation. Since this is a global control, affecting all blood vessels in the body in the same way, the appearance of symmetric frequencies in DPPG data taken from different parts of the body is not surprising.

However, the power spectra for the group of patients with confirmed DVT (by DUS), sometimes reveal additional low frequencies in the DPPG data taken from the thrombosed limb (e.g., see figure 9.6). These components seem to occur at similar frequencies to the oscillations observed in section 9.3.2. Initially, it was thought that these frequencies may be associated with the presence of the DVT, causing a cycle of distal damming and release of blood. However, as was the case with the low frequency components observed in section 9.3.2, such additional low frequencies also occur in the power spectra of the DPPG signals taken from the limbs without DVT.

Fig 9.6: The power spectra, between 0cpm-10cpm, of DPPG data taken from a patient with DVT (positive patient number 19, who had an acute ileo-femoral DVT). *The spectra are normalised, compared to the maximum power in each.*

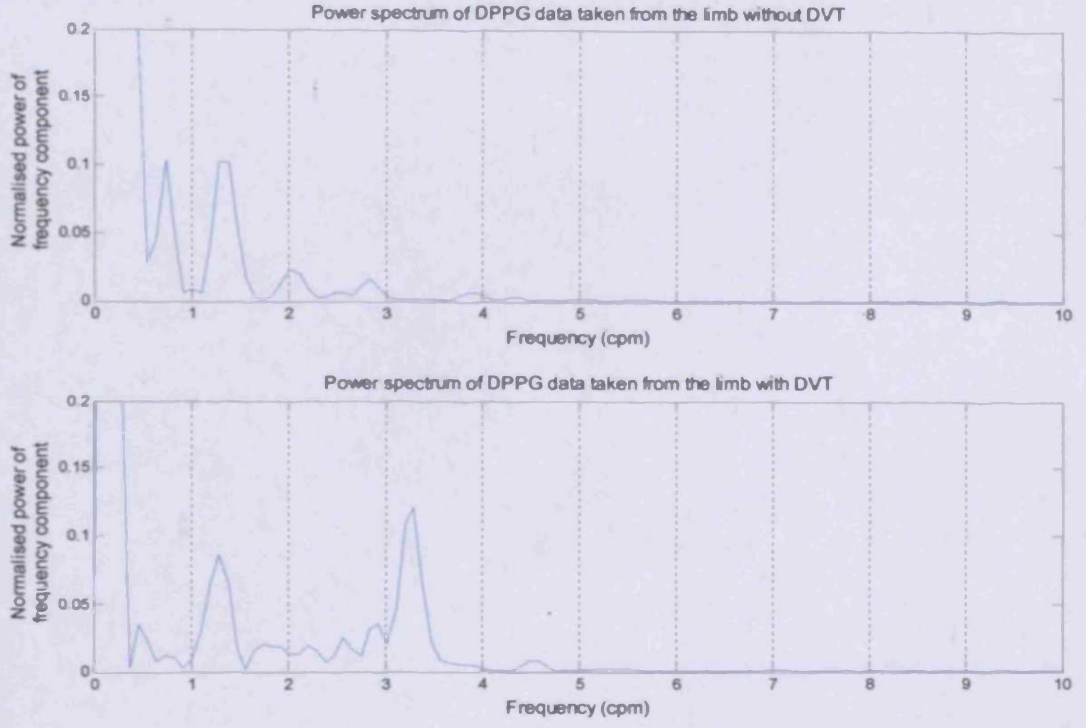

Asymmetry in the low frequency band is also observed in the DPPG data taken from the patients who were not diagnosed as having DVT. (A similar effect was also observed in PI-1, when considering the power spectra of DPPG signals taken from volunteers without venous disease.) Therefore, the presence of a DVT may not be the cause of the additional low frequencies. Since the low frequency region of the DPPG power spectrum is believed to be affected by local controls of blood flow (in addition to global, neurogenic control) it is possible that these non-symmetric peaks may be caused by local conditions around the foot, e.g. temperature variations. During the data collection in the patient investigation, the feet were covered by a blanket to try and minimise cooling. However, since no attempt was made to monitor temperature (or any other conditions such as blood pressure etc.) it is difficult to determine the source of the low frequencies.

9.3.3.2 Cardiac frequencies (>~40cpm)

At the cardiac frequencies, there does not seem to be any significant difference between the power spectra of the DPPG signals taken from the left and the right foot (in power or frequency). This is true for patients with or without DVT (e.g., see figure 9.7). The reason for this may be that, since that the cardiac pulsations are conveyed to the microcirculation via the arterial side of the circulation (see PI-1), the presence of a DVT may not affect the microcirculation pulsations to a great extent.

9.3.3.3 Breathing frequencies

The breathing component in the power spectra of the DPPG signals is not always clearly visible. (That is not to say that a breathing component does not exist, just that it cannot easily be seen with the naked eye.) However, for those patients who were confirmed negative for DVT (by DUS), and where the breathing component is distinguishable, it can always be observed in the power spectra from both limbs. However, this is not always the case for those patients with confirmed DVT. The power spectrum of the DPPG signal taken from the foot of the limb with the DVT often exhibits a reduction in the prominence of the breathing component or, in some cases, it becomes indistinguishable from neighbouring frequencies (e.g., see figure 9.7). Therefore, it seems to be the case that the presence of a DVT in the deep veins of the leg can affect the process by which the effect of breathing is communicated to the microcirculation of the foot of the same limb. This may be similar to what is observed during DUS examinations for DVT, where phasic venous blood flow in the deep veins of the lower limb, caused by breathing, becomes less pronounced or often disappears when a DVT is present in the same limb (see section 2.5.2). A similar effect was also observed in PI-2 during thigh compression of a volunteer without venous disease. During compression, the breathing component of the power spectrum diminished for the DPPG signal taken from the foot of the ipsilateral limb. This was not observed for the DPPG signal taken from the limb that was not compressed.

Fig 9.7: Two examples of the power spectra of DPPG data taken from patients in this study.
- 1a and 1b are obtained from the right and left foot of a patient without DVT.
- 2a and 2b are obtained from the right and left foot of a patient with a DVT in the left leg.

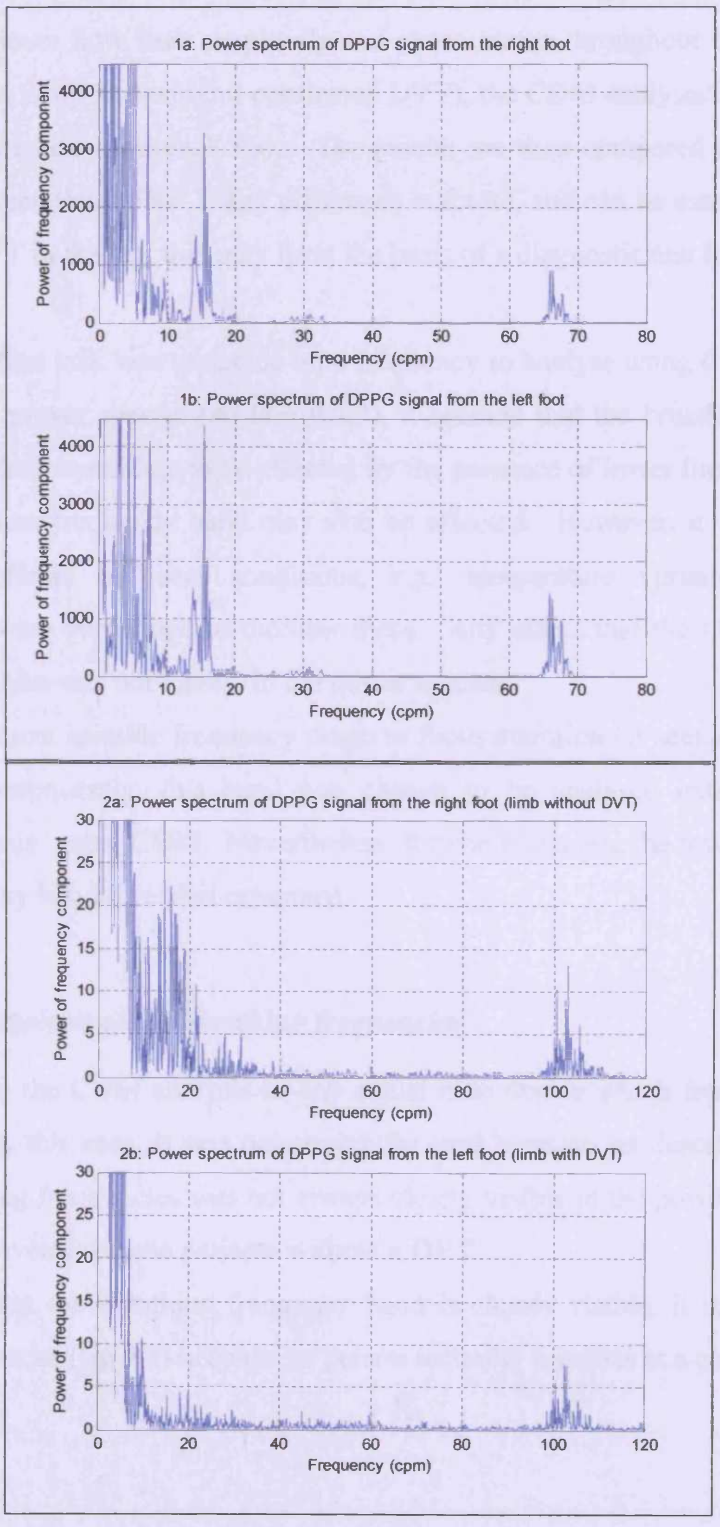

9.3.4 Complex demodulation of the DPPG signals

Examination of the power spectra of the DPPG signals in the previous section provided a hint as to which frequencies may be affected by the presence of lower limb DVT. In this section, these frequencies are analysed more closely, using complex demodulation (CDM), to discover how their amplitude and phase varies throughout the DPPG data. For each patient (with and without confirmed DVT), the CDM analysis is performed on the DPPG data taken from each foot. The results are then compared to look for any difference between the limbs. If any difference is found, and can be associated with the presence of DVT in the leg, this may form the basis of a diagnostic test for DVT.

Therefore, the first task was to decide on a frequency to analyse using CDM. From the analysis of the power spectra (section 9.3.3), it seemed that the breathing component was the most likely candidate to be affected by the presence of lower limb DVT. It was noted that the low frequency band may also be affected. However, it was difficult to exclude the effects of local conditions, e.g., temperature variations, since no investigations were performed to monitor these. Any effect that the DVT has on the cardiac frequencies was not visible in the power spectra.
Therefore, the most suitable frequency range to focus attention on seemed to be that of breathing. Consequently, this band was chosen to be analysed extensively in the following analysis, using CDM. Nevertheless, for completeness, the low frequency and cardiac frequency bands are also examined.

9.3.4.1 CDM analysis of the breathing frequencies

The first step in the CDM analysis of any signal is to decide which frequency is to be investigated. In this case, it was not straightforward because, as described above, the band of breathing frequencies was not always clearly visible in the power spectra of the DPPG signals, even for those patients without a DVT.
In addition, when the breathing frequency band is clearly visible, it is spread over a range of frequencies (fig 9.8) because no person naturally breathes at a constant rate.

Fig 9.8: An example of the power spectrum of a DPPG signal taken from the sole of the foot, illustrating the band of frequencies associated with breathing (coloured green).

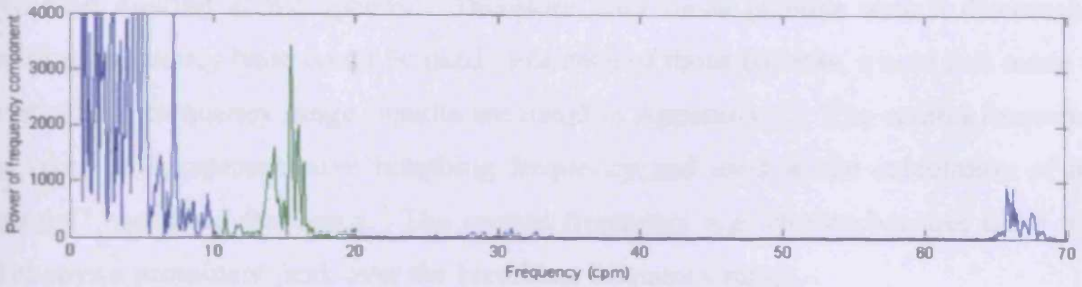

Asking the patients to breath at a constant rate (possibly in time with a metronome) or measuring the rate of spontaneous breathing during the investigation may have alleviated this problem. However, it was felt that both these procedures would have introduced unwelcome complications into any DVT test developed using the system (in which, one of its main strengths is simplicity). Also, in the case of breathing with a metronome, it is likely that patient compliance would be a problem. Patients may find it difficult to keep time with the metronome, especially confused or elderly patients. There may also be circumstances where controlled breathing may not be possible, e.g., when patients are unconscious, on the operating table or recovering from operations etc. These patients are at a high risk of developing DVT and any new diagnostic test should ideally be available to them all.

Therefore, it was decided to try and determine the breathing rate directly from the DPPG data. However, since the breathing frequency band could not always be clearly determined by visual inspection of the power spectrum, an alternative method was required to decide which breathing frequency was to be used in the CDM analysis. Two different methods were considered and are described below.

9.3.4.1.1 Method-A: An "average" breathing frequency

The first method was somewhat simple and involved finding an "average" breathing frequency for all of the patients investigated. CDM was then performed at that single frequency for all patients.

The "average" frequency was found by inspecting the power spectra of the DPPG signals from each patient (calculated as described in section 9.3.3) and involved no more than looking at the spectra. Therefore only those patients with a discernable breathing frequency band could be used. For each of those patients, a note was made of the breathing frequency range (results are listed in Appendix J). The central frequency was taken as a representative breathing frequency and used in the calculation of the "average" breathing frequency. The central frequency was chosen because there was not always a prominent peak over the breathing frequency range.

The "average" breathing frequency was found to be 21.0cpm for the group of patients with DVT and 19.7cpm for the group of patients without DVT (table 9.3). The mean of these two values (20.4cpm) was chosen to be used in the CDM analysis*.

Table 9.3: Statistics describing the breathing frequencies observed in the power spectra of the DPPG signals acquired in the patient study.

Patient Group (Number of patients where the breathing range was clearly observable)	Minimum breathing frequency observed (cpm, 1dp)	Maximum breathing frequency observed (cpm, 1dp)	Mean breathing frequency range (cpm, 1dp)	Mean central breathing frequency (cpm, 1dp)	std central breathing frequencies (cpm, 1dp)
Positive DVT (34/65)	10.0	32.0	6.0	21.0	4.2
Negative DVT (45/77)	8.0	30.0	6.0	19.7	3.6

Next, a suitable low pass filter (LPF) had to be selected for use in CDM. A 10cpm filter width was chosen so that the range of frequencies included in the CDM analysis was 20.4±10cpm. This seemed sensible since it is unlikely that the breathing frequency of any person would normally be much outside this range. In addition, the filter width is at least twice the standard deviation of all the central breathing frequencies recorded for

* It must be remembered here that the "average" breathing frequency is not the average of all the patients in the study but is used represent all the patients. The "average" frequency was calculated using only those patients where the breathing frequency range could be clearly seen in the power spectra (true for 34/65 patients with confirmed DVT and 45/77 without DVT). For this reason, inverted commas are used when referring to the average frequency.

both positive and negative DVT patients (table 9.3). Therefore, even though the minimum and maximum breathing frequencies recorded are 8cpm and 32cpm (and just outside the CDM analysis range) at least 95% of central breathing frequencies will be included in the analyses, since the central breathing frequencies for both positive and negative DVT patients approximate a normal distribution (fig 9.9)*. In fact, all central breathing frequencies, except that corresponding to negative patient number 33 (central breathing frequency=10cpm; breathing frequency range, 8-12cpm) were within the range passed by the LPF.

* All Q-Q plots, boxplots and statistical calculations (Mann-Whitney tests and correlation coefficients) were calculated using SPSS 11 (SPSS Inc, Chicago, Illinois, USA).

Fig 9.9: Q-Q plots illustrating the approximate normal distribution of the central breathing frequencies.

Values of central breathing frequency are plotted against the expected values if they were from a normal distribution. Points will cluster around a straight line if the data are from a normal distribution.

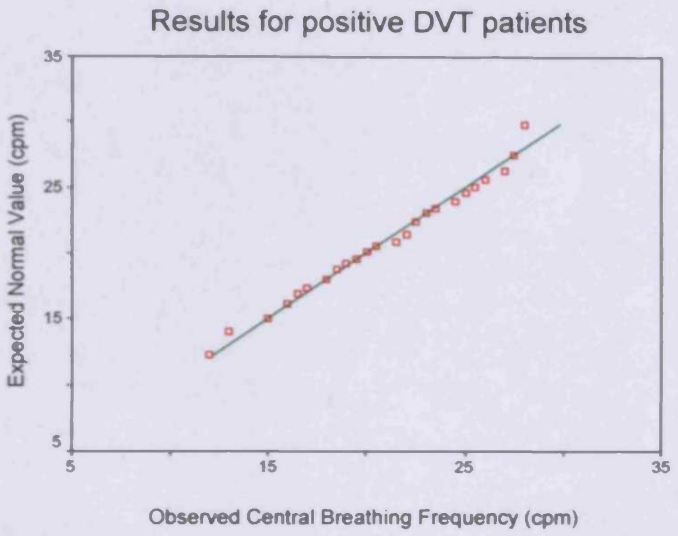

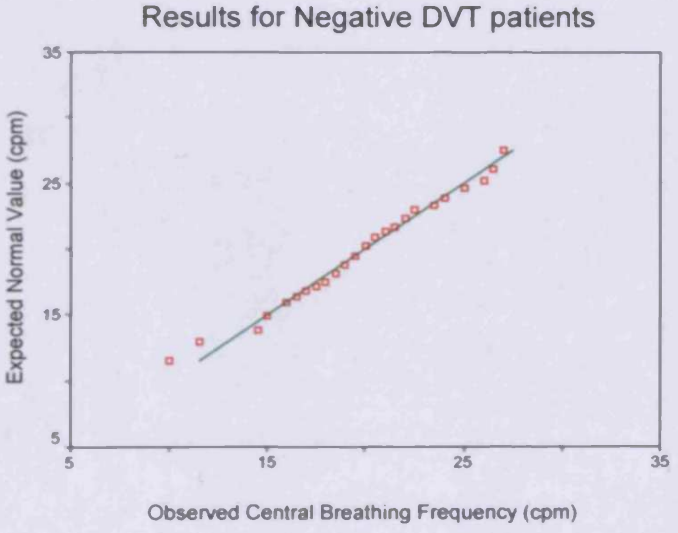

It was thought that choosing a wide LPF would compensate for the fact that the CDM frequency and the actual breathing frequency of the patients were not the same. Provided that the filter is wide enough, the true breathing frequency should always make a contribution to the results (see figure 9.10). If there are no other significant frequencies within the range passed by the filter then the breathing frequency will make the most significant contribution to the CDM output. For this reason, it was thought

undesirable to further extend the lower bound of the filter width because frequencies below 10cpm may be caused by local or neurogenic controls in the microcirculation (see PI-1). The same applies to the upper bound and the cardiac frequencies.

Fig 9.10: Power spectrum of a DPPG signal, illustrating the range of frequencies analysed using a 10cpm LPF width in CDM.

The black vertical line at 20.4cpm illustrates the frequency chosen for CDM. The dashed lines at 20.4±10cpm illustrate the frequency range included in the CDM analysis (all frequencies in the grey shaded area are excluded from the analysis).

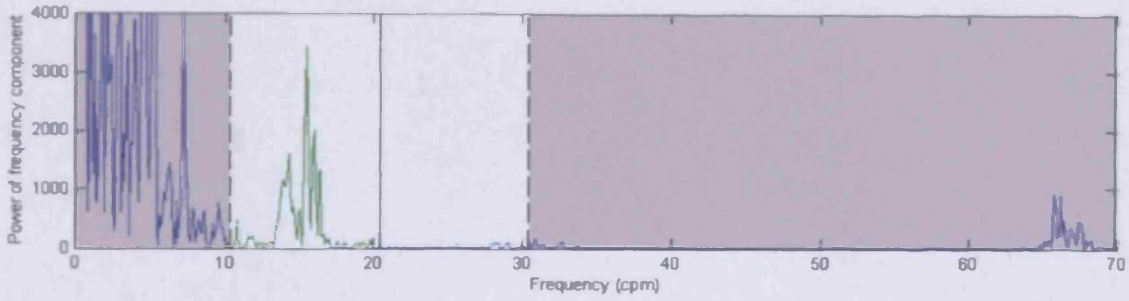

Nevertheless, a large filter width, combined with a disparity between the CDM and the actual breathing frequency, will affect the outputs from the CDM analyses. The amplitude and phase outputs from CDM will be different to those obtained if the CDM frequency was equal to the actual breathing frequency and a narrow LPF was used to isolate it (an idea explored further in Appendix B). However, this was not a major concern in this study since it was not the absolute CDM output values that were of interest but rather the difference between the CDM outputs from the left and right foot of each patient. There is no reason why the breathing frequency in the DPPG signal should be different in both feet, since the origin of the frequency is the same, i.e., pressure variations in the thorax and abdomen (see section 1.3). Therefore, the difference between the breathing frequency and the CDM frequency will be the same for the DPPG signals taken from both feet. Also, any effects on the CDM outputs caused by a large filter width should be the same for each foot and "cancel out" when compared (in the absence of any other physiological processes causing frequencies within the range passed by the filter).

9.3.4.1.1.1 Results of the CDM analysis using method-A[*]

Each of the 284 DPPG signals, obtained from the 142 patients, were analysed by CDM. A frequency of 20.4cpm was chosen for the analyses and a 10cpm LPF width was used. (The filter was a 5th order[•] Butterworth type.) The CDM outputs describe how the amplitude and phase of the selected frequency varies over time. An example for one patient is given in figure 9.11.

Fig 9.11: An example of the CDM outputs for a single patient. (Positive patient number 2, who had a popliteal vein DVT in the left leg.)

The top graph shows how the amplitude of the 20.4cpm component varies over the time that the DPPG data were recorded. The bottom graph shows the corresponding output for the phase.
The blue lines are calculated from DPPG data taken from the right foot. The red lines are calculated from DPPG data taken from the left foot.

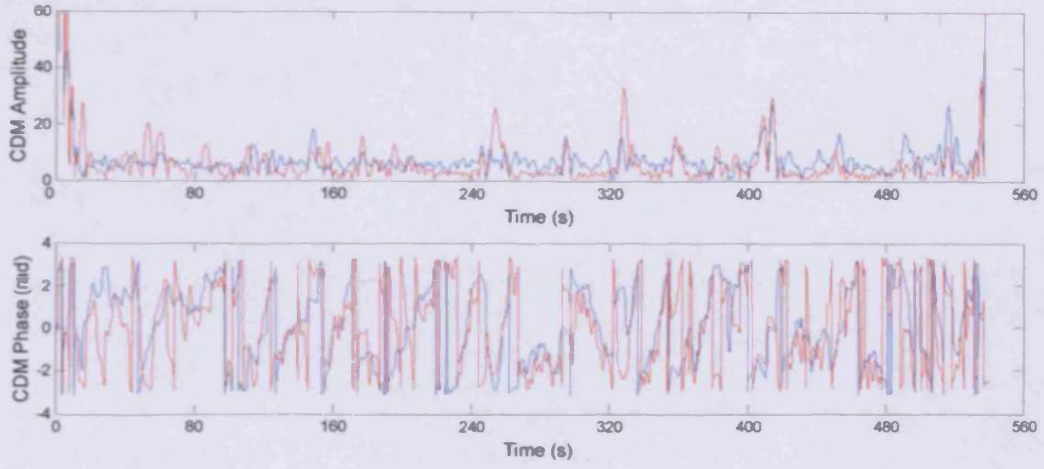

For patients with lower limb DVT, it was hypothesised that the amplitude of the breathing frequency would be smaller, on average, in the DDPG data taken from the ipsilateral limb. This was based on the knowledge that DVT is known to disrupt the phasic nature of venous blood flow (caused by breathing) in the large veins of the lower

---

[*] The MATLAB code used to implement the analysis for method-A can be found in Appendix C.

[•] The filter order was chosen as a compromise between the length of filter ringing and "roll-off" steepness in the transition band. The steepness of the cut off, when moving from the passband to the stopband, increases with filter order but so does the length of the filter ringing (section 5.3.2). The filter ringing causes disturbances to the CDM outputs. Since the disturbances were removed before the CDM outputs were examined further (described in greater detail below), the filter ringing had to be kept at a reasonable level.

limb (section 2.5.2). Also, it was observed in section 9.3.3.3 that DVT tends to reduce the amplitude of the breathing frequency band in the power spectra of DPPG signals.

Looking at the CDM amplitude outputs for the patients with DVT, the amplitude did appear to be generally smaller in the data taken from the limb with DVT in 20/65 cases (positive patient numbers 2, 6, 7, 9, 10, 11, 12, 15, 18, 20, 29, 30, 45, 47, 50, 53, 57, 59, 62, 65). However, this was not always observed and in three cases the amplitude of the breathing component tended to be lower in the leg without DVT (positive patient numbers 14, 16, 17). For these three cases, all the DVTs were at the level of the popliteal vein or more proximal.
For the patients without DVT, the amplitude of the breathing component tended to be similar for both limbs. However, amplitude discrepancies could be seen in the results for some of these patients (negative patient numbers 12, 23, 24, 31, 33, 38, 52, 63, 66, 68). In 5/10 of these cases, the amplitude was lower in the leg that was not scanned by DUS (since a bilateral scan was not requested by the referring physician). In these cases, even though there was a lack of clinical suspicion, it is impossible to be certain that a DVT was not present in the leg that was not scanned. (For the same reason, it is impossible to completely rule our bilateral DVT in the positive patients.)

To investigate more objectively the relationship between the CDM amplitude output and the presence of lower limb DVT, the mean absolute difference between the CDM amplitude outputs from both limbs was calculated. For each patient, this gives a single numerical value that quantifies any overall difference in the CDM amplitude outputs for the data taken from both limbs. Based on the observations above, the mean absolute difference in amplitude was expected to be generally lower for those patients who do not have a DVT. Therefore, it was thought that these values could be used as an indicator for DVT.

9.3.4.1.1.2 Mean absolute amplitude difference (MAAD) results

Before calculating the MAAD values, it was necessary to remove sections of the CDM output data that were significantly affected by filter ringing. As a result of the "filtfilt" function used to implement the filtering process in MATLAB, disturbances occur at both the start and the end of the CDM output data (section 5.4.2). An example of this

can be seen in figure 9.11. Consequently, following the procedure described in Appendix D, the first and last 112 data values of the CDM amplitude outputs were not used in the MAAD calculations.

For each patient, the MAAD was calculated using the following equation,

$$MAAD = \frac{\sum_{n} \left| A^{R}{}_{n} - A^{L}{}_{n} \right|}{N} \qquad \text{Equation 9.1}$$

$A^{R}{}_{n}$ is the n^{th} value in the CDM amplitude output from the right foot.

$A^{L}{}_{n}$ is the n^{th} value in the CDM amplitude output from the left foot.

N is the total number of values in the CDM amplitude output (equal for both feet).

The MAAD was calculated for each of the 142 patients. The results are displayed in figure 9.12 and figure 9.13.

Fig 9.12: The MAAD values for each patient in the investigation.
(CDM frequency = 20.4cpm. LPF width = 10cpm)
Each point represents the MAAD value for one patient.

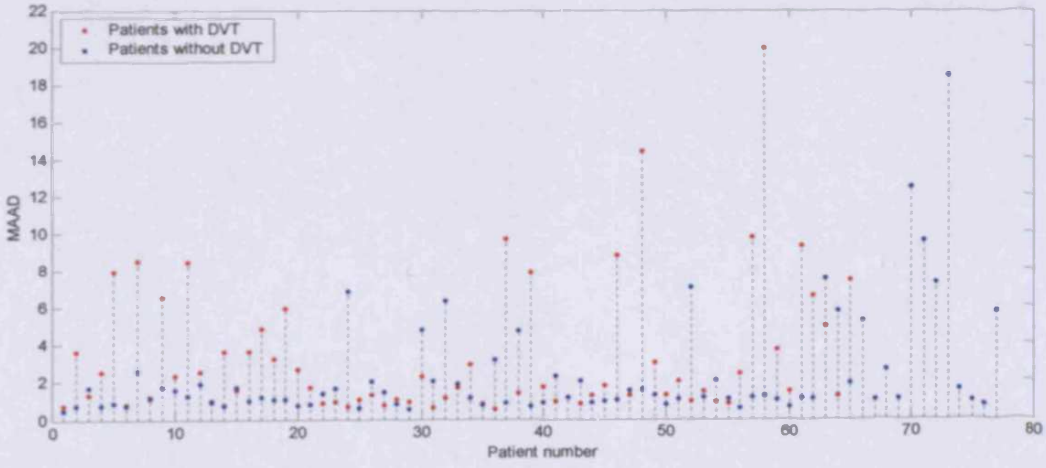

Fig 9.13: Boxplots of the MAAD values.

The box represents the interquartile range, containing 50% of the values. The line across the box indicates the median value. The lines protruding from the box extend to the highest and lowest values, excluding outliers and extreme values. Values between 1.5 and 3 box lengths from the upper or lower edge of the box are classified as outliers and are represented by circles. Extreme values are marked with an asterisk and represent those values that are greater than 3 box lengths from the upper or lower edge of the box.

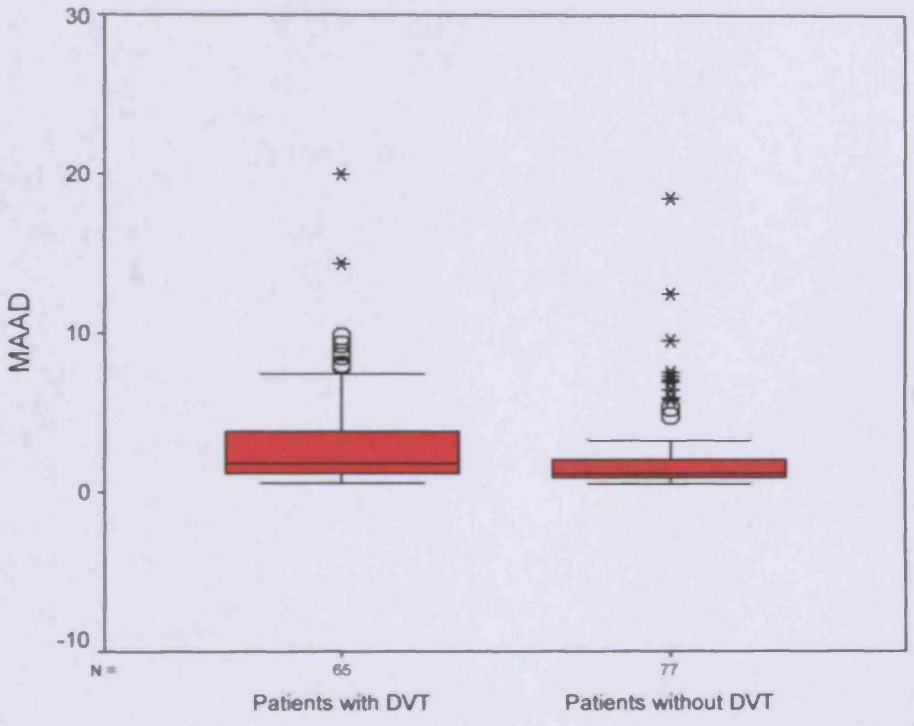

Figure 9.12 does not seem to show any overall difference in the MAAD values between the two groups of patients. Although there are some large MAAD values for patients with confirmed DVT, large values also occur in the results from those patients without DVT. This is consistent with observations of the CDM amplitude outputs in the previous section.

The boxplots (fig 9.13) show that the interquartile range of the MAAD values is wider for the patients with DVT. The median MAAD value is also slightly larger (1.6985 compared to 1.1725 for those without DVT). However, there is a considerable overlap between the two groups.

To test whether the MAAD values from the two patient groups can be considered as being from separate populations, the non-parametric Mann-Whitney test (2-tailed) was used. This test was chosen since the MAAD values from both categories of patients are

totally independent but tend not to be normally distributed. A Mann-Whitney test on the MAAD values from the two groups gives $p<0.05$ ($p=0.018$, 3dp) suggesting that the null hypothesis of no difference in MAAD values between the two groups may be rejected. However, since the p-value is not negligible, compared to the 0.05 significance level, this conclusion may not be definitive. In addition, the large number of outliers and extreme MAAD values in the boxplots of both patient groups (fig 9.13) does not improve confidence in the conclusion. Therefore, it seems that the MAAD values do not give a good indication of the presence of lower limb DVT.

9.3.4.1.1.3 Mean absolute phase difference (MAPD) results

In addition to the CDM amplitude outputs, the phase outputs were also considered. In a similar procedure, the phase outputs were analysed by calculating the mean absolute difference between the results from both limbs. The mean absolute phase difference was expected to be greater for patients with DVT because of the disturbances caused to the phasic blood flow in the veins.

As with the CDM amplitude outputs, the first and last 112 data points of the phase outputs were removed before calculating the MAPD values (following the procedure described in Appendix D). This was required to remove the effects of filter ringing on the CDM outputs.

The MAPD values were then calculated using the following equation,

$$MAPD = \frac{\sum_{n} \left| \phi^{R}{}_{n} - \phi^{L}{}_{n} \right|}{N} \qquad \text{Equation 9.2}$$

ϕ^{R}_{n} is the n^{th} value of the CDM phase output from the right foot.

ϕ^{L}_{n} is the n^{th} value of the CDM phase output from the left foot.

N is the total number of values in the CDM phase output (equal for both feet).

The MAPD was calculated for each of the 142 patients. The results are displayed in figure 9.14 and figure 9.15.

Fig 9.14: The MAPD values for each patient in the investigation.
(CDM frequency = 20.4cpm. LPF width = 10cpm)

Each point represents the MAPD value for one patient.
The black, horizontal line represents the minimum MAPD of all the patients with DVT (0.5710radians).

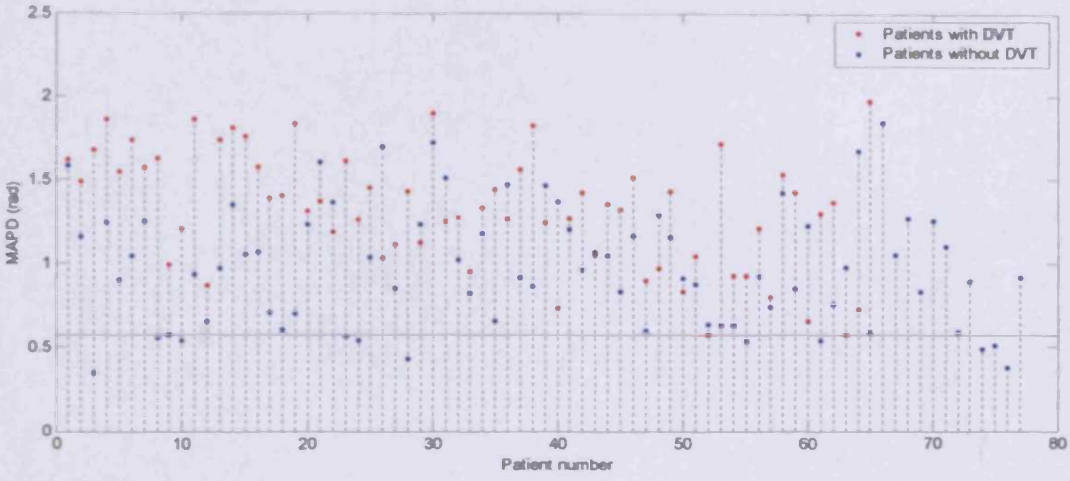

Fig 9.15: Boxplots of the MAPD values.
(A description of the features of the boxplot can be found in figure 9.13.)

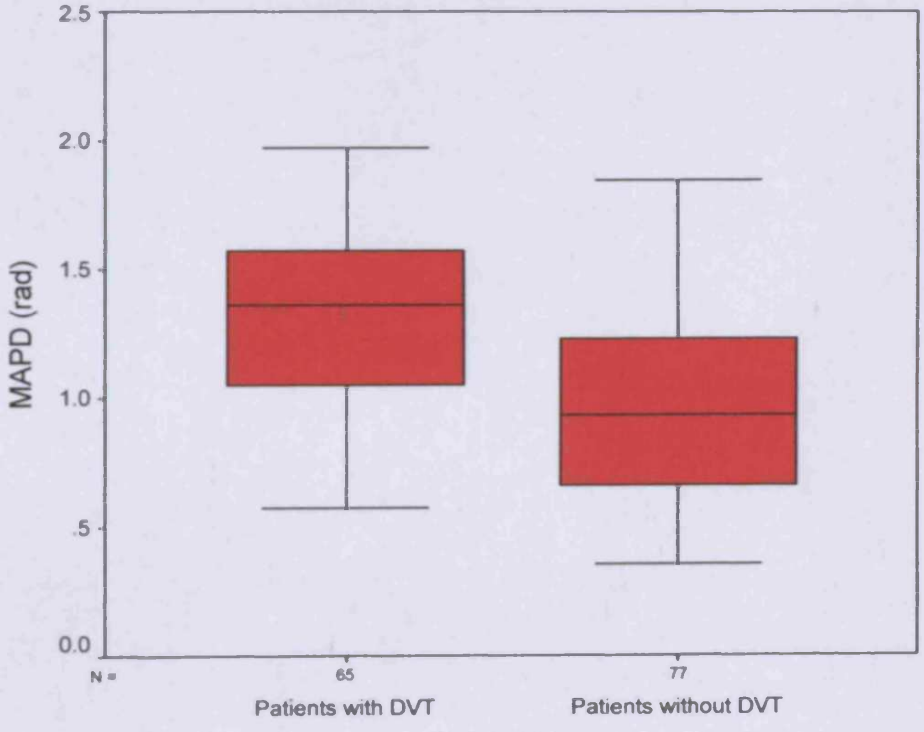

Figure 9.14 seems to show that the MAPD values for the patients with DVT are generally larger than for the patients without DVT. There are 12 patients without DVT for which the corresponding MAPD value is below the minimum MAPD value for those patients with DVT.

An indication of a difference between the two groups of patients can also be seen in the boxplots (fig 9.15). The interquartile range of MAPD values is similar for the two groups of patients but occurs at larger MAPD values for the patients with DVT. The median MAPD value is also larger for the patients with DVT (1.3558radians compared to 0.9317radians for those without DVT). However, there is an overlap between the two patient groups.

To test whether the MAPD values from the two groups of patients can be considered to be from different populations, the Mann-Whitney test (2-tailed) was again used, since the MAPD values seemed to deviate from a normal distribution. A Mann-Whitney test on the MAPD values of the two groups gives $p<0.05$ ($p=0.000$, 3dp) suggesting that the null hypothesis of no difference in MAPD values between the two groups may be rejected.

This suggests that the MAPD value may be able to give an indication of the presence of lower limb DVT. For example, a DVT test could be formed by setting an empirical threshold MAPD value such that all patients with a lower value are classified as not having DVT. The threshold value of the test should be set so that the sensitivity is 100%, i.e., all patients with DVT should be classified as positive by test, since it is important not to miss any cases of DVT. Therefore, the threshold value must be set equal to, or less than, the minimum MAPD for any patient who tested positive for DVT with the gold standard (DUS). From figure 9.14, it can be seen that, for the group of patients in this study, a threshold value of 0.5710 radians would meet such a requirement. If this value was used as the threshold value, the DVT test would have the statistics shown in table 9.4. (Definitions of the test statistics can be found in Appendix K.)

Table 9.4 Statistics of a DVT test using the MAPD value as an indicator for DVT and a threshold of 0.5710 radians.
(CDM frequency = 20.4cpm. LPF width = 10cpm)

Number of true positives (compared to DUS)	65
Number of false positives (compared to DUS)	65
Total number of positive test results	130

Number of true negatives (compared to DUS)	12
Number of false negatives (compared to DUS)	0
Total number of negative test results	12

Sensitivity	100.0% (1dp)	(65/65)
Specificity	15.6% (1dp)	(12/77)
Negative predicting value	100.0% (1dp)	(12/12)
Positive predicting value	50.0% (1dp)	(65/130)
Accuracy	54.2% (1dp)	(77/142)

Because the sensitivity is fixed at 100%, all those patients who were diagnosed as having DVT with DUS would also test positive with the MAPD-DPPG test. However, only 15.6% (12/77) of those patients without a DVT would be confirmed negative by the test. The other 84.4% (65/77) would be false positives.

For any diagnostic test, such a low specificity is undesirable since it could lead to unnecessary administration of treatments. In the case of DVT, this may be anticoagulant drugs. However, the MAPD-DPPG test may be suitable for DVT screening. In this case, a high negative predicting value is desirable to be confident that any negative test result is correct and no further investigation is required. Fixing the sensitivity at 100% automatically sets the negative predicting value to 100%. Therefore, all patients with a negative test result would not require further treatment. However, for those with a positive test result, further investigation would still be necessary because the low positive predicting value of the MAPD-DPPG test (50.0%) means that only half of those patients would actually have a DVT.

Therefore, it is envisaged that the MAPD-DPPG test may be used as a screening tool, preceding more established DVT diagnostic tests such as DUS or venography. Such a precursor test is desirable because the unreliability of clinical diagnosis of DVT leads to a large number of referrals for objective testing, many of which turn out to be negative

(section 2.5). A quick and simple screening test would reduce the number of such patients before they are scanned with relatively expensive and time consuming DUS or venography.

There are, however, screening tests for DVT that are currently in use. The D-dimer test is probably the most popular. The sensitivity of this test has been reported to be greater than 90%, with specificity in the range 30-50%, depending on the type of assay used (section 2.5.3). However, the big disadvantage of D-dimer is its invasive nature, requiring a blood sample. The DPPG system, on the other hand, is non-invasive.

Nevertheless, if the MAPD-DPPG test is to form the basis of a screening (or diagnostic) test for DVT, it would be desirable to improve its specificity from 15.6%. One way to do this may be to increase the threshold MAPD value. However, it can be seen from figure 9.14, that it is impossible to do this without introducing false negative results and decreasing the sensitivity. Therefore, to increase the specificity, while maintaining the sensitivity at 100%, the separation of MAPD values between the two patient groups must be increased*.

Improving the way the data are analysed by CDM may help to achieve this. Therefore, it was decided to look more closely at the selection of the breathing frequency used in the CDM analysis. Until now, an "average" value for the breathing frequency was used for all the patients. This was calculated by looking at the power spectra of the DPPG data from each patient. A large LPF width was chosen so that a wide band of frequencies, centred on the "average" breathing frequency, was used in the CDM analysis. This frequency band was likely to include the actually breathing frequency of each patient. However, the effect that employing such a large LPF width has on the CDM outputs is uncertain (e.g., see Appendix B). In addition, the process of selecting individual breathing frequencies by eye and calculating an "average" value introduces unwelcome subjectivity into the analysis. This also proved to be difficult because the breathing component was not always clearly visible in the power spectra of the DPPG signals.

Therefore, rather than using a one size fits all "average" frequency for CDM, it was thought appropriate to try and develop a more objective method to determine the breathing frequency of each individual patient. This is described in method-B.

---

* Artefacts caused by patient movement or recalibration may have affected the DPPG data. Removing such artefacts may improve the specificity of the test. This is discussed further in section 9.3.4.1.2.3.

9.3.4.1.2 Method-B: Objective determination of the breathing frequency of each patient

This method is based upon the following assumptions:

- There is a finite range of frequencies within which all spontaneous breathing occurs. For example, Stefanovska et al. (1999) find this range to be between 9cpm and 24cpm. In this study, the minimum and maximum breathing frequency observed, by eye, in the power spectra of the DPPG data were 8cpm and 32cpm (table 9.3). It is unlikely that the breathing frequency of any person would normally be outside this range.
- It is assumed that breathing is the only, or the main physiological process that causes frequencies between the low (<~10cpm) and high (>~40cpm) frequency regions of the DPPG power spectrum (see PI-1).
- Breathing should normally affect blood flow in both legs in the same way, since any changes are caused by a single source, i.e. pressure variations in the thorax and abdomen (see section 1.3). Therefore, changes in the DPPG signal, at the breathing frequency, should normally be the same and in phase for signals taken from corresponding locations on each limb.

If CDM is performed many times over the range of possible breathing frequencies and the MAPD is calculated each time, it is postulated that the frequency with the lowest MAPD will be that due to breathing[♦]. The CDM outputs corresponding to this breathing frequency should then be used in the MAPD-DPPG test (fig 9.16[a]).
For those patients with confirmed lower limb DVT, the MAPD is expected to be consistently large over the breathing frequency range analysed if the breathing component in the DPPG signal is disrupted, or absent, when a DVT is present. Therefore, a dip in MAPD over this range may be less prominent, or even

[♦] Due to the filtering process used in CDM, the calculated MAPD between the breathing components of the DPPG signals from both limbs may not be exactly zero. Although the actual breathing frequency in the DPPG signals taken from the both limbs may be in phase, the influence of unwanted frequencies passed through the finite width of the LPF will introduce disturbances in the CDM output (see Appendix B). Nevertheless, the actual breathing frequency should be more in phase than any other frequency over the analysed range if breathing is assumed to be the main physiological process occurring.

indistinguishable. Nevertheless, selection of the minimum MAPD should still be justified since any MAPD value should approximate that of the true breathing frequency (e.g., fig 9.16[b]).

Figure 9.16[a] clearly shows a decrease in MAPD within the breathing frequency range. However, a significant decrease in MAPD is also evident in the cardiac range (>~40cpm). This was expected since there was no reason to believe that the microcirculation cardiac pulsations would be greatly out of phase between the limbs. The decrease in MAPD at higher frequencies is related to harmonics of the cardiac frequency.

Fig 9.16: Selection of the minimum MAPD value for use in the MAPD-DPPG test.
Each MAPD value is plotted against the various frequencies used in CDM (using a 5cpm, 10th order LPF).
The dotted lines bound the frequencies between 10-40cpm.

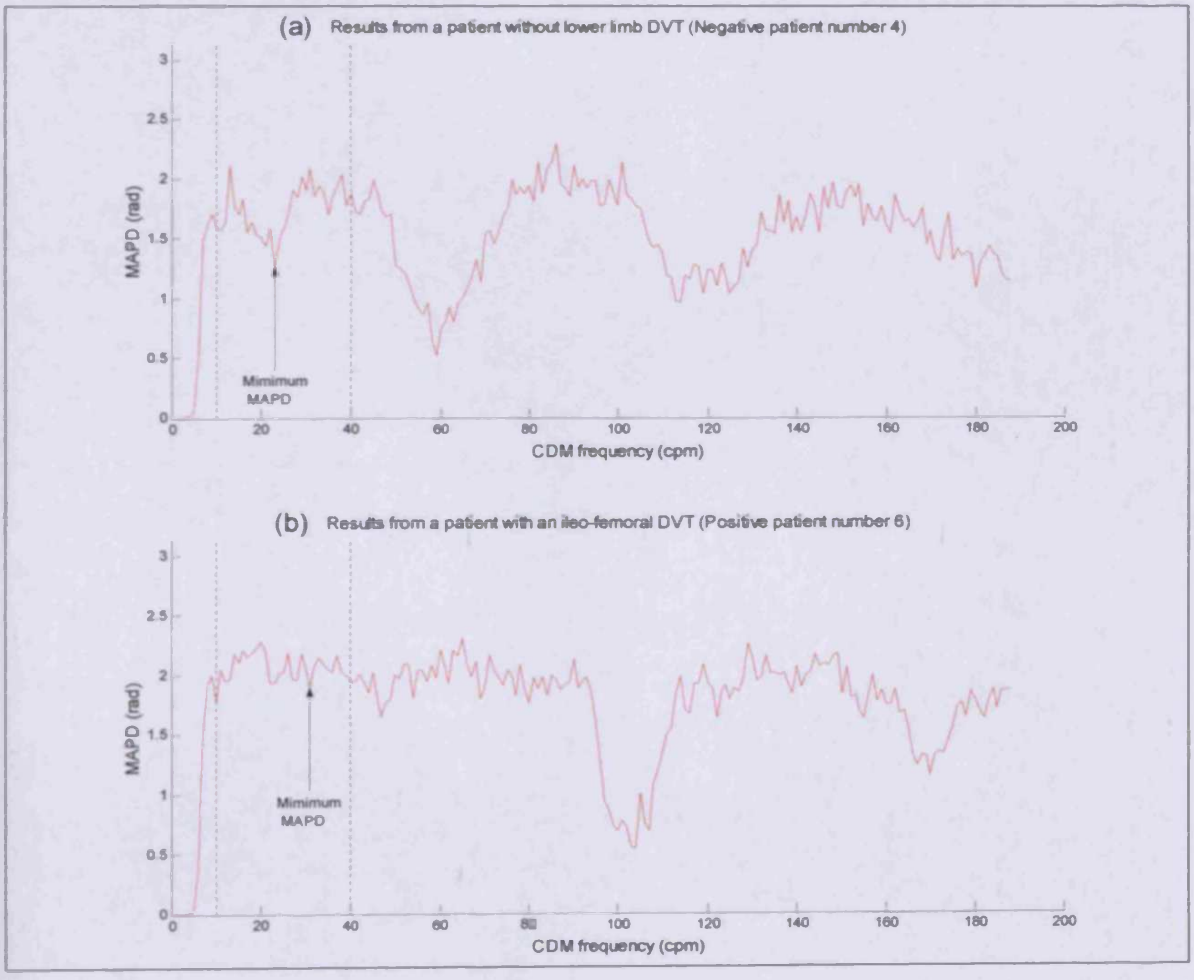

Having decided on a method to determine the breathing frequency, an appropriate LPF had to be selected for use in CDM. Because method-B does not use a fixed breathing frequency for all patients, the choice of LPF could be more flexible than in method-A. The filter does not need to be wide enough to cover the whole range of possible breathing frequencies (except possibly to cover a slight variation about the mean breathing frequency of each person). Instead, different filter widths can be investigated to determine their effect on the calculated minimum MAPD value. An example of this is given in figure 9.17[a] and figure 9.17[b], where the MAPD is calculated at various frequencies, up to the Nyquist frequency, using three different LPFs.

Fig 9.17: The effect of changing the LPF width on the MAPD values.
Each MAPD value is plotted against the various frequencies used in CDM.

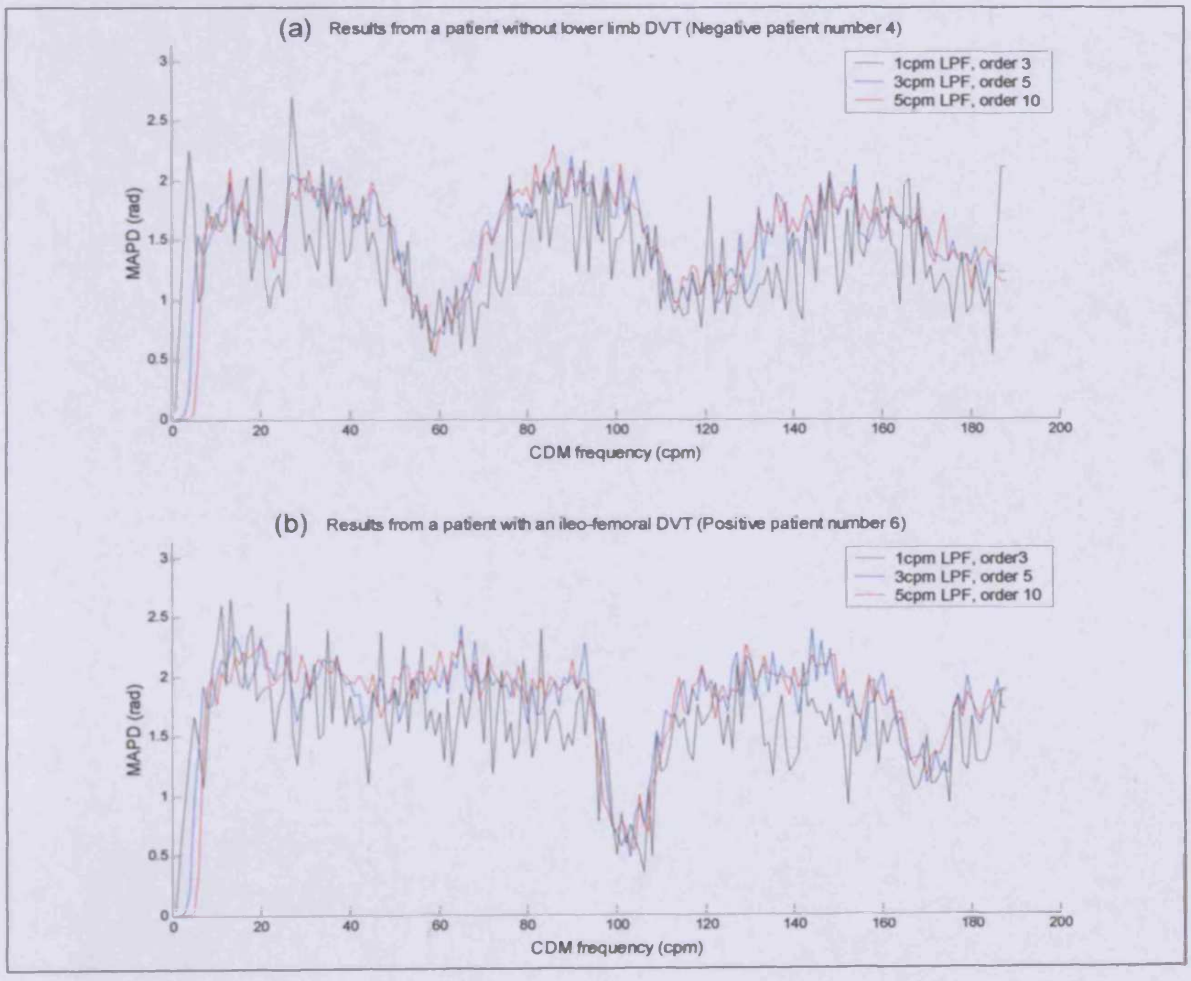

Figure 9.17[a] clearly shows a minimum MAPD in the breathing frequency range for the results of all three LPFs. However, the minimum MAPD is not exactly the same for each filter, nor is the frequency at which it occurs. Therefore, the statistics of any DVT test, using the minimum MAPD value to separate positive from negative cases, may depend on the width of the LPF used in CDM.

Figure 9.17[a] and figure 9.17[b] also indicate that larger LPF widths tend to produce a smoother curve with less variation in MAPD over the whole frequency range. However, it may be unwise to use a very large filter width in the breathing frequency analysis in case the breathing frequency is very low, say 10cpm. Performing CDM at this frequency with a very wide LPF may extend the range of frequencies passed by the filter into the low frequency region of the DPPG power spectrum that is dominated by local and neurogenic controls (PI-1 found these frequencies to be <~10cpm). It is also undesirable for the CDM analysis to encroach on the region of the power spectrum dominated by cardiac frequencies. Heart rates seldom occur at less than 36cpm, except in highly trained athletes (Stefanovska et al., 1999) and the CDM analysis should not extend to frequencies much greater than this.
In addition, figure 9.17[a] and figure 9.17[b] show that the MAPD calculation breaks down at very low frequencies. The frequency, to which this effect extends, increases with the width of the LPF. (It can also be shown that the breakdown extends to higher frequencies when the filter order is decreased, for a constant filter width). Therefore, if the breathing frequencies of the patients are likely to be >~8cpm (from table 9.3), it would be unwise to use a LPF filter very much wider than ~5cpm.

Therefore, the appropriate frequency range from which to calculate the minimum MAPD seems to be between 8-35cpm, using a LPF with a width no larger than 5cpm in CDM.

9.3.4.1.2.1 Results of the CDM analysis using method-B[§]

9.3.4.1.2.2 MAPD results using different LPFs

For each patient, CDM was performed at frequencies between 8-35cpm, in steps of 1cpm. From the CDM phase outputs, the MAPD value corresponding to each frequency was calculated using equation 9.2 (following removal of sections of data at the start and the end of the CDM phase outputs to remove disturbances caused by the LPF. The length of data removed depended on the LPF, as described in Appendix D). The minimum MAPD over the frequency range was then selected as the value to be used in the DVT test. From this point onwards, when describing the results from method-B, any reference to MAPD will mean the minimum MAPD over the 8-35cpm frequency range.

To assess the influence of the LPF on the calculated MAPD, three different filter widths (1cpm, 3cpm and 5cpm) were compared. The filter orders were 3 5 and 10 respectively (chosen as a compromise between the length of ringing and "roll-off" steepness in the transition band, as described in section 9.3.4.1.1.1). The results of implementing method-B are presented below.

Boxplots of the MAPD results (figures 9.18, 9.19 and 9.20) suggest that the two groups of patients (with and without lower limb DVT, confirmed by DUS) are distinguishable. Although there is an overlap in the MAPD values from the two groups, the median value for patients with DVT is always larger than that for patients without DVT. The interquartile range of MAPD values is similar for the two groups of patients but occurs at larger MAPD values for the patients with DVT.

For each of the three different LPFs, a Mann-Whitney test (2-tailed) on the MAPD results from the two patient groups gives $p<0.05$ (p=0.000, 3dp) indicating that the MAPD values can be considered as being from two separate populations.

[§] The MATLAB code used to implement the analysis for method-B can be found in Appendix C.

Fig 9.18: Boxplots of MAPD values using a 1cpm LPF width.
(A description of the features of the boxplot can be found in figure 9.13.)

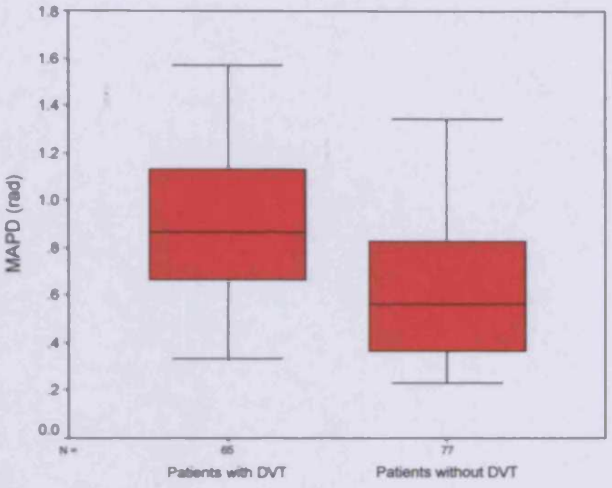

Fig 9.19: Boxplots of MAPD values using a 3cpm LPF width.
(A description of the features of the boxplot can be found in figure 9.13.)

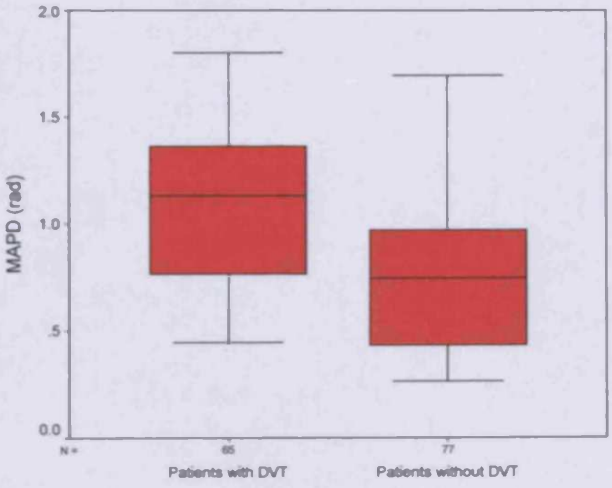

Fig 9.20: Boxplots of MAPD values using a 5cpm LPF width.
(A description of the features of the boxplot can be found in figure 9.13.)

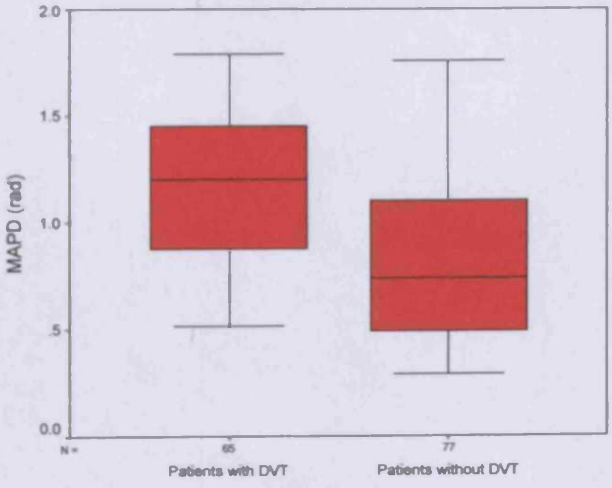

The statistical difference between the two groups of patients indicates that it may be possible to develop a DVT test based on method-B, using an empirical threshold MAPD value as a cut-off between a positive and a negative test result. As described in method-A (section 9.3.4.1.1.3), the threshold MAPD value must be set so that the sensitivity of the test is 100% and no cases of DVT are missed. Therefore, the threshold value should be no greater than the lowest MAPD for all those patients who were confirmed positive for DVT by DUS. If the threshold value is set at this level, the MAPD-DPPG test for DVT, using method-B, would have the statistics shown in table 9.5.

Table 9.5: Statistics of the MAPD-DPPG test for DVT, using method-B.

		LPF width		
		1cpm	3cpm	5cpm
Sensitivity	(1dp)	100.0%	100.0%	100%
Specificity	(1dp)	16.9%	18.2%	20.8%
Negative predicting value	(1dp)	100.0%	100.0%	100.0%
Positive predicting value	(1dp)	50.4%	50.8%	51.6%
Accuracy	(1dp)	54.9%	55.6%	57.0%

The performance of the test seems to depend on the LPF chosen for CDM. Specificity, positive predicting value and accuracy all improved with increasing LPF width. The best specificity achieved was 20.8% using the 5cpm LPF. This is an improvement in specificity, compared to the DVT test using method-A (specificity, 15.6%), but is still not significantly greater than that offered by other diagnostic/screening tests for DVT. For example, in section 9.3.4.1.1.3 it was noted that the specificity of a D-dimer test for DVT may be around 50%, depending on the type of assay used. In fact, studies using DPPG with dorsiflexions of the foot have shown a 47% specificity (Tan and da Silva, 1999). Therefore, if the MAPD-DPPG test is to be considered a serious alternative, it was considered necessary to improve the specificity of the test even further.

To do this, several factors were considered that may have had a detrimental effect on the DPPG signal during the data collection (e.g., recalibration, patient movement etc.). It

was hoped that by removing or reducing the influence of any artefacts caused by these factors, the specificity of the test would improve.
The length of DPPG data used in the CDM analysis was also considered, since all results so far have been calculated using the whole of the DPPG data collected from each patient (~10min). It was thought that analysing smaller portions of the data may improve the test results by reducing the possibility of artefacts. However, any improvements may be offset by having less data available to calculate the MAPD value.

The results of these investigations are described below.

9.3.4.1.2.3 The effect of artefacts on the specificity of the MAPD-DPPG test

Artefacts are defined here as disturbances in the DPPG signal that are caused by non-physiological factors. Three causes were considered: Patient movement, the influence of talking and recalibration during data collection.

Patient movement:

DPPG is very susceptible to artefacts caused by movement. Therefore, all patients were asked to remain perfectly still throughout the 10 minutes while the DPPG data were being collected. However, this is difficult. Lying absolutely still for this length of time is likely to cause unease. Consequently, some patients (mainly the more elderly patients) were observed to adjust their body position during the test. Such movement is likely to disturb the DPPG signal. If carried out gently, the movement may cause no more than a slow change in DPPG amplitude. However, larger more rapid movements may cause more prominent changes in the DPPG signal. This is especially true for movement of the same limb to which the DPPG probe is attached.

Each time the patient moved in this way, they were reminded to try and remain still and a record of the movement was noted down. If the movement was large, and towards the beginning of the data collection period, the procedure was restarted. However, if the movement was small, so that the amplitude change of the DPPG signal was small and gradual, rather than large and abrupt, the data collection was not restarted. This was also the case if the movement occurred towards the end of the data collection period and

restarting the procedure would have been inconvenient for the patient (especially those who had been diagnosed with DVT and were eager to receive treatment).

There were 3 patients who were very restless during the test (positive patient numbers 39 and 58; negative patient number 36). In addition, on 3 occasions, the patient's feet began to involuntarily shake (positive patient numbers 1 and 30; negative patient number 48).

It is difficult to account for patient movement artefacts when analysing the DPPG data. Even if the location of the artefact within the data is known, it is not possible to remove it without influencing the rest of the data. Sharp peaks, which exist for a short time, could be removed and the data interpolated over this period. However, it may not be sensible to apply filtering techniques because this could also remove frequencies within the signal, caused by the various physiological processes described in PI-1. Such frequencies are observed over a wide range from the very low frequencies, caused by local or neurogenic controls of the microcirculation, to the high frequencies associated with cardiac pulsations and the breathing frequencies in between.
Therefore, it was decided not to make any corrections for the movement artefacts in the DPPG signals. In any case, it was thought that such artefacts may not greatly affect the calculated MAPD, which is an average value, when the whole 10 minutes of data are used. However, any disturbances may be more important if shorter lengths of the signal are analysed. The effect of analysing different lengths of the DPPG data is investigated in section 9.3.4.1.2.4.

Influence of talking on the DPPG signal:

The MAPD is calculated after performing CDM at frequencies over the range 8-35cpm. These frequencies within the DPPG signal are believed to be caused by the process of breathing (see PI-1). Therefore, each patient was asked to remain silent throughout the investigation because it was thought that talking may have prevented the patient from breathing at a regular rate. Taking short breaths in between speaking may have reduced the periodicity of the phasic venous blood flow, caused by breathing, and consequent microcirculation blood volume changes. As a result, the breathing frequency could

have been less well defined in the DPPG signal, resulting in an unclear minimum MAPD over the 8-35cpm breathing range.
Nevertheless, 8 patients continually ignored this request and continued talking during the investigation (positive patient numbers 32, 41, 44 and 64; negative patient numbers 36, 61, 63 and 68).

It is difficult to remove disturbances in the DPPG signal caused by talking. The DPPG data for the patients who talked during the investigations could have been excluded from all the analyses but it was decided not to do this. If talking is limited to short periods, it may not have an overly detrimental effect on the calculated MAPD, which is an average value, when the whole 10 minutes of data are used. In addition, any disturbance to the venous blood flow, caused by talking, is likely to affect both the lower limbs in the same way (in the absence of disease). Therefore, since the MAPD is a comparison of the phase of the breathing component in the DPPG signal taken from each foot, any artefacts caused by talking may cancel out when calculating the difference.

DPPG recalibration during data collection:

The largest artefact in the DPPG data is probably due to recalibration. As described in section 9.3.2, a slow drift in the DPPG signal during data collection from some patients resulted in the signal going out of the measurement range of the instrument. In these cases, the DPPG device had to be recalibrated to bring the DPPG signal back into the measurable range. In some cases, the patient was asked if it would be OK to restart the test. However, in 22/142 cases, recalibration was performed while data collection was taking place to avoid patient inconvenience (especially for those who had been diagnosed with DVT and were eager to receive treatment). Recalibration was performed during the test for positive patient numbers 5, 7, 11, 19, 37, 39, 46, 48, 57, 58, 61, 62, 63, 65 and negative patient numbers 7, 32, 64, 70, 71, 72, 73, 77.

The calibration procedure results in large, abrupt changes in the DPPG signal. These changes do not occur in the same way for both DPPG channels and are likely to significantly affect the calculated MAPD. Since the changes in the DPPG signal are so considerable, it was decided that the MAPD values calculated from these signals should

not be included when determining the statistics of the MAPD-DPPG test. The statistics of the test, following exclusion of the data affected by re-calibration, are displayed in table 9.6.

Table 9.6: MAPD-DPPG test statistics, excluding all data affected by recalibration.

- *Positive patient numbers 5, 7, 11, 19, 37, 39, 46, 48, 57, 58, 61, 62, 63 and 65 were excluded from the analyses.*
- *Negative patient numbers 7, 32, 64, 70, 71, 72, 73 and 77 were excluded from the analyses.*

		LPF width		
		1cpm	3cpm	5cpm
Sensitivity	(1dp)	100.0%	100.0%	100.0%
Specificity	(1dp)	18.8%	20.3%	23.2%
Negative predicting value	(1dp)	100.0%	100.0%	100.0%
Positive predicting value	(1dp)	47.7%	48.1%	49.0%
Accuracy	(1dp)	53.3%	54.2%	55.8%

Comparing the MAPD-DPPG test statistics with those in table 9.5, it can be seen that the positive predicting value and the accuracy are slightly lower when the signals affected by recalibration are removed. However, there is a modest improvement in specificity for all filter widths (increasing by 1.9%, 2.1% and 2.4% respectively for the 1cpm, 3cpm and 5cpm LPFs).

This may not necessarily indicate that recalibration adversely affects the specificity of the test. The increase in specificity when the recalibrated data are removed may simply be the result of a change in the total number of MAPD values from which to calculate the statistics. Removing a different set of 22 patient data (14 random positives and 8 random negatives) would also produce a change in specificity, as illustrated in figure 9.21.

However, an important point to note is that all the MAPD values for the data affected by recalibration (from patients with and without DVT, diagnosed with DUS) were large enough to be classed as positive in the MAPD-DPPG test. This was true for the 3 different LPF widths. Therefore, it seems likely that recalibration does disrupt the DPPG data sufficiently to produce false positive results.

Fig 9.21: A boxplot of 500 MAPD-DPPG test specificities.

Each specificity was calculated after removing 14 random positive patients and 8 random negative patients from the CDM analyses (MAPD values for use in the MAPD-DPPG test were calculated using a 5cpm LPF in CDM).

(A description of the features of the boxplot can be found in figure 9.13.)

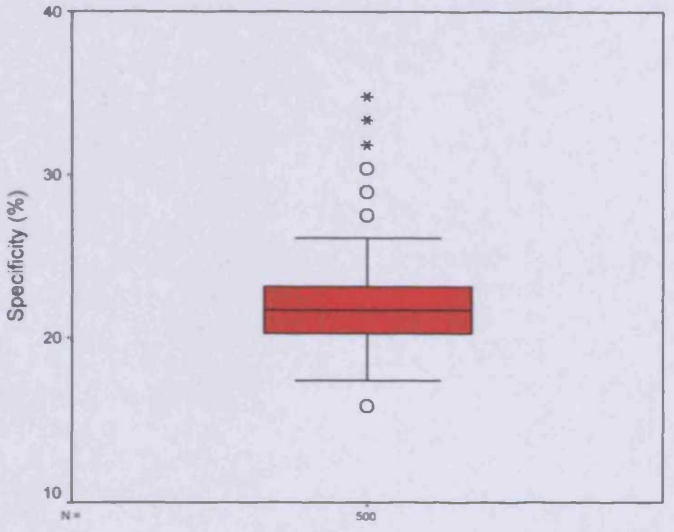

9.3.4.1.2.4 The effect of DPPG signal length on the specificity of the MAPD-DPPG test

Up until this point, all MAPD values have been calculated using the whole length of the DPPG data taken from each patient (~10min). However, analysing smaller sections of the data may help to improve the specificity of the test by reducing the amount of artefact, e.g., caused by patient movement, within the analysed section.

On the other hand, looking at smaller sections of the DPPG data may have a detrimental effect since the MAPD is an average value. The MAPD may be more likely to show a phase difference between the breathing components of the DPPG signals when more data are available to calculate it.

Apart from possible improvements in specificity, reducing the amount of DPPG data required in the analysis would also be an advantage in any real life application of the test. This would reduce the time needed to acquire the data and speed up the time taken to complete the test, resulting in a faster turnaround of patients and greater efficiency.

The effect of analysing different lengths of the DPPG data on the statistics of the MAPD-DPPG test is shown in the following tables. In each case, the first 4min, 6min and 8min of the DPPG data collected from each patient are analysed♦. Tables 9.7, 9.8 and 9.9 show the results when the data from all the patients are analysed. Tables 9.10, 9.11 and 9.12 show the results after excluding those patients for which recalibration took place at any time during the DPPG data collection (positive patient numbers 5, 7, 11, 19, 37, 39, 46, 48, 57, 58, 61, 62, 63 and 65; negative patient numbers 7, 32, 64, 70, 71, 72, 73 and 77). Excluding all these patients for each DPPG data length was considered necessary to allow a fair comparison of the test statistics, even if the recalibration did not occur during the period of data analysed. For example, recalibration 5 minutes after the start of the DPPG data collection will not have any influence on the MAPD value calculated using the first 4 minutes of the signal. Nevertheless, excluding all the patient data affected by recalibration, at any time, provides an equal number of MAPD values from each group of positive and negative patients from which to calculate the test statistics. If this was not the case, any difference in the test statistics when analysing different lengths of the DPPG signal may have been caused by differing numbers of MAPD values from each group of patients rather than the length of the DPPG signal.

♦ To prevent the effects of filter ringing from influencing the results, large disturbances in the CDM phase outputs were removed before calculating the MAPD values. For the 1cpm, 3cpm and 5cpm LPFs, 109s, 60s and 72s of data were removed from the start and the end of the CDM output data (see Appendix D). Therefore, the initial length of DPPG data used in the analyses needed to be greater than 218s, 120s and 142s respectively, for each LPF. Consequently, signal lengths less than approximately 4minutes could not be compared.

Tables 9.7, 9.8 and 9.9: MAPD-DPPG test statistics using different lengths of the DPPG signal.

(The grey shaded box in table 9.9 indicates that the negative predicting value could not be calculated because no patients were diagnosed negative for DVT by the MAPD-DPPG test.)

Table 9.7: LPF width, 1cpm

		First 4min	First 6min	First 8min	Whole data
Sensitivity	(1dp)	100.0%	100.0%	100.0%	100.0%
Specificity	(1dp)	1.3%	11.7%	10.4%	16.9%
Negative predicting value	(1dp)	100.0%	100.0%	100.0%	100.0%
Positive predicting value	(1dp)	46.1%	48.5%	47.7%	50.4%
Accuracy	(1dp)	46.5%	51.8%	50.7%	54.9%

Table 9.8: LPF width, 3cpm

		First 4min	First 6min	First 8min	Whole data
Sensitivity	(1dp)	100.0%	100.0%	100.0%	100.0%
Specificity	(1dp)	9.1%	14.3%	22.1%	18.2%
Negative predicting value	(1dp)	100.0%	100.0%	100.0%	100.0%
Positive Predicting value	(1dp)	48.1%	49.2%	51.2%	50.8%
Accuracy	(1dp)	50.7%	53.2%	57.1%	55.6%

Table 9.9: LPF width, 5cpm

		First 4min	First 6min	First 8min	Whole data
Sensitivity	(1dp)	100.0%	100.0%	100.0%	100.0%
Specificity	(1dp)	0.0%	14.3%	24.7%	20.8%
Negative predicting value	(1dp)		100.0%	100.0%	100.0%
Positive predicting value	(1dp)	45.8%	49.2%	52.1%	51.6%
Accuracy	(1dp)	45.8%	53.2%	58.6%	57.0%

Tables 9.10, 9.11 and 9.12: MAPD-DPPG test statistics using different lengths of the DPPG signal. (Excluding all data for which re-calibration took place during the investigation.)

Table 9.10: LPF width, 1cpm

		First 4min	First 6min	First 8min	Whole data
Sensitivity	(1dp)	100.0%	100.0%	100.0%	100.0%
Specificity	(1dp)	1.4%	21.7%	14.5%	18.8%
Negative predicting value	(1dp)	100.0%	100.0%	100.0%	100.0%
Positive predicting value	(1dp)	42.9%	48.1%	45.4%	47.7%
Accuracy	(1dp)	43.3%	54.6%	50.0%	53.3%

Table 9.11: LPF width, 3cpm

		First 4min	First 6min	First 8min	Whole data
Sensitivity	(1dp)	100.0%	100.0%	100.0%	100.0%
Specificity	(1dp)	24.6%	21.7%	24.6%	20.3%
Negative predicting value	(1dp)	100.0%	100.0%	100.0%	100.0%
Positive predicting value	(1dp)	49.5%	48.1%	48.5%	48.1%
Accuracy	(1dp)	56.7%	54.6%	55.9%	54.2%

Table 9.12: LPF width, 5cpm

		First 4min	First 6min	First 8min	Whole data
Sensitivity	(1dp)	100.0%	100.0%	100.0%	100.0%
Specificity	(1dp)	17.4%	17.4%	27.5%	23.2%
Negative predicting value	(1dp)	100.0%	100.0%	100.0%	100.0%
Positive predicting value	(1dp)	47.2%	46.7%	49.5%	49.0%
Accuracy	(1dp)	52.5%	52.1%	57.6%	55.8%

Tables 9.7-9.12 show that there are changes in the statistics of the MAPD-DPPG test when different lengths of the DPPG signal are analysed. However, the changes do not seem to follow a consistent pattern when comparing the results for each LPF. Figure 9.22 summarises how the specificity varies with the length of the DPPG signal used in the analyses and also with the LPF used in CDM. (It is worth remembering here that the cut off MAPD value in each test is set so that the sensitivity and negative predicting value are fixed at 100%. This is required to ensure that all those patients with DVT (confirmed with DUS) are also found positive by the MAPD-DPPG test. Therefore, the usefulness of the MAPD-DPPG test is ultimately determined by its specificity, which indicates the ability of test to rule out DVT.)

Fig 9.22: The specificity of the MAPD-DPPG test using different lengths of the DPPG data and different LPF widths.

- *The solid lines connect the values of specificity that were calculated using the DPPG data from all patients.*
- *The dotted lines connect the values of specificity that were calculated following the removal of DPPG data affected by recalibration.*

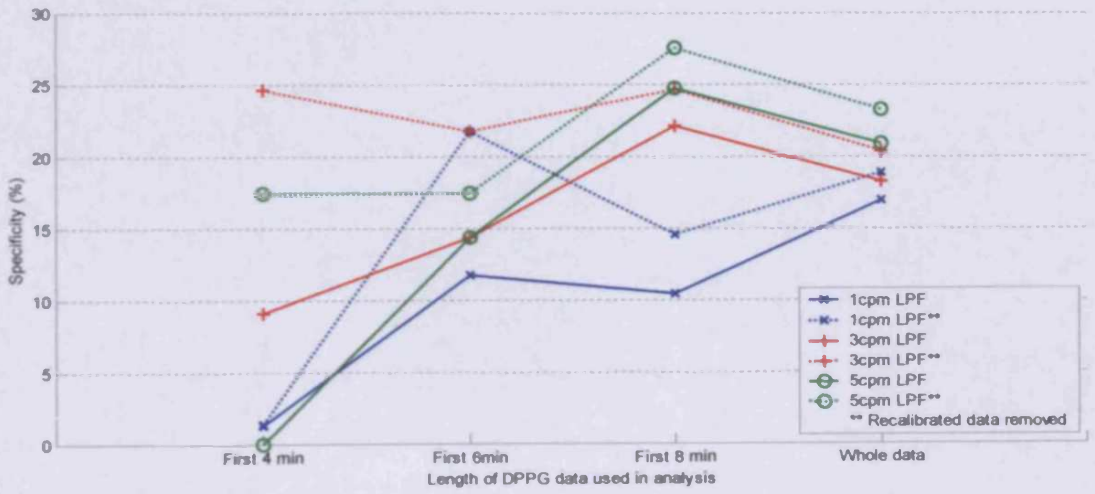

From figure 9.22 it can bee seen that:

- Removing the recalibrated data improves specificity. This is observed for all LPF widths and lengths of DPPG signal analysed. However, as mentioned above (section 9.3.4.1.2.3), this may simply be the result of changes in the total number of patients used to calculate the specificity.

- The specificity shows a tendency to increase when the DPPG data length is increased from 4minutes to 6minutes. However, as the length of the DPPG data increases beyond this, no definitive pattern emerges between DPPG data length and the specificity. Initially, it was thought that the specificity would increase with increasing length of the DPPG signal because any artefacts in the data may be less important when the MAPD is averaged over a longer length of data. However, it is difficult to draw any such conclusions from figure 9.22. More patient data is required to investigate this further.

- Conclusions concerning the LPF width are also less than definitive. It appears that, when at least 8 minutes of the DPPG signal is used in the CDM analysis, the specificity increases with increasing LPF width, whether or not the recalibrated data are removed. It was thought that the reason for this may be a consequence of the true breathing frequency moving out of the analysed range when a very narrow LPF is used in CDM. The range of frequencies included in each CDM analysis is given by "*selected frequency* $\pm$ *LPF width*". Therefore, if the actual breathing frequency of the patient tends to wander around the selected breathing frequency, it has more chance of being included in the analysis as the width of the LPF increases. However, a pattern of increasing specificity with LPF width is not observed for DPPG data lengths less than 8minutes. Here, the specificity changes with LPF width in a more variable way.

The best specificity (27.5%) is obtained when the first 8 minutes of DPPG data are analysed using a 5cpm LPF and all the data affected by recalibration are excluded from the analysis.

9.3.4.1.3 Conclusions regarding the CDM analyses at the breathing frequencies

Using method-B, i.e., selecting the minimum MAPD over a 8-35cpm breathing frequency range, improved the specificity of the MAPD-DPPG test compared to method-A, in which an "average" breathing frequency was used to calculate the MAPD. The specificity increased from 15.6% to 20.8% when a 5cpm LPF width was used in the CDM analysis (section 9.3.4.1.2.2).

Removing all the patient data affected by recalibration increased the specificity of the MAPD-DPPG test even further. A specificity of 23.2% was achieved using a 5cpm LPF width (section 9.3.4.1.2.3). However, it remains uncertain whether the improvement was due to removing the data affected by recalibration or a consequence of changing the number of MAPD values available to calculate the specificity. Nevertheless, it was observed that all the MAPD values calculated for those patients without DVT (confirmed with DUS) were above the threshold for DVT in the MAPD-DPPG test, indicating that recalibration may disturb the data sufficiently to generate false positive results.

Analysis of different lengths of the DPPG data (section 9.3.4.1.2.4) led to inconclusive results. No clear trend was observed between the length of DPPG data and the specificity of the MAPD-DPPG test, except figure 9.22 showed a significant improvement in specificity when 6minutes of data, or longer, were used in the CDM analyses. This was postulated to be due to artefacts in the data (e.g., caused by patient movement) being less important when the MAPD is averaged over a longer period of time.
Increasing the LPF width also seemed to improve specificity but, as with DPPG data length, there was not a clear trend.

Overall, the best specificity for the MAPD-DPPG test (27.5%) was achieved using method-B, the first 8 minutes of DPPG data and a 5cpm LPF width in CDM (excluding the DPPG data where recalibration took place during the data collection).

9.3.4.1.4 Alternative influences on the MAPD value, other than DVT

It is appropriate to consider whether factors, other that DVT, had any influence on the calculated MAPD values. Although there is statistical evidence indicating that the MAPD is different for the two groups of patients (with and without DVT, confirmed with DUS) the presence of the thrombus may not be the only distinguishing factor between the two groups. Some other disease, e.g., venous insufficiency, varicose veins etc., may also influence the MAPD values, which just happens to correspond to the split observed when the patients are classified as positive or negative for DVT (by DUS). Alternatively, it may be a combination of factors causing a difference between the MAPD values of the two patient groups.

The medical history of each patient used in the study was not comprehensive enough to assess the effect of conditions other than DVT on the calculated MAPD values. However, it may be that, as a person ages, the vascular system becomes more dysfunctional and the MAPD-DPPG test detects a degeneration of the vascular system as a whole, not just the effects of DVT. Since the age of each patient could be obtained from the patient records, it was possible to test this association.

To do this, the set of results that gave the best MAPD-DPPG test specificity were considered. The best specificity (27.5%) was obtained using the first 8 minutes of DPPG data and a 5cpm LPF width in CDM (excluding DPPG data where recalibration took place during the data collection).

Figure 9.23 plots the MAPD value versus age for each patient. The plot does not indicate a strong correlation between the two variables and this was confirmed by correlation statistics. The Pearson correlation coefficient gave a non-significant (p=0.831, 2-tailed), slightly negative (r=-0.020) correlation between MAPD and age, ruling out a linear relationship between the variables. The Pearson correlation coefficient works best when the data do not form a skewed distribution and have no outliers. Figure 9.23 suggests that this is the case for the MAPD-age data. However, Spearman's rank correlation coefficient was also calculated, which uses a ranking system that does not depend on the distribution of the original data and is less influenced by the presence of outliers. This test also gave a non-significant (p=0.853, 2-

tailed) slightly negative (ρ=-0.17) correlation between MAPD and age, ruling out a linear relationship between the two variables.

Fig 9.23: Correlation between MAPD and age for each patient.

Each point represents a single patient (49 patients with DVT confirmed with DUS; 68 patients with no DVT confirmed with DUS).

(Excluding patients for which recalibration took place during the data collection (see section 9.3.4.1.2.3) and those for which less than 8 minutes of DPPG data were collected, i.e., positive patient numbers 21 and 29. The age of negative patient number 20 was not available.)

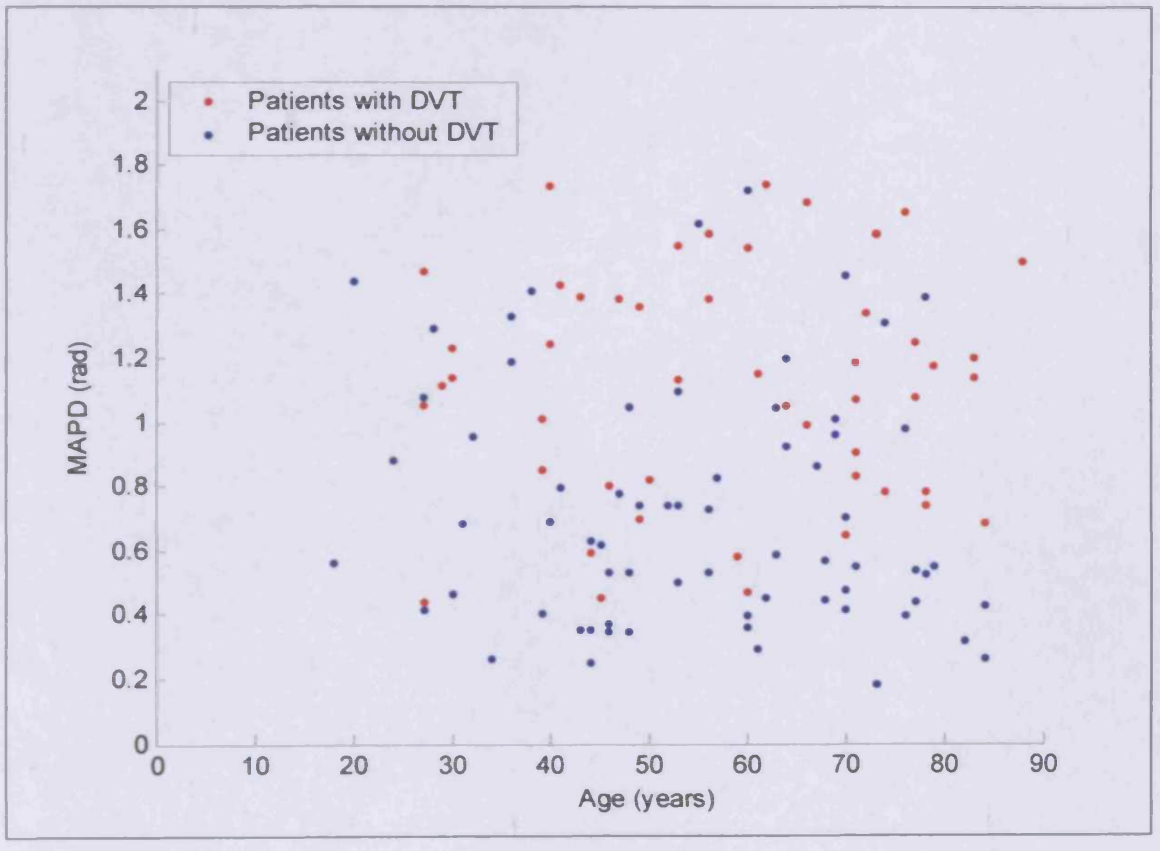

9.3.4.1.5 Relationship between DVT location and MAPD value

Due to the large number false positive diagnoses, the MAPD-DPPG test seems more suited to screening out patients without DVT rather than used as a diagnostic test for the condition. Nevertheless, within the group of patients who were diagnosed (true) positive with the MAPD-DPPG test, it was thought important to consider whether there is any association between the MAPD value and the location of the DVT in the limb.

To do this, DVT location was broadly split into two categories. An above knee (AK) DVT was defined as one that occurs in the popliteal vein or more proximally. A below knee (BK) DVT was defined as one that occurs distal to the level of the popliteal vein. Bilateral DVTs were classed as AK if at least one DVT was AK.

In real life applications of the test, an ability to distinguish between AK and BK-DVT could be advantageous when deciding on a DVT management strategy to follow. For example, it has been suggested that treatment can be withheld for small calf vein DVTs, which may dissolve spontaneously, in favour of repeat testing to check for propagation to more proximal levels (section 2.6). However, it has always been recognised that AK-DVTs may lead to fatal complications and require immediate treatment.

DVT is thought to most commonly originate in the small veins of the calf before increasing in size and propagating to more proximal regions (section 2.2). Therefore, one might expect generally larger AK-DVTs to disturb venous blood flow more than smaller BK-DVTs. In addition, multiple veins in the calf provide alternative pathways for the venous blood to flow even if one of the veins is occluded. This is not the case for the larger, more proximal veins.

Therefore, the MAPD-DPPG test may be able to distinguish between AK and BK-DVTs depending on the level of the disturbance caused to the venous blood flow and, consequently, the DPPG signal. For example, it may be that the range of MAPD values for those patients with DVT can be split into two groups representing BK-DVTs and AK-DVTs. If BK-DVTs disturb venous blood flow to a lesser extent than AK DVTs, the corresponding MAPD value may be smaller.

Relationship between MAPD and AK or BK-DVT:

To look for an association between DVT location and MAPD value, the set of results that gave the best MAPD-DPPG test specificity using method-B were considered. The best specificity (27.5%) was obtained using the first 8 minutes of DPPG data and a 5cpm LPF width in CDM (excluding the DPPG data where recalibration took place during the data collection).

Table 9.13 lists those patients who were classified as having AK or BK-DVT from the 65 patients diagnosed as positive for DVT with DUS (see Appendix H). In total, there were 42 patients with AK-DVT and 23 patients with BK-DVT. Figure 2.4 compares the MAPD results for the AK and BK DVT groups.

Table 9.13: List of patients with AK or BK-DVT, as diagnosed with DUS.

The numbers in red and blue indicate those patients not included in the MAPD-DPPG test (therefore the MAPD value was not available).

- *The numbers in red indicate the patients for which the DPPG device was recalibrated during the first 8 minutes of the investigation.*
- *The numbers in blue indicate the patients for which less than 8 minutes of DPPG data were collected.*

	Positive patient number
AK-DVT	1, 2, 3, 5, 6, 9, 11, 12, 14, 15, 16, 17, 18, 19, 22, 25, 27, 28, 30, 31, 33, 34, 36, 37, 38, 40, 41, 42, 43, 45, 46, 47, 49, 50, 51, 53, 57, 58, 61, 63, 64, 65
BK-DVT	4, 7, 8, 10, 13, 20, 21, 23, 24, 26, 29, 32, 35, 39, 44, 48, 52, 54, 55, 56, 59, 60, 62

Fig 9.24: Boxplots of MAPD values for patients with AK and BK-DVT.
(A description of the features of the boxplot can be found in figure 9.13.)

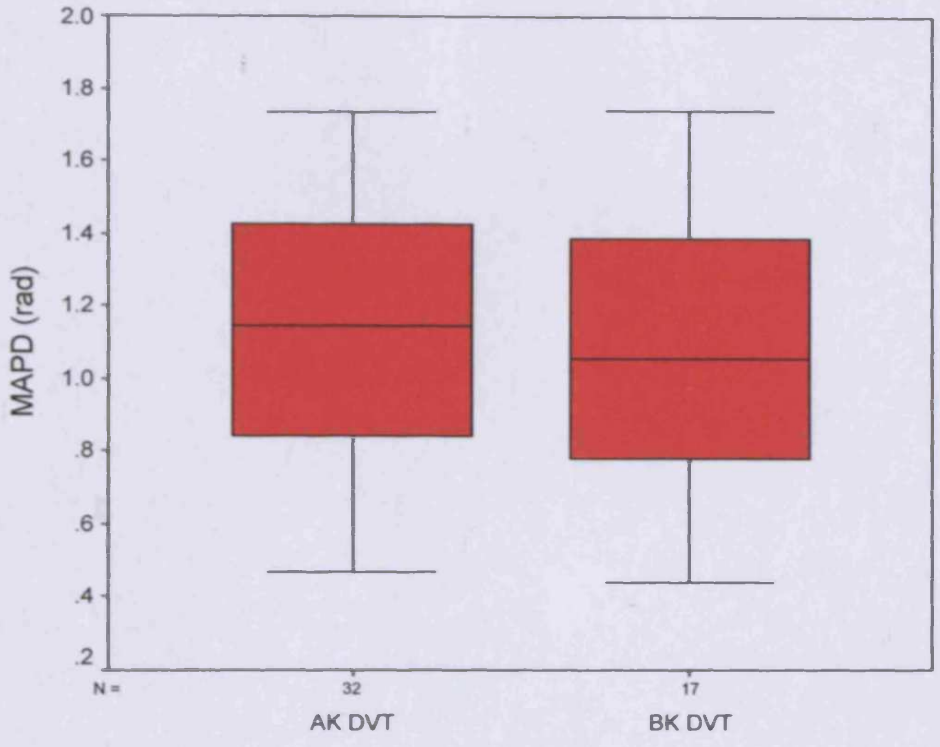

The boxplots (fig 9.24) do not show a clear difference between the MAPD values from the patients with AK and BK-DVT. The range, interquartile range and median of the MAPD values from the two groups of patients are all similar. A Mann-Whitney test (2-tailed) on the MAPD values from the AK and BK groups gave, $p>0.05$ ($p=0.324$, 3dp) suggesting that the null hypothesis of no difference between the two groups, based on the MAPD values, cannot be rejected.

Therefore there appears to be no statistical difference between the MAPD values from the two groups of patients with AK and BK-DVT. Even if the MAPD-DVT test is able to identify a DVT, it does not seem able to identify the location of the DVT in the lower limb from DPPG probes placed on the soles of the feet.

However, it may be that the amount by which the vessel lumen is occluded by the DVT has a greater influence on the MAPD value than the location of the DVT in the limb. This would be likely if the disruption to the phasic blood flow in the large veins of the lower limbs correlates with the degree of vessel occlusion. For small DVTs, phasic venous blood flow may still occur with only little disruption, leading to small MAPD

values, compared to those for larger DVTs where venous blood flow becomes continuous. Therefore, small non-occlusive DVTs may be associated with small MAPD values regardless of their location in the lower limb. The DUS results used in this study did not always provide information about the degree of occlusion when a DVT was present because the initial remit of this study was only to detect DVT in the lower limbs using DPPG, so this information was not required. Therefore, the association between vessel occlusion and MAPD value could not be investigated here.

9.3.4.1.6 Limitations of the MAPD-DPPG test

The above analyses indicate that it is possible to detect DVT in the lower limbs by signal processing DPPG signals collected from the soles of the feet. The DVT test procedure requires no more from the patients than to remain still and in a supine position while the DPPG data are collected. This is a distinct advantage over current PPG tests for DVT which require active patient participation, usually via dorsiflexions of the foot. Therefore, the new test can be performed on the majority of individuals, not just those who are mentally or physically able to perform the exercises. However, the test is not without its limitations and these deserve further consideration.

The MAPD compares the phase of the breathing component in the DPPG signals from both limbs. The MAPD value was shown to be generally larger for those patients with DVT. However, it cannot specify which limb the DVT resides in. The breathing component in the DPPG data from the limb with DVT was not found to lag or lead the corresponding component in the limb without DVT, only to be disrupted. For example, if the mean phase difference (MPD) is calculated from the CDM outputs instead of the mean *absolute* phase difference (MAPD), no statistical separation is found between the groups of patients with or without DVT, as illustrated by the boxplots in figure 9.25.

Fig 9.25: Boxplots showing the MPD of the breathing frequency components (established using method-B), calculated using 8 minutes of DPPG data taken from the soles of the feet.

The results exclude those patients for which recalibration took place during the data collection (see section 9.3.4.1.2.3).

- *For patients with DVT, the MPD was calculated from the phase of the breathing component in the data taken from the limb with DVT minus that of the limb without DVT.*
- *For patients without DVT, the MPD was calculated from the phase of the breathing component in the data taken from the left limb minus that of the right limb.*

(A description of the features of the boxplot can be found in figure 9.13.)

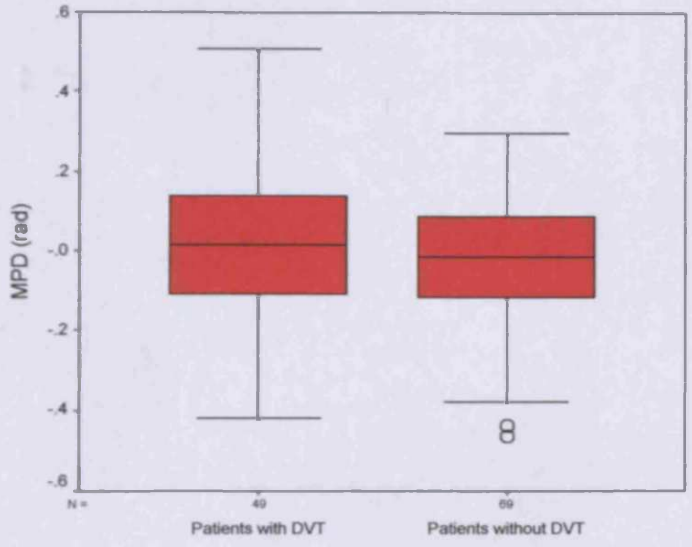

It is also uncertain how well the test would perform in the case of bilateral lower limb DVT. The test compares the breathing component of the DPPG signal between two limbs. Therefore, if the breathing component is disrupted in both limbs it is likely that the MAPD value would still be large. Previous studies suggest that the incidence of bilateral DVT may be quite significant. Using ultrasound bilaterally, Miller et al. (1998) found bilateral DVT in 15% of 250 positive cases of DVT when only unilateral signs and symptoms were present. For patients with unilateral, bilateral or no signs and symptoms of DVT, Naidich et al. (1996) found the incidence of bilateral DVT to be 44% for those who tested positive for DVT, using ultrasound bilaterally (38% for those with only unilateral signal and symptoms). However, the effect of bilateral DVT on the MAPD value could not be investigated further in this study because bilateral DUS scanning was not carried out unless requested by the referring clinician. Therefore, in

most cases, when DVT was diagnosed with DUS, it was not possible to tell whether bilateral DVT was present. There was one case where bilateral DVT was confirmed by DUS (femoral DVT in the left limb and posterior tibial vein DVT in the right limb; both partially recanalised). However, this patient was excluded from the analyses because the DPPG device had to be recalibrated during the data collection. Therefore, to determine the effect of bilateral DVT on the MAPD value, further investigation is required.

All DPPG data in the patient investigation were collected by placing the probes at the same location on each limb, i.e., the soles of the feet. Placing the probes on symmetrical parts of the body was thought necessary to ensure that any phase difference caused by observing the breathing component at unequal distances along the limb would be minimised. However, because of this, the test may not be suitable for use on amputees. The probes could be placed at the lowest point on the amputated limb and at the corresponding location on the contralateral limb, but any DVT distal to this location could be missed.

The influence of venous or arterial disease, other then DVT, on the DPPG signal and the MAPD value remains uncertain. Allen and Murray (2000) demonstrated that cardiac pulsations in PPG signals taken from the toes of both lower limbs were out of phase and had a different shape when arterial disease was present in one of the limbs. However, in this study, arterial disease was thought unlikely to affect the breathing component of the DPPG signal since it is understood to be derived from the venous side of the circulation (see PI-1). Nevertheless, other venous diseases may influence the MAPD value. However, not enough information was collected in this study to investigate this in any great detail. Further investigation is required to determine the effect of other diseases on the MAPD value.

9.3.4.2 CDM analysis of the cardiac frequencies

Examination of the power spectra of the DPPG signals in section 9.3.3 did not reveal any significant differences at the cardiac frequencies (>~40cpm) when lower limb DVT was present. Nevertheless, for completeness, it was felt that these frequencies should also be analysed by CDM. Therefore, in a similar way to the breathing frequencies, the MAAD and MAPD values were calculated for each patient. These values were then compared between the groups of patients with and without DVT (confirmed with DUS) and their possible use in a DVT test considered.

As always, the first step in CDM analysis is to decide which frequency is to be investigated. Since the cardiac rate was not independently measured during the DPPG data collection in the patient investigation, the appropriate frequency had to be derived from the power spectra of the DPPG signals themselves. Since the cardiac frequencies could be clearly seen in the power spectra of almost all (139/142) the DPPG signals, it was thought appropriate to select each cardiac frequency by eye*. This involved no more than looking at the power spectra and making a note of the appropriate frequency. However, one complication was that the heart rate varies over the time that the DPPG data are collected (due to nervous system controls etc.). In addition, the amplitude of the cardiac frequency may be modulated by lower frequency components. Both of these processes result in a band of cardiac frequencies in the power spectra rather than a single peak. Since only one frequency can be examined at any one time using CDM, a representative frequency had to be chosen. This was taken to be the central frequency in the observed cardiac band, which was considered to represent an "average" cardiac frequency, modulated by lower frequencies, causing the sidebands. An example illustrating how the cardiac frequency was selected is shown in figure 9.26.

* Method-A or method-B, developed for analysis of the breathing frequencies, were not considered the best way to analyse the cardiac frequencies. These methods were developed because it was not always possible to see the breathing frequency range in the power spectra of the DPPG data. Therefore, a breathing frequency, specific to each patient, could not always be selected by eye. However, this was possible for the cardiac frequencies, which occur at higher frequencies than those due to any other physiological processes and were therefore easy to pick out.

Fig 9.26: An example illustrating selection of the cardiac frequency for CDM.

The dashed red lines represent the range frequencies in the cardiac band. The solid red line represents the frequency selected for CDM.
(The power spectrum is that of the DPPG data collected from negative patient number 5.)

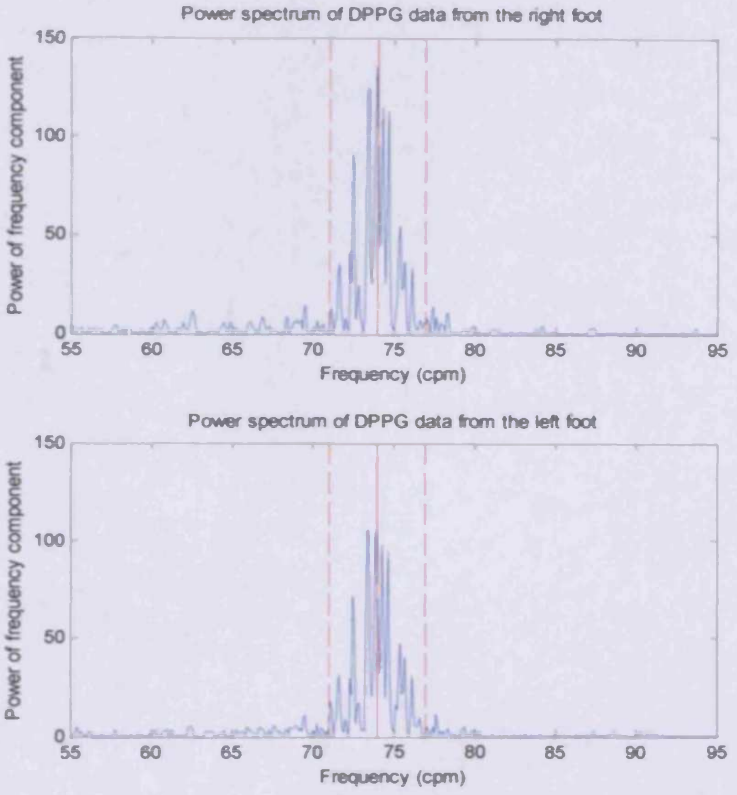

The cardiac ranges for all the patients are listed in Appendix L. The mean range of cardiac frequencies was 9.4Hz for the patients with DVT and 9.4Hz for the patients without DVT. Therefore, a 5cpm LPF width was chosen for use in the CDM analyses of all patients. This LPF is wide enough so that any variation in cardiac frequency will be included in the band of frequencies passed through the filter. Since the cardiac frequencies generally occur at much higher values than those corresponding to any other physiological process (the next highest are due to breathing and do not usually occur above 40cpm), the CDM analyses should not be contaminated by other frequencies as a result of choosing a 5cpm LPF width.

9.3.4.2.1 Results of the CDM analysis of the cardiac frequencies[**]

CDM was performed at the selected cardiac frequency for each patient and a 5cpm, 10^{th} order LPF was used in the analysis. To investigate the effect of using different lengths of DPPG data in the analyses, the first 4minutes, 6minutes and 8minutes of data were considered in addition to the whole length of data collected from each patient.
The analyses were performed on the DPPG signals from all the patients in the study except those for which the signal was recalibrated during the data collection (positive patient numbers 5, 7, 11, 19, 37, 39, 46, 48, 57, 58, 61, 62, 63 and 65; negative patient numbers 7, 32, 64, 70, 71, 72, 73 and 77). Also, positive patient numbers 33 and 38 and negative patient number 34 were excluded from the analyses because the cardiac frequency band could not be clearly seen in the power spectra of the DPPG data.
For the analysis using 6minutes of DPPG data, positive patient number 21 was excluded because less than 6minutes of data were collected for this patient. For the analysis using 8minutes of DPPG data, positive patient numbers 21 and 29 were excluded for the same reason.

The CDM outputs describe how the amplitude and phase of the selected cardiac frequency varies over time. From these outputs, the MAAD and MAPD values were calculated as previously described in equation 9.1 and equation 9.2. These values were then compared to look for any difference between the groups of patients with and without DVT (confirmed with DUS). The results are presented below.

9.3.4.2.1.1 MAAD results

Figure 9.27 shows boxplots comparing the MAAD values when different lengths of DPPG data were analysed. From these plots, it can be seen that, for all lengths of DPPG data, the median MAAD value is smaller for the patients with DVT and the values within the box, representing the interquartile range, are spread over a narrower range. However, there seems to be a considerable overlap between the two patient groups.
The results of a Mann-Whitney test (2-tailed) on the MAAD values from the two patient groups are given in table 9.14. When the whole length of the DPPG data is used, the

[**] The MATLAB code used to implement the analysis can be found in Appendix C.

test gives $p>0.05$ ($p=0.077$), indicating no statistical difference in MAAD between the two groups of patients. However, when 4minutes, 6minutes and 8minutes of DPPG data are considered, the test gives $p<0.05$ (0.028, 0.046 and 0.046 respectively) suggesting that the null hypothesis of no difference in MAAD between the two groups may be rejected. However, these p-values may not be small enough to render this conclusion particularly convincing and the large number of outliers and extreme values in the boxplots do not improve confidence.

In any case, even if a statistical difference does exist between the two groups of patients, a DVT test based on the MAAD values may not be feasible due to the large overlap. If a threshold MAAD value was selected for a DVT test, such that all patients with a greater MAAD are classified as positive, the statistics of the test would be as shown in table 9.15. (The threshold MAAD value fixes the sensitivity at 100%, preventing any false negative diagnoses). In all but one case, the specificity is 0%, indicating that the test is incapable of separating positive from negative DVT patients. When the whole length of the DPPG data is used, the specificity becomes 1.5%, but this only results in 1 out of 68 patients without DVT being diagnosed correctly. The other 98.5% (67/68) are false positives. Therefore, it seems that the MAAD would not be an appropriate value to use in a test for lower limb DVT.

Fig 9.27: Boxplots of the MAAD values for different lengths of DPPG data used in the CDM analyses.

(A description of the features of the boxplots can be found in figure 9.13.)

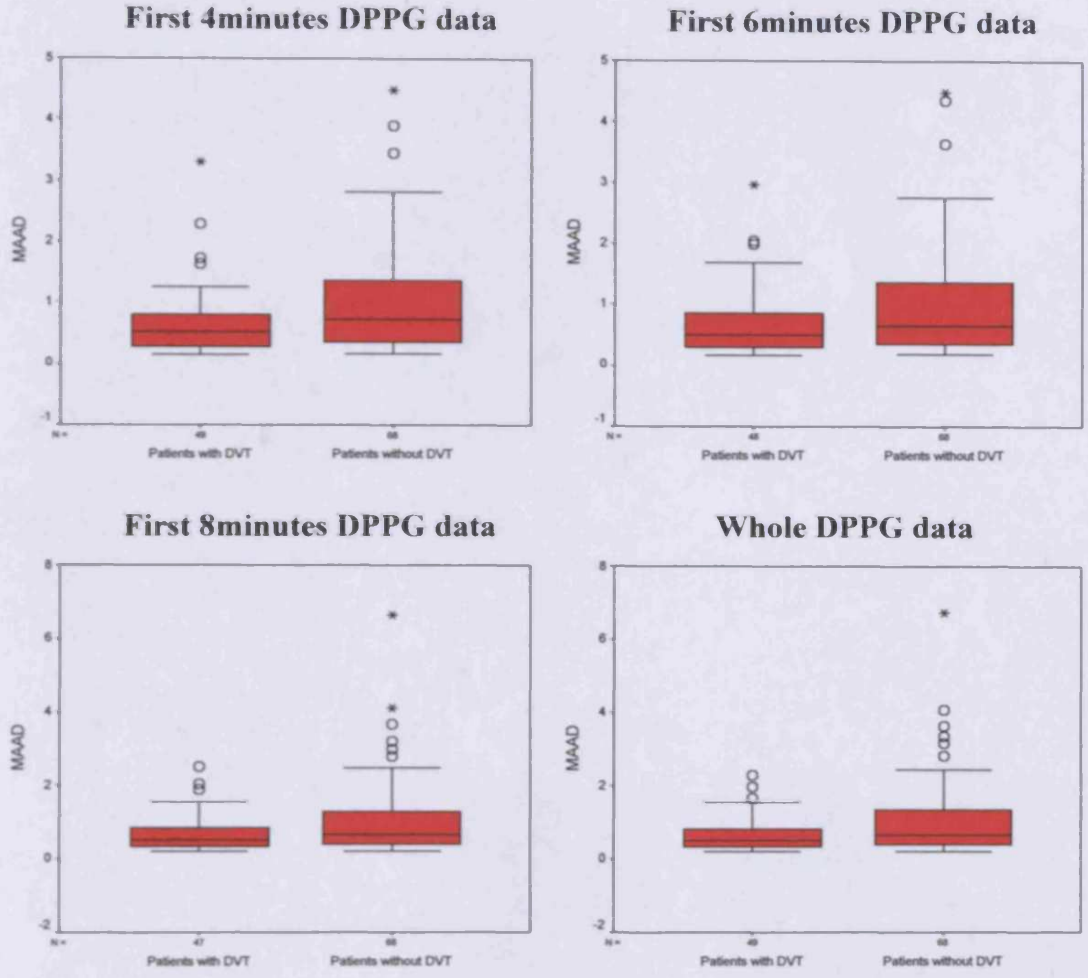

Table 9.14: Results of a Mann-Whitney test on the MAAD values from the two groups of patients (with and without lower limb DVT, confirmed with DUS).

	First 4min	First 6min	First 8min	Whole data
p-value (3dp)	0.028	0.046	0.046	0.077

Table 9.15: Test statistics of a MAAD-DPPG test, using different lengths of DPPG data.

(The grey shaded boxes indicate that the negative predicting value could not be calculated because no patients were diagnosed negative by the MAAD-DPPG test.)

		First 4min	First 6min	First 8 min	Whole data
Sensitivity	(1dp)	100.0%	100.0%	100.0%	100.0%
Specificity	(1dp)	0.0%	0.0%	0.0%	1.5%
Negative predicting value	(1dp)				100.0%
Positive predicting value	(1dp)	41.9%	41.4	40.9%	42.2%
Accuracy	(1dp)	41.9%	41.4	40.9%	42.7%

9.3.4.2.1.2 MAPD results

Boxplots comparing the MAPD values for the different lengths of DPPG data used in the CDM analyses are shown in figure 9.28. In all cases, the median MAPD value is smaller for the patients without DVT and the values within the box, representing the interquartile range, are spread over a narrower range. However, as was the case for the MAAD values, there is a considerable overlap between the MAPD values from the two patient groups.

The results of Mann-Whitney tests (2-tailed) on the MAPD values from the two patient groups all show $p<0.05$ (table 9.16), suggesting that the null hypothesis of no difference in MAPD between the two groups can be rejected. The boxplots show several outliers and extreme values but, even so, it is difficult to argue against the results of the Mann-Whitney tests, since the p-values are much less than the 0.05 significance level. This result was somewhat surprising bearing in mind that no clear difference was observed in the power spectra of the DPPG signals, at the cardiac frequencies, from the patients with and without DVT (section 9.3.3.2). It was assumed that the cardiac pulsations, derived from the arterial side of the circulation, would not be influenced by an obstruction in the deep veins.

Nevertheless, as with the MAAD values, even though there is statistical evidence for a difference in MAPD values between the groups of patients with and without DVT, the large overlap between the two groups renders a DVT test, based on the values, impracticable. For example, as before, a threshold MAPD value can be selected such that all patients with a greater MAPD are classified as positive for DVT and those with a lower MAPD are classed as negative. This sets the sensitivity to 100% and prevents any false negative diagnoses. For the MAPD values obtained from the cardiac frequencies, the statistics of such a test would be those shown in table 9.17. At best the test is only able to correctly diagnose 5 out of 68 patients without the condition. Such a low specificity (7.4%) would be much less than reasonably expected in a test for lower limb DVT.

Fig 9.28: Boxplots of the MAPD values for different lengths of DPPG data used in the CDM analyses.

(A description of the features of the boxplots can be found in figure 9.13.)

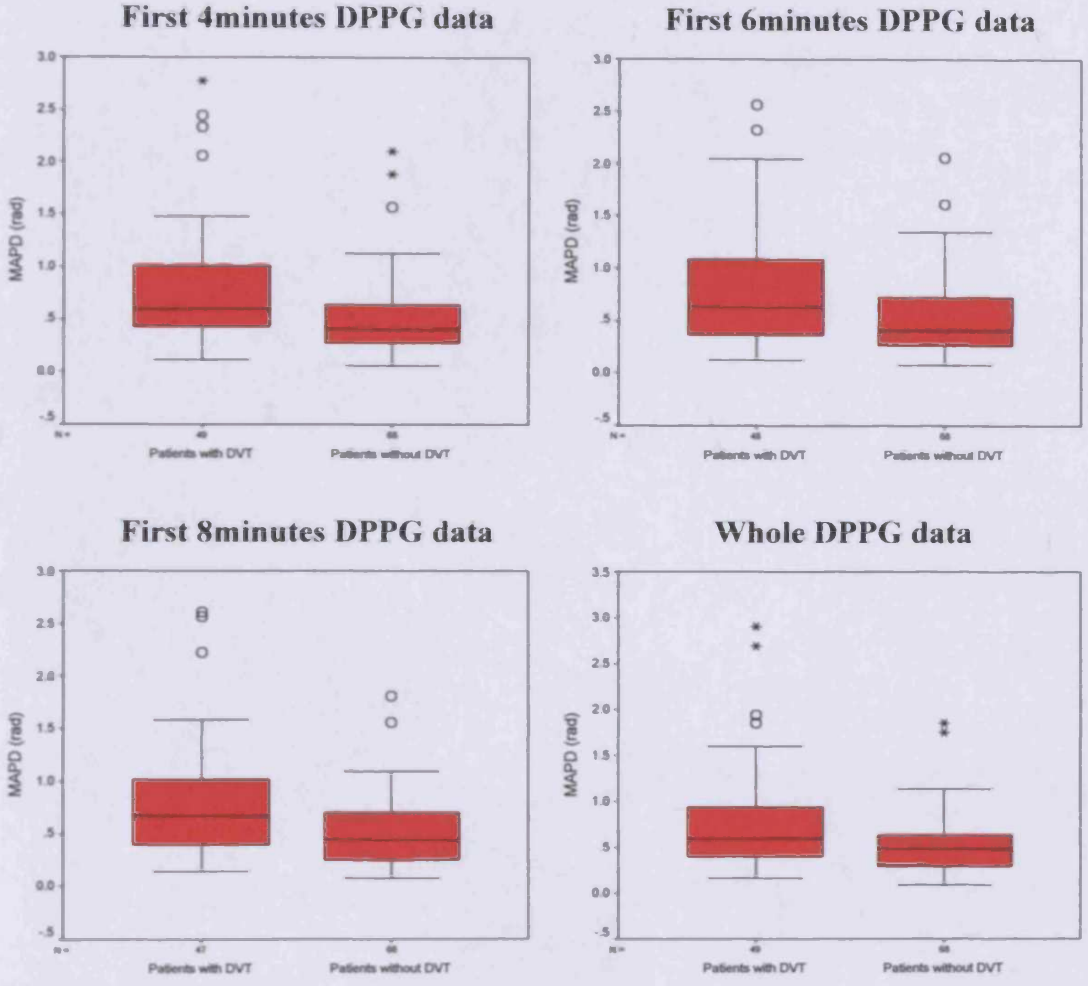

Table 9.16: Results of a Mann-Whitney test on the MAPD values from the two groups of patients (with and without lower limb DVT, confirmed with DUS).

	First 4min	First 6min	First 8min	Whole data
p-value (3dp)	0.001	0.004	0.003	0.002

Table 9.17: Test statistics of a MAPD-DPPG test, using different lengths of DPPG data.

		First 4min	First 6min	First 8 min	Whole data
Sensitivity	(1dp)	100.0%%	100.0%	100.0%	100.0%
Specificity	(1dp)	5.9%	5.9%	7.4%	5.9%
Negative predicting value	(1dp)	100.0%%	100.0%	100.0%	100.0%
Positive predicting value	(1dp)	43.4%	42.9%	42.7%	43.4%
Accuracy	(1dp)	45.3%	44.8%	45.2%	45.3%

9.3.4.2.2 Conclusions regarding the CDM analyses at the cardiac frequencies

CDM analysis of the cardiac frequencies was not expected to show any difference between the patients with and without DVT. This was based on the reasoning that, since the cardiac component of the DPPG signal is derived from the arterial side of the circulation (see PI-1), thrombus in the deep veins should not disturb this process.
From the CDM outputs (amplitude and phase), the MAAD and MAPD values were calculated. Mann-Whitney tests on the MAAD values indicated little statistical difference between the patients with and without DVT. Statistical evidence was greater when the MAPD values were considered but a large overlap between the two patient groups prevents development of a useful DVT test. A maximum test specificity of 7.4% was achieved when the sensitivity was fixed at 100%.

The fact that any statistical evidence existed for a difference in the MAPD values between the two groups of patients was surprising. However, previous studies have shown phase differences between cardiac pulsations in the PPG signal, measured at different locations on the periphery of the body, to be associated with the presence of arterial disease. For example, Allen and Murray (2000) took simultaneous PPG recordings at the toes, thumbs and ears. For those without significant arterial disease, the cardiac components of the PPG signals recorded at the three sites were shown to be a similar shape and oscillating in phase. However, for a patient with unilateral iliac arterial occlusive disease, significant changes were observed in the PPG signals taken from the toes. The shape of the cardiac pulses were different and the pulse arrival times were out of phase.
Therefore, if arterial disease was present in the patients used in this study, this may have influenced the MAPD values. However, the presence of arterial disease was not tested during the DUS examinations so no data were available on the prevalence of arterial disease in the patients. Therefore, it is impossible to conclude whether arterial disease had any influence on the MAAD or MAPD values.

9.3.4.3 CDM analysis of the low frequencies

In PI-1, it was described that the low frequency components in the power spectra of the DPPG signals can be attributed to several different physiological processes. There is nervous system control of the microcirculation, which is a global process (affecting the whole body) and therefore may be responsible for the symmetric frequencies observed in the DPPG signals taken from the left and right limbs in the patient study (section 9.3.3.1). There are also local controls of the microcirculation that depend on conditions around the vessels and these were postulated to be the cause of the asymmetric frequencies observed in the DPPG signals. In addition, body temperature or skin surface temperature may affect microcirculation blood flow via local or global control.

It is possible that lower limb DVT could affect the above processes, altering their influence on the DPPG signal. Previous studies have related changes in the low frequency components to other diseases, e.g., the correlation between the low frequency oscillations in PPG signals (caused by nervous system control) taken at various locations around the body was found to diminish when diabetic neuropathy is present (Nitzan et al., 1998).
In the case of DVT, an increase in the surface temperature of the affected limb is often observed and this effect has been utilised in DVT diagnosis using thermography (section 2.5.9). Such temperature increases are likely to cause changes to the microcirculation blood flow, which could possibly be detected using PPG. Changes in the PPG signal, brought about by skin temperature variations, have previously been observed. For example, Kamal et al. (1989) describe a decrease in the amplitude of the PPG reflection signal and changes to the spectral power (increased ratio between the high and low frequency bands) at higher skin temperatures.
Alternatively, it may be possible to directly observe changes to the venous blood flow caused by the DVT itself.

However, analysis of the low frequencies was found to be problematic using CDM. Initial difficulties were encountered when selecting a frequency to use in the analysis. The methods used to select representative breathing and cardiac frequencies did not seem applicable to the low frequency case. As described above, there are several

processes that may cause low frequency components in the power spectrum of a DPPG signal. Therefore, it did not seem appropriate to select a single, average frequency to represent the whole region, as was the case in method-A for the breathing frequency region. For the same reason, the procedure used in method-B did not seem to be appropriate here (i.e. selecting a minimum MAPD over the 0-10cpm region). There may be multiple minima from which to chose, depending on the influence of the global controls on the microcirculation. Also, the MAPD calculation was shown to break down at very low frequencies (section 9.3.4.1.2) unless a very narrow LPF is used. Therefore, the MAPD information obtained may not be reliable.

In addition, even though the low frequency region of the DPPG power spectrum tends to have greater power than the breathing or cardiac regions (e.g., see figure 9.7), clear peaks cannot always be seen, making them difficult to select by eye. Where prominent peaks were observed, it was not possible to associate a particular peak with a corresponding physiological process because no additional measurements were made to monitor the factors that may have caused the low frequencies (e.g., blood pressure or temperature). This was also confused by the fact that both global and local controls exist, making it difficult to determine whether the presence of non-symmetric frequencies in the power spectra were due to local microcirculation controls or the presence of a DVT.

Therefore, the best way to analyse the low frequency region with CDM seemed to be to perform multiple analyses over the whole range of frequencies, from 0cpm to 10cpm, using a very narrow LPF. The MAAD and MAPD results for each frequency can then be compared to look for a difference when lower limb DVT is present. However, this approach relies on the assumption that the processes that cause the low frequency terms result in oscillations at approximately the same frequency in all people and do not vary significantly about a mean frequency, which seems unlikely.

Performing the CDM analyses between 0-10cpm, in steps of 1cpm, using a 1cpm LPF width (3^{rd} order) produced no statistical evidence for a difference between the two groups of patients at any frequency, based on the MAAD values (table 9.18). However, for the MAPD values, there did seem to be evidence to suggest a difference when frequencies greater than 5cpm were analysed. However, there was a significant overlap in the MAPD values from the two patient groups and a DVT test based on the MAPD results at any of these frequencies was found not to be practicable.

Table 9.18: Mann-Whitney test statistics (2-tailed) following CDM at frequencies between 0-10cpm (using 8 minutes of DPPG data and a 1cpm LPF width).

The test compares the MAAD and MAPD values between the two groups of patients (with and without DVT, confirmed with DUS).

CDM frequency (cpm)	*p*-value for MAAD values (3dp)	*p*-value for MAPD values (3dp)
0	0.047	1.000
1	0.054	0.989
2	0.924	0.163
3	0.702	0.935
4	0.946	0.598
5	0.346	0.002
6	0.598	0.012
7	0.486	0.003
8	0.714	0.024
9	0.393	0.021
10	0.785	0.007

However, since table 9.18 suggests a statistical difference in the MAPD values from the two patient groups, further investigation of the low frequency region may be worthwhile using more suitable analysis techniques. A speculative attempt to do this involved integrating the power spectra of the DPPG signals over the low frequency region (0-10cpm). The ratio of the power for the signals taken from both feet was then compared between the two groups of patients. In addition, the power under the low frequency range was compared with the power under the breathing frequency range and the cardiac frequency range. However, none of these approaches provided evidence for a statistical difference between the patients with and without DVT.

9.4 Future work

The investigations in this study were not carried out blind, i.e., the results of the gold standard DVT tests (DUS) were known before the DPPG data were analysed. This was necessary to be able to look for any differences in the DPPG data collected from patients with and without DVT. It also allowed a threshold MAPD value to empirically be set that distinguishes between the two patient groups in the new DPPG test. Therefore, in this study, it was certain that all those patients who tested positive for DVT with DUS also tested positive with the MAPD-DPPG test. The concern was limiting the number of false positive test results to improve the specificity.
In order to verify the sensitivity and specificity of the MAPD-DPPG test, it would be necessary to undertake a further blinded study on a group of suspected DVT patients.

It was noted in section 9.3.4.1.5, that it is useful for clinicians to have an indication about the size and location of a DVT when deciding on a management strategy for the condition. However, no relationship was found between the MAPD value (calculated using the breathing component of the DPPG signal) and the location of the DVT in the lower limb. It was suggested that the degree of occlusion of the vessel lumen may have a greater influence on the MAPD value, but not enough information could be obtained from the DUS scan results to investigate this further.
However, to determine the location of the DVT, an extension to the current apparatus is envisaged that uses multiple pairs of DPPG probes placed along the lower limbs (fig 9.29). For such a set-up, one may expect the MAPD value to be lower for any pair of probes placed proximal to a DVT in the limb. It was observed in PI-2 that the power spectra of DPPG signals taken from the foot and positions along the leg contain similar information, i.e. oscillations at low frequencies, breathing frequencies and cardiac frequencies. Therefore, there should be no reason why DPPG signals from multiple probes placed along the limb cannot be compared.

Fig 9.29: Possible addition to the DPPG apparatus to determine the location of the DVT in the limb.
DPPG probes are placed at the level of the knee (level 1) and on the soles of the feet (level2).

For an AK-DVT, it may be expected that: *MAPD(level 1)> threshold for DVT*
AND
MAPD(level 2)> threshold for DVT

For a BK-DVT, it may be expected that: *MAPD(level 1)< threshold for DVT*
AND
MAPD(level 2)> threshold for DVT

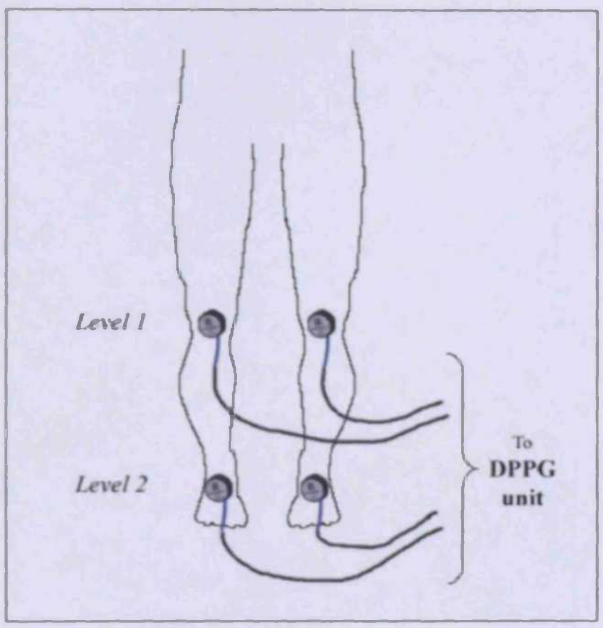

Like the original 2-probe set-up, this system would not be able to specify which leg the DVT resides in, unless a comparison of the DPPG signals from probes on the same limb can provide some information regarding this. Nevertheless, if the specificity of the MAPD-DPPG test could be improved (while maintaining the sensitivity at 100%) the 4-probe DPPG system could have the potential to provide a powerful diagnostic tool. The specificity may be improved by looking more closely at artefact removal from the DPPG signals (especially those caused by movement) or by using more powerful analysis techniques, such as neural networks. In addition, if the MAPD value can be shown to correlate with the degree of vessel occlusion caused by the DVT, the diagnostic information obtained from the 4-probe test could approach that provided by venography or DUS.

9.5 Overall conclusions

Previous studies have shown that PPG can be used to investigate vascular disease in the body. To investigate venous disease (especially venous insufficiency or DVT), the system is most commonly used to measure the quantity of blood expelled from the microcirculation of the leg during a simple foot exercise and the consequent refill time. Most research involving signal processing of the PPG signal to diagnose vascular disease has considered the low frequency changes caused by nervous system controls or the high frequency changes caused by cardiac pulsations. For example, it has been suggested that PPG could be used to assess the function of the autonomic nervous system in diabetics (Nitzan et al., 1998). Allen and Murray (1995) developed a neural network to predict arterial disease based on the shape of the arterial pulse measured at the big toe. They also demonstrated that the cardiac pulse arrival time at different parts of the body can give an indication of arterial disease (Allen and Murray, 2000). Use of the breathing frequency component in the DPPG signal seems to have been limited to monitoring breathing rates (e.g., Lindberg et al. (1992), Olsson et al. (2000)). However, this study has produced evidence to suggest that analysis of the breathing frequency can be used to indicate the presence of DVT in the lower limbs. To do this, 284 DPPG signals were collected from the soles of both feet of 142 patients (65 with DVT diagnosed with DUS and 77 without the condition) while they remained motionless and supine. Using CDM to compare the signals from both feet, the mean absolute phase difference (MAPD) between the breathing frequency components was shown to be statistically greater for those patients who had lower limb DVT. This allowed a threshold MAPD value to be selected that could be used as an indicator of DVT. After considering the artefacts within the DPPG data, the amount of DPPG data required in the analysis and the effect of the LPF width in CDM, the best MAPD-DPPG test for DVT was shown to have the statistics given in table 9.19.

Table 9.19: Statistics of the MAPD-DPPG test, following CDM analysis of the breathing frequency in the DPPG signals.

Sensitivity	100.0% (1dp)
Specificity	27.5% (1dp)
Negative predicting value	100.0% (1dp)
Positive predicting value	49.5% (1dp)
Accuracy	57.6% (1dp)

By careful selection of the threshold MAPD value, the sensitivity of the test was fixed at 100% so that all cases of DVT, within the group of patients analysed, were detected by the new DPPG test. However, this resulted in a specificity of 27.5%, which is fairly low for a diagnostic test. Nevertheless, since the negative predicting value is 100%, it is envisaged that the system could be used as a screening device to complement current gold standard tests, i.e., venography or DUS. Such screening tests are desirable because clinical diagnosis of DVT is unreliable and it is estimated that up to 90% of those sent for objective testing do not have the condition (section 2.5). Performing a quick preliminary test for DVT reduces the number of patients requiring relatively expensive and time consuming DUS or invasive venography. However, there are screening tests that are currently available to perform such a task, e.g., D-dimer, which has a reported sensitivity greater than 90% and a specificity up to 50%, depending on the type of assay used (section 2.5.3). Even current PPG tests for DVT, employing dorsiflexions of the foot, have been shown to achieve a sensitivity of 100% and specificity of 47% (section 2.5.4). There are also clinical scoring systems that assist the DVT screening process (section 2.5.5). Therefore, if the MAPD-DPPG test is to compete with these currently available DVT screening procedures, further improvement to the specificity would be required.

However, the MAPD-DPPG test does have significant advantages. For example, the test is non-invasive, whereas D-dimer requires a blood sample to be taken by suitably qualified medical staff. Also, the MAPD-DPPG test can be performed with minimal training and so does not require highly trained operators like venography or DUS. The technique does not require active patient participation, unlike the current PPG dorsiflexion test for DVT, and can therefore be performed on almost anybody, including immobile patients who are at a high risk of developing DVT. The main disadvantage of the test is that its accuracy seems to improve when longer lengths of DPPG signals are analysed (section 9.3.4.1.2.4). The best test statistics (table 9.19) were obtained when 8 minutes of DPPG data were used to calculate the MAPD value. Having to collect data for this length of time may reduce the usefulness of the test in a busy clinical setting. Nevertheless, because the DPPG device is portable and can be powered by a rechargeable battery, it can be performed almost anywhere. Other advantages of the

new DPPG test are that the procedure is painless, with almost no risk to the patient, it is without side effects and it is inexpensive.

Appendix A

Calculating the magnitude and phase angle of a complex number

A complex number, z, can be written as:

$$z = a + ib \qquad \text{or} \qquad z = |z|e^{i\phi} = |z|(\cos\phi + i\sin\phi)$$

where,

a is the real part of the complex number
b is the imaginary part of the complex number
i is an imaginary number, where $i^2 = -1$
$|z|$ is the magnitude of the complex number
ϕ is the angle between the complex "vector" and the real axis on an Argand diagram (fig A.1)

Fig A.1: Representation of a complex number on an Argand diagram.

$\Re$ represents the real axis. $\Im$ represents the imaginary axis. The complex number, $z = a + ib$, is represented by a point on the diagram and ϕ is the angle between the real axis and a line connecting that point to the origin.

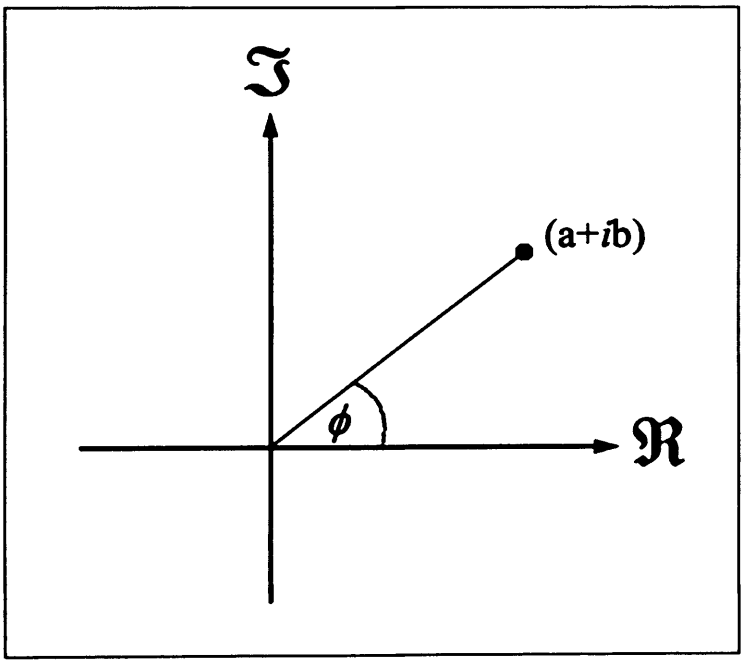

The angle, ϕ, is given by,

$$\phi = \tan^{-1}\left(\frac{b}{a}\right)$$

(The angle, ϕ, is sometimes referred to as the "complex argument" or the "complex phase".)

The magnitude of z is given by,

$$|z| = \left(a^2 + b^2\right)^{1/2}$$

Appendix B

The effect of a finite LPF width in CDM

To obtain amplitude and phase information about a single frequency using CDM would require an infinitely narrow LPF. In reality, it is impossible to design such a filter. There will always be a finite pass band resulting in unwanted information about neighbouring frequencies. Therefore, it is important to consider the effect such frequencies have on the results of CDM. While an in depth analysis of the filtering process in CDM would be too great for this appendix, the example below gives an indication of the problems associated with a finite LPF width.

Consider a signal which is comprised of the sum of two sinusoidal frequency components, 15cpm and 20cpm. The 20cpm component has an amplitude 5 times greater than the 15cpm component.

$$y = y_{15} + y_{20} = \cos\left[2\pi\left(\tfrac{15}{60}\right)t\right] + 5\cos\left[2\pi\left(\tfrac{20}{60}\right)t\right] \qquad \text{Equation B.1}$$

The power spectrum of the signal is illustrated in figure B.1.

Fig B.1: Power spectrum of the signal given in equation B.1.

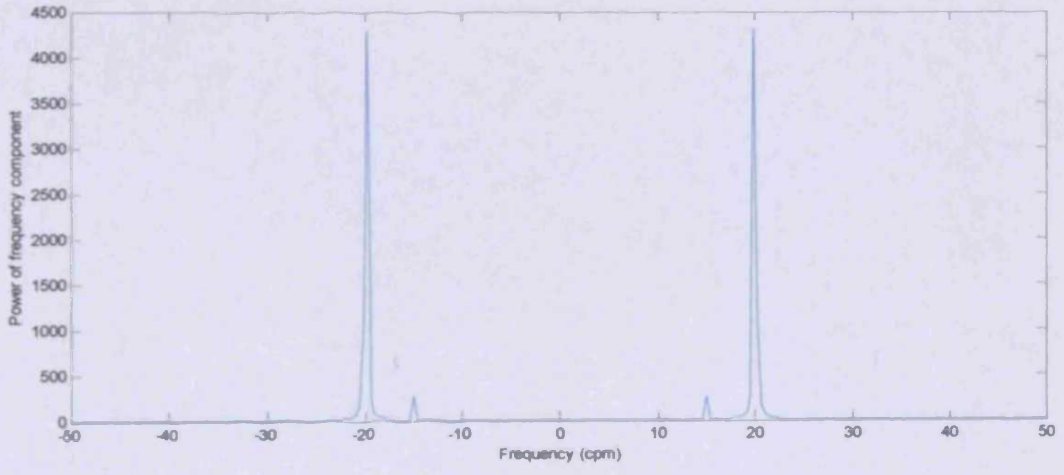

Performing CDM on the signal in equation B.1 gives the outputs A_t and ϕ_t, which describe how the amplitude and phase of a particular selected frequency varies over time. However, the outputs depend on the width of the LPF employed in the analysis. This is illustrated below using 20cpm as the frequency chosen for CDM.

CDM at 20cpm

As described in section 5.2.1, the first stage in the process of CDM is to shift the entire power spectrum of the signal so that the frequency of interest moves to zero frequency units. Following this, the LPF is applied to the adjusted signal, which removes all frequency components, except those within its passband (fig B.2).

Fig B.2: Power spectrum of the adjusted signal showing the passband of two different LPFs (cf. figure B.1 above).

The vertical dashed lines indicate the range of frequencies passed by a 2cpm LPF.
The vertical dot-dashed lines indicate the range of frequencies passed by a 10cpm LPF.

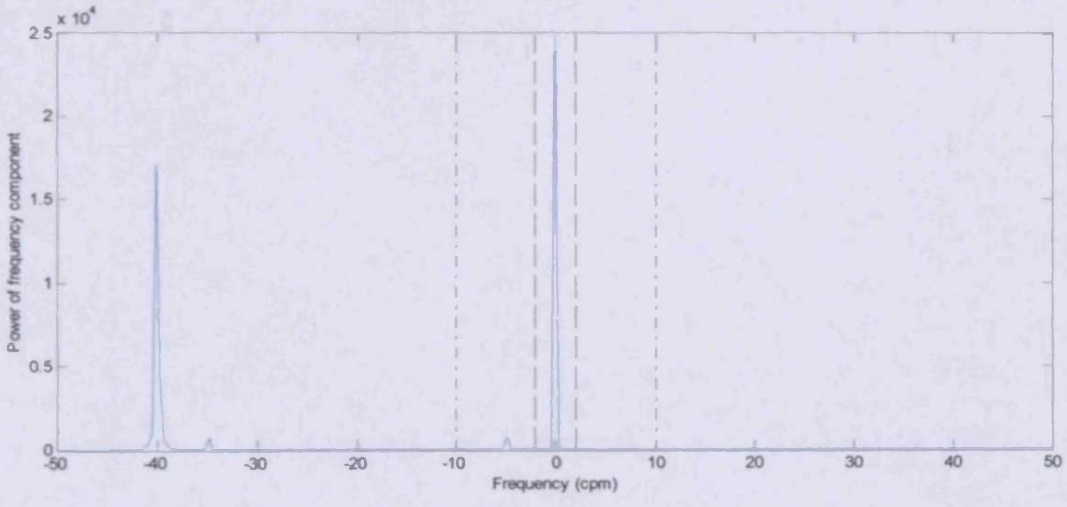

The CDM outputs, A_t and ϕ_t, are calculated using the filtered signal and therefore depend on the width of the LPF. This is examined below where CDM is performed twice, each time at 20cpm. In the first case, the LPF is made narrow enough (2cpm) to remove all components from the signal, other than the one of interest. Consequently, it is shown that the CDM outputs, A_t and ϕ_t, closely resemble the amplitude and phase variations of the 20cpm component in the original signal (equation B.1). In the second case, the LPF filter (10cpm) is incapable of removing all the unwanted components and this adversely affects the CDM outputs.

CDM using a 2cpm LPF:

Performing CDM at 20cpm on the signal described in equation B.1, using a 2cpm LPF, produces an output for A_t and ϕ_t as shown in figure B.3.

Fig B.3: Results for A_t and ϕ_t following CDM at 20cpm using a 2cpm LPF.

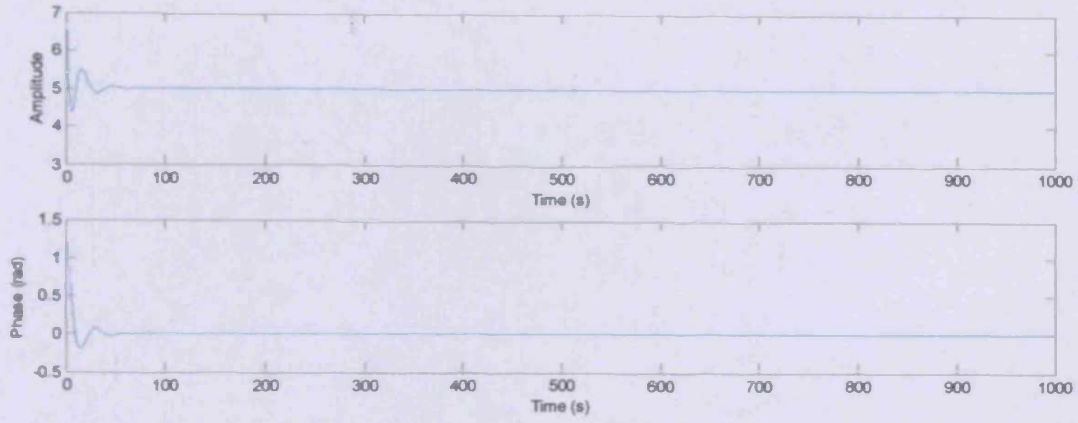

Apart from some transient effects at the start (associated with the filtering process, described in section 5.3.1.2), the output clearly shows that both the amplitude and the phase of the 20cpm component are constant in time, with a magnitude of 5 and 0 respectively. This agrees with the properties of the original signal (equation B.1).

CDM using a 10cpm LPF:

Performing CDM at 20cpm on the signal described in equation B.1, using a 10cpm LPF, produces an output for A_t and ϕ_t as shown in figure B.4.

Fig B.4: Results for A_t and ϕ_t following CDM at 20cpm using a 10cpm LPF.

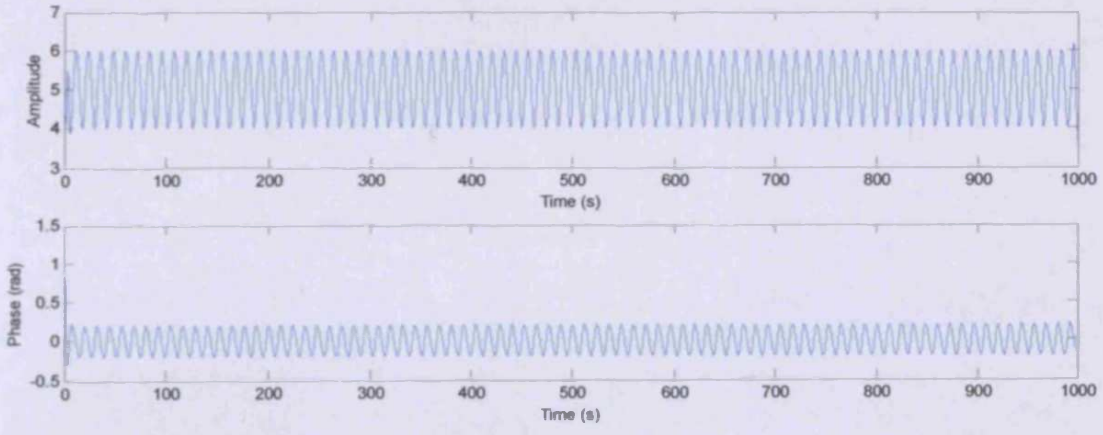

In this case, the amplitude and phase outputs are very much different from those in figure B.3 and do not agree with the amplitude and phase of the 20cpm component in the original signal (equation B.1). This difference occurs because the LPF was not narrow enough to remove all the unwanted components from the signal (see figure B.2).

The presence of the additional frequencies in the CDM analysis influences the calculated values of A_t and ϕ_t.

The influence of the additional frequencies let through by the LPF depends on their amplitude, compared to that of the frequency selected for CDM. For example, if the amplitude of the 15cpm component in equation B.1 was 0.1, instead of unity, and CDM was performed again at 20cpm using a 10cpm LPF, the outputs, A_t and ϕ_t, would more closely resemble those of the 20cpm component (fig B.5).

Fig B.5: Results for A_t and ϕ_t when the amplitude of the 15cpm component in equation B.1 is 0.1.

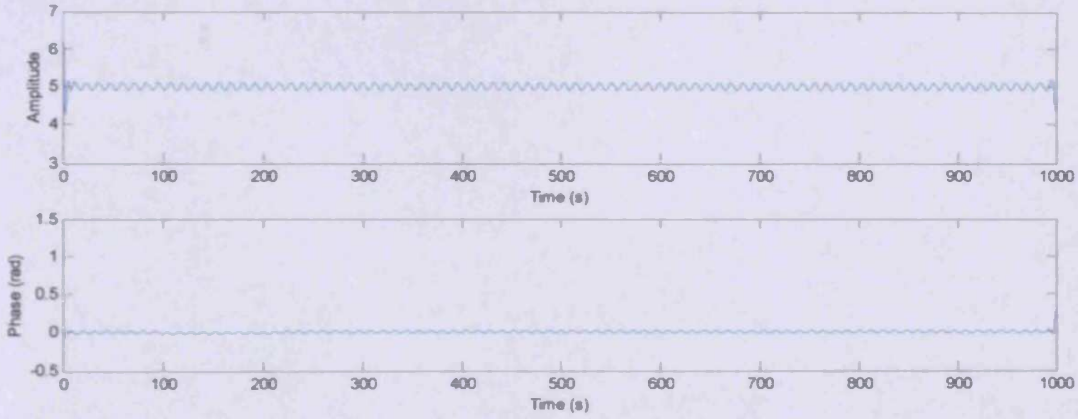

Therefore, the ability of CDM to precisely describe A_t and ϕ_t for a particular frequency clearly depends on the width of the LPF and the magnitude of any unwanted frequencies that are passed by the filter.

For a more detailed consideration of low pass filtering in CDM see, e.g., Bloomfield (2000).

Appendix C

MATLAB programs used to analyse the DPPG data in this study

The MATLAB programs, used to analyse the DPPG data in this study, are presented in the following order:

1. The code used to implement method-A in the CDM analysis of the breathing frequencies in section 9.3.4.1.1.
2. The code used to implement method-B in the CDM analysis of the breathing frequencies in section 9.3.4.1.2.
3. The code used to implement CDM analysis of the cardiac frequencies in section 9.3.4.2.
4. The code used to generate a list of filenames containing the patient data.

1. MATLAB code used to implement method-A in section 9.3.

```
function [MAAD_pos,MAPD_pos,MAAD_neg,MAPD_neg]=Analyse_breathing_constant    %Outputs MAAD and MAPD v
                                                                             %with and without DVT

Ringing_length=112;                    %Sets the length of "filter ringing" to be removed from the start and the end of the C
freq=20.4/60;                          %Sets the frequency to be analysed by CDM
[B,A]=butter(5, (10/60)/(6.25/2),'low'); %Sets the coefficients A and B that define the width and order of the LPF, for use in

for  m=1:2                             %Loops through the whole program twice - for positive patients then negative patien
  if m==1
    Make_list_DVT                      %Loads a list containing the location and file names of the data from patients with c
  else
    Make_list_no_DVT                   %Loads a list containing the location and file names of the data from the patients wit
  end

[L, w] = size(list_path);
h = waitbar(0,['Calculating for group ', num2str(m), '/2. Please wait...']);    %Plots a "progress bar" on the screen

for p = 1:L                            %Cycles through the CDM analysis for each patient in the list

  dataname=[list_path(p,:) list_name(p,:) ]; %Stores the path and file name of the data set to be analysed in this loop
  dat=load(dataname);                  %Loads the data set in the location defined by 'dataname'

  for k=1:2                            %This loop analyses each column of data in 'dat' (The 2 columns correspond to DPP
  data=dat(:,k);

  %-------------------------Performs CDM-------------------------
  t=1:length(data);t=t*0.16;t=t';      %Lists of times that each value in 'data' was sampled - assumes a sampling frequenc
  w=2*pi*freq;                         %Angular form of frequency 'freq'
  cdm=2*data.*exp(-i*w*t);             %Performs the multiplication required for CDM
  cdm_filt = ( filtfilt( B, A, cdm ) ); %Applies the low pass filter. The coefficients 'A' and 'B' define the cut-off frequency
  amplitude=abs(cdm_filt);             %Calculates the instantaneous amplitude variations of the frequency 'w'
  phase=angle(cdm_filt);               %Calculates the instantaneous phase variations of the frequency 'w'
  %-------------------------------------------------------------
```

```
%----------Removes filter ringing effects from the beginning and the end of the CDM outputs 'amplitude' and 'phase'----------
amplitude((length(amplitude)-Ringing_length+1):length(amplitude))=[ ];     %Filter ringing removed from the end of 'amplit
phase((length(amplitude)-Ringing_length+1):length(amplitude))=[ ];         %Filter ringing removed from the end of 'phase'
amplitude(1:Ringing_length)=[ ];                                           %Filter ringing removed from the beginning of '
phase(1:Ringing_length)=[ ];                                               %Filter ringing removed from the beginning of t
%-------------------------------------------------------------------------------------------------------------------------

eval( [ 'am', num2str(k), '=amplitude;' ] ); %Saves the CDM 'amplitude' output with a tag indicating which column of 'data' it w
eval( [ 'ph', num2str(k), '=phase;' ] );     %Saves the CDM 'phase' output with a tag indicating which column of 'data' it was a
end

if m==1
  MAAD_pos(p)=mean(abs(am2-am1));  %Stores the MAAD for the patients with DVT
  MAPD_pos(p)=mean(abs(ph2-ph1));  %Stores the MAPD for the patients with DVT
else
  MAAD_neg(p)=mean(abs(am2-am1));  %Stores the MAAD for the patients without DVT
  MAPD_neg(p)=mean(abs(ph2-ph1));  %Stores the MAPD for the patients without DVT
end

waitbar(p/L)                       %Updates the "progress bar"

end
close(h)                           %Closes the "progress bar"
end
```

2. MATLAB code used to implement method-B in section 9.3.

```
function [MAPD_pos, MAPD_neg]=Analyse_8_35cpm(A,B)          %Outputs MAPD values from the program, for patients wi

Data_length=3000;                                  %Sets the length of DPPG data required in the analysis
Ringing_length=450;                                %Sets the length of "filter ringing" to be removed from the start and the end of the CL

for  m=1:2                                         %Loops through the whole program twice - for positive patients then negative patient
   if m==1
      Make_list_DVT                                %Loads a list containing the location and file names of the data from patients with co
   else
      Make_list_no_DVT                             %Loads a list containing the location and file names of the data from the patients wit
   end

[L, w] = size(list_path);
h = waitbar(0,['Calculating MAPD values for group ', num2str(m), '/2. Please wait...']);    %Plots a "progress bar" on the screen

for p = 1:L                                        %Cycles through the CDM analysis for each patient in the list
  for n = 1:28                                     %This loop performs CDM at 28 different frequencies

   freq=(n+7)/60;                                  %Performs CDM at frequencies from 8-35cpm

   dataname=[list_path(p,:) list_name(p,:) ];          %Stores the path and file name of the data set to be analysed in this loop
   dat=load(dataname);                                 %Loads the data set in the location defined by 'dataname'

   dat=dat(1:Data_length,:);                       %Adjusts the length of 'dat' to analyse - depending on the value of 'Data_length'

   for k=1:2                                       %This loop analyses each column of data in 'dat' (The 2 columns correspond to DPP
   data=dat(:,k);

   %-------------------------Performs CDM-------------------------
   t=1:length(data);t=t*0.16;t=t';                 %Lists of times that each value in 'data' was sampled - assumes a sampling frequency
   w=2*pi*freq;                                    %Angular form of frequency 'freq'
   cdm=2*data.*exp(-i*w*t);                        %Performs the multiplication required for CDM
   cdm_filt = ( filtfilt( B, A, cdm ) );           %Applies the low pass filter. The coefficients 'A' and 'B' define the cut-off frequency
```

```
amplitude=abs(cdm_filt);                %Calculates the instantaneous amplitude variations of the frequency 'w'
phase=angle(cdm_filt);                  %Calculates the instantaneous phase variations of the frequency 'w'
%-------------------------------------------------------------

%----------Removes filter ringing effects from the beginning and the end of the CDM outputs 'amplitude' and 'phase'----------
amplitude((length(amplitude)-Ringing_length+1):length(amplitude))=[ ];    %Filter ringing removed from the end of 'amplitu
phase((length(amplitude)-Ringing_length+1):length(amplitude))=[ ];        %Filter ringing removed from the end of 'phase'
amplitude(1:Ringing_length)=[ ];                                          %Filter ringing removed from the beginning of 'a
phase(1:Ringing_length)=[ ];                                              %Filter ringing removed from the beginning of th
%-------------------------------------------------------------------------------------------------------------------------

eval( [ 'am', num2str(k), '=amplitude;' ] ); %Saves the CDM 'amplitude' output with a tag indicating which column of 'data' it w
eval( [ 'ph', num2str(k), '=phase;' ] );     %Saves the CDM 'phase' output with a tag indicating which column of 'data' it was d
end

%----------Calculates MAPD----------
MAPD_result(n)=mean(abs(ph2-ph1));      %Stores 32 values of MAPD (for each frequency between 8-35cpm) in MAPD_results
%-----------------------------------

end

if m==1
   MAPD_pos(p)=min(MAPD_result);        %Stores the minimum MAPD in the breathing region, for the patients with DVT
else
   MAPD_neg(p)=min(MAPD_result);        %Stores the minimum MAPD in the breathing region, for the patients without DVT
end

waitbar(p/L)                            %Updates the "progress bar"

end
close(h)                                %Closes the "progress bar"
end
```

3. MATLAB code used to implement CDM analysis of the cardiac frequencie

```
%Cardiac frequencies for CDM are stored in variables which are constructed before the program is run and stored in the workspa
%The variable 'frequencies1' should contain consecutive cardiac frequencies (cpm) for the list of patients in Make_list_DVT.
%The variable 'frequencies2' should contain consecutive cardiac frequencies (cpm) for the list of patients in Make_list_no_DVT.

function [MAAD_pos,MAPD_pos,MAAD_neg,MAPD_neg]=Analyse_cardiac(frequencies1,frequencies2)      %Outputs MA
                                                                                              %values for p
                                                                                              %DVT
Data_length=3000;                       %Sets the length of data for analysis
Ringing_length=450;                     %Sets length of filter ringing fto be removed
[B,A]=butter(10, (5/60)/(6.25/2),'low'); %Sets the coefficients A and B that define the width and order of the LPF, for use in C

for  m=1:2                              %Loops through the whole program twice - for positive patients then negative patient
  if m==1
    Make_list_DVT                       %Loads a list containing the location and file names of the data from patients with co
  else
    Make_list_no_DVT                    %Loads a list containing the location and file names of the data from the patients witl
  end

[L, w] = size(list_path);
h = waitbar(0,['Calculating for group ', num2str(m), '/2. Please wait...']);      %Plots a "progress bar" on the screen

for p = 1:L                             %Cycles through the CDM analysis for each patient in the list

  eval(['freq=frequencies', num2str(m), '(p)/60;']);  %Loads the cardiac frequency to be analysed by CDM
  dataname=[list_path(p,:) list_name(p,:) ];          %Stores the path and file name of the data set to be analysed in this loop
  dat=load(dataname);                                 %Loads the data set in the location defined by 'dataname'

  dat=dat(1:Data_length,:);                           %Adjusts the length of 'dat' to analyse - depending on the value of 'Data_leng

  for k=1:2                                           %This loop analyses each column of data in 'dat' (The 2 columns correspond
                                                      %and left foot)
  data=dat(:,k);
```

```
%-------------------------Performs CDM-------------------------
t=1:length(data);t=t*0.16;t=t';          %Lists of times that each value in 'data' was sampled - assumes a sampling fi
w=2*pi*freq;                             %Angular form of frequency 'freq'
cdm=2*data.*exp(-i*w*t);                 %Performs the multiplication required for CDM
cdm_filt = ( filtfilt( B, A, cdm ) );    %Applies the low pass filter. The coefficients 'A' and 'B' define the cut-off fre
amplitude=abs(cdm_filt);                 %Calculates the instantaneous amplitude variations of the frequency 'w'
phase=angle(cdm_filt);                   %Calculates the instantaneous phase variations of the frequency 'w'
%-------------------------------------------------------------

%----------Removes filter ringing effects from the beginning and the end of the CDM outputs 'amplitude' and 'phase'----------
amplitude((length(amplitude)-Ringing_length+1):length(amplitude))=[ ];   %Filter ringing removed from the end of 'amplitu
phase((length(amplitude)-Ringing_length+1):length(amplitude))=[ ];       %Filter ringing removed from the end of 'phase'
amplitude(1:Ringing_length)=[ ];                                         %Filter ringing removed from the beginning of 'a
phase(1:Ringing_length)=[ ];                                             %Filter ringing removed from the beginning of thi
%-----------------------------------------------------------------------------------------------------------------------------

eval( [ 'am', num2str(k), '=amplitude;' ] );   %Saves the CDM 'amplitude' output with a tag indicating which column of 'd
eval( [ 'ph', num2str(k), '=phase;' ] );       %Saves the CDM 'phase' output with a tag indicating which column of 'data'
end

if m==1
  MAAD_pos(p)=mean(abs(am2-am1));              %Stores the MAAD for the patients with DVT
  MAPD_pos(p)=mean(abs(ph2-ph1));              %Stores the MAPD for the patients with DVT
else
  MAAD_neg(p)=mean(abs(am2-am1));              %Stores the MAAD for the patients without DVT
  MAPD_neg(p)=mean(abs(ph2-ph1));              %Stores the MAPD for the patients without DVT
end

waitbar(p/L)                                   %Updates the "progress bar"

end
close(h)                                       %Closes the "progress bar"
end
```

4. MATLAB code used to generate a list of filenames containing the p

---

```
%This program generates a list of filenames where the DPPG data are stored for the 65 patients who were positive for DVT
%(called by 'Make_list_DVT' in the main program).
%A similar program was used to generate a list of filenames where the DPPG data are stored for the 77 patients who did not have
% (called by 'Make_list_no_DVT' in the main program).

list_path = [
        'C:\PhD\DVT_Study\DVT\';...%1
        'C:\PhD\DVT_Study\DVT\';...%2
        'C:\PhD\DVT_Study\DVT\';...%3
        'C:\PhD\DVT_Study\DVT\';...%4
        'C:\PhD\DVT_Study\DVT\';...%5
        'C:\PhD\DVT_Study\DVT\';...%6
        'C:\PhD\DVT_Study\DVT\';...%7
        'C:\PhD\DVT_Study\DVT\';...%8
        'C:\PhD\DVT_Study\DVT\';...%9
        'C:\PhD\DVT_Study\DVT\';...%10
        'C:\PhD\DVT_Study\DVT\';...%11
        'C:\PhD\DVT_Study\DVT\';...%12
        'C:\PhD\DVT_Study\DVT\';...%13
        'C:\PhD\DVT_Study\DVT\';...%14
        'C:\PhD\DVT_Study\DVT\';...%15
        'C:\PhD\DVT_Study\DVT\';...%16
        'C:\PhD\DVT_Study\DVT\';...%17
        'C:\PhD\DVT_Study\DVT\';...%18
        'C:\PhD\DVT_Study\DVT\';...%19
        'C:\PhD\DVT_Study\DVT\';...%20
        'C:\PhD\DVT_Study\DVT\';...%21
        'C:\PhD\DVT_Study\DVT\';...%22
        'C:\PhD\DVT_Study\DVT\';...%23
        'C:\PhD\DVT_Study\DVT\';...%24
        'C:\PhD\DVT_Study\DVT\';...%25
        'C:\PhD\DVT_Study\DVT\';...%26
        'C:\PhD\DVT_Study\DVT\';...%27
```

```
'C:\PhD\DVT_Study\DVT\';...%28
'C:\PhD\DVT_Study\DVT\';...%29
'C:\PhD\DVT_Study\DVT\';...%30
'C:\PhD\DVT_Study\DVT\';...%31
'C:\PhD\DVT_Study\DVT\';...%32
'C:\PhD\DVT_Study\DVT\';...%33
'C:\PhD\DVT_Study\DVT\';...%34
'C:\PhD\DVT_Study\DVT\';...%35
'C:\PhD\DVT_Study\DVT\';...%36
'C:\PhD\DVT_Study\DVT\';...%37
'C:\PhD\DVT_Study\DVT\';...%38
'C:\PhD\DVT_Study\DVT\';...%39
'C:\PhD\DVT_Study\DVT\';...%40
'C:\PhD\DVT_Study\DVT\';...%41
'C:\PhD\DVT_Study\DVT\';...%42
'C:\PhD\DVT_Study\DVT\';...%43
'C:\PhD\DVT_Study\DVT\';...%44
'C:\PhD\DVT_Study\DVT\';...%45
'C:\PhD\DVT_Study\DVT\';...%46
'C:\PhD\DVT_Study\DVT\';...%47
'C:\PhD\DVT_Study\DVT\';...%48
'C:\PhD\DVT_Study\DVT\';...%49
'C:\PhD\DVT_Study\DVT\';...%50
'C:\PhD\DVT_Study\DVT\';...%51
'C:\PhD\DVT_Study\DVT\';...%52
'C:\PhD\DVT_Study\DVT\';...%53
'C:\PhD\DVT_Study\DVT\';...%54
'C:\PhD\DVT_Study\DVT\';...%55
'C:\PhD\DVT_Study\DVT\';...%56
'C:\PhD\DVT_Study\DVT\';...%57
'C:\PhD\DVT_Study\DVT\';...%58
'C:\PhD\DVT_Study\DVT\';...%59
'C:\PhD\DVT_Study\DVT\';...%60
'C:\PhD\DVT_Study\DVT\';...%61
'C:\PhD\DVT_Study\DVT\';...%62
'C:\PhD\DVT_Study\DVT\';...%63
```

```
        'C:\PhD\DVT_Study\DVT\';...%64
        'C:\PhD\DVT_Study\DVT\';  %65

];

save Dat_list_path.mat list_path

list_name = [
        'DVT_Patient01.dat';...1
        'DVT_Patient02.dat';...2
        'DVT_Patient03.dat';...3
        'DVT_Patient04.dat';...4
        'DVT_Patient05.dat';...%5
        'DVT_Patient06.dat';...%6
        'DVT_Patient07.dat';...%7
        'DVT_Patient08.dat';...%8
        'DVT_Patient09.dat';...%9
        'DVT_Patient10.dat';...%10
        'DVT_Patient11.dat';...%11
        'DVT_Patient12.dat';...%12
        'DVT_Patient13.dat';...%13
        'DVT_Patient14.dat';...%14
        'DVT_Patient15.dat';...%15
        'DVT_Patient16.dat';...%16
        'DVT_Patient17.dat';...%17
        'DVT_Patient18.dat';...%18
        'DVT_Patient19.dat';...%19
        'DVT_Patient20.dat';...%20
        'DVT_Patient21.dat';...%21
        'DVT_Patient22.dat';...%22
        'DVT_Patient23.dat';...%23
        'DVT_Patient24.dat';...%24
        'DVT_Patient25.dat';...%25
        'DVT_Patient26.dat';...%26
        'DVT_Patient27.dat';...%27
```

```
'DVT_Patient28.dat';...%28
'DVT_Patient29.dat';...%29
'DVT_Patient30.dat';...%30
'DVT_Patient31.dat';...%31
'DVT_Patient32.dat';...%32
'DVT_Patient33.dat';...%33
'DVT_Patient34.dat';...%34
'DVT_Patient35.dat';...%35
'DVT_Patient36.dat';...%36
'DVT_Patient37.dat';...%37
'DVT_Patient38.dat';...%38
'DVT_Patient39.dat';...%39
'DVT_Patient40.dat';...%40
'DVT_Patient41.dat';...%41
'DVT_Patient42.dat';...%42
'DVT_Patient43.dat';...%43
'DVT_Patient44.dat';...%44
'DVT_Patient45.dat';...%45
'DVT_Patient46.dat';...%46
'DVT_Patient47.dat';...%47
'DVT_Patient48.dat';...%48
'DVT_Patient49.dat';...%49
'DVT_Patient50.dat';...%50
'DVT_Patient51.dat';...%51
'DVT_Patient52.dat';...%52
'DVT_Patient53.dat';...%53
'DVT_Patient54.dat';...%54
'DVT_Patient55.dat';...%55
'DVT_Patient56.dat';...%56
'DVT_Patient57.dat';...%57
'DVT_Patient58.dat';...%58
'DVT_Patient59.dat';...%59
'DVT_Patient60.dat';...%60
'DVT_Patient61.dat';...%61
'DVT_Patient62.dat';...%62
'DVT_Patient63.dat';...%63
```

```
    'DVT_Patient64.dat';...%64
    'DVT_Patient65.dat';  %65
];

save Dat_list_name.mat list_name
```

Appendix D

Removing the effects of filter ringing from the CDM outputs

When a digital filter is applied to a signal, the output is affected by "ringing", which causes a large disturbance at the start of the filtered signal but eventually settles down with time (section 5.3.1.2). Before analysing the outputs from CDM, it was thought necessary to remove this effect. The LPFs used in the CDM analyses in this study are the Butterworth type. The impulse response of this type of filter continues indefinitely but decays with time. Therefore, an appropriate cut-off time can be selected where the ringing effect may be considered insignificant. A reasonable cut-off time was considered to be that for which the absolute amplitude of the impulse response of the filter becomes always less than 0.5% of the initial overshoot.

For example, the impulse response of a low pass Butterworth filter is shown in figure D.1.

Fig D.1: The impulse response of low pass Butterworth filter with cut-off frequency 3cpm and filter order 5.

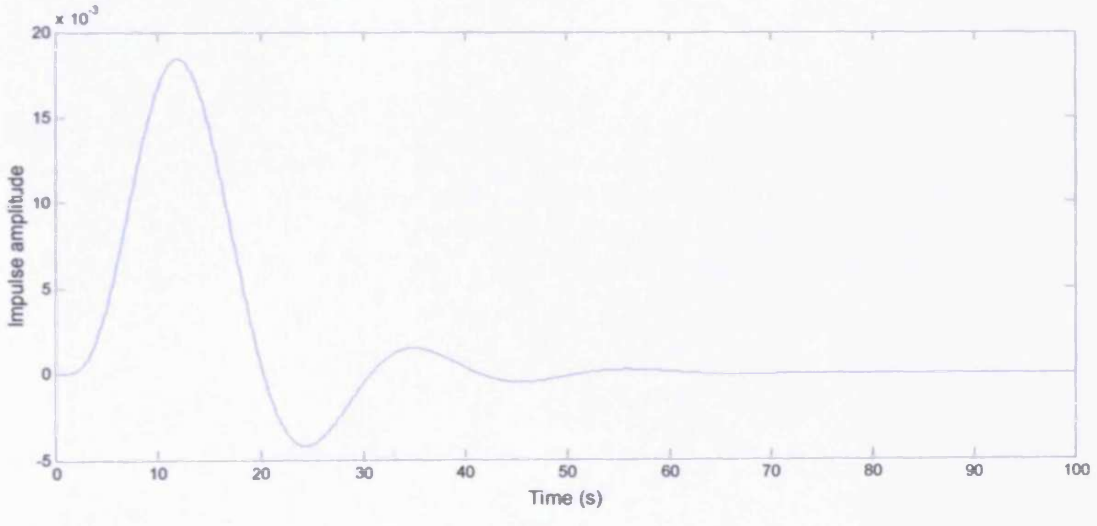

The absolute amplitude of the impulse response is shown in figure D.2. The shaded area indicates the region where the absolute amplitude of the impulse response is always less than 0.5% of the initial overshoot. The 0.5% cut-off time is the dashed vertical line indicating the beginning of this region.

Fig D.2: The absolute amplitude of the impulse response of a low pass Butterworth filter with cut-off frequency 3cpm and filter order 5.

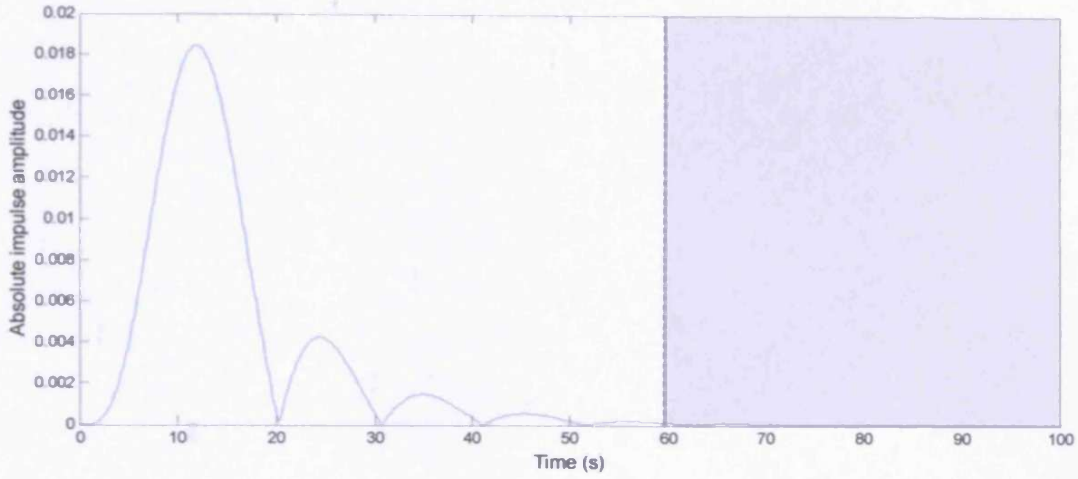

For the LPFs used in this study, the 0.5% cut-off time occurs at the values given in table D.1 (calculated using a sampling frequency of 6.25Hz).

Table D.1: Time after the start of the filtered signal when the absolute amplitude of the impulse response becomes always less than 0.5% of the initial overshoot.

Cut-off frequency of low-pass Butterworth filter (cpm)	Filter order	0.5% cut-off time (s)
1	3	109.4s (1dp)
3	5	59.7s (1dp)
5	10	72.0s (1dp)
10	5	17.9s (1dp)

Appendix E

DPPG data collected in Preliminary Investigation 1

The following plots show the DPPG data described in Chapter 7. In each case, the blue line represents the data recorded with the DPPG probe which was placed 10cm above the medial malleolus. The green line represents the data recorded with the DPPG probe which was placed at the medial aspect of the leg, just below the knee.
The two red, vertical, dashed lines in each plot bound the section of data that were used to calculate power spectra. The power spectra are displayed in Appendix F.

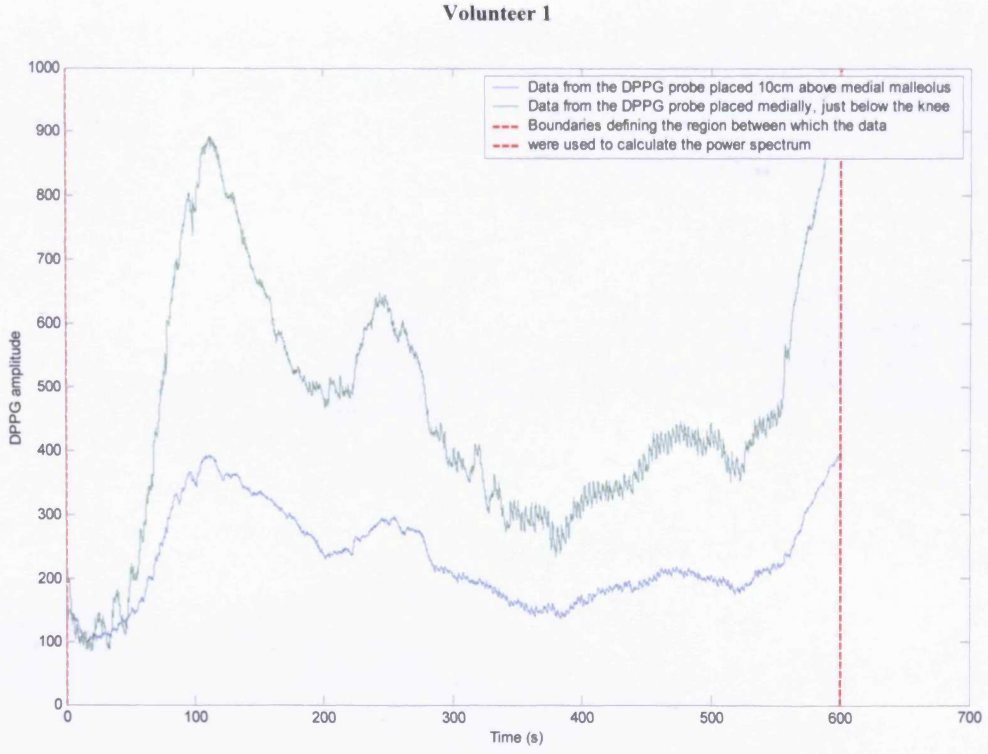
Volunteer 1
Data from the DPPG probe placed 10cm above medial malleolus
Data from the DPPG probe placed medially, just below the knee
Boundaries defining the region between which the data
were used to calculate the power spectrum
DPPG amplitude
Time (s)
0
100
200
300
400
500
600
700
800
900
1000

Volunteer 2

Before 1st red line: DPPG device calibration

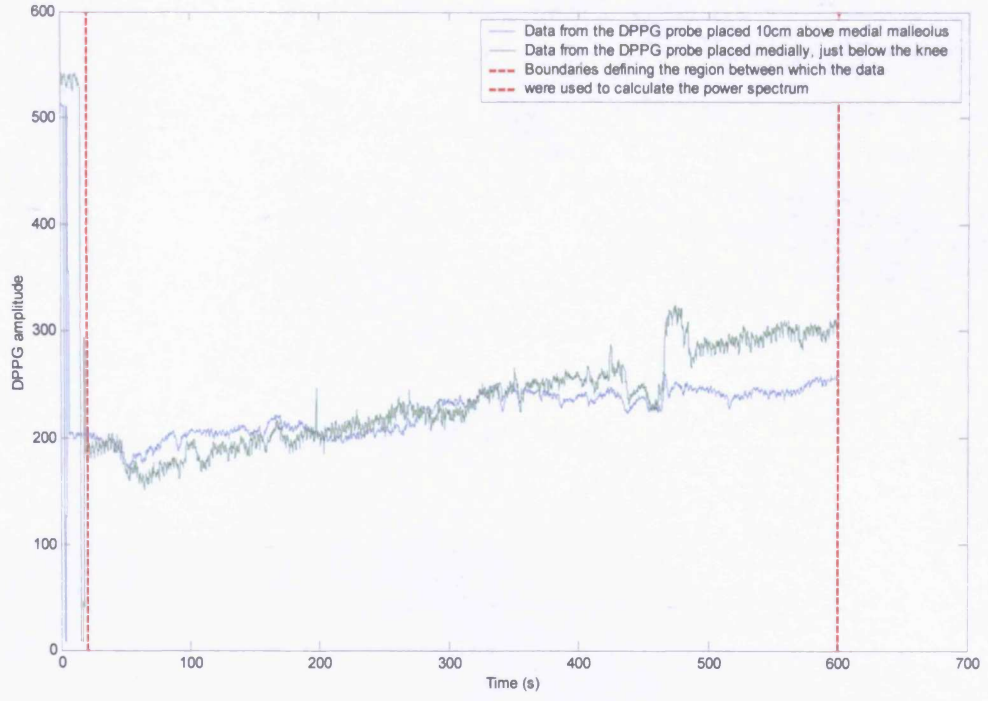

Volunteer 3

Before 1st red line: DPPG device calibration *After 2nd red line: Subject movement*

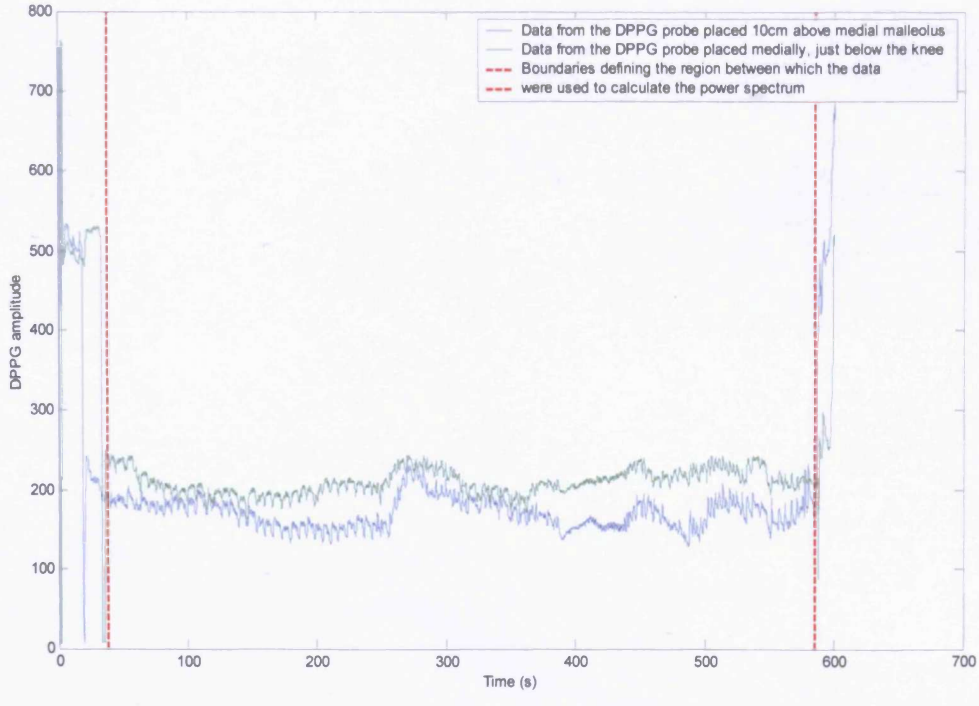

Volunteer 4

Before 1st red line: DPPG device calibration Data acquisition stopped at 563s (9min 23s)

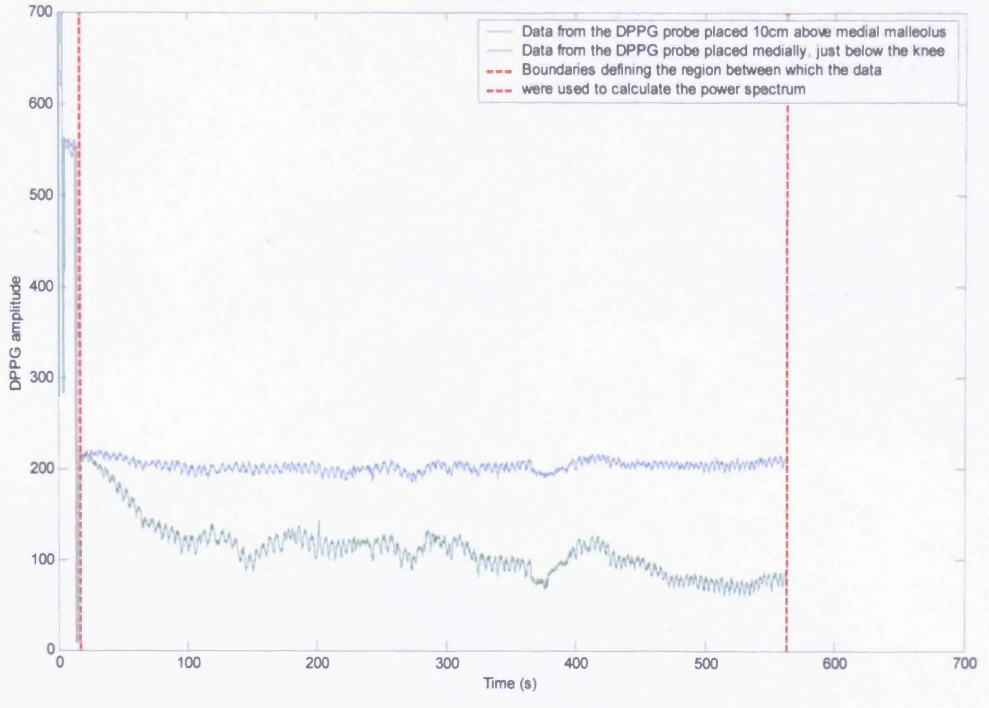

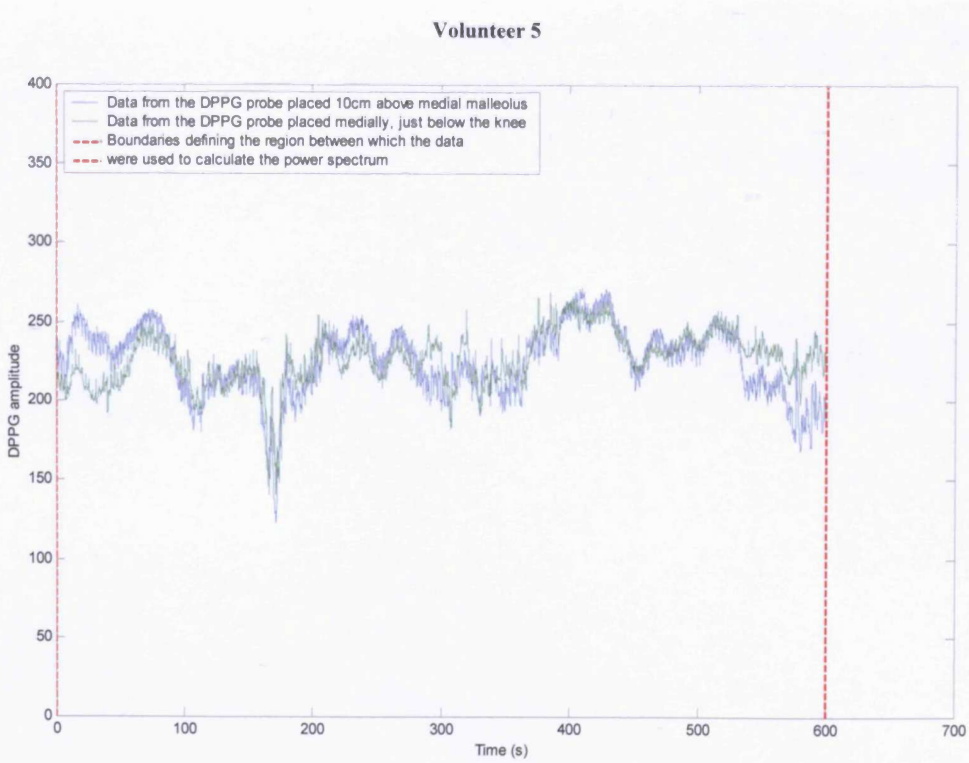
Volunteer 5
Data from the DPPG probe placed 10cm above medial malleolus
Data from the DPPG probe placed medially, just below the knee
Boundaries defining the region between which the data
were used to calculate the power spectrum
DPPG amplitude
Time (s)
0
50
100
150
200
250
300
350
400
0
100
200
300
400
500
600
700

Appendix F

Power spectra of the DPPG data collected in Preliminary Investigation 1

The following plots show the power spectra of the DPPG data presented in Appendix E. Each spectrum is normalised, compared to the maximum power.

Volunteer 1

Power spectra between 0cpm and 187.5cpm

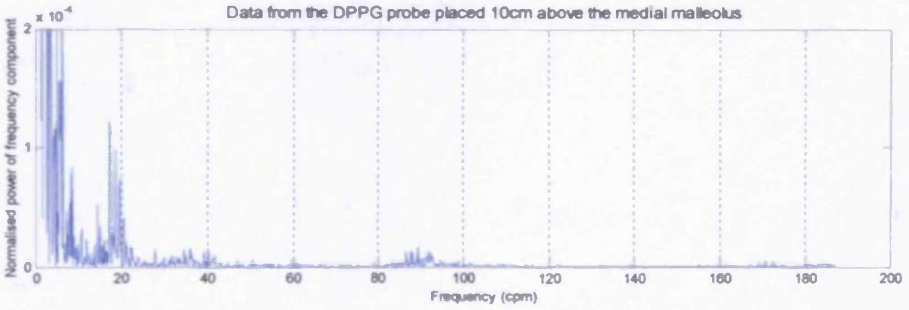

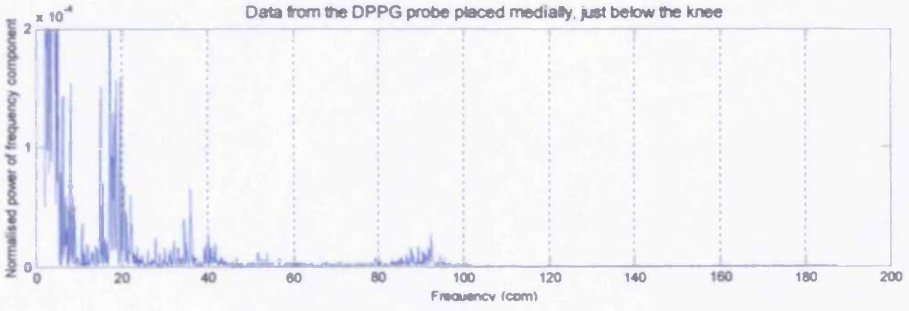

Power spectra between 0cpm and 10cpm

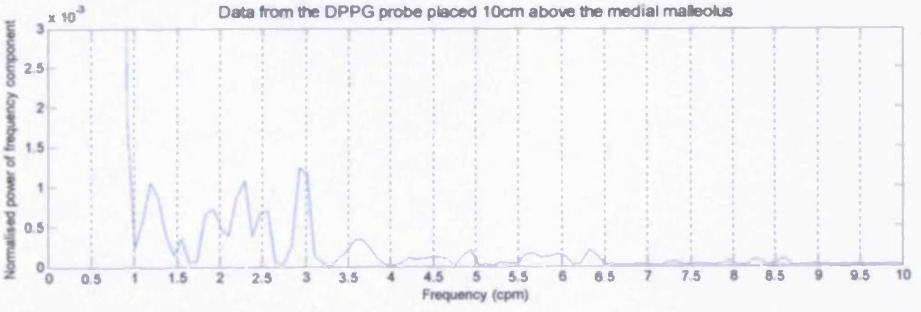

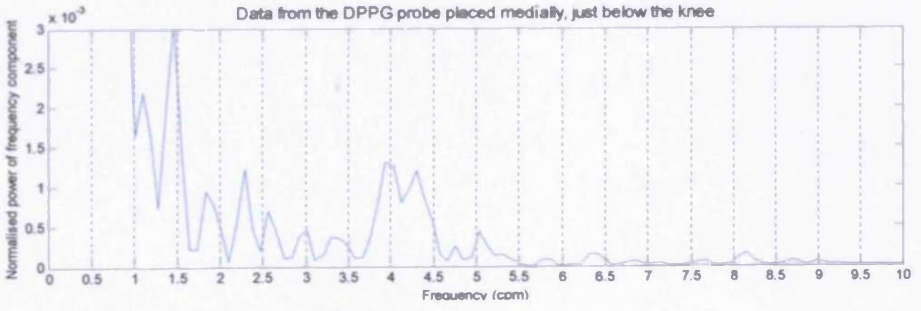

Volunteer 2

Power spectra between 0cpm and 187.5cpm

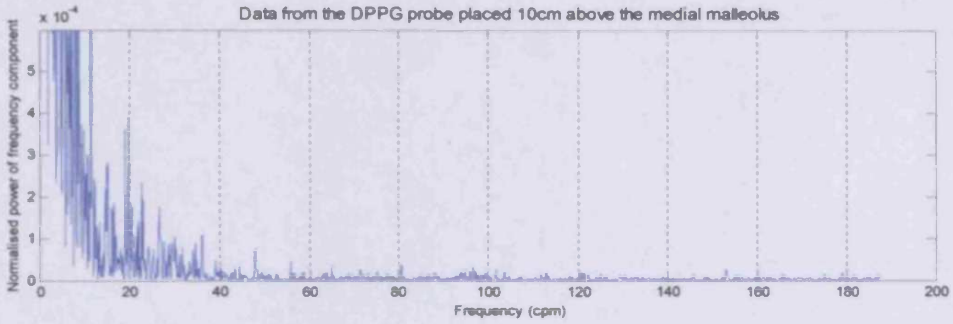

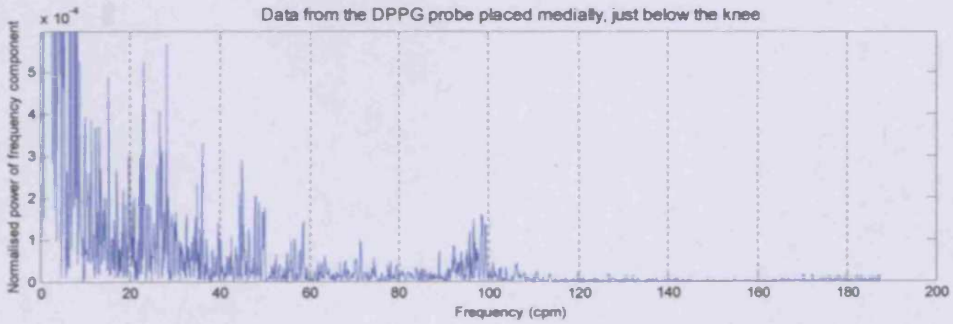

Power spectra between 0cpm and 10cpm

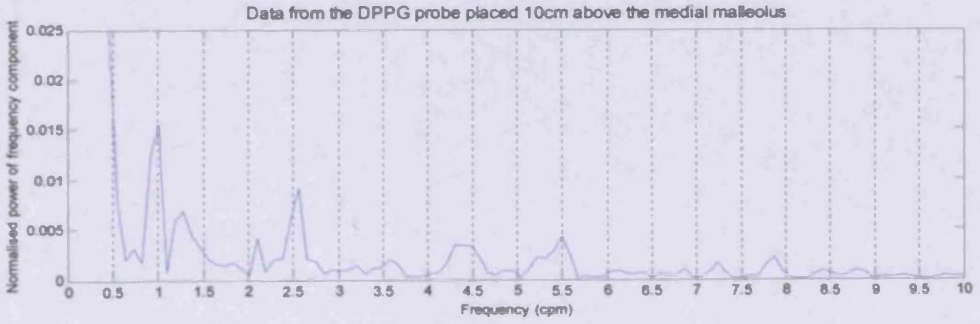

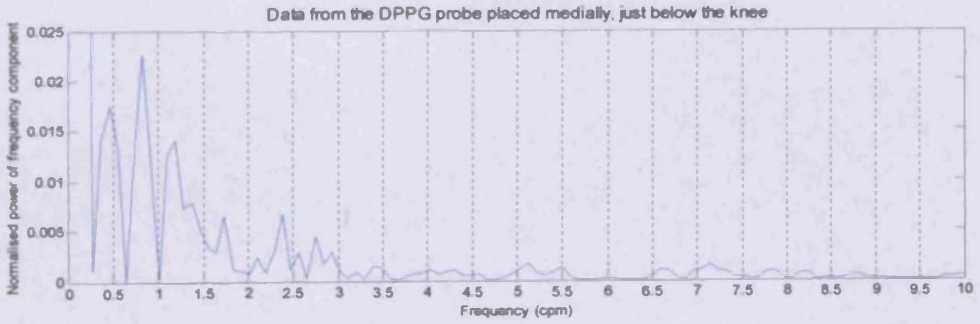

Volunteer 3

Power spectra between 0cpm and 187.5cpm

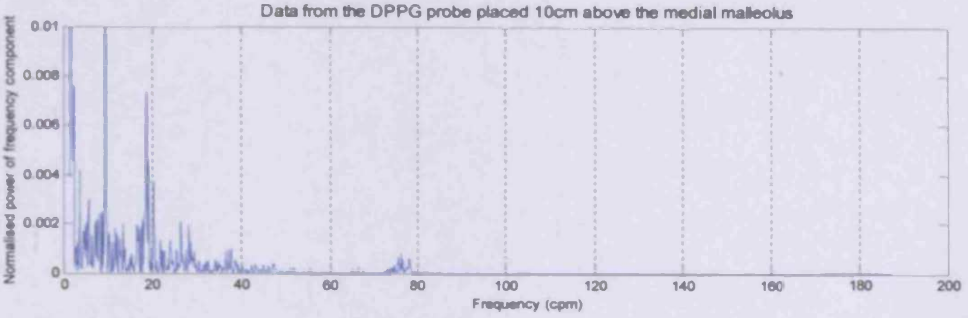

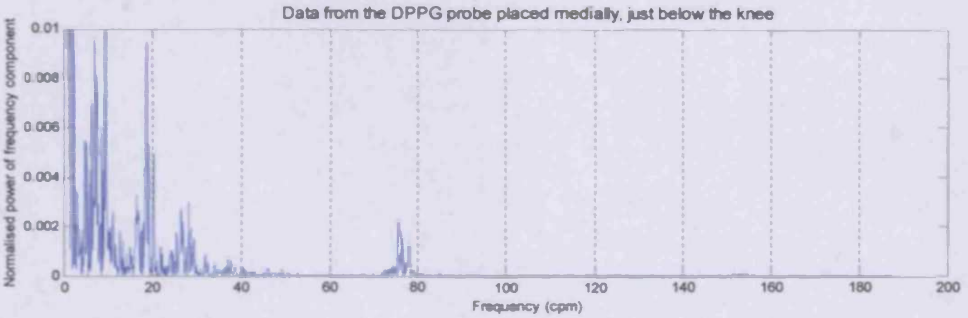

Power spectra between 0cpm and 10cpm

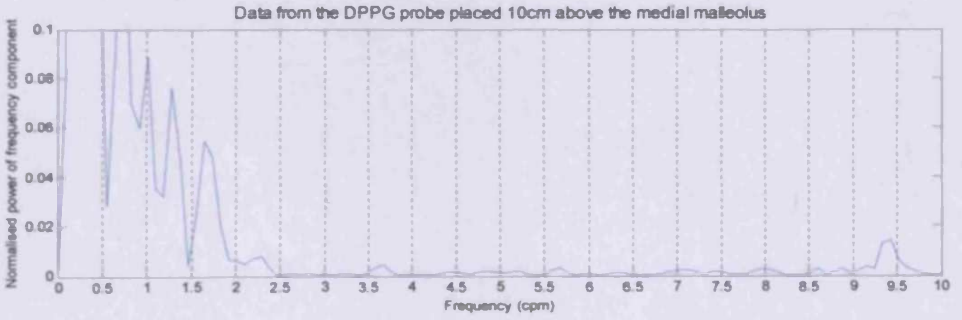

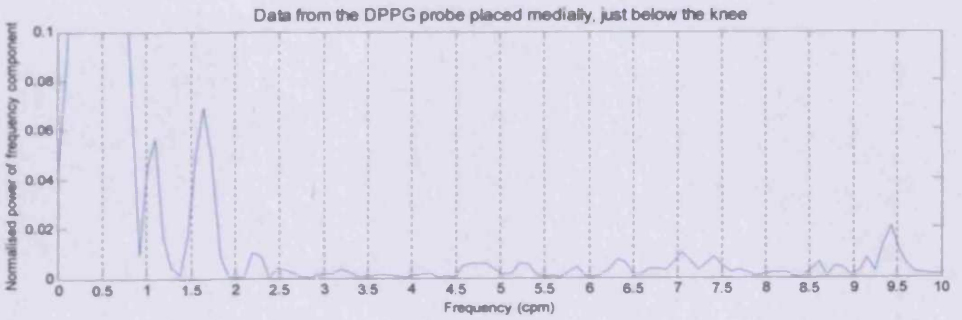

Volunteer 4

Power spectra between 0cpm and 187.5cpm

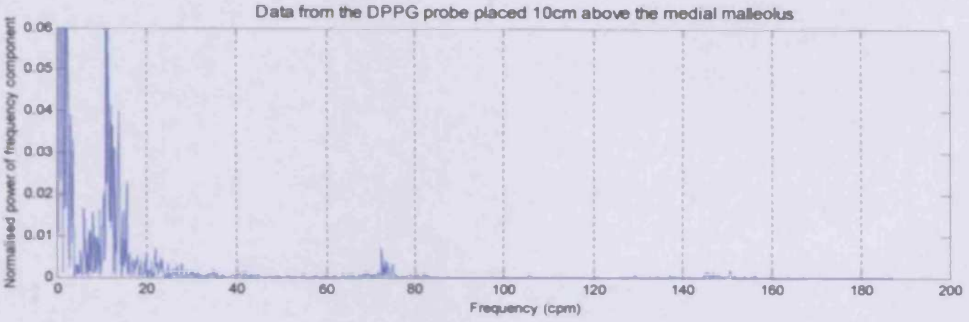

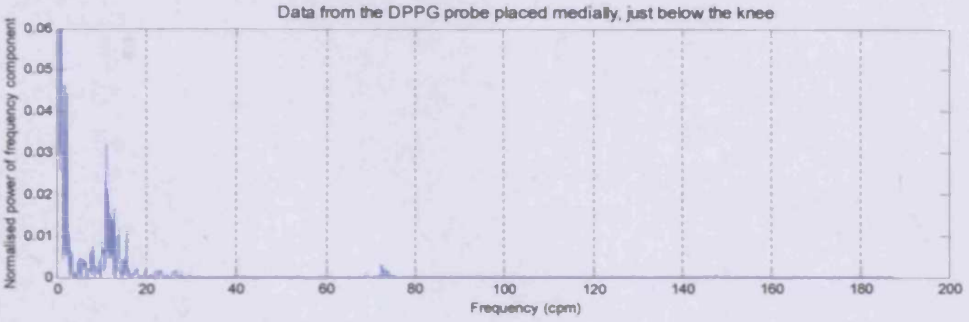

Power spectra between 0cpm and 10cpm

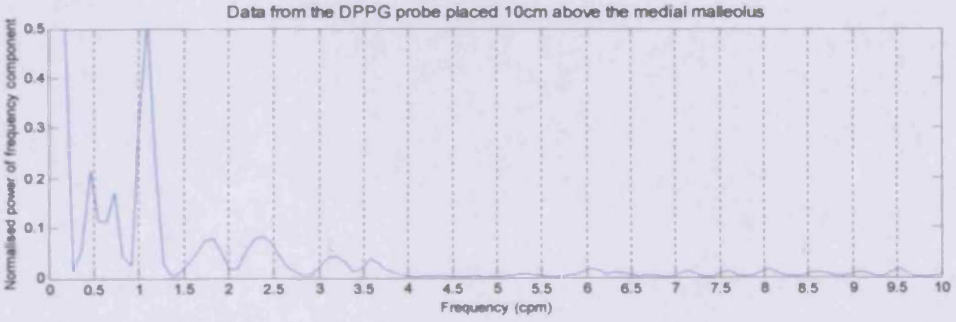

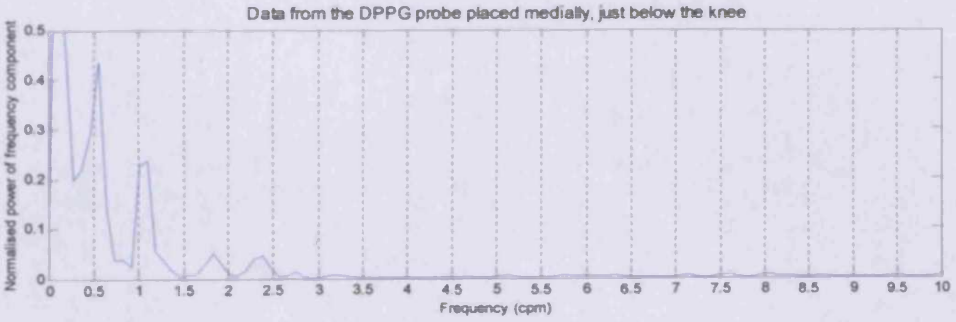

Volunteer 5

Power spectra between 0cpm and 187.5cpm

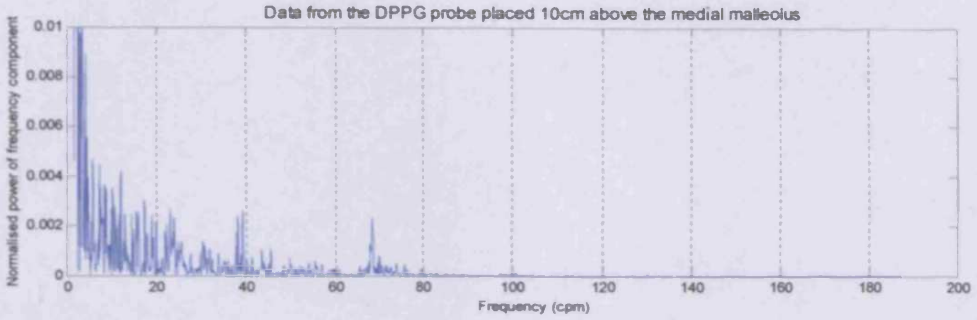

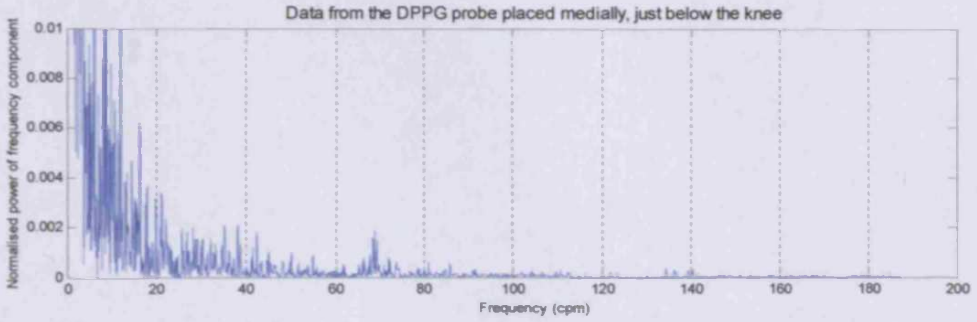

Power spectra between 0cpm and 10cpm

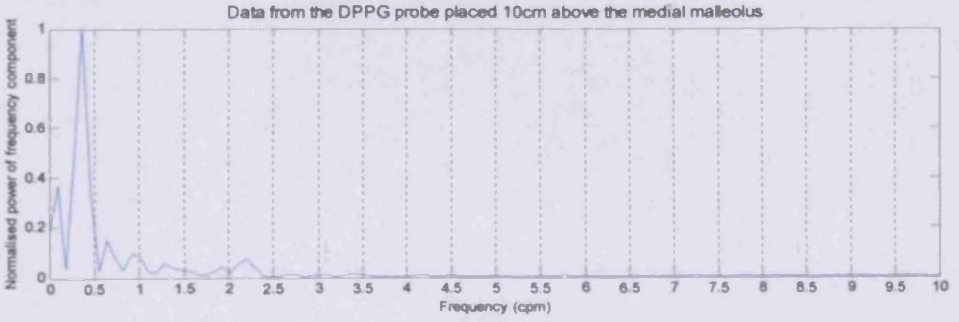

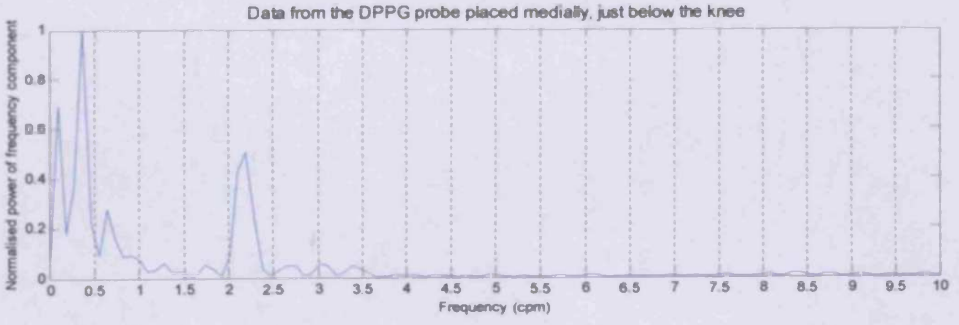

Appendix G

Copies of the information sheet and consent form used in the patient study

---

Patient Information Sheet

"Measurement of Venous Blood Flow Using Photoplethysmography"

A photoplethysmograph (PPG) is a device that uses infrared light (like normal light but with lower energy) to measure changes in an amount of blood. Measurement probes are attached to the skin with sticky pads and infrared light is shone from the probes onto the skin. The amount of light that returns to the probes depends on the amount of blood in the vessels of the skin.

It has been suggested that PPG may be used as a test for deep vein thrombosis (DVT). Currents tests for DVT, including venography and Doppler ultrasound, are time consuming, expensive and require specialist operators. However, PPG may be able to offer a quick, simple, cost effective test for DVT that can be performed anywhere and by anyone. A distinct advantage of such a system would be the ability to test for DVT away from a hospital setting.

Your participation will involve sitting on a bed, relaxed and motionless for 10min. Two PPG probes will be taped to the soles of your feet. The procedure is painless and will in no way affect your normal investigation for DVT. There are no harmful effects associated with PPG. If any discomfort is experienced, the test will be stopped.

If you have any concerns or questions, please contact Mr G John on 029 2074 2015 who will be happy to discuss these matters with you.

We would be most grateful for your help, but you are under no obligation to take part in the study. If you agree, you will be free to change your mind at any time without your normal investigation being affected.

Thank you.

Patient Consent Form

"Measurement of Venous Blood Flow Using Photoplethysmography"

Please fill in this form yourself, ticking the boxes where provided.

1. Have you read and understood the patient information sheet? Yes☐ No☐
   You may keep a copy if you wish.
2. Have you had the opportunity to discuss this study, and ask any questions? Yes☐ No☐
3. Have you had satisfactory answers to all of your questions? Yes☐ No☐
4. Have you received enough information about the study? Yes☐ No☐
5. Who has given you an explanation about the study?

   Dr/Mr/Mrs.....

6. Sections of your medical notes relating to your participation in the study may be inspected by responsible individuals from the Department of Medical Physics. All personal details will be treated as STRICTLY CONFIDENTIAL.

   Do you give you permission for these individuals to have access to your records? Yes☐ No☐

7. Do you understand that you are free to withdraw from the study:

- At any time?
- Without having to give a reason?
- Without affecting your medical care?
- That details of your participation up to the time of withdrawal will be stored anonymously on file and may be used in the final analysis of data?

  Yes☐ No☐

8. Have you had sufficient time to come to your decision? Yes☐ No☐
9. Do you agree to participate in this study? Yes☐ No☐

PATIENT Name .....
Date .....
Signed .....

WITNESS Name .....
Date .....
Signed .....

I have explained the study to the above patient and he/she has indicated his/her willingness to take part.

INVESTIGATOR Name.....
Date.....
Signed .....

Appendix H

Summary of the DUS scan results and relevant medical history for the patients who participated in this study

---

The following tables show:

i. The DUS scan results for the patients who participated in this study.
ii. Any relevant details given on the doctor's request form and the results of any previous or subsequent DUS scans at the same hospital (UHW).

i. Doppler ultrasound scan results

Patients with confirmed DVT

Patient Number	Diagnosis
1	Left leg. Extensive acute ileo-femoral DVT.
2	Left leg. Acute popliteal DVT. No extension into femoral vein noted.
3	Left leg. There is an acute femoral DVT extending up to proximal SFV level.
4	Right leg. There is an acute plug of thrombus in one of the peroneal veins. The thrombus is partially occlusive. No evidence of any fem-pop DVT. There is fluid effusion behind the knee and in the proximal calf.
5	Left leg: There is a femoral DVT, which is extending up to the distal SFV level. There is partial recanalisation of the thrombus and appearance suggests it is 1-2 months old. Right leg: Popliteal vein is patent but there is a posterior tibial vein DVT, some partial recanalisation and appearance suggest 1-2 months old.
6	Left leg. Extensive acute ileo-femoral DVT, extending proximally to confluence of common iliac vein and IVC but not extending into IVC.
7	Left leg. There is an acute peroneal DVT.
8	Left leg. There is an acute peroneal DVT. No extension into fem-pop veins.
9	Right leg. Extensive acute femoral DVT extending proximally to common femoral level.
10	Right leg. No evidence of any fem-pop DVT. There is a small plug of isolated clot in one of the posterior tibial veins otherwise no further below knee DVT.
11	Left leg. There is an extensive acute ileo-femoral DVT.
12	Left leg. Acute femoral DVT extending up to mid SFV level.
13	Right leg. Acute posterior tibial vein DVT affecting one of the paired veins and no evidence of any extension into fem-pop veins.
14	Left leg. Acute femoral DVT extending to confluence with deep femoral vein.
15	Right leg. Acute distal femoral DVT extending just up to the distal external iliac veins.
16	Left leg. Acute popliteal DVT extending up to distal femoral level.
17	Left leg. Extensive acute DVT extending proximally to popliteal level. No femoral extension.
18	Right leg. Acute popliteal DVT. No evidence of any extension into femoral vein.
19	Left leg. Acute ileo-femoral DVT
20	Right leg. Acute DVT in the post tibial veins. Extensive post thrombotic changes above knee also some thrombo-phlebitis in the LSV below knee.
21	Right leg. Extensive clot in the below knee peroneal veins. Veins are well distended

	and the clot is quite anechoic. Appears to be an acute DVT.
22	Right leg. Acute femoral DVT extending up to confluence of the SFV and PFV. CFV is patent above.
23	Right leg. Acute posterior tibial DVT. No extension into fem-pop veins noted.
24	Left leg. Isolated acute peroneal DVT affecting one of the paired veins. No evidence of any DVT in fem-pop veins.
25	Left leg. Extensive femoral DVT extending up to proximal CFV where the thrombus is partially occlusive.
26	Right leg. Acute peroneal DVT. No extension into fem-pop veins noted.
27	Right leg. There is an acute femoral DVT extending up to the groin level. CFV is patent above.
28	Right leg. There is an acute popliteal DVT.
29	Right leg. There is an acute peroneal DVT affecting one of the paired veins. No extension into the fem-pop veins. There is also some superficial thrombo-phlebitis in the below knee LSV.
30	Right leg: There is an acute clot in the iliac and common femoral vein. There is no fem-pop DVT. This looks like as if it is a primary iliac vein DVT. Incidentally, there is a 5.3cm AAA containing significant intraluminal thrombus.
31	Left leg. There is an acute femoral DVT extending proximally to the confluence with the deep femoral vein.
32	Right leg. No evidence of any acute fem-pop DVT, but there is an extensive below knee DVT. The veins are quite distended and this looks like a relatively acute DVT.
33	Right Leg. There is an acute femoral vein DVT extending up to the SFV level.
34	Right leg. There is an acute femoral DVT extending up to the proximal thigh level.
35	Right leg. There is an acute peroneal DVT. No evidence of any proximal extension.
36	Left leg. There is an acute clot in the iliac vein, which is extending into the common iliac and proximal external iliac vein. The clot appears partially occlusive in parts. No evidence of any infra-inguinal clot.
37	Right leg. There is an acute femoral DVT extending to the confluence of the femoral and deep femoral veins.
38	Right leg. Extensive acute ileo-femoral DVT.
39	Right leg. There is an acute DVT in one of the peroneal veins. This does not extend into the fem-pop segment.
40	Left leg. There is an acute DVT extending from the calf veins up to the mid SFV.
41	Right leg. There is an acute popliteal DVT with the thrombus extending up from the peroneal veins.
42	Left leg. There is an acute femoral DVT extending up to the level of the groin. CFV patent above.
43	Left leg. There are extensive chronic changes in the calf veins consistent with the previous DVT. However, there is an acute DVT in one of the posterior tibial veins extending into the distal popliteal vein.
44	Right leg. There is an acute peroneal DVT affecting one of the paired veins. No evidence of any fem-pop DVT.
45	Right leg. There is a small plug of partially occlusive thrombus in the femoral vein just below the bifurcation. No evidence of any further fem-pop or calf vein DVT.
46	Left leg. There is a popliteal vein DVT with the thrombus extending in from one of the paired peroneal veins. There is a duplicated popliteal vein with thrombus in one. The other popliteal vein is patent as is the femoral vein.
47	Left leg. There is an acute DVT in the posterior tibial veins and one of the peroneal veins which is extending into the distal popliteal vein.
48	Left leg. There is an acute peroneal DVT. This does not extend into the popliteal vein.
49	Right leg. There is an acute ileo-femoral DVT. There is also an acute thrombus in the PFV and LSV.
50	Right leg. Extensive acute calf vein DVT running into the popliteal vein.
51	Right leg. There is an extensive acute femoral DVT extending proximally to common femoral level.
52	Left leg. There is an acute peroneal DVT. No fem-pop extension.
53	Left leg. There is an acute iliac/common femoral DVT but no evidence of any

	femoral or popliteal DVT below. There is a left transplanted kidney and there are complex cystic areas in the region of the kidney. History of Ca - ? pelvic pathology.
54	Right leg. There is an acute peroneal DVT in both branches of the peroneal vein. No proximal extension into popliteal.
55	Positive. Right leg. There is an acute clot in the peroneal and intra-muscular calf veins. No proximal extension into the popliteal vein.
56	Right leg. There is a peroneal DVT, which is beginning to resolve, and I would think consistent with a history of 3-4 weeks. No evidence of any proximal extension into fem-pop segment.
57	Left leg. There is DVT in the femoral vein extending proximally to confluence with deep femoral vein. This is most probably an acute DVT.
58	Left leg. There is a partially occlusive acute DVT extending up to the mid CFV.
59	Right leg. There is acute DVT in one of the paired peroneal, which does not extend into the popliteal vein.
60	Right leg: There is acute DVT in one of the paired peroneal veins in the calf. This is not extending into the popliteal vein. Left leg: No evidence of any acute fem-pop or calf vein DVT on duplex.
61	Left leg. Extensive acute calf and popliteal vein DVT confirmed on duplex.
62	Left leg. Extensive acute below knee DVT in posterior tibial and peroneal veins. No extension into fem-pop segment.
63	Left leg. There is an acute ileo-femoral DVT. Right leg. No obvious ileo-femoral DVT.
64	Left leg. Acute femoral DVT extending up to CFV in the groin.
65	Right leg. There is an acute ileo-femoral DVT.

Patients with no confirmed DVT

Patient Number	Diagnosis
1	Left leg: No evidence of any acute fem-pop or calf vein DVT on duplex.
2	Left leg: No evidence of any acute fem-pop or calf vein DVT on duplex.
3	Right leg: No evidence of any acute fem-pop or calf vein DVT on duplex.
4	Left leg: No evidence of any acute fem-pop DVT on duplex. In the calf there are post thrombotic changes in the posterior tibial veins suggestive of a previous DVT but no evidence of any acute DVT.
5	Right leg: Some post thrombotic changes in the peroneal veins suggestive of a small previous DVT but no evidence of any acute DVT. Gross oedema noted below knee.
6	Left leg: No evidence of any obvious DVT in fem-pop or calf veins on duplex. There is evidence of a ruptured Baker's cyst in the medial aspect of the knee.
7	Bilateral scan: No evidence of any acute fem-pop or calf vein DVT on duplex.
8	Right leg. No evidence of any fem-pop or calf vein DVT on duplex. There is superficial thrombo-phlebitis in the LSV just below the knee.
9	Right leg. No evidence of any acute fem-pop or calf vein DVT on duplex.
10	Left leg. No evidence of any acute fem-pop or calf vein DVT on duplex.
11	Right leg. No evidence of any acute fem-pop or calf vein DVT on duplex. There is evidence of superficial thrombo-phlebitis in the distal calf LSV.
12	Right leg. No evidence of any acute fem-pop or calf vein DVT on duplex.
13	Left leg. No evidence of any acute fem-pop or calf vein DVT on duplex.
14	Left leg. No evidence of any acute fem-pop or calf vein DVT on duplex.
15	Right leg. No evidence of any acute fem-pop or calf vein DVT on duplex.
16	Bilateral scan. No evidence of any acute fem-pop or calf vein DVT on duplex.
17	Right leg. No evidence of any acute fem-pop or calf vein DVT on duplex.
18	Left leg. No evidence of any acute fem-pop or calf vein DVT on duplex.
19	Left leg. No evidence of any acute fem-pop or calf vein DVT in duplex.
20	Left leg. No evidence of any acute fem-pop or calf vein DVT on duplex.
21	Bilateral scan. No evidence of any acute fem-pop or calf vein DVT on duplex.

22	Right leg. No evidence of any acute fem-pop or calf vein DVT on duplex. There are several enlarged lymph nodes in the groin - ? Some degree of lymph obstruction.
23	Left leg. No evidence of any acute fem-pop or calf vein DVT on duplex.
24	Right leg. No evidence of any acute fem-pop or calf vein DVT on duplex.
25	Left leg. No evidence of any acute fem-pop or calf vein DVT on duplex.
26	Left leg. No evidence of any acute fem-pop or calf vein DVT on duplex.
27	Left leg. No evidence of any acute fem-pop or calf vein DVT on duplex.
28	Left leg. No evidence of any acute fem-pop or calf vein DVT on duplex.
29	Left leg. No evidence of any acute fem-pop or calf DVT on duplex.
30	Right leg. No evidence of any acute fem-pop DVT on duplex. In the calf there are post thrombotic changes in the peroneal veins suggestive of a previous DVT but no evidence of any acute DVT.
31	Right leg. No evidence of any acute fem-pop or calf vein DVT on duplex.
32	Right leg. No evidence of any acute fem-pop or calf vein DVT on duplex.
33	Left leg. No evidence of any acute fem-pop or calf vein DVT on duplex.
34	Left leg. No evidence of any acute fem-pop or calf vein DVT on duplex.
35	Left leg. No evidence of any acute fem-pop or calf vein DVT on duplex.
36	Left leg. No evidence of any acute fem-pop or calf vein DVT on duplex.
37	Left leg. No evidence of any acute fem-pop or calf vein DVT on duplex.
38	Right leg. No evidence of any acute fem-pop or calf vein DVT on duplex.
39	Bilateral scan. No evidence of any acute iliac, fem-pop or calf vein DVT on duplex.
40	Left leg. No evidence of any acute fem-pop or calf vein DVT on duplex.
41	Right leg. No evidence of any acute fem-pop or calf vein DVT on duplex.
42	Left leg. No evidence of any acute fem-pop or calf vein DVT on duplex.
43	Left leg. No evidence of any acute fem-pop or calf vein DVT on duplex.
44	Right leg. No evidence of any fem-pop DVT on duplex. Calf veins not fully seen but no obvious calf vein DVT on duplex.
45	Right leg. No evidence of any acute fem-pop or calf vein DVT on duplex.
46	Right leg. Extensive post thrombotic changes in the calf veins, but no evidence of any acute DVT. No evidence of any acute thrombo-phlebitis.
47	Right leg. No evidence of any acute fem-pop or calf vein DVT on duplex.
48	Left leg. No evidence of any obvious DVT in fem-pop or calf veins on duplex. There is evidence of a ruptured Baker's cyst in the medial aspect of the knee trekking down the calf.
49	Left leg. No evidence of any acute fem-pop or calf vein DVT on duplex.
50	Left leg. No evidence of any acute fem-pop or cal vein DVT on duplex.
51	Right leg. No evidence of any acute fem-pop or calf vein DVT on duplex. No evidence of any Baker's cyst.
52	Left leg. No evidence of any acute fem-pop or calf vein DVT on duplex.
53	Right leg. No evidence of any acute fem-pop or calf vein DVT on duplex.
54	Left leg. No evidence of any acute fem-pop or calf vein DVT on duplex.
55	Left leg. No evidence of any fem-pop or calf vein DVT on duplex.
56	Left leg. No evidence of any acute fem-pop or calf vein DVT on duplex.
57	Left leg. No evidence of any acute fem-pop or calf vein DVT on duplex. Deep venous reflux noted particularly in one of the paired posterior tibial veins and in the distal SFV.
58	Left leg. No evidence of any acute fem-pop or calf vein DVT on duplex. There is evidence of a Baker's cyst in the medial aspect of the knee.
59	Right leg. No evidence of any acute fem-pop or calf vein DVT on duplex.
60	Right leg. No evidence of any fem-pop or calf vein DVT on duplex.
61	Left leg. No evidence of any acute fem-pop or calf vein DVT on duplex. There is superficial thrombo-phlebitis in the prominent vein at the back of the calf.
62	Right leg. There is resolving chronic thrombus in the peroneal veins and deep venous reflux in the popliteal vein consistent with an acute DVT a few months ago. No current fem-pop or calf vein acute DVT.
63	Left leg. No evidence of any acute fem-pop or calf vein DVT on duplex.
64	Right leg. Some post thrombotic changes in the leg but no evidence of any acute iliac,

	fem-pop or calf vein DVT.
65	Bilateral. No evidence of any acute fem-pop or calf vein DVT bilaterally on duplex. Chronic cellulites affecting both legs.
66	Right leg. No evidence of any acute fem-pop or calf vein DVT on duplex.
67	Bilateral scan. No evidence of any acute fem-pop or calf vein DVT bilaterally on duplex.
68	Left leg. There are extensive post thrombotic changes throughout the leg especially below the knee but there is no obvious acute DVT.
69	Right leg. Extensive post thrombotic changes in the calf veins, but no evidence of any acute DVT.
70	Left leg. No evidence of any acute fem-pop or calf vein DVT on duplex.
71	Left leg. No evidence of any obvious DVT in the fem-pop or calf veins on duplex. There is evidence of a large ruptured Baker's cyst in the medial aspect of the knee tracking down the calf.
72	Left leg. No evidence of any acute fem-pop or calf vein DVT on duplex.
73	Left leg. No evidence of any acute fem-pop or calf vein DVT on duplex.
74	Right leg. No evidence of any fem-pop DVT on duplex. Calf veins not fully seen but no obvious calf vein DVT on duplex.
75	Right leg. No evidence of any acute fem-pop or calf vein DVT on duplex.
76	Right leg. No evidence of any acute fem-pop or calf vein DVT on duplex.
77	Left leg. No evidence of any acute fem-pop or calf vein DVT on duplex.

ii. Relevant details on the doctor's request form and results of previous or subsequent Doppler ultrasound scans

Patients with confirmed DVT

Patient Number	Details on Request Form	Details of previous or subsequent DUS scans
1	Increased swelling in the left leg for 5 days. Previous history rheumatoid arthritis. On sulphasalazine. Splenectomy ~20yrs ago.	N/A
2	Left leg swelling. Mild cellulitis.	N/A
3	Query DVT left calf.	N/A
4	Had a total knee replacement on 14/5/03 and has right ankle oedema.	N/A
5	Left calf swelling on and off for weeks – painful last few days. Feels hot. Query DVT.	N/A
6	Admitted with swelling and pain left thigh and calf. Tender superficial veins. Had total hip replacement. Pain now worse upper left thigh.	Subsequent scan 22-04-04: Left leg: The common and external iliac veins remain chronically occluded. The collateralisation is mainly via pelvic cross over to the right SFJ. The collateralisation in the pelvis does not look particularly good. The femoral vein has recanalised reasonably well and the popliteal and below knee veins are patent and competent (these were not involved previously). There is no significant superficial incompetence at present. In conclusion chronic occlusion of iliac system.
7	Painful swollen left leg. Previous DVT. Oral contraceptive pill. Pitting, pedal oedema. Pain in calf on dorsiflexion.	N/A
8	Four weeks in plaster. Painful left calf.	N/A
9	Very swollen and tense right calf. This has been present for several weeks, but does not seem to be getting better or worse. Oedematous and tense but not red and hot. Query DVT.	30-05-01 No significant evidence of acute DVT bilaterally on duplex. All the deep veins are patent and competent. No significant chronic disease noted.
10	Swelling, redness, right calf. History of injury to right leg days ago. Query DVT.	N/A
11	Previous surgery to abdomen, now has hot swollen calf. Left leg.	24-10-00 Left leg: No evidence of any acute fem-pop DVT on duplex. Reflux in posterior tibial veins. Possible chronic changes.
12	Two weeks post total hip replacement. Left calf swollen and tender.	N/A
13	Pain in right calf worsening over last 24hrs. Difficult to weight-bear on that leg. Tender right calf. No swelling.	N/A
14	Pain started in knee after prolonged kneeling. Now whole left calf very hot and tender. Clinically ruptured Baker's cyst but need to exclude DVT.	N/A
15	Swollen right calf and thigh. Query DVT.	N/A
16	Left calf pain and swelling. Tender calf and heavy smoker.	N/A
17	Swollen left leg. Smoker 20+ per day. Alchohol 84+units/wk.	N/A
18	Swollen right lower leg. Possible previous bite. No previous DVT	N/A

19	Two days ago sudden onset of red, swollen, warm, tender left leg below and above knee. Query DVT. On aspirin and bendrofluazide. Has atrial flutter.	N/A
20	Swollen, tender right calf. Previous PE. Previous multiple DVTs.	30-12-1999 In the LEFT lower limb there is evidence of acute DVT in the distal SFV, popliteal, posterior tibial and peroneal veins. The thrombus appears fresh and echolucent (<1 week old). No recanalisation noted. The common femoral and proximal SFV appear patent. In the RIGHT lower limb there is evidence of post-thrombotic changes throughout the femoro-popliteal and calf deep veins with scarring and DVI noted. No evidence of any acute thrombus observed. 22-05-03 In the RIGHT lower limb there is evidence of post-thrombotic changes throughout the femoro-popliteal and calf deep veins with scarring and DVI noted. No evidence of any acute thrombus observed.
21	Recent fractured ankle. Limb in plaster. Previous PE. Now has swollen calf. On warfarin. Query DVT.	N/A
22	Presents with pain and swelling in the right calf. No history of trauma.	N/A
23	Has single vessel coronary artery disease (1998). He presents with left ankle and calf pain with some ankle oedema.	Subsequent scan 10-10-03: Right leg – There is an acute posterior tibial DVT. No extension into fem-pop veins noted.
24	Ten 10 days post-natal. She has a tender left lower calf but no swelling. Probably muscular pain.	N/A
25	Swollen left calf (>Right). Pain. Erythema.	N/A
26	Right leg painful and slight swelling.	N/A
27	Pain and swelling in the right calf. Carcinoma caecum in 2003 – lymph node positive. Need to check pelvis.	N/A
28	Previous left sided DVT. Complaining of tense and tender right calf.	25-02-03 Left leg: There is an acute femoral DVT extending up to the level of the groin.
29	Query DVT.	N/A
30	Previous muscle-invasive disease of bladder. Swollen right calf.	N/A
31	Adenocarcinoma of the pancreas. Swollen left leg.	N/A
32	History of Achilles tendon repair 12 weeks ago. Immobilised in cast. Previous DVTs. On warfarin. Swelling and pain in right leg/calf.	14-10-03 There is an isolated posterial tibial DVT affecting one of the paired veins. No evidence of any fem-pop DVT.
33	Painful swelling in right leg. Previous DVT in the left leg. On aspirin.	N/A
34	Swelling and pain in right calf for 5 days. Some oedema.	N/A
35	Previous DVT. Has been in part plaster for fractured ankle. On warfarin. Now complains of pain in the right calf, which is more swollen/firmer than the left. Query right, below knee DVT.	22-10-01 Right leg: Extensive below knee DVT affecting both the posterior tibial and peroneal veins. No popliteal extension.

36	Pain in left leg with swelling – thigh and calf. Query femoral DVT or ruptured Baker's cyst.	N/A
37	Swollen right calf/leg since fractured left hip. Oedema and swelling for 3 days.	N/A
38	Swelling and tender right leg. Query DVT.	N/A
39	Swollen and painful right leg for 3 days. Calf pain on dorsiflexion of right ankle. Query DVT.	N/A
40	Painful swollen left calf. Query DVT.	N/A
41	Previous history of DVT in the left calf. Right calf tender. Has a poor perforating vein in the right calf.	N/A
42	Swelling. Query DVT.	N/A
43	Pregnant. Family history DVT. Pain in left calf.	N/A
44	Recent right knee arthroscopy. Increased right leg swelling.	N/A
45	Query right calf DVT after total hip replacement.	N/A
46	Swollen left leg and increased shortness of breath. Nodes in left groin. Query DVT.	N/A
47	Four days history of pain and swelling in the left calf. Query DVT.	N/A
48	Achilles tendon repair. Left leg in plaster. Now tender, warm to palpation. Increased swelling. Query DVT.	N/A
49	Two weeks history of hot, swollen, painful right leg.	14-11-02 Deep fem-pop patent and competent. Extensive post thrombotic changes below knee bilaterally.
50		06-06-02 Left leg: Extensive post thrombotic changes in the popliteal and calf veins but no evidence of any acute DVT.
51	Tender, swollen calf highly suggestive of a DVT.	09-03-04 Left leg: No evidence of any acute fem-pop or calf vein DVT on duplex.
52	Recent hospital stay. Now complains of tenderness in left calf. Left calf larger than right.	N/A
53	Developed groin/upper leg pain on walking. After stopping, the pain subsides. Associated oedema of the left leg has occurred. Recently had major maxillofacial surgery for a squamous cell carcinoma, which has led relatively immobility. A smoker, but there is no previous history/family history of DVT. Oedema to mid shin left leg. Scar from coronary artery bypass graft left leg (no previous oedema).	N/A
54	Swollen right calf. Raised D-dimer. Two weeks post op.	N/A
55	Fractured foot in plaster for one week. No swelling or redness. Pain in postero-lateral aspect of calf.	N/A
56	Swelling of right leg since coming out of hospital two weeks ago.	N/A
57	Previous popliteal – femoral DVT. Factor V	03-02-00

	Leiden. Now complains of pain in thigh.	All the deep veins in the LEFT lower limb appear patent and competent with no significant evidence of any previous or acute DVT (common femoral, superficial femoral, popliteal, gastrocnemius, posterior tibial and peroneal veins). There is evidence of acute superficial thrombophlebitis in the calf LSV, which is distended with echolucent thrombus. 11-02-00 Left leg: There is an acute popliteal DVT extending up to the proximal popliteal region. Note - the superficial thrombophlebitis has now spread through the LSV to groin region but is not extending into the deep system at SFJ.
58	Isolated marked swelling of left leg to knee.	N/A
59	Painful, swollen right calf. Most likely a ruptured Baker's cyst.	02-04-03 Right leg. No evidence of any acute fem-pop or calf vein DVT on duplex.
60	Previous DVT and PE. On clexane, starting warfarin.	N/A
61	Painful swollen left calf. Query DVT.	N/A
62	Left total knee replacement 3 weeks ago. Increased swelling and pain in left calf. Query DVT.	N/A
63	Swollen feet and calf (left larger than right).	N/A
64	Developed swelling of left ankle and left calf.	N/A
65	Coronary artery bypass graft 2 weeks ago. Transient ischaemic attack 5 days ago. Now increased swelling and tenderness. Right calf swollen to thigh.	N/A

Patients with no confirmed DVT

Patient Number	Details on Request Form	Details of previous or subsequent DUS scans
1	Left lower leg pain. Tender and slightly swollen.	N/A
2	Left leg in plaster for 6 weeks. Swelling, Erythema and pain in calf. Query DVT.	N/A
3	Painful right calf. Superficial phlebitis. Tender right calf.	N/A
4	Previous DVT. Recent pain in left leg.	28-07-99 Extensive calf vein DVT in posterior tibial and peroneal veins but no extension into popliteal vein. 11-10-00 Right leg: No evidence of any acute fem-pop or calf vein DVT on duplex.
5	Swelling in right calf.	N/A
6	Left leg swelling. History of diabetes and hypertension. Query Ruptured Baker's cyst. Query DVT.	Left leg: No evidence of any fem-pop or calf vein DVT on duplex.

7	Complains of chest pain. Pain in both legs. Query DVT.	N/A
8	Leg red, swollen and hot. Query DVT.	N/A
9	Query DVT in right leg.	N/A
10	Possible 2 week old DVT. Swollen left, painful calf. Left calf tense and more oedematous than right.	N/A
11	Recent aeroplane flight. Superficial thrombophlebitis. Previous varicose vein surgery.	N/A
12	Had a carotid endarterectomy on right side. Has a painful swelling of the right calf. Has a history of transient ischaemic attack, hypertension, left carotid artery occlusion and >90% stenosis of right carotid artery. Also has a history of ischemic heart disease and hypercholesterolaemia. No definitive signs of DVT but a very high risk and history suggestive of DVT.	N/A
13	Recent aeroplane flight. Left calf tenderness.	N/A
14	Red hot swollen left calf and foot. Recent aeroplane flight.	N/A
15	Previous history of DVT and PE. Recent aeroplane flight. Pain and swelling in right calf.	N/A
16	Recent aeroplane flight. Pain and swelling both calves. Calf tenderness bilaterally. A Smoker. On combined oral contraceptive pill. Family history of DVT. Query DVT.	N/A
17	Recent aeroplane flight. Increased swelling in right leg. Previous DVT.	26-01-01 Left leg: There is a peroneal DVT affecting just one of the peroneal veins. The other peroneal vein appears patent, as do the PTVs. No evidence of any extension into fem-pop veins.
18	Had surgery 3 weeks ago (laparoscopic cholecystectomy and now has painful, tender calf. Homan's sign positive. Oedema.	N/A
19	Swollen left leg. Oedema and tender calf.	N/A
20	Tender swollen calf. Query DVT.	N/A
21	Multiple plane flights in past week including 2 long haul flights. Bilateral lower leg and foot oedema. No calf tenderness. Query DVT.	N/A
22	Swollen right leg. Query DVT.	N/A
23	Bruise on left calf one week ago. Cramp like pains. Left calf larger than right and tender. Taking oral contraceptive pill. Family history of DVT.	N/A
24	Swollen right lower leg. Knee injury 2 weeks ago. Aspirated. Now has swollen, painful and hard lower leg.	N/A
25	Query left calf DVT. Taking combined oral contraceptive pill.	N/A
26	Pain and tenderness in left calf. Pregnant.	N/A
27	Sudden onset of severe left calf pain. Muscular ibuprofen not helping. On HRT.	N/A
28	Had arthroscopy to left knee 2 weeks ago.	N/A

	Now has a swollen and painful left calf. Tender to palpation.	
29	Recent aeroplane flight. Swollen, tender left calf. On Femodene.	N/A
30	Pain in left calf and thigh. Bladder operation in 2003. Also had a previous DVT several years ago.	N/A
31	Pain in right calf. An occasional smoker.	N/A
32	Pain and slight swelling in right lower calf. Family history of DVT. Tender calf.	N/A
33	Painful left calf. Query DVT.	N/A
34	Left ankle swollen. Query DVT.	29-12-98 Left leg: No evidence of any fem-pop or calf vein DVT on duplex. There appears to be some thrombo-phlebitis in the short saphenous vein.
35	Previous antenatal DVT. History of varicose veins and superficial phlebitis. Now has tenderness body of gastrocnemius on the right side extending to the back of the thigh. Query DVT.	N/A
36	Pain in the left calf and previous history of DVT in right.	13-06-02 Right leg: There are very extensive post thrombotic changes but no evidence of any acute DVT. The appearance suggests that the popliteal and calf veins were affected by the clot with poor recanalisation especially below the knee.
37	Previous DVT and multiple PEs. On Warfarin. Left knee replacement 11 days ago. Swelling and pain in calf.	N/A
38	Previous varicose veins, eczema and ulcers in the right leg. Swelling and pain in the right calf. Query DVT.	N/A
39	Suspicious of PE. V/Q (ventilation-perfusion scan) negative. ECG changes.	03-03-04 No evidence bilaterally of any acute fem-pop or calf vein DVT on duplex. Normal response to valsalva in groin bilaterally.
40	Pain and tenderness in medial left calf. Family history of thrombosis. A smoker. Homan's sign positive. Query DVT.	N/A
41	Pain in right calf. Leg has been in plaster. Overweight. Family history DVT. A smoker.	N/A
42	Swollen left leg.	N/A
43	Pain in the left calf and slight swelling. Overweight. Recent riding injury.	N/A
44	Painful swollen right calf/lower leg. Varicose veins in the right leg. Tender, hot right lower calf. Homan's sign positive.	N/A
45	Pain in the right calf and along the medial aspect of the thigh. Family history of thromboembolism.	N/A
46	Query DVT in the right calf. Lower leg tender. Previous PE (1995) and DVT in right calf.	N/A
47	Query DVT. Taking oral contraceptive pill.	N/A

48	Sudden increase in lower leg swelling. History of Baker's cyst.	N/A
49	Sudden onset of pain and swelling in the left calf. Tender.	N/A
50	Swollen left leg with varicosities. Not tender or red. No sign of oedema or thrombophlebitis.	N/A
51	Painful right knee. Non smoker. No history of DVT.	N/A
52	Raised D-dimer (615).	N/A
53	Recent aeroplane flight. Sudden onset of pain and swelling in the right calf with cellulites. High body mass index.	N/A
54	Sudden onset of swelling in the left calf. Not tender but feels hot compared to the right leg.	N/A
55	Complains of pain from the heel of the left foot up into the left calf. Left calf is swollen and tender.	N/A
56	Pain in the left calf. No swelling but tender. Recent aeroplane flight. Taking oral contraceptive pill until 3 days ago.	N/A
57	Recent aeroplane flight. Has had two previous DVTs in the left leg. Complains of cramp-like symptoms in the left leg.	N/A
58	Painful and tender left calf. Decreased mobility.	N/A
59	Right calf swollen and red. Tender and aching calf.	N/A
60	Complains of pain in the leg.	N/A
61	Swollen, tender and warm left calf. Increasing in severity and inflamed. No risk factors for DVT, although may be secondary to a bite or thrombophlebitis.	N/A
62	Swollen right calf. Pitting oedema.	N/A
63	Severe pain in the left calf. Query DVT.	N/A
64	Query DVT in the right leg. Factor V Leiden. Recent aeroplane flight. Previous DVTs.	30-07-98 Right leg: Extensive ileo-femoral DVT extending proximally to the common iliac vein. 07-03-00 Reflux in the right femoral veins but recanalised and quite widely patent. No acute DVT. 08-05-01 Right leg: There is evidence of an acute peroneal DVT affecting one of the pair of veins. No evidence of any proximal extension. Evidence of extensive post thrombotic changes throughout the veins. 05-02-03 Right leg: Extensive post thrombotic changes but no evidence of any acute DVT.
65	Inflammation and swelling in the lower legs (right greater than left). History of asthma, gout and back pain. Calf is hot, swollen and tender.	N/A
66	Pain and swelling in the right foot. History of	N/A

	high cholesterol.	
67	Recent aeroplane flight. Has a painful, swollen calf. Shiny appearance. Possible DVT in the right leg.	N/A
68	Taking warfarin. Previous PE and DVT. Sudden onset of swelling in the left calf. Painful.	N/A
69	Sudden onset of swelling in the right leg. Painful. History of previous DVT.	25-03-03 Right leg: No evidence of any fem-pop DVT. There is extensive acute peroneal DVT affecting both branches of the peroneal veins.
70	Polycythaemia. Tender left calf. No clinical evidence of DVT other than specific tenderness.	N/A
71	Swollen and painful left calf. Raised D-dimer (1463).	N/A
72	History of mycotic aneurysm. Increased swelling of the left leg. Query DVT. Recent coach trip.	N/A
73	Knee replacement 7 months ago. Now has swelling and discomfort of calf on the left side. History of hypertension and lumbar canal stenosis.	N/A
74	History of Baker's cysts.	N/A
75	Swelling. Query DVT.	N/A
76	Pain in the right lower leg.	N/A
77	Swelling and pain in the left ankle and calf. Recent holiday abroad. Query DVT.	N/A

Appendix I

DPPG data collected in the patient investigation

Presented here are the DPPG data collected in the patient investigation (Chapter 9).

For the patients with lower limb DVT (confirmed with DUS), the green line corresponds to data taken from the limb with DVT. The blue line corresponds to data taken from the limb without DVT (except patient number 5 who had bilateral DVT).

For the patients with no lower limb DVT, the green line corresponds to data taken from the left limb. The blue line corresponds to data taken from the right limb.

Data from patients with lower limb DVT confirmed with DUS

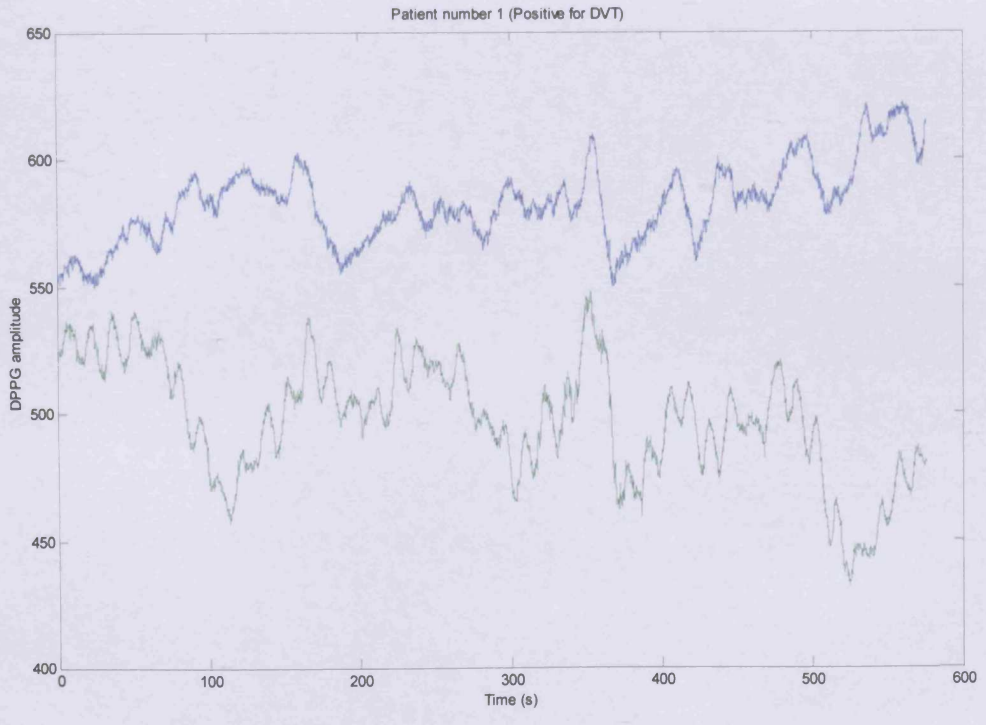
Patient number 1 (Positive for DVT)
650
600
550
500
450
400
DPPG amplitude
0
100
200
300
400
500
600
Time (s)

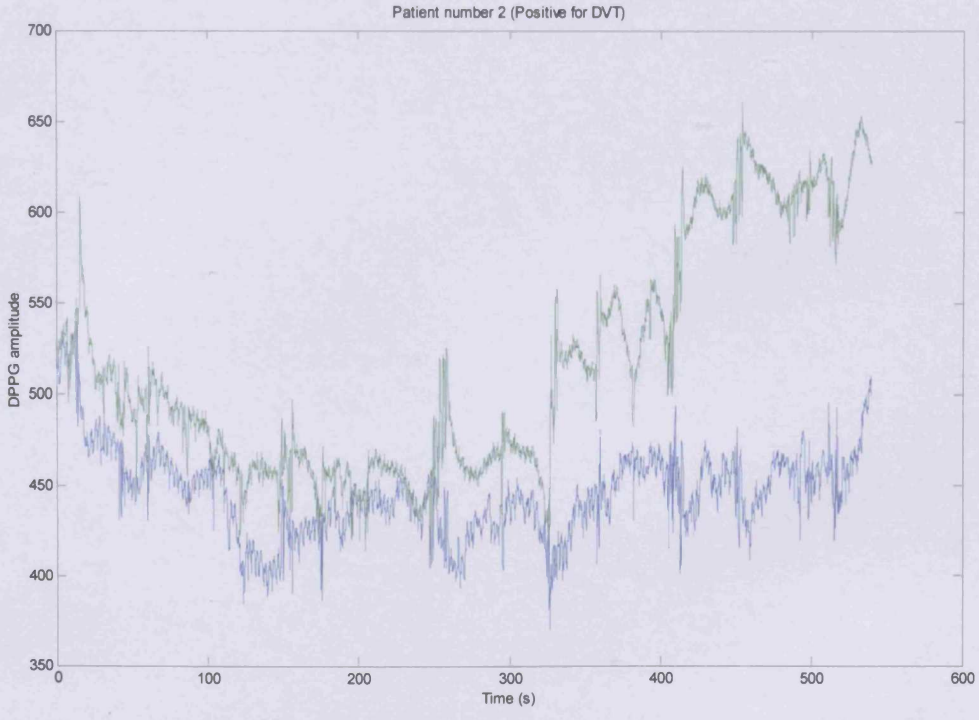
Patient number 2 (Positive for DVT)
DPPG amplitude
Time (s)
700
650
600
550
500
450
400
350
0
100
200
300
400
500
600

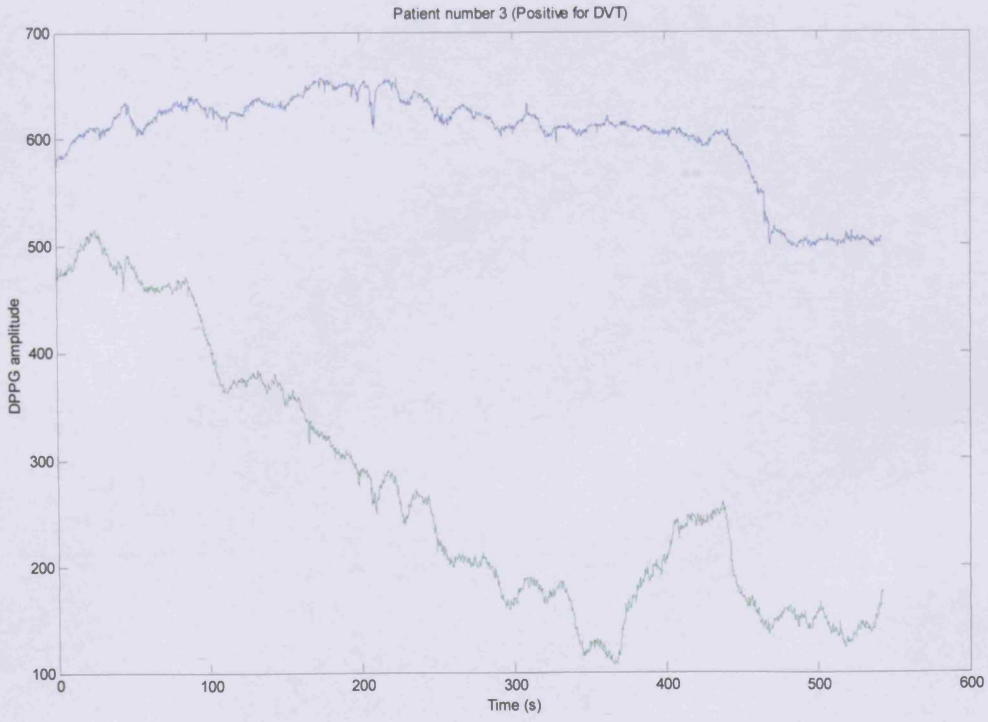
Patient number 3 (Positive for DVT)
DPPG amplitude
Time (s)
700
600
500
400
300
200
100
0
100
200
300
400
500
600

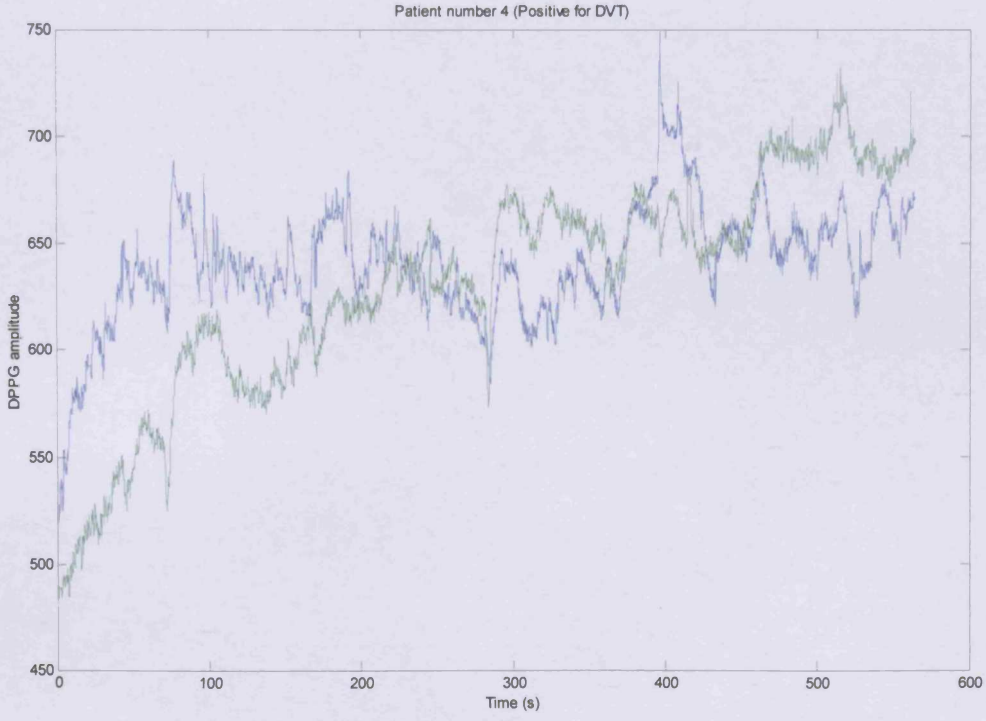
Patient number 4 (Positive for DVT)
DPPG amplitude
Time (s)
750
700
650
600
550
500
450
0
100
200
300
400
500
600

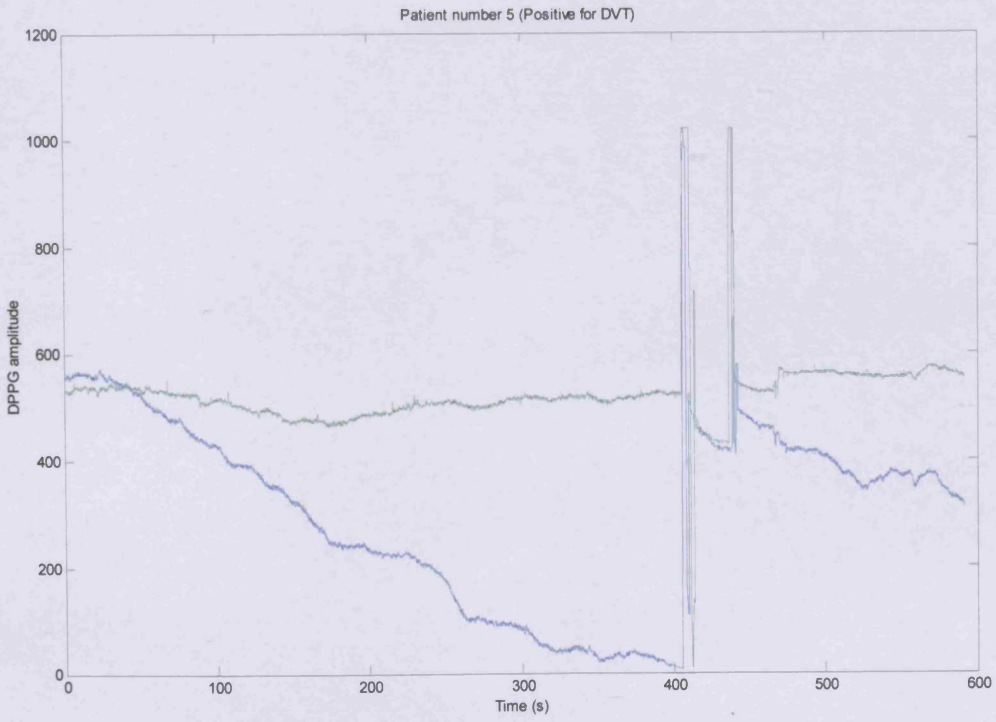
Patient number 5 (Positive for DVT)
DPPG amplitude
Time (s)
0
200
400
600
800
1000
1200
0
100
200
300
400
500
600

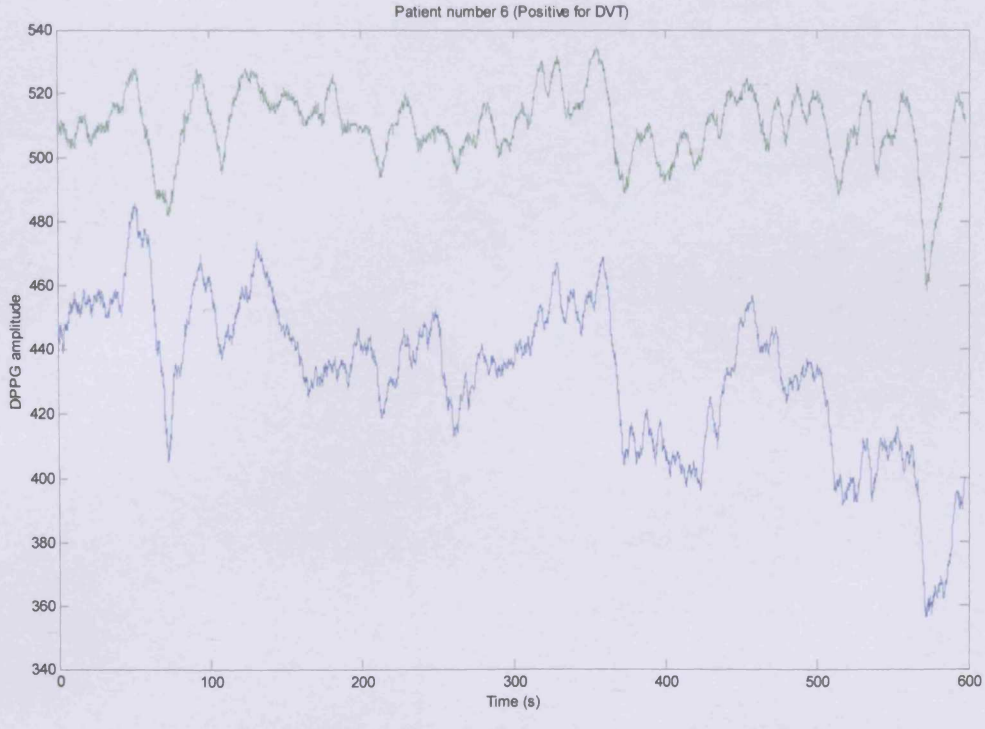
Patient number 6 (Positive for DVT)
DPPG amplitude
Time (s)
540
520
500
480
460
440
420
400
380
360
340
0
100
200
300
400
500
600

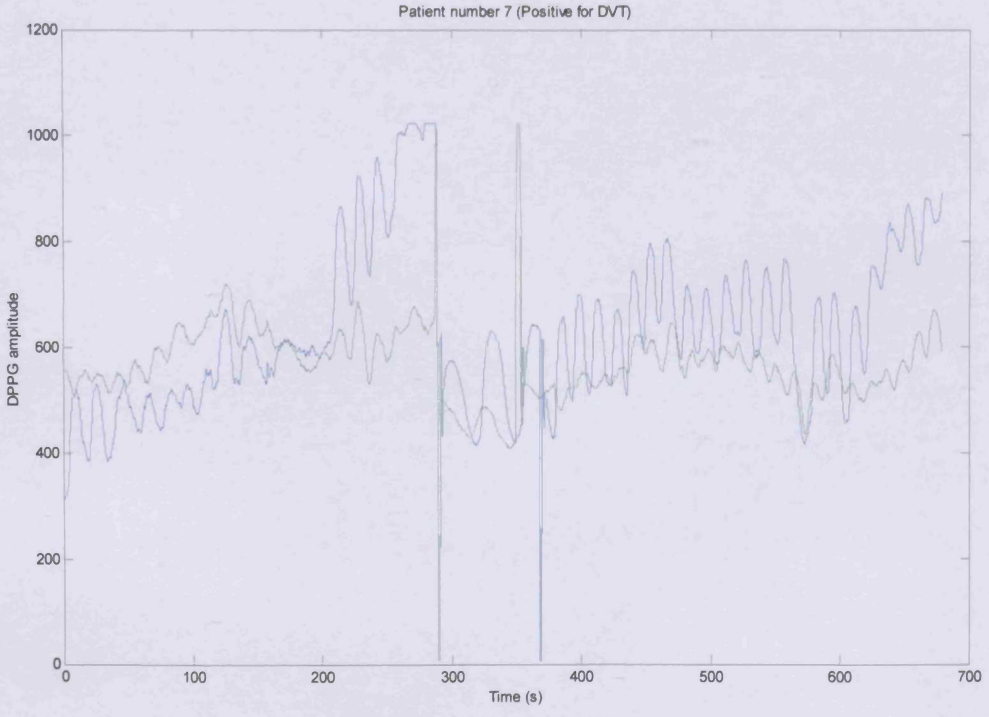
Patient number 7 (Positive for DVT)
DPPG amplitude
Time (s)
0
200
400
600
800
1000
1200
0
100
200
300
400
500
600
700

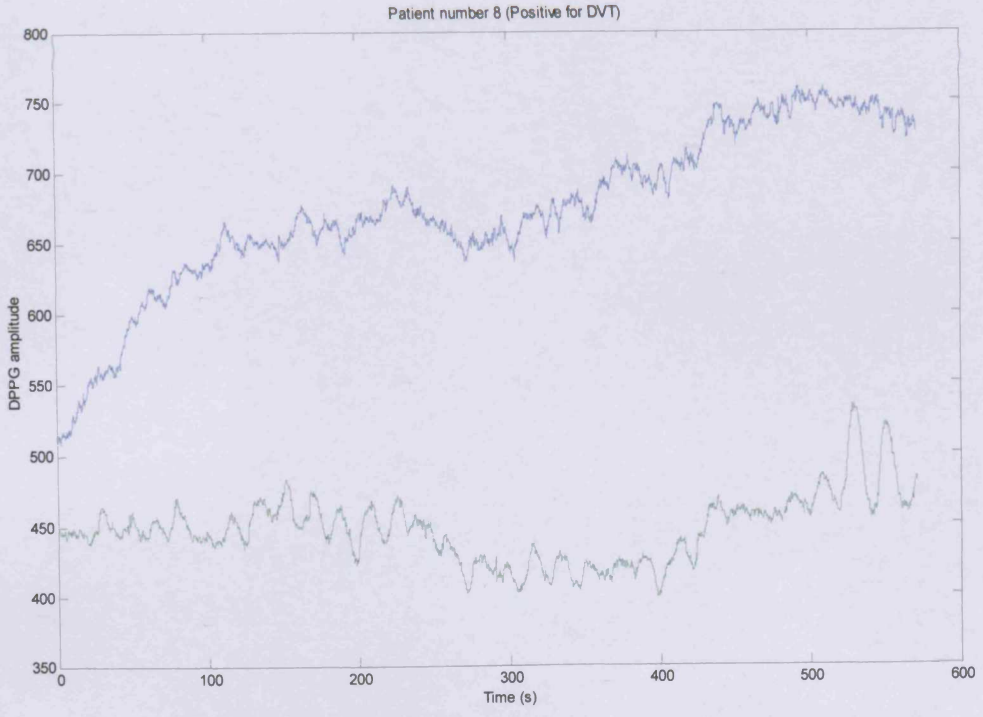
Patient number 8 (Positive for DVT)
DPPG amplitude
Time (s)
800
750
700
650
600
550
500
450
400
350
0
100
200
300
400
500
600

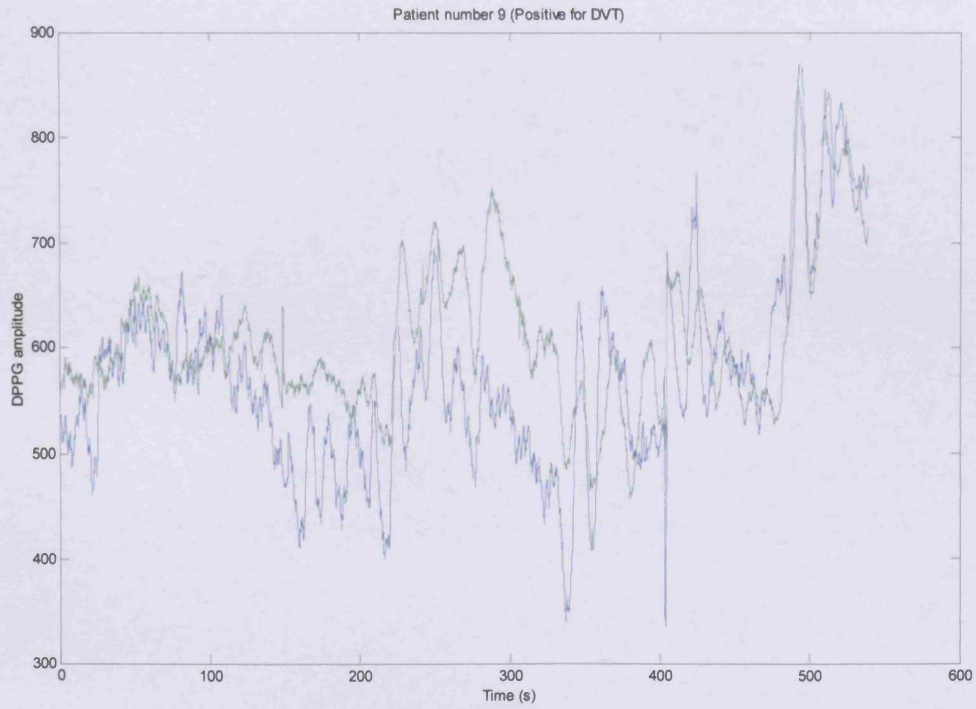
Patient number 9 (Positive for DVT)
DPPG amplitude
Time (s)
900
800
700
600
500
400
300
0
100
200
300
400
500
600

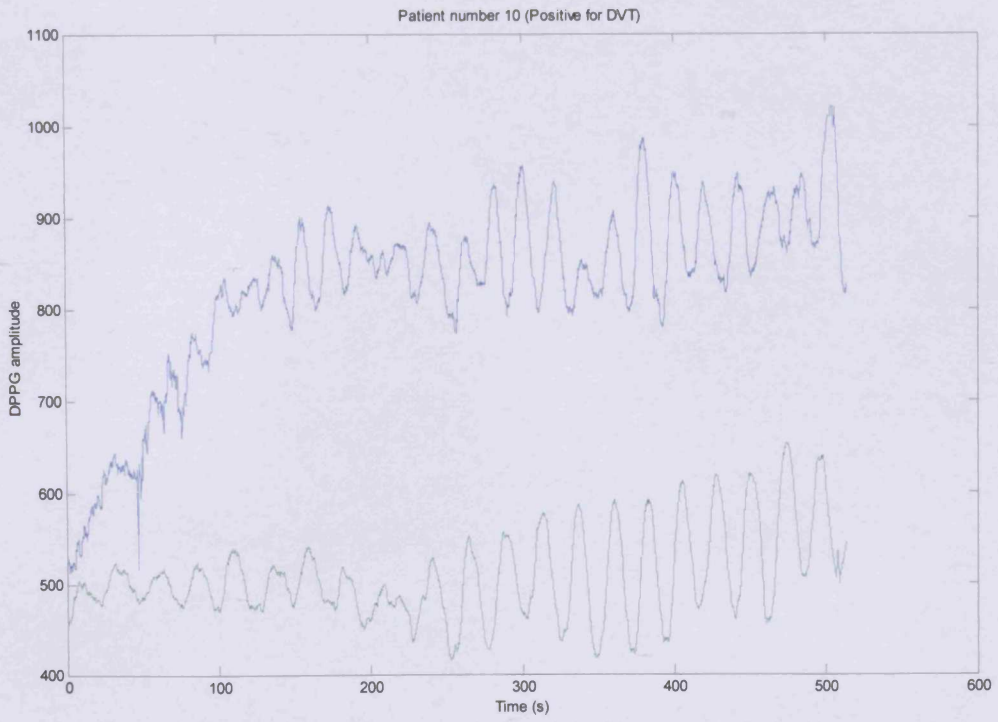
Patient number 10 (Positive for DVT)
DPPG amplitude
Time (s)
1100
1000
900
800
700
600
500
400
0
100
200
300
400
500
600

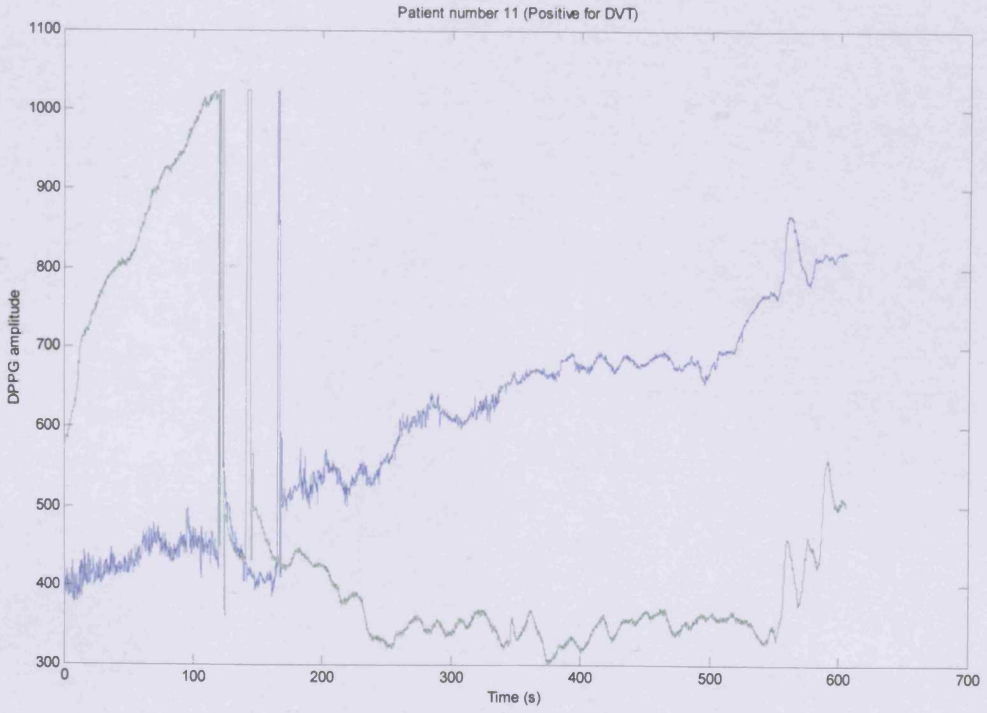
Patient number 11 (Positive for DVT)
DPPG amplitude
Time (s)
1100
1000
900
800
700
600
500
400
300
0
100
200
300
400
500
600
700

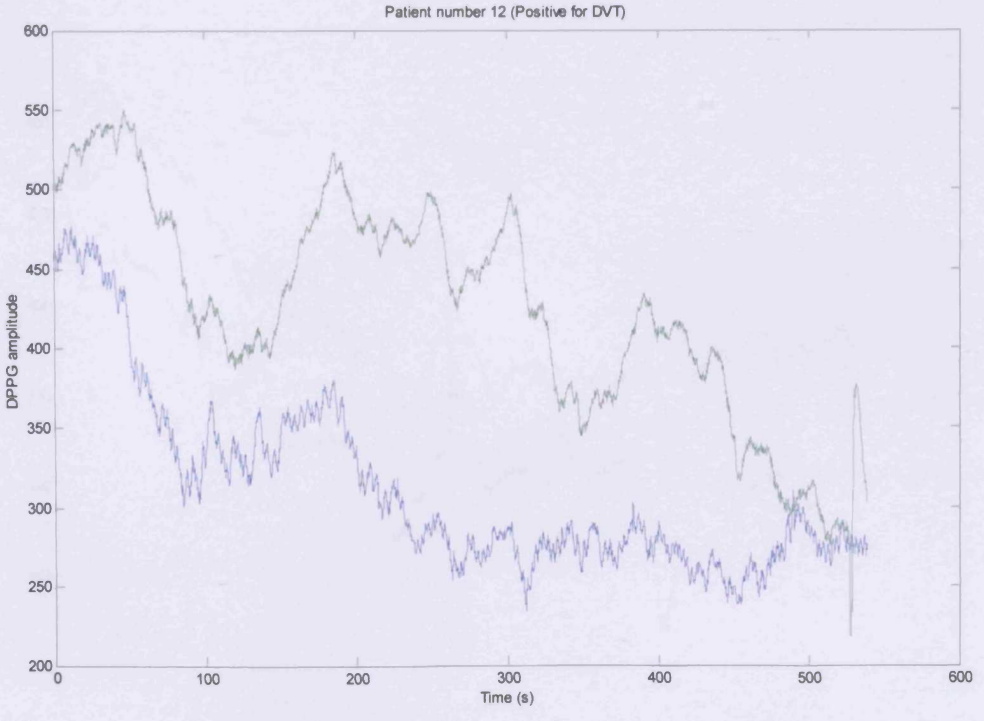
Patient number 12 (Positive for DVT)
DPPG amplitude
Time (s)
600
550
500
450
400
350
300
250
200
0
100
200
300
400
500
600

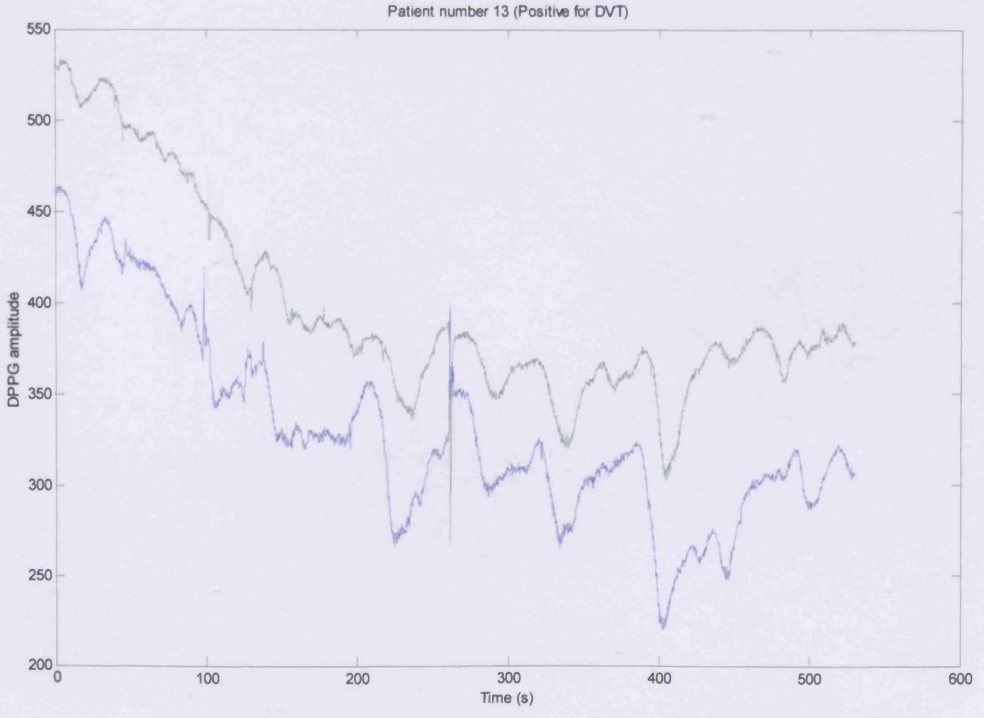
Patient number 13 (Positive for DVT)
DPPG amplitude
Time (s)
550
500
450
400
350
300
250
200
0
100
200
300
400
500
600

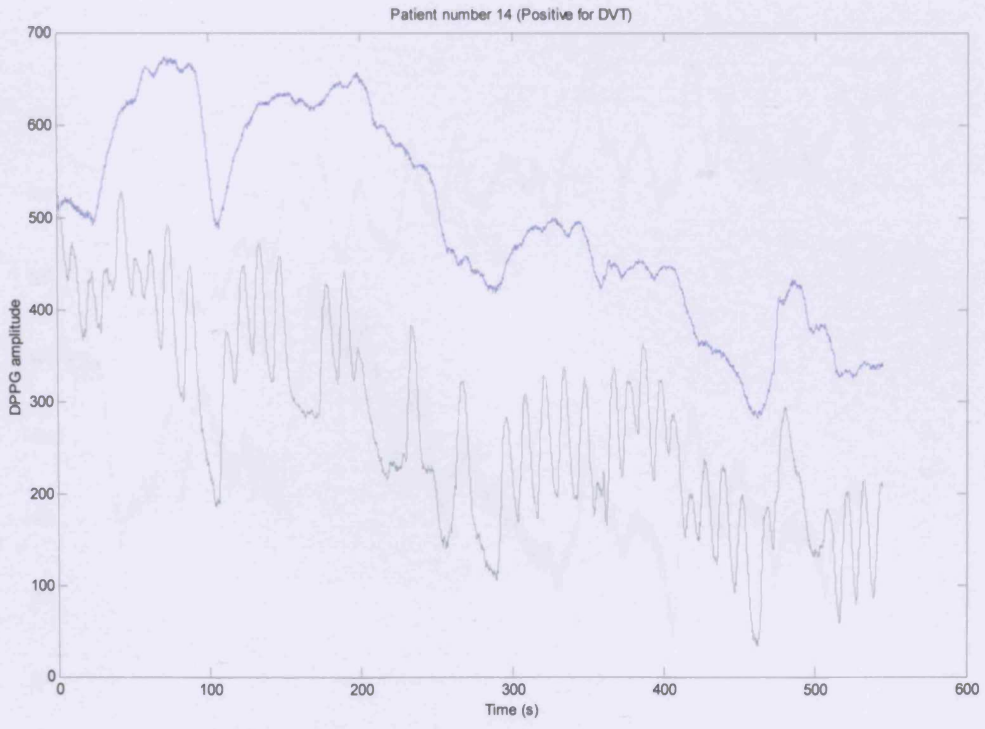
Patient number 14 (Positive for DVT)
DPPG amplitude
Time (s)
0
100
200
300
400
500
600
700

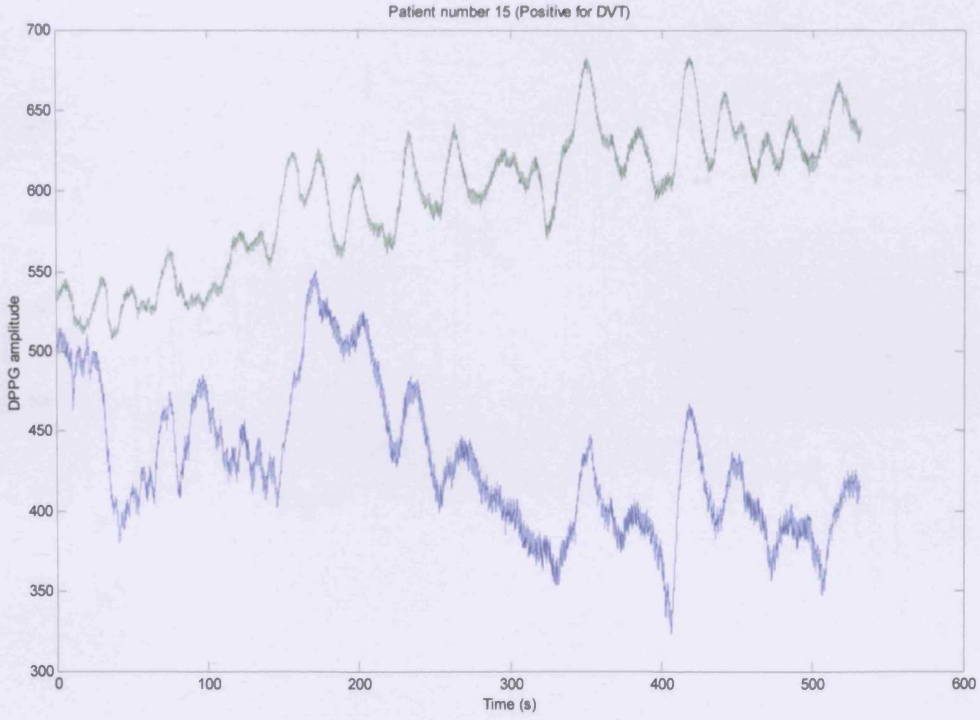
Patient number 15 (Positive for DVT)
DPPG amplitude
Time (s)
700
650
600
550
500
450
400
350
300
0
100
200
300
400
500
600

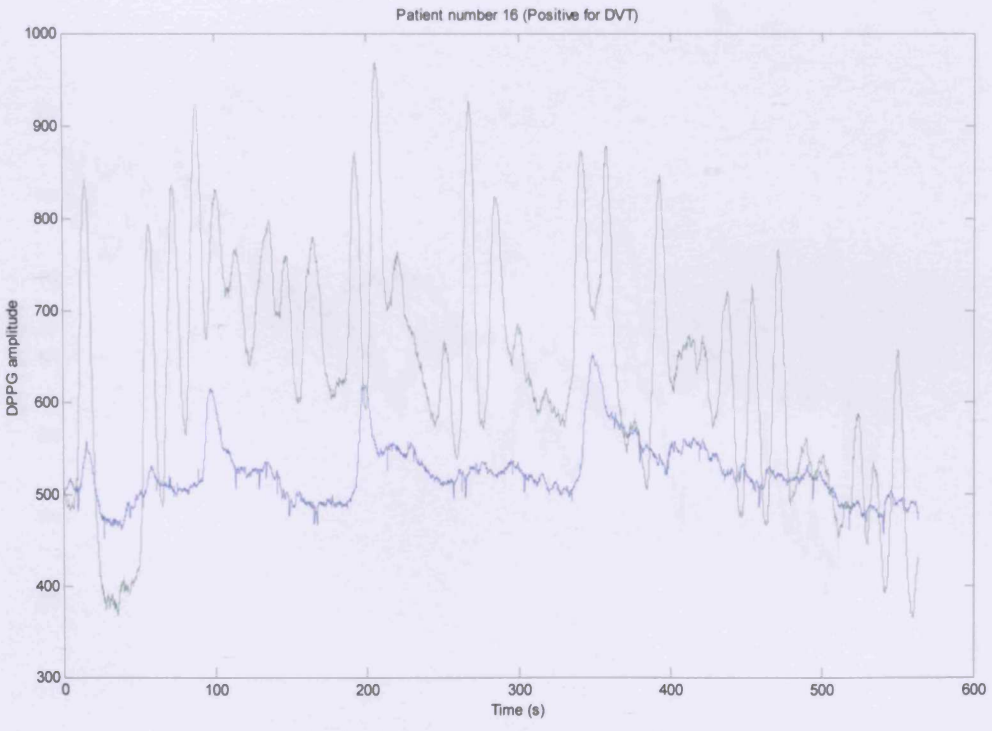
Patient number 16 (Positive for DVT)
DPPG amplitude
Time (s)
1000
900
800
700
600
500
400
300
0
100
200
300
400
500
600

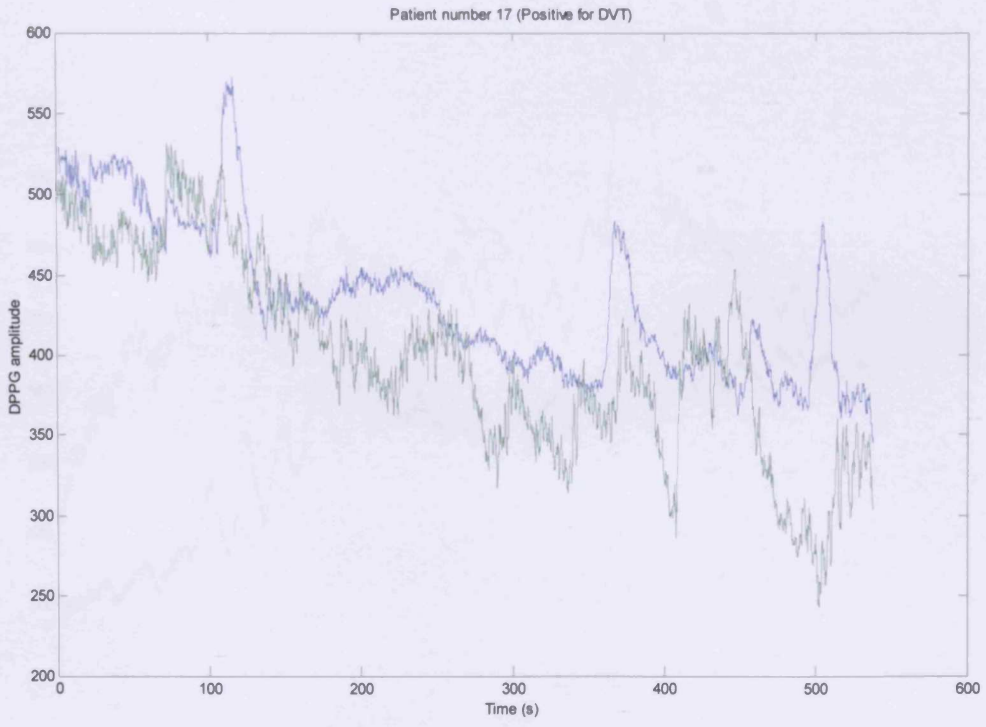
Patient number 17 (Positive for DVT)
DPPG amplitude
Time (s)
600
550
500
450
400
350
300
250
200
0
100
200
300
400
500
600

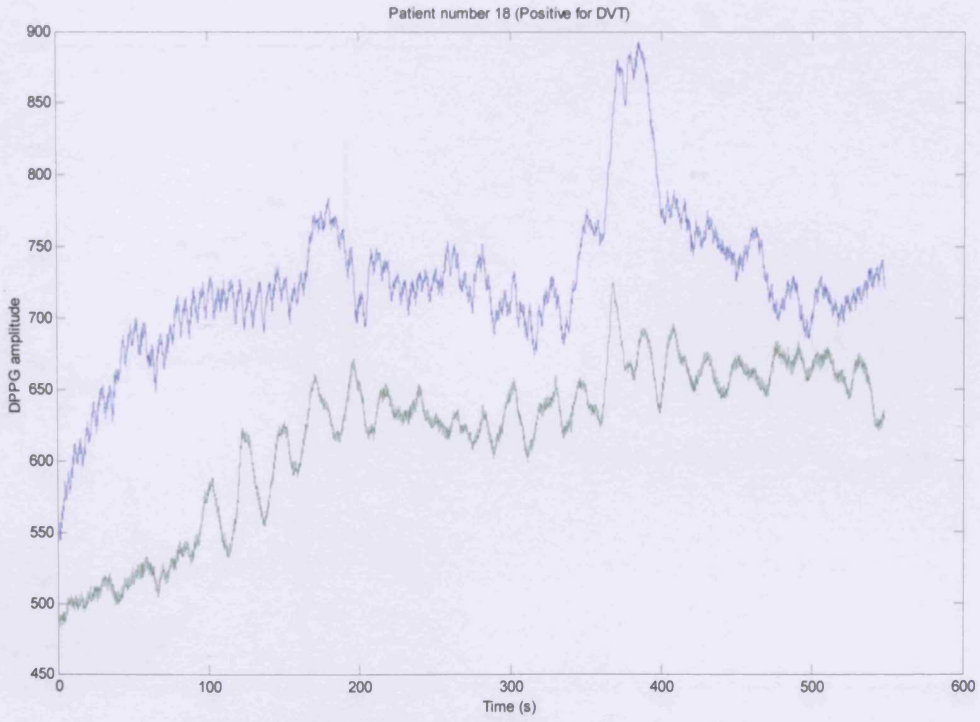
Patient number 18 (Positive for DVT)
DPPG amplitude
Time (s)
900
850
800
750
700
650
600
550
500
450
0
100
200
300
400
500
600

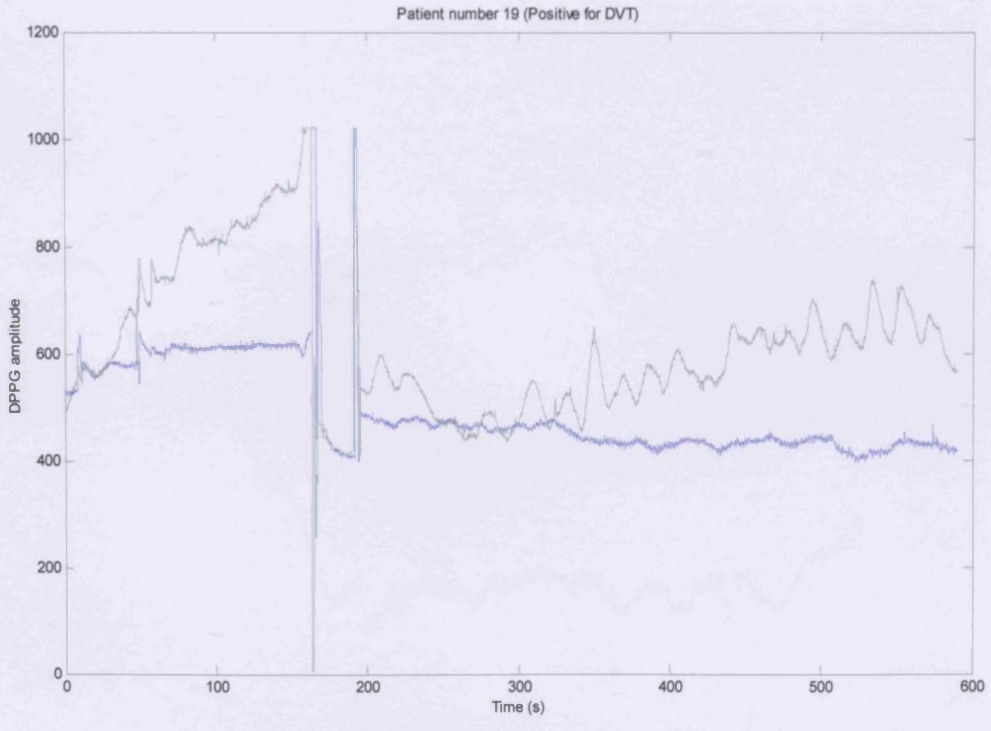
Patient number 19 (Positive for DVT)
DPPG amplitude
Time (s)
0
200
400
600
800
1000
1200
0
100
200
300
400
500
600

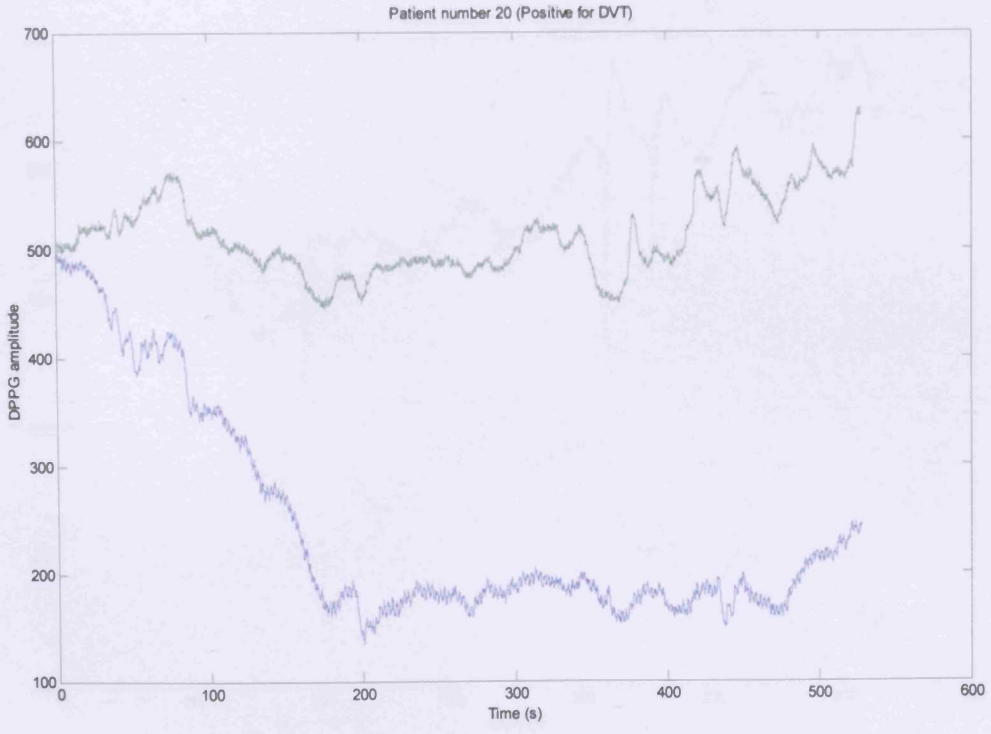
Patient number 20 (Positive for DVT)
DPPG amplitude
Time (s)
700
600
500
400
300
200
100
0
100
200
300
400
500
600

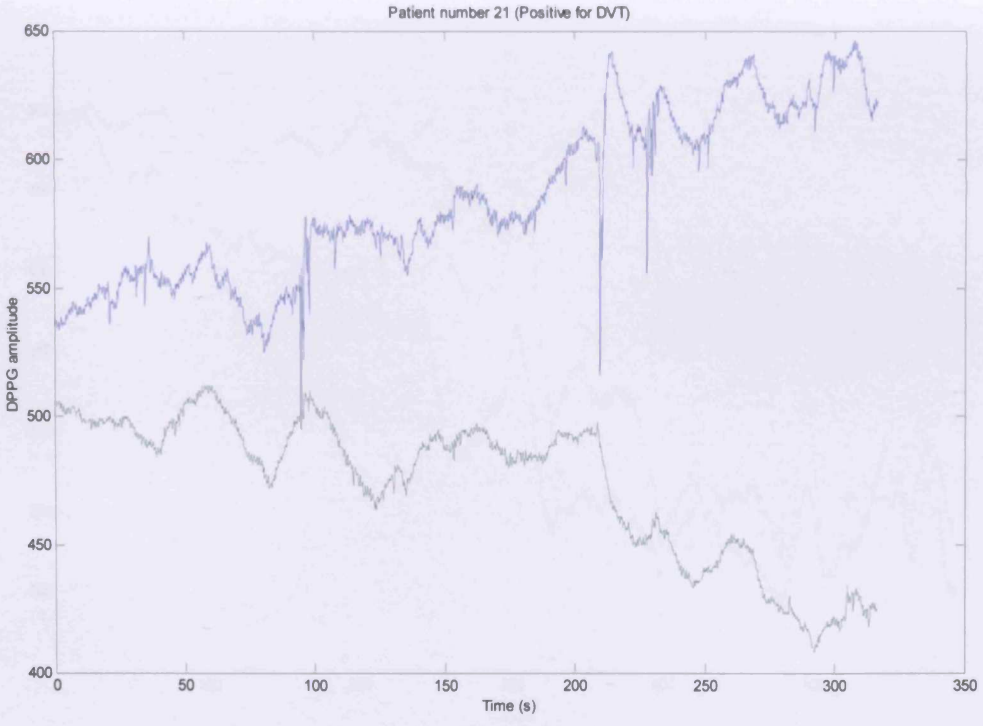
Patient number 21 (Positive for DVT)
DPPG amplitude
Time (s)
650
600
550
500
450
400
0
50
100
150
200
250
300
350

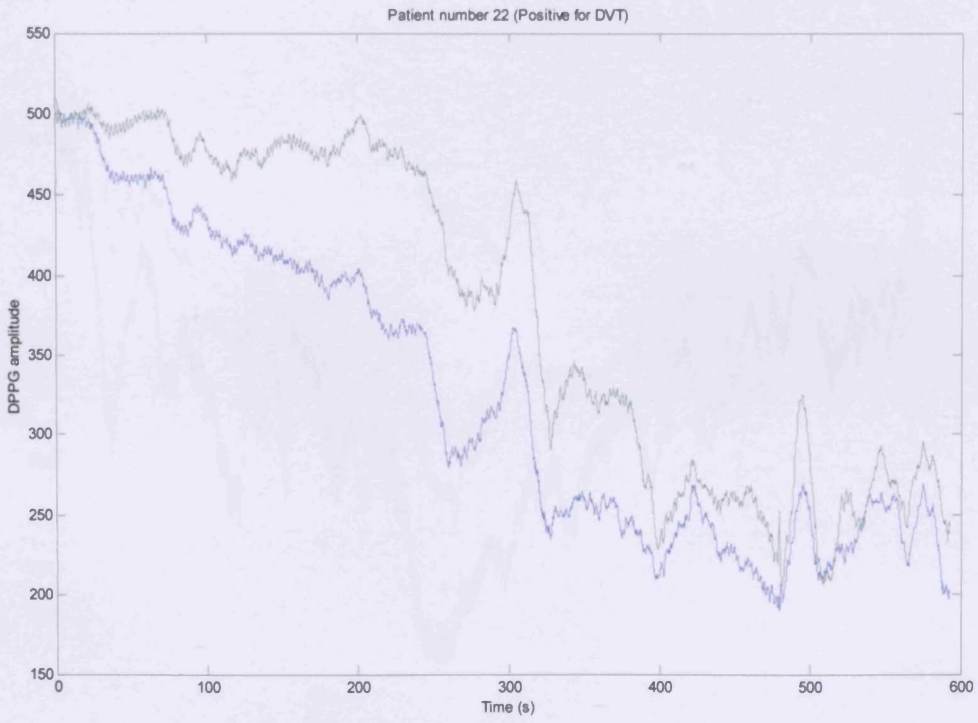
Patient number 22 (Positive for DVT)
DPPG amplitude
Time (s)
550
500
450
400
350
300
250
200
150
0
100
200
300
400
500
600

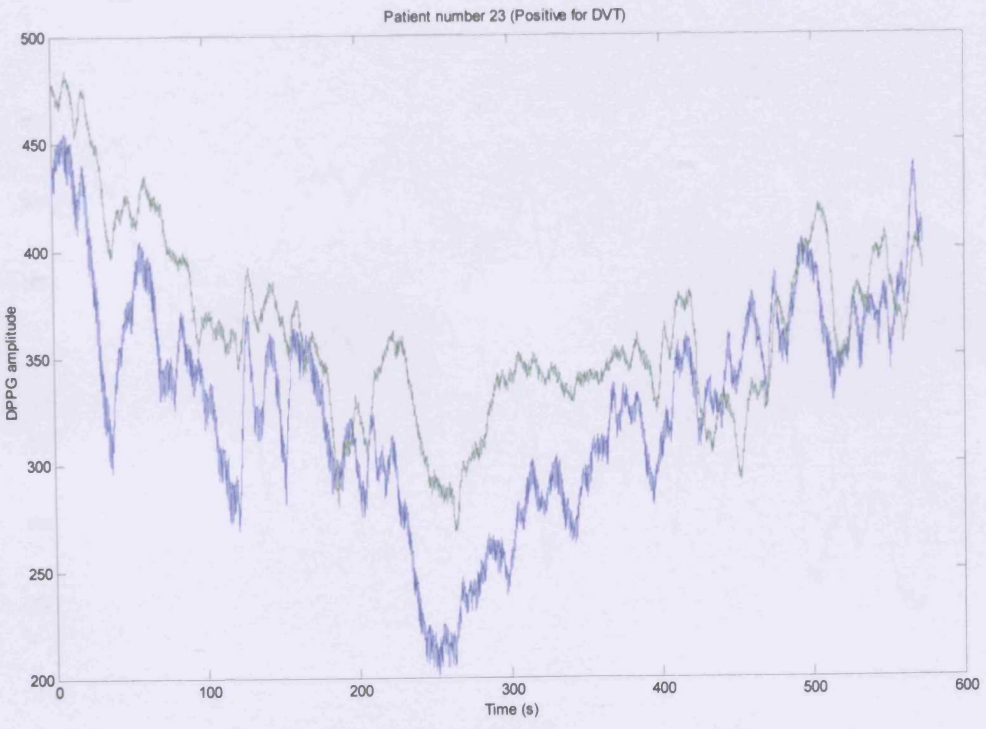
Patient number 23 (Positive for DVT)
DPPG amplitude
Time (s)
500
450
400
350
300
250
200
0
100
200
300
400
500
600

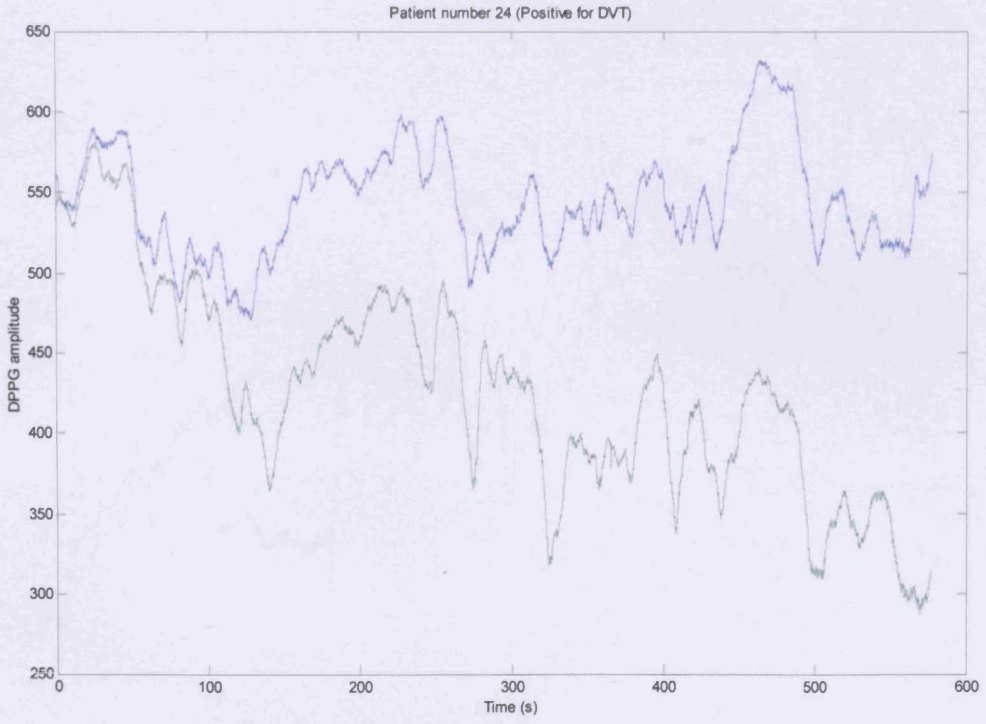
Patient number 24 (Positive for DVT)
DPPG amplitude
Time (s)
650
600
550
500
450
400
350
300
250
0
100
200
300
400
500
600

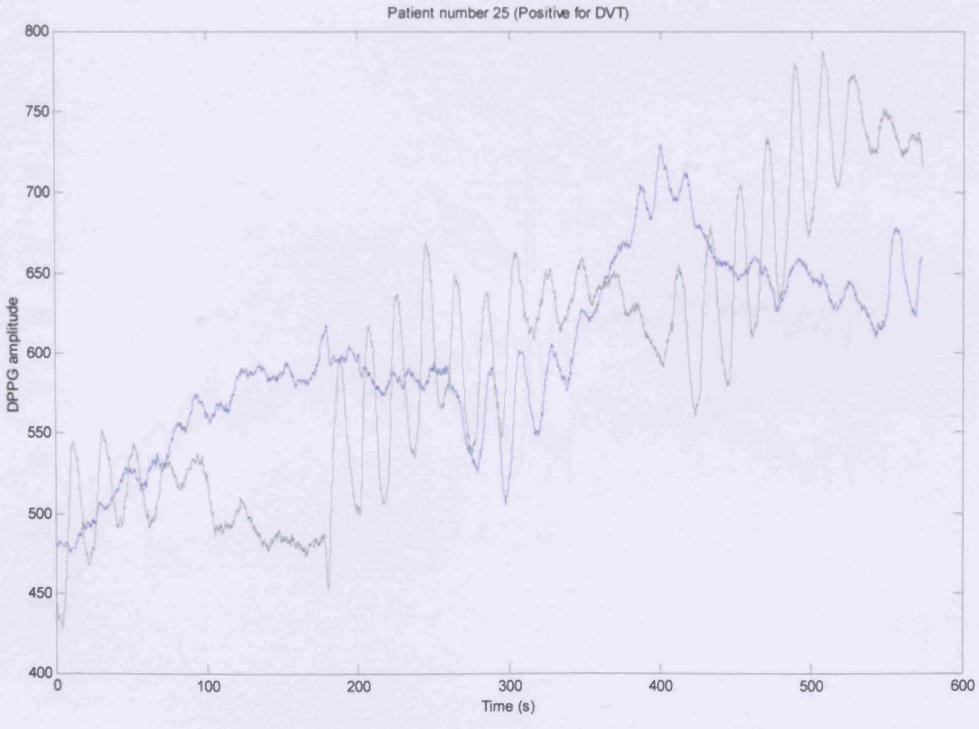
Patient number 25 (Positive for DVT)
DPPG amplitude
Time (s)
800
750
700
650
600
550
500
450
400
0
100
200
300
400
500
600

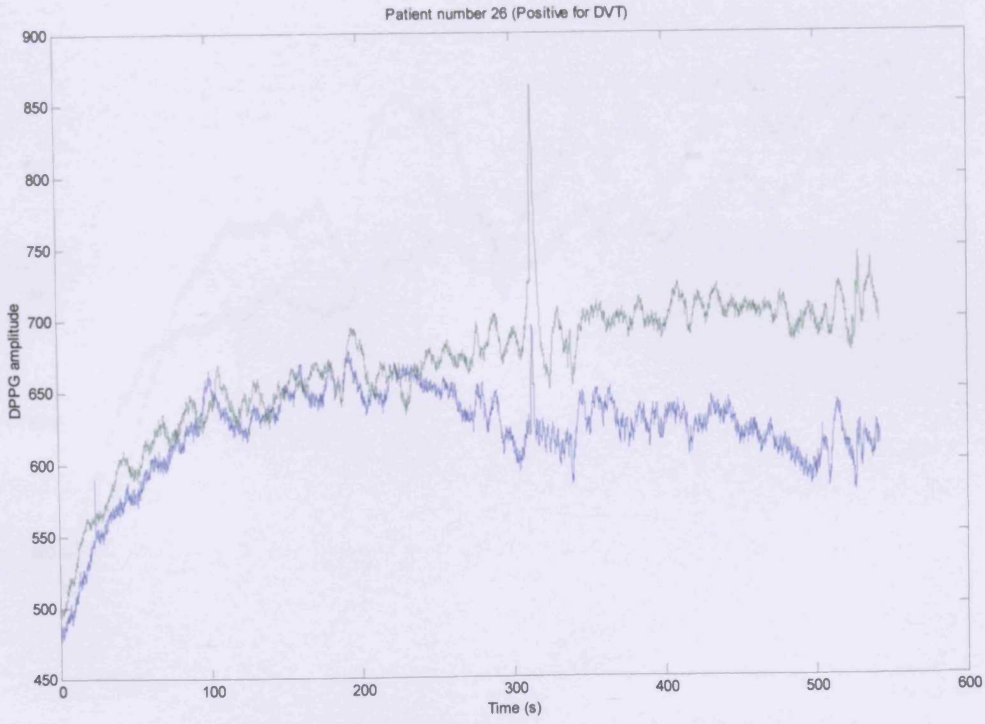
Patient number 26 (Positive for DVT)
DPPG amplitude
Time (s)
900
850
800
750
700
650
600
550
500
450
0
100
200
300
400
500
600

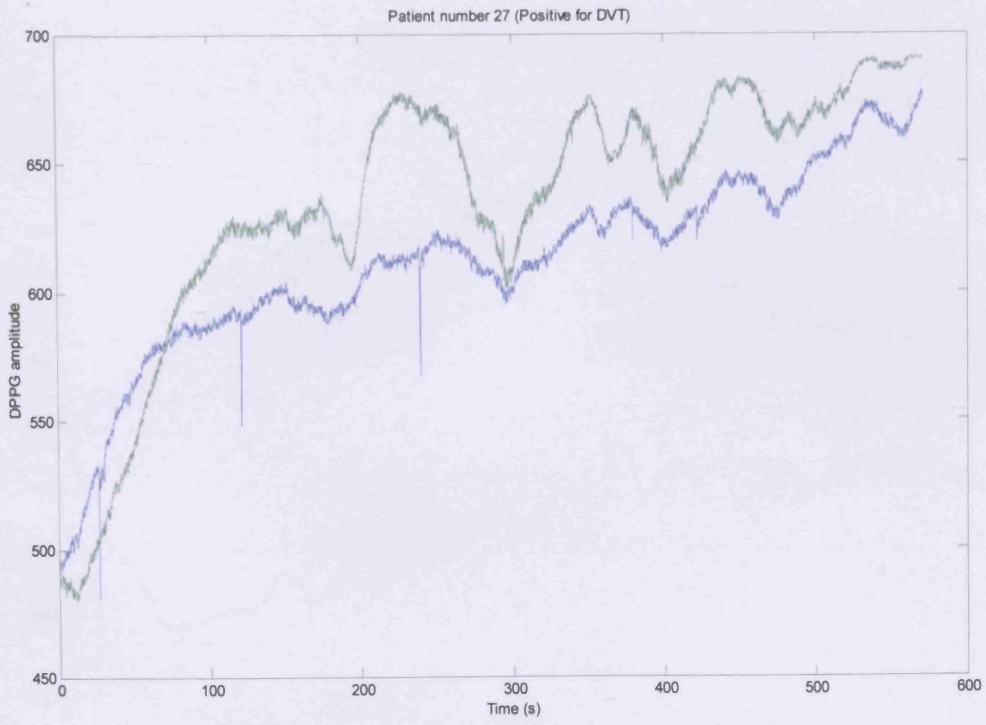
Patient number 27 (Positive for DVT)
DPPG amplitude
Time (s)
700
650
600
550
500
450
0
100
200
300
400
500
600

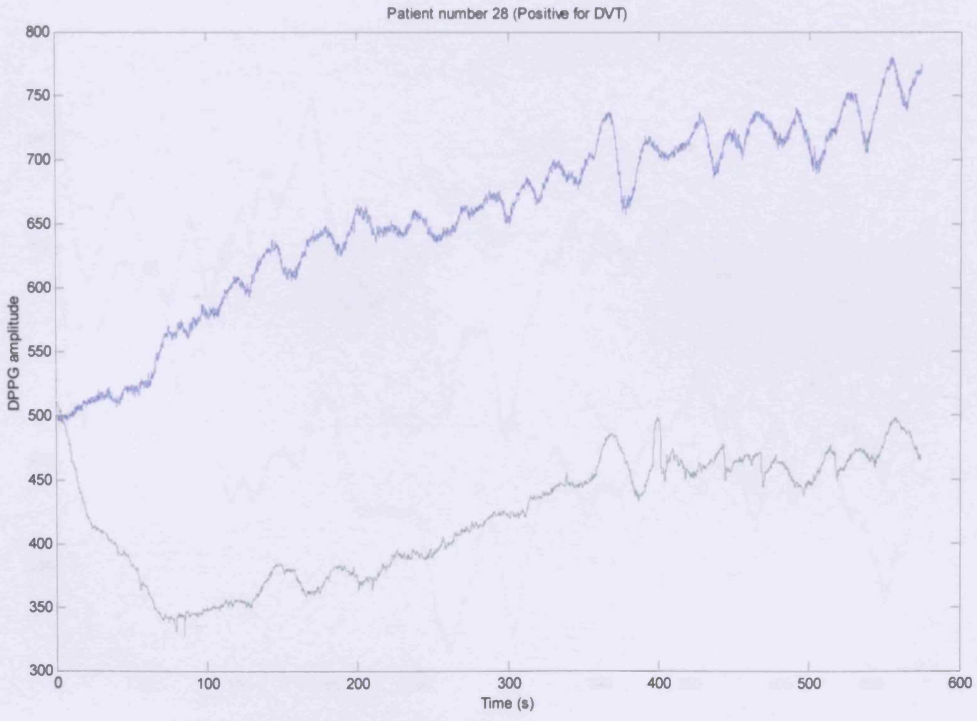
Patient number 28 (Positive for DVT)
DPPG amplitude
Time (s)
800
750
700
650
600
550
500
450
400
350
300
0
100
200
300
400
500
600

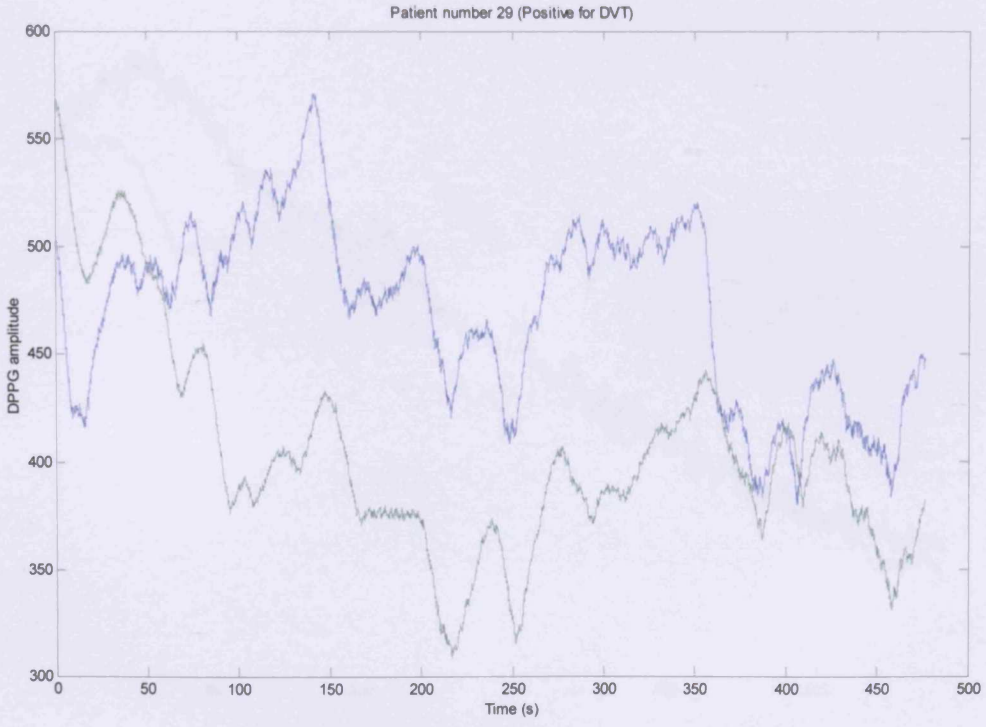
Patient number 29 (Positive for DVT)
DPPG amplitude
Time (s)
600
550
500
450
400
350
300
0
50
100
150
200
250
300
350
400
450
500

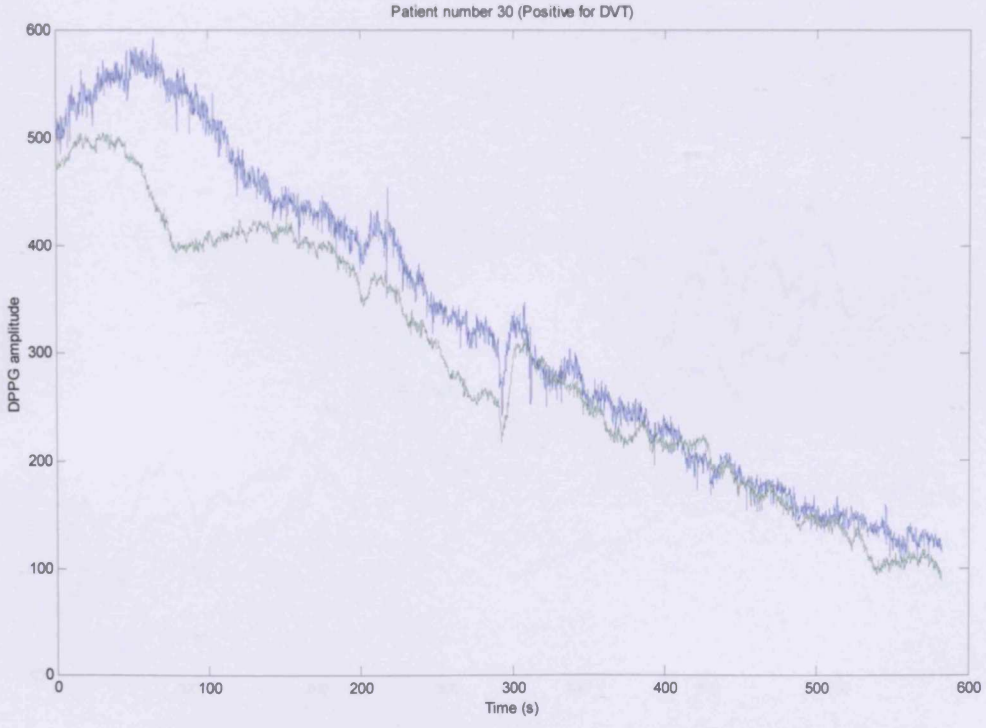
Patient number 30 (Positive for DVT)
DPPG amplitude
Time (s)
0
100
200
300
400
500
600

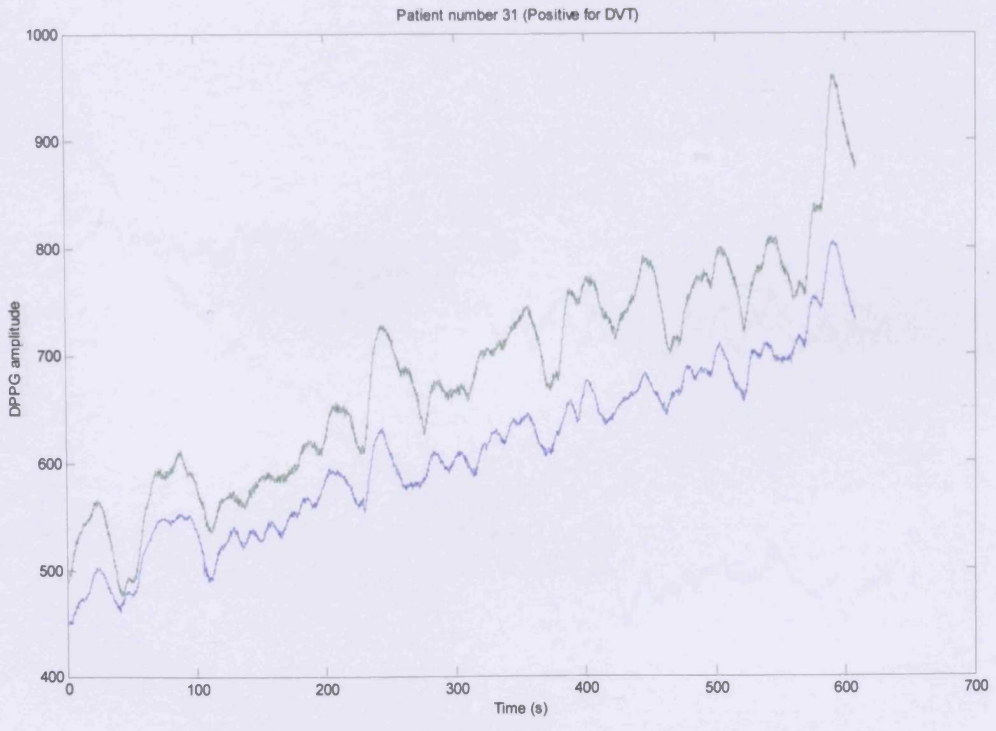
Patient number 31 (Positive for DVT)
DPPG amplitude
Time (s)
1000
900
800
700
600
500
400
0
100
200
300
400
500
600
700

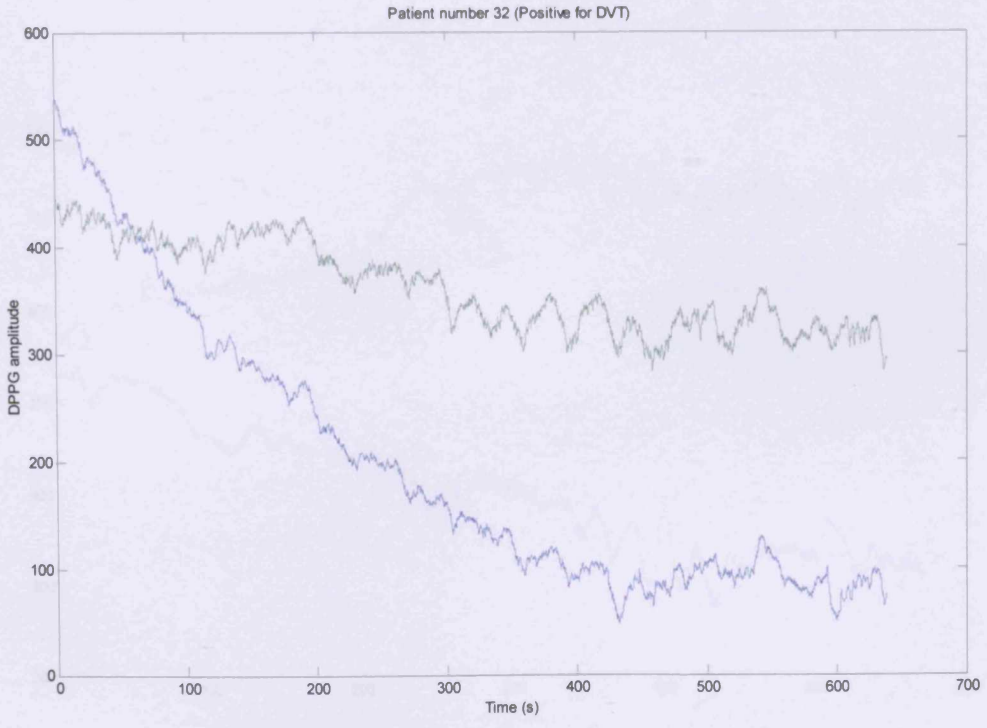
Patient number 32 (Positive for DVT)
DPPG amplitude
Time (s)
0
100
200
300
400
500
600
700

Patient number 33 (Positive for DVT)
DPPG amplitude
Time (s)
900
800
700
600
500
400
300
200
0
100
200
300
400
500
600

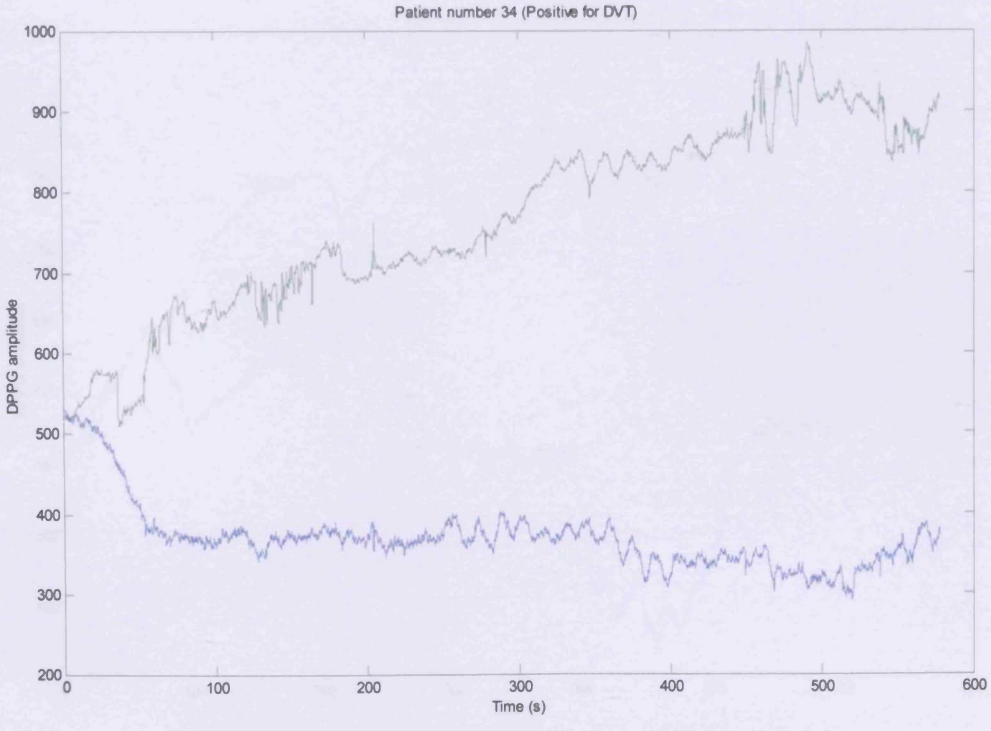
Patient number 34 (Positive for DVT)
DPPG amplitude
Time (s)
1000
900
800
700
600
500
400
300
200
0
100
200
300
400
500
600

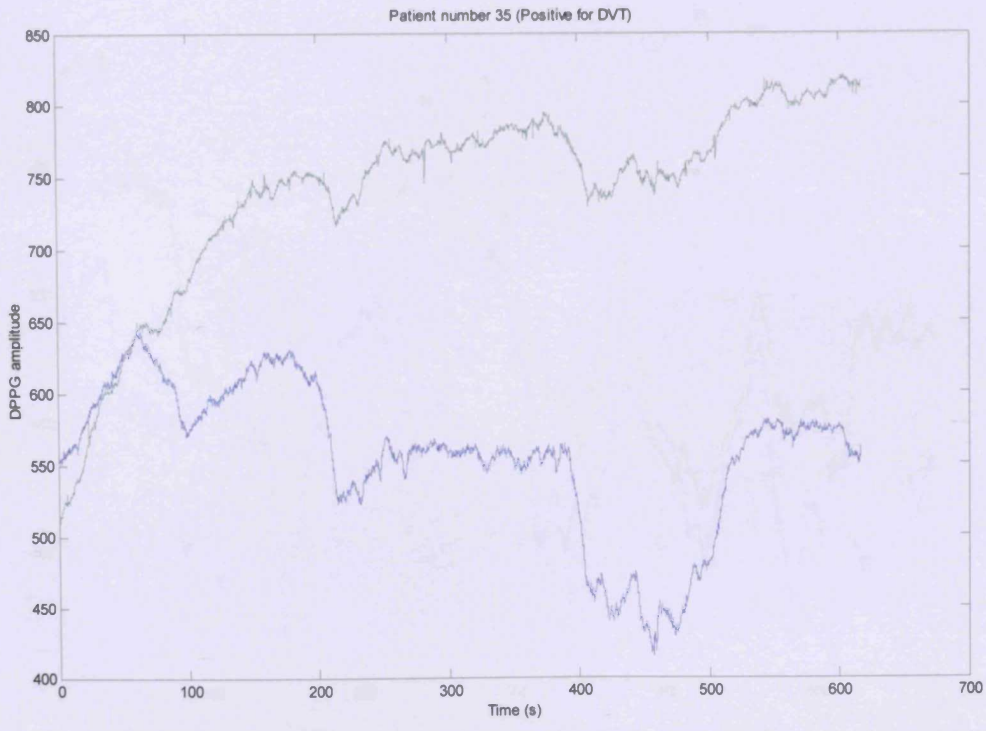
Patient number 35 (Positive for DVT)
DPPG amplitude
Time (s)
850
800
750
700
650
600
550
500
450
400
0
100
200
300
400
500
600
700

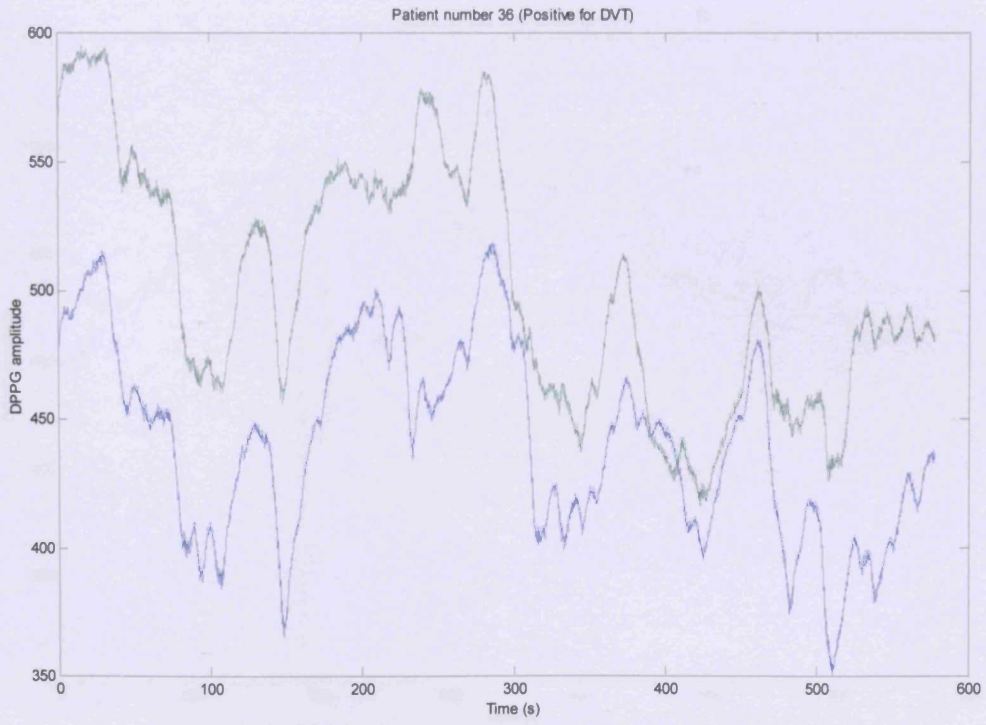
Patient number 36 (Positive for DVT)
DPPG amplitude
Time (s)
600
550
500
450
400
350
0
100
200
300
400
500
600

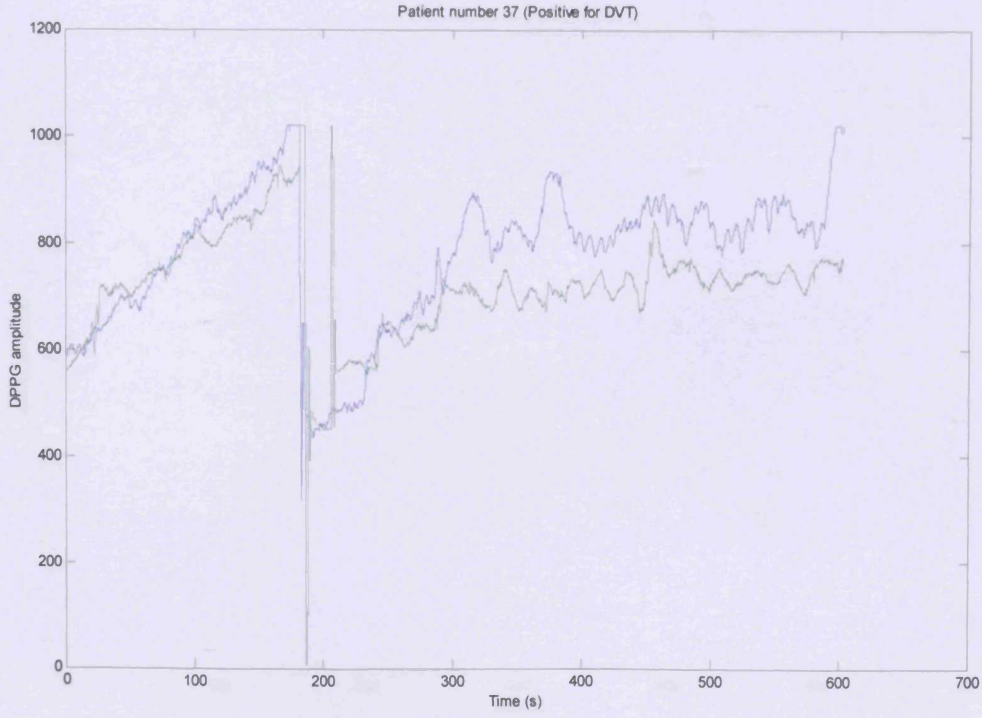
Patient number 37 (Positive for DVT)
DPPG amplitude
Time (s)
0
200
400
600
800
1000
1200
0
100
200
300
400
500
600
700

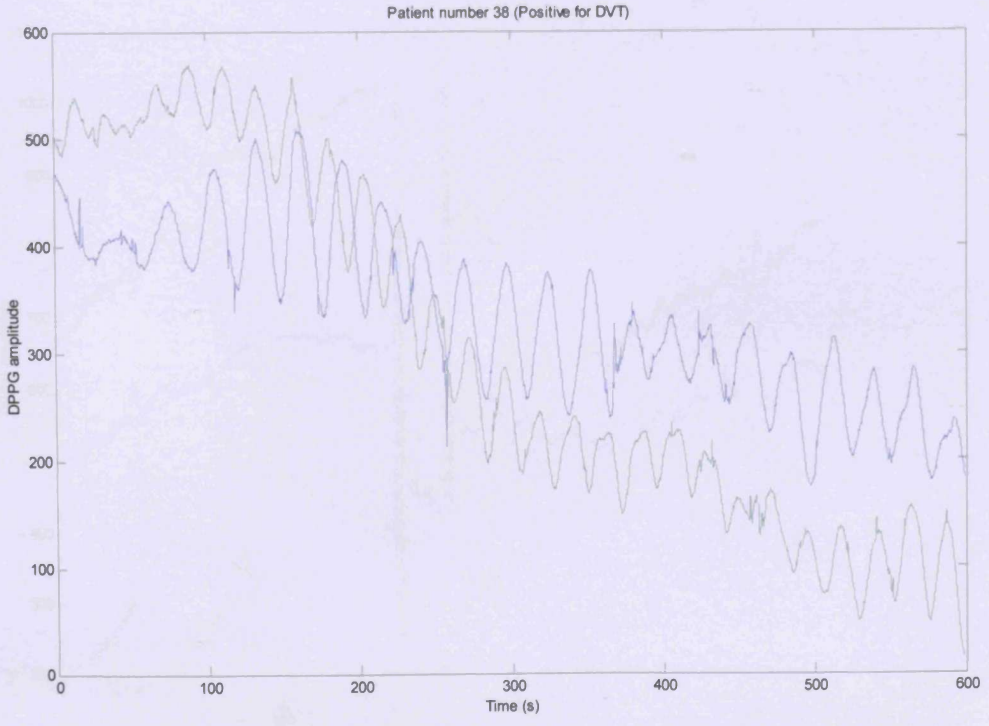
Patient number 38 (Positive for DVT)
DPPG amplitude
Time (s)
0
100
200
300
400
500
600

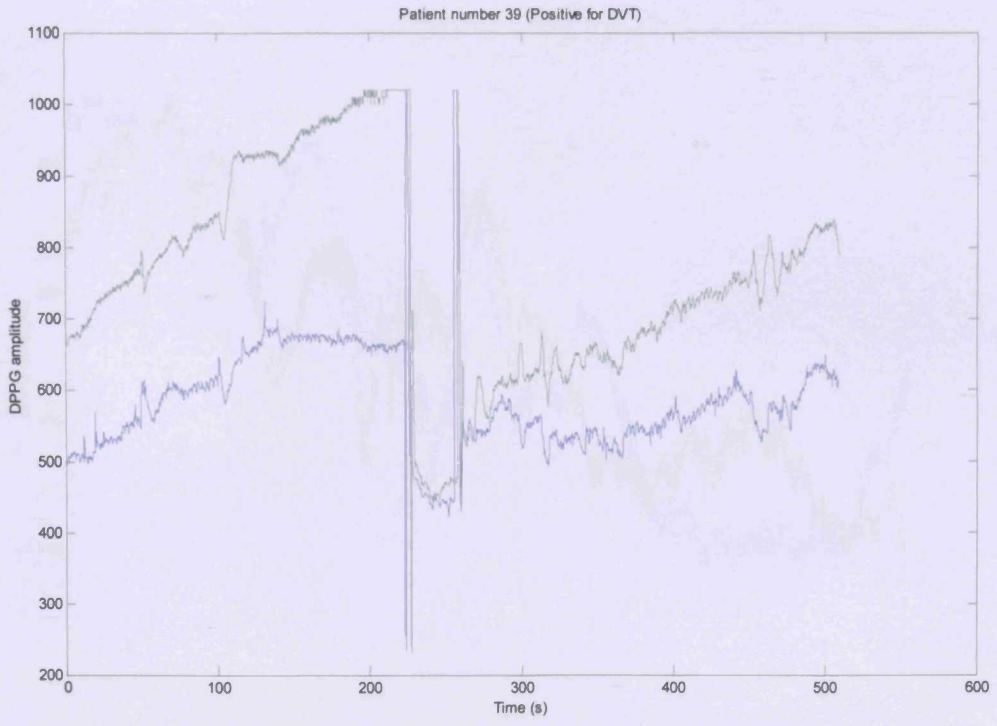
Patient number 39 (Positive for DVT)
DPPG amplitude
Time (s)
1100
1000
900
800
700
600
500
400
300
200
0
100
200
300
400
500
600

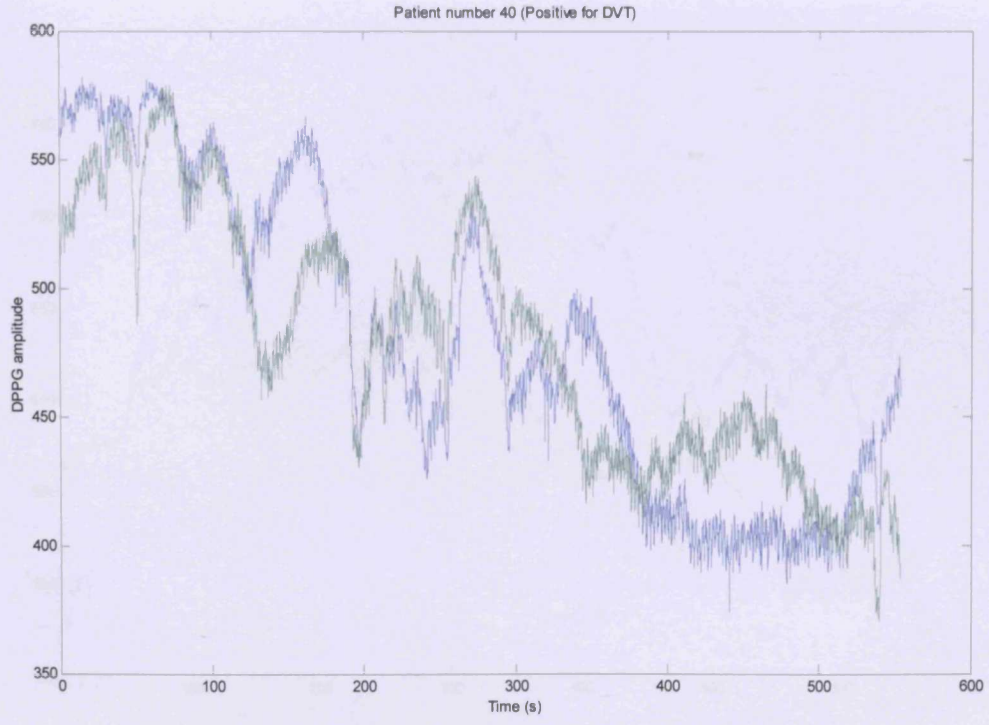
Patient number 40 (Positive for DVT)
DPPG amplitude
Time (s)
600
550
500
450
400
350
0
100
200
300
400
500
600

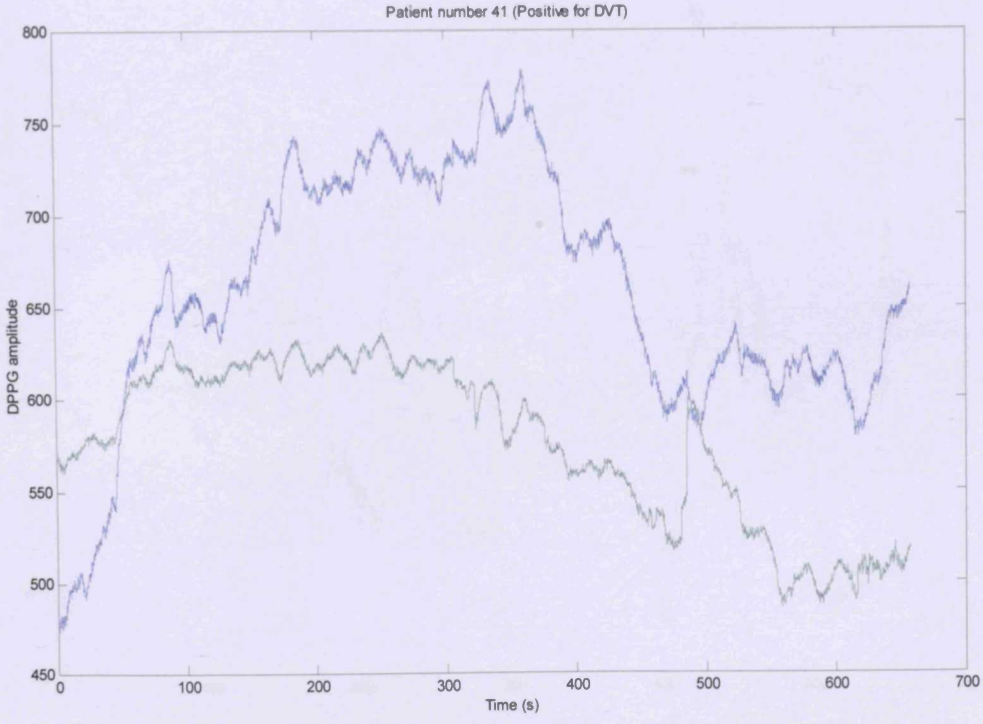
Patient number 41 (Positive for DVT)
DPPG amplitude
Time (s)
800
750
700
650
600
550
500
450
0
100
200
300
400
500
600
700

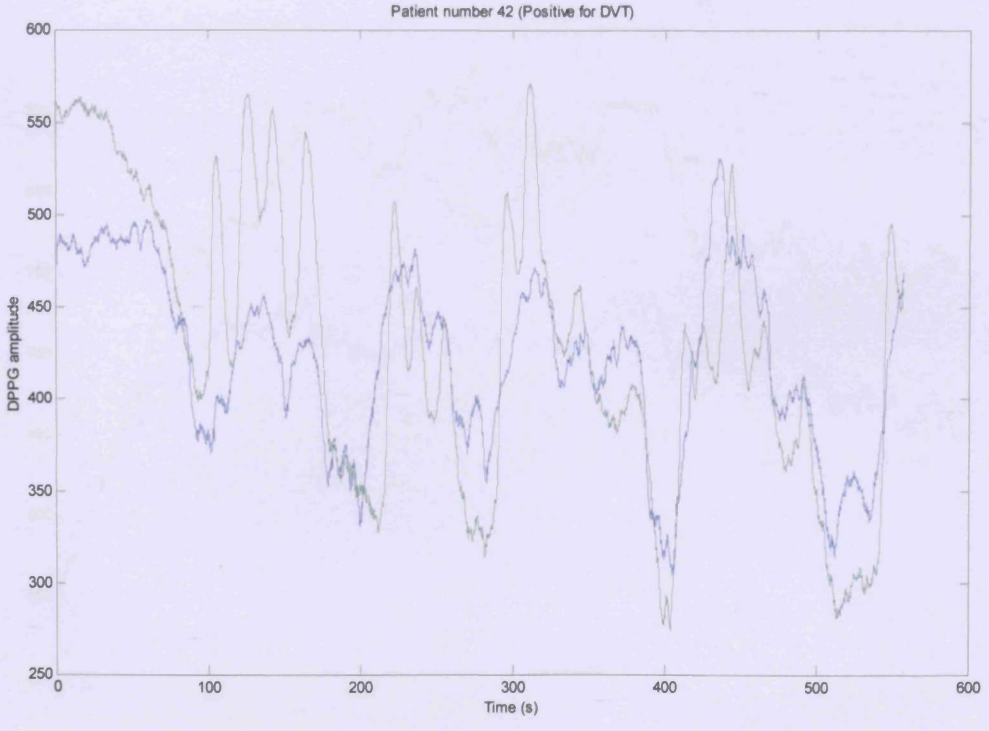
Patient number 42 (Positive for DVT)
DPPG amplitude
Time (s)
600
550
500
450
400
350
300
250
0
100
200
300
400
500
600

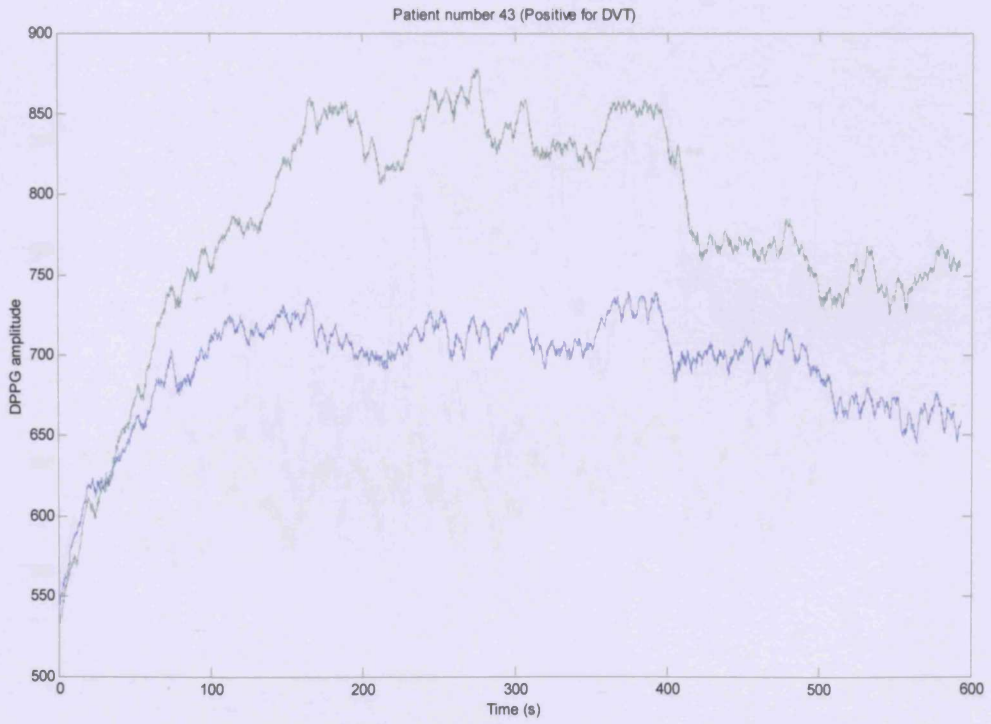
Patient number 43 (Positive for DVT)
DPPG amplitude
Time (s)
900
850
800
750
700
650
600
550
500
0
100
200
300
400
500
600

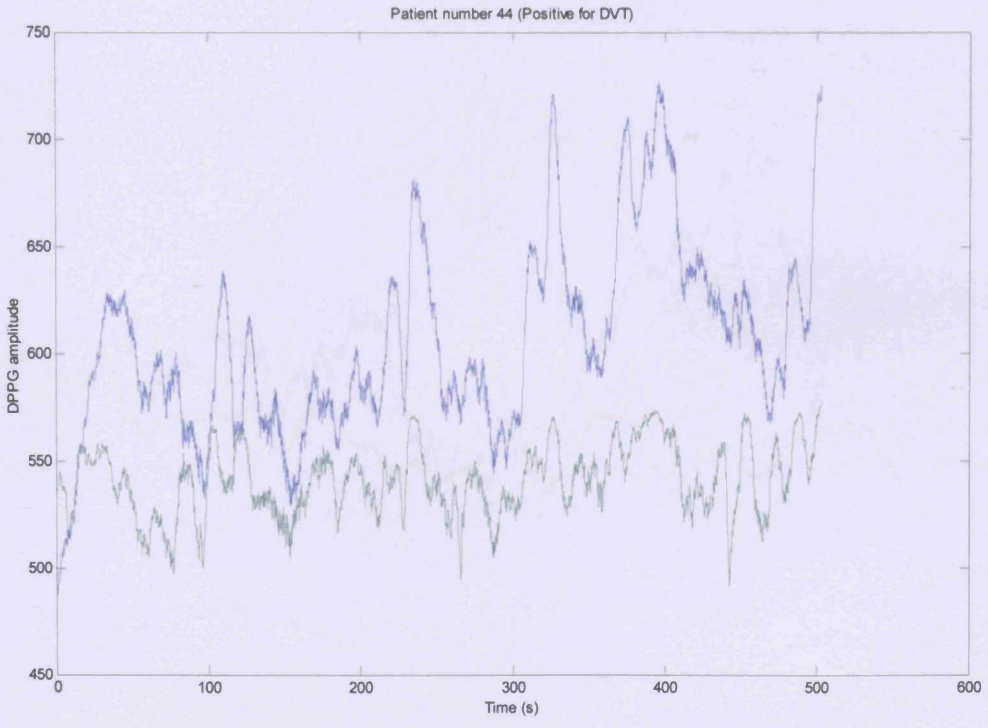
Patient number 44 (Positive for DVT)
DPPG amplitude
Time (s)
750
700
650
600
550
500
450
0
100
200
300
400
500
600

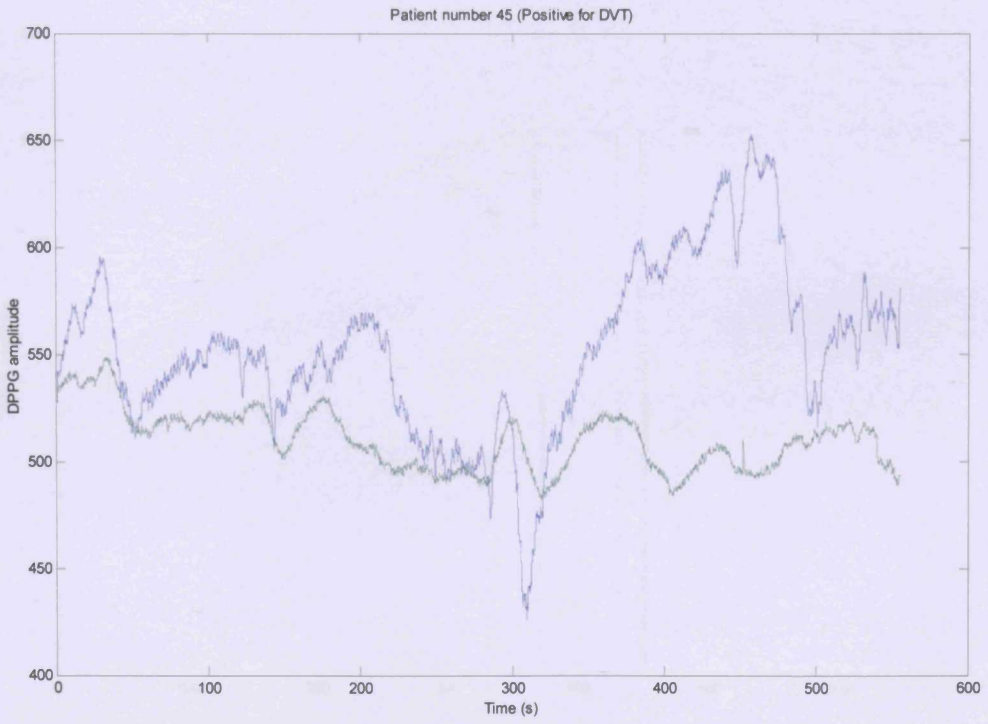
Patient number 45 (Positive for DVT)
DPPG amplitude
Time (s)
700
650
600
550
500
450
400
0
100
200
300
400
500
600

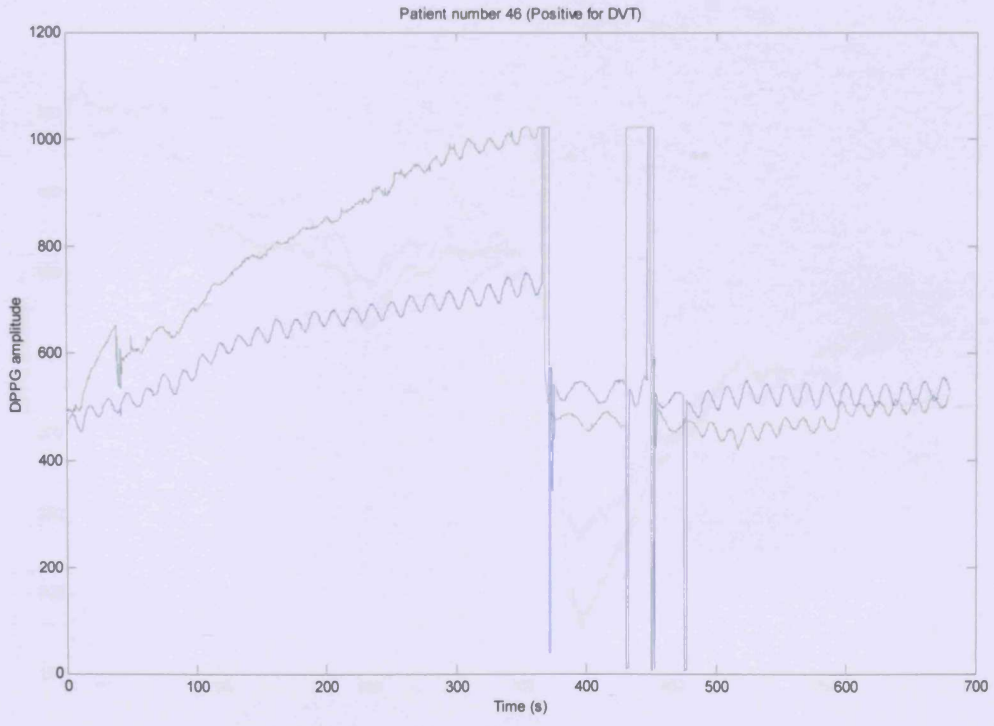
Patient number 46 (Positive for DVT)
DPPG amplitude
Time (s)
0
200
400
600
800
1000
1200
0
100
200
300
400
500
600
700

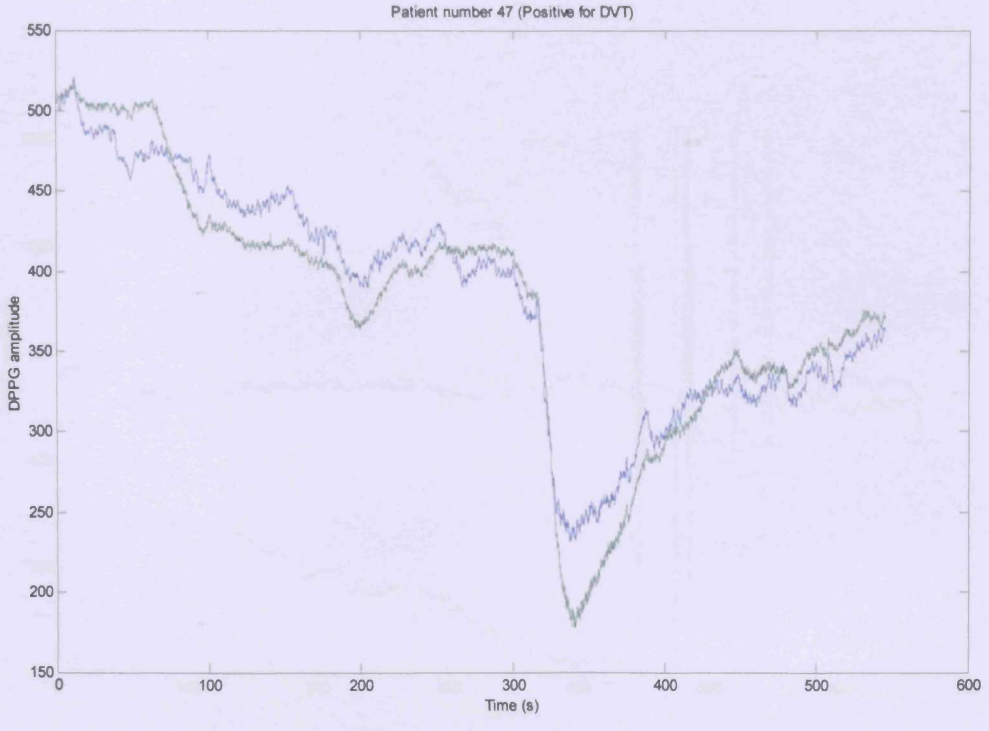
Patient number 47 (Positive for DVT)
DPPG amplitude
Time (s)
550
500
450
400
350
300
250
200
150
0
100
200
300
400
500
600

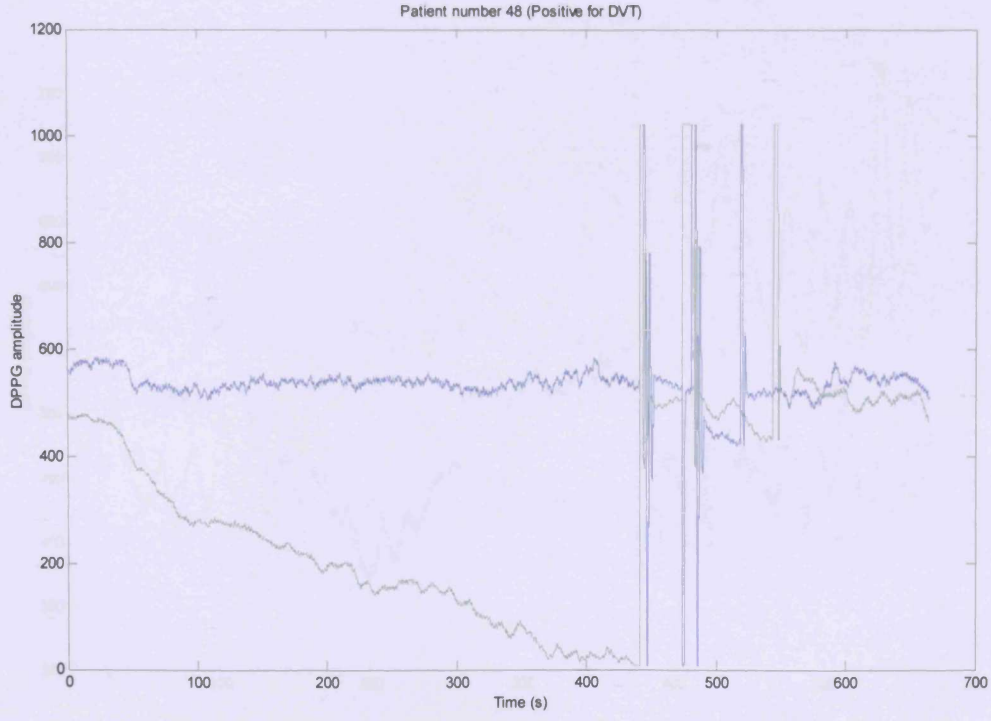
Patient number 48 (Positive for DVT)
DPPG amplitude
Time (s)
0
200
400
600
800
1000
1200
0
100
200
300
400
500
600
700

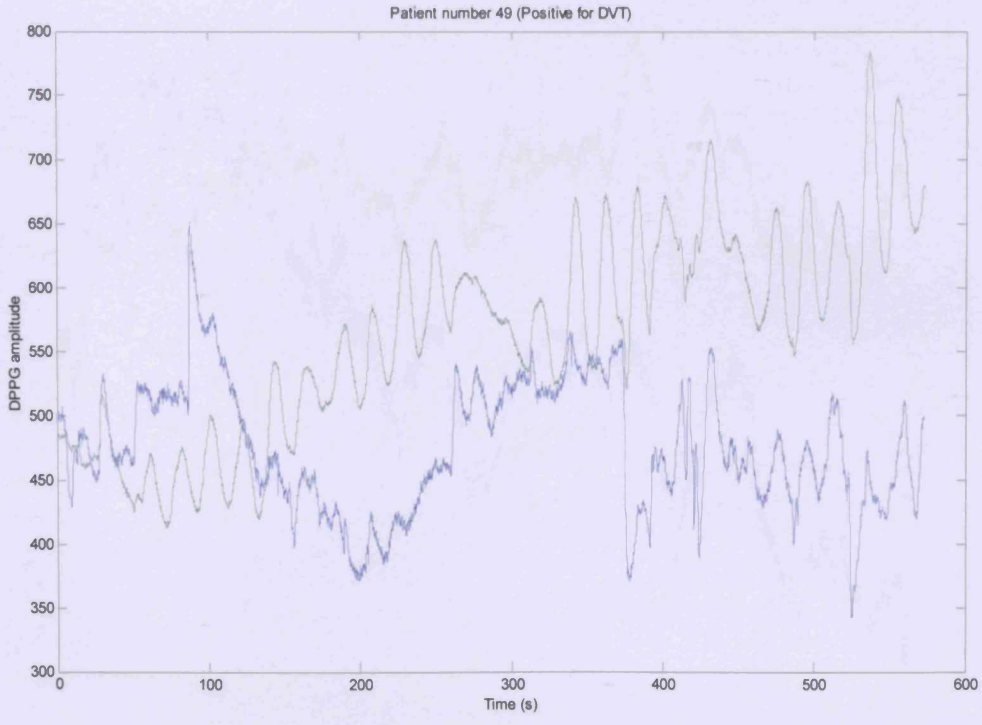
Patient number 49 (Positive for DVT)
DPPG amplitude
Time (s)
800
750
700
650
600
550
500
450
400
350
300
0
100
200
300
400
500
600

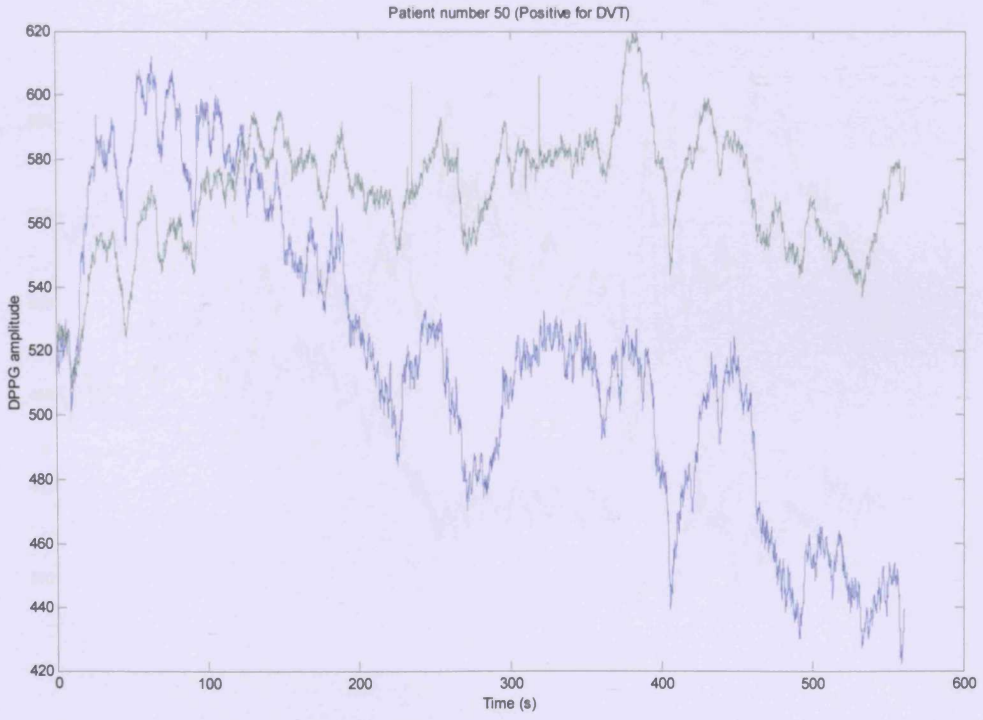
Patient number 50 (Positive for DVT)
DPPG amplitude
Time (s)
620
600
580
560
540
520
500
480
460
440
420
0
100
200
300
400
500
600

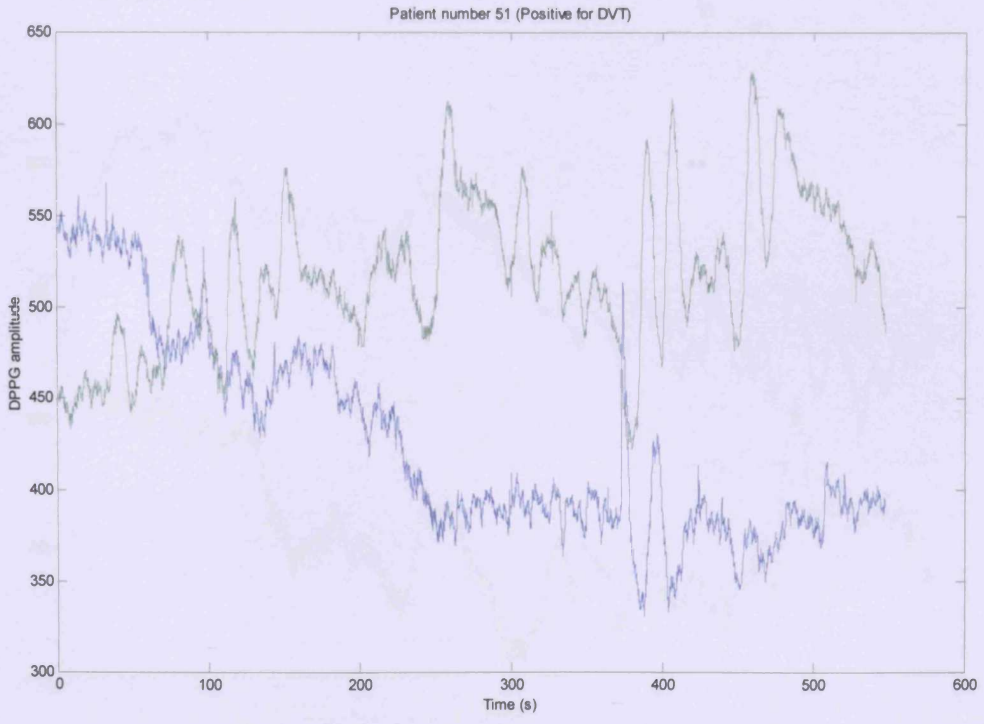
Patient number 51 (Positive for DVT)
DPPG amplitude
Time (s)
650
600
550
500
450
400
350
300
0
100
200
300
400
500
600

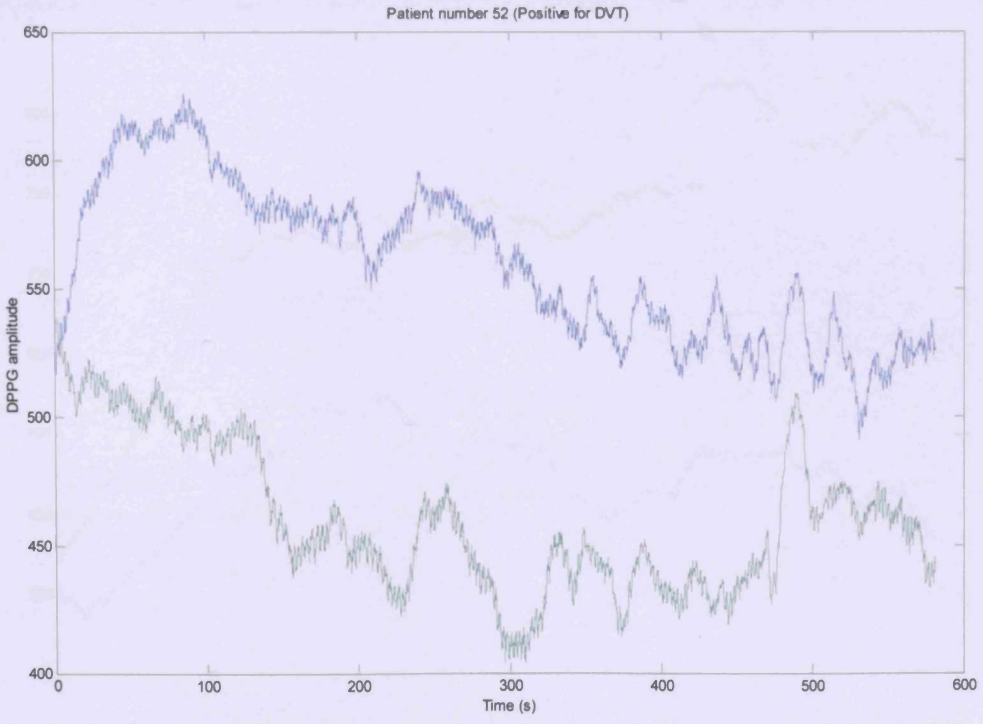
Patient number 52 (Positive for DVT)
DPPG amplitude
Time (s)
650
600
550
500
450
400
0
100
200
300
400
500
600

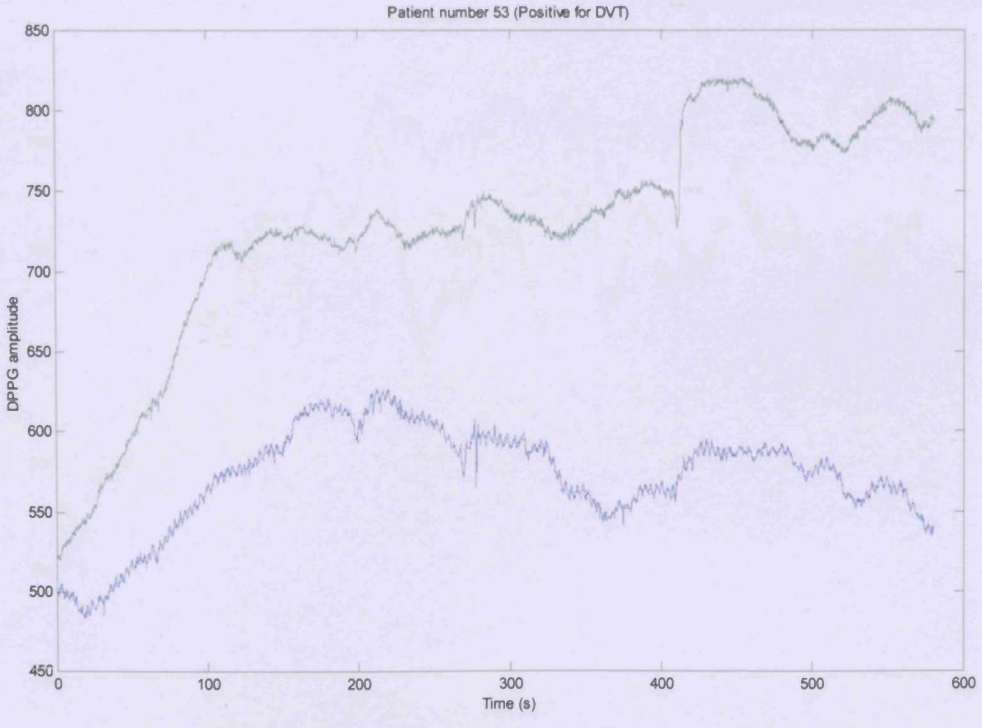
Patient number 53 (Positive for DVT)
DPPG amplitude
Time (s)
850
800
750
700
650
600
550
500
450
0
100
200
300
400
500
600

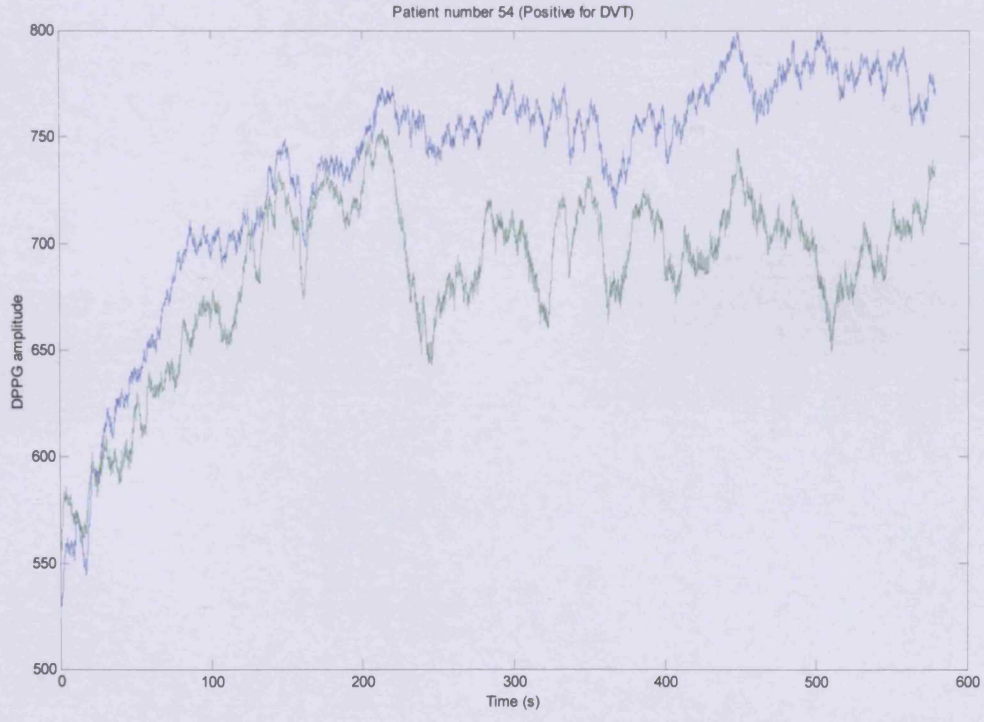
Patient number 54 (Positive for DVT)
DPPG amplitude
Time (s)
800
750
700
650
600
550
500
0
100
200
300
400
500
600

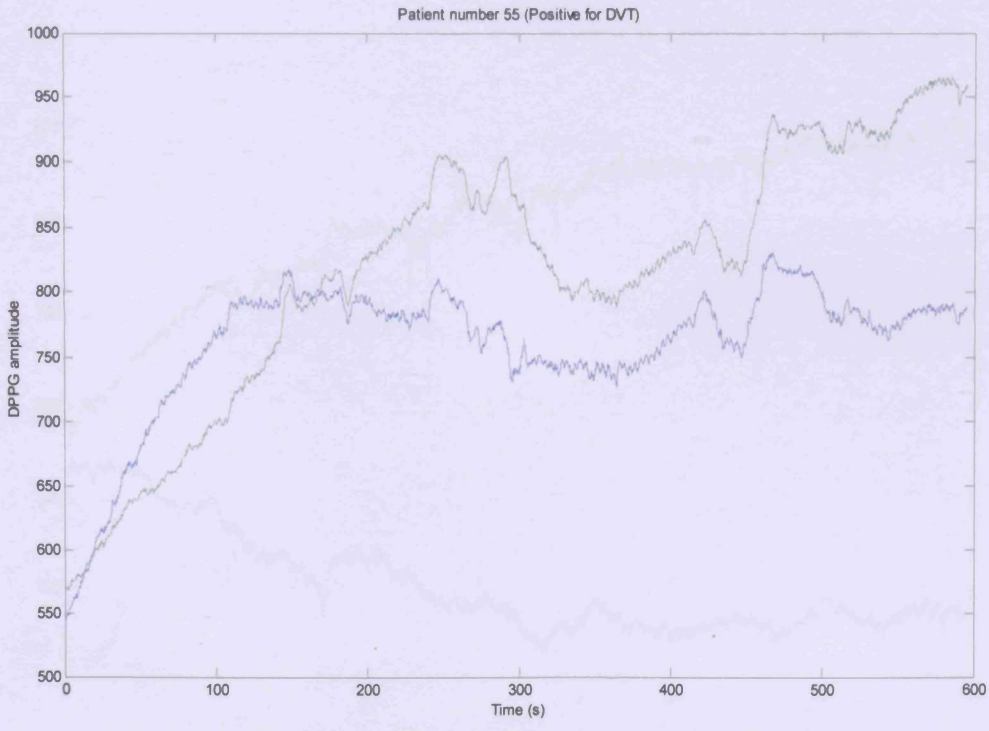
Patient number 55 (Positive for DVT)
DPPG amplitude
Time (s)
1000
950
900
850
800
750
700
650
600
550
500
0
100
200
300
400
500
600

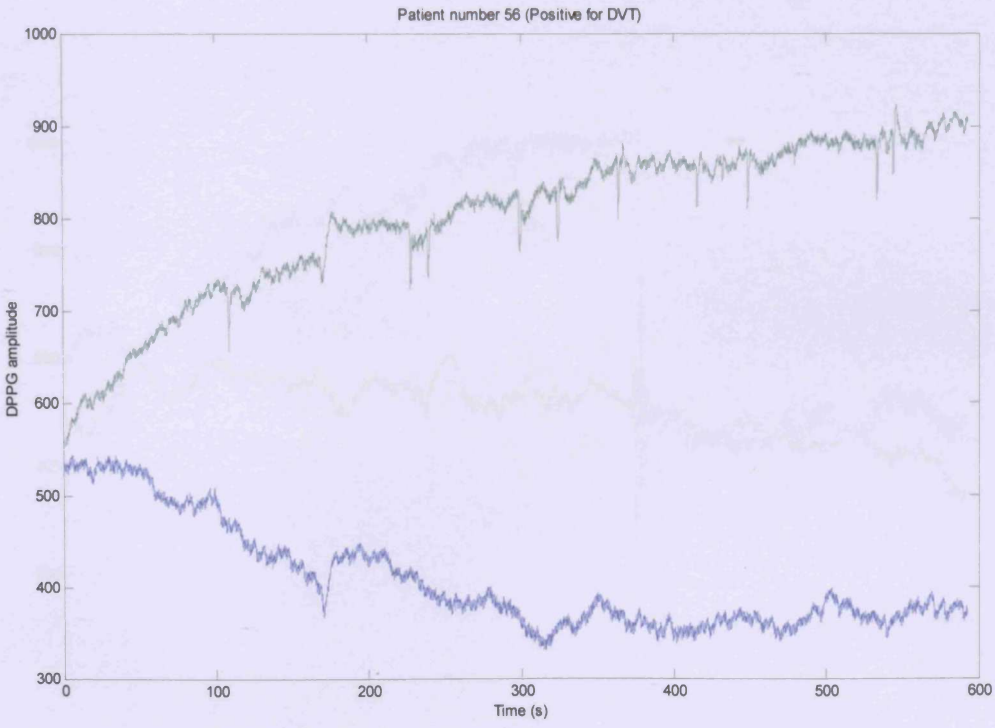
Patient number 56 (Positive for DVT)
DPPG amplitude
Time (s)
1000
900
800
700
600
500
400
300
0
100
200
300
400
500
600

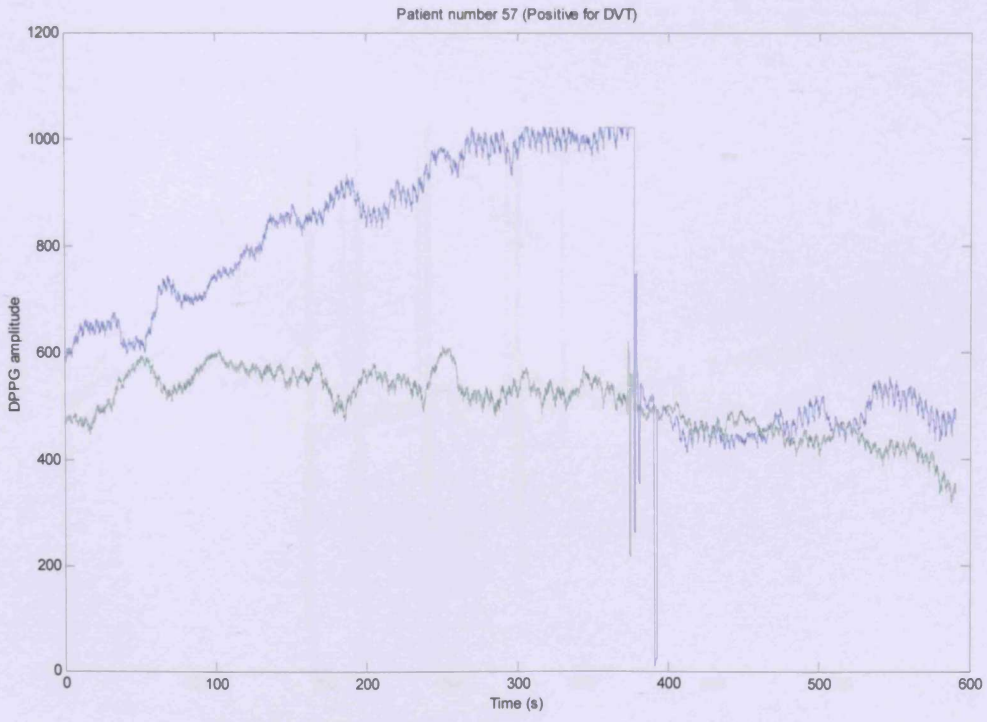
Patient number 57 (Positive for DVT)
DPPG amplitude
Time (s)
0
200
400
600
800
1000
1200
0
100
200
300
400
500
600

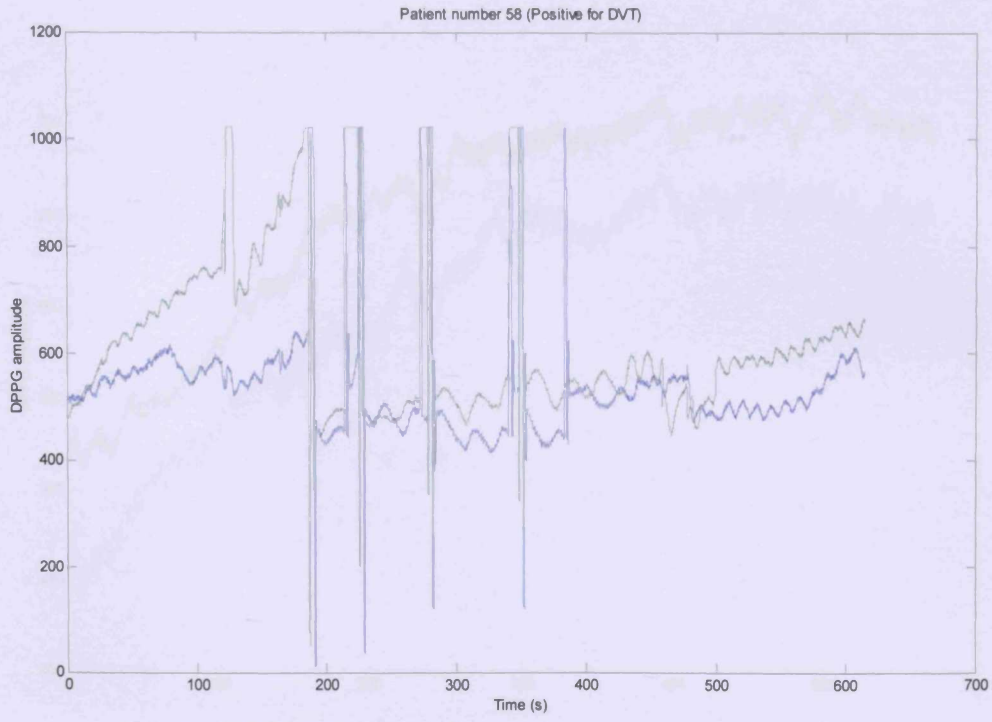
Patient number 58 (Positive for DVT)
DPPG amplitude
Time (s)
0
200
400
600
800
1000
1200
0
100
200
300
400
500
600
700

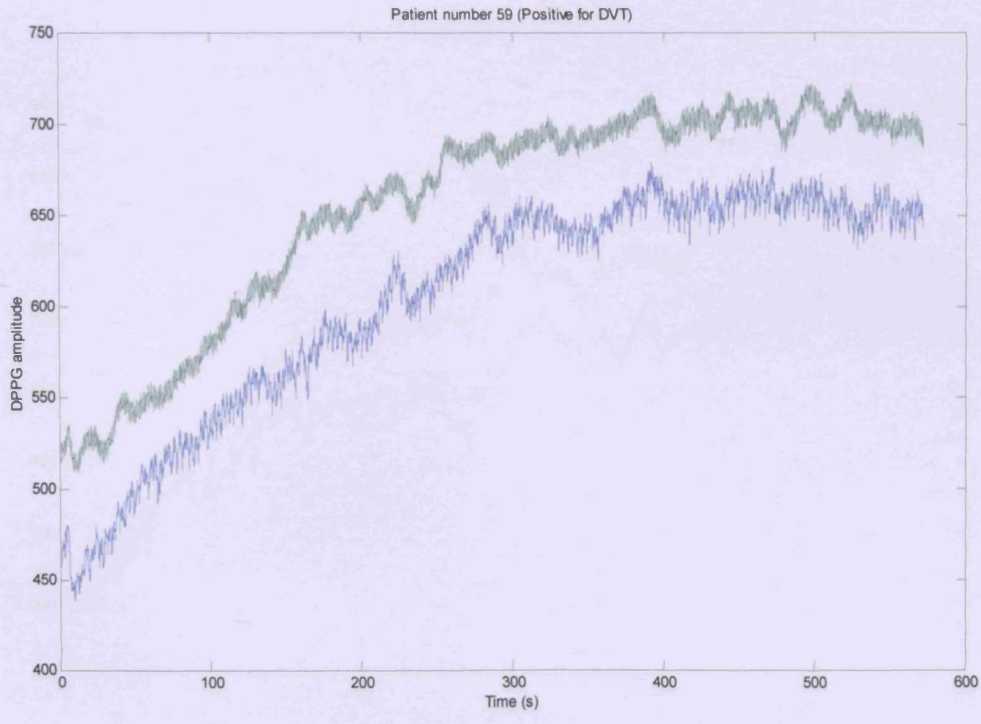
Patient number 59 (Positive for DVT)
DPPG amplitude
Time (s)
750
700
650
600
550
500
450
400
0
100
200
300
400
500
600

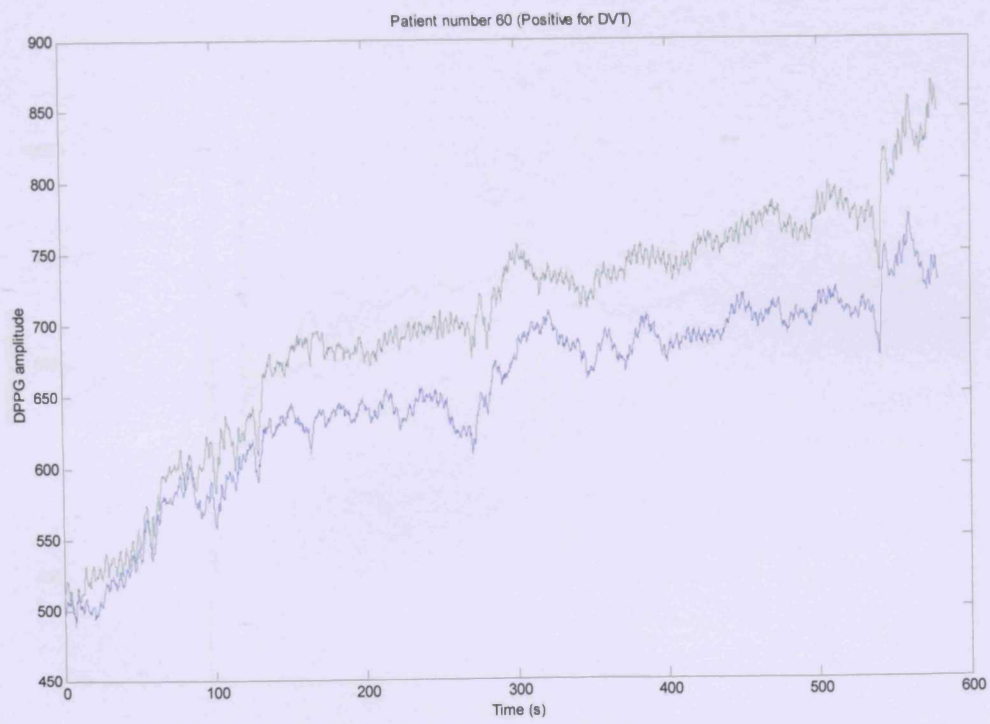
Patient number 60 (Positive for DVT)
DPPG amplitude
Time (s)
900
850
800
750
700
650
600
550
500
450
0
100
200
300
400
500
600

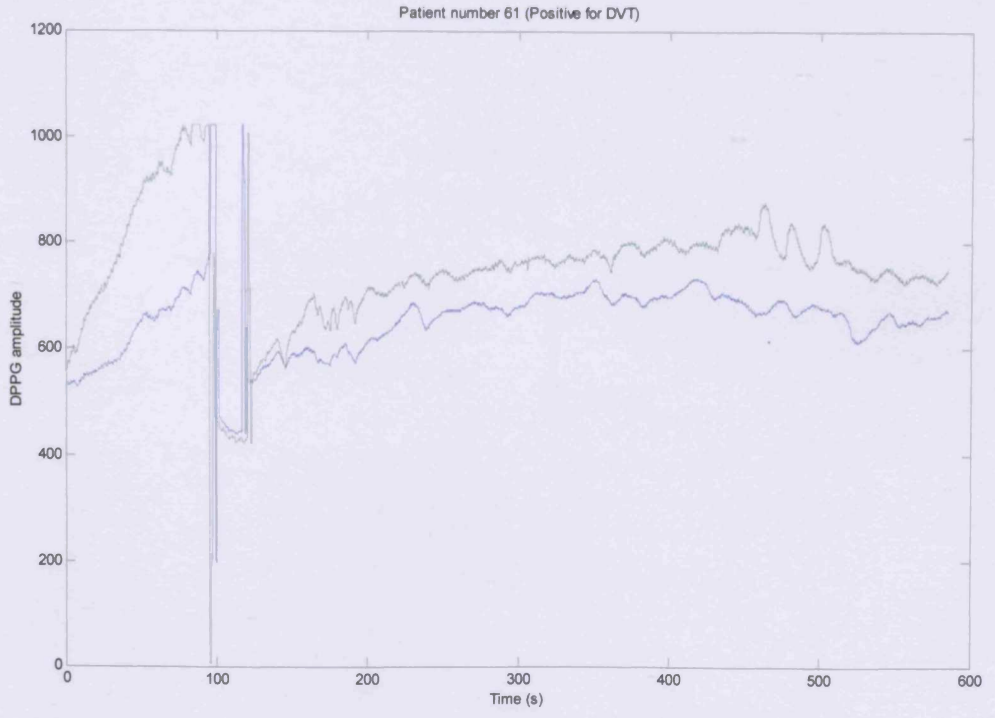
Patient number 61 (Positive for DVT)
DPPG amplitude
Time (s)
0
200
400
600
800
1000
1200
0
100
200
300
400
500
600

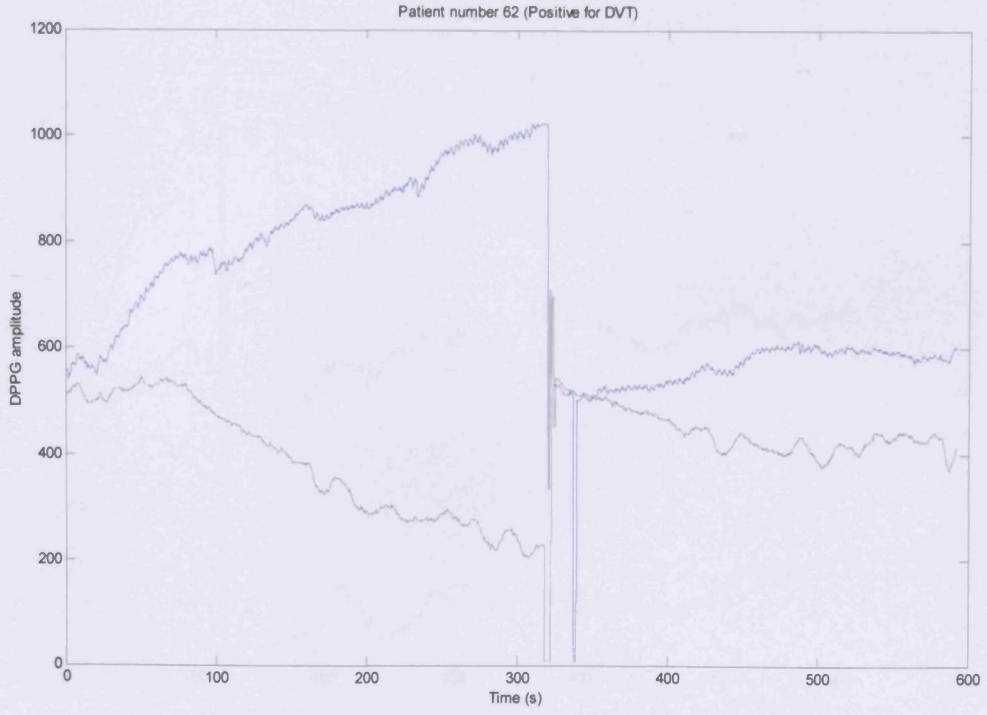
Patient number 62 (Positive for DVT)
DPPG amplitude
Time (s)
0
200
400
600
800
1000
1200
0
100
200
300
400
500
600

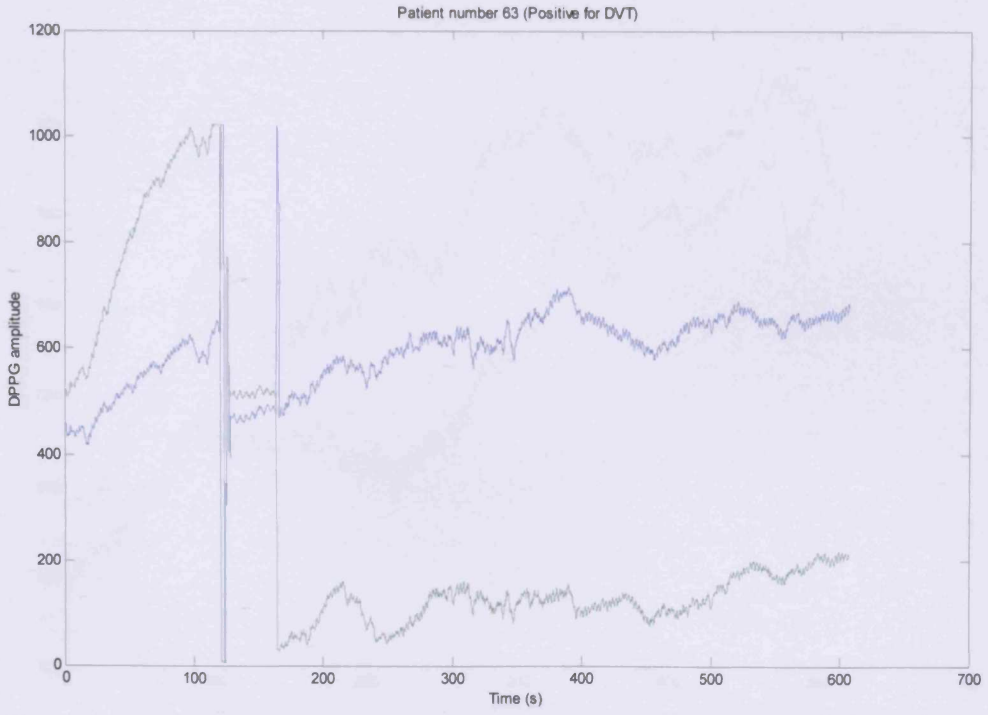
Patient number 63 (Positive for DVT)
DPPG amplitude
Time (s)
0
200
400
600
800
1000
1200
0
100
200
300
400
500
600
700

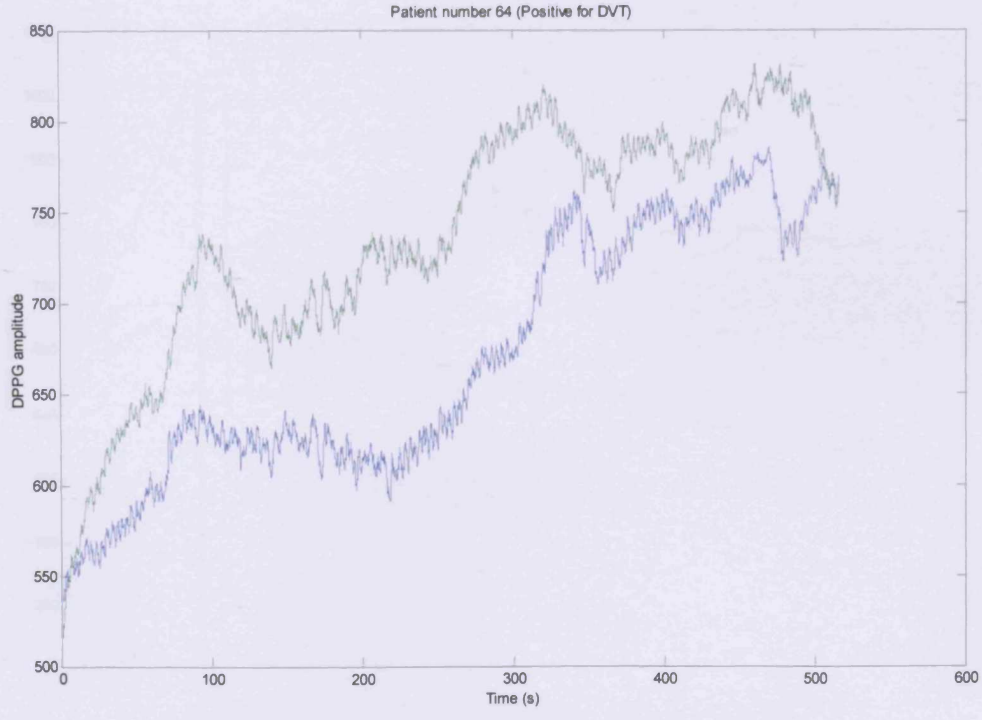
Patient number 64 (Positive for DVT)
DPPG amplitude
Time (s)
850
800
750
700
650
600
550
500
0
100
200
300
400
500
600

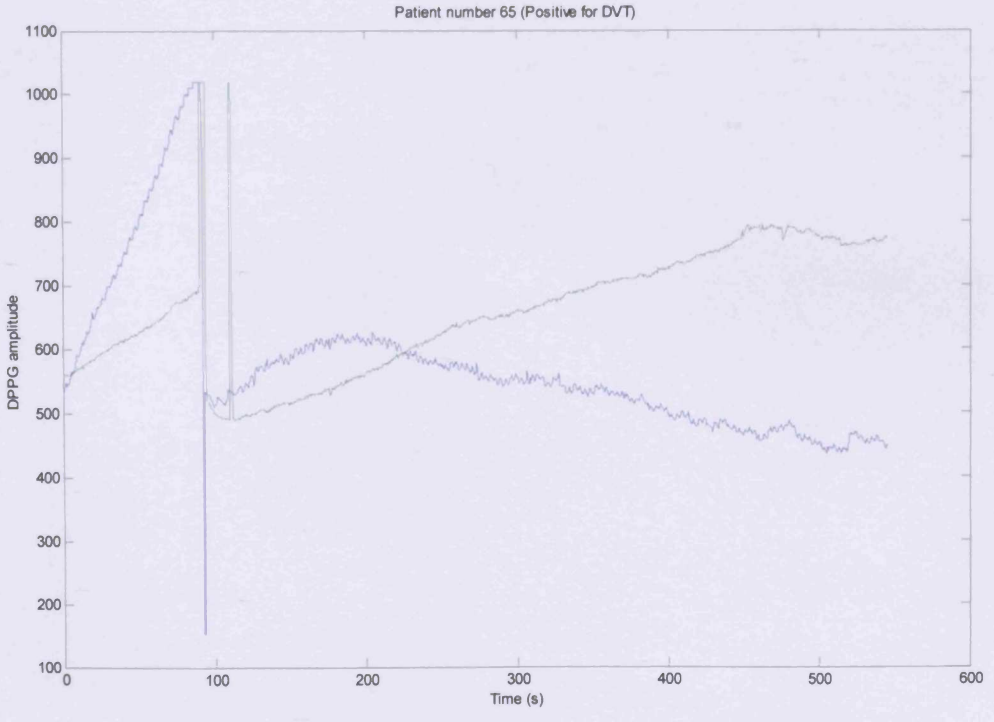
Patient number 65 (Positive for DVT)
DPPG amplitude
Time (s)
1100
1000
900
800
700
600
500
400
300
200
100
0
100
200
300
400
500
600

Data from patients with no lower limb DVT

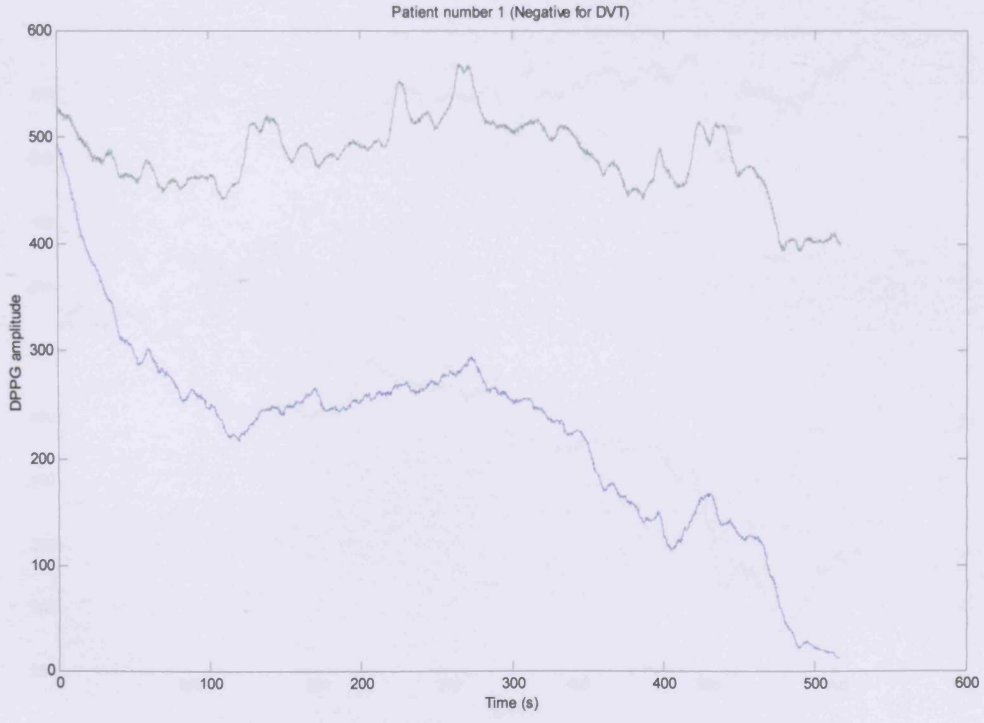
Patient number 1 (Negative for DVT)
DPPG amplitude
Time (s)
0
100
200
300
400
500
600

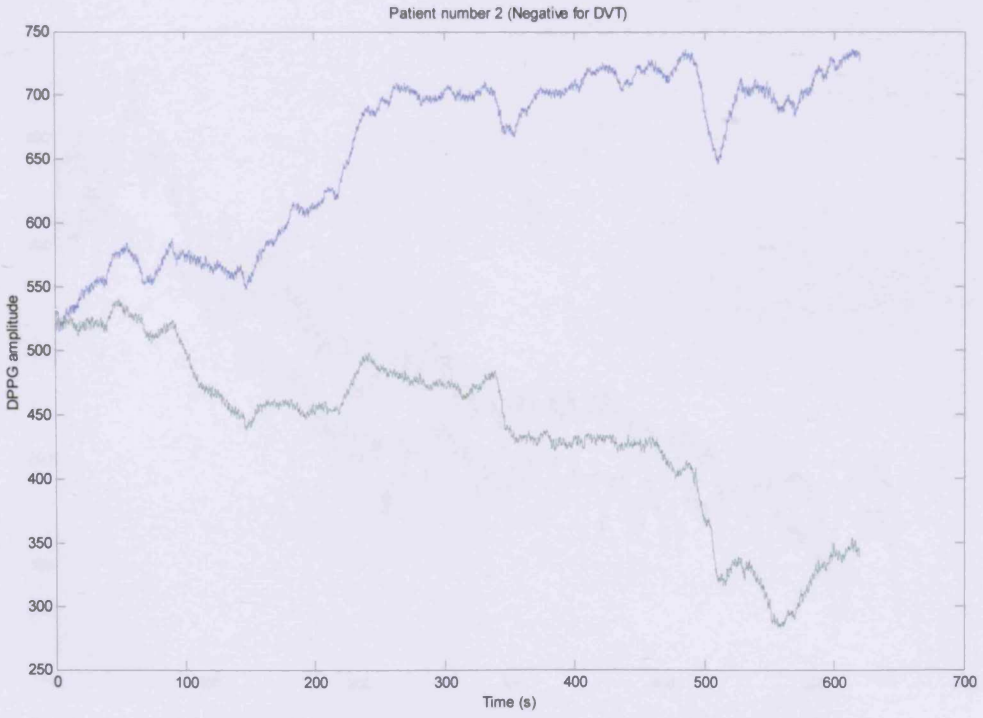
Patient number 2 (Negative for DVT)
DPPG amplitude
Time (s)
750
700
650
600
550
500
450
400
350
300
250
0
100
200
300
400
500
600
700

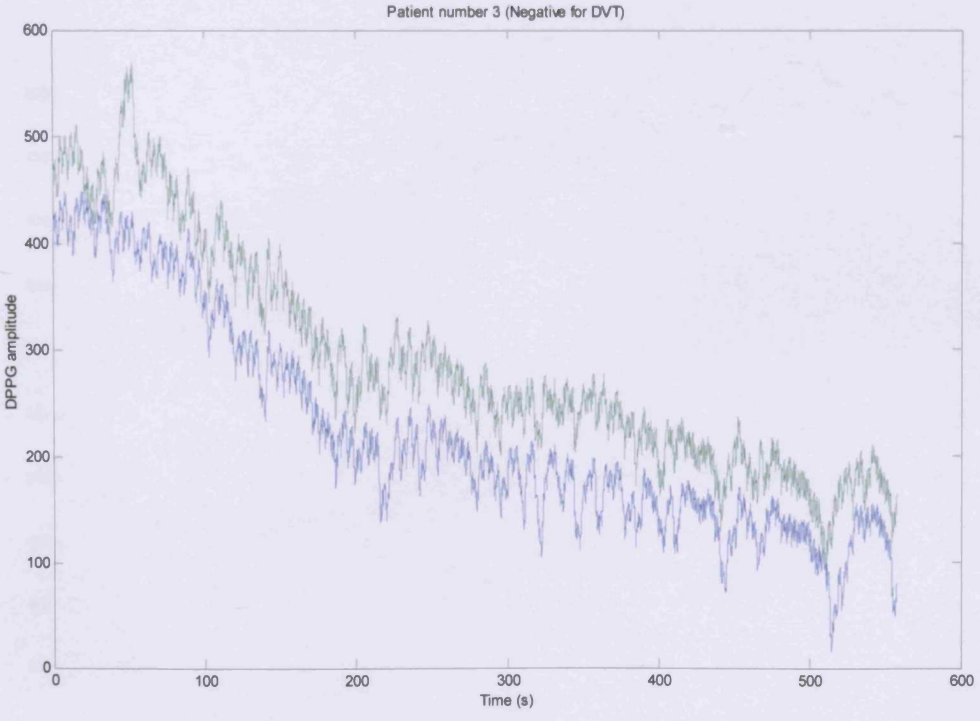
Patient number 3 (Negative for DVT)
DPPG amplitude
Time (s)
0
100
200
300
400
500
600

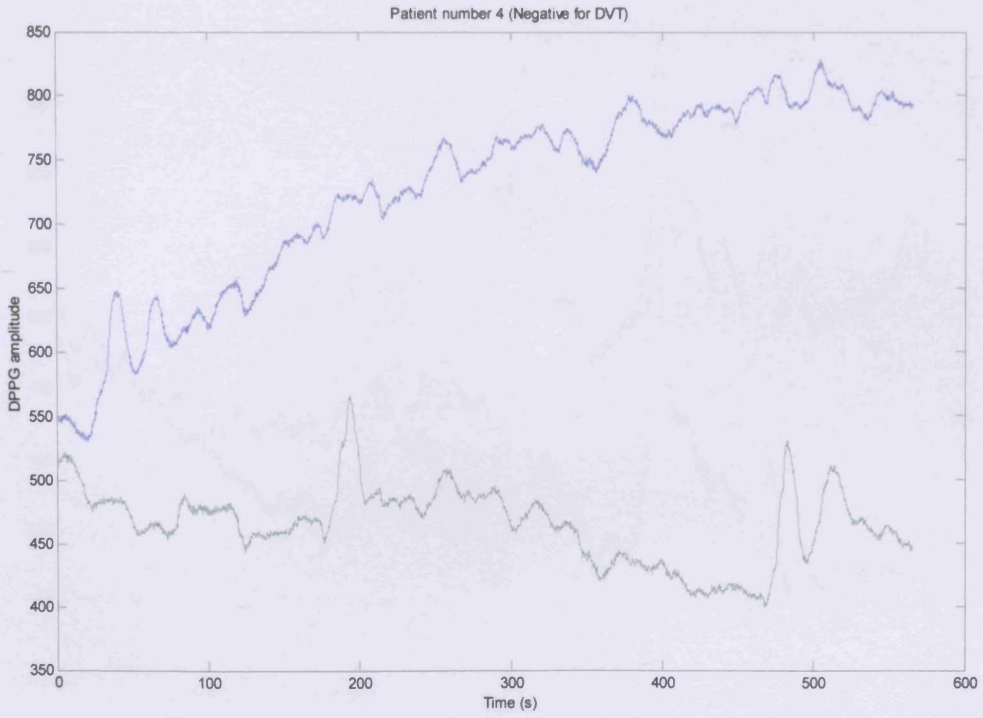
Patient number 4 (Negative for DVT)
DPPG amplitude
Time (s)
850
800
750
700
650
600
550
500
450
400
350
0
100
200
300
400
500
600

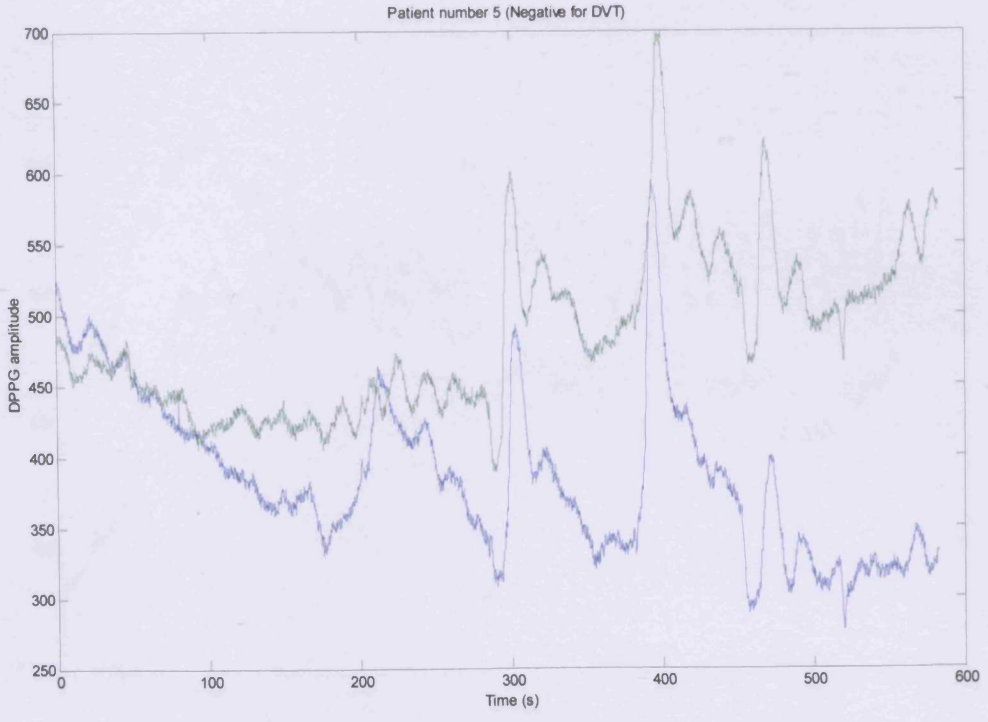
Patient number 5 (Negative for DVT)
DPPG amplitude
Time (s)
700
650
600
550
500
450
400
350
300
250
0
100
200
300
400
500
600

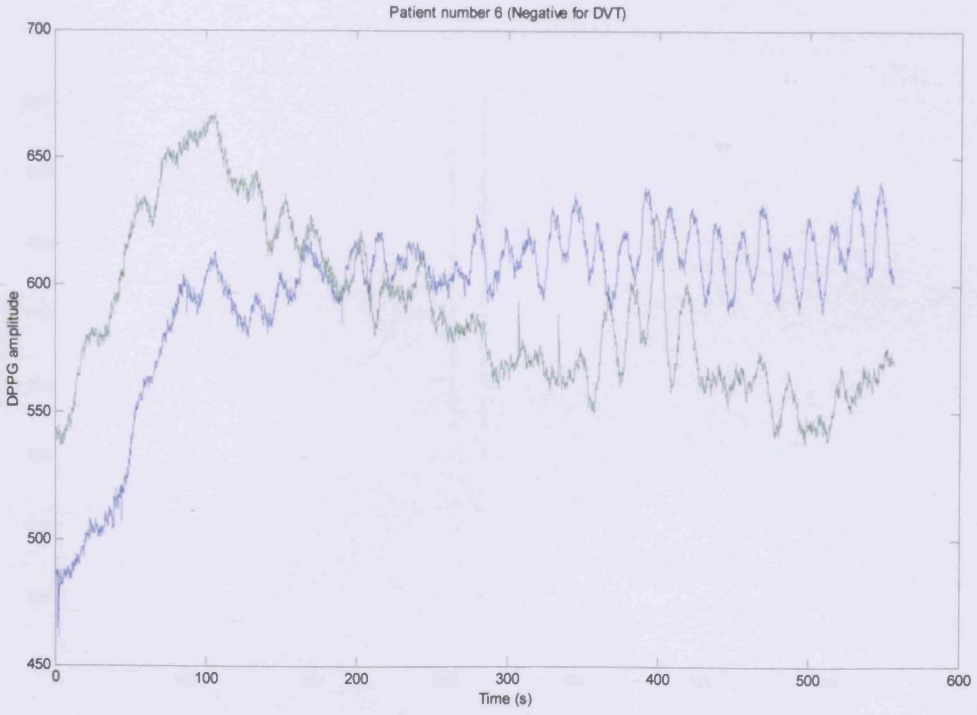
Patient number 6 (Negative for DVT)
DPPG amplitude
Time (s)
700
650
600
550
500
450
0
100
200
300
400
500
600

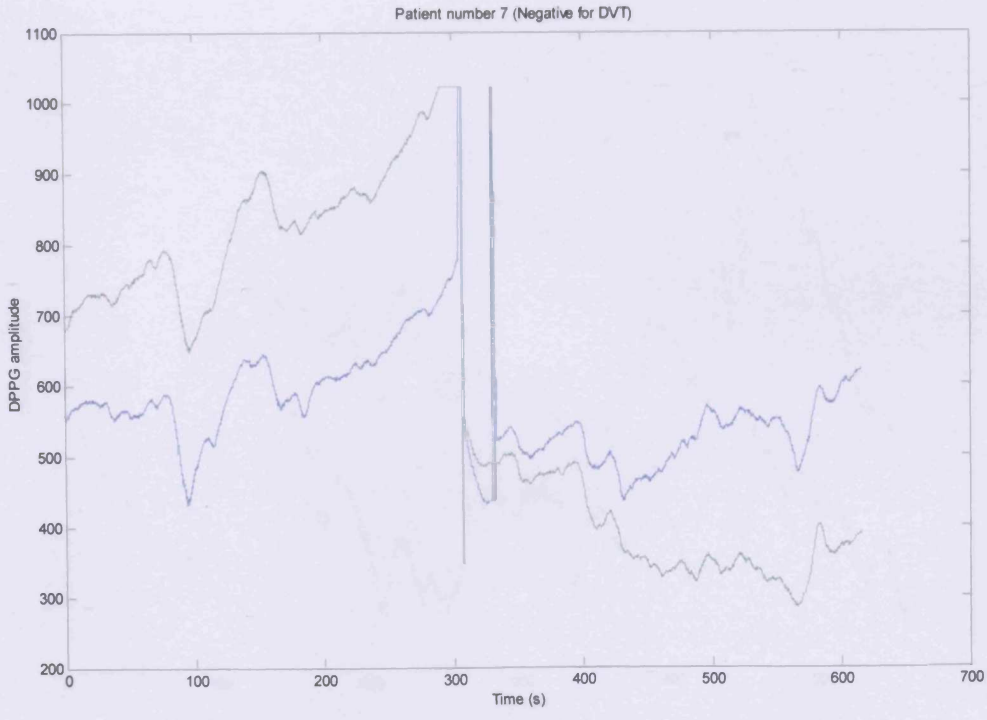
Patient number 7 (Negative for DVT)
DPPG amplitude
Time (s)
1100
1000
900
800
700
600
500
400
300
200
0
100
200
300
400
500
600
700

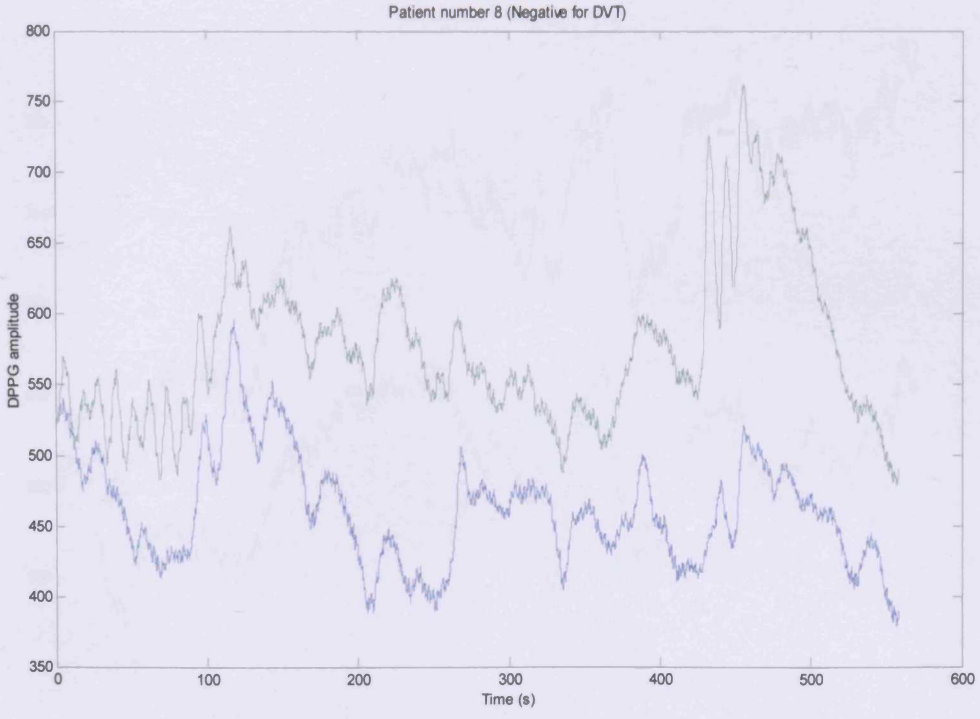
Patient number 8 (Negative for DVT)
DPPG amplitude
Time (s)
800
750
700
650
600
550
500
450
400
350
0
100
200
300
400
500
600

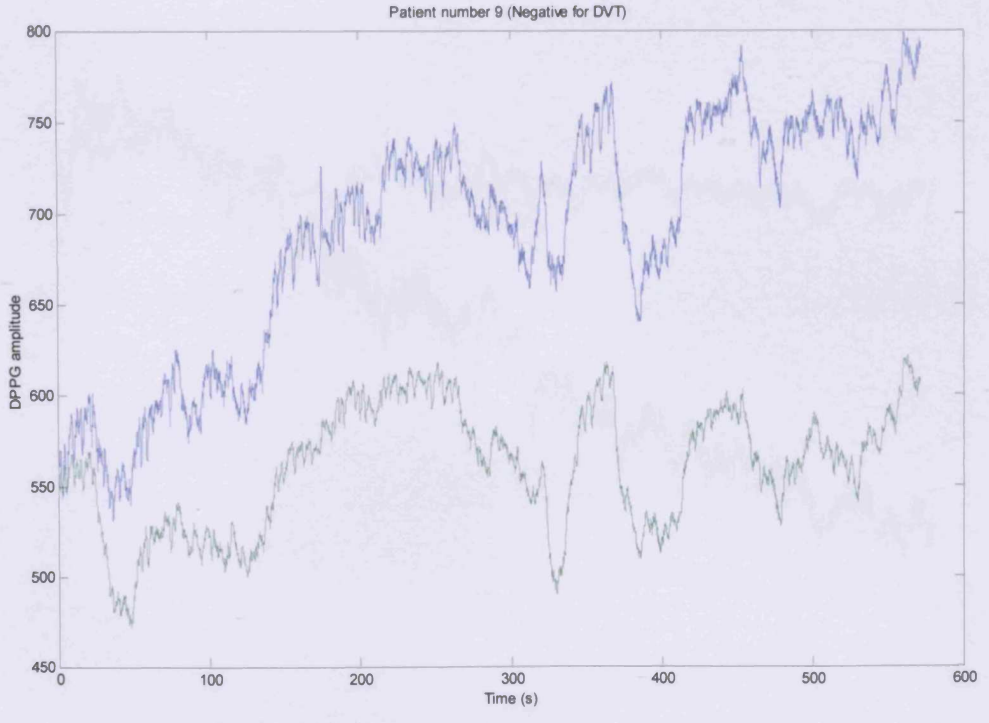
Patient number 9 (Negative for DVT)
DPPG amplitude
Time (s)
800
750
700
650
600
550
500
450
0
100
200
300
400
500
600

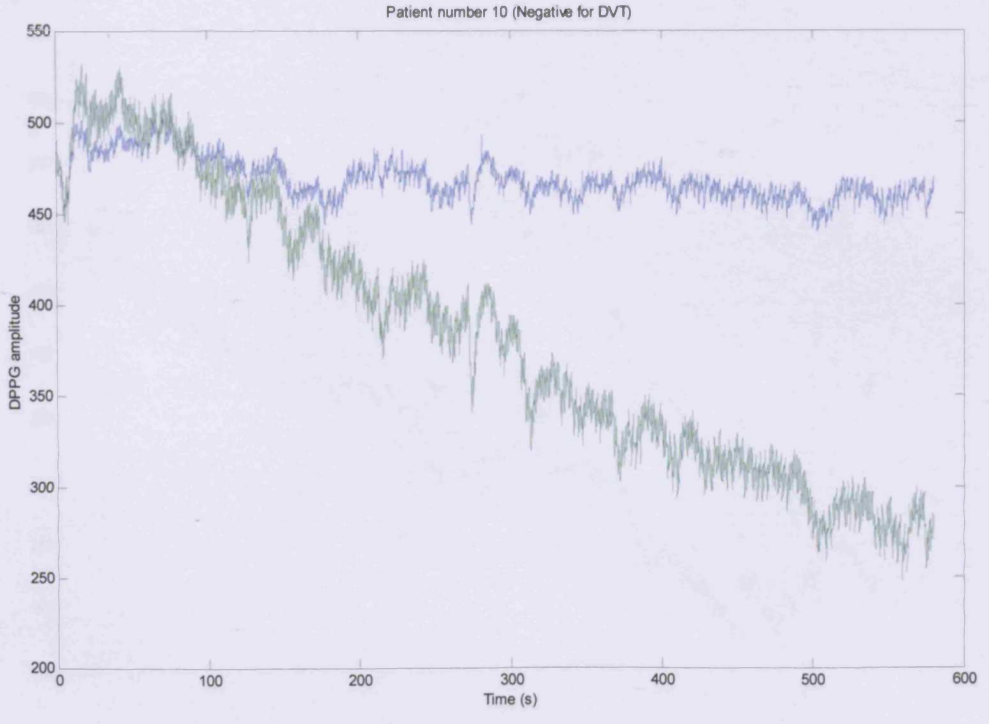
Patient number 10 (Negative for DVT)
DPPG amplitude
Time (s)
550
500
450
400
350
300
250
200
0
100
200
300
400
500
600

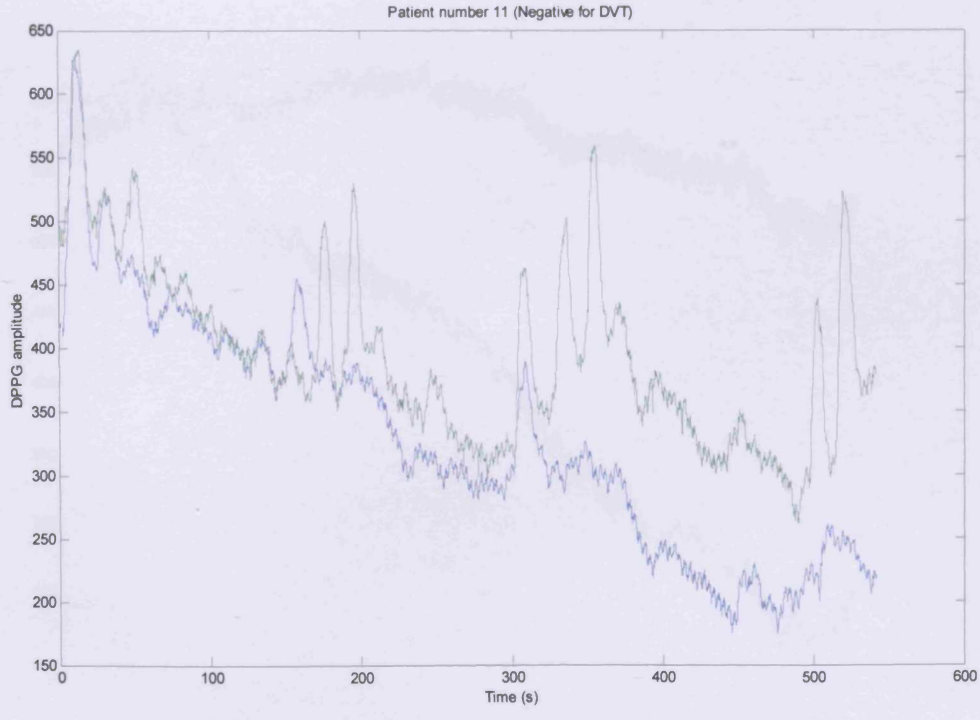
Patient number 11 (Negative for DVT)
DPPG amplitude
Time (s)
650
600
550
500
450
400
350
300
250
200
150
0
100
200
300
400
500
600

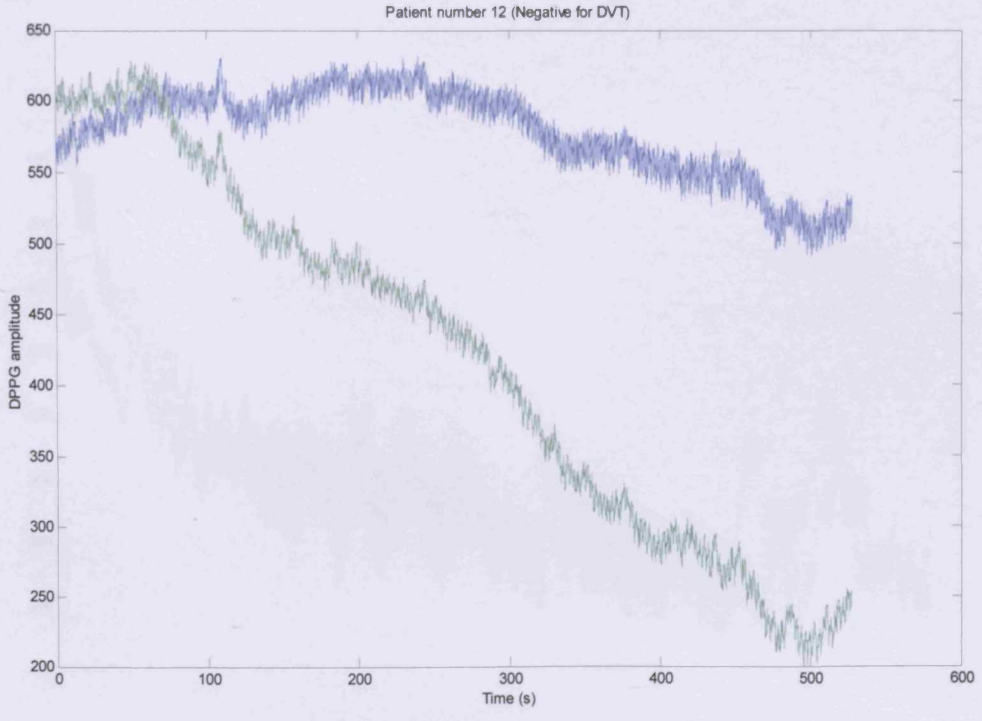
Patient number 12 (Negative for DVT)
DPPG amplitude
Time (s)
650
600
550
500
450
400
350
300
250
200
0
100
200
300
400
500
600

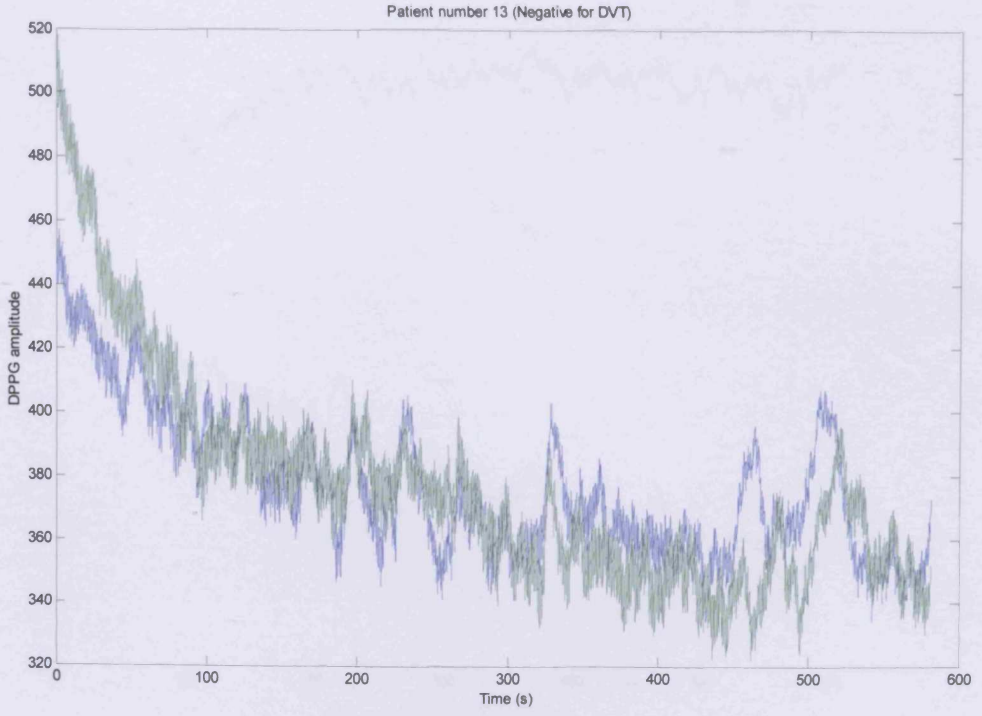
Patient number 13 (Negative for DVT)
DPPG amplitude
Time (s)
520
500
480
460
440
420
400
380
360
340
320
0
100
200
300
400
500
600

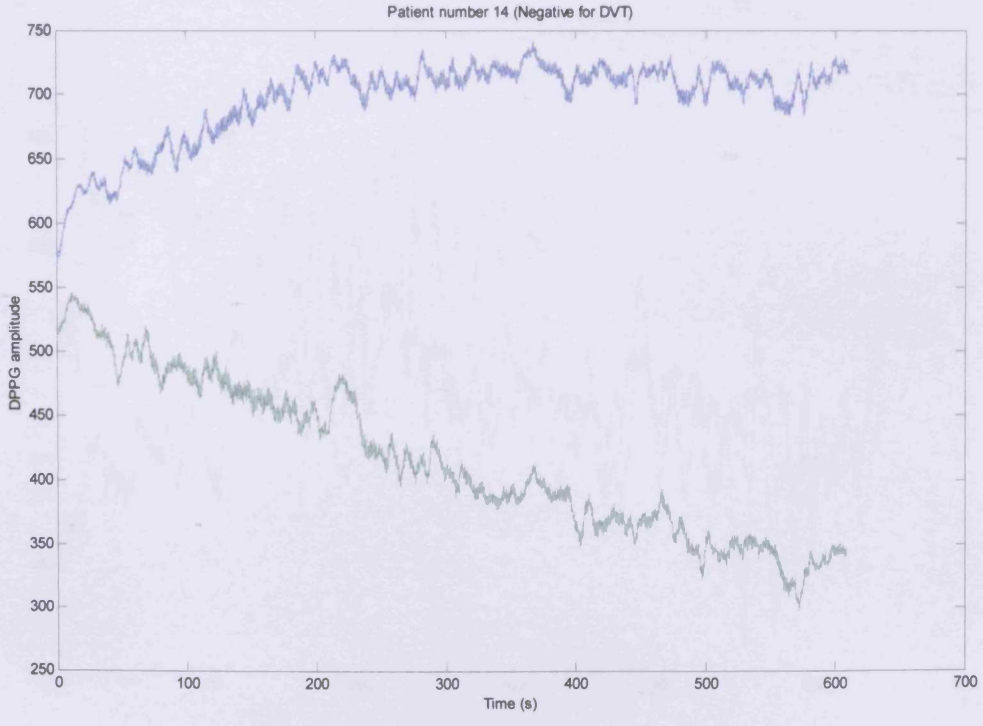
Patient number 14 (Negative for DVT)
DPPG amplitude
Time (s)
750
700
650
600
550
500
450
400
350
300
250
0
100
200
300
400
500
600
700

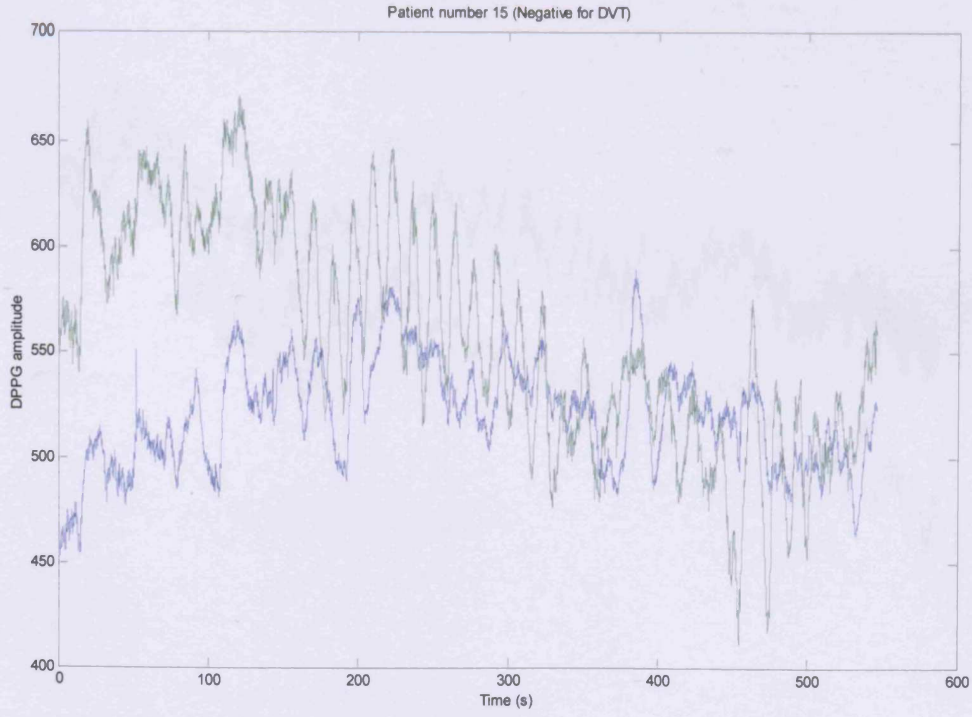
Patient number 15 (Negative for DVT)
DPPG amplitude
Time (s)
700
650
600
550
500
450
400
0
100
200
300
400
500
600

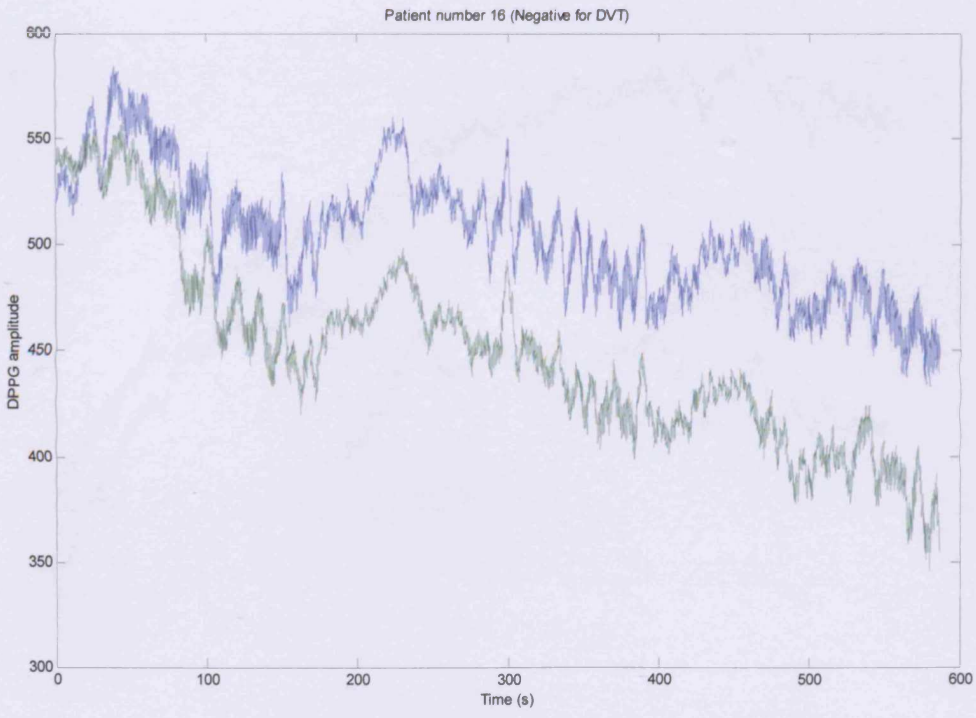
Patient number 16 (Negative for DVT)
DPPG amplitude
Time (s)
600
550
500
450
400
350
300
0
100
200
300
400
500
600

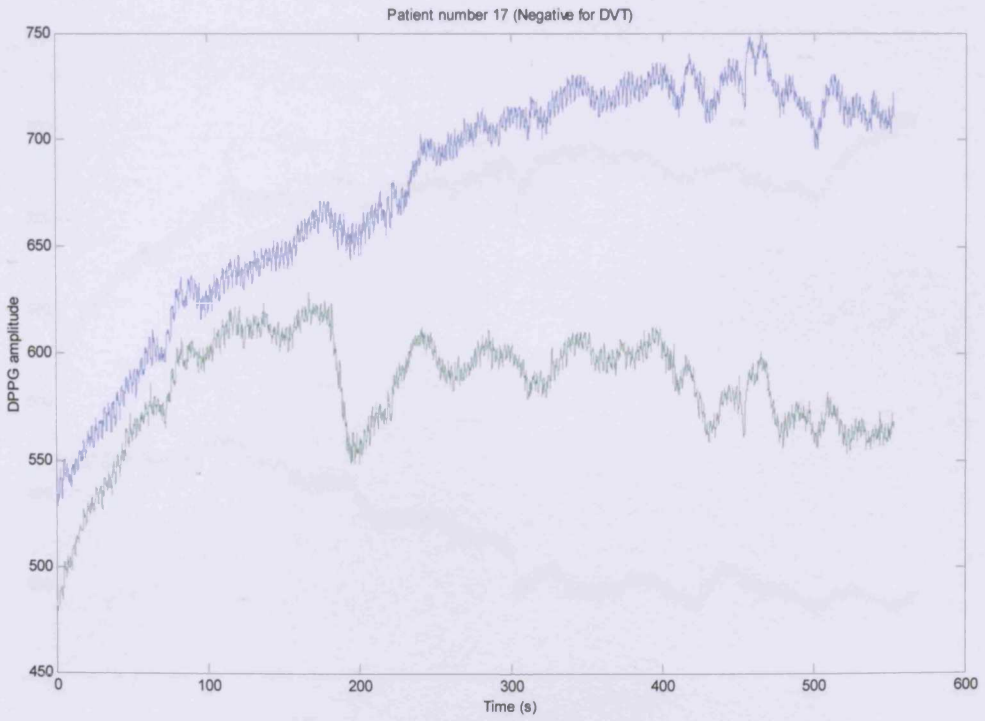
Patient number 17 (Negative for DVT)
DPPG amplitude
Time (s)
750
700
650
600
550
500
450
0
100
200
300
400
500
600

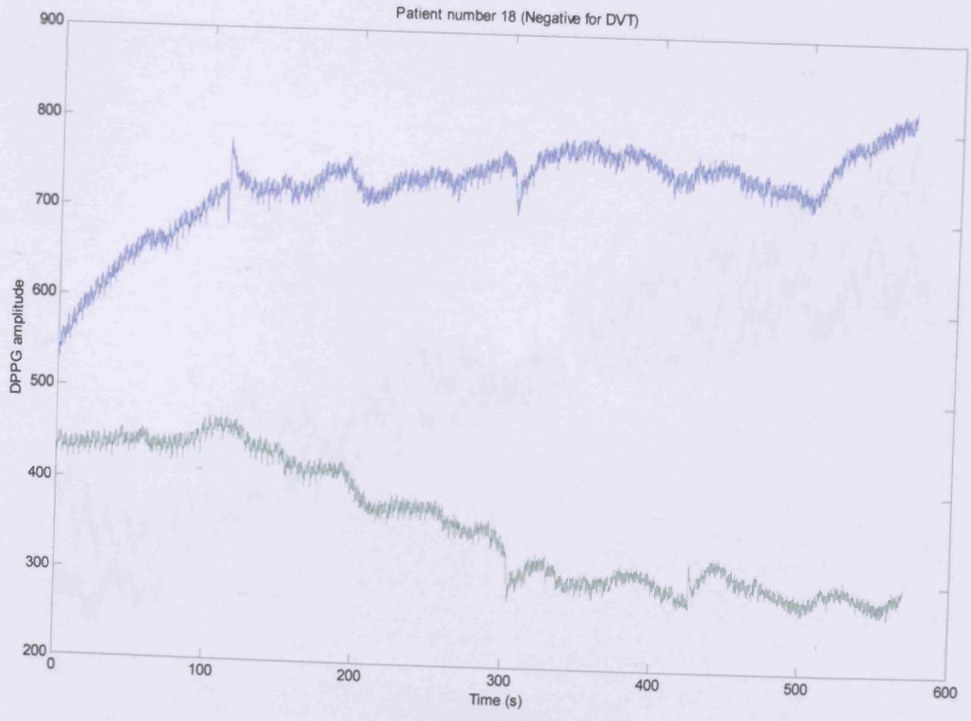
Patient number 18 (Negative for DVT)
DPPG amplitude
Time (s)
900
800
700
600
500
400
300
200
0
100
200
300
400
500
600

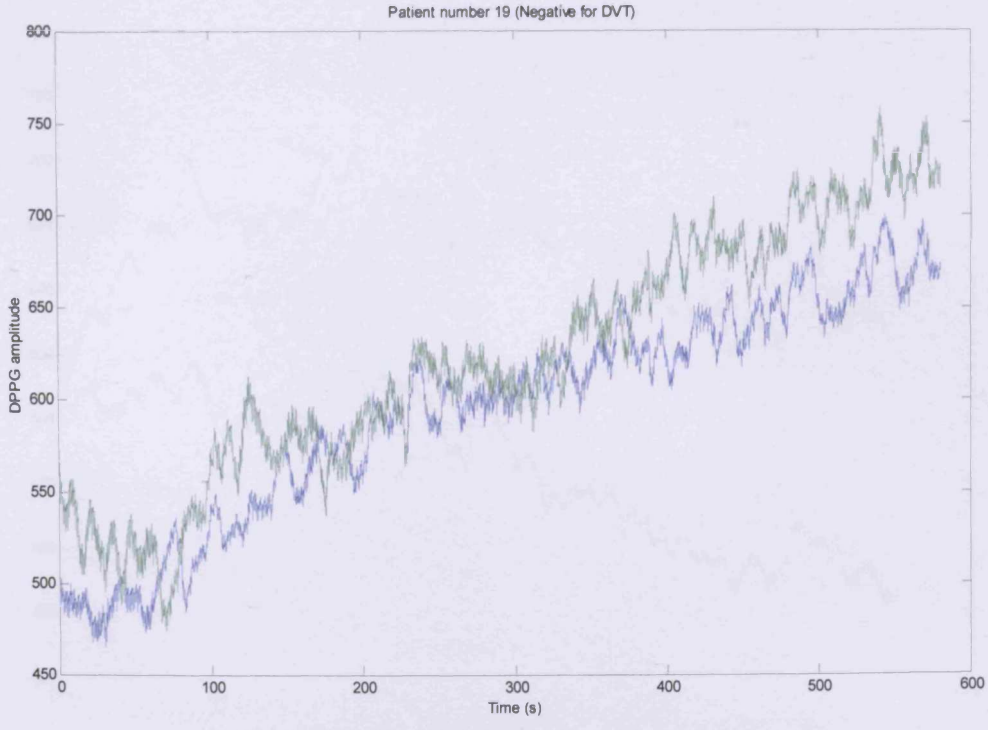
Patient number 19 (Negative for DVT)
DPPG amplitude
Time (s)
800
750
700
650
600
550
500
450
0
100
200
300
400
500
600

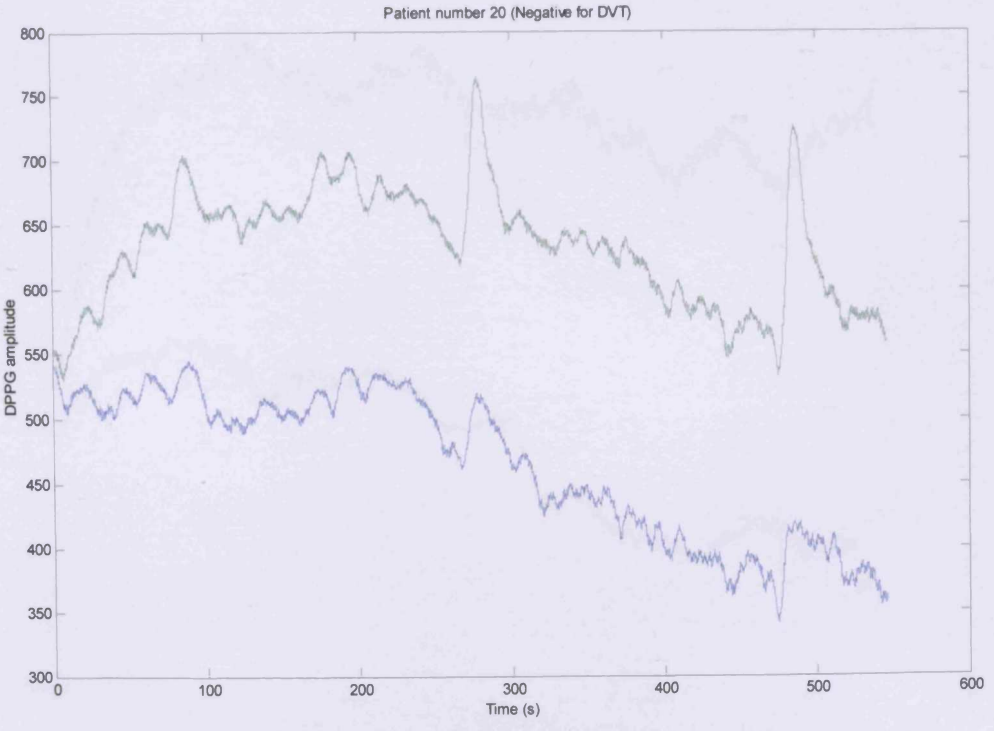
Patient number 20 (Negative for DVT)
DPPG amplitude
Time (s)
800
750
700
650
600
550
500
450
400
350
300
0
100
200
300
400
500
600

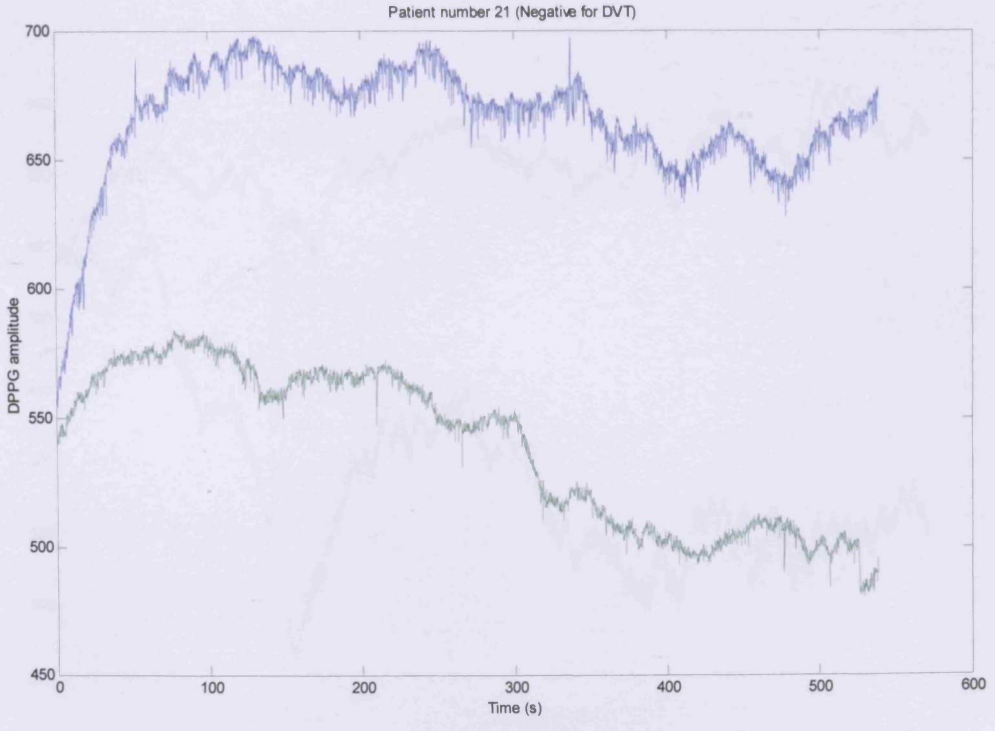
Patient number 21 (Negative for DVT)
DPPG amplitude
Time (s)
700
650
600
550
500
450
0
100
200
300
400
500
600

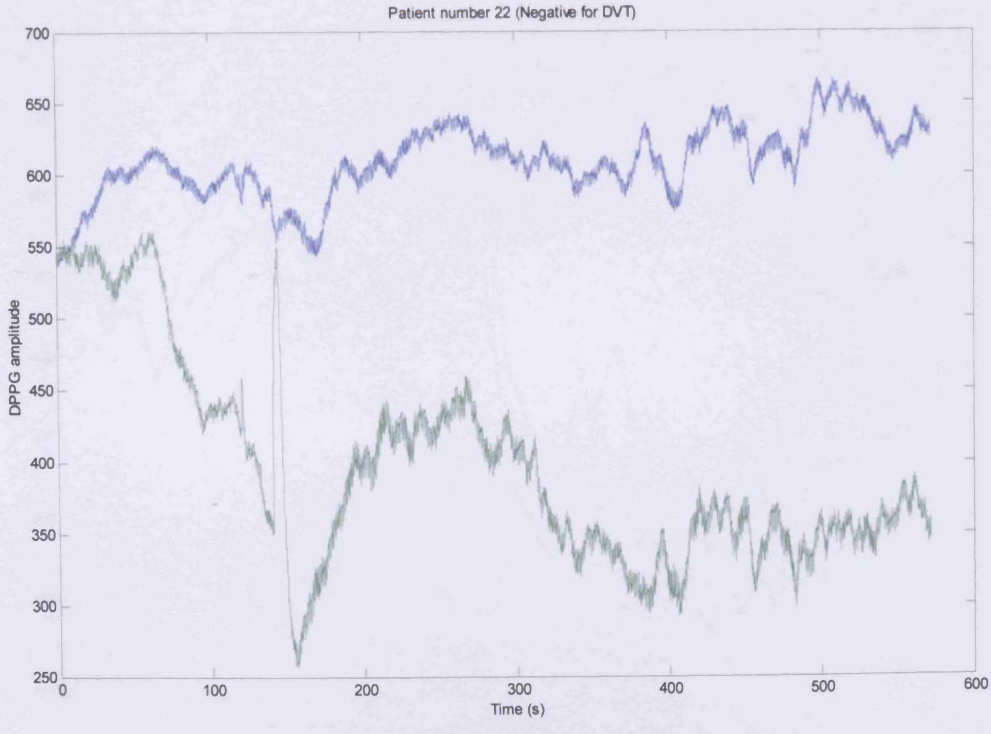
Patient number 22 (Negative for DVT)
DPPG amplitude
Time (s)
700
650
600
550
500
450
400
350
300
250
0
100
200
300
400
500
600

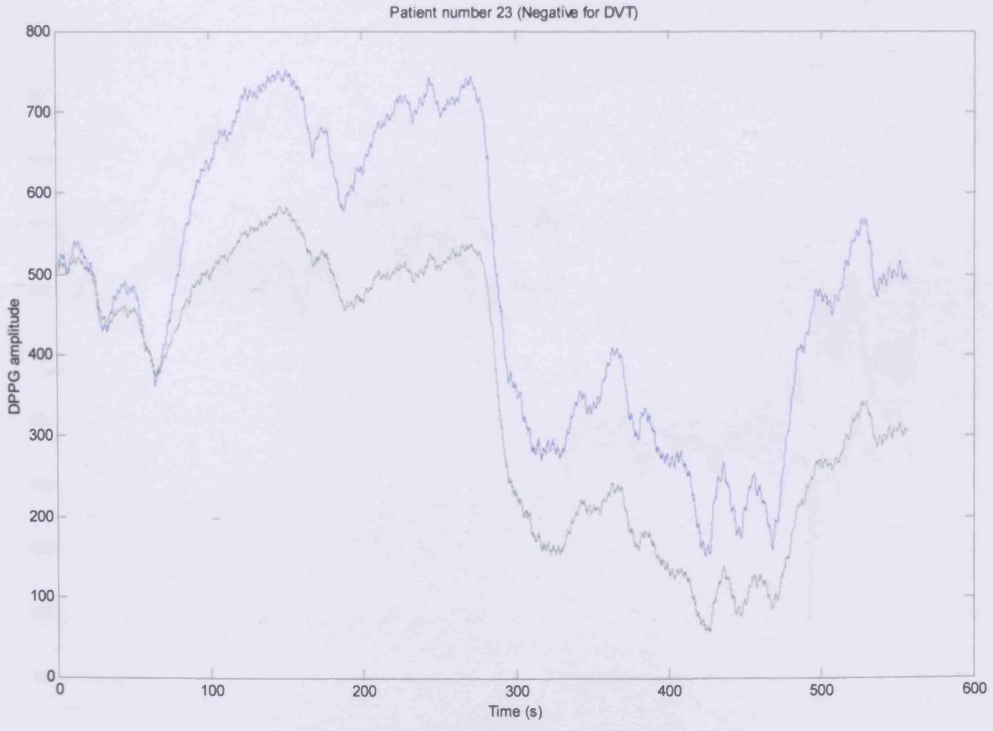
Patient number 23 (Negative for DVT)
DPPG amplitude
Time (s)
0
100
200
300
400
500
600
700
800

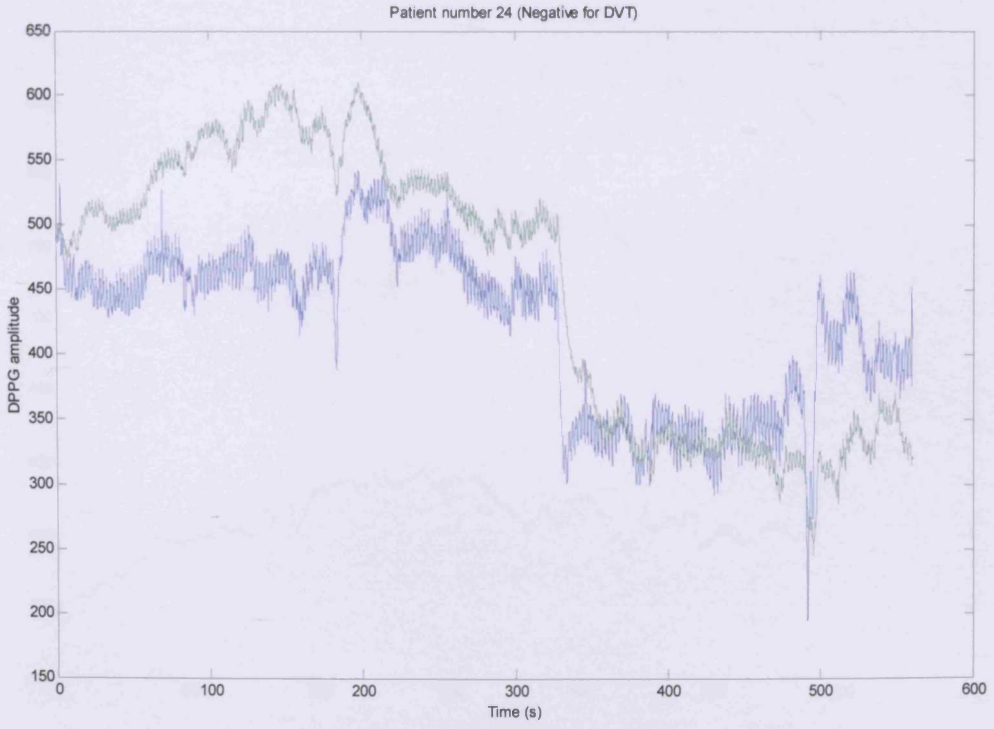
Patient number 24 (Negative for DVT)
DPPG amplitude
Time (s)
650
600
550
500
450
400
350
300
250
200
150
0
100
200
300
400
500
600

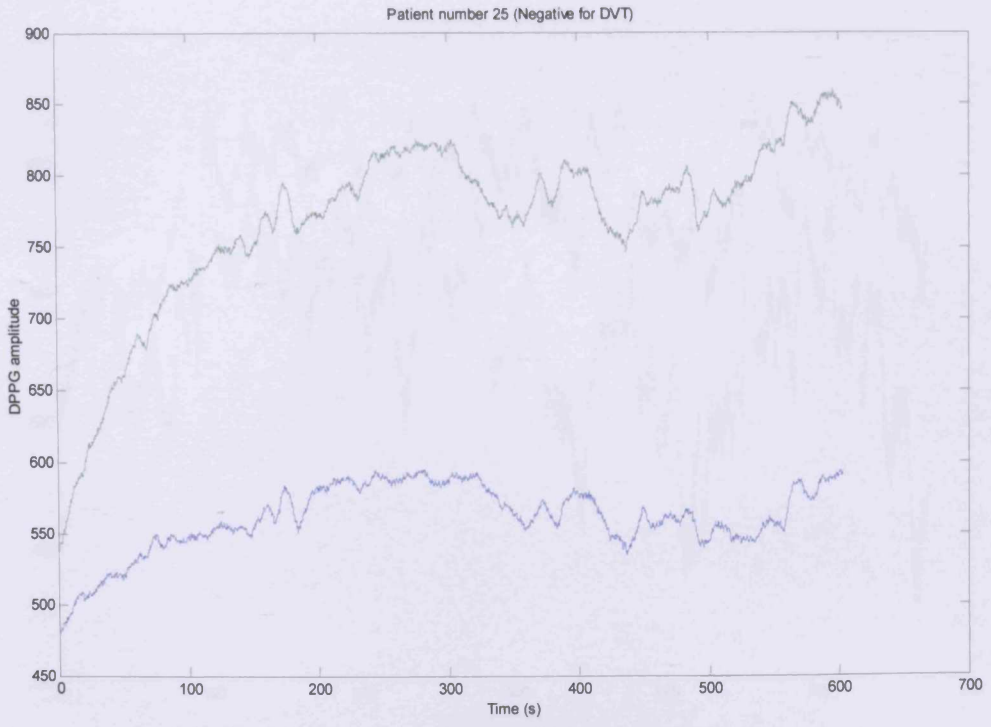
Patient number 25 (Negative for DVT)
DPPG amplitude
Time (s)
900
850
800
750
700
650
600
550
500
450
0
100
200
300
400
500
600
700

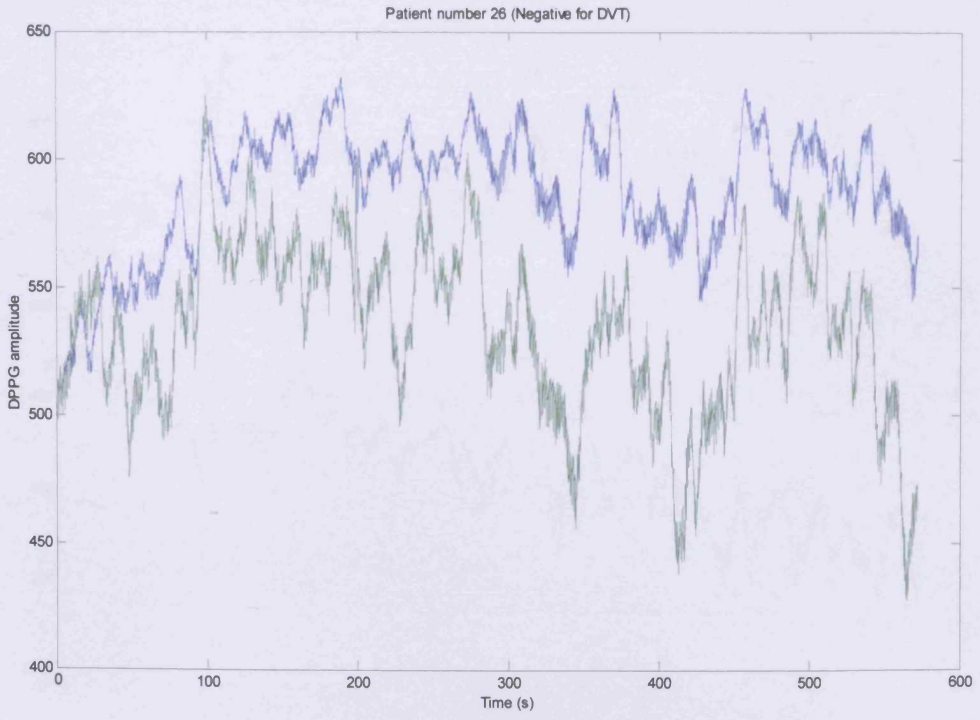
Patient number 26 (Negative for DVT)
650
600
550
500
450
400
DPPG amplitude
0
100
200
300
400
500
600
Time (s)

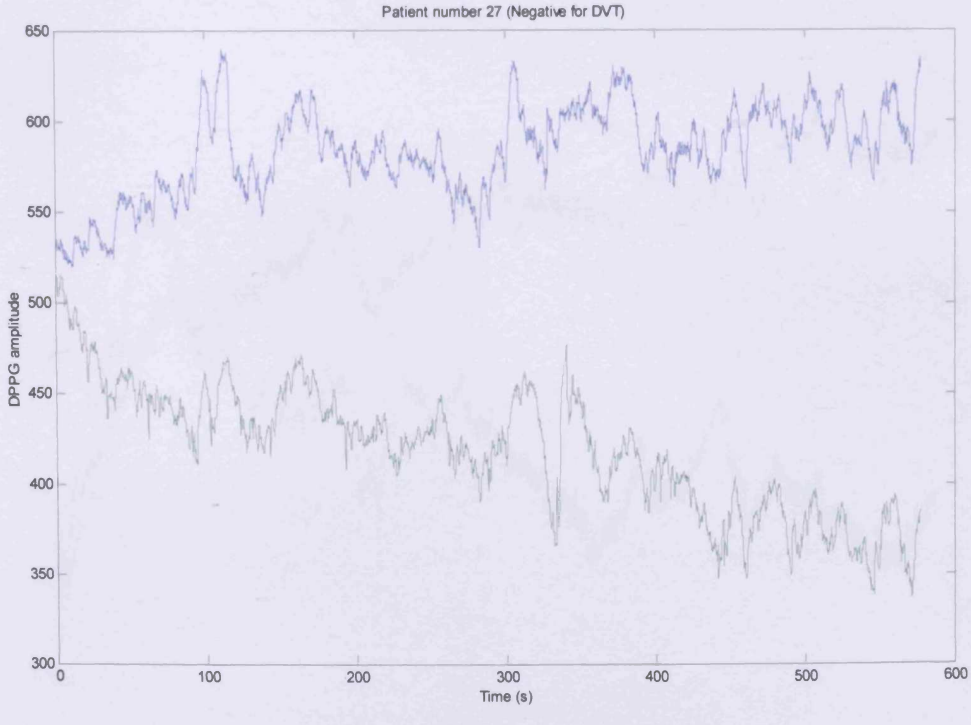
Patient number 27 (Negative for DVT)
650
600
550
500
450
400
350
300
DPPG amplitude
0
100
200
300
400
500
600
Time (s)

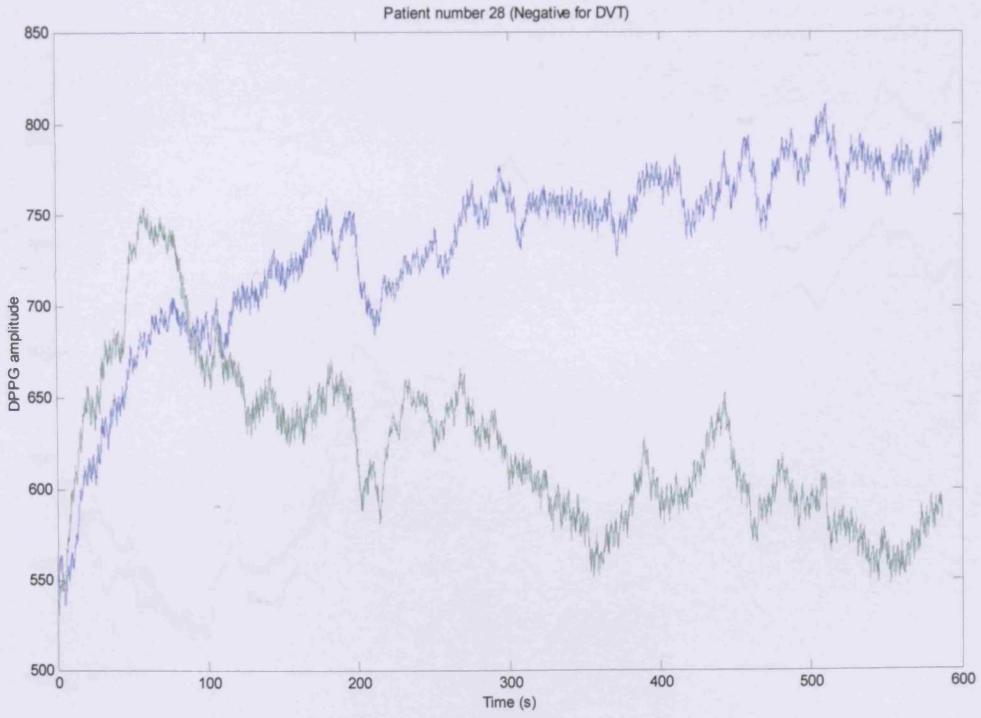
Patient number 28 (Negative for DVT)
DPPG amplitude
Time (s)
850
800
750
700
650
600
550
500
0
100
200
300
400
500
600

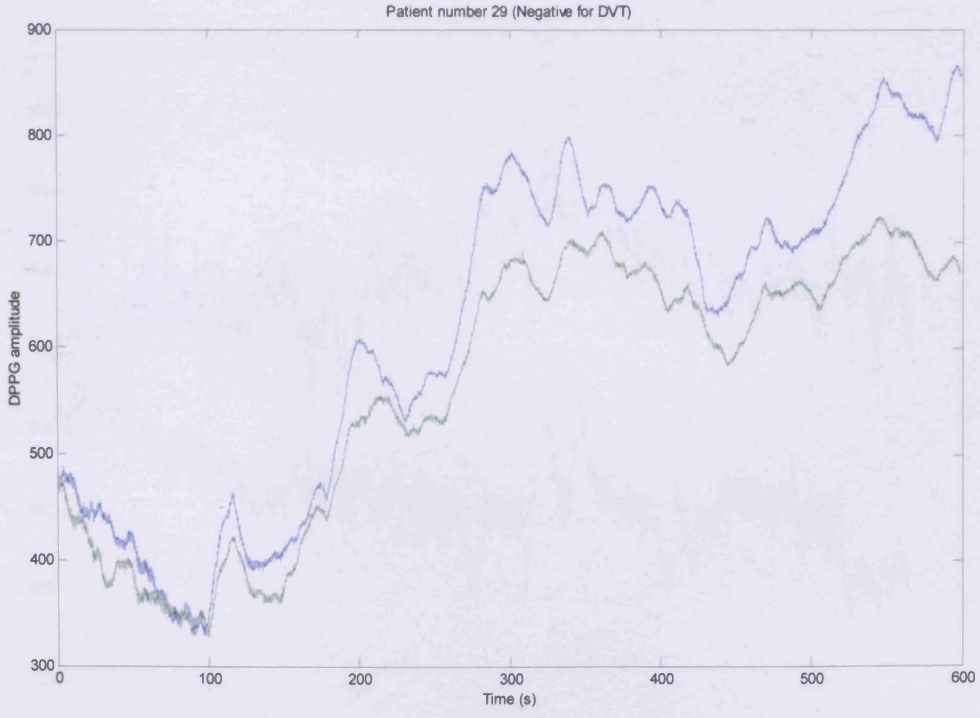
Patient number 29 (Negative for DVT)
DPPG amplitude
Time (s)
900
800
700
600
500
400
300
0
100
200
300
400
500
600

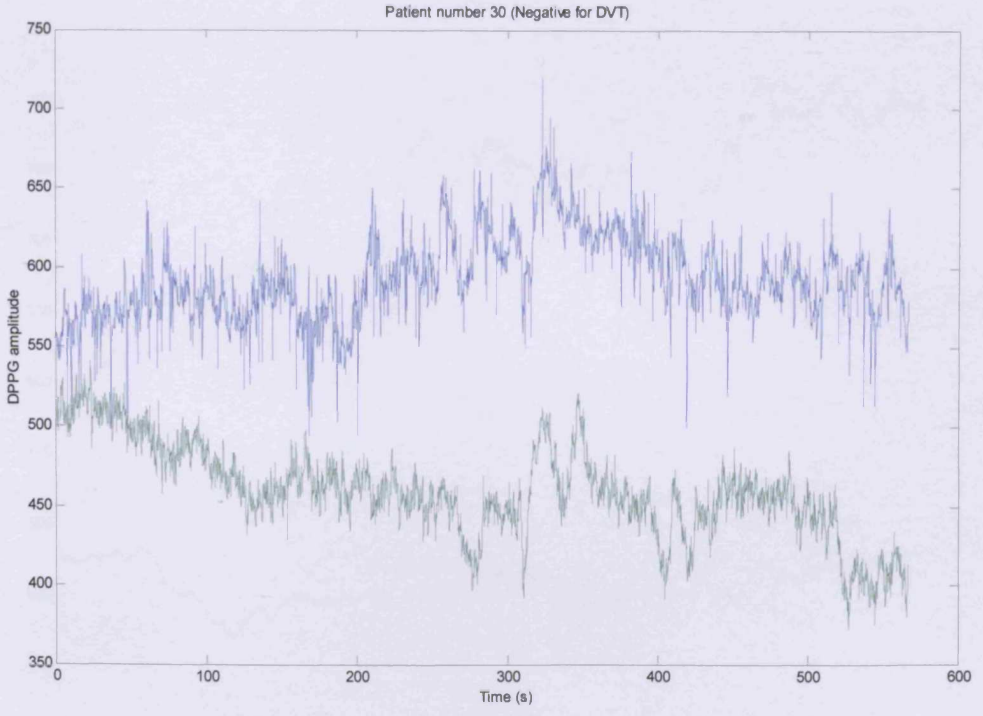
Patient number 30 (Negative for DVT)
DPPG amplitude
Time (s)
750
700
650
600
550
500
450
400
350
0
100
200
300
400
500
600

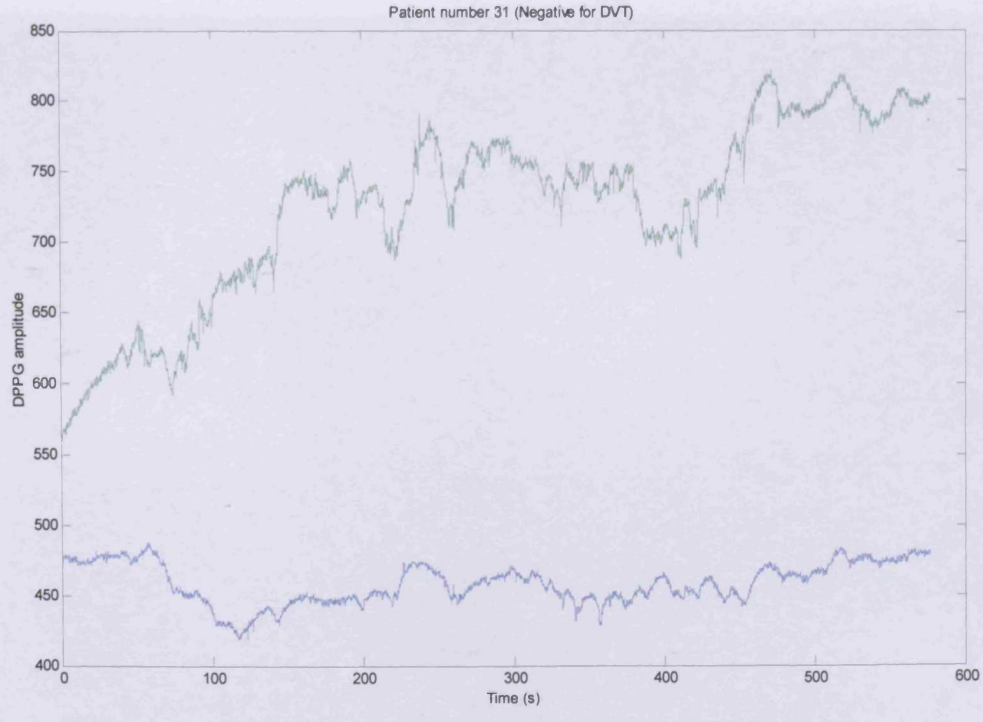
Patient number 31 (Negative for DVT)
DPPG amplitude
Time (s)
850
800
750
700
650
600
550
500
450
400
0
100
200
300
400
500
600

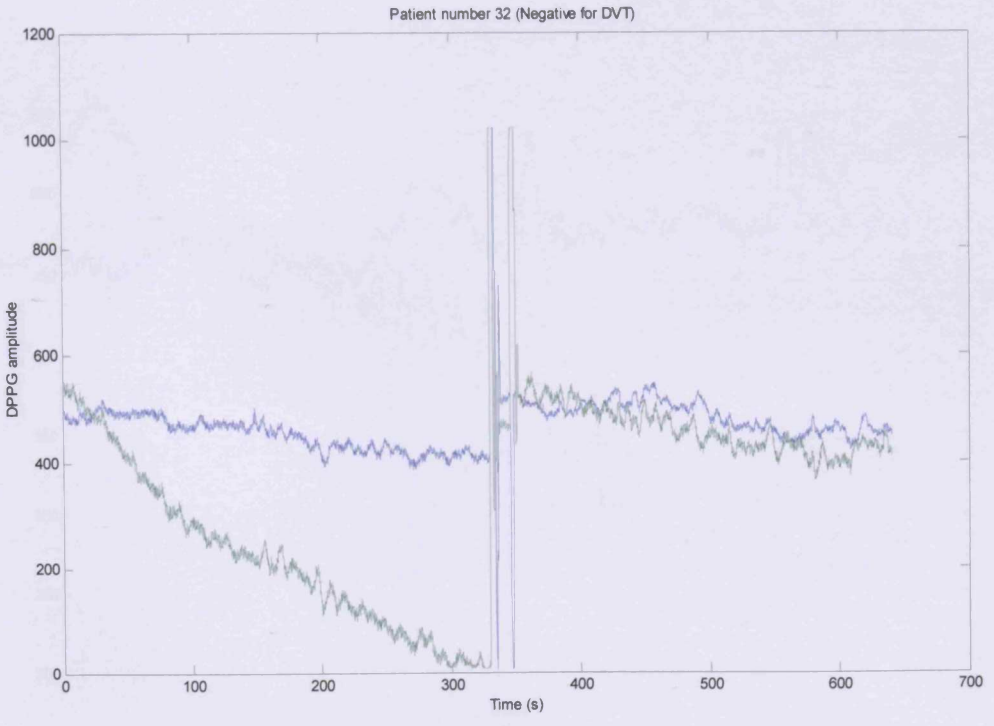
Patient number 32 (Negative for DVT)
DPPG amplitude
Time (s)
0
200
400
600
800
1000
1200
0
100
200
300
400
500
600
700

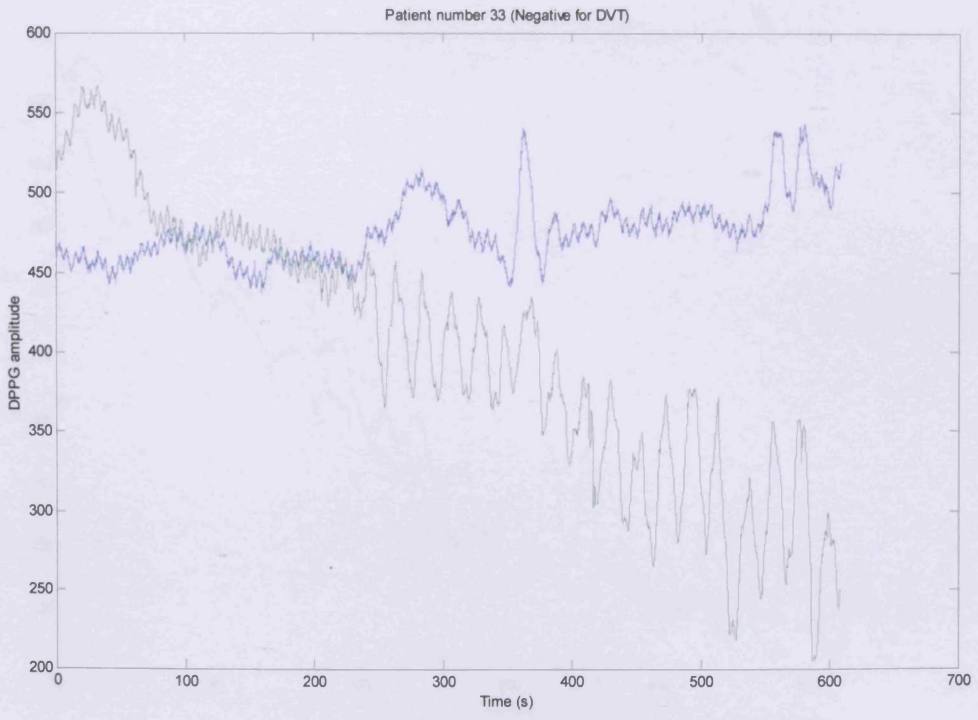
Patient number 33 (Negative for DVT)
DPPG amplitude
Time (s)
600
550
500
450
400
350
300
250
200
0
100
200
300
400
500
600
700

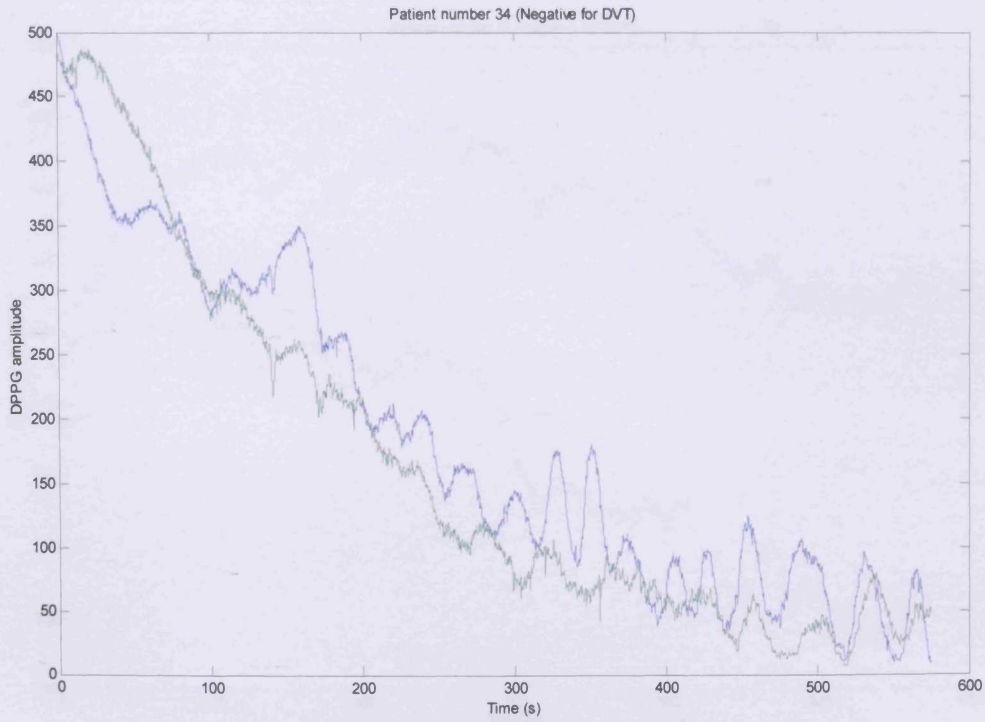
Patient number 34 (Negative for DVT)
DPPG amplitude
Time (s)
0
50
100
150
200
250
300
350
400
450
500
0
100
200
300
400
500
600

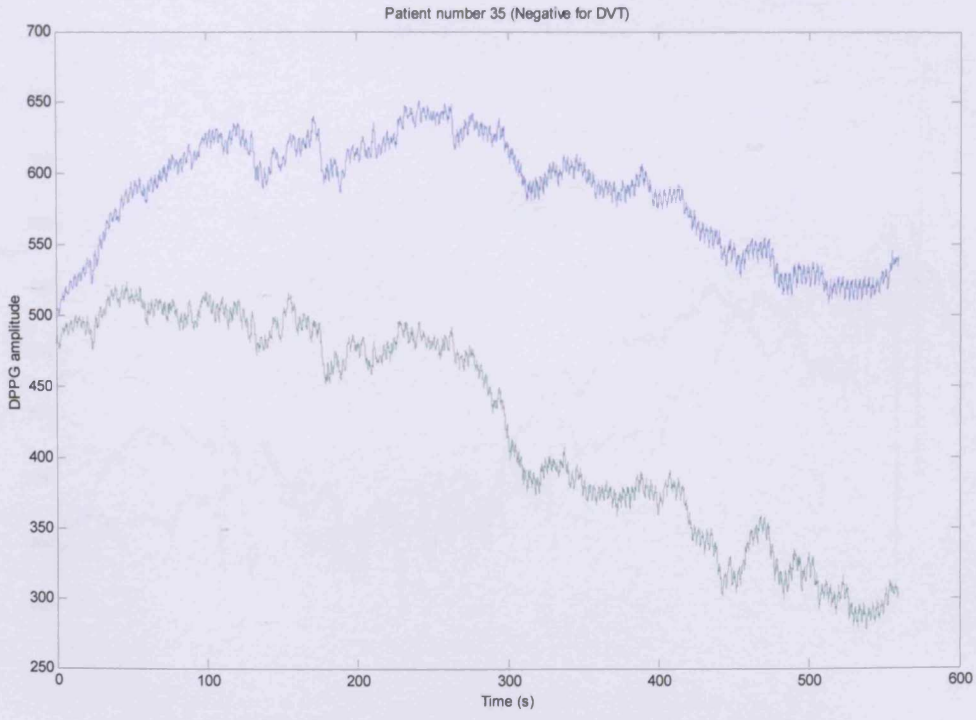
Patient number 35 (Negative for DVT)
DPPG amplitude
Time (s)
700
650
600
550
500
450
400
350
300
250
0
100
200
300
400
500
600

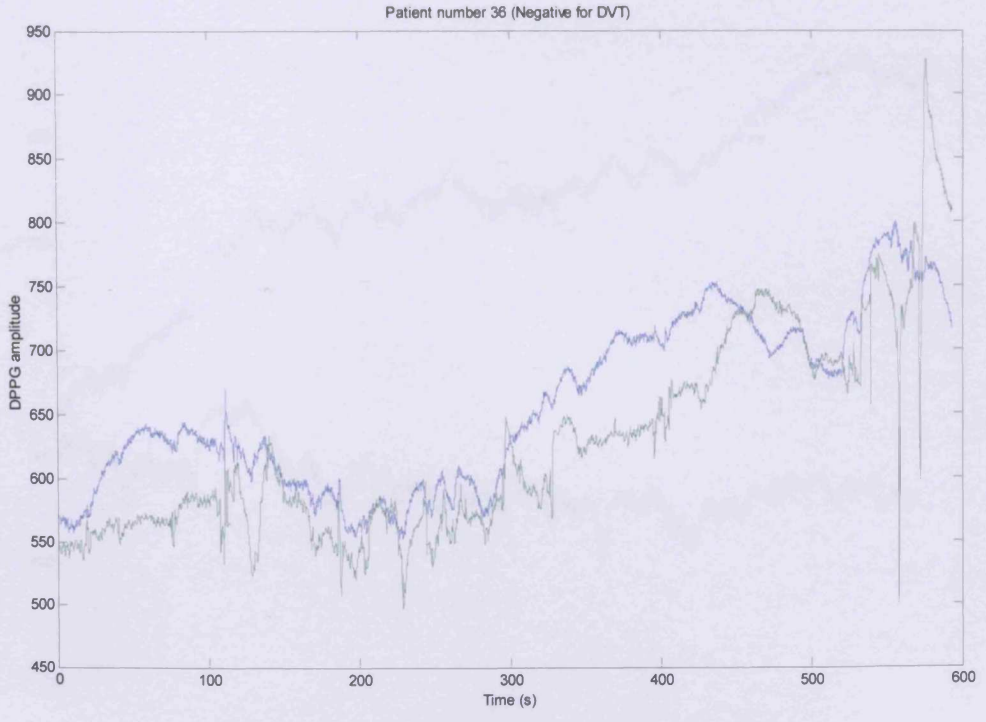
Patient number 36 (Negative for DVT)
DPPG amplitude
Time (s)
950
900
850
800
750
700
650
600
550
500
450
0
100
200
300
400
500
600

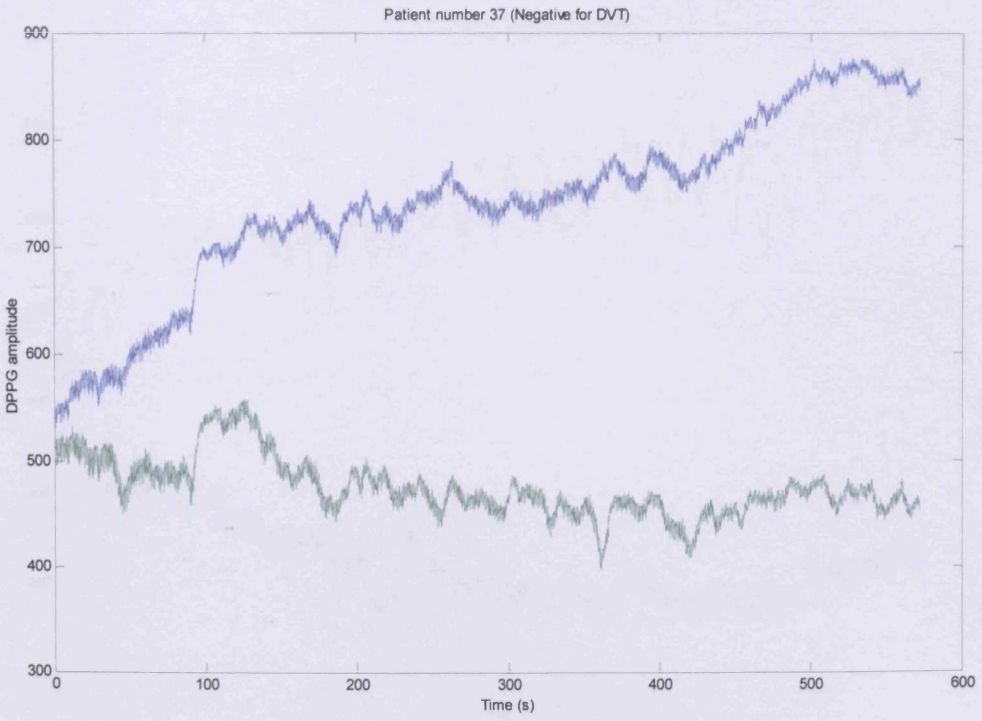
Patient number 37 (Negative for DVT)
DPPG amplitude
Time (s)
900
800
700
600
500
400
300
0
100
200
300
400
500
600

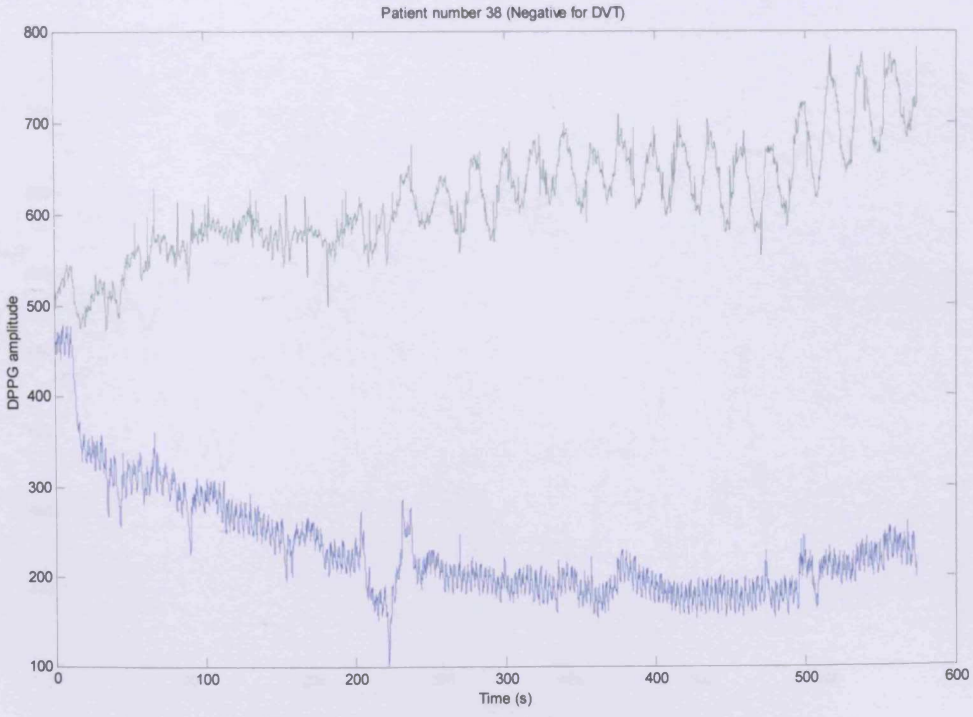
Patient number 38 (Negative for DVT)
DPPG amplitude
Time (s)
800
700
600
500
400
300
200
100
0
100
200
300
400
500
600

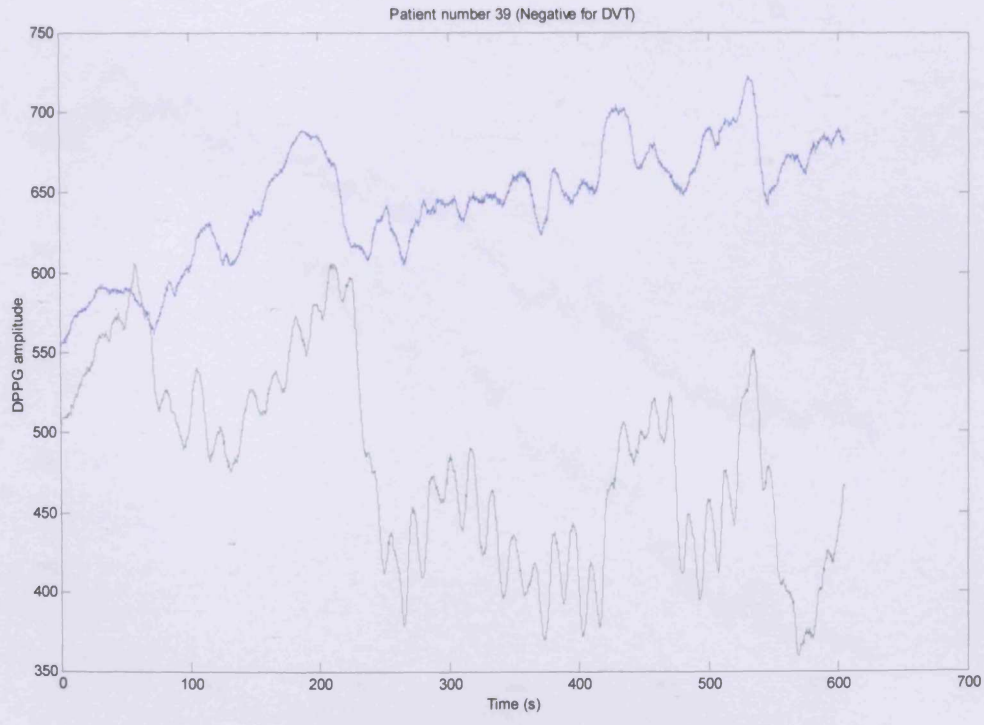
Patient number 39 (Negative for DVT)
DPPG amplitude
Time (s)
750
700
650
600
550
500
450
400
350
0
100
200
300
400
500
600
700

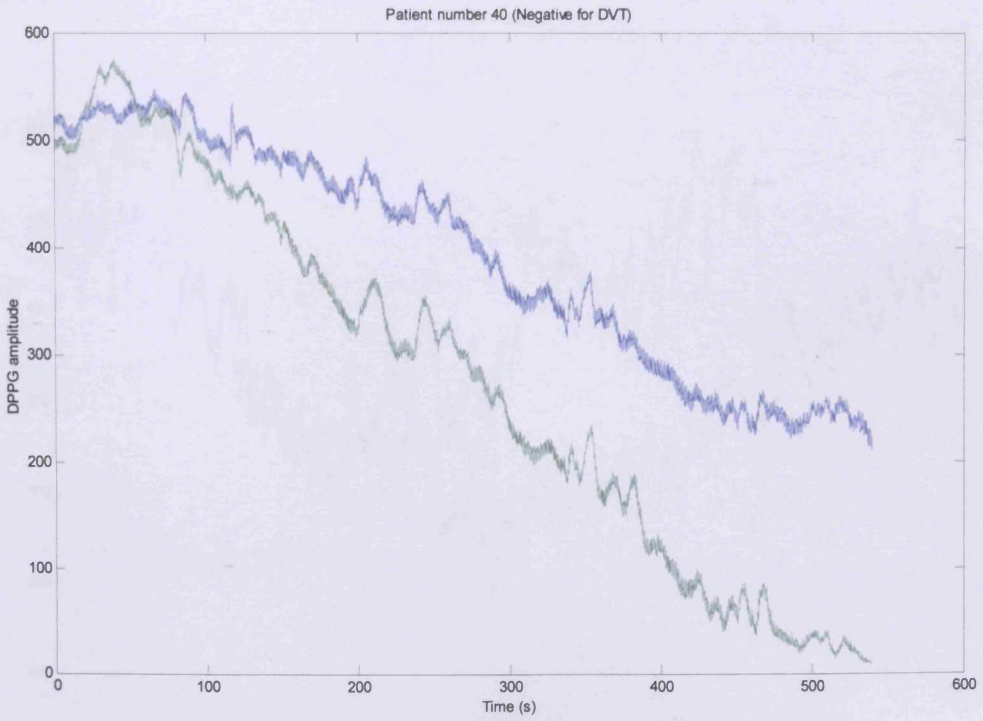
Patient number 40 (Negative for DVT)
DPPG amplitude
Time (s)
0
100
200
300
400
500
600

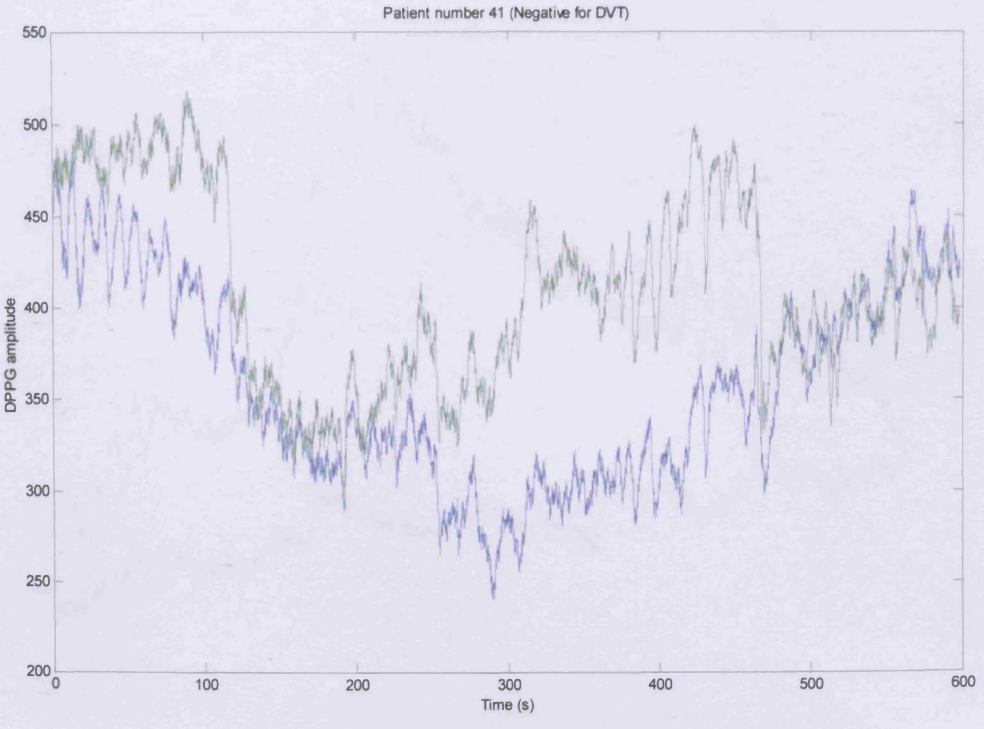
Patient number 41 (Negative for DVT)
DPPG amplitude
Time (s)
550
500
450
400
350
300
250
200
0
100
200
300
400
500
600

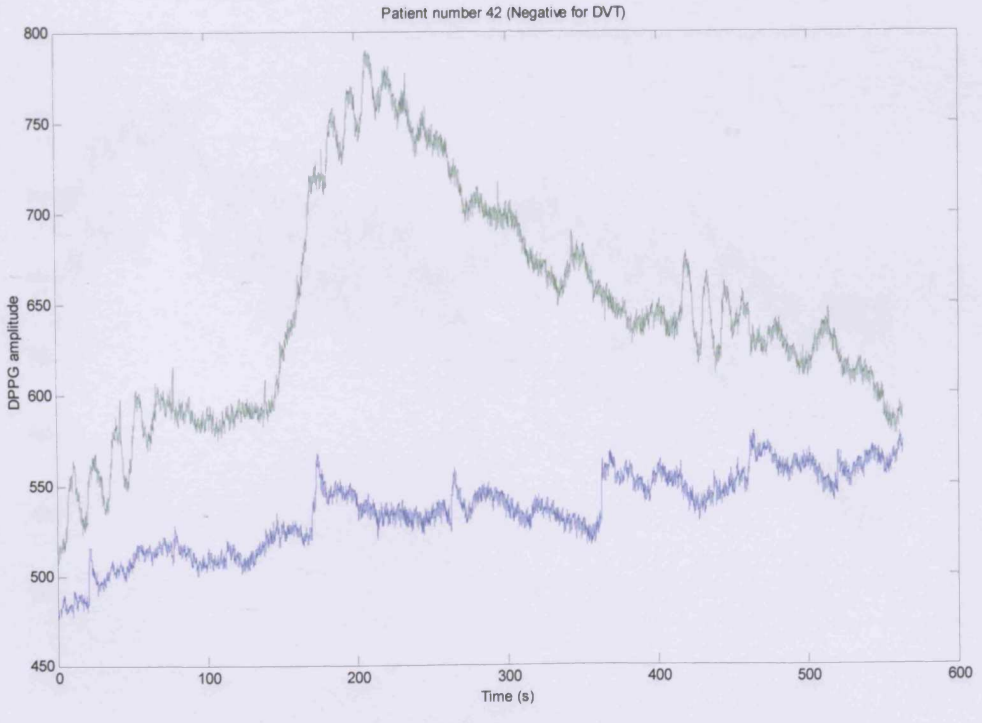
Patient number 42 (Negative for DVT)
DPPG amplitude
Time (s)
800
750
700
650
600
550
500
450
0
100
200
300
400
500
600

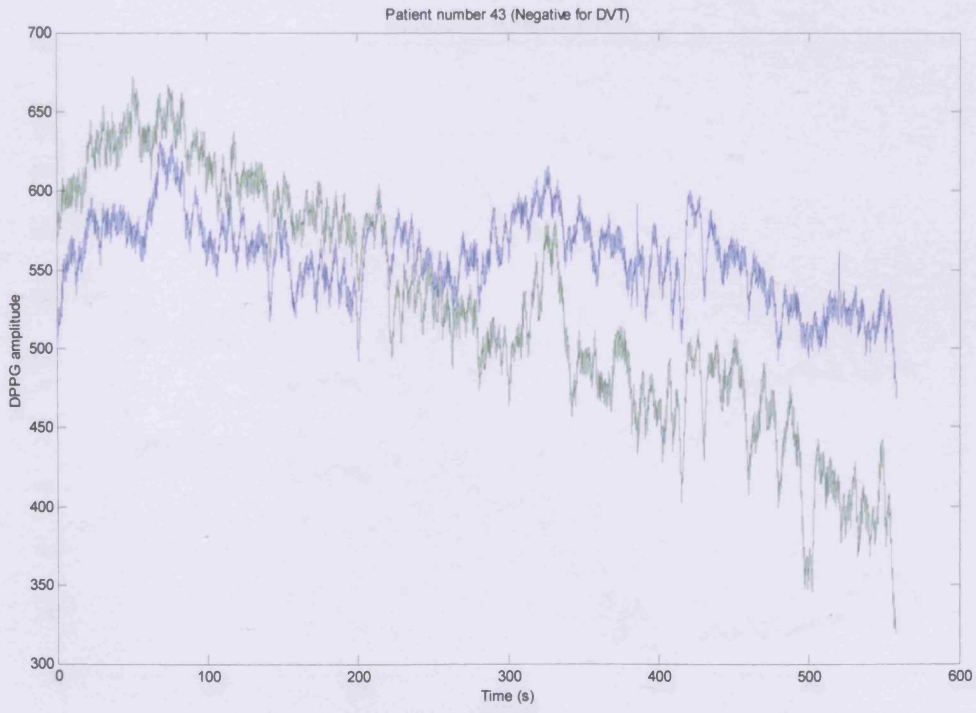
Patient number 43 (Negative for DVT)
DPPG amplitude
Time (s)
700
650
600
550
500
450
400
350
300
0
100
200
300
400
500
600

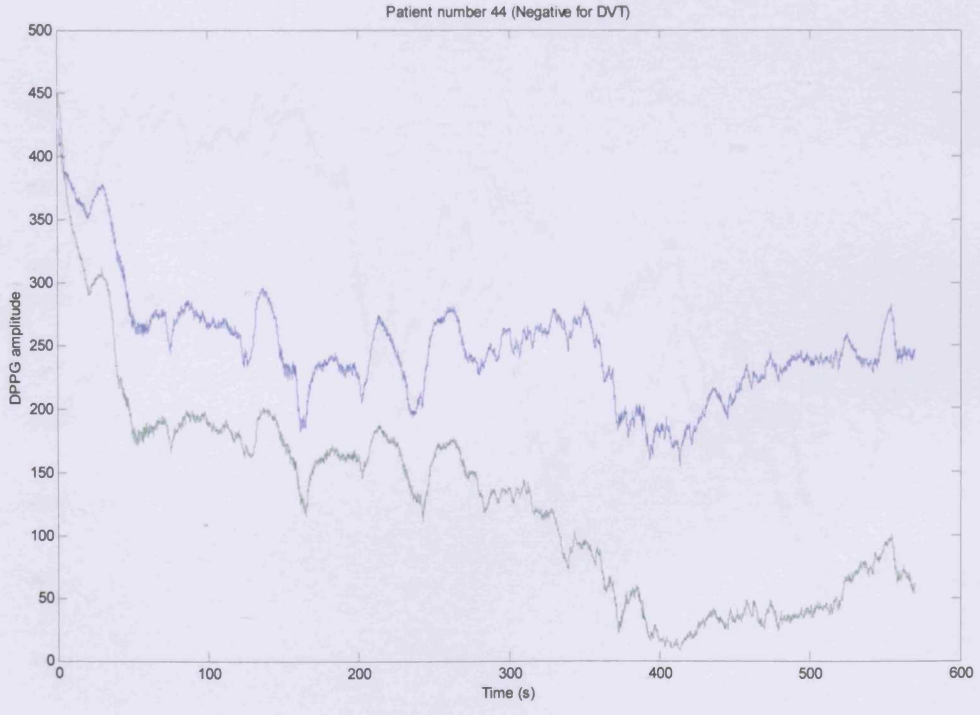
Patient number 44 (Negative for DVT)
DPPG amplitude
Time (s)
0
50
100
150
200
250
300
350
400
450
500
0
100
200
300
400
500
600

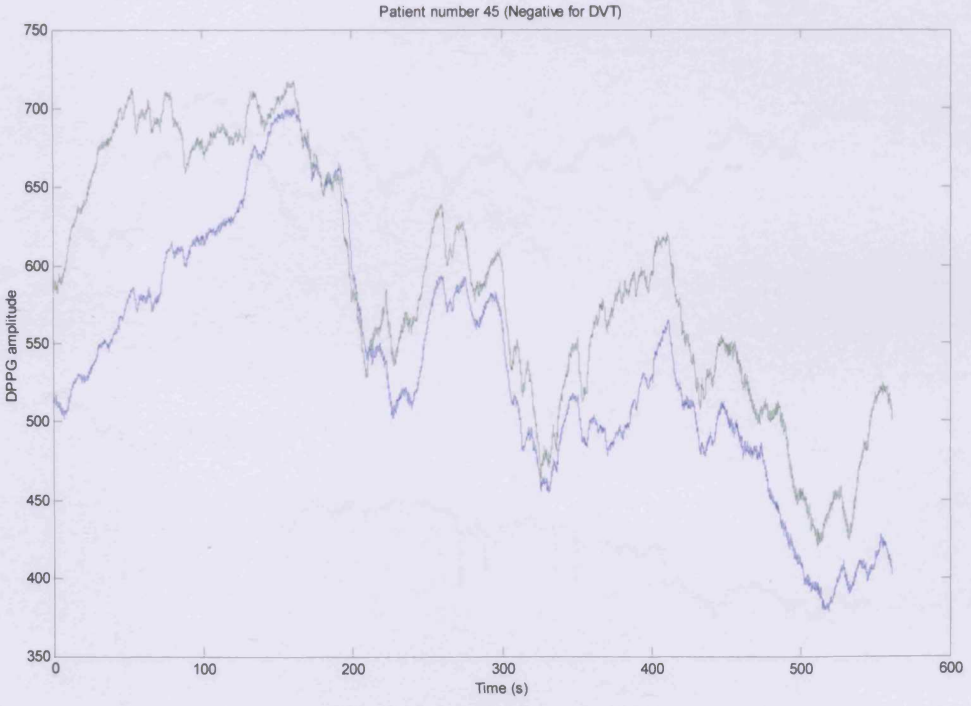
Patient number 45 (Negative for DVT)
DPPG amplitude
Time (s)
750
700
650
600
550
500
450
400
350
0
100
200
300
400
500
600

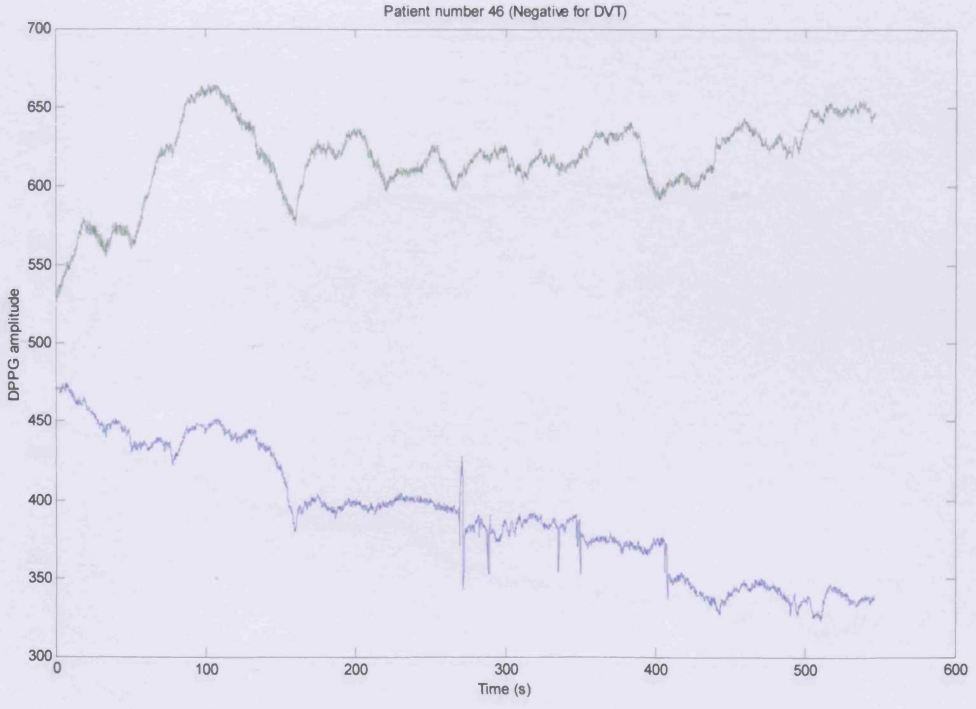
Patient number 46 (Negative for DVT)
DPPG amplitude
Time (s)
700
650
600
550
500
450
400
350
300
0
100
200
300
400
500
600

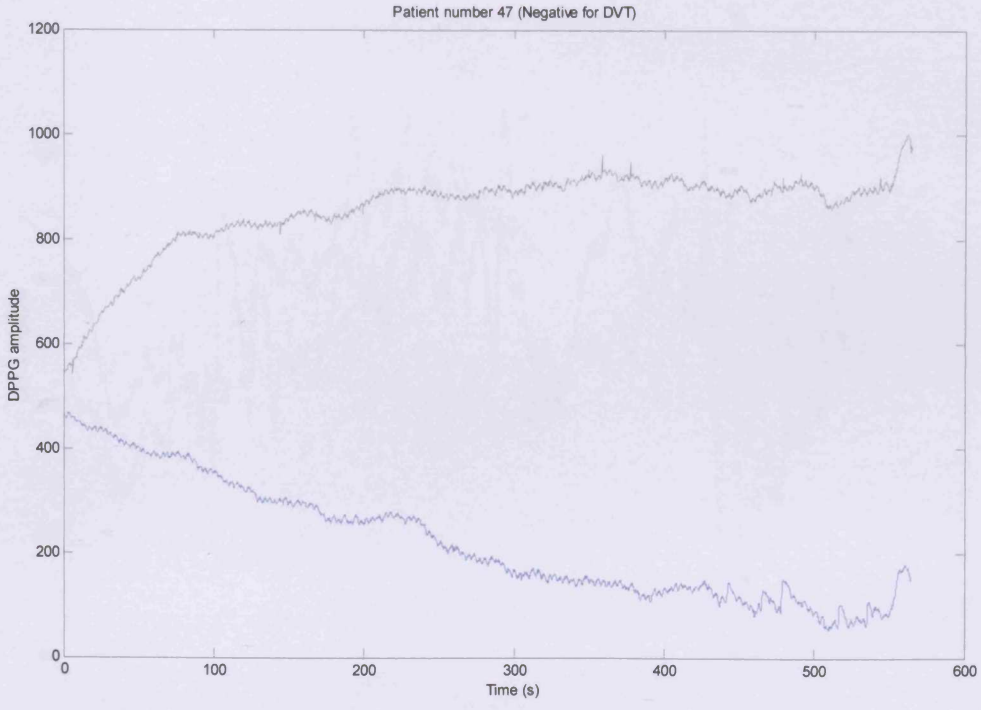
Patient number 47 (Negative for DVT)
DPPG amplitude
Time (s)
0
200
400
600
800
1000
1200
0
100
200
300
400
500
600

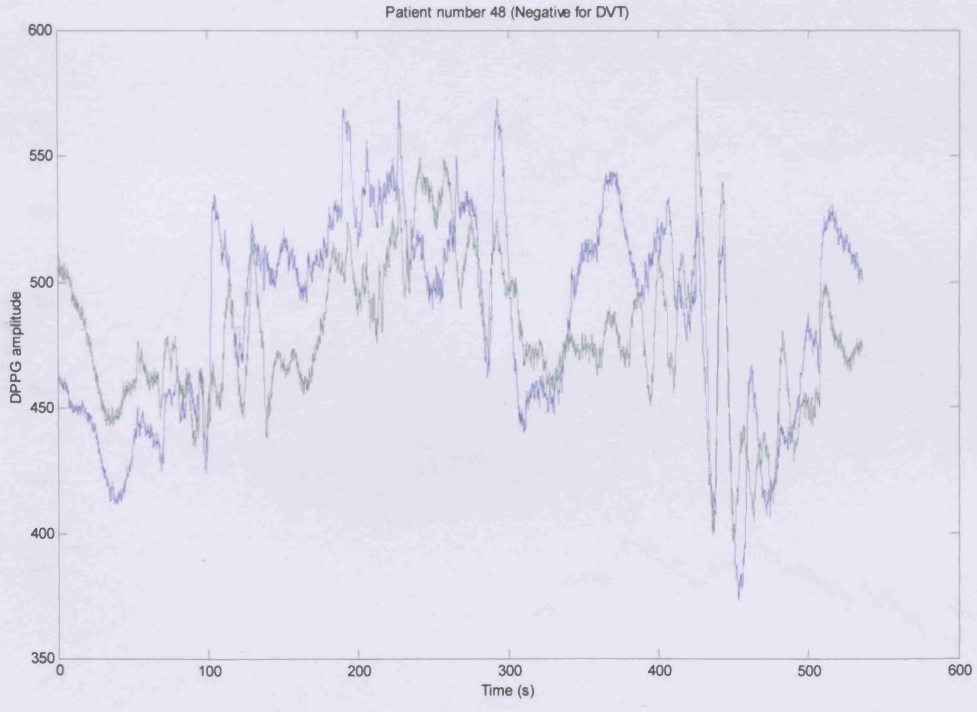
Patient number 48 (Negative for DVT)
DPPG amplitude
Time (s)
600
550
500
450
400
350
0
100
200
300
400
500
600

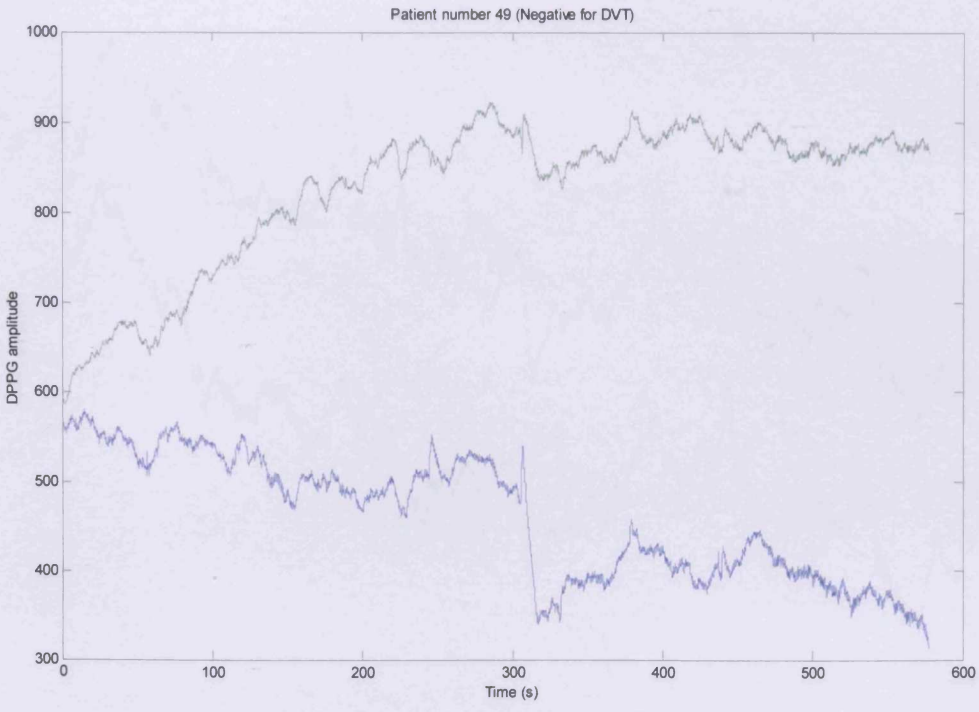
Patient number 49 (Negative for DVT)
DPPG amplitude
Time (s)
1000
900
800
700
600
500
400
300
0
100
200
300
400
500
600

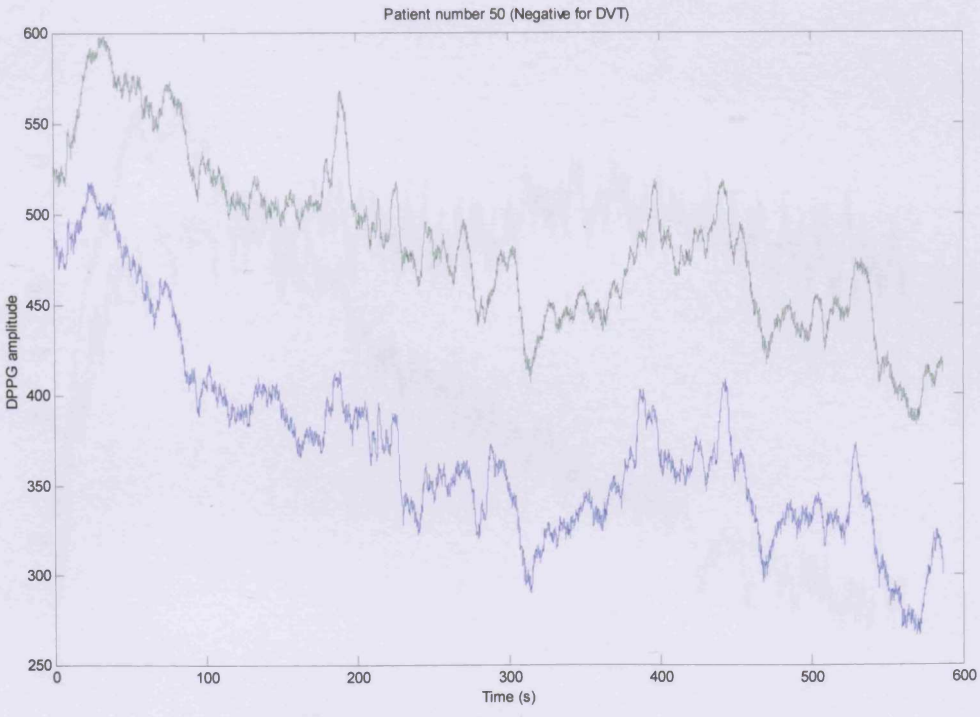
Patient number 50 (Negative for DVT)
DPPG amplitude
Time (s)
600
550
500
450
400
350
300
250
0
100
200
300
400
500
600

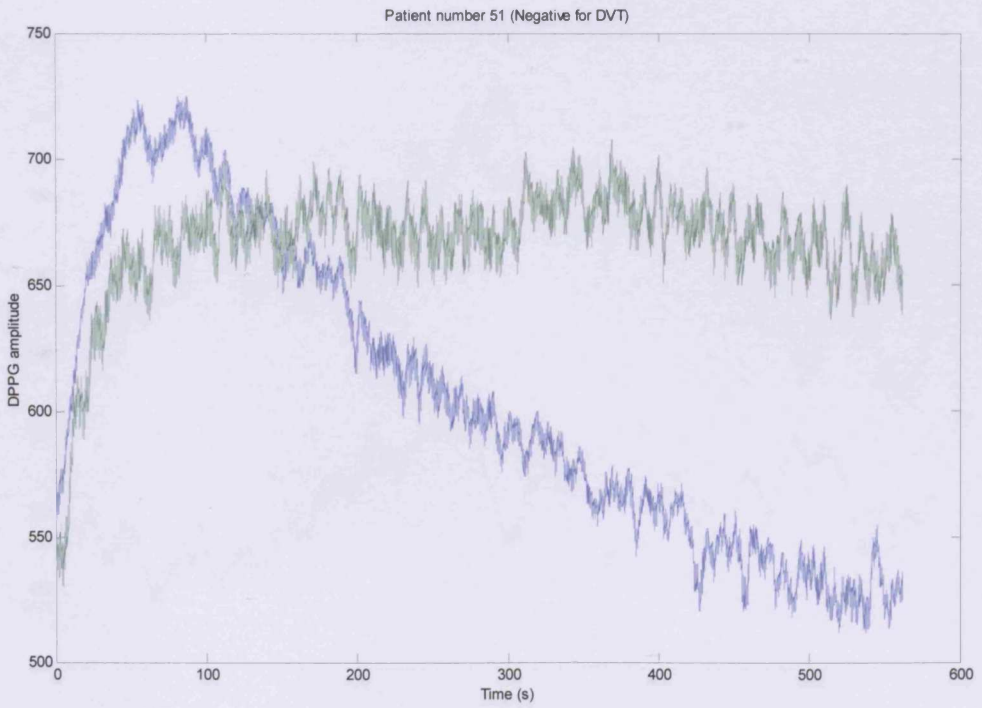
Patient number 51 (Negative for DVT)
DPPG amplitude
Time (s)
750
700
650
600
550
500
0
100
200
300
400
500
600

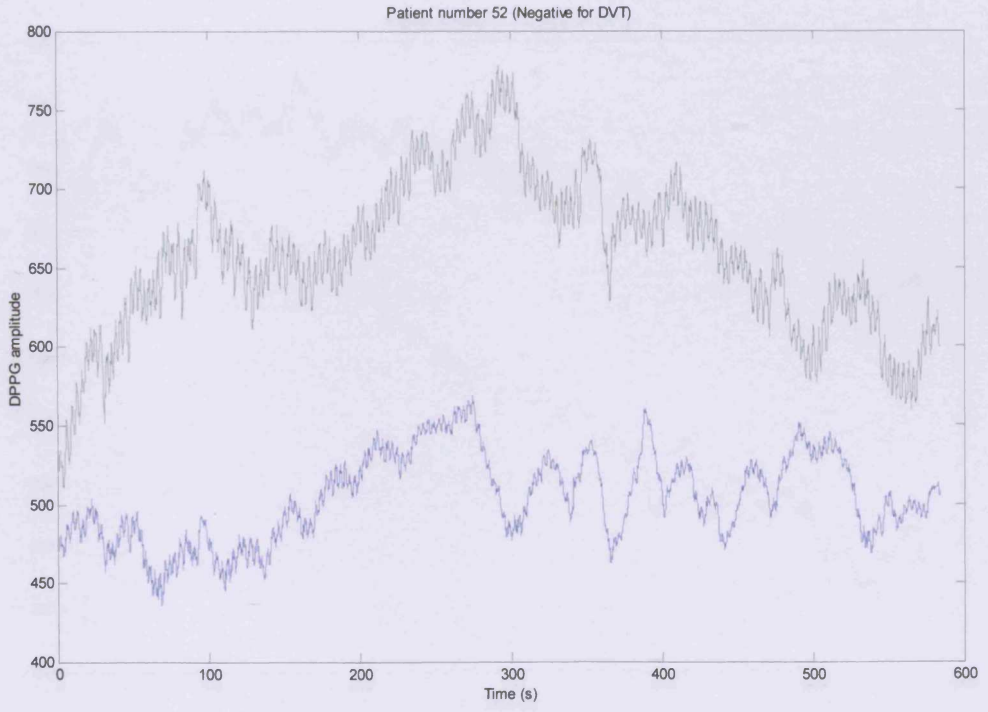
Patient number 52 (Negative for DVT)
DPPG amplitude
Time (s)
800
750
700
650
600
550
500
450
400
0
100
200
300
400
500
600

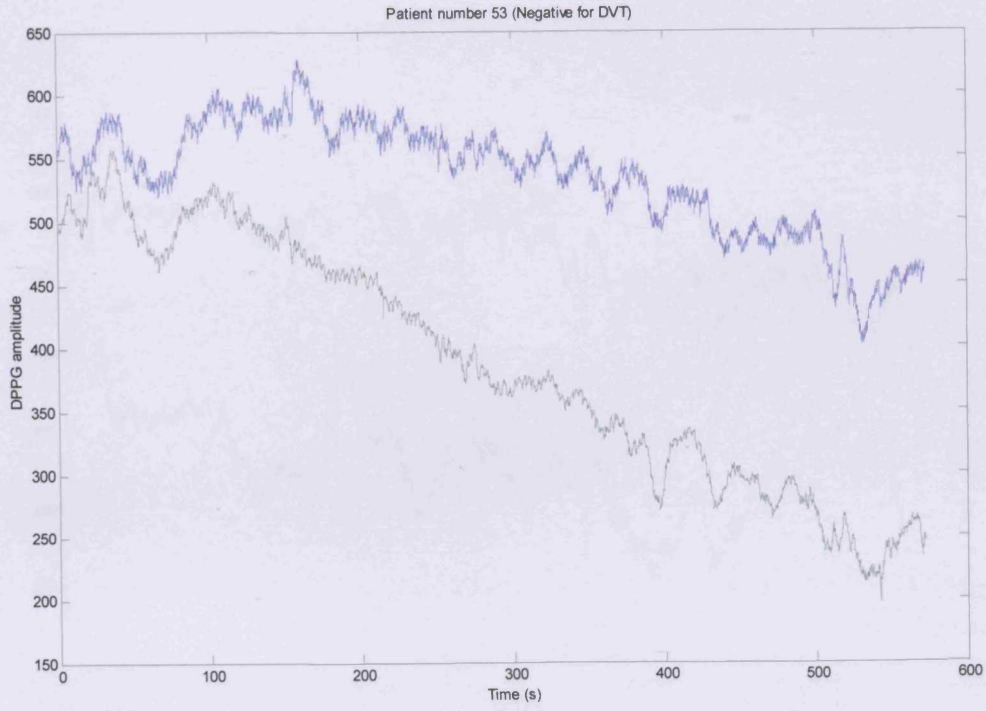
Patient number 53 (Negative for DVT)
DPPG amplitude
Time (s)
650
600
550
500
450
400
350
300
250
200
150
0
100
200
300
400
500
600

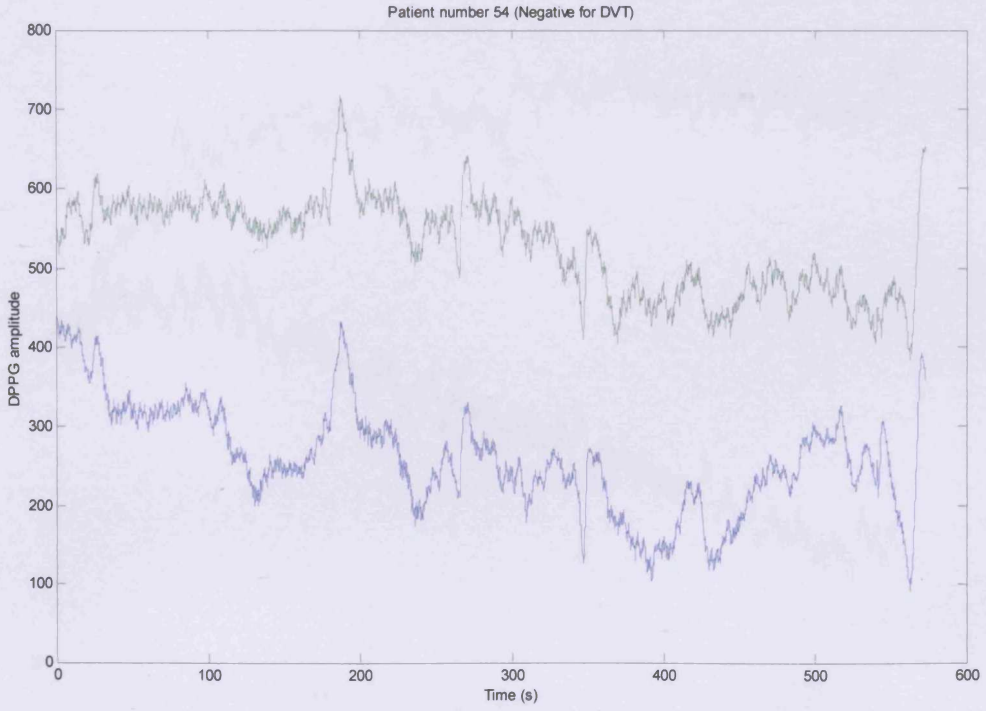
Patient number 54 (Negative for DVT)
DPPG amplitude
Time (s)
800
700
600
500
400
300
200
100
0
0
100
200
300
400
500
600

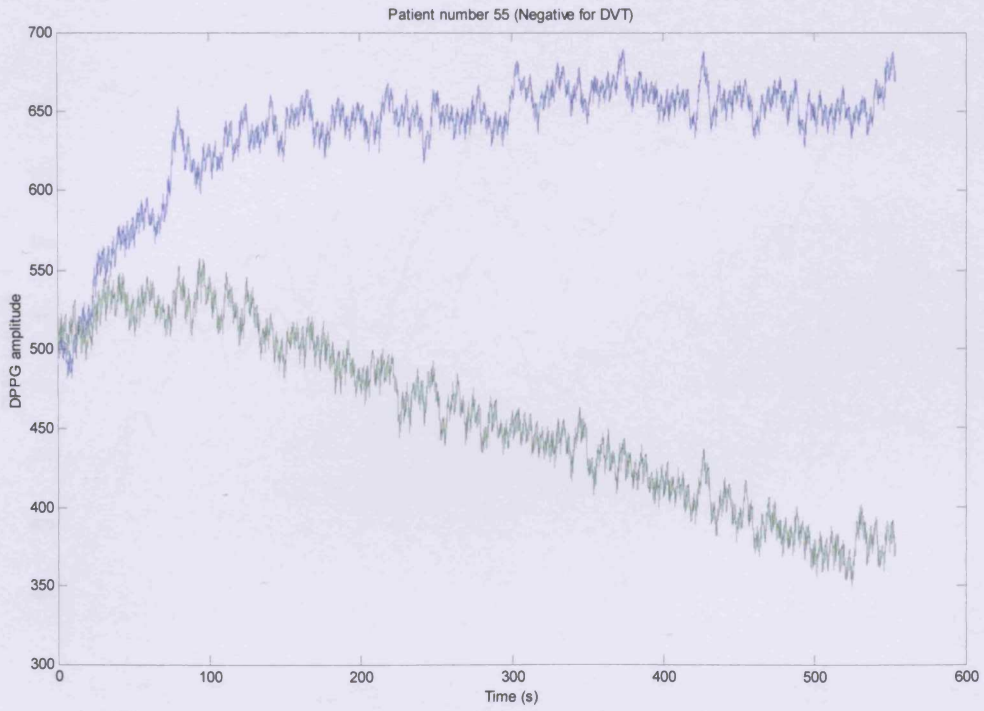
Patient number 55 (Negative for DVT)
DPPG amplitude
Time (s)
700
650
600
550
500
450
400
350
300
0
100
200
300
400
500
600

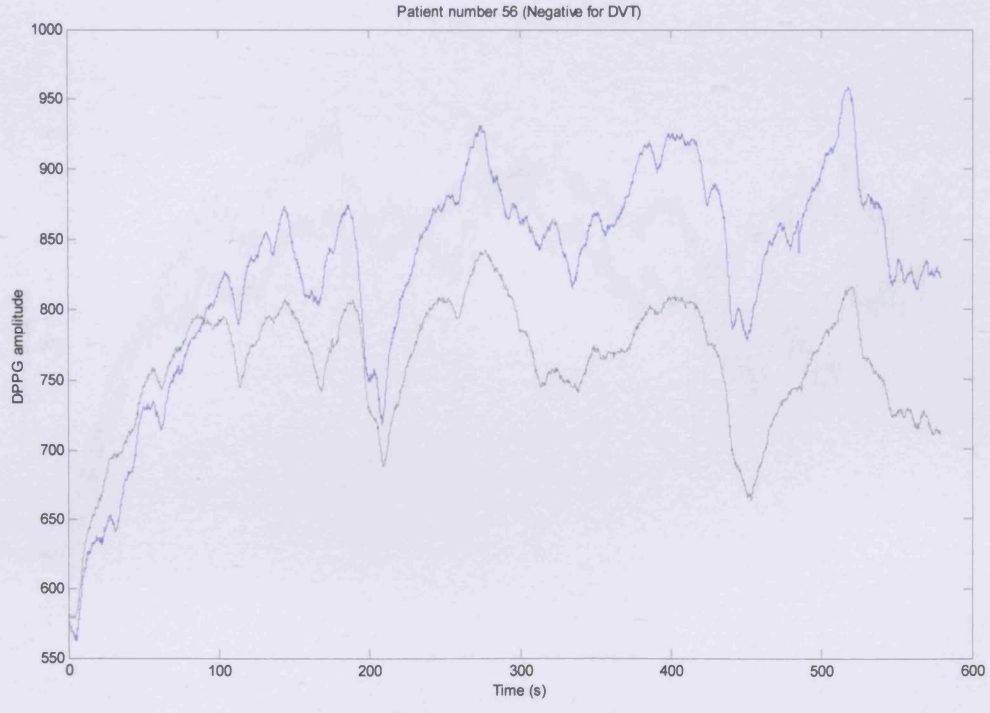
Patient number 56 (Negative for DVT)
DPPG amplitude
Time (s)
1000
950
900
850
800
750
700
650
600
550
0
100
200
300
400
500
600

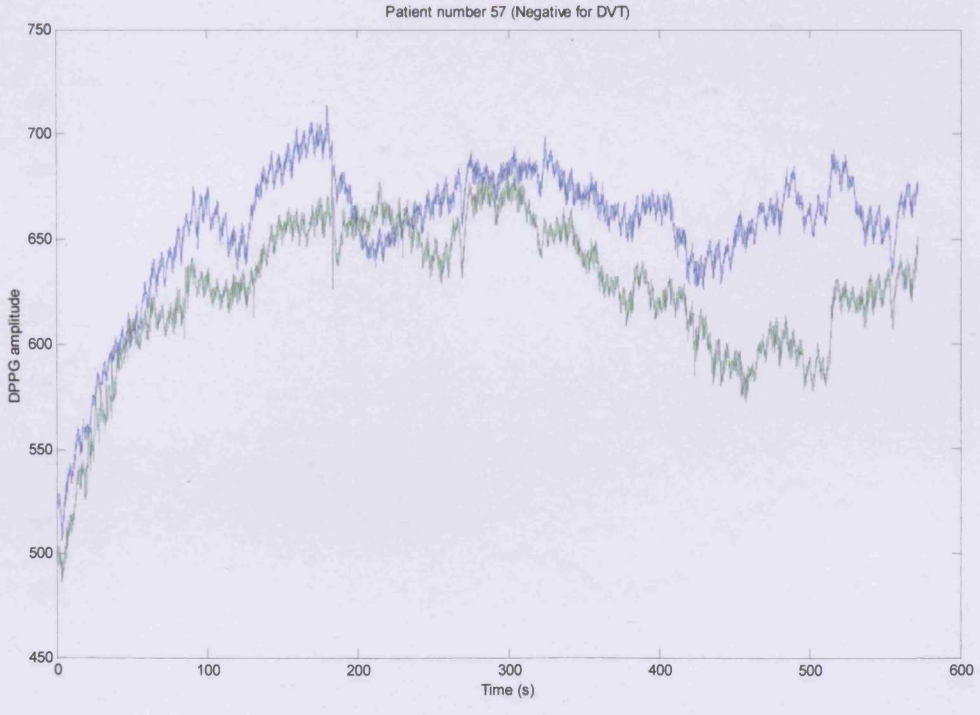
Patient number 57 (Negative for DVT)
DPPG amplitude
Time (s)
750
700
650
600
550
500
450
0
100
200
300
400
500
600

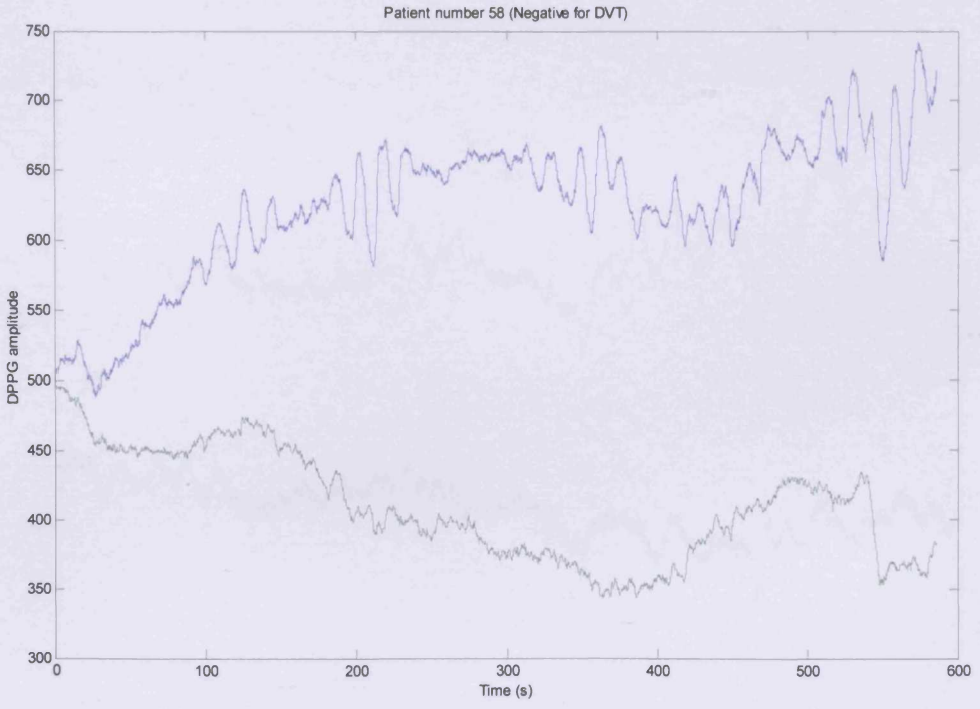
Patient number 58 (Negative for DVT)
DPPG amplitude
Time (s)
750
700
650
600
550
500
450
400
350
300
0
100
200
300
400
500
600

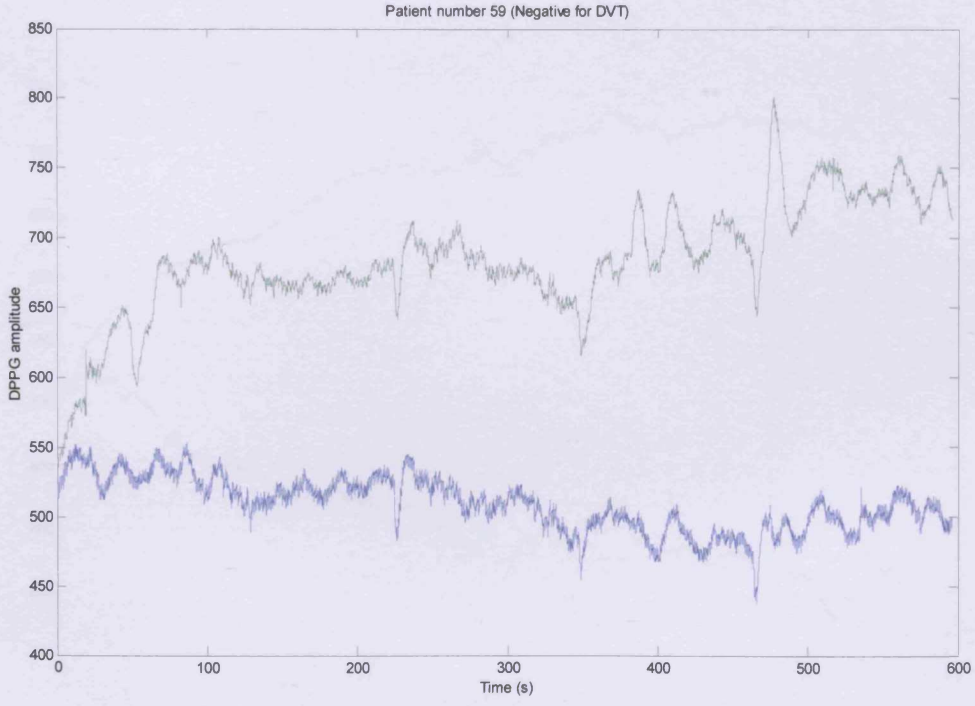
Patient number 59 (Negative for DVT)
DPPG amplitude
Time (s)
850
800
750
700
650
600
550
500
450
400
0
100
200
300
400
500
600

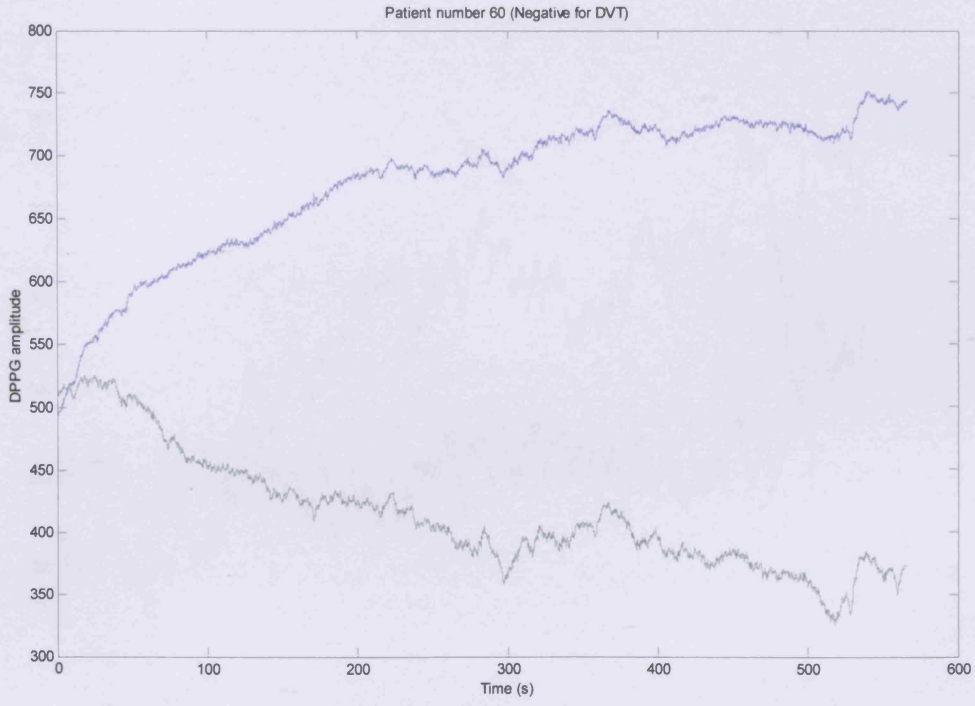
Patient number 60 (Negative for DVT)
DPPG amplitude
Time (s)
800
750
700
650
600
550
500
450
400
350
300
0
100
200
300
400
500
600

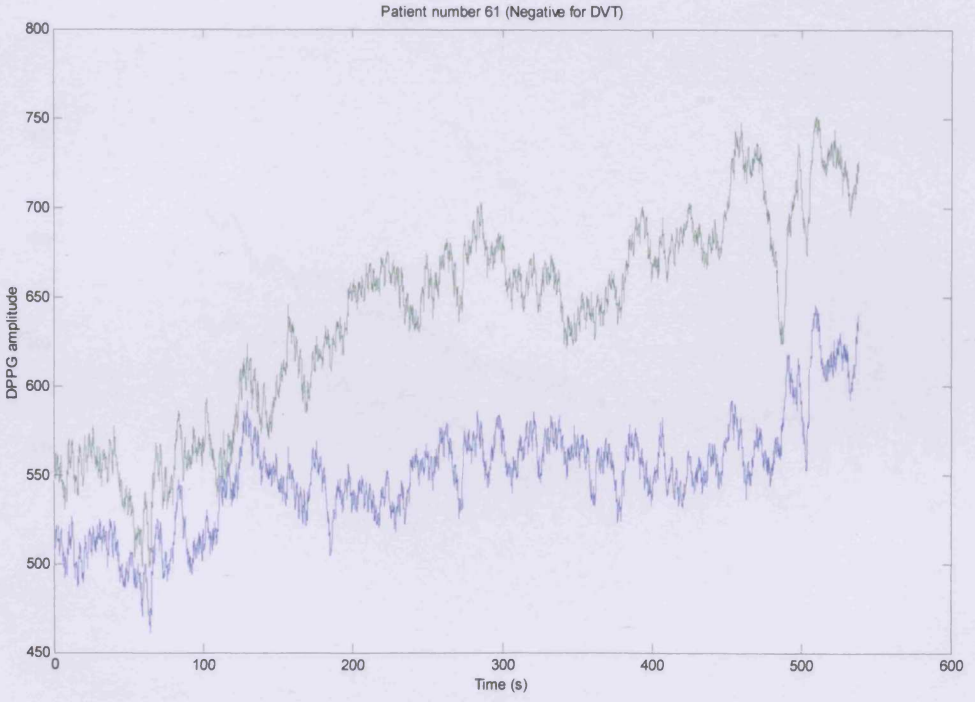
Patient number 61 (Negative for DVT)
DPPG amplitude
Time (s)
800
750
700
650
600
550
500
450
0
100
200
300
400
500
600

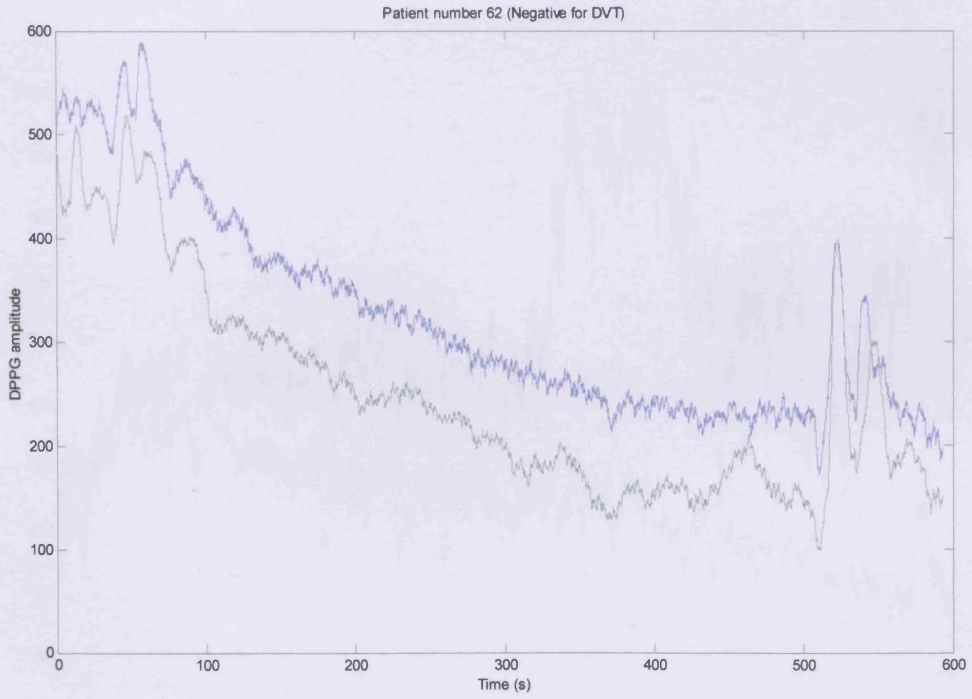
Patient number 62 (Negative for DVT)
DPPG amplitude
Time (s)
0
100
200
300
400
500
600

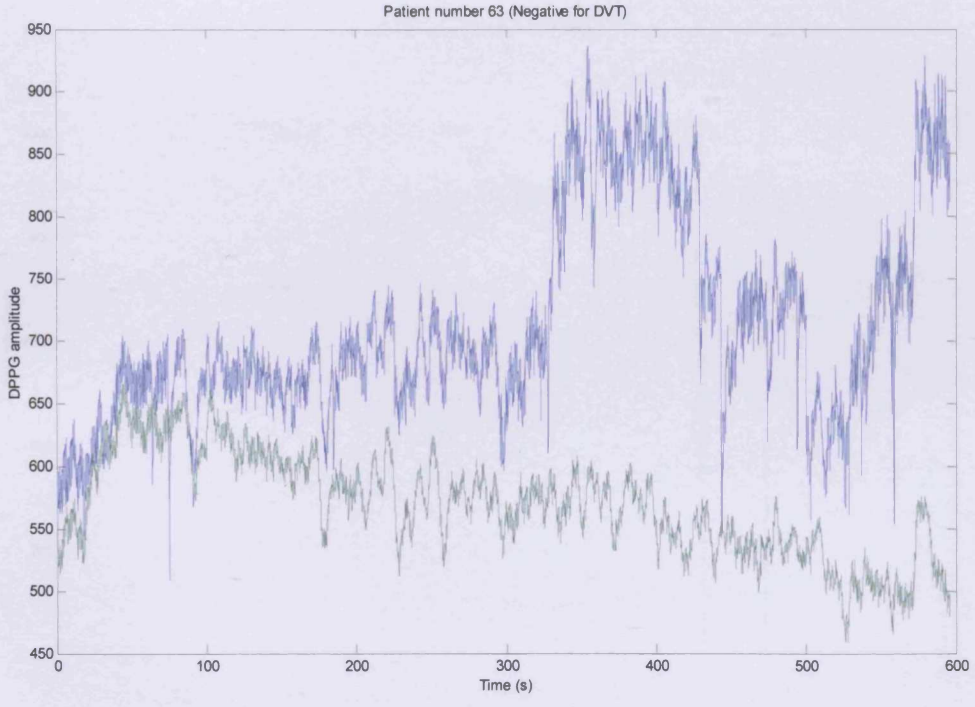
Patient number 63 (Negative for DVT)
DPPG amplitude
Time (s)
950
900
850
800
750
700
650
600
550
500
450
0
100
200
300
400
500
600

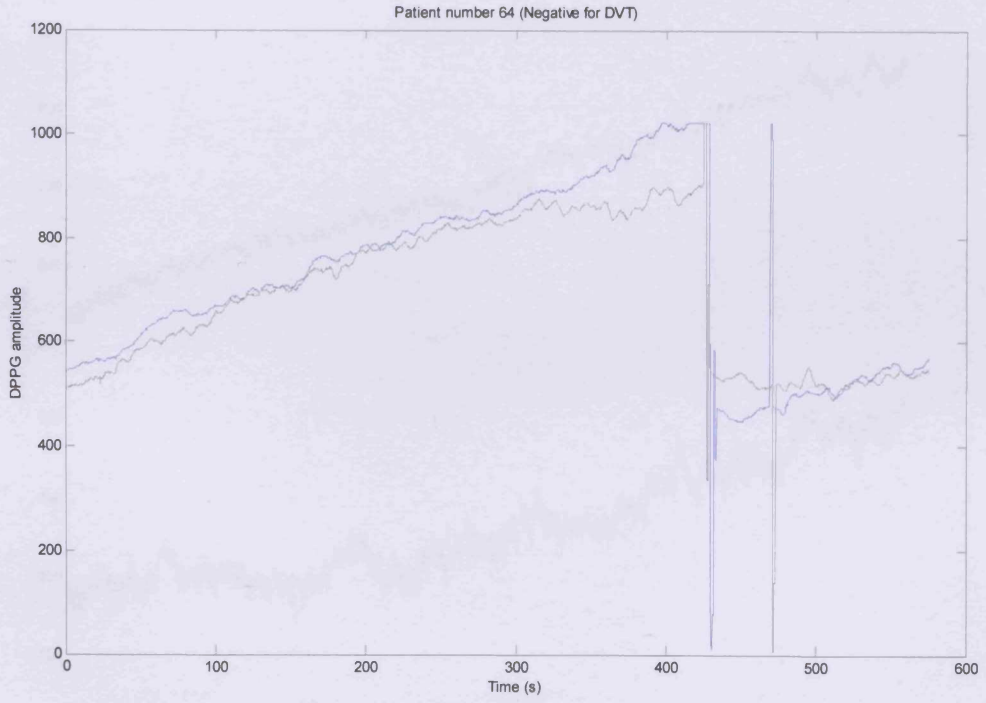
Patient number 64 (Negative for DVT)
DPPG amplitude
Time (s)
0
200
400
600
800
1000
1200
0
100
200
300
400
500
600

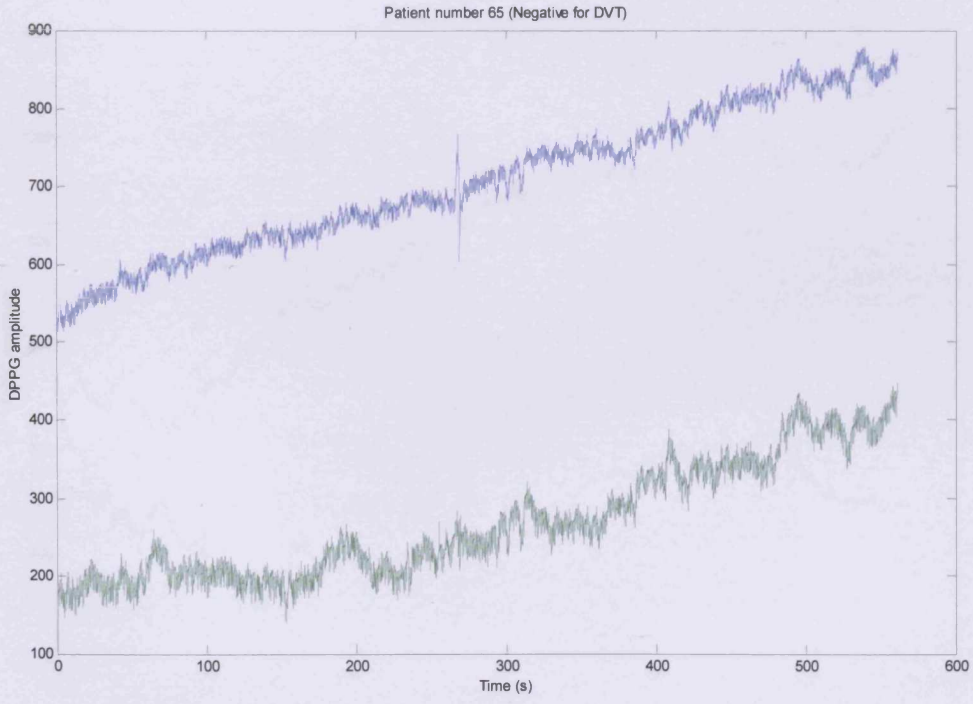
Patient number 65 (Negative for DVT)
DPPG amplitude
Time (s)
900
800
700
600
500
400
300
200
100
0
100
200
300
400
500
600

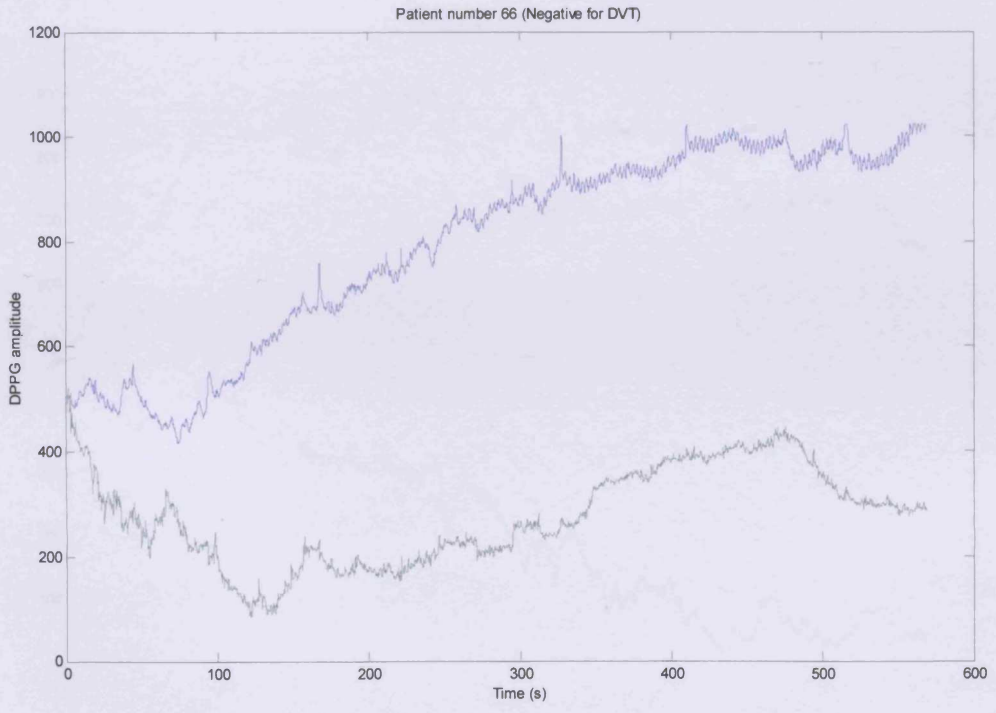
Patient number 66 (Negative for DVT)
DPPG amplitude
Time (s)
0
200
400
600
800
1000
1200
0
100
200
300
400
500
600

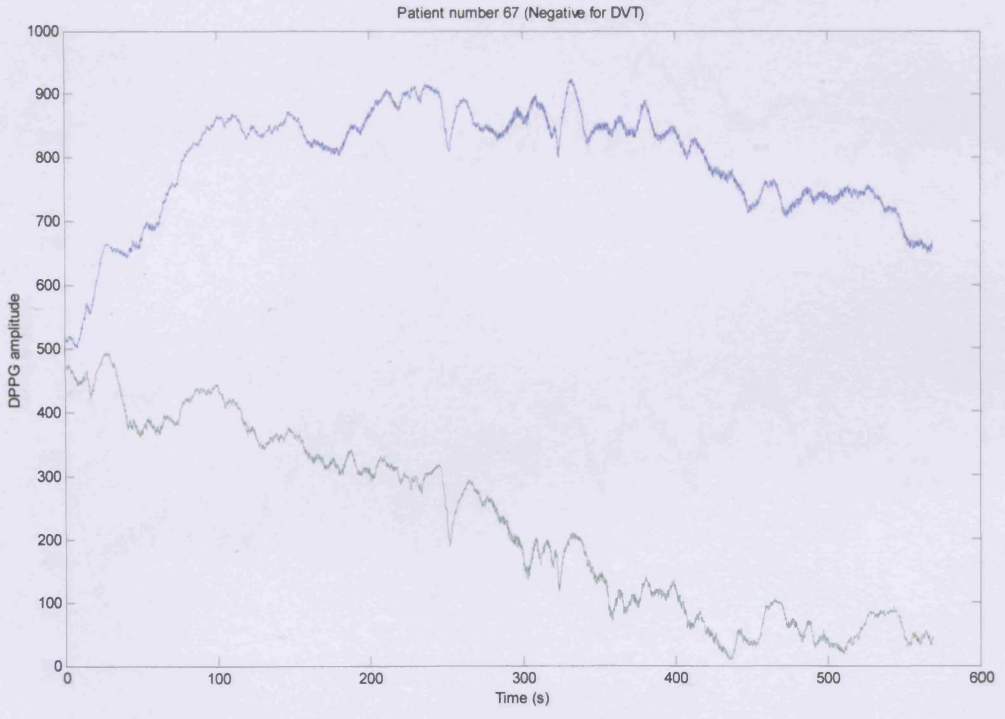
Patient number 67 (Negative for DVT)
DPPG amplitude
Time (s)
0
100
200
300
400
500
600
700
800
900
1000

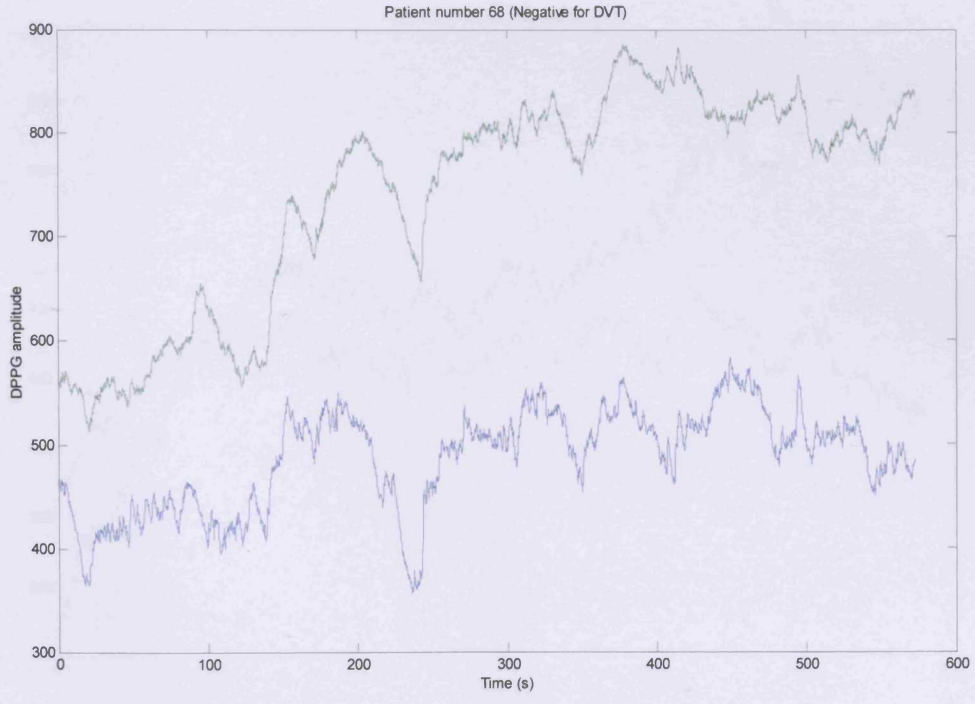
Patient number 68 (Negative for DVT)
DPPG amplitude
Time (s)
900
800
700
600
500
400
300
0
100
200
300
400
500
600

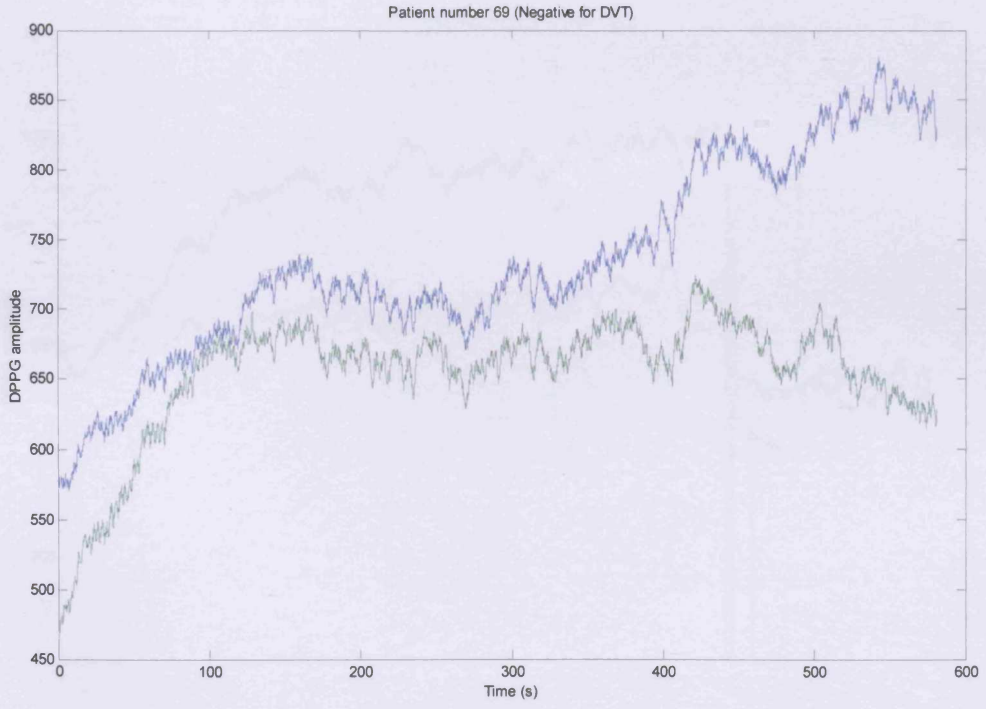
Patient number 69 (Negative for DVT)
DPPG amplitude
Time (s)
900
850
800
750
700
650
600
550
500
450
0
100
200
300
400
500
600

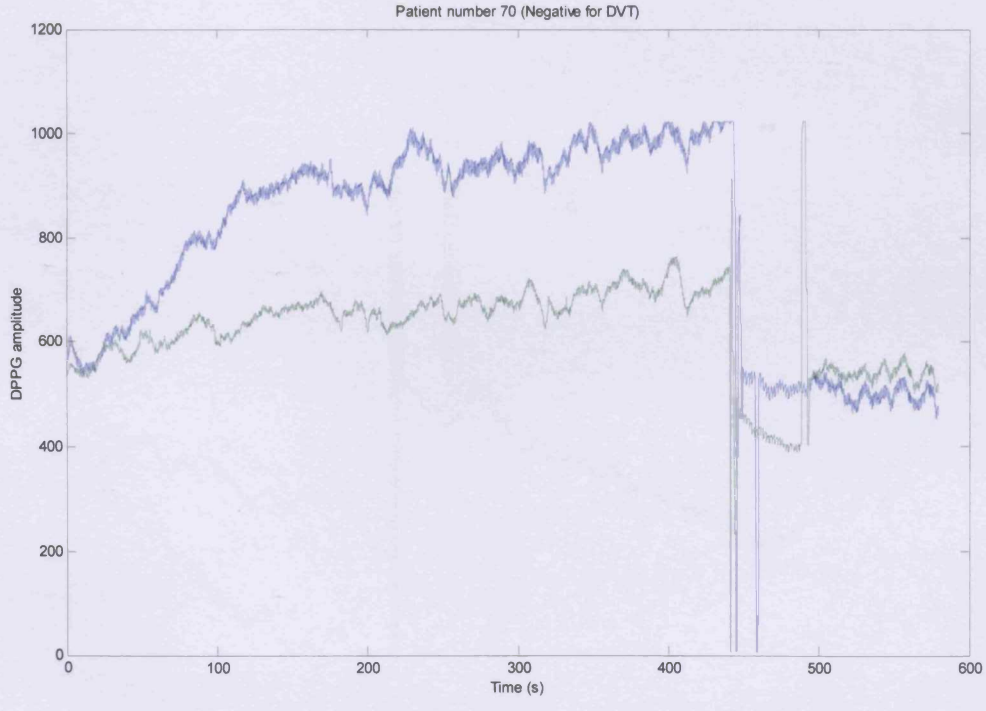
Patient number 70 (Negative for DVT)
DPPG amplitude
Time (s)
0
200
400
600
800
1000
1200
0
100
200
300
400
500
600

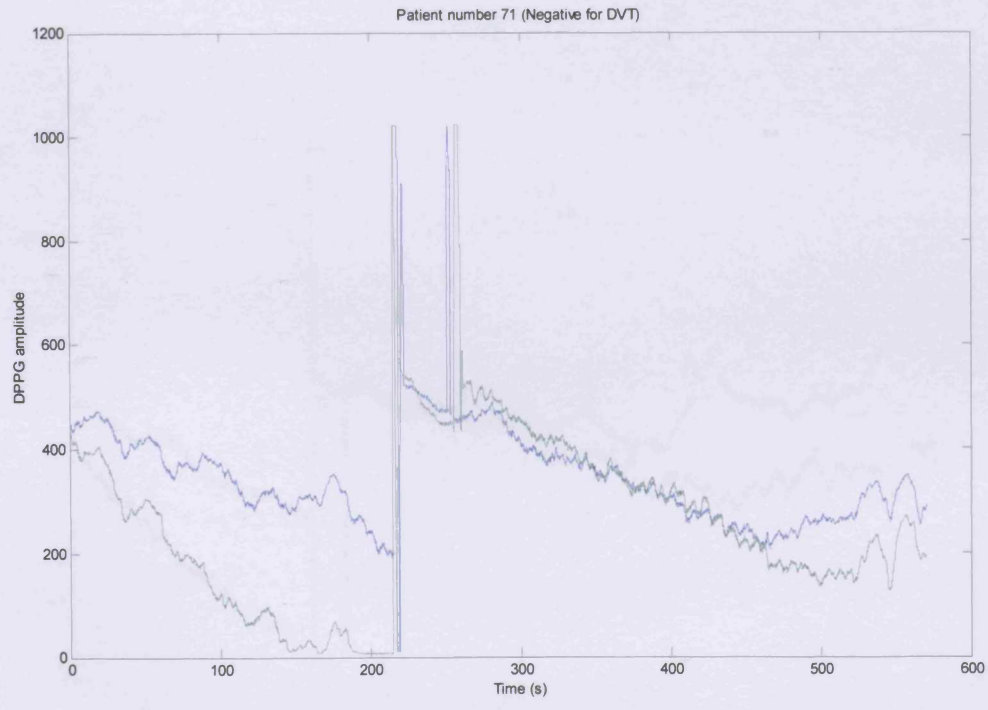
Patient number 71 (Negative for DVT)
DPPG amplitude
Time (s)
0
200
400
600
800
1000
1200
0
100
200
300
400
500
600

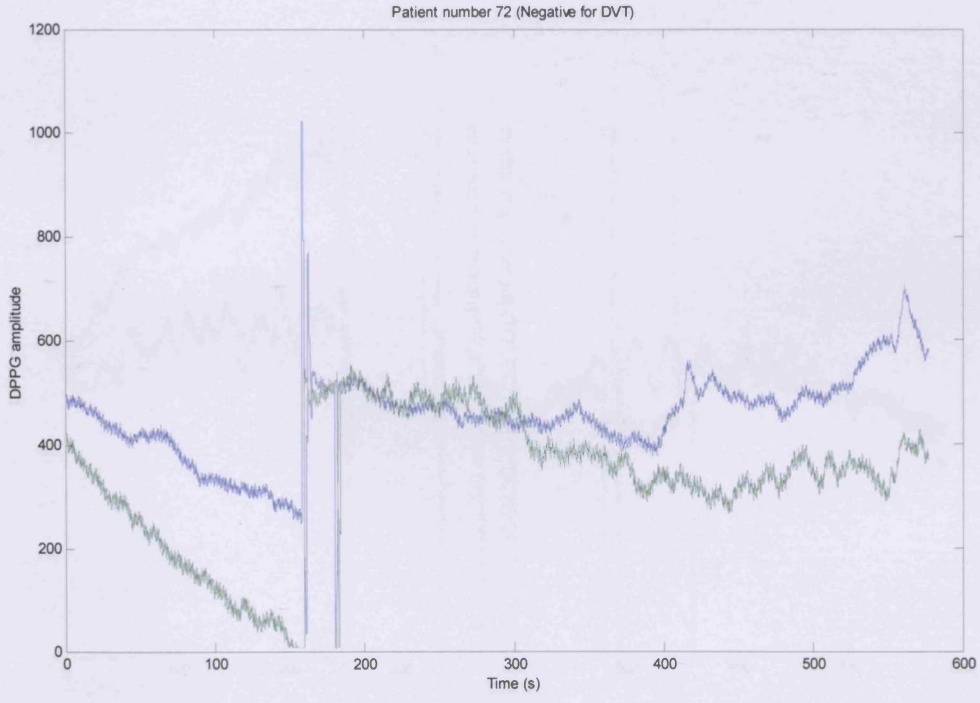
Patient number 72 (Negative for DVT)
DPPG amplitude
Time (s)
0
200
400
600
800
1000
1200
0
100
200
300
400
500
600

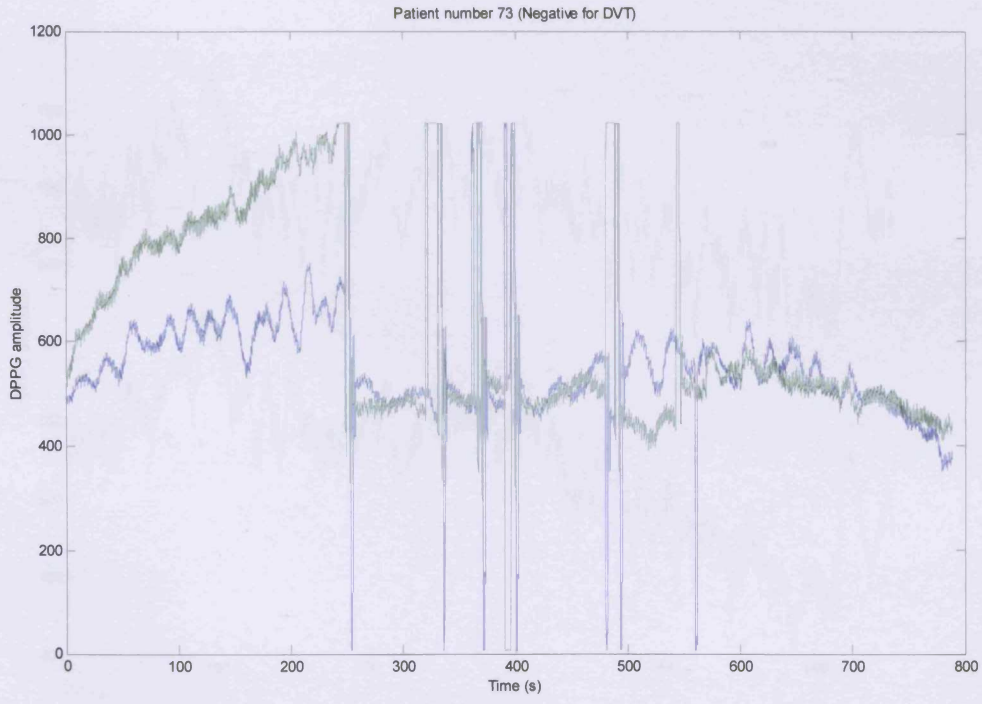
Patient number 73 (Negative for DVT)
DPPG amplitude
Time (s)
0
200
400
600
800
1000
1200
0
100
200
300
400
500
600
700
800

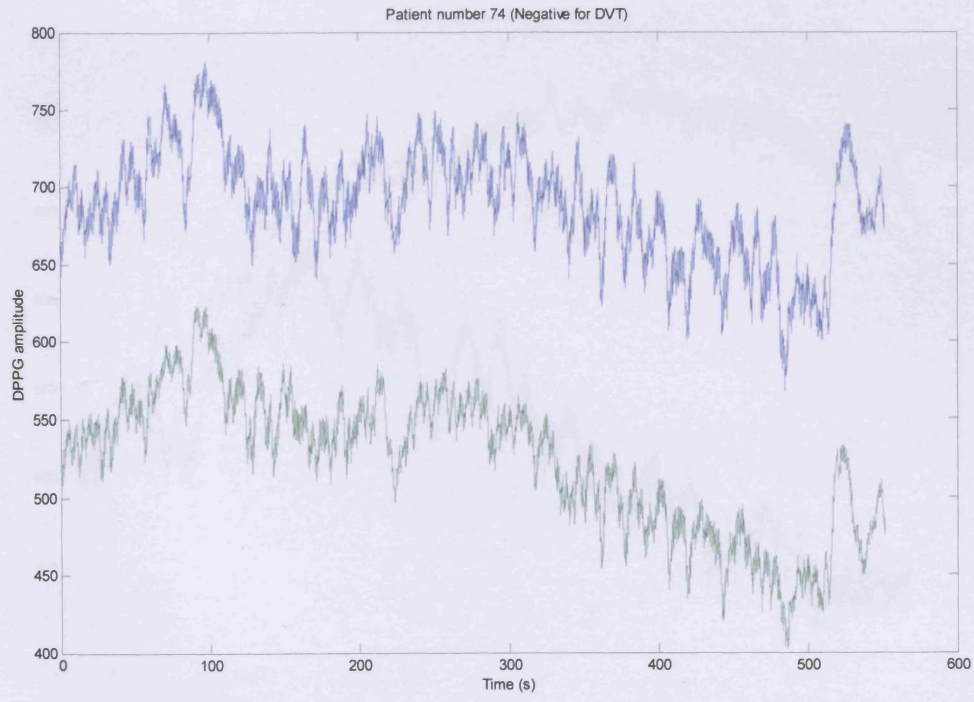
Patient number 74 (Negative for DVT)
DPPG amplitude
Time (s)
800
750
700
650
600
550
500
450
400
0
100
200
300
400
500
600

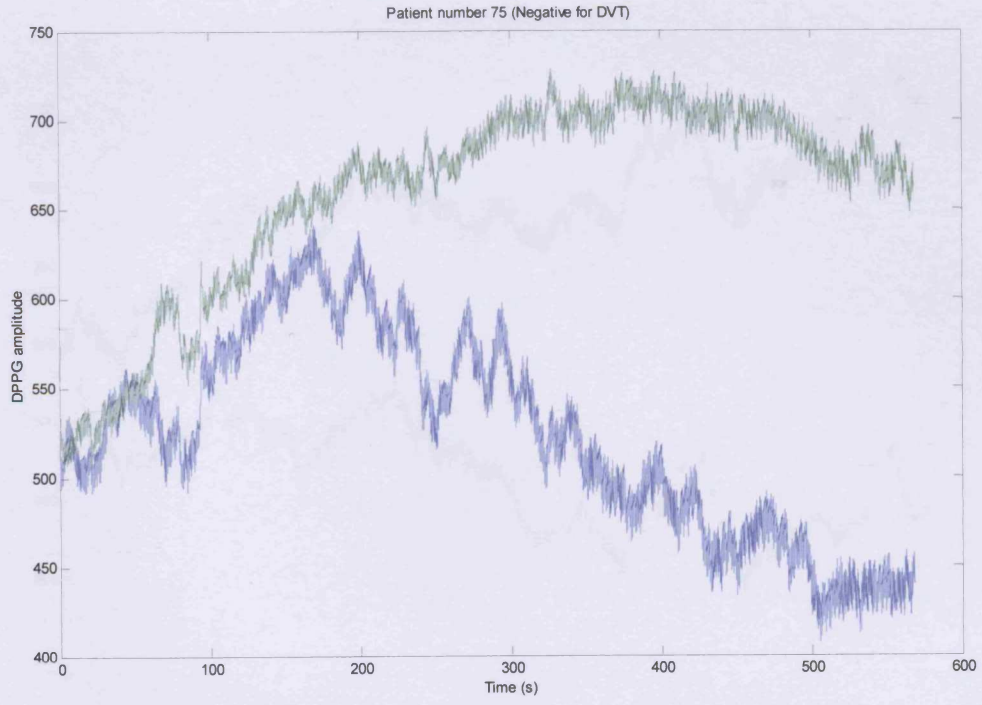
Patient number 75 (Negative for DVT)
DPPG amplitude
Time (s)
750
700
650
600
550
500
450
400
0
100
200
300
400
500
600

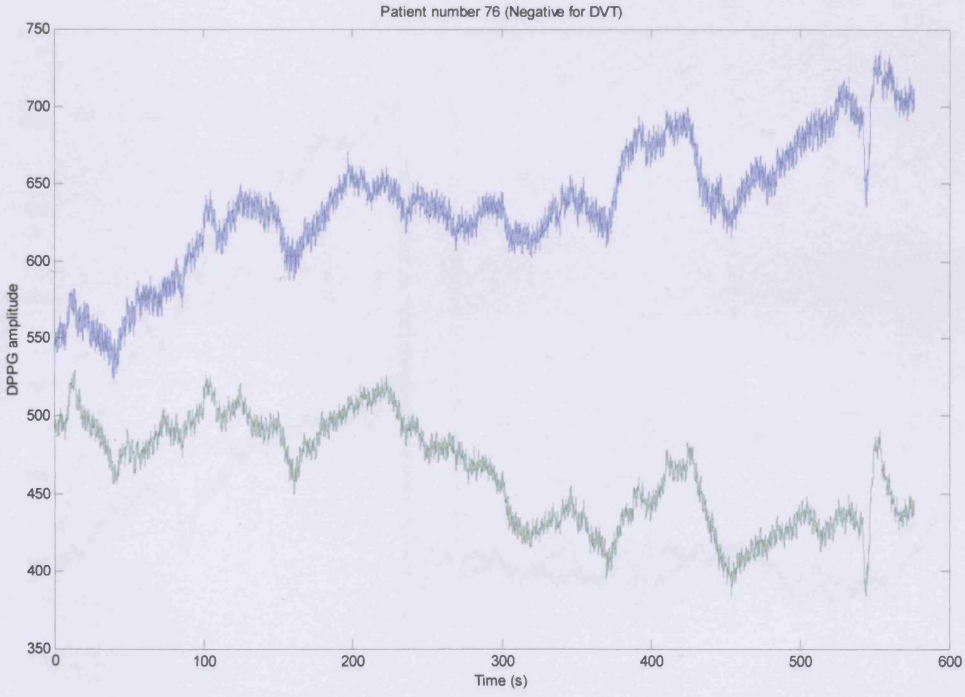
Patient number 76 (Negative for DVT)
DPPG amplitude
Time (s)
750
700
650
600
550
500
450
400
350
0
100
200
300
400
500
600

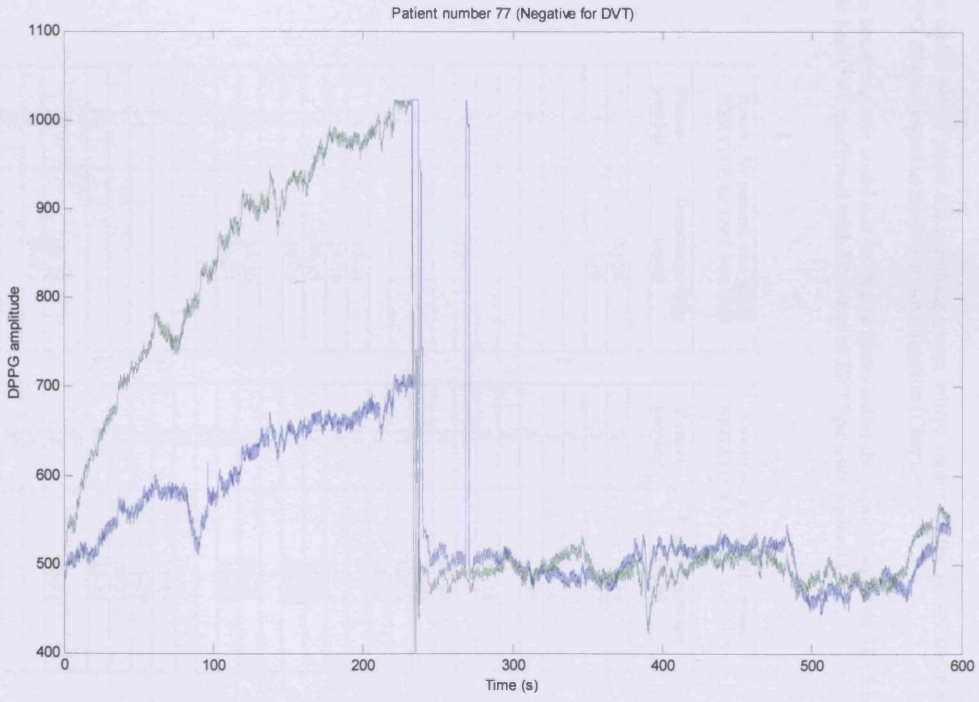
Patient number 77 (Negative for DVT)
DPPG amplitude
Time (s)
1100
1000
900
800
700
600
500
400
0
100
200
300
400
500
600

Appendix J

Breathing frequencies in the power spectra of the DPPG data collected in the patient investigation

---

The tables below show the breathing range, where visible, in the power spectra of the DPPG data collected in the patient investigation (Chapter 9).

The breathing rate could not be clearly identified in the power spectra of 31/65 patients who had DVT confirmed with DUS and in 32/77 patients without DVT.

Results for patients who tested **POSITIVE** for DVT with DUS	
Patient number	**Breathing range (cpm)**
1	
2	20-24
3	24-28
4	
5	
6	
7	
8	
9	16-21
10	
11	
12	
13	
14	19-24
15	25-30
16	20-25
17	16-24
18	
19	24-30
20	21-24
21	
22	
23	
24	
25	
26	
27	
28	18-23
29	18-22
30	
31	10-14
32	
33	19-25
34	22-25
35	14-20
36	10-16

Results for patients who tested **NEGATIVE** for DVT with DUS	
Patient number	**Breathing range (cpm)**
1	
2	24-29
3	13-17
4	
5	20-24
6	15-19
7	
8	20-25
9	
10	12-24
11	17-20
12	18-23
13	18-21
14	
15	
16	18-22
17	22-28
18	
19	20-24
20	15-23
21	
22	
23	18-22
24	25-29
25	20-23
26	22-25
27	
28	17-22
29	
30	
31	
32	20-24
33	8-12
34	
35	16-26
36	

37	
38	
39	19-26
40	22-28
41	23-26
42	
43	
44	
45	22-27
46	24-27
47	12-24
48	24-32
49	
50	15-24
51	
52	16-28
53	10-20
54	15-22
55	
56	
57	13-19
58	
59	15-23
60	13-19
61	26-29
62	12-21
63	20-26
64	
65	15-21

37	15-25
38	19-23
39	15-22
40	22-30
41	
42	13-19
43	
44	12-17
45	
46	12-18
47	13-19
48	10-20
49	
50	
51	16-20
52	15-20
53	15-23
54	
55	14-20
56	16-21
57	
58	
59	18-30
60	15-25
61	
62	17-22
63	
64	14-19
65	
66	19-25
67	
68	
69	
70	
71	
72	18-30
73	17-22
74	
75	14-23
76	18-23
77	8-15

Appendix K

Definitions of sensitivity, specificity, positive predicting value, negative predicting value and accuracy

---

***Sensitivity*: The ability of a test to correctly detect disease.**

$$Sensitivity = \frac{N_{correct+}}{N_{disease}} \times 100$$

$N_{correct+}$: Number of correct positive tests compared to the gold standard.

$N_{disease}$: Total number with disease diagnosed by the gold standard.

***Specificity*: The ability of a test to correctly rule out disease.**

$$Specificity = \frac{N_{correct-}}{N_{normal}} \times 100$$

$N_{correct-}$: Number of correct negative tests compared to the gold standard.

N_{normal}: Total number with no disease detected by the gold standard.

***Positive Predicting Value (PPV)*: Indicates whether a positive test result is likely to be correct.**

$$PPV = \frac{N_{correct+}}{N_{tot+}} \times 100$$

$N_{correct+}$: Number of correct positive tests compared to the gold standard.

N_{tot+}: Total number of positive tests.

***Negative Predicting Value (NPV)*: Indicates whether a negative test result is likely to be correct.**

$$NPV = \frac{N_{correct-}}{N_{tot-}} \times 100$$

$N_{correct-}$: Number of correct negative tests compared to the gold standard.

N_{tot-}: Total number of negative tests.

***Accuracy*: The overall ability of a test to give a correct diagnosis.**

$$Accuracy = \frac{N_{correct\pm}}{N_{total}} \times 100$$

$N_{correct\pm}$: Number of correct positive and negative tests compared to the gold standard.

N_{total} : Total number of tests.

Appendix L

Cardiac frequencies in the power spectra of the DPPG data collected in the patient investigation

---

The tables below show the range of cardiac frequencies observed in the power spectra of the DPPG data collected in the patient investigation (Chapter 9).

The cardiac rate could not be clearly identified in the power spectra of 2/65 patients who had DVT confirmed with DUS and in 1/77 patients without DVT.

Results for patients who tested **POSITIVE** for DVT with DUS	
Patient number	**Cardiac range (cpm)**
1	125-130
2	77-87
3	58-66
4	75-85
5	70-80
6	99-106
7	91-110
8	54-68
9	82-88
10	78-84
11	93-98
12	87-95
13	72-79
14	57-65
15	75-83
16	73-81
17	95-99
18	78-90
19	111-122
20	64-68
21	56-68
22	88-98
23	90-104
24	102-118
25	84-88
26	85-90
27	93-97
28	60-71
29	81-93
30	59-75
31	120-124
32	71-84
33	------
34	98-104
35	60-74
36	79-91

Results for patients who tested **NEGATIVE** for DVT with DUS	
Patient number	**Cardiac range (cpm)**
1	67-71
2	80-84
3	66-69
4	54-68
5	71-77
6	75-81
7	66-78
8	58-63
9	97-105
10	54-60
11	84-90
12	68-74
13	56-65
14	47-53
15	66-80
16	71-79
17	64-70
18	62-65
19	78-93
20	56-70
21	86-94
22	80-86
23	72-86
24	78-82
25	80-88
26	80-96
27	61-69
28	80-94
29	67-80
30	87-92
31	53-64
32	71-83
33	72-77
34	------
35	78-85
36	66-73

37	65-72
38	------
39	77-98
40	85-90
41	64-72
42	60-70
43	82-92
44	83-89
45	80-85
46	100-112
47	98-104
48	74-85
49	85-92
50	80-103
51	75-85
52	105-122
53	62-68
54	80-85
55	62-76
56	95-99
57	77-86
58	72-78
59	64-73
60	55-64
61	78-86
62	94-101
63	86-106
64	112-119
65	71-76

37	82-90
38	71-80
39	98-107
40	72-82
41	97-106
42	81-87
43	68-79
44	77-88
45	70-82
46	70-80
47	75-83
48	79-89
49	69-80
50	59-74
51	70-82
52	66-70
53	66-77
54	55-63
55	90-94
56	80-100
57	91-99
58	101-112
59	71-80
60	70-80
61	81-90
62	55-63
63	63-77
64	62-72
65	64-76
66	70-84
67	92-112
68	73-86
69	90-106
70	66-78
71	94-108
72	90-98
73	57-65
74	65-73
75	73-81
76	54-60
77	72-76

Bibliography

Abramowitz HB, Queral LA, Flinn WR, Nora PF Jr, Peterson LK, Bergan JJ and Yao JST. The use of photoplethysmography in the assessment of venous insufficiency: A Comparison to venous pressure measurements. *Surgery* 1979; **86 (3):** 434-41

Allen J, Murray A. Prospective assessment of an artificial neural network for the detection of peripheral vascular disease from lower limb pulse waveforms. *Physiol Meas* 1995; **16 (1):** 29-38

Allen J, Murray A. Similarity in bilateral photoplethysmographic peripheral pulse wave characteristics at the ears, thumbs and toes. *Physiol Meas* 2000; **21 (3):** 369-77

Anand SS, Wells PS, Hunt D, Brill-Edwards P, Cook D, Ginsberg JS. Does this patient have deep vein thrombosis? *JAMA* 1998; **279 (14):** 1094-9

Anderson DR, Lensing AW, Wells PS, Levine MN, Weitz JI, Hirsh J. Limitations of impedance plethysmography in the diagnosis of clinically suspected deep-vein thrombosis. *Ann Intern Med 1993*; **118 (1):** 25-30

Anderson RR, Parrish JA. The optics of human skin. *J Invest Dermatol* 1981; **77 (1):** 13-9

Anderson FA Jr, Wheeler HB. Physician practices in the management of venous thromboembolism: A community-wide survey. *J Vasc Surg* 1992; **16 (5):** 707-14

Anderson FA Jr, Wheeler HB, Goldberg RJ, Hosmer DW, Patwardhan NA, Jovanovic B, Forcier A, Dalen JE. A population-based perspective of the hospital incidence and case-fatality rates of deep vein thrombosis and pulmonary embolism. The Worcester DVT Study. *Arch Intern Med* 1991; **151 (5):** 933-8

Baglin T, Luddington R, Brown K, Baglin C. Incidence of recurrent venous thromboembolism in relation to clinical and thrombophilic risk factors: prospective cohort study. *Lancet* 2003; **362 (9383):** 523-6

Bank I, Mac Gillavry MR, Brandjes DPM, Büller HR. Does the location of deep venous thrombosis of the leg determine the risk of the post-thrombotic syndrome? *J Thromb Haemost* 2003; **1 (9):** 2058-9

Beasley R, Raymond N, Hill S, Nowitz M, Hughes R. eThrombosis: the 21st Century variant of venous thromboembolism associated with immobility. *Eur Respir J* 2003; **21 (2):** 374-6

Belcaro G, Nicolaides AN, Veller M. 1995. Venous Disorders: A Manual of Diagnosis and Treatment. London, UK: WB Saunders Company

Bernardi L, Radaelli A, Solda PL, Coats AJS, Reeder M, Calciati A, Garrard CS, Sleight P. Autonomic control of skin microvessels: Assessment by power spectrum of photoplethysmographic waves. *Clinical Science* 1996; **90 (5):** 345-55

Berne RM, Levy MN. 1998. Physiology. 4th edition. St. Louis, Missouri: Mosby

Blažek V, Schultz-Ehrenburg U. 1996. Quantitative Photoplethysmography: Basic Facts and Examination Tests for Evaluating Vascular Functions. Düsseldorf: VDI Verlag

Bloomfield P. 2000. Fourier Analysis of Time Series: An Introduction. 2nd edition. New York: Wiley

Bounameaux H, de Moerloose P, Perrier A, Reber G. Plasma measurement of D-dimer as diagnostic aid in suspected venous thromboembolism: an overview. *Thromb Haemostas.* 1994; **71 (1):** 1-6

Bradley MJ, Spencer PA, Alexander L, Milner GR. Colour flow mapping in the diagnosis of the calf deep vein thrombosis. *Clin Radiol* 1993; **47 (6):** 399-402

Brandjes DPM, Büller HR, Heijboer H, Huisman MV, de Rijk M, Jagt H, ten Cate JW. Randomised trial of effect of compression stockings in patients with symptomatic proximal-vein thrombosis. *Lancet* 1997; **349 (9054):** 759-62

Bray JJ, Cragg PA, Macknight ADC, Mills RG. 1999. Lecture Notes on Human Physiology. 4th edition. Oxford: Blackwell Science

Brotman DJ, Segal JB, Jani JT, Petty BG, Kickler TS. Limitations of D-dimer testing in unselected inpatients with suspected venous thromboembolism. *Am J Med* 2003; **114 (4):** 276-82

Browse NL, Burnand KG, Irvine AT, Wilson NM. 1999. Diseases of the Veins. 2nd edition. London, UK: Arnold

Chawla R, Kumarvel V, Girdhar KK, Sethi AK, Indrayan A, Bhattacharya A. Can pulse oximetry be used to measure systolic blood pressure?. *Anesth Analg* 1992; **74 (2):** 196-200

Chengelis DL, Bendick PJ, Glover JL, Brown OW, Ranval TJ. Progression of superficial venous thrombosis to deep vein thrombosis. *J Vasc Surg* 1996; **24 (5):** 745-9

Clagett GP, Anderson FA Jr, Heit J, Levine M, Wheeler HB. Prevention of venous thromboembolism. *Chest* 1995; **108 (Suppl 4):** 312S-334S

Dexter L, Folch-Pi W. Venous thrombosis. An account of the first documented case. *JAMA* 1974; **228 (2):** 195-6

Diamond S, Goldbweber R, Katz S. Use of D-dimer to aid in excluding deep venous thrombosis in ambulatory patients. *Am J Surg* 2005; **189 (1):** 23-6

Dorlas JC. Nijboer JA. Photo-electric plethysmography as a monitoring device in anaesthesia. Application and interpretation. *Br J Anaesth* 1985; **57 (5):** 524-30

Fowkes FJ, Price JF, Fowkes FG. Incidence of diagnosed deep vein thrombosis in the general population: systematic review. *Eur J Vasc Endovasc Surg* 2003: **25 (1):** 1-5

Fowl RJ, Strothman GB, Blebea J, Rosenthal GJ, Kempczinski RF. Inappropriate use of venous duplex scans: an analysis of indications and results. *J Vasc Surg* 1996; **23 (5):** 881-5

Fraser DGW, Moody AR, Morgan PS, Martel AL, Davidson I. Diagnosis of lower-limb deep venous thrombosis: A prospective blinded study of magnetic resonance direct thrombus imaging. *Ann Intern Med* 2002; **136 (2):** 89-98

Fronek A, Vanderweijer I. Noninvasive determination of venomuscular efficiency. *J Vasc Surg* 2003; **37 (4):** 839-41

Ganong WF. 1999. Review of Medical Physiology. 19th edition. Stamford, Connecticut: Appleton & Lange

Giltvedt J, Sira A, Helme P. Pulsed multifrequency photoplethysmograph. *Med & Biol Eng & Comput* 1984; **22 (3):** 212-15

Ginsberg JS, Wells PS, Hirsh J, Panju AA, Patel MA, Malone DE, McGinnis J, Stevens P, Brill-Edwards P. Reevaluation of the sensitivity of impedance plethysmography for the detection of proximal deep vein thrombosis. *Arch Intern Med* 1994; **154 (17):** 1930-3

Guyton AC, Hall JE. 2000. Textbook of Medical Physiology. 10th edition. Philadelphia, Pennsylvania: WB Saunders Company

Hansson PO, Welin L, Tibblin G, Eriksson H. Deep vein thrombosis and pulmonary embolism in the general population. 'The Study of Men Born in 1913'. *Arch Intern Med* 1997; **157 (15):** 1665-70

Harris LM, Curl GR, Booth FV, Hassett JM Jr, Leney G, Ricotta JJ. Screening for asymptomatic deep vein thrombosis in surgical intensive care patients. *J Vasc Surg* 1997; **26 (5):** 764-9

Heijboer H, Buller HR, Lensing A, Turpie A, Colly LP, ten Cate JW. A Comparison of real-time compression ultrasonography with impedance plethysmography for the diagnosis of deep-vein thrombosis in symptomatic outpatients. *N Engl J Med* 1993; **329 (19):** 1365–9

Hertzman AB. The blood supply of various skin areas as estimated by the photoelectric plethysmograph. *Am J Physiol* 1938; **124 (2):** 328-40

Hertzman AB, Dillon JB. Applications of photoelectric plethysmography in peripheral vascular disease. *Am Heart J* 1940a; **20 (6):** 750-61

Hertzman AB, Dillon JB. Distinction between arterial, venous and flow components in photoelectric plethysmography in man. *Am J Physiol* 1940b; **130 (1):** 177-85

Hyers TM, Hull RD, Morris TA, Tapson V. Antithrombotic therapy for venous thromboembolic disease. *Chest* 2001; **119 (Suppl 1):** 176S–193S

Jackson MR. Diagnosis and management of venous thrombosis in the surgical patient. *Semin Thromb Hemost* 1998; **24 (Suppl 1):** 67-76

Janes S, Ashford N. Use of a simplified clinical scoring system and D-dimer testing can reduce the requirement for radiology in the exclusion of deep vein thrombosis by over 20%. *Br J Haematol* 2001; **112 (4):** 1079-82

Kahn SR, Ginsberg JS. Relationship between deep venous thrombosis and the postthrombotic syndrome. *Archives of Internal Medicine* 2004; **164 (1):** 17-26

Kamal AAR, Harness JB, Irving G, Mearns AJ. Skin photoplethysmography - a review. *Comput Methods Programs Biomed* 1989; **28 (4):** 257-69

Kearon C. Noninvasive diagnosis of deep vein thrombosis in postoperative patients. *Semin Thromb Hemost* 2001; **27 (1):** 3-8

Kelly J, Rudd A, Lewis RR, Hunt BJ. Plasma D-dimers in the diagnosis of venous thromboembolism. *Arch Int Med* 2002; **162 (7):** 747-56

Lensing AW, Prandoni P, Prins MH, Büller HR. Deep-vein thrombosis. *Lancet* 1999; **353 (9151):** 479-85

Lindberg L-G, Öberg PÅ. Photoplethysmography. Part 2. Influence of light source wavelength. *Med Biol Eng Comput* 1991; **29 (1):** 48-54

Lindberg L-G, Ugnell H, Öberg PÅ. Monitoring of respiratory and heart rates using a fibre-optic sensor. *Med & Biol Eng & Comput* 1992; **30 (5):** 533-7

Line BR. Pathophysiology and diagnosis of deep venous thrombosis. *Seminars in Nuclear Medicine* 2001; **31 (2):** 90-101

Lynn PA. 1993. An Introduction to the Analysis and Processing of Signals. 3rd edition. London, UK: Macmillan

Mannucci PM. Venous thrombosis: The history of knowledge. *Pathophysiol Haemost Thromb* 2002; **32 (5-6):** 209-12

Markel A, Manzo RA, Bergelin RO, Strandness DE Jr. Pattern and distribution of thrombi in acute venous thrombosis. *Arch Surg* 1992; **127 (3):** 305-9

Martini FH. 1989. Fundamentals of Anatomy and Physiology. 4th edition. New Jersey: Prentice Hall

Maskell NA, Cooke S, Meecham Jones DJ, Prior JG, Butland RJA. The use of automated strain gauge plethysmography in the diagnosis of deep vein thrombosis. *Br J Radiol* 2002; **75 (896):** 648-51

Messina LM, Sarpa MS, Smith MA, Greenfield LJ. Clinical significance of routine imaging of iliac and calf veins by color flow duplex scanning in patients suspected of having acute lower extremity deep venous thrombosis. *Surgery* 1993; **114 (5):** 921-7

Miller N, Obrand D, Tousignant L, Gascon I, Rossignol M. Venous duplex scanning for unilateral symptoms: When do we need a contralateral evaluation? *Eur J Vasc Endovasc Surg* 1998; **15 (1):** 18-23

Moser KM, Fedullo PF, LitteJohn JK, Crawford R. Frequent asymptomatic pulmonary embolism in patients with deep venous thrombosis. *JAMA* 1994; **271 (3):** 223-5

Molitor H, Kniazuk M. A new bloodless method for continuous recording of peripheral circulatory changes. *J Pharmacol Exp Ther* 1936; **57:** 6-18

Morris Rh J. 2000. The Effects of Intermittent Compression on Lower Limb Blood Flow. PhD Thesis, University of Wales, Cardiff

Moser KM, LeMoine JR. Is embolic risk conditioned by location of deep venous thrombosis? *Ann Intern Med* 1981; **94 (1):** 439-44

Moyle JTB. 2002. Pulse Oximetry. 2nd edition. London, UK: BMJ Books

Mukherjee D, Andersen CA, Sado AS, Bertoglio MC. Use of light reflection rheography for diagnosis of axillary or subclavian venous thrombosis. *Am J Surg* 1991; **161 (6):** 651-6

Murray WB, Foster PA. The peripheral pulse wave: Information overlooked. *J Clin Monit* 1996; **12 (5):** 365-77

Naidich JB, Torre JR, Pellerito JS, Smalberg IS, Kase DJ, Crystal KS. Suspected deep venous thrombosis: Is US of both legs necessary? *Radiology* 1996; **200 (2):** 429-31

Nakajima K, Tamura T, Miike H. Monitoring of heart and respiratory rates by photoplethysmography using a digital filtering technique. *Medical Engineering & Physics* 1996; **18 (5):** 365-72

Nicolaides AN, Miles C. Photoplethysmography in the assessment of venous insufficiency. *J Vasc Surg* 1987; **5 (3):** 405-12

Nicolaides AN, Sumner DS. 1991. Investigation of Patients with Deep Vein Thrombosis and Chronic Venous Insufficiency. London, UK: Med-Orion

Nijboer JA, Dorlas JC and Mahieu HF. Photoelectric plethysmography - some fundamental aspects of the reflection and transmission method. *Clin Phys Physiol Meas* 1981; **2 (3):** 205-15

Nilsson L, Johansson A, Kalman S. Monitoring of respiratory rate in postoperative care using a new photoplethysmographic technique. *J Clin Monit Comput* 2000; **16 (4);** 309-15

Nilsson L, Johansson A, Kalman S. Respiratory variations in the reflection mode photoplethysmographic signal. Relationships to peripheral venous pressure. *Med Biol Eng Comput* 2003; **41 (3):** 249-54

Nitzan M, Babchenko A, Khanokh B. Very low frequency variability in arterial blood pressure and blood volume pulse. *Med & Biol Eng & Comput* 1999; **37 (1):** 54-8

Nitzan M, Babchenko A, Khanokh B, Landau D. The variability of the photoplethysmographic signal – a potential method for the evaluation of the autonomic nervous system. *Physiol Meas* 1998; **19 (1):** 93-102

Olsson E, Ugnell H, Oberg PA and Sedin G. Photoplethysmography for simultaneous recording of heart and respiratory rates in newborn infants. *Acta Paediatrica* 2000; **89 (7):** 853-61

Passman MA, Moneta GL, Taylor LM Jr, Edwards JM, Yeager RA, McConnell DB, Porter JM. Pulmonary embolism is associated with the combination of isolated calf vein thrombosis and respiratory symptoms. *J Vasc Surg* 1997; **25 (1):** 39-45

Philbrick JT, Becker DM. Calf deep venous thrombosis. A wolf in sheep's clothing? *Arch Intern Med* 1988; **148 (10):** 2131-8

Phillips GW. Review of venous vascular ultrasound. *World J Surg* 2000; **24 (2):** 241-8

Prandoni P, Lensing AWA; Cogo A, Cuppini S, Villalta S, Carta M, Cattelan AM, Polistena P, Bernardi E, Prins MH. The long-term clinical course of acute deep venous thrombosis. *Ann Intern Med* 1996; **125 (1):** 1-7

Rose SC, Zwiebel WJ, Nelson BD, Priest DL, Knighton RA, Brown JW, Lawrence PF, Stults BM, Reading JC, Miller FJ. Symptomatic lower extremity deep venous thrombosis: Accuracy, limitations, and role of color duplex flow imaging in diagnosis. *Radiology* 1990: **175 (3):** 639-44

Rosfors S. Venous photoplethysmography: Relationship between transducer position and regional distribution of venous insufficiency. *J Vasc Surg* 1990; **11 (3):** 436-40

Rubin BG, Reilly JM, Sicard GA, Botney MD. Care of patients with deep venous thrombosis in an academic medical center: limitations and lessons. *J Vasc Surg* 1994; **20 (5):** 698-704

Rutgers PH, Kitslaar PJ, Ermers EJ. Photoplethysmography in the diagnosis of superficial venous valvular incompetence. *Br J Surg* 1993; **80 (3):** 351-3

Sadiq S, Chithriki M. Arterial pressure measurements using infrared photosensors: comparison with CW Doppler. *Clin Physiol* 2001; **21 (1):** 129-32

Sandler DA, Martin JF. Autopsy proven pulmonary embolism in hospital patients: Are we detecting enough deep vein thrombosis? *J R Soc Med* 1989; **82 (4):** 203-5

Smith SW. 1999. The Scientist and Engineer's Guide to Digital Signal Processing. 2nd edition. San Diego: California Technical Publishing

Sproule, M W. Alcorn, D J. Reid, A W. The value of light reflection rheography as a screening tool for deep venous thrombosis. *Br J Radiol* 1997; **70 (836):** 782-5

Stacey MC, Rashid P, Hoskin SE, Pearce CA. Influence of arterial disease, age and active ulceration on venous refilling time measured by photoplethysmography. *Cardiovasc Surg* 1996; **4 (3):** 368-71

Stefanovska A, Bračič M, Kvernmo HD. Wavelet analysis of oscillations in the peripheral blood circulation measured by laser Doppler technique. *IEEE Transactions on Biomedical Engineering* 1999; **46 (10):** 1230-9

Tan YK and da Silva AF. Digital photoplethysmography in the diagnosis of suspected lower limb DVT: Is it useful? *Eur J Vasc Endovasc Surg* 1999; **18 (1):** 71-9

Tapson VF, Carroll BA, Davidson BL, Elliott CG, Fedullo PF, Hales CA, Hull RD, Hyers TM, Leeper KV Jr, Morris TA, Moser KM, Raskob GE, Shure D, Sostman HD, Taylor Thompson B. The diagnostic approach to acute venous thromboembolism. Clinical practice guideline. *Am J Respir Crit Care Med* 1999; **160 (3):** 1043-66

Tarnay TJ, Rohr PR, Davidson AG, Stevenson MM, Byars EF, Hopkins GR. Pneumatic calf compression, fibrinolysis and the prevention of deep venous thrombosis. *Surgery* 1980; **88 (4):** 489-96

Vanek VW. Meta-analysis of effectiveness of intermittent pneumatic compression devices with a comparison of thigh-high to knee-high sleeves. *Am Surg* 1998; **64 (11):** 1050-8

Veraart JC, Joost van der Kley AM, Neumann HA. Digital photoplethysmography and light reflection rheography. A clinical comparison. *J Dermatol Surg Oncol* 1994; **20 (7):** 470-3

Wells PS, Hirsh J, Anderson DR, Lensing AW, Foster G, Kearon C, Weitz J, D'Ovidio R, Cogo A, Prandoni P, Girolami A, Ginsberg JS. Accuracy of clinical assessment of deep-vein thrombosis. *Lancet* 1995; **345 (8961):** 1326-30

Wells PS, Anderson DR, Bormanis J, Guy F, Mitchell M, Gray L, Clement C, Robinson KS, Lewandowski B. Value of assessment of pretest probability of deep-vein thrombosis in clinical management. *Lancet* 1997; **350 (9094):** 1795–8

Wells PS, Anderson DR, Rodger M, Forgie M, Kearon C, Dreyer J, Kovacs G, Mitchell M, Lewandowski B, Kovacs MJ. Evaluation of D-dimer in the diagnosis of suspected deep-vein thrombosis. *N Engl J Med* 2003; **349 (13):** 1227-35

White RH. The epidemiology of venous thromboembolism. *Circulation* 2003; **107 (Suppl 1):** I-4 – I-8

White RH, McGahan JP, Daschbach MM, Hartling RP. Diagnosis of deep-vein thrombosis using duplex ultrasound. *Ann Intern Med* 1989; **111 (4):** 297-304

Zierler BK. Ultrasonography and diagnosis of venous thromboembolism. *Circulation* 2004; **109 (Suppl 1):** I-9 – I-14